Series Editor R. R. Gupta

Volume Editor S. Eguchi

Bioactive Heterocycles II

Springer

8
Topics in Heterocyclic Chemistry

Series Editor: R. R. Gupta

Topics in Heterocyclic Chemistry
Series Editor: R. R. Gupta

Recently Published and Forthcoming Volumes

Bioactive Heterocycles II

Volume Editor: Shoji Eguchi

With contributions by

M. Ariga · H. Fujii · A. B. Hendrich · H. Ichinose · K. Matsumoto
K. Michalak · N. Motohashi · S. Murata · H. Nagase · N. Nishiwaki
N. Shibata · T. Toru · F. Urano · O. Wesołowska
T. Yamamoto · M. Yamashita

The series *Topics in Heterocyclic Chemistry* presents critical reviews on "Heterocyclic Compounds" within topic-related volumes dealing with all aspects such as synthesis, reaction mechanisms, structure complexity, properties, reactivity, stability, fundamental and theoretical studies, biology, biomedical studies, pharmacological aspects, applications in material sciences, etc. Metabolism will be also included which will provide information useful in designing pharmacologically active agents. Pathways involving destruction of heterocyclic rings will also be dealt with so that synthesis of specifically functionalized non-heterocyclic molecules can be designed.

The overall scope is to cover topics dealing with most of the areas of current trends in heterocyclic chemistry which will suit to a larger heterocyclic community.

As a rule contributions are specially commissioned. The editors and publishers will, however, always be pleased to receive suggestions and supplementary information. Papers are accepted for *Topics in Heterocyclic Chemistry* in English.

In references *Topics in Heterocyclic Chemistry* is abbreviated *Top Heterocycl Chem* and is cited as a journal.

Springer WWW home page: springer.com
Visit the THC content at springerlink.com

Springer is a part of Springer Science+Business Media

springer.com

© Springer-Verlag Berlin Heidelberg 2007

Series Editor

Prof. R. R. Gupta

10A, Vasundhara Colony
Lane No. 1, Tonk Road
Jaipur-302 018, India
rrg_vg@yahoo.co.in

Volume Editor

Emeritus Prof. Shoji Eguchi

Dept. Molecular Design and Engineering
Graduate School of Engineering
Nagoya University
Furo-cho
464-8603 Nagoya, Aichi-ken
Japan
eguchi@lilac.ocn.ne.jp

Editorial Board

Topics in Heterocyclic Chemistry
Also Available Electronically

For all customers who have a standing order to Topics in Heterocyclic Chemistry, we offer the electronic version via SpringerLink free of charge. Please contact your librarian who can receive a password or free access to the full articles by registering at:

springerlink.com

If you do not have a subscription, you can still view the tables of contents of the volumes and the abstract of each article by going to the SpringerLink Homepage, clicking on "Browse by Online Libraries", then "Chemical Sciences", and finally choose Topics in Heterocyclic Chemistry.

You will find information about the

– Editorial Board
– Aims and Scope
– Instructions for Authors
– Sample Contribution

at springer.com using the search function.

Preface

As part of the series *Topics in Heterocyclic Chemistry*, this volume titled *Bioactive Heterocycles II* presents comprehensive and up-to-date reviews on selected topics regarding synthetic as well as naturally occurring bioactive heterocycles.

The first chapter, "High Pressure Synthesis of Heterocycles Related to Bioactive Molecules" by Kiyoshi Matsumoto, presents a unique high-pressure synthetic methodology in heterocyclic chemistry. Basic principles and fruitful examples for pericyclic reactions, such as Diels-Alder reactions, 1,3-dipolar reactions, and also for ionic reactions, such as S_N and addition reactions, are discussed. The review will be of considerable interest to heterocyclic chemists and synthetic chemists.

The second chapter, "Ring Transformation of Nitropyrimidinone Leading to Versatile Azaheterocyclic Compounds" by Nagatoshi Nishiwaki and Masahiro Ariga, presents a very critical review on novel ring transformations of dinitropyridones and nitropyrimidinones based on the work of his group. Addressed in this review is the synthesis of functionalized molecules, such as nitroanilines, nitropyridines, and nitrophenols, by the ring transformation of dinitropyridones as the nitromalonaldehyde equivalent. Ring transformations of nitropyrimidinones with dinucleophiles to 4-pyridones, pyrimidines and 4-aminopyridines, and to polyfunctinal pyridones with 1,3-dicarbonyl compounds, etc., are also discussed. This review may attract the interest of synthetic chemists as well as heterocyclic chemists in the life science fields.

The third chapter, "Synthesis of Thalidomide" by Norio Shibata, Takeshi Yamamoto and Takeshi Toru, describes a modern synthetic aspect of thalidomide.

This drug has had a disastrous medical history due to its teratogenicity, however, its recently found efficacy toward so-called incurable diseases, such as leprosy, AIDS, and various cancers, has revived researchers' interest, in particular for the production of optically pure isomers. From this point of view, this article may be attractive to medicinal and pharmaceutical chemists, and also heterocyclic and synthetic chemists.

The fourth chapter, "Rational Drug Design of delta Opioid Receptor Agonist TAN-67 from delta Opioid Receptor Antagonist NTI" by Hiroshi Nagase and Hideaki Fujii, presents the fascinating and successful drug design of delta opioid receptor agonist TAN-67 from delta opioid receptor antagonist NTI

based on the work by Nagase and his coworkers. The drug design requires a high level of synthetic technology in order to provide designed molecules for pharmacological evaluations. This article represents a very brilliant example of molecular design and may attract much attention from researchers in the fields of pharmacology, medicinal chemistry, and organic synthesis.

The fifth chapter, "Tetrahydrobiopterin and Related Biologically Important Pterins" by Shizuaki Murata, Hiroshi Ichinose and Fumi Urano, describes a modern aspect of pteridine chemistry and biochemistry. Pteridine derivatives play a very important role in the biosynthesis of amino acids, nucleic acids, neurotransmitters and nitrogenmonooxides, and metabolism of purine and aromatic amino acids. Some pteridines are used in chemotherapy and for the diagnosis of various diseases. From these points of view, this article will attract considerable attention from medicinal and pharmaceutical chemists, and also heterocyclic chemists and biochemists.

The sixth chapter, "Preparation, Structure and Biological Property of Phosphorus Heterocycles with a C-P Ring System" by Mitsuji Yamashita presents a very critical review of novel phosphorus heterocycles. The review discusses aliphatic 4-, 5-, 6- and 7-membered C-P-C heterocycles, aromatic C-P-C heterocycles, and various C-P-O type heterocycles including phospha sugars. Synthetic aspects, structural studies, and the biological properties of these phosphorus heterocycles are also addressed. This chapter may attract the interest of synthetic chemists as well as heterocyclic and heteroatom chemists in the life science fields.

The final chapter, "The Role of the Membrane Actions of Phenothiazines and Flavonoids as Functional Modulators" by K. Michalak, O. Wesolowska, N. Motohashi and A. B. Hendrich, presents a very comprehensive review on important biological effects of phenothiazines and flavonoids due to interactions with membrane proteins and the lipid phase of membranes. The discussion includes the influence of these heterocycles on model and natural membranes, modulation of MDR transporters by these heterocycles, and the effects of these heterocycles on ion channel properties. This review may attract much interest from medicinal and pharmaceutical chemists as well as heterocyclic chemists in the life science fields.

I hope that our readers find this series to be a useful guide to modern heterocyclic chemistry. As always, I encourage both suggestions for improvement and ideas for review topics.

Nagoya, March 2007   Shoji Eguchi

Contents

Contents of Volume 6

Bioactive Heterocycles I

Volume Editor: Eguchi, S.
ISBN: 978-3-540-33350-0

High-Pressure Synthesis of Heterocycles Related to Bioactive Molecules

Kiyoshi Matsumoto

Department of Pharmaceutical Sciences, Faculty of Pharmacy,
Chiba Institute of Science, Choshi, 288-0025 Chiba, Japan
kmatsumoto@cis.ac.jp

Abstract The present article describes 1) how to perform high-pressure experiments; and 2) the most recent examples of synthetic applications of high-pressure mediated pericyclic reactions, such as inter- and intramolecular Diels–Alder reactions, 1,3-dipolar reactions, and multicomponent cycloadditions to heterocycles related to biologically interesting molecules. The article also extends to ionic reactions in a similar fashion, though not many examples have been investigated. The scope and limitations are also described when necessary.

Keywords Addition reaction · 1,3-Dipolar reaction · Diels–Alder reaction · High pressure · Substitution reaction

Abbreviations
Ac   Acetyl
AcOEt   Ethyl acetate

Aq	Aqueous
BHT	2,6-Di-*tert*-butyl-4-methylphenol
Bn	Benzyl
BOC	*tert*-Butoxycarbonyl
Cbz	Benzyloxycarbonyl
DCM	Dichloromethane
DEGD	Diglyme ethylene glycol dimethyl ether
DHP	Dihydrofuran
DMAD	Dimethylacetylene dicarboxylate
DMAP	4-(Dimethylamino)pyridine
DME	1,2-Dimethoxyethane
DMF	Dimethylformamide
DMSO	Dimethyl sulfoxide
13DPR	1,3-Dipolar reaction
ee	Enantiomeric excess
EtOH	Ethanol
EuFOD	Europium tris(6,6,7,7,8,8,8-heptafluoro-2,2-dimethyl-3,5-octanedionate)
fod	Tris(6,6,7,7,8,8,8-heptafluoro-2,2-dimethyl-3,5-octanedionate)
HJR	Hilbert–Johnson reaction
HMPA	Hexamethylphosphoric triamide
IEDAR	Intermolecular Diels–Alder reaction
IRDAR	Intramolecular Diels–Alder reaction
MATBr	Methylaluminum bis(2,4,6-tribromophenoxide)
MCC	Multicomponent cycloaddition
MCR	Multicomponent reaction
MeOH	Methanol
MOM	Methoxymethyl
NMP	*N*-Methylpyrrolidine
Pet. Et	Petroleum ether
PTFE	Polytetrafluoroethylene (Teflon®)
Pyr	Pyridine
rt	Room temparature
SES	β-(Trimethylsilyl)ethanesulfonyl
TADDOL	$\alpha,\alpha,\alpha',\alpha'$-Tetraaryl-4,5-dimethoxy-1,3-dioxolane
TBDMS	*tert*-Butyldimethylsilyl
tBu	Tertiary butyl
TCNE	Tetracyanoethylene
TEA	Triethylamine
Temp	Temperature
THF	Tetrahydrofuran
THP	2-Tetrahydropyranyl
TMED	Tetramethylethylenediamine
Tol	*p*-Tolyl
Ts	*p*-Toluenesulfonyl

1
Introduction

1.1
A Short Note on High-Pressure Chemistry

High pressure is encountered in the deep sea, inside the earth, and on other planets. High pressure is likely to have been an agent in the geochemical conditions that formed coal and oil deposits [1]. Even more, biological and physicochemical arguments in support of a high-pressure origin for life on Earth have been recently reviewed [2]. It is interesting to research the change of molecules at high pressure because the pressure affects molecular environments. When covalent bond formation takes place, the model is simply assumed that one molecule collides with another molecule. But it has been clarified that solvent, concentration, temperature, and pressure around the molecules actually affect the reaction. The use of extreme conditions such as ultrahigh pressure in materials science and industry led to the successful preparation of synthetic diamond, ruby, and borazone as early as the 1950s [3, 4]. Around 1980, high-pressure apparatus, such as autoclave apparatus, became popular. But until then the utility of high pressure in organic synthesis had not been widely explored in spite of its potential. Of the many parameters that could be changed to improve the results of synthetic transformation, much attention has been paid to the study of electronic and steric effects by chemical modification of substrates and reagents, to thermal and photochemical effects, to the use of catalysts such as Lewis acids and bases, and to phase-transfer reagents. Sonochemistry, flash vacuum pyrolysis and other thermal processes, electroorganic transformations, reactions with solid-supported reagents and catalysts [5], and solvent-free organic synthesis [6] have also been employed. Supercritical fluids have also been used, and this can often be an alternative to the use of organic solvents under high pressure [7]. In particular, microwave techniques [8] are now quite popular because of the wide availability as well as quite easy operation, and even an ordinary microwave oven being successfully used.

Interest has been generated in the high-pressure method since it was demonstrated that high pressure is not only useful in effecting cycloaddition reactions, but also several kinds of ionic reactions [9–16]. The aim of the present article is to review recent examples of the use of high pressure for the synthesis of heterocycles related to biologically interesting molecules, and to predict some further possibilities. The present review covers either representative or most recent examples.

1.2
Basic Principles

At present, most methods of organic synthesis are based on chemical modification of reagents and catalysts. Nevertheless, frequent use has recently been made of "distinctive" techniques, such as ultrasound, flash vacuum pyrolysis, electroorganic, microwave, supercritical, solvent-free (or otherwise solid sate), and even plasma conditions, for syntheses of organic materials. The high-pressure technique is one of the most developed nonconventional tools for the preparation of either new or known compounds. Chemical reactions at high pressure require conditions characterized by high number densities of the reacting particles. Thus, considerable degrees of intense intermolecular interactions take place depending on the applied pressures. In terms of the potential energy of interactions as a function of the distance between molecules or atoms, the repulsive part of the relationship is mainly discussed. At lower number densities, interactions of this type take place only at higher temperature, but within a limited time interval determined by the impact parameters. At higher pressure, the duration of these strong interactions is much longer. This phenomenon may lead to a considerable increase in the reaction rates (Fig. 1).

In principle, the fundamental equation for the effect of high pressure on a reaction rate constant was deduced by Evans and Polanyi on the basis of transition state theory:

$$(\partial \ln k/\partial P)_T = -\Delta V^{\ddagger}/RT, \tag{1}$$

where $\Delta V^{\ddagger}(= V^{\ddagger} - V^R)$ is called the volume of activation and is the difference between the volume ($V^{\ddagger}$) of the activated complex, including molecule(s) of the solvation shell, and the volume (V^R) of the reactant molecule(s) associated with the solvent molecule(s), measured at constant pressure and temperature.

In general, formation of a bond, concentration of charge, and ionization during the transition state lead to a negative volume of activation, whereas
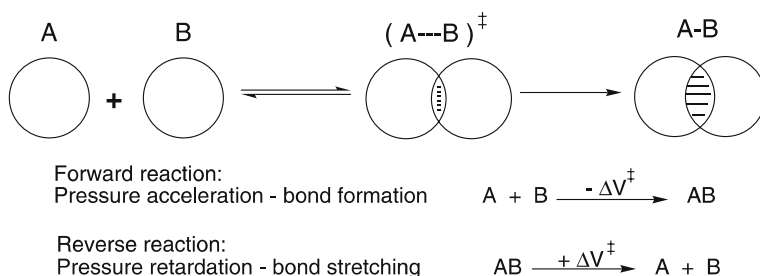
Fig. 1 High-pressure effects on organic reactions

cleavage of a bond, dispersal of charge, neutralization of the transition state, and diffusion control lead to a positive volume of activation. For reactions in which the polarity of the transition state changes, the influence of the solvent on $\Delta V^{\ddagger}$ is of importance. Thus, the types of organic reactions in which rate enhancement is expected on application of pressure may be summarized, as a preparative or synthetic guide, as follows:

1. Reactions in which molecularity decreases in the products; e.g., cycload-ditions, condensations.
2. Reactions which proceed via cyclic transition states; e.g., Claisen and Cope rearrangements.
3. Reactions which take place through dipolar transition states; e.g., Menschutkin reactions, electrophilic aromatic substitution.
4. Reactions that do not take place or otherwise occur in low yields due to steric hindrance in transition states.

As described above, the activation volume is the difference in partial molar volume between the transition state and the initial state. From a synthetic point of view this could often be approximated by the difference in the molar volume between the reactant(s) and product(s). Partial molar activation volumes, which can be divided into a structural part and a solvent-dependent part, are of considerable value in speculating about the nature of the transition state. This thermodynamic property has led to many studies on the mechanism of organic reactions.

From Eq. 1, the application of pressure accelerates reactions which have a negative volume of activation. The system does not strictly obey the ideal rate equation above ~ 1.0 GPa since the activation volume is itself pressure dependent; the values of $\Delta V^{\ddagger}$ generally decrease as pressure increases. Innumerable data on $\Delta V^{\ddagger}$ are now available. If the $\Delta V^{\ddagger}$ value is not available for a reaction type of interest, $\Delta S^{\ddagger}$ data may serve as a guide. Indeed, a linear relationship of $\Delta V^{\ddagger}$ with $\Delta S^{\ddagger}$ has been reported for a variety of reactions.

The differences between the units can be ignored when the exact numerical values are not under consideration, unless otherwise we need the nature of activation volumes in order to obtain some aspects of the reaction mechanism, e.g., 1 kbar = 100 MPa = 1000 kg/cm^2 = 1000 atm = 7.5×10^5 mmHg. This is indeed the case in high-pressure synthetic chemistry or preparation under pressure. In the Système International d'Unités (SI units) adopted by the Conférence Générale des Poids et Mesures and endorsed by the International Organization for Standardization, the unit of force is the Newton (N), which is equal to kilogram $\times$ (meter per second) per second and is written as kg m s^{-2}. The SI unit of pressure is one Newton per square meter (N m^{-2}) which is called a Pascal (Pa); 1 bar = 10^5 Pa; thus, the Pa is used in this chapter as an approximate equivalent to other units (Table 1).

Table 1 The units of pressure

	kbar	MPa	kg/cm^2	atm	mmHg
1 kbar	1	100	1019.7	986.92	7.5006×10^5
1 MPa	0.01	1	10.197	9.8692	7.5006×10^3
1 kg/cm^2	9.8067×10^{-4}	9.8067×10^{-2}	1	0.9678	735.6
1 atm	1.0132×10^{-3}	1.0132×10^{-1}	1.0132	1	760.0
1 mmHg	1.333×10^{-6}	1.333×10^{-4}	1.3595×10^{-3}	1.3158×10^{-3}	1

1.3
Effects of Pressure on Various Properties of Solvents

Before performing high-pressure experiments, it is essential to have knowledge of the effects of pressure on various physical properties of the solvent, such as freezing temperature, density, viscosity, solubility, compressibility, dielectric constant, and conductivity, although unfortunately sufficient data on all these properties are often unavailable. The less polar solvents have higher compressibilities and are therefore more constricted by ionic or dipolar solutes than the more polar solvents, which exhibit smaller compressibilities owing to the strong intermolecular interactions.

The melting point of liquids is raised by increasing the pressure; this effect amounts to $\sim$ 15–20 °C per 100 MPa. Tables 2 and 3 summarize the freezing temperatures [3] and the viscosity of common solvents at high pressure, respectively [14].

The solubility of solids in liquids often decreases as the pressure is raised, the reagents often crystallizing out from the solvents. The viscosity of liquids increases by approximately two times every 100 MPa, thus diffusion control of the reaction is important.

1.4
High-Pressure Apparatus and Experimental Procedures

This review gives only a brief account of the equipment used in high-pressure organic synthesis [14, 16]. The most general and convenient method for obtaining high pressures is disproportion, i.e., application of Pascal's principle. Particularly in organic synthesis, a piston–cylinder device may be most satisfactory. A maximum pressure of ca. 5.0 GPa is obtainable with such a device when constructed of cemented tungsten carbide. Although miscellaneous types of piston and cylinder apparatus have been devised, depending on the purpose of the experiments, they consist essentially of a high-pressure vessel, a pressure gauge (usually Bourdon or manganin or strain gauges), a pump,

Table 2 Freezing temperatures of common solvents at high pressure

Compound	Freezing temperature (°C)		
	0.1 MPa	at high pressure	(GPa)
Acetic acid	16.6	37.5	(0.1)
Acetone	– 94.8	20	(0.8)
Aniline	– 6.1	15.5	(0.1)
Benzene	5.5	33.4	(0.1)
Benzyl alcohol	– 10.0	0.2	(0.1)
Bromobenzene	– 30.6	– 10.7	(0.1)
Butanol	– 89.8	– 77.2	(0.1)
t-Butyl alcohol	25.5	58.1	(0.1)
Carbon disulfide	– 111.6	– 98.0	(0.1)
Carbon tetrachloride	– 22.9	12.1	(0.1)
Chlorobenzene	– 45.5	– 28.1	(0.1)
Chloroform	– 61.0	– 45.2	(0.1)
Cyclohexane	6.5	58.9	(0.1)
Cyclohexanol	25.4	62.3	(0.1)
Diethylene glycol	– 10.5	0	(0.57)
Ethyl acetate	– 83.6	25	(1.21)
Ethanol	– 117.3	– 108.5	(0.1)
Diethyl ether	– 116.3	35	(1.2)
Ethylene glycol	– 17.4	0	(0.32)
Formic acid	8.5	20.6	(0.1)
Hexane	– 95.3	30	(1.02)
Methanol	– 97.7	25	(3.0)
Dichloromethane	– 96.7	– 85.8	(0.1)
Nitromethane	– 28.6	– 14.4	(0.1)
Phenol	40.7	53.9	(0.1)
Propanol	– 126.1	25	(5.0)
2-Propanol	– 89.5	25	(5.0)
Toluene	– 95.1	30	(0.96)
Water	0.0	– 9.0	(0.1)

and an intensifier. The source of high pressure is due to the intrusion of a piston into the cylinder (Fig. 2).

Many kinds of flexible sample tubes have been devised. Four different kinds of sample containers are shown in Fig. 3. In all cases, either polytetrafluoroethylene (PTFE) or metal bellows are used, and there is at least one threaded hole for withdrawal. For high-pressure reactions at temperatures of up to ca. 60 °C, several kinds of commercially available syringes and polyethylene tubes have also been used.

Table 3 Ratio of viscosity at pressure P and 0.1 MPa (η_p/η_1) of common solvents

Compound	Viscosity [η_p/η_1]	
	P = 0.1 GPa (30 °C)	0.4 GPa (30 °C)
Acetone	1.68	4.03
Benzene	2.22	–
Bromobenzene	1.83	7.89
Butanol	2.09	8.60
i-Butyl alcohol	2.44	16.0
Carbon disulfide	1.44	3.23
Carbon tetrachloride	2.24	–
Chlorobenzene	1.79	7.36
Bromoethane	1.67	4.28
Chloroethane	1.75	4.46
Methyl cyclohexane	2.44	–
Ethyl acetate	1.81	6.58
Ethanol	1.58	4.14
Diethyl ether	2.11	6.20
Hexane	2.15	8.2
Methanol	1.47	2.96
o-Xylene	2.05	–
m-Xylene	1.95	9.27
n-Propanol	1.92	6.86
2-Propanol	2.20	9.60
Toluene	1.95	7.89
Water	3.27	–
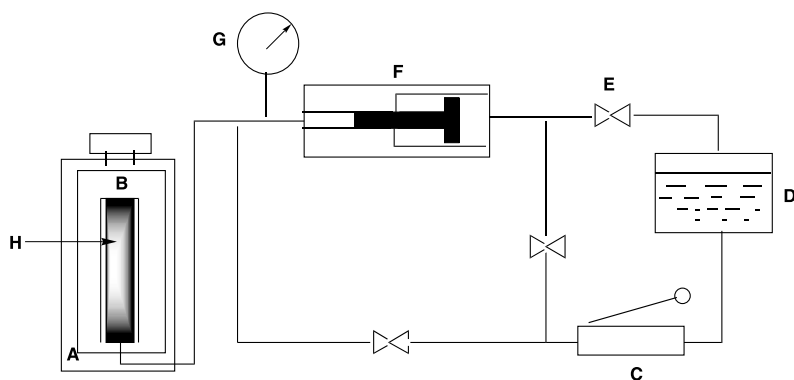
Fig. 2 An example of schematic diagram of high-pressure apparatus. *A* Heater; *B* double-wall pressure vessel; *C* hand pump or electronic pump; *D* oil reservoir; *E* valve; *F* intensifier; *G* gauge; *H* flexible sample container
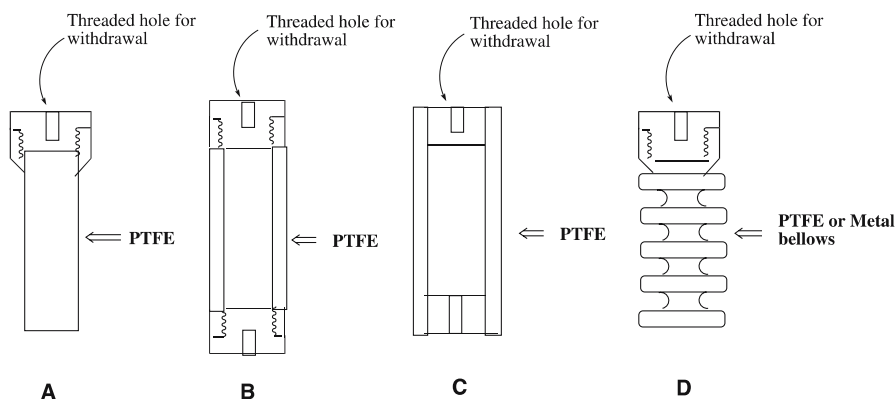
Fig. 3 Examples of flexible sample containers used at high pressures

In most preparative experiments under high pressure, the procedure is as follows: pressure is applied at room temperature (rt) to a sample tube containing the reagents and, if necessary, catalysts and solvent, before the temperature is raised, if required. After a suitable time, the heater is switched off. After cooling to rt, the pressure is carefully released, and the sample tube is removed from the vessel. When the reaction at high pressure does not take place at ambient temperature, according to GC, TLC, NMR, or other analytical techniques, an increase of pressure and/or temperature might be effective. In certain cases, the use of a catalyst may lead to success.

2
Pericyclic Reactions

Of the wide variety of pericyclic reactions, cycloadditions have been most extensively studied both for mechanistic and synthetic aspects. Cycloaddition reactions have been defined, classified, and reviewed in two fashions [17, 18]. Cycloadditions can be facilitated under a variety of conditions, such as addition of catalysts, application of high-temperature or high-pressure conditions, or use of microwave techniques, etc. As a result, the conditions of cycloaddition reactions can usually be selected in such a way as to accommodate sensitive functionality in the substrate. An application of the high-pressure technique to this type of reaction is anticipated to be extremely fruitful on both kinetic ($\Delta V^{\ddagger} < 0$) and thermodynamic ($\Delta V < 0$) grounds. Indeed, activation volumes of cycloadditions range from -7 to $-50\ cm^3\ mol^{-1}$. It is noteworthy that high-pressure conditions often improve the yield of cycloadditions and, in some cases, afford the opposite configuration of the cycloadducts compared with conventional methods [19–21].

2.1
Intermolecular Diels–Alder Reactions

Since Diels and Alder discovered nearly 75 years ago the formation of a 1 : 1 adduct in the reaction of cyclopentadiene with 1,4-benzoquinone, the Diels–Alder reaction, the prototype of [4 + 2] cycloadditions, has become indispensable to synthetic chemists and has the advantages of excellent stereospecificity, predictable *endo* stereoselectivity, and regioselectivity. Furthermore, it serves as an indirect and general method for the introduction and/or conversion of functional groups, through suitable bond-breaking reactions of an initially formed adduct. Intermolecular Diels–Alder reactions (IEDARs) exhibit a large negative volume of activation (ca. – 25 to – 45 cm^3/mol), together with a large negative volume of reaction. Among high-pressure mediated reactions, preparative IEDARs have been most extensively explored.

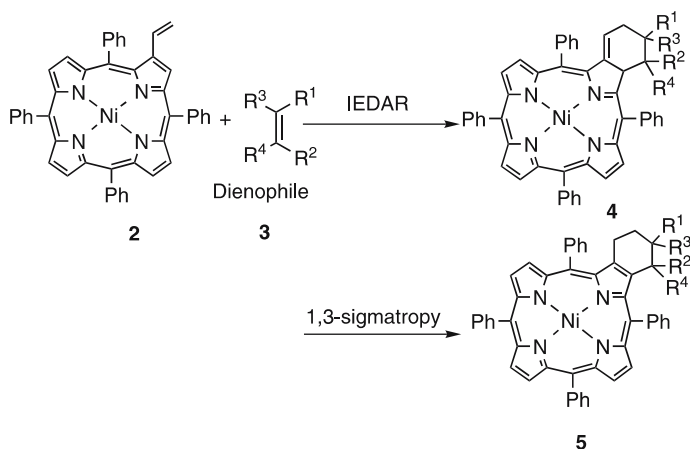As one of the key steps toward manzamine B, the reaction of dihydropyridone with Danishefsky's diene was performed. At a high pressure of 1.5 GPa, the reaction proceeded cleanly to give 66% yield of the adduct **1**, whereas under thermal conditions (in *p*-cymene at 200–220 °C, 18 h) **1** was produced in 53% yield (Scheme 1) [22].
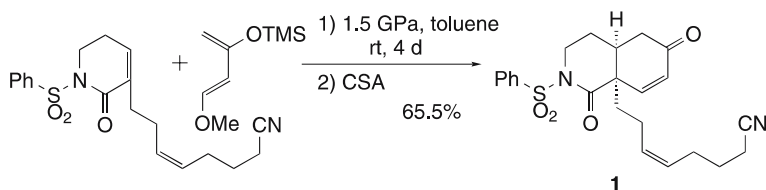
Scheme 1 IEDAR of dihydropyridone with Danishefsky's diene [22]

Porphyrins and their synthetic analogues have been extensively investigated because of their increasingly diverse applications in fields ranging from catalysis to biomedical science. One of the most general and simplest methods for modification of the porphyrin core would be attachment of additional moieties by the IEDAR of vinyl porphyrins with electron-deficient dienophiles. However, the dienophiles so far used are limited to highly active ones, such as tetracyanoethylene (TCNE) and dimethyl acetylenedicarboxylate; the generality of this method has not been demonstrated. Ni(II) β-vinyl-*meso*-tetraphenylporphyrin (**2**) undergoes IEDAR with such usual dienophiles as *N*-aryl and *N*-alkyl maleimides, dimethyl fumarate, dimethyl maleate, and methyl acrylates to give the six-membered condensed porphyrins which form from the IEDA adducts, followed by 1,3-hydrogen shifts as illustrated in Scheme 2. The yields of the adducts were highly improved by applied pressure [23, 24].

Entry	Dienophile				equiv.	Pressure (GPa)	Yield, %	
	R^1	R^2	R^3	R^4			4	5
1	CON(Et)CO		H	H	3.1	Amb.	43	1.1
					3.2	0.6	–	53
2	CO_2Me	H	CO_2Me	H	3.4	Amb.	26	13
					3.4	0.6	–	73

Amb. = Ambient pressure

Scheme 2 IEDAR of Ni(II) β-vinyl-*meso*-tetraphenylporphyrin (**2**) [23, 24]

Numerous Amaryllidaceae alkaloids include phenanthridine skeletons, one of whose constructive methods constitutes an IEDA strategy. In some cases, the functionality on the dienophile influences the stereochemistry of cycloaddition reactions under high-pressure conditions. For example, the reactions of (*E*)-buta-1,3-dienyl acetate (**6**) and the quinolin-2(1*H*)-ones **7** gave rise to different configurations in the products **8** and **9**, depending on the functional groups at the 4-position of **7** (Scheme 3). These results reflect
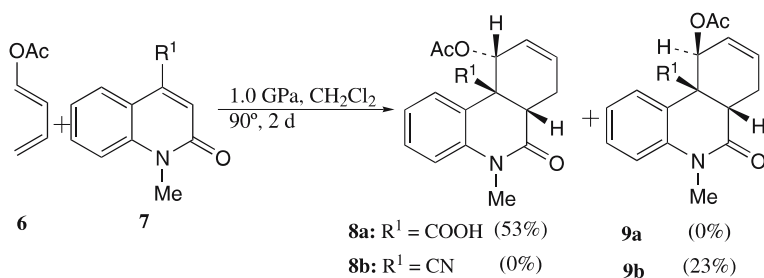
Scheme 3 Reactions of (*E*)-buta-1,3-dienyl acetate (**6**) with 2(1*H*)-quinolones **7** [25]

different activation energies (E_a) for the *endo* and *exo* adducts **8** and **9**, respectively. For R = COOH, the calculated E_a values for *endo* vs *exo* addition to **8a** and **9a**, respectively, were reported as 33.5 vs 34.2 kcal/mol. In the case of R = CN, the corresponding values for **8b** and **9b** were 36.9 vs 35.9 kcal/mol, respectively, indicating that the pathway with the smaller activation volume was preferred under high-pressure conditions [25]. Analogous IEDARs were also reported [26].

Madangamine A (**10**) is a pentacyclic alkaloid produced by marine sponge *Xestospongia ingens*. This compound is of interest both because of its unique structure and the fact that it shows significant in vitro cytotoxic activity toward a number of tumor cell lines, including human lung A549, brain U373, and breast MCF-7. A concise approach to the tricyclic core **11** of **10** was achieved in terms of high-pressure IEDARs (Scheme 4) [27]. This reaction was unsuccessful under thermal conditions.

madangamine A

10

SES = β - (trimethylsilyl)ethanesulfonyl-

PMB = *p*-MeOC$_6$H$_4$CH$_2$O$^-$
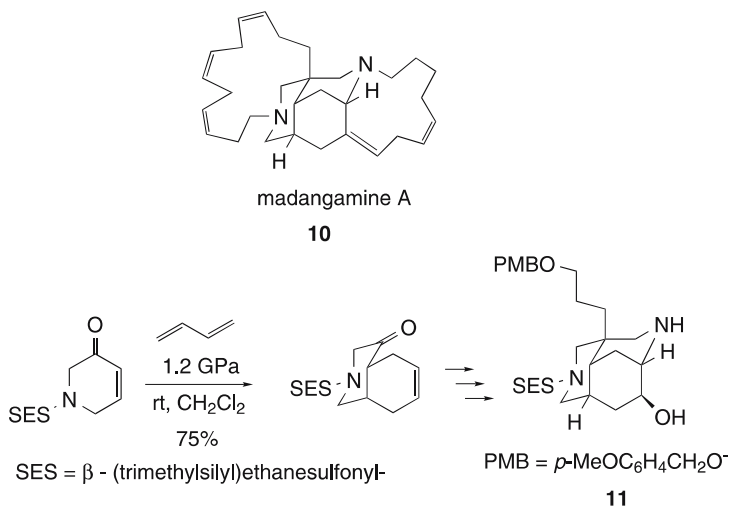
Scheme 4 Construction of tricyclic core **11** via IEDAR [27]

Indoles often serve as dienophiles whose IEDARs lead to nitrogen-containing polycycles useful in the synthesis of biologically active alkaloids. A recent example for the combination of Lewis acid catalyst and high pressure is the reaction of 2,3-dimethylbuta-1,3-diene (**12**) with the indole **13**. As shown in Scheme 5, quantitative yields of the adducts **14** and **15** were obtained under high-pressure conditions. Interestingly, the combination of high pressure and ZnCl$_2$ as catalyst afforded mainly the opposite configuration in **15** [28]. It is worth noting that all-carbon IEDARs are kinetically favored, which is in accord with the observed higher reactivity of the aromatic C $=$ C bond relative to the (unaffected) formyl group in the indole, producing **14** exclusively (in the absence of catalyst) under high pressure. Both SnCl$_4$ and
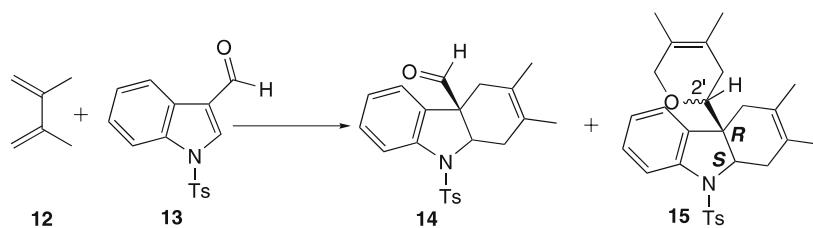
sealed tube, toluene, 195°, 80 h	(85%), **14:15** = 100:0
toluene, ZnCl₂, 110°, 80 h	(77%), **14:15** = 87:13; **15**: 2'R
1.6GPa, CH₂Cl₂, 50°, 48 h	(100%), **14:15** = 100:0
1.2GPa, CH₂Cl₂, ZnCl₂, 25°, 48 h	(100%), **14:15** = 2:98; **15**: 2'S

Scheme 5 Effect of pressure and catalyst in the reaction of dimethylbutadiene (**12**) with the indole **13** [28]

ZnCl₂ accelerate the second IEDAR, in which the *trans* (e.g., 2'R) cycloadduct was formed via an *anti*-type transition state under thermal conditions. In contrast, at high pressure, the corresponding *cis* (e.g., 2'S) cycloadduct were formed via a *syn*-type transition state, which has a smaller activation volume (data not given).

Although the furan unit has become an important diene in the synthesis of natural products, 2-vinylfurans have been less exploited. In certain cases, a high-pressure mediated IEDAR is useful for this type of furan. For example, the reaction of methyl 5-ethenyl-2-methylfuran-3-carboxylate (**16**)

| ether, reflux, 7 d | (0%) |
| 1.1GPa, CH₂Cl₂, 30°, 7 d | (23%) |

| ether, reflux, 7 d | (0%) |
| 1.1GPa, CH₂Cl₂, 30°, 7 d | (51%) |
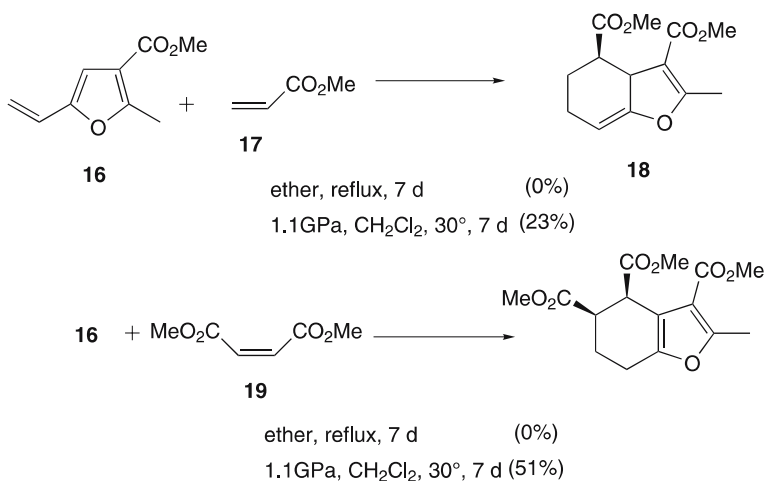
Scheme 6 Reactions of methyl 5-ethenyl-2-methylfuran-3-carboxylate (**16**) with methyl acrylate (**17**) and dimethyl maleate **19** under thermal and high-pressure conditions [29]

and methyl acrylate (**17**) afforded the adduct **18**, without concomitant aromatization, albeit in low yield (23%) [29]. It is noted that, in the case of the similar reaction between **16** and dimethyl maleate (**19**), the resulting adduct underwent aromatization via C = C migration.

As previously described, furans are one of most versatile starting materials for natural and bioactive molecules since the resulting adducts, 7-oxabicyclo[2.2.1]heptanes, are of highly practical importance as a variety of functionalizations of the adducts are possible. Because of the aromatic character of furans, conventional IEDARs are often unsuccessful; thus, there are many examples of IEDARs that were performed at high pressure [9–14]. Therefore, this methodology is still employed by many research groups. For example, in order to construct the CD ring of the anticancer agent paclitaxel (Taxol®), the reactions of several furans **20** with citraconic anhydride (**21**) were preliminarily studied under high pressure. Furan (**20**: R = H) with citraconic anhydride (**21**) afforded the *exo* adduct **22** (R = H) diastereoselectively, whereas 2-substituted furans **20** gave an approximately 1 : 1 mixture of *exo* regioisomers **22** and **23** [30].

| R	Yield	22/23
EtO_2C	0%	–
$^{t}BuO_2CCH_2$	54%	1:1
MeO_2CCH_2	59%	5:6
$BnOCH_2$	31%	7:5
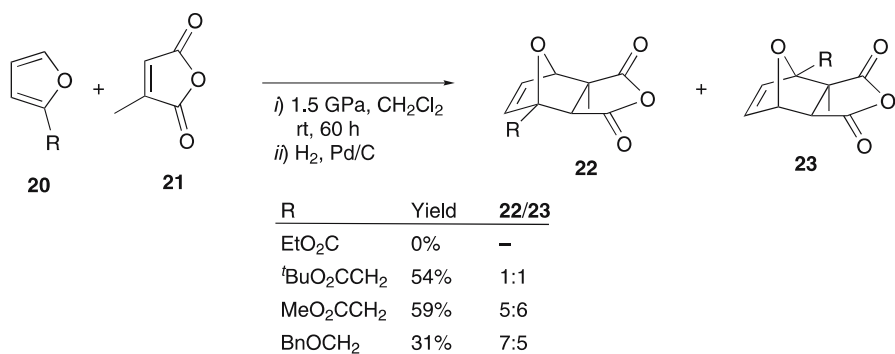
Scheme 7 IEDARs of furans **20** with citraconic anhydride **21** [30]

Cantharidin (**24**) [31] represents the simplest known inhibitor of the serine/threonine protein phosphatases 1 and 2A, and can be isolated from dried beetles (*Cantharis vesycatoria*). The simplest synthesis of **24** from furan and dimethylmaleic anhydride met with failure, even at pressures as high as 6.0 GPa either at rt or at temperatures of up to 350 °C, presumably due to the thermodynamic instability of the adduct at normal pressure, e.g., when pressure is released [32]. However, if this reaction could be carried out in the presence of Pd/C and H_2, **24** might be obtained in one step. Nevertheless, high-pressure cycloaddition turned out to be very useful for the synthesis of cantharidin and its derivatives [31–33]. For instance, (±)-palasonin was synthesized from furan and citraconic anhydride (**21**) at 0.8 GPa for 138 h, followed by hydrogenation over Pd/C. Neither high temperatures nor
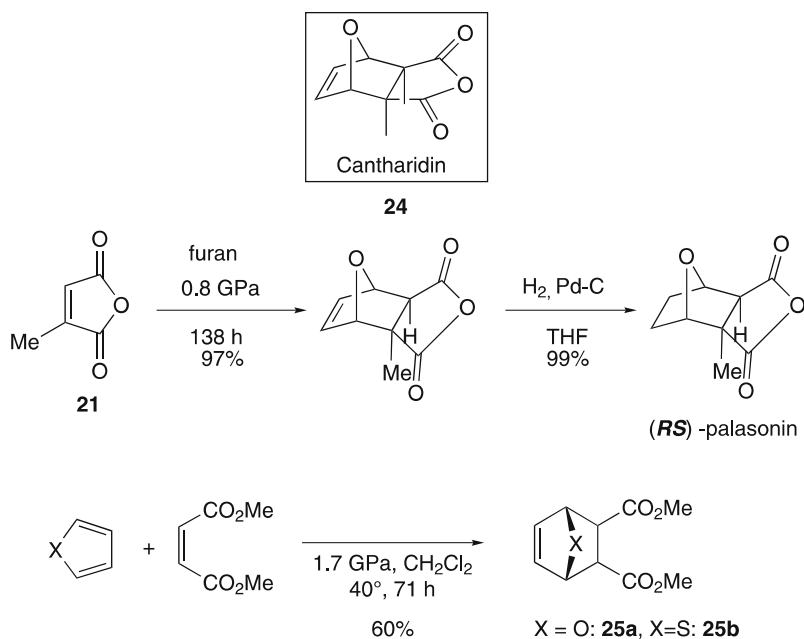
Scheme 8 A simple synthesis of cantharidin analogues [33, 34]

Grieco conditions (LiClO$_4$, Et$_2$O, H$_2$O) are effective in this transformation at atmospheric pressure. The two cantharidin analogues **25** displaying PP1 selectivity were obtained by high-pressure IEDARs of furan and thiophene with dimethyl maleate (Scheme 8). They possess PP1 selectivity (> 40- and > 30-fold selectivity) over PP2A. Both **25a** and **25b** exhibited a moderate PP1 activity with IC$_{50}$ values of 50 and 12.5 µM, respectively; however, the corresponding monoester of **25a** showed no such selectivity [34]. Similarly, simple and alkyl-substituted cycloalkenones such as **26** undergo IEDARs with sulfanylfuran **27** and, to a lesser extent, with 3-phenylsulfanylfuran **28** to afford the adducts, albeit in poor yields (Scheme 9) [35].

R		P	t	Yield
Me	**27**	1.5 GPa	48 h	23%
Ph	**28**	1.5 GPa	72 h	–
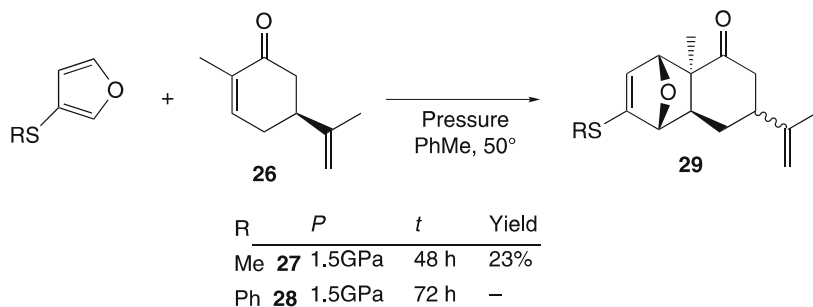
Scheme 9 IEDARs of sulfanylfurans **27** and **28** with cycloalkenones **26** [35]

Pyrrole is believed to be more aromatic than furan, with an aromatic stabilization energy estimated to be $100-130\,kJ\,mole^{-1}$, thus only with such extremely powerful dienophiles as tetrakis(trifluoromethyl)Dewar thiophene were the IEDA adducts isolated. Therefore, several attempts to achieve an IEDAR with pyrroles using high pressure have been made [9–14].

Epibatidine (**30**), an alkaloid isolated from the skin of the Ecuadorian poison frog *Epipedobates tricolor*, was reported as a novel, highly potent, nonopioid analgesic agent and a specific agonist of central nicotinic acetylcholine receptors (nAChRs). The high-pressure IEDAR of *N*-methoxycarbonylpyrrole (**31**) with phenyl vinyl sulfone produced a mixture of *endo*- and *exo*-5-phenylsulfonyl-7-methoxycarbonyl-7-azabicyclo[2.2.1]hept-2-ene (**32**), which was desulfonylated in the usual fashion to give **33**, followed by reductive Heck reactions and treatment with Me₃SiI, affording epibatidine analogues (Scheme 10) [36].
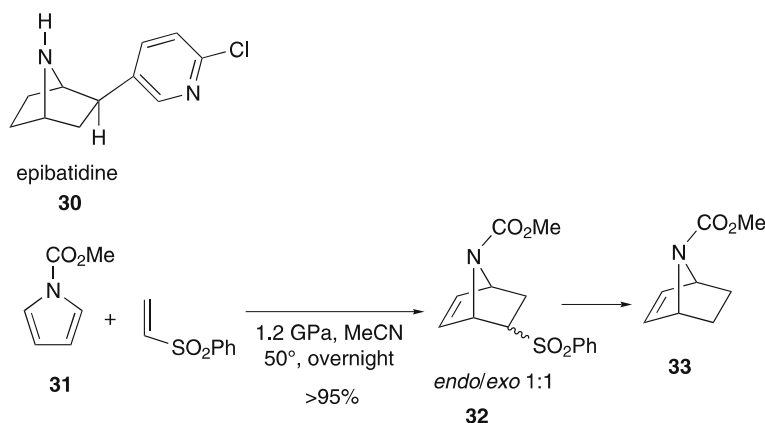
Scheme 10 A facile synthesis of the intermediates of epibatidine analogues via high-pressure IEDARs of pyrrole **31** [36]

It is known that thiophene (**34**) is more aromatic than pyrrole and does not undergo IEDAR under conventional conditions. However, almost 25 years ago, it was reported that the reaction with maleic anhydride (**35**) at $1.2-2.0\,GPa$ and a temperature of $100\,°C$ produced the *exo* adduct **36** in 40% yield [37]. Recently, highly improved results have been attained under high-pressure and solvent-free conditions (Scheme 11) [38].

2-Pyrones usually behave as aliphatic compounds, and therefore a number of IEDARs were reported with both electron-deficient and electron-rich dienophiles, but these adducts are prone to lose CO_2 under conventional conditions. Thus, a number of examples that retain the useful CO_2 moiety have appeared via recourse to high-pressure strategy [9–14].
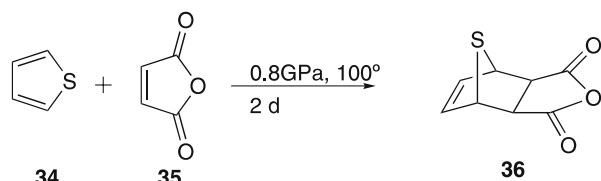
34:35	Solvent	Yield (%)
1 : 1	CH_2Cl_2	19
4 : 1	CH_2Cl_2	21
4 : 1	solvent-free	93
2 : 1	solvent-free	87

Scheme 11 IEDAR of thiophene (**34**) with maleic anhydride (**35**) under high-pressure/ solvent-free conditions [38]

The palmarumycins are a group of fungal metabolites isolated from *Coniothyrium* sp. Specifically, palmarumycin CP1 (**37**) may be considered as the parent member of this group, with others displaying a range of hydroxylation, unsaturation, or epoxidation. Several of them exhibit antibacterial, antifungal, or potentially anticancer activity. One of the simplest approaches to the palmarumycin skeleton would be IEDARs of 3-methoxy-2-pyrone (**38**) with benzoquinone monoacetals **39**, as exemplified in Scheme 12 [39]. However, in this case, no high-pressure conditions seem to be essential because of the need for aromatization. Rather than high pressure, microwave irradiation might be a method of choice.

2-Pyridones are classified as aromatic heterocycles (estimated aromatic stabilization energy: about 100 kJ/mol). Indeed, they undergo electrophilic

R[1]	R[2]	Conditions	Yield
H	H	1.2 – 1.5 GPa	quant.
H	H	0.1 MPa, PhH, reflux	55%
H	Me	1.2 – 1.5 GPa	quant.
MeO	H	1.2 – 1.5 GPa	quant.
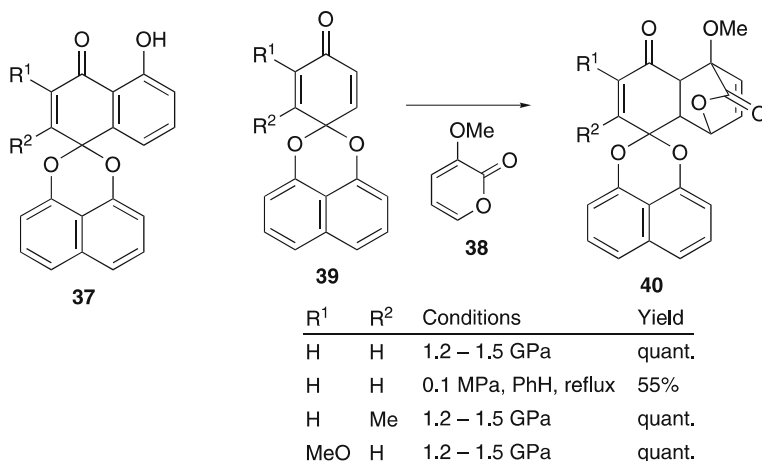
Scheme 12 Synthetic approaches to the palmarumycins [39]

substitution at the 3- and 5-positions. In connection with the strategic view-point for construction of the isoquinuclidine skeleton, their IEDARs are of considerable interest. 2-Pyridones are much more inert to dienophiles than 2-pyrones, the initial adducts often losing an RHCO group under conventional conditions. These difficulties are partly surmounted by recourse to the high-pressure technique [9–14]. Cyclooctyne (**41**) is the smallest cyclic alkyne that is stable at rt. In particular, its cycloadditions and subsequent ring enlargement have been utilized for construction of medium- and large-ring compounds [40]. Some 2-pyridones **42** underwent high-pressure IEDARs with cyclooctyne (**41**) to give the corresponding stable bridged tricyclic adducts **43** in moderate to good yields (Scheme 13) [41].


Pyridones			Pressure	Temp	Time	Yield
R^1	R^2	R^3	(GPa)	(°C)	(d)	(%)
CH$_3$	H	H	0.8	90	10	77
CH$_2$Ph	H	H	0.8	90	10	80
CH(CH$_3$)$_2$	H	H	0.8	90	10	62
CH$_3$	H	CH$_3$	0.8	90	10	70
CH$_3$	CH$_3$	H	0.8	90	10	16
CH$_3$	OCH$_3$	H	0.8	60	5	4
CH$_3$	OCH$_3$	H	0.8	90	10	24
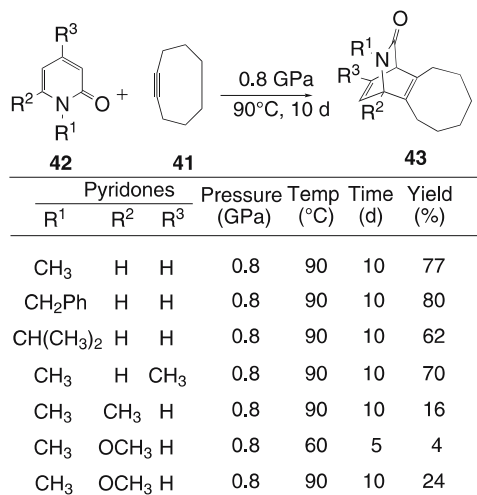
Scheme 13 IEDARs of 2-pyridones **42** with cyclooctyne (**41**) at 0.8 GPa [41]

The IEDAR of tetramethyl-4*H*-pyrazole (**44**) with 2,5-dihydrofurans **45** was accomplished only by high pressure in the strict absence of any acid traces, giving the adduct **46** in 74% yield. Attempts to perform the reaction at temperatures up to 150 °C by using microwave irradiation (700 W, 3 min, resulting in decomposition) and standard activation with TFA or LiClO$_4$ failed (Scheme 14) [42].
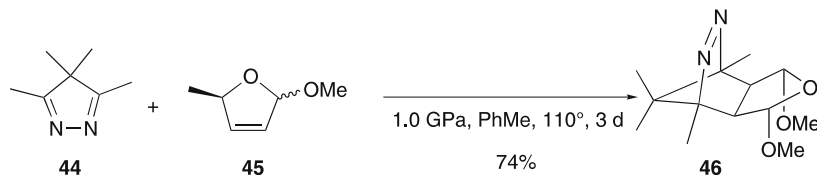
Scheme 14 IEDAR of tetramethyl-4*H*-pyrazole (**44**) with 2,5-dihydrofurans **45** [42]

Recently, the intriguing IEDA adducts **48** of 1-germa-2,3,4,5-tetraphenyl-1,1-dimethyl-2,4-cyclopentadiene (**47**) with *N*-methylmaleimide and maleic anhydride were prepared by high-pressure reactions (Scheme 15) [43].
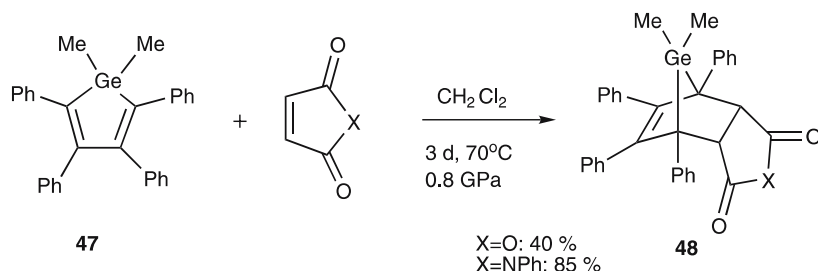
Scheme 15   IEDAR of 1-germa-2,3,4,5-tetraphenyl-1,1-dimethyl-2,4-cyclopentadiene (**47**) [43]

Hetero IEDARs offer a useful protocol for construction of oxa- and aza-cycles. In particular, dihydropyrans are useful intermediates for a variety of biologically intriguing compounds. Thus, many examples of high-pressure mediated IEDARs of dienes with dienophiles possessing carbonyl groups have been reported [9–14, 44, 45]. One of the simplest approaches to sugars and sugar-like polyhydroxylated compounds from noncarbohydrate substrates would be such hete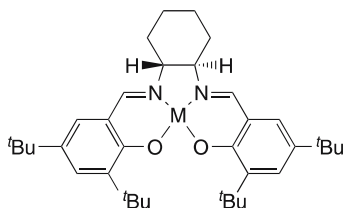ro IEDARs. A recent example of this type of reaction is an enantioselective high-pressure IEDAR of 1-methoxybuta-1,3-diene (**49**) with *tert*-butyldimethylsilyloxyacetaldehyde (**50**) catalyzed by (salen)Co(II) (**53**), (salen)Co(III)Cl (**54**), and (salen)Cr(III)Cl (**55**) complexes. The reaction afforded, in good yield (up to 90%) and with both high diastereoselectivity (up to 92%) and enantioselectivity (up to 94% ee), the hydroxymethyl(methoxy)tetrahydropyrans **51** and **52** (Scheme 16) [46].

Alternatively, the inverse electron-demand hetero IEDARs of α,β-unsaturated carbonyl compounds with enol ethers serve as a short and attractive route to dihydropyrans. For instance, the use of Lewis acids such as Eu(fod)$_3$ along with high-pressure afforded a high yield of the dihydropyran **56**, as shown in Scheme 17 [47]. Analogous and more synthetically extensive results including dihydrothiopyrans were also reported [48–52].

The desperate search for effective anticancer and anti-HIV therapeutic agents has greatly stimulated research on specifically modified sugars. Synthesis of the dihydropyrans **59**, incorporating annelated spirocyclopropane moieties, has been accomplished by means of an inverse-demand hetero IEDAR of methyl *trans*-4-benzyloxy-2-oxo-3-butenoate (**57**) onto benzyl (cyclopropylidenemethyl) ether (**58**) as the key step (Scheme 18) [53]. Further transformations led to 3-benzylated α- and β-anomeric benzylspiro[2]-deoxy-(D,L)-*arabino*-hexopyranoside-2,1′-cyclopropanes **60**.
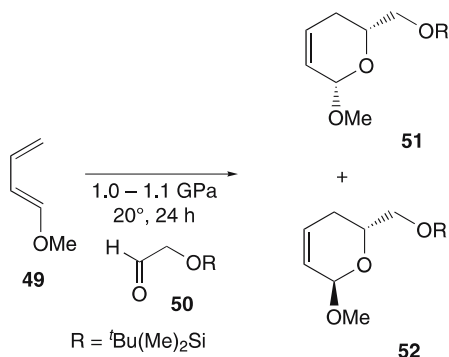
Catalyst (mol%)	Solvent	Yield (%)	**51/52**	**51** (ee)	**52** (ee)
53 (5)	CH₂Cl₂	61	93:7	93	73
53 (2)	CH₂Cl₂	52	93:7	92	70
53 (0.5)	CH₂Cl₂	30	90:10	81	43
53 (2)	PhMe	33	88:12	75	48
53 (5)	CH₂Cl₂	52	95:5	94	74
53 (2)	CH₂Cl₂	47	95:5	94	79
54 (2)	CH₂Cl₂	32	81:19	75	32
55 (5)	CH₂Cl₂	80	91:9	84	66
55 (2)	CH₂Cl₂	70	95:5	85	65
55 (2)	PhMe	84	96:4	87	78
55 (2)	CH₂Cl₂	88	93:7	83	69

53 M = Co

54 M = CoCl

55 M = CrCl

Scheme 16 Enantioselective high-pressure IEDAR of 1-methoxybuta-1,3-diene (**49**) with *tert*-butyldimethylsilyloxyacetaldehyde (**50**) catalyzed by (salen)Co(II) (**53**) and (salen)Cr(III)Cl (**55**) complexes [46]

One of the simplest preparations of the pyridine skeleton would be hetero IEDARs of nitriles with dienes, which would, however, be highly limited because of the small number of activated dienes and nitriles. The hetero IEDARs of 2,3-dimethyl-1,3-butadiene (**61**) with perfluorooctanon-itrile (**62**) at 0.15 GPa and 50 °C afforded 3,4-dimethyl-6-perfluoroheptyl-
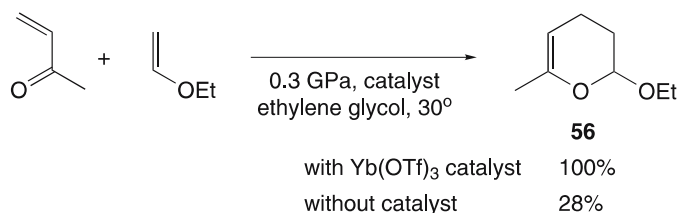
Scheme 17 Hetero IEDAR of an α,β-unsaturated carbonyl compound with enol ether: a highly efficient synthesis of the dihydropyran **56** [47]
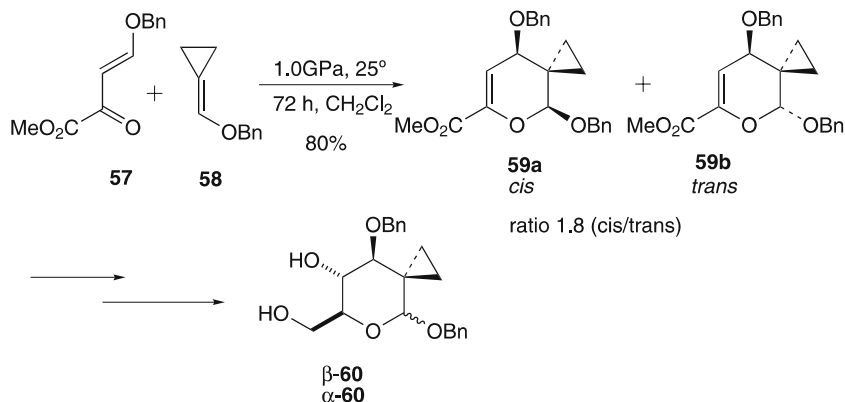
Scheme 18 Synthesis of 3-benzylated α- and β-anomeric benzylspiro[2]-deoxy-(D,L)-*arabino*-hexopyranoside-2,1′-cyclopropanes **60** via spirocyclopropane-annelated dihydropyrans **59** [53]

3,5-dihydropyridine (**63**), along with 3,4-dimethyl-6-perfluoroheptyl-3,5-pyridine (**64**) though only in low yields, the former gradually eliminating hydrogen to give **64** (Scheme 19) [54]. A higher pressure like 0.8 GPa might highly improve the yields.

Activated imines can also serve as dienophiles and the resulting adducts, piperidine-derived ring systems, constitute the skeleton of many naturally occurring alkaloids. They exhibit a variety of biological activities and are found in numerous therapeutic agents. Thus, a short and efficient synthesis of highly functionalized tetrahydropyridines is attained by high-pressure aza-IEDAR, employing the imine **65** (Scheme 20) [55]. The reaction was applied to the stereoselective synthesis of a pipecolic acid derivative.

Heterocyclic compounds which have, as a common structural feature, a tetracyclic pyrido[2,3,4-*kl*]acridine system often offer striking biological activities such as antitumor activities. Specifically, a facile synthesis of ascididemine (**70**) was achieved by high-pressure IEDAR of 6*H*-4-bromopyrido[2,3,4-*kl*]acridin-6-one (**69**) with propanal dimethylhydrazone

(**68**), albeit in low yield of 21%, whereas **71** with **68** gave **72**, an isomer of ascididemine (**70**) in moderate yield (Scheme 21) [56].

Pressure	Time (h)	63	64
0.1 MPa	2	1.6	4.4
0.1 MPa	67	23.7	10.2
0.1 MPa	98	27.0	0.5
0.15 GPa	2	5.6	7.8
0.15 GPa	4	8.0	8.5
0.15 GPa	5.5	12.0	13.3
0.15 GPa	29	29.1	20.8
0.15 GPa	44	28.6	
0.15 GPa	67	31.3	
0.15 GPa	98	26.4	
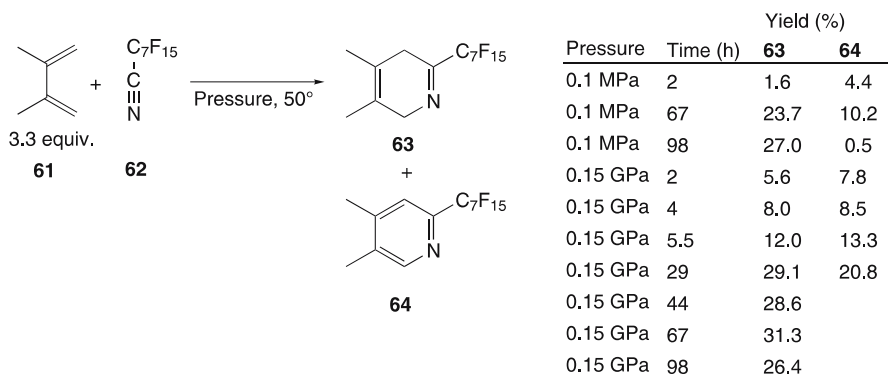
Scheme 19 Synthesis of pyridine **64** by hetero IEDAR of the diene **61** with nitrile **62** [54]

R^1	R^2	Yield (%)
AcO	BnO_2CCH_2	89
AcO	$BnO(CH_2)_2$	91
BnO	$^tBu(Me)_2SiO$	62
$^tBu(Me)_2SiO$	$BnO(CH_2)_2$	60
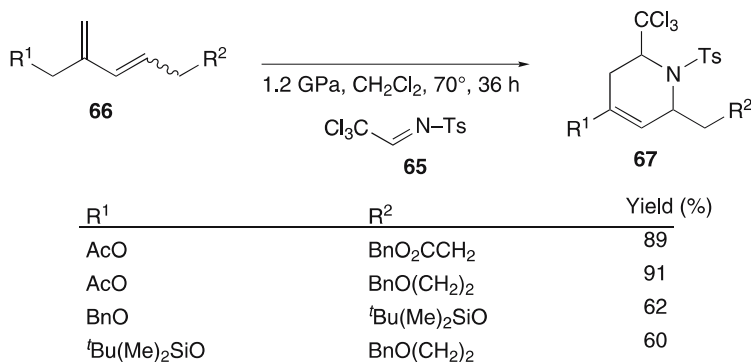
Scheme 20 Synthesis of tetrahydropyridines [55]
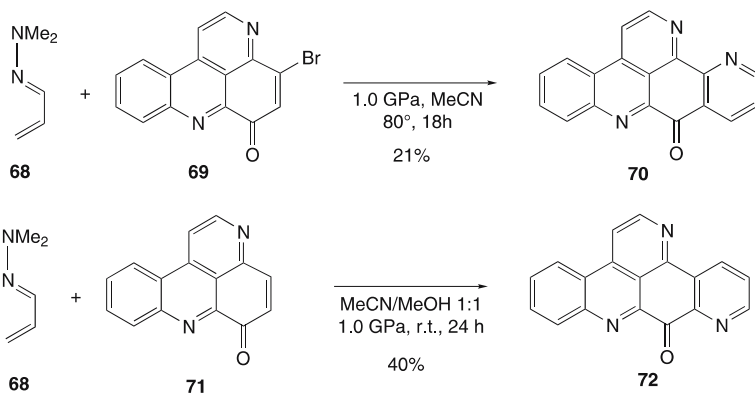
Scheme 21 A simple synthesis of ascididemine (**70**) via aza-IEDAR [56]

2.2
Intramolecular Diels–Alder Reactions

In recent years, there has been considerable interest in synthetic applications of intramolecular Diels–Alder reactions (IRDARs), because the intramolecular reaction can offer some advantages over the intermolecular version, especially an increased reaction rate and higher selectivity. IRDARs allow the regioselective and stereospecific introduction of multiple stereogenic centers. Therefore, these reactions have become a powerful method for the synthesis of polycyclic natural products. Pressure effects of IRDARs of **73** were investigated in comparison with sigmatropic reactions such as the Cope rearrangement of (*Z*)-1,3,5-hexatriene (**75**) (Scheme 22) [57, 58]. It has been proved that the $-\Delta V^{\ddagger}$ values of the former are at lea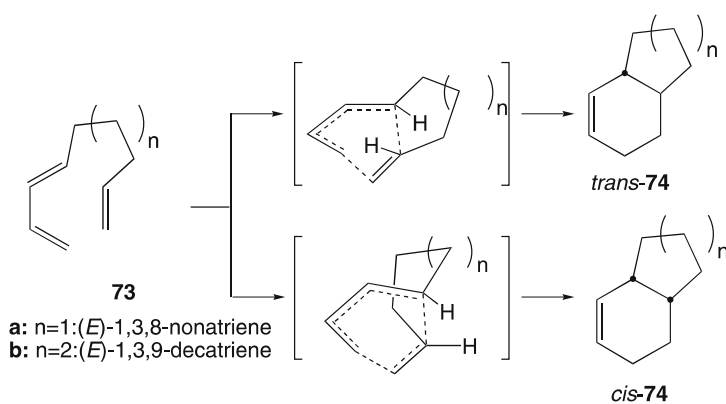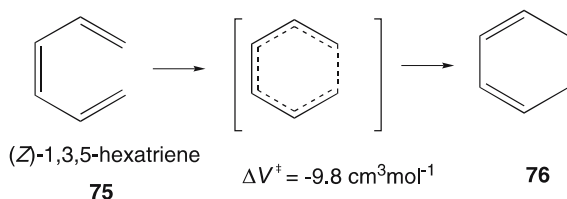st two times those of the latter. Importantly, large negative activation volumes ranging from -24 to $-37\ cm^3\ mol^{-1}$, as well as large negative volume changes, have been found for

73
a: n=1:(*E*)-1,3,8-nonatriene
b: n=2:(*E*)-1,3,9-decatriene

n	Temp./°C	73 to *trans*-74		73 to *cis*-74	
		$\Delta V^{\ddagger}$	ΔV	$\Delta V^{\ddagger}$	ΔV
1	153.2	-24.8	-28.5	-24.8	-37.4
2	172.5	-35.0	-32.0	-37.4	-45.4

All volumes are given in $cm^3 mol^{-1}$.

(*Z*)-1,3,5-hexatriene

75

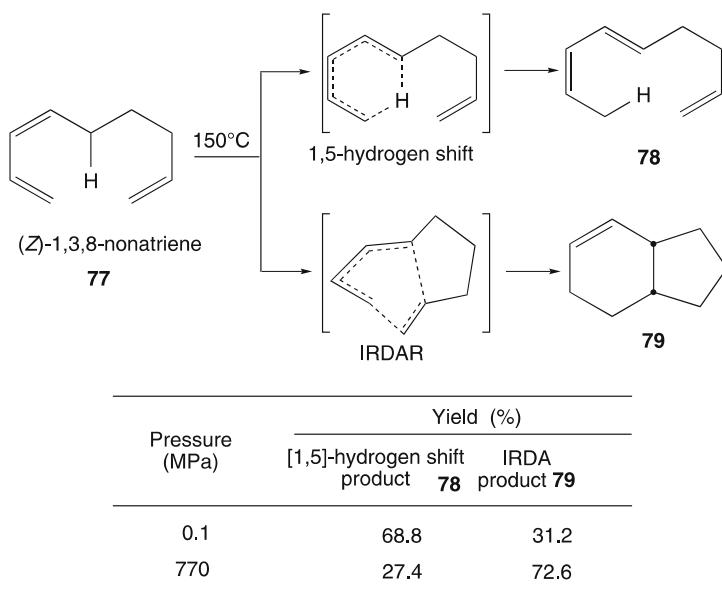$\Delta V^{\ddagger} = -9.8\ cm^3 mol^{-1}$ **76**

Scheme 22 Pressure effects on IRDARs of **73** and Cope reaction of **75** [57, 58]
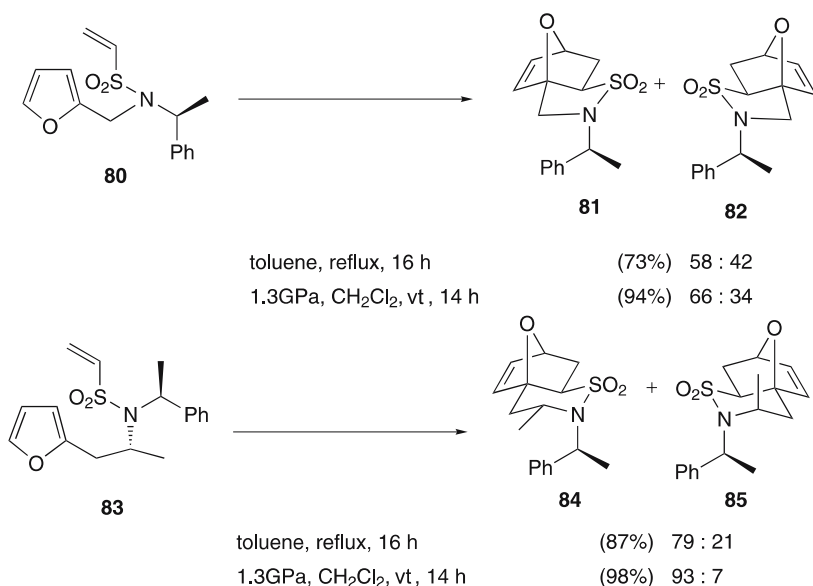
this type of IRDAR. In another example, the IRDAR of (*Z*)-1,3,8-nonatriene (**77**) is highly favored over 1,5-hydrogen sigmatropy to **78** by applied pressure (Scheme 23) [57, 58]. At atmospheric pressure and 150 °C, the 1,5-hydrogen shift predominated over the IRDAR in the yields, whereas even at 0.77 GPa, the ratio of the yields was completely reversed. Thus, high pressure is expected to be extremely fruitful in this type of IRDAR. Indeed, a considerable number of high-pressure mediated IRDARs have already proved useful for construction of the skeleton of bioactive molecules [44, 45].

Sultams have been recognized to be useful for medicinal chemistry [59]. The preparation of enantiomerically pure δ- and γ-sultams was achieved by a high-pressure IRDAR. As high as at 1.3 GPa, the sulfone **80** smoothly underwent an IRDAR to give both slightly higher yield and asymmetric induction than under thermal conditions in refluxing toluene at ambient pressure. The *exo*-sultam **81** predominated over the *endo*-sultam **82** by the chiral (*S*)-1-phenylethyl substitution. In contrast, the vinylsulfonamide **83**, in which double stereodifferentiation is anticipated by the presence of two stereogenic centers, gave rise to a higher diastereoselectivity noted for the high-pressure cycloaddition by virtue of both stereogenic elements present in **83**. The equatorial disposition of the methyl group on the δ-sultam **84** dominated the stereochemical outcome of the reaction, the diastereoisomer **85** being formed as the minor product (Scheme 24) [60].

Thermal or high-pressure induced IRDARs of the triene **86**, featuring either a sulfonate or sulfonamide moiety connecting a diene and a dienophile,

Pressure (MPa)	Yield (%)	
	[1,5]-hydrogen shift product **78**	IRDA product **79**
0.1	68.8	31.2
770	27.4	72.6

Scheme 23 Pressure effects on competitive IRDAR and 1,5-hydrogen shift of **77** [57, 58]

toluene, reflux, 16 h   (73%) 58 : 42
1.3GPa, CH$_2$Cl$_2$, vt , 14 h   (94%) 66 : 34

toluene, reflux, 16 h   (87%) 79 : 21
1.3GPa, CH$_2$Cl$_2$, vt , 14 h   (98%) 93 : 7

Scheme 24 IRDARs of *N*-1-phenylethyl-substituted vinylsulfonamides **80** and **83** under thermal and high-pressure conditions [60]

were found to proceed with moderate diastereoselectivity to give the sultones **87** and **88**. It is interesting to note that the ratio is reversed under high pressure compared to thermal conditions. Presumably, under high-pressure conditions, the reaction takes place via a more compact *endo*-type transition state (Scheme 25) [61]. Similar IRDARs with high diastereoselectivity were also reported [62].

	1.3 GPa, CH$_2$Cl$_2$, rt		Toluene, BHT, reflux	
	87 : 88	Yield (%)	**87 : 88**	Yield (%)
X = O, R^1 = Me, R^2 = H, R^3 = Me	1.0 : 2.0	78	1.4 : 1.0	64
X = N, R^1 = Me, R^2 = H, R^3 = Me	1.0 : 1.9	81	1.6 : 1.0	61
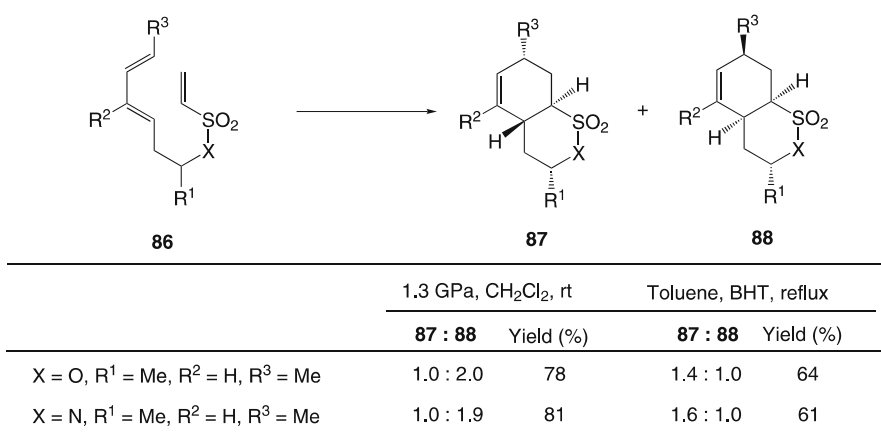
Scheme 25 IRDARs of vinylsulfonate and vinylsulfonamide **86** [61]

Scheme 26 Synthetic approaches toward phorbols via the high-pressure mediated IRDARs of furans **89** [64]
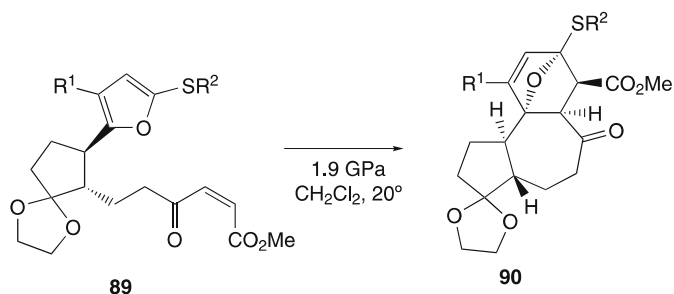
R^1	R^2	t (h)	Yield (%)
H	Bn	15	66
Me	Ph	15	–
Me	Bn	19	45
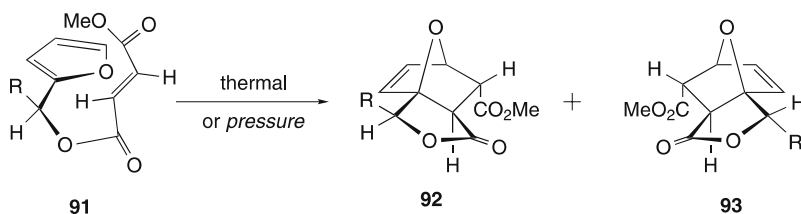
Diester R	Method	Yield (% :**92**+**93**)	Ratio of **92**:**93**	de %
Me	high pressure	96	55 : 45	10
	thermal	41	55 : 45	10
Et	high pressure	36	68 : 32	36
i-Pr	high pressure	90	90 : 10	80
	thermal	31	78 : 22	56
t-Bu	high pressure	92	93 : 7	86
	thermal	44	92 : 8	84
neo-Pen	high pressure	93	69 : 31	38
Ph	high pressure	49	23 : 77	54

Thermal reaction: acetone, 40°C, 5-7 days.
equilibrium was reached, but starting material remained.
High pressure reaction: acetone, 40°C, 0.7 GPa, 18 h.

Scheme 27 Asymmetric IRDARs of furfuryl fumarates **91** under thermal and high-pressure conditions [65]

R^1	R^2	P	Solvent	T	t	95 Yield (%)
H	CN	0.1 MPa	toluene	reflux	24 h	68
H	EtOOC	0.1 MPa	toluene	reflux	24 h	70
H	CN	1.0 GPa	CH$_2$Cl$_2$	rt	overnight	65
H	EtOOC	1.0 GPa	CH$_2$Cl$_2$	rt	overnight	76
Ph	CN	0.1 MPa	toluene	reflux	24 h	52
Ph	EtOOC	0.1 MPa	toluene	reflux	24 h	74
Ph	EtOOC	1.0 GPa	CH$_2$Cl$_2$	rt	overnight	63
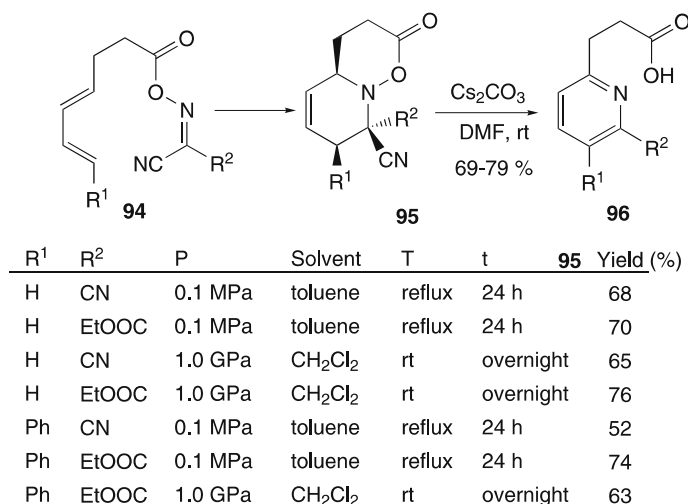
Scheme 28 Regioselective synthesis of pyridines via IRDARs of oximinomalonates **94** [68]

Tricyclic structures (A, B, and C rings) **90** possessing the functionality and stereochemistry inherent in phorbol [63] and its analogues were constructed in one step by a high-pressure IRDAR. The nature of the 2-thioether substituent on the furan was critical for the success of the reaction; a range of high-pressure conditions with the phenylthiofuran **89** (R^1 = Me, R^2 = Ph) led either to the recovery of starting material or decomposition (Scheme 26) [64].

Asymmetric IRDARs of optically active furfuryl fumarates **91** were investigated under thermal and high-pressure conditions. The diastereoselectivities observed increased with the size of the tether substituents, achieving up to 86% in the case of R = *t*-Bu, though in the case of R = *neo*-Pen only 38% de was obtained. It is concluded the diastereoselectivity observed was thermodynamically controlled (Scheme 27) [65]. An IRDA ring-expansion approach toward taxinine (a carbocylic compound) [66] utilizing both Lewis acids and high pressure has been reported [67].

Finally, the thermal and high-pressure mediated IRDARs of an oximino-malonate dienophile **94** tethered to a dienic carboxylic acid offer a facile method for regioselective synthesis of substituted pyridines **96** after aromatization of the adducts **95** with Cs$_2$CO$_3$ (Scheme 28) [68].

2.3
1,3-Diploar Reactions

The 1,3-dipolar reaction (13DPR), whether concerted or not, undoubtedly rivals Diels–Alder reactions in ubiquity as well as synthetic utility [69], and its synthetic potential is still far from being exhausted. Both inter- and intramolecular 1,3-dipolar cycloadditions represent an efficient method for the

syntheses of a wide variety of carbo- and heterocyclic compounds, including natural products.
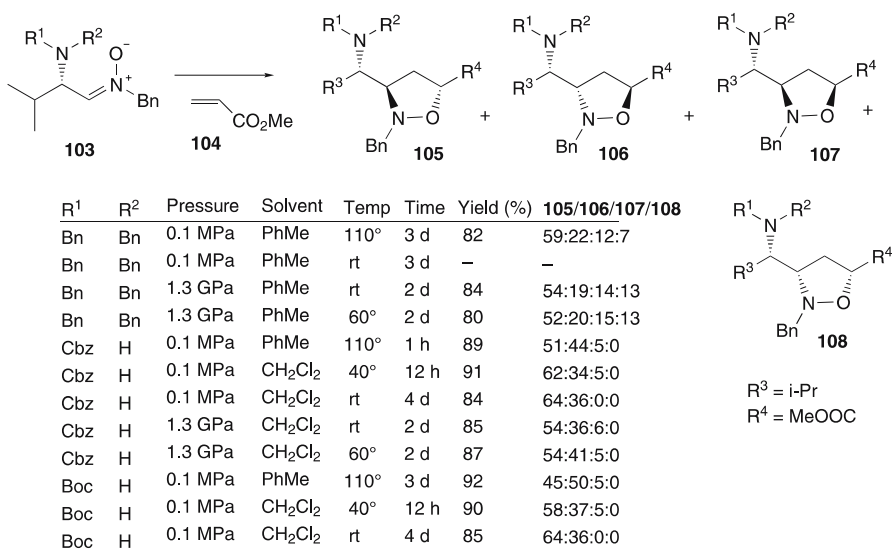
The activation volume for 1,3-dipolar cycloaddition reactions is typically highly negative (ca. – 18 to – 32 cm^3 mol^{-1}). In spite of the broad applicability of 1,3-dipolar cycloadditions in organic synthesis, high-pressure data are still rare compared to Diels–Alder reactions. Among other reasons, this is partly due to the fact that the formation of 1,3-dipoles often involves a bond-breaking process and partly because, in certain cases, 1,3-dipoles are prone to dimerization. Classical examples of synthetic applications of high-pressure 13DPRs have already been compiled [44].

The growing interest in the synthesis of aza-C-disaccharides is associated with the search for new selective glycosidase inhibitors [70–72]. One of the simplest and most elegant approaches to this skeleton would be 13DPRs of hydroxylated nitrones. 13DPRs of the enantiomerically pure, hydroxylated nitrones **97** and **100** to the glycols **98** and **101** are accelerated by applied pressure, giving the adducts **99** and **102**, respectively (Scheme 29). In the reaction leading to the cyclic glycoside **102**, the D-tartaric acid derived nitrone **100** is assumed to approach **101** from the α face (bottom). The stereoselectivity is apparently controlled by the 3-BnO substituent of the glycal as well as by the *t*-BuO group next to the nitrone double bond. Thus, the process has proven to allow direct access to stereodifferentiated tricyclic isoxazolidines like **102**, which may serve as key intermediates to pseudo aza-C-disaccharides [73]
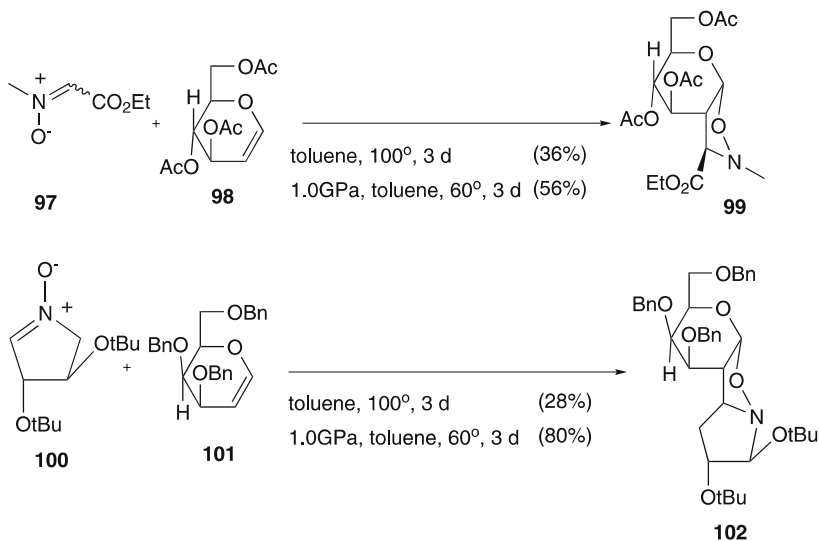
Scheme 29 13DPRs of the enantiopure hydroxylated nitrones **97** and **100** with the glycals **98** and **101** [73]

Analogously, the L-valine derived nitrones **103** react with methyl acrylate (**104**) to produce the corresponding diastereomeric 3,5-disubstituted isoxazolines **105–108**. In the case of the dibenzyl-substituted nitrones, in addition to 3,5-disubstituted isoxazolines, the 3,4-disubstituted isoxazolines were also obtained in low yields. High pressure just served to decrease the reaction time. The major products **105** were found to have the C-3/C-6 *erythro* and C-3/C-5 *trans* relative configuration (Scheme 30) [74].


R^1	R^2	Pressure	Solvent	Temp	Time	Yield (%)	105/106/107/108
Bn	Bn	0.1 MPa	PhMe	110°	3 d	82	59:22:12:7
Bn	Bn	0.1 MPa	PhMe	rt	3 d	–	–
Bn	Bn	1.3 GPa	PhMe	rt	2 d	84	54:19:14:13
Bn	Bn	1.3 GPa	PhMe	60°	2 d	80	52:20:15:13
Cbz	H	0.1 MPa	PhMe	110°	1 h	89	51:44:5:0
Cbz	H	0.1 MPa	CH$_2$Cl$_2$	40°	12 h	91	62:34:5:0
Cbz	H	0.1 MPa	CH$_2$Cl$_2$	rt	4 d	84	64:36:0:0
Cbz	H	1.3 GPa	CH$_2$Cl$_2$	rt	2 d	85	54:36:6:0
Cbz	H	1.3 GPa	CH$_2$Cl$_2$	60°	2 d	87	54:41:5:0
Boc	H	0.1 MPa	PhMe	110°	3 d	92	45:50:5:0
Boc	H	0.1 MPa	CH$_2$Cl$_2$	40°	12 h	90	58:37:5:0
Boc	H	0.1 MPa	CH$_2$Cl$_2$	rt	4 d	85	64:36:0:0

R^3 = i-Pr
R^4 = MeOOC

Scheme 30 13DPRs of L-valine derived nitrones **103** with methyl acrylate (**104**) [74]

The thermal and high-pressure 13DPRs of various *Z*- and *E*-nitrones, e.g., **109**, with alkyl vinyl ethers, e.g., **110**, catalyzed by a variety of chiral oxazaborolidines, e.g., **113**, were carried out with little success. As exemplified in Scheme 31, conversion was achieved only up to 38% ee [75].

A putative type of 13DPRs, or otherwise formal [3 + 2] cycloadditions of 5-alkoxyoxazoles **114** with the carbonyl dipolarophile **115**, were performed either under high pressure or 0.1 MPa, catalyzed by tin(IV) chloride as illustrated in Scheme 32, the regiochemical results being generally complex [76].

13DPRs of organic azides with alkenes and alkynes have long been known to give triazoles and a high-pressure mediated version of this reaction has also been well investigated [9–14, 44]. A recent example is 13DPRs with morpholino-1,3-butadienes and an α-ethynyl-enamine [77].

Finally, nonactivated nitriles do not usually undergo a 13DPR with a 1,3-dipole. However, nitrones like **120–123** react with a variety of normal nitriles to afford the corresponding 2,3-dihydro-1,2,4-oxadiazoles in moderate
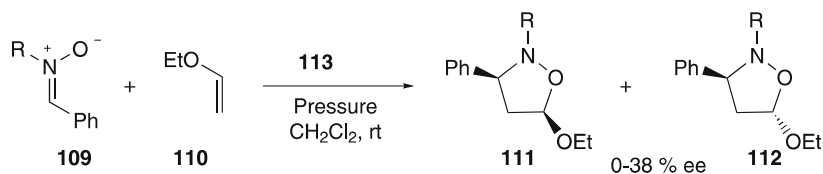
| R	Pressure	**113**	Time (h)	Yield (%)	**111/112**
Me	0.1 MPa	20 mol %	18	64	40:60
Me	0.2 GPa	none	18	84	42:58
Me	0.2 GPa	20 mol%	18	56	37:63
Ph	0.1 MPa	20 mol%	21	14	100:0
Ph	0.2 GPa	none	18	60	38:62
Ph	0.2 GPa	20 mol%	19	80	40:60
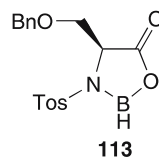
Scheme 31 13DPRs of nitrones **109** with alkyl vinyl ethers **110** catalyzed by chiral oxazaborolidine **113** [75]
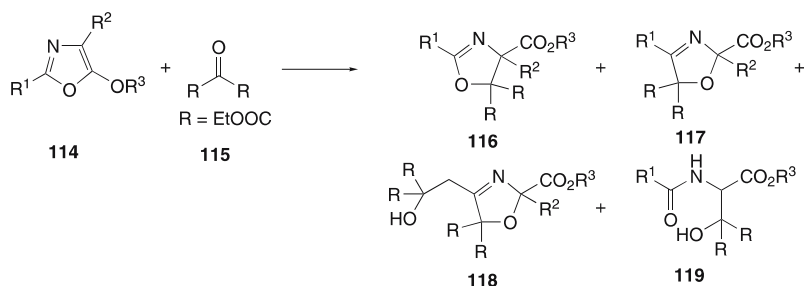
R^1	R^2	R^3	Pressure	Catalyst	Solvent	Temp	Time (h)	Yield (%)
Me	H	Et	0.1 MPa	$SnCl_4$	MeCN	rt	72	16(**116**), 31 (**119**)
Me	H	Et	0.85 GPa	$ZnCl_4$	MeCN	40°	68.5	73 (**116/117** 96:4),9(**119**)
Me	H	Et	0.1 MPa	none	xylene	reflux	24	10 (**117**)
Me	4-MeO-C_6H_4	Me	0.1 MPa	$SnCl_4$	MeCN	rt	33	56(**116/117** 94:6)
Me	4-MeO-C_6H_4	Me	0.1 MPa	$SnCl_4$	MeCN	rt	62	40 (**114/117** 30:70)
Me	4-MeO-C_6H_4	Me	0.85 GPa	none	MeCN	40°	120	47 (**117/118** 21:26)
Me	4-MeO-C_6H_4	Me	0.85 GPa	none	MeCN	40°	120	45 (**118**)

Scheme 32 Formal [3 + 2] cycloadditions of 5-alkoxyoxazoles **114** with diethyl oxomalonate (**115**) [76]

yields [78]. In contrast, under a high pressure of 1.0 GPa, the reaction temperature and time were able to be greatly decreased. For example, reaction of the adamantane-derived nitrone **120** with benzonitrile for 15 h at 150 °C in sealed tube gave a 51% yield of the adduct **124**, whereas at 1.0 GPa and 100 °C for only 1 h **124** was obtained in 71% yield [79].

120 121 122 123

120

PhCN

toluene

150°C (sealed tube), 15h: 51 %
100°C, (1.0GPa),   1h: 71 %

124
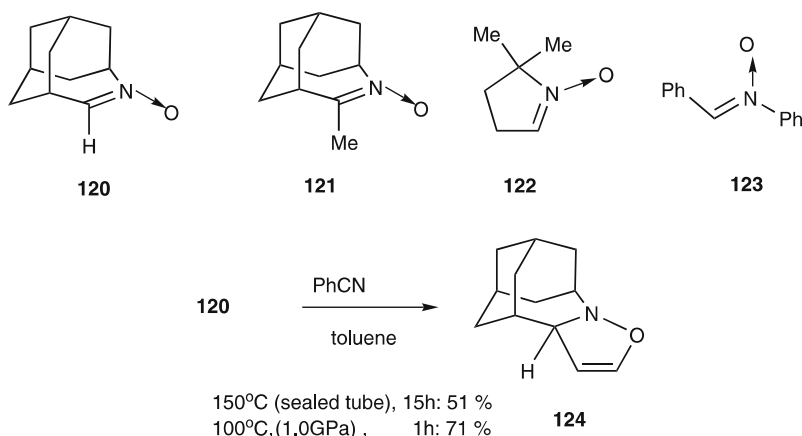
**Scheme 33** 13DPRs of nitrones with nitriles [79]

2.4
Other Pericyclic Reactions

2.4.1
[2 + 2] Cycloadditions

The formal [2 + 2] cycloaddition is a useful method for cyclobutane and oxetane ring formation. Thermal, concerted [2 + 2] cycloadditions are disallowed by orbital symmetry. Heteroallenes, such as ketenes with two π bonds, are thought to undergo thermal concerted cycloaddition either via a $[_\pi 2_s +_\pi 2_s +_\pi 2_s]$ or a $[_\pi 2_s +_\pi 2_a]$ process. Otherwise, [2 + 2] cycloadditions could take place stepwise via either a biradical or a zwitterionic intermediate. [2 + 2] Cycloadditions have large negative activation volumes, with $\Delta V^\ddagger$ values in the range of – 20 to – 50 cm^3 mol^{-1} for concerted and – 25 to – 45 cm^3 mol^{-1} for polar or stepwise reactions [11]. High-pressure conditions are, therefore, expected to be useful for [2 + 2]-type cycloadditions, though

R—NCO +

0.8 GPa
100°C, 20 h

R	Yield (%)
Me	71
Et	92
Bu	77
C$_6$H$_{11}$	68
t-Bu	23
Bn	100

125 126 127
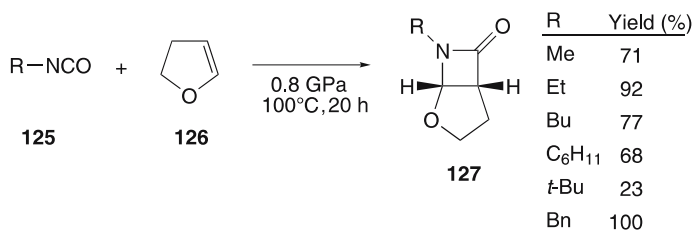
Scheme 34 [2 + 2] Cycloadditions of alkyl isocyanates **125** with 2,3-dihydrofuran (**126**) [80]

not many practical examples of high-pressure mediated [2 + 2] cycloadditions have been reported. Classical examples are compiled in [44].
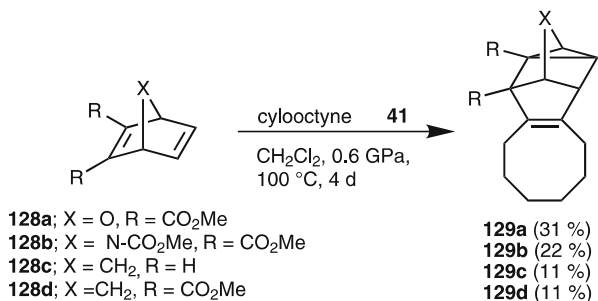
One of the most facile methods for construction of the β-lactam skeleton would be [2 + 2] cycloadditions of isocyanates to alkenes. However, the [2 + 2] cycloadditions of alkyl or aryl isocyanides with either 2,3-dihydrofuran or vinyl ethers often fails under normal conditions. High pressure can surmount this difficulty in certain cases. For instance, alkyl isocyanates **125** underwent [2 + 2] cycloadditions with such cyclic vinyl ethers as **126** to produce the β-lactams **127** (Scheme 34) [80].

2.4.2
[2 + 2 + 2] Cycloadditions

The homo-Diels–Alder reactions of norbornadiene with dimethylacetylene dicarboxylate (DMAD) and TCNE are reported to have activation volumes of about $-30\ cm^3\ cm^{-1}$ and classical examples have already been reviewed [10].

Neither dimethyl oxanorbornadiene-2,3-dicarboxylate (**128a**) nor the related analogues **128b–d** reacted with cyclooctyne [40] at 100 °C in a sealed

128a; X = O, R = CO₂Me
128b; X = N-CO₂Me, R = CO₂Me
128c; X = CH₂, R = H
128d; X = CH₂, R = CO₂Me

129a (31 %)
129b (22 %)
129c (11 %)
129d (11 %)

Scheme 35 Homo-Diels–Alder reactions of dimethyl oxanorbornadiene-2,3-dicarboxylate and related compounds **128** with cyclooctyne [81]
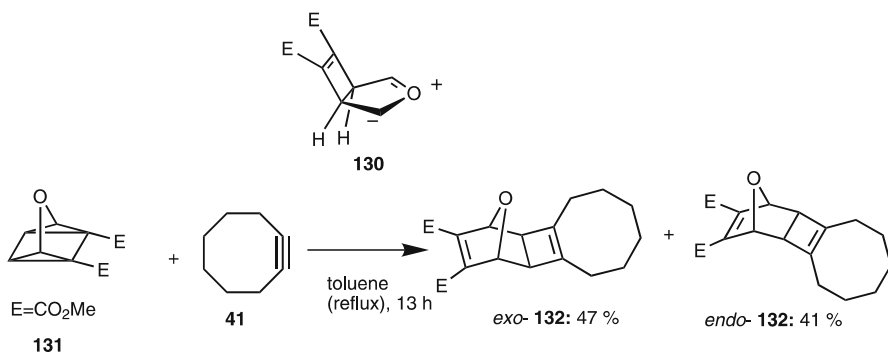
**Scheme 36** A first example of inverse-electron demand [π2 + σ2 + σ2] cycloaddition [82]

tube. In contrast, at 0.6 GPa and 100 °C the same reaction took place to give the corresponding adducts **129a–d** in moderate yields (Scheme 35) [81].

In connection with this, dimethyl oxaquadricyclane-2,3-dicarboxylate (**131**) was initially assumed to behave as a carbonyl ylide **130** toward cyclooctyne [81]. However, this proved to be not the case by an X-ray analysis of the adduct *exo*-**132**, but a first example of an inverse-electron demand [$\pi 2 + \sigma 2 + \sigma 2$] cycloaddition (Scheme 36) [82].

2.4.3
Multicomponent Cycloadditions (MCCs)

Multicomponent reactions (MCRs) are very efficient in organic synthesis, and have represented a rapid upsurge in the literature [83]. High-pressure conditions have proved to be useful for MCRs, and even for double MCRs [83]. For example, 3-[(*E*)-2-nitroethenyl]pyridine (**133**), the benzyl vinyl ether **134**, and *N*-phenylmaleimide underwent a three-component cycloaddition, through tandem IEDA/13DPRs, to afford the bicyclic nitroso acetal **135** as a single stereoisomer, whereas the adduct **136** was obtained as a mixture of three diastereoisomers when methyl acrylate was used instead of *N*-phenylmaleimide (Scheme 37) [84]. The alkaloid family of pyrrolidizines has, in certain cases, shown amnesia-reversal activity related to Alzheimer's disease, and in another cases, viral and retroviral suppression activities including against HIV as well as glycosidase inhibitory properties.
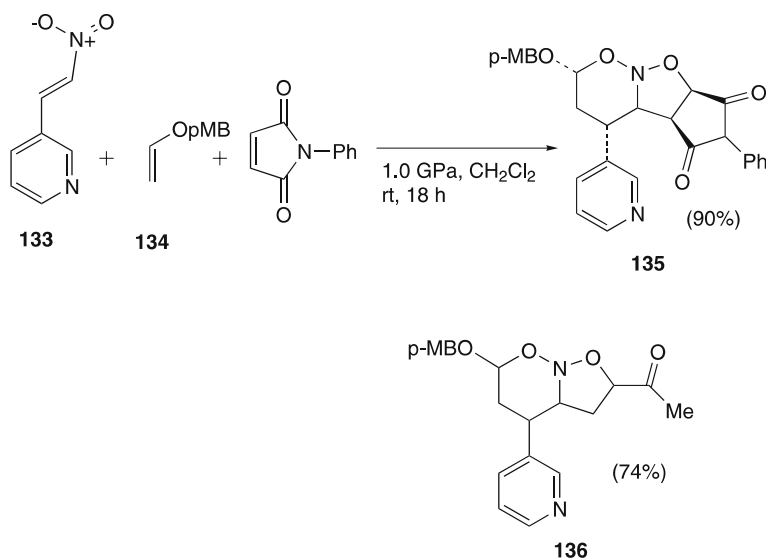
Scheme 37 Three-component cycloaddition of 3'-pyridyl-β-nitroethene (**133**), vinyl ether **134**, and *N*-phenylmaleimide [84]

Similar three-component cycloadditions have been accomplished under heterogeneous and high-pressure conditions, where one reactant was immobilized [85]. Finally, high-pressure mediated MCRs have already been overviewed [86].

3
Ionic Reactions

High pressure is generally effective in accelerating those reactions that involve either an ionization process or a dipolar transition state [9].

3.1
S_N Reactions

This type of reaction is usually promoted by applied pressure and some of the examples have been reviewed by us [87]. The Menschutkin reaction of the phenazine **137** with the allyl bromide **138** occurs only in poor yield with elimination of HBr from **138**, whereas at 1.2 GPa and rt the reaction constitutes a total synthesis of phenazinomycin (**139**), a rare type of phenazine antibiotic, albeit only in 20% yield (Scheme 38) [88].
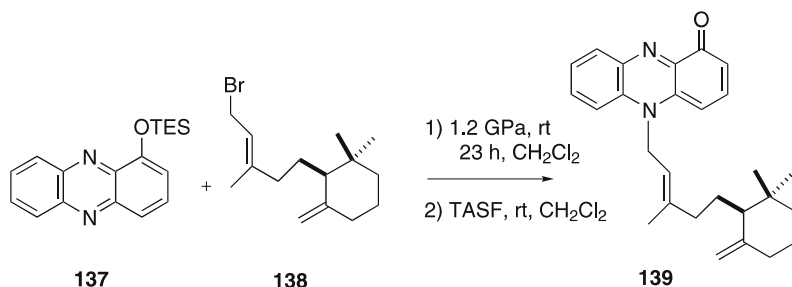
Scheme 38 High-pressure mediated total synthesis of phenazinomycin (**139**) [88]

In a preliminary study toward the total synthesis of the kopsane alkaloid **140**, which may exhibit cholinergic activity, the formal [3 + 2] annulation reaction of 3-alkylindoles with 1,1-cyclopropane diesters was studied in the presence of Yb(OTf)$_3$ either at elevated temperature or at high pressure. For example, N-methyltetrahydrocarbazole (**141**) with styryl-substituted cyclopropane **142** produced a mixture of diastereomeric adducts **143a** and **143b** (3 : 1) in 49% yield at 1.3 GPa for 7 days (Scheme 39) [89].

Nucleophilic aromatic substitution (S_NAr) reactions are not, in general, facile and usually require the presence of at least one strongly electron-withdrawing group, such as a nitro group, or otherwise a very good leav-
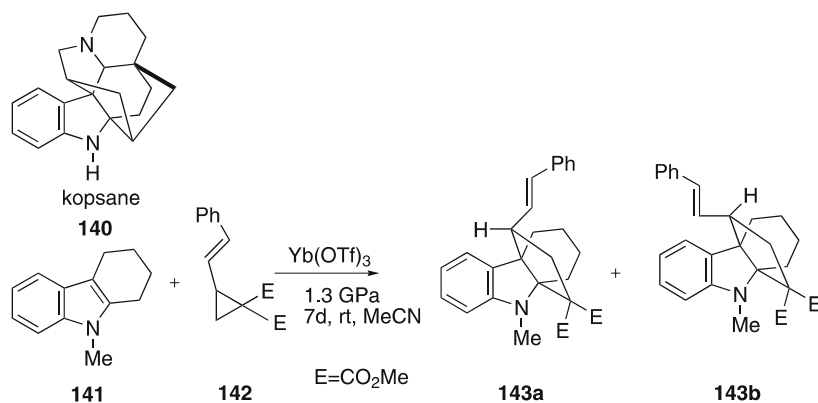
Scheme 39 Formal [3 + 2] approach to a tetracyclic subunit of kopsane alkaloid **140** [89]
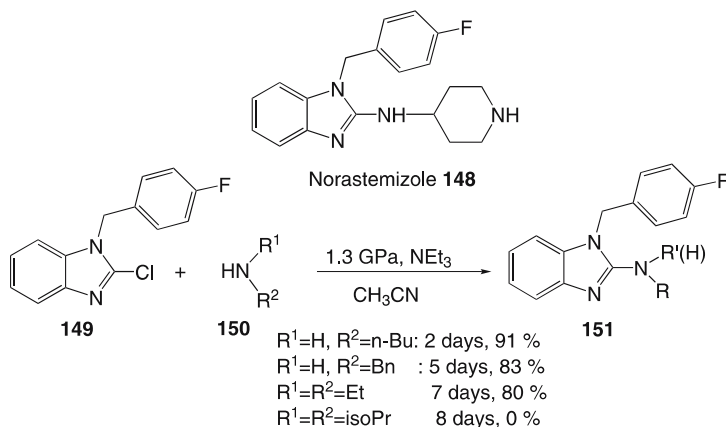
ing group like a diazonium cation in the aromatic ring. The overall volumes of activation for the reactions have been found to be negative, $- 10$ to $- 30\,cm^3\,mol^{-1}$ for the methoxide ion. $S_N Ar$ reactions involving neutral nucleophiles, such as butylamine and piperidine, result in a net charge separation in the transition states, so that highly negative activation volumes have been reported, amounting to ca. $- 70\,cm^3\,mol^{-1}$. Unfortunately, however, the high-pressure technique had not been employed for this type of reaction for synthetic purposes until Ibata et al. and ourselves reported in 1987 that activated halogenobenzenes and halogenopyridines could undergo an $S_N Ar$ reaction with primary and secondary amines without a Lewis acid catalyst at moderate temperatures when performed at 0.6–0.8 GPa. The synthetic applications of high-pressure amino $S_N Ar$ reactions that have been performed by our group up to around 1995 are reviewed in [87, 90].

This high-pressure methodology was later used by several groups, e.g., for the preparation of 4-(dimethylamino)pyridine (DMAP) derivatives [91] and oligoanilines [92]. More intriguingly, the synthesis of enantiomerically pure C-6 substituted pyrazolo[3,4-*d*]pyrimidines **147** has been performed by $S_N Ar$ reaction of 4-amino-6-chloro-1-phenylpyrazolo[3,4-*d*]pyrimidine (**145**) under high-pressure conditions at ambient temperature. Conventional synthetic conditions (reflux at 0.1 MPa) were unsuccessful. The *S* enantiomer displayed higher affinity and selectivity for the adenosine A1 receptor than the *R* enantiomer (Scheme 40) [93].
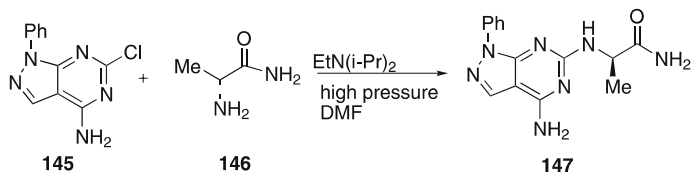
Scheme 40 Enantioselective $S_N Ar$ reaction of **145** with the chiral (*S*)-amine **146** [93]

A similar reaction was applied to an approach to norastemizole (**148**) and its analogues, which are of significant medicinal interest due to their wide range of biological activity. However, no reaction took place either with bulky amines such as isopropyl amine or with aromatic amines such as anisyl amine (Scheme 41) [94]. An alternative method is a palladium-catalyzed amination of **149** based on the Buchwald method [95].

Norastemizole **148**

R^1=H, R^2=n-Bu: 2 days, 91 %
R^1=H, R^2=Bn   : 5 days, 83 %
R^1=R^2=Et   7 days, 80 %
R^1=R^2=isoPr   8 days, 0 %

Scheme 41 High-pressure amino S$_N$Ar reaction of 2-chlorobenzimidazole (**149**) [94]

The high-pressure reaction of 2-methylfuran with alkyl glyoxylates, catalyzed by a chiral (salen)Co(II) complex, is reported to afford the corresponding Friedel–Crafts products both in moderate yield and enantioselectivity [96].

3.2
Addition Reactions

The utility of the high-pressure technique in addition reactions, such as aldol reactions and Michael reactions, is already well known [9, 97]. Perhaps a multicomponent version of reactions is more important in the synthesis of heterocycles. Notably, classical examples are illustrated by the Hantzsch synthesis of 1,4-dihydropyridine and pyrrole synthesis, the Radziszeski imidazole synthesis, the Biginelli reaction for dihydropyrimidinone synthesis, and the Bucherer–Bergs hydantoin synthesis. More recently, the tricyclic diamino ketone from octahydro-2*H*-quinolin-2-one was prepared by Scheiber and Nemes using a double Mannich condensation [98]. Unfortunately, there seems no notable example of high-pressure applications to heterocyclic synthesis, though effects of high pressure just up to 0.3 GPa on the Biginelli reaction have been reported [99].

As an extension of the successful Strecker reaction under high pressure [83], a heterocyclic version of this reaction was investigated by us but met with very limited success. For example, 1 equivalent of 1,2-diacetylbenzene (152) with 1,2-diaminobenzene (153) and TMSCN (2.4 equivalents) afforded 5,6,11,12-tetrahydro-6,11-dimethyldibenzo[*b*,*f*][1,4]diazocine-6,11-dicarbonitrile (154), albeit only in 17% yield in one step. A similar reaction of cyclohexane-1,2-dione (155) with 153 produced 1,2,3,4,5,10-hexahydrophenazine-4a,10a-dicarbonitrile (156) in 13% yield along with the aromatized product, 1,2,3,4-tetrahydrophenazine (157) (Scheme 42). However, similar attempts with other diketones, such as 2,5-hexanedione, 2,3-butadiene, and 9,10-phenanthrenequinone, met with failure, either giving a complex mixture of products or well known and commercially available product possessing a pyrazine skeleton [100].
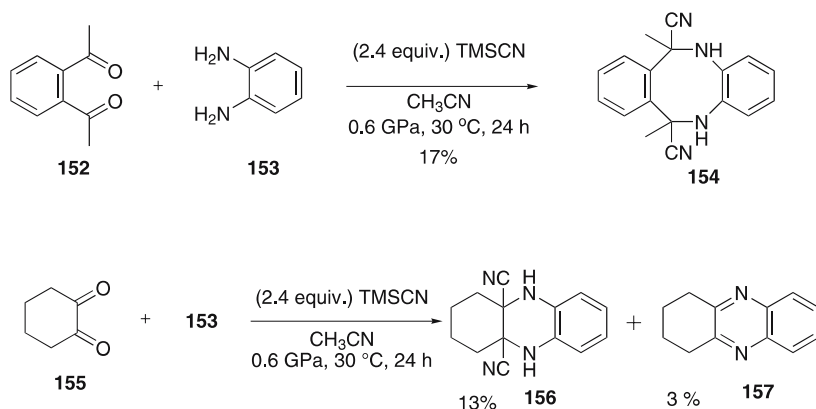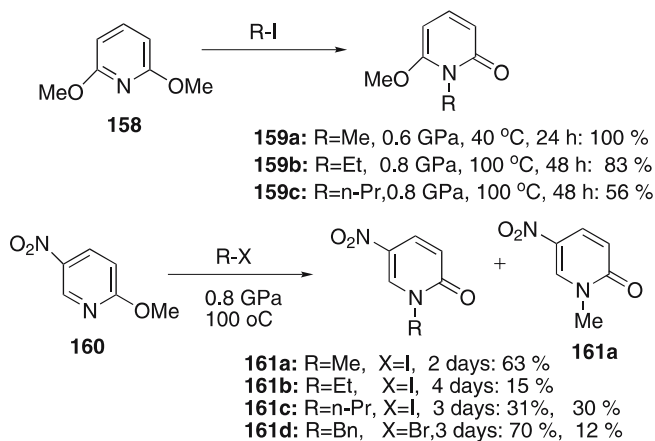

Scheme 42 Multicomponent Strecker reaction of diketones 152 and 155 with 1,2-diaminobenzene (153) [100]

3.3
Other Ionic Reactions

Irreversible lactim–lactam tautomerization was recognized a long time ago and is generally achieved by either heat or catalysts. One of the synthetic applications was reported by Knorr as early as 1897. Later, this reaction was first applied to the synthesis of pyrimidine nucleoside by Johnson and Hilbert, thus being called the Hilbert–Johnson reaction (HJR). The reaction has been employed as one of protocols for the preparation of pyrimidine nucleosides. The biological and medicinal interest in pyrimidine affords further impetus to prepare new types of derivatives. Because of the synthetic utility of the HJR for synthesis of pyrimidine nucleosides, a more sophisticated version of the HJR has been developed by Vorbrüggen (the silyl HJR : VHJR) employ-

ing silyloxypyrimidines rather than alkoxypyrimidines with the aid of Lewis acids, such as AlCl$_3$, SnCl$_4$, and Me$_2$SiSO$_3$CF$_3$ [101]. In particular, the VHJR was used, as one of the key steps, for the total synthesis of the anthelmintic agent hikizimycin [102]. The HJR is amenable to dimethoxypyridines but requires more harsh conditions, probably because of the less electron-deficient nature than pyrimidines. The classical HJRs under high pressure offer a facile synthesis of 2-pyridones. Typical results are summarized in Scheme 43 [103]. Even highly electron-deficient pyridines like **160** were forced to undergo HJRs, albeit needing several days. In view of the postulated mechanism [104, 105], **161** presumably has arisen by reaction of liberated MeX with **160** because of the longer reaction times than in the case of the reaction with **158**. It is anticipated that this methodology would be amenable to a modified VHJR under neutral conditions for exploitation of synthetic applications to pyrimidine nucleosides, which is in progress in our group.

159a: R=Me, 0.6 GPa, 40 °C, 24 h: 100 %
159b: R=Et, 0.8 GPa, 100 °C, 48 h: 83 %
159c: R=n-Pr, 0.8 GPa, 100 °C, 48 h: 56 %

161a: R=Me, X=I, 2 days: 63 %
161b: R=Et, X=I, 4 days: 15 %
161c: R=n-Pr, X=I, 3 days: 31%, 30 %
161d: R=Bn, X=Br, 3 days: 70 %, 12 %

Scheme 43 HJR of 2,6-dimethoxypyridine (**158**) and 2-methoxy-5-nitropyridine (**160**) with haloalkanes [103]

4
Concluding Remarks

In view of the present stage of organic synthesis it is possible to design and construct a desired molecule, partly based upon computer-aided molecular modeling and partly based upon our own chemical history, inspiration, and philosophy. The utility of a high-pressure strategy to accomplish a desired reaction that is not otherwise accessible is well documented. Therefore, high-pressure technology has already become a routine technique for synthetic chemists. As exemplified above, this technique (0.1–2.0 GPa) is applied mainly in liquid systems and is a valuable and necessary tool which can be

employed to stimulate reluctant organic reactions that take place too slowly, require too high temperatures, or are hindered by steric or electronic factors. Furthermore, it has proved to be useful in order to increase selectivity among alternative products, since both regio- and stereoselectivities change with pressure if there is a difference in activation volumes. Among nonconventional methods such as sonochemistry (ultrasound), flash vacuum pyrolysis, microwave irradiation, and supercritical fluids (most related to high pressure), the basic principles are most discrete as described in Eq. 1, thus in certain cases being extremely useful for elucidation of reaction mechanisms. On the other hand, it is not so easy to maintain a high-pressure apparatus if we use over 0.8 GPa. Since the microwave method is easy to operate and inexpensive, the author suggests that readers should use microwave irradiation first but does not recommend materials having a low boiling point. This short review shows clearly that the high-pressure technique for laboratory use now has an assured role specifically in fine chemical research such as drug synthesis. The author believes that the high-pressure technique will find more and more successful applications as a facile and useful methodology in various synthetic reactions. Commercial applications of high-pressure techniques may become even more probable, especially in the pharmaceutical sciences. Finally, high-pressure methodology has proven to constitute a field of green chemistry, providing atom-economic as well as environmentally friendly tactics in organic synthesis.

References

1. Sharma A, Scott JH, Cody GD, Fogel ML, Hazen RM, Hemley RJ, Huntress WT (2002) Science 295:1514
2. Daniel I, Oger P, Winter R (2006) Chem Soc Rev 35:858
3. Hamann SD (1957) Physico-chemical effects of pressure. Butterworths, London
4. Bridgman PW (1952) The physics of high pressure. Bell, London
5. Ho TL (1981) Distinctive techniques for organic synthesis. World Scientific, Toh Tuck Link, Singapore
6. Tanaka K, Toda F (2000) Chem Rev 100:1025
7. Arai Y, Sako T, Takebayashi Y (2002) Supercritical fluids: molecular interactions, physical properties and new applications. Springer, Berlin
8. Eycken EV, Kappe CO (2006) Microwave-assisted synthesis of heterocycles. Springer, Berlin
9. Matsumoto K, Uchida T, Sera A (1985) Synthesis 1
10. Matsumoto K, Sera A (1985) Synthesis 999
11. Matsumoto K, Acheson R (eds) (1991) Organic synthesis at high pressures. Wiley, New York

12. van Eldik R, Klärner FG (2002) High pressure chemistry. Wiley, Weinheim
13. Jenner G (2005) Tetrahedron 61:3621
14. Matsumoto K, Ibata T (1999) Choukoatsu yuki gosei. Nakanishiya, Kyoto
15. Isaacs NS (1981) Liquid phase high pressure chemistry. Wiley, New York
16. Holzapfel WB, Isaacs NS (1997) High-pressure techniques in chemistry and physics. Oxford University Press, Oxford
17. Huisgen R (1968) Angew Chem Int Ed Engl 7:321
18. Woodward R, Hoffmann R (1970) The conservation of orbital symmetry. Academic, San Diego
19. Tietze LF, Steck PL (2002) High pressure chemistry. Wiley, Weinheim, p 239
20. Chmielewski M, Jurczak J (1987) J Carbohydr Chem 6:1
21. Tietze LF, Kettschau GJ, Gewert JA, Schuffenhauer A (1998) Curr Org Chem 2:19
22. Torisawa Y, Ali MA, Tavet F, Kageyama A, Aikawa M, Fukui N, Hino T, Nakagawa M (1996) Heterocycles 42:677
23. Matsumoto K, Kimura S (2000) Heterocycl Commun 6:31
24. Matsumoto K, Kimura S, Morishita T, Misumi Y, Hayashi N (2000) Synlett 233
25. Fujita R, Oikawa K, Yoshisuji T, Okuyama Y, Nakano H, Matsuzaki H (2003) Chem Pharm Bull 51:295
26. Minuti L, Taticchi A, Gacs-Baitz E, Marrocchi A (1998) Tetrahedron 54:10891
27. Matzanke N, Gregg RJ, Weinreb SM (1997) J Org Chem 62:1920
28. Chrétien A, Chataigner I, Hélias NL, Piettre SR (2003) J Org Chem 68:7990
29. Drew MGB, Jahans A, Harwood LM, Apoux SABH (2002) Eur J Org Chem 3589
30. Beusker P, Aben RWG, Seerden J-PG, Smits JMM, Scheeren HW (1998) Eur J Org Chem 2483
31. Dauben WG, Gerdeo J, Smith DB (1985) J Org Chem 50:2576
32. Matsumoto K, Hashimoto S, Ikemi Y, Otani S, Uchida T (1986) Heterocycles 24:1835
33. Dauben WD, Lam JYL, Guo ZR (1996) J Org Chem 61:4816
34. McCluskey A, Keane MA, Walkom CC, Bowyer MC, Sim ATR, Young DJ, Sakoff JA (2002) Bioorg Med Chem Lett 12:391
35. Rao HSP, Murali R, Taticchi RA, Scheeren HW (2001) Eur J Org Chem 2869
36. Seerden J-PG, Tulp MTM, Scheeren HW, Kruse CG (1998) Bioorg Med Chem 6:2103
37. Kotsuki H, Kitagawa S, Nishizawa H, Tokoroyama T (1978) J Org Chem 43:1471
38. Kumamoto K, Fukada I, Kotsuki H (2004) Angew Chem Int Ed 43:2015
39. Coutts IGC, Allcock RW, Scheeren HW (2000) Tetrahedron Lett 41:9105
40. Heber D, Roesner P, Tochtermann W (2005) Eur J Org Chem 4231
41. Matsumoto K, Ciobanu M, Yoshida M, Uchida T (1997) Heterocycles 45:15
42. Exner E, Hochstrate D, Keller M, Klärner F-G, Prinzbach H (1996) Angew Chem Int Ed Engl 35:2256
43. Margetic D, Murata Y, Komatsu K, Eckert-Maksic M (2006) Organometallics 25:111
44. Matsumoto K, Hamana H, Iida H (2005) Helv Chim Acta 88:2033
45. Kotsuki H, Kumamoto K (2005) Yuki Gosei Kagaku Kyokaishi 63:770
46. Malinowska M, Kwiatkowski P, Jurczak J (2004) Tetrahedron Lett 45:7693
47. Jenner G, Ben Salem RB (2000) New J Chem 24:203
48. Vandenput DAL, Scheeren HW (1995) Tetrahedron 51:8383
49. Aben HM, de Gelder R, Scheeren HW (2002) Eur J Org Chem 3126
50. Al-Badri H, Maddaluno N, Masson JS, Collignon N (1999) J Chem Soc Perkin Trans 1 2255
51. Al-Badri H, Collignon N, Maddaluno N, Masson JS (2000) Chem Commun 1191
52. Al-Badri H, Collignon N, Maddaluno J, Masson JS (2000) Tetrahedron 56:3909

53. de Meijere A, Leonov A, Heiner T, Noltemeyer M, Bes MT (2003) Eur J Org Chem 472
54. Junge H, Oehme G (1998) Tetrahedron 54:11027
55. Schürer SC, Blechert S (1999) Tetrahedron Lett 40:1877
56. Álvarez M, Feliu L, Ajana W, Joule JA, Fernández-Puentes JL (2000) Eur J Org Chem 849
57. Klärner FG, Wurche F (1998) Koatsuryoku no Kagaku to Gijyutsu 8:104
58. Diedrich MK, Klärner FG (1998) J Am Chem Soc 120:6212
59. Wanner J, Harned AM, Probst DA, Poon KW, Klein TA, Snelgrove KA, Hanson PR (2002) Tetrahedron Lett 43:917
60. Rogatchov VO, Bernsmann H, Schwab P, Fröhlich R, Wibbeling B, Metz P (2002) Tetrahedron Lett 23:4753
61. Plietker B, Seng D, Fröhlich R, Metz P (2000) Tetrahedron 56:873
62. Galley G, Pätzel M (1996) J Chem Soc Perkin Trans 1 2297
63. Hoppe W, Brandl F, Strell I, Rohrl Gassmann I, Hecker E, Bartsch H, Kreibich G, Szczepanski CV (1967) Angew Chem Int Ed Engl 6:809
64. Brickwood AC, Drew MGB, Harwood LM, Ishikawa T, Marais P, Morisson V (1999) J Chem Soc Perkin Trans 1 913
65. Butz T, Sauer J (1997) Tetrahedron Asymmetry 8:703
66. Hosoyama H, Shigemori H, Tomida A, Tsuro T, Kobayashi J (1999) Bioorg Med Chem Lett 9:389
67. Phillips JA, Morris JC, Abell AD (2000) Tetrahedron Lett 41:2723
68. Bland DC, Rausdenbush BC, Weinreb SM (2000) Org Lett 2:4007
69. Padwa A, Pearson WH, Taylor EC, Wipf P (2003) Synthetic applications of 1,3-dipolar cycloaddition chemistry toward heterocycles and natural products. Wiley, New York
70. Krähenbühl K, Picasso S, Vogel P (1997) Bioorg Med Chem Lett 7:893
71. Dong W, Jespersen T, Bols M, Skrydstrup T, Sierks MR (1996) Biochemistry 35:2788
72. Zou W (2005) Curr Top Med Chem 5:1363
73. Cardona F, Salanski P, Chmielewski M, Valenza S, Goti A, Brandi A (1998) Synlett 1444
74. Blanarikov-Hlobilova I, Kubanova Z, Fisera L, Cyranski MK, Salanski P, Jurczak J, Pronayova JN (2003) Tetrahedron 59:3333
75. Seerden J-PG, Boeren MMM, Scheeren HW (1997) Tetrahedron 53:11843
76. Suga H, Shi X, Ibata T, Kakehi A (2001) Heterocycles 55:1711
77. Brunner M, Maas G, Klärner F-G (2005) Helv Chim Acta 88:1813
78. Yu Y, Ohno M, Eguchi S (1995) J Chem Soc Perkin Trans 1 1417
79. Yu Y, Fujita H, Ohno M, Eguchi S (1995) Synthesis 498
80. Taguchi Y, Tsuchiya T, Oishi A, Shibuya I (1996) Bull Chem Soc Jpn 69:1667
81. Matsumoto K, Taketsuna H, Ikemi Y, Kakehi A, Uchida T, Otani S (1998) Heterocycles 49:79
82. Matsumoto K, Taketsuna H, Kim J-C, Kakehi A (2001) J Heterocycl Chem 38:1233
83. Matsumoto K, Kim J-C, Iida H, Hamana H, Kumamoto K, Kotsuki H, Jenner G (2005) Helv Chim Acta 88:1734
84. Kuster GJT, Steeghs RHJ, Scheeren HW (2001) Eur J Org Chem 553
85. Kuster GJT, Scheeren HW (2000) Tetrahedron Lett 41:515
86. van Berkom WA, Kuster GJT, Scheeren HW (2003) Mol Divers 6:271
87. Ciobanu M, Matsumoto K (1997) Liebigs Ann Recuil 623
88. Kinoshita Y, Kitahara T (1997) Tetrahedron Lett 38:4993
89. England DB, Kuss TDO, Keddy RG, Kerr MA (2001) J Org Chem 66:4704

90. Matsumoto K (1994) Synthetic applications of amino S_NAr reactions under high pressure. In: Taniguchi Y, Senoo M, Hara K (eds) High pressure liquids and solutions. Elsevier, Amsterdam, pp 119–135
91. Kotsuki H, Sakai H, Shinohara T (2000) Synlett 116
92. Brown CL, Muderawan I, Wayan Y, David J (2003) Synthesis 251
93. Poulsen S.-A. Young DJ, Quinn RJ (2001) Bioorg Med Chem Lett 11:191
94. Barrett IC, Kerr MA (1999) Tetrahedron Lett 40:2439
95. Ahman J, Buchwald SL (1997) Tetrahedron Lett 38:6363
96. Kwiatkowski P, Wojaczynska E, Jurczak J (2003) Tetrahedron Asymmetry 14:3643
97. Misumi Y, Matsumoto K (2002) Angew Chem Int Ed 41:1031
98. Scheiber P, Nemes P (1994) Liebigs Ann Chem 1033
99. Jenner G (2004) Tetrahedron Lett 45:6195
100. Kumamoto K, Iida H, Hamana H, Kotsuki H, Matsumoto K (2005) Heterocycles 66:675
101. Seela F, Peng X (2006) Curr Top Med Chem 6:867
102. Ikemoto N, Schreiber SL (1990) J Am Chem Soc 112:9657
103. Matsumoto K, Ikemi Y, Suda M, Iida H, Hamana H (2007) Heterocycles 72:187
104. Ulbricht TLV (1962) Angew Chem 74:767
105. Ueda T, Ohtsuka H (1973) Chem Pharm Bull 21:1451

Ring Transformation of Nitropyrimidinone Leading to Versatile Azaheterocyclic Compounds

Nagatoshi Nishiwaki (✉) · Masahiro Ariga

Department of Chemistry, Osaka Kyoiku University, Asahigaoka 4-698-1, Kashiwara, 582-8582 Osaka, Japan
nishi@cc.osaka-kyoiku.ac.jp

Abstract The ring transformation (RTF) is a powerful protocol for preparing polyfunctionalized compounds not easily available by alternative procedures. Dinitropyridone and nitropyrimidinone are excellent substrates for this reaction. Dinitropyridone behaves as the synthetic equivalent of unstable nitromalonaldehyde to give nitroanilines, nitropyridines, and nitrophenols. On the other hand, nitropyrimidinone causes three kinds of RTF reactions. When nitropyrimidinone reacts with dinucleophilic reagent at the 2- and the 6-positions, 4-pyridones, pyrimidines, and 4-aminopyridines are formed, in which pyrimidinone behaves as the synthetic equivalent of activated diformylamine. Nitropyrimidinone also behaves as the equivalent of α-nitroformylacetic acid to furnish 3-nitro-2-pyridones when the RTF reaction occurs at the 4- and the 6-positions. Nitropyrimidinone reveals nucleophilicity at the 3-position and electrophilicity at the 6-position with loss of an imino group. This structural feature enables the synthesis of 2-pyridones upon treatment with 1,3-dicarbonyl compounds. The RTF reactions of pyridone and pyrimidinone prove to be a useful protocol for syntheses of versatile azaheterocyclic compounds having multi-functionalities.

Keywords Ammonium acetate · Nitro compounds · Pyridone · Pyrimidinone · Ring transformation

Abbreviations
RTF   Ring transformation
TCRT   Three components ring transformation

1
Chemical Behavior of a Nitro Group

Nitro compounds constitute a large family among organic compounds and are widely used for various purposes [1–3]. The nitro group is one of the useful functional groups because of the following properties.

a) As the Electron-Withdrawing Group

The nitro group behaves as the electron-withdrawing group by both inductive and resonance effects. The inductive electron-withdrawing ability can be estimated by comparing pKa values of substituted acetic acids. While chloroacetic and dichloroacetic acids have pKa values of 2.86 and 1.29, respectively, the pKa value of nitroacetic acid is 1.68. These facts indicate the electron-withdrawing inductive effect of a nitro group is a match for that of two chloro groups. The resonance effect of a nitro group also diminishes the electron density of the β- and the δ-carbons through the conjugated system. As a result, not only α-carbon but also these carbons become highly electron-deficient.

b) As the Activating Group

The electron-withdrawing nitro group activates various skeletons. Although most halobenzenes cause no change upon treatment with nucleophile, nitrated ones easily undergo the nucleophilic substitution. The activation by a nitro group is also observed in the Diels-Alder reaction, in which nitroalkene behaves as a good dienophile. The nitro group significantly increases the acidity of α-hydrogen to form nitronate easily. The nitronate possesses both nucleophilic and electrophilic sites, thus it is often used for syntheses of heterocyclic compounds. Furthermore, the nitro group assists the adjacent carbon–carbon bond cleavage since stable nitronate anion is readily eliminated. As shown here, nitro compounds play an important role in organic reactions due to these chemical behaviors.

c) Chemical Conversion to Other Functionalities

The nitro group is converted to versatile functionalities. A carbon–carbon double bond can be produced from nitroalkane by elimination of a nitro group with vicinal hydrogen as nitrous acid. The Nef reaction is also often used for transformation from nitroalkanes to ketones. The most useful chemical modification of a nitro group is the reduction furnishing oximes and amines, and further chemical conversion to various functionalities can be performed via diazonium salts.

The above diversity of a nitro group surely provides a valuable tool in organic syntheses. However, the chemistry of heterocyclic compounds substituted with a nitro group has not been studied enough since their preparation is often difficult, especially electron-deficient pyridines and pyrimidines derivatives are not easily available. While nitration is a powerful method for direct introduction of a nitro group to the aromatic ring, the pyridine nuclei cannot be nitrated under generally used conditions. Direct nitration of pyridines at the 3-position is realized when a combination of nitrogen pentoxide and sulfur dioxide is employed [4]. If nitric acid is employed as the nitrating agent, modification of the pyridine ring should be performed. Pyridine N-oxide is readily nitrated at the 4-position by nitric acid because its electron density is increased by electron-donating ability of the oxygen atom [5]. Alternatively, pyridone derivatives are also usable as the substrate for nitration since aromaticity of the N-substituted 2-pyridone becomes considerably lower but it is still an aromatic compound showing somewhat aromaticity as shown in Scheme 1. The nitration proceeds at the 3- or the 5-positions to afford 3-nitro, 5-nitro and 3,5-dinitropyridones. These nitropyridones are expected to reveal high electrophilicity, and reactions with various kinds of nucleophiles afford polyfunctionalized azaheterocyclic compounds.
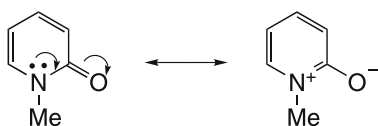

Scheme 1 Resonance structures of *N*-methyl-2-pyridone

2
Ring Transformation (RTF) Reaction

A great number of heterocyclic compounds have been employed for functional materials such as medicines, agricultural chemicals, dyes, organic electroluminescence, etc. It is necessary to construct libraries containing a large

number of compounds with variety for effective research of new functional materials. Functionalized heterocyclic compounds are especially useful for the present purpose because they are also used as the key synthetic intermediates leading to versatile compounds. However, direct modification of the heterocyclic compounds like pyridine is rather difficult than that of the benzene ring. Thus, supplementary protocols for modification of heterocyclic compounds should be developed. The built-in method is one of the convenient procedures in which a building block having a functional group is condensed with another component to construct polyfunctionalized compounds.

The ring transformation (RTF) reaction is known to be another supplementary method. Since this protocol provides polyfunctionalized compounds that are not easily prepared, its synthetic utility is quite high. The RTF reaction is a restructuring reaction involving "scrap and build" of the substrate. Namely, the partial structure (B) of the substrate (A + B) is transferred to the reagent (C) forming a new ring system (B + C) accompanied by elimination of the leaving group (A) (Scheme 2). This chemistry has been energetically investigated in which van der Plas and his co-workers have contributed to a great degree, and research for finding new RTF reactions or new substrates is still one of the challenging projects even now [6–9].
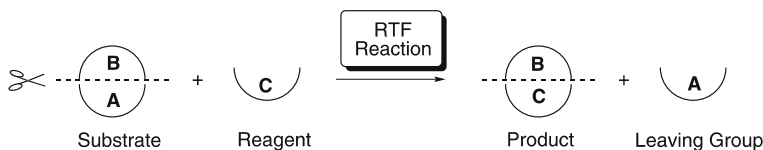
Scheme 2 Basic concept of the RTF reaction

Several kinds of reaction patterns are known in the RTF reaction. The nucleophilic RTF reaction uses a combination of dinucleophilic substrate and dielectrophilic reagent. Electron-deficient cyclic compounds having a good leaving group are suitable substrates in this kind of reaction [10–12]. Nitropyridines are known to cause the nucleophilic RTF reactions whose electron density is diminished by a nitro group besides by the ring nitrogen. However, employment of somewhat severe conditions such as strong base and high temperature are required for destroying aromaticity of the pyridine nuclei [7]. Furthermore, effective RTF reaction is surely realized if the substrate has a good leaving group as the partial structure. From this viewpoint, 3,5-dinitro-2-pyridone **1** is considered to overcome these drawbacks, namely pyridone **1** is a highly electron-deficient compound with low aromaticity, and its N1 – C2 – C3 moiety is easily eliminated as a stable nitroacetamide anion (Scheme 3). We have actually shown dinitropyridone **1** is an excellent substrate for the RTF reactions. Recently, we have focussed on its azaanalogs, nitropyrimidinones **2** and **3** having similar structural features to **1**. In this
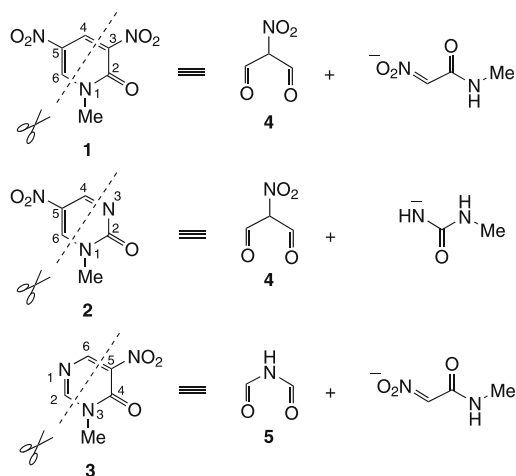
Scheme 3 Nitropyridone and nitropyrimidinones

article, we would like to review our works on RTF reactions using these substrates in the past decade.

3
Preparation of Substrates

Substrates **1–3** are readily prepared with a few steps as illustrated in Scheme 4. After methylation of pyridine with dimethyl sulfate, oxidation with potassium ferricyanide in the presence of sodium hydroxide leads
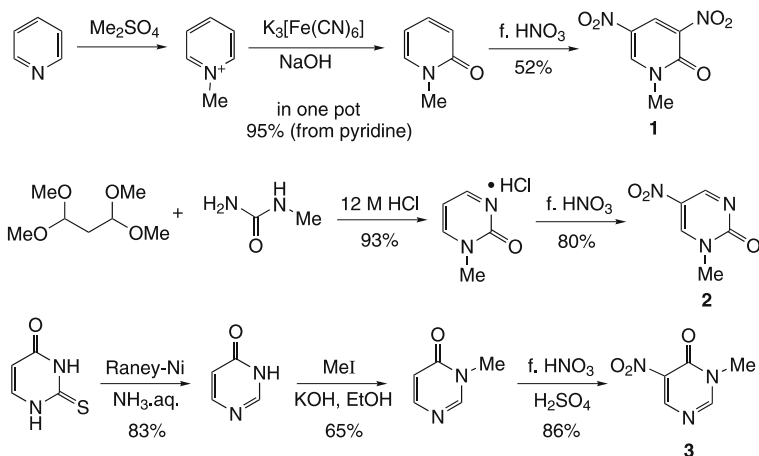

Scheme 4 Preparative methods for substrates

to 1-methyl-2-pyridone [13]. These reactions are conducted in one pot. 1-Methylpyrimidin-2(1H)-one is obtained as the white precipitates just after mixing N-methylurea and 1,1,3,3-tetramethoxypropane in concentrated hydrochloric acid [14]. Preparation of 3-Methylpyrimidin-4(3H)-one is performed by reduction of 2-thiouracil with Raney-nickel followed by methylation with methyl iodide [15]. Nitration of N-methylated pyridone and pyrimidinones is performed upon treatment with fuming nitric acid to give substrates for the RTF reactions, namely dinitropyridone 1 and nitropyrimidinones 2 and 3.

4
Aminolysis of Nitropyridone and Nitropyrimidinones

The electron deficiency and electrophilicity of dinitropyridone 1 and nitropyrimidinones 2 and 3 are estimated before beginning the study on RTF reactions by conducting aminolysis. When pyridone 1 is allowed to react with amines in a pyridine solution, aminolysis easily proceeds to afford azadienamines 6 having a nitro group (Scheme 5). However, this reaction suffers from side reaction forming adduct 7 by which pyridone 1 is consumed by eliminated anionic N-methylnitroacetamide [16]. On the other hand, nitropyrimidinone 2 is a more convenient precursor for azadienamines 6 in higher yields [17]. In this case, eliminated anionic N-methylurea is trapped by methanol, leading to methyl carbamate 8 that cannot react with pyrimidinone 2 at all. These facts indicate the 4- and the 6-positions of 1 and 2 are highly electrophilic to react with nucleophilic reagents easily.
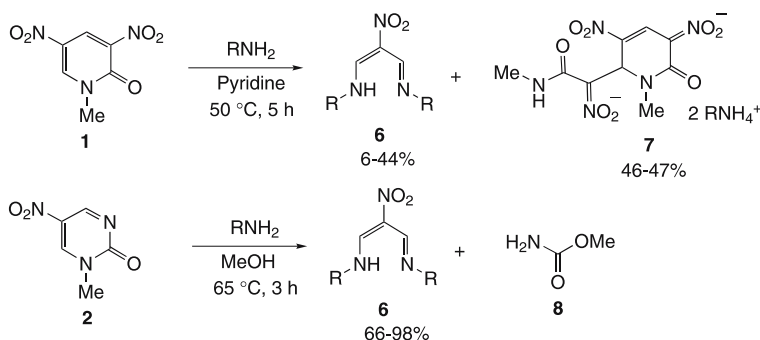
Scheme 5 Preparation of nitroazadienamines

Azadienamines 6 are usable as the β-diketiminate ligands that have a nitro group in the carbon framework. Many reports dealing with diketiminate ligands are found in the literature since their complexes have recently

drawn attention as a polymerization catalyst [18]. However, β-diketiminate having an electron-withdrawing group is rarely seen except for cyano derivative [19–21], hence the diketiminate having a nitro group is expected to show novel property that has not been observed for other diketiminate ligands. Nitroazadienamines **6** actually form complexes with copper(I) to afford bis(β-diketiminato)copper(II) complex **9a** [22, 23], mononuclear complex **9b** [22, 24] and head-to-tail linear polymer complex **9c** [22, 24] as illustrated in Scheme 6. Their coordination patterns are varied with substituents on the nitrogen atoms of **6**.
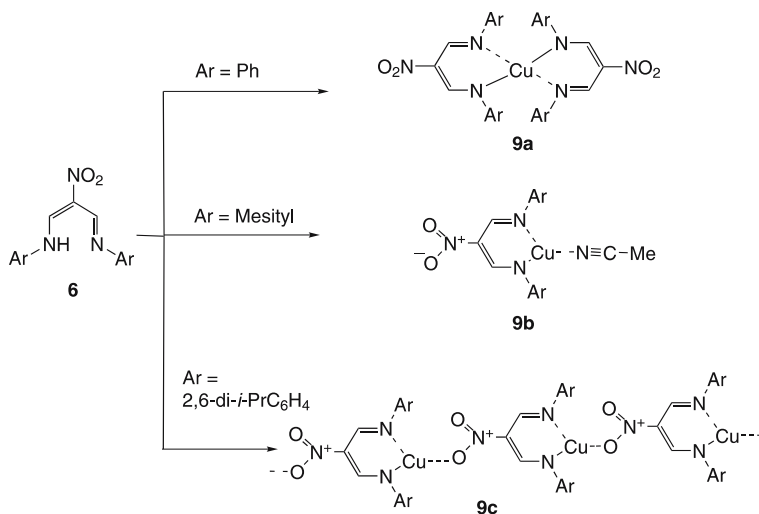
Scheme 6 Complexes of azadienamines with copper(I)

When azadienamines **6** is charged on a silica gel column at room temperature, formylated nitroenamine **10** is effectively produced by half hydrolysis [25] (Scheme 7). Formylnitroenamine **10** can be used as the building block for built-in method to afford versatile nitro azaheterocyclic compounds [26] and nitrophenols [27] in reactions with dinucleophilic reagents.

Nitropyrimidinone **3** has also electrophilic sites, the 2-and the 6-positions, which are attacked by amines to yield nitroenamines having a carbamoyl group **11** in good yields [28]. Nitroenamine **11** is converted to polyfunctionalized pyridone **12a** upon treatment with sodium enolate of ethyl 3-oxobutanoate **13a** [29].

Nitroenamine derivatives are typical push-pull alkenes, and have been widely used in organic syntheses [3, 30, 31]. Although their synthetic utility is quite high, functionalized ones are not often employed because of their difficult preparation. Hence, the aminolysis of pyrimidinones **2** and **3** is regarded as a new preparative method for functionalized nitroenamines **10** and **11**.
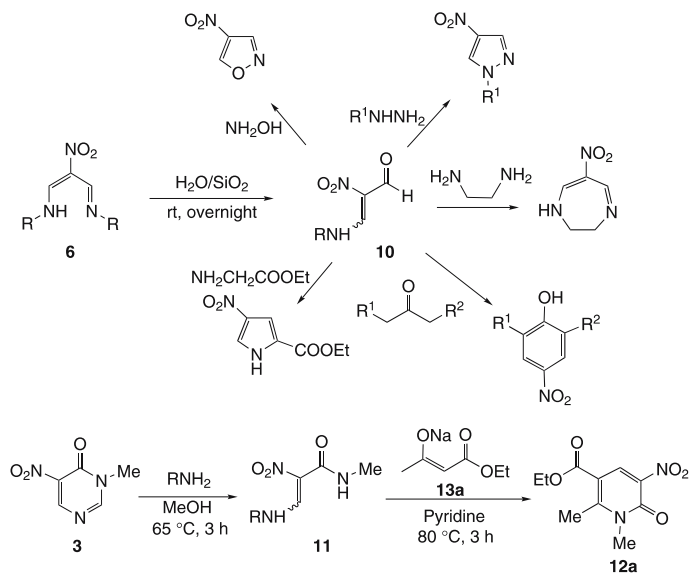
Scheme 7 Functionalized nitroenamines

5
RTF Reaction

5.1
Suitable Substrates for the RTF Reaction

On the basis of results obtained in the last section, it is confirmed that both nitropyrimidinones **2** and **3** have two electrophilic sites respectively similar to dinitropyridone **1**. These electrophilic positions are considered to react with dinucleophilic reagents to cause RTF reactions.

As illustrated in Scheme 3, the C4 – C5 – C6 moiety of pyridone **1** and that of pyrimidinone **2** behave as the synthetic equivalent of nitromalonaldehyde **4**. Nitromalonaldehyde **4** often appears as the synthon in the retrosyntheses for a variety of nitro compounds, but it cannot be actually employed for organic syntheses because of instability. Thus, its sodium salt has been used as the synthetic equivalent for a long time [32]. The sodium salt is prepared from furfural via mucobromic acid accompanied by somewhat troublesome manipulations [33], and the insolubility of the sodium salt into general organic solvents obliges us to conduct reactions in the aqueous medium or in the highly polar solvent. Furthermore, crude sodium salt should be handled as a potentially explosive material because it is sensitive to impact and thermally unstable. Despite the problems mentioned here, sodium salt is still widely used in organic syntheses due to the lack of other efficient reagents.

From this viewpoint, dinitropyridone **1** and nitropyrimidinone **2** would be supplementary synthetic equivalents of **4** treatable in organic media with considerable safety instead of sodium nitromalonaldehyde. Dinitropyridone **1** is a more suitable substrate for the RTF reaction compared to nitropyrimidinone **2** since the stable nitroacetamide anion is more readily eliminated than anionic urea.

On the other hand, the C2 – N1 – C3 moiety of pyrimidinone **3** behaves as the synthetic equivalent of activated diformylamine **5** accompanied by elimination of anionic nitroacetamide [34]. Diformylamine **5** is the simplest secondary amide, however it has not been extensively used in organic syntheses due to its low reactivity. The carbonyl group of diformylamine has carbamoyl properties rather than formyl ones, and thus nucleophilic substitution proceeds in reactions using **5** [35, 36]. The sole example employing diformylamine as an aldehyde is the intramolecular Wittig reaction leading to pyrrole derivatives [37, 38]. The RTF reaction using nitropyrimidinone **3** would provide a C – N – C unit as a building block in the new ring systems.

5.2
RTF Reaction Using Enolate Ion

As the dinucleophilic reagent, sodium enolates of 1,3-dicarbonyl compounds can be used. When dinitropyridone **1** is treated with sodium enolate **13b** derived from diethyl 3-oxopentanedioate, the RTF reaction proceeds to give 2,6-bis(ethoxycarbonyl)-4-nitrophenol **14b** in 91% yield [39]. Enolates of ethyl 3-oxobutanoate **13a** and 2,4-pentadione **13c** similarly react to give corresponding functionalized 4-nitrophenols **14a** and **14c**, respectively.

A plausible mechanism for this reaction is shown in Scheme 8. The nucleophilic attack of the enolate **13** occurs at the 4-position of pyridone **1** to form an adduct intermediate **15**, and then regenerated enolate attacks at the 6-position, leading to bicyclic intermediate **16**. The order of these nucleophilic attacks is not a serious problem because the same product is obtained even though the 6-position is attacked prior to the 4-position. The following elimination of anionic nitroacetamide from **16** affords RTF product, nitrophenol **14**.

In this reaction, another mechanism can be proposed as illustrated in Scheme 9. Namely, the ring opening reaction of pyridone **1** proceeds after addition of enolate **13** to form the open-chain intermediate **17** instead of bicyclic one **16**, and then its cyclization yields nitrophenol **14**. However, this mechanism is excluded by the following experimental facts. When the reaction is conducted at a low temperature, the bicyclic compound **18** is isolated, which is transformed to nitrophenol **14** upon heating with base (Scheme 10) [39].
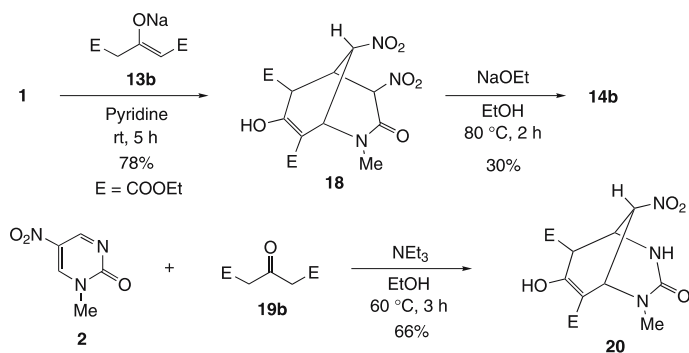
On the other hand, nitropyrimidinone **2** is considered to reveal different reactivity from pyridone **1** since the leaving group, anionic *N*-methylurea, is less stable than anionic *N*-methylnitroacetamide. Actually, polyfunction-
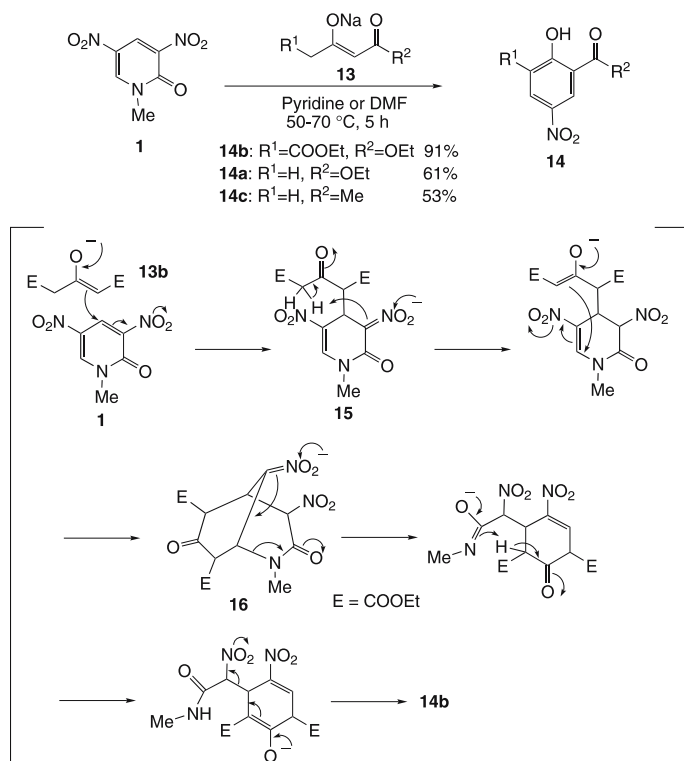
Scheme 8 RTF reaction leading to nitrophenol derivative
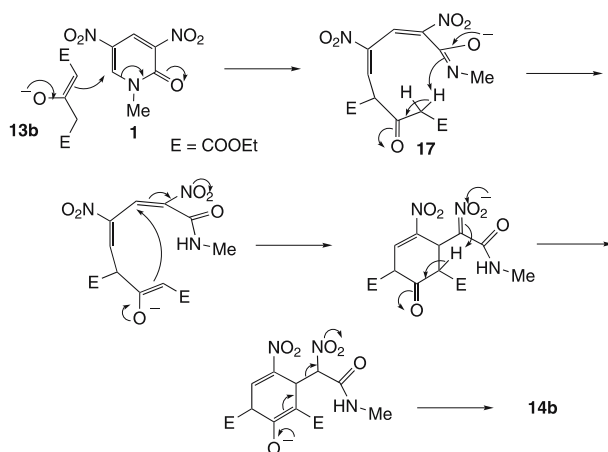
Scheme 9 Another mechanism via open-chain intermediate

Scheme 10 Isolation of bicyclic compounds

alized bicyclic compound **20** is isolated to our expectation in the reaction with diethyl 3-oxopentanedioate **19b** and triethylamine, in which conversion of **19b** to enolate **13b** is not necessary beforehand [40]. This experimental fact also supports the mechanism, including a bicyclic intermediate **16** as shown in Scheme 8.

Nitropyrimidinone **3** is also confirmed to be a suitable substrate for RTF reaction. When pyrimidinone **3** is allowed to react with diethyl 3-oxopentanedioate **19b** in the presence of triethylamine, the RTF reaction effectively proceeds to afford 3,5-bis(ethoxycarbonyl)-4-pyridone **21b** (Scheme 11). The C2 – N1 – C6 moiety of pyridone **21b** is derived from **3**, which means that nitropyrimidinone **3** behaves as the synthetic equivalent of activated diformylamine **5**. While 2,4,6-heptanetrione **19d** causes the RTF reaction under the same conditions, giving **21d**, ethyl 3-oxobutanoate requires conversion to sodium enolate **13a** for preparation of **21a**, due to the presence of only a single active methylene group [40].
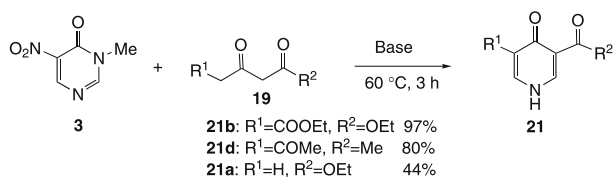
Scheme 11 Synthesis of 3,5-difunctionalized 4-pyridones

5.3
Three Components Ring Transformation (TCRT)

As mentioned, dinitropyridone **1** and nitropyrimidinone **3** are highly electrophilic, and these substrates undergo RTF reactions to give nitrophenols **14** and 4-pyridone **21** upon treatment with β-keto esters or β-diketones.

1,3-Dicarbonyl compounds **19** surely behave as the excellent dinucleophilic reagents for the RTF reactions, however, only several kinds of RTF products can be obtained due to limited availability of these reagents. In order to improve the synthetic utility of the RTF reaction, other reagents such as simple ketones **22** must be used. In this case, another nucleophile or activating reagent should be employed, and this kind of RTF reaction is called "three components ring transformation (TCRT)".

5.3.1
Synthesis of 4-Nitroanilines

Since simple ketones **22** are less reactive compared to 1,3-dicarbonyl compounds **19**, improvement of the nucleophilicity of the α-carbon is required by conversion to enamines. When dinitropyridone **1** is treated with acetone **22a** in the presence of amines, 2,6-disubstituted 4-nitroanilines **23a–c** are produced in good yields (Table 1). In this reaction, the enamine is formed in situ, and attacks stepwise at the 4- and the 6-position of pyridone **1** to afford bicyclic intermediate from which anionic nitroacetamide is eliminated leading to nitroaniline derivative **23**. It is possible to synthesize unsymmetrical nitroanilines having different substituents at the 2- and the 6-positions by changing ketones **22**, and modification of the amino group is also achieved by using other amines [41].

**Table 1** TCRT reaction leading to nitroaniline derivatives
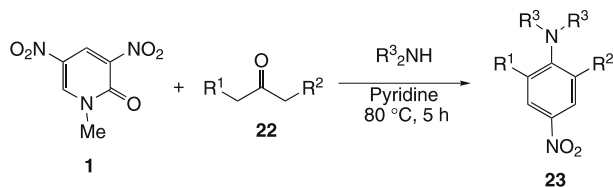
R^1	R^2	Ketone	R_2^3NH	Product	Yield/%
H	H	**22a**	Pyrrolidine	**23a**	95
H	H	**22a**	Et$_2$NH	**23b**	93
H	H	**22a**	BuNH$_2$	**23c**	93
Me	H	**22b**	Pyrrolidine	**23d**	98
Me	Me	**22c**	Pyrrolidine	**23e**	58
H	COOEt	**19b**	Pyrrolidine	**23f**	85

5.3.2
Syntheses of Nitropyridines and Pyrimidines

As shown in the previous section, N-alkyl nitroanilines **23** are obtained in the reaction of pyridone **1** with ketones **22** in the presence of amines. In this case, amines are introduced as the dialkylamino substituents. On the contrary, different reactivity is observed when ammonia is used instead of amines. The TCRT reaction proceeds to afford 2,3-dialkyl-5-nitropyridines **24** upon treatment of pyridone **1** with ketones **22** in the presence of ammonia (Table 2) [42, 43]. The C4 – C5 – C6 unit is derived from pyridone **1**, the C2 – C3 unit is derived from ketone, and the ring nitrogen (N1) is from ammonia, namely the new ring consists of three components. As electrophilic nitration of pyridines is quite difficult, the present TCRT will be an alternative method for preparation of nitropyridine derivatives.

In this reaction, enamines **25** are usable as the reagent, which sometimes gives better results than ketones **22**. The present TCRT is applicable to versatile aliphatic, aromatic and heteroaromatic ketones to afford corresponding nitropyridines **24**, respectively. In cases of aromatic ketones **22g–l**, higher

**Table 2** Synthesis of nitropyridine derivatives
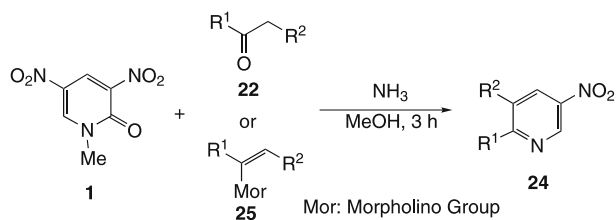
R^1	R^2	Temp/°C		Yield/%[a]
$-(CH_2)_4-$		65	**d**	83 (90)
$-(CH_2)_3-$		65	**e**	27 (37)
i-Pr	H	65	**f**	36
Ph	H	65	**g**	44 (90)
Ph	H	120[b]	**g**	81
Ph	Me	65	**h**	10 (50)
4-MeC$_6$H$_4$	H	120[b]	**i**	73
4-NO$_2$C$_6$H$_4$	H	120[b]	**j**	27
2-Pyridyl	H	120[b]	**k**	72
2-Furyl	H	120[b]	**l**	62
H	i-Pr	100[b]	**m**	52

[a] Yields of **24** in reactions using enamine **25** is given in parentheses
[b] Temperature in a sealed tube

reaction temperature using a sealed tube is necessary for effective TCRT. Furthermore, aldehyde can be used as the reagent, giving 3,5-disubstituted pyridine **24m**.

This kind of TCRT is also observed in the reactions of nitropyrimidinone **3** with ketones and methanolic ammonia, which leads to 4,5-disubstituted pyrimidines **26** [44, 45]. This reaction is initiated by the successive addition of ammonia and ketone at the 2- and the 6-positions of pyrimidinone **3**. The intramolecular cyclization between the amino and the carbonyl groups furnishes bicyclic intermediate **27**, and then anionic nitroacetamide is eliminated to afford pyrimidine **26** (Scheme 12).

26d: R^1,R^2=(CH$_2$)$_4$ 85%^{a}
26e: R^1,R^2=(CH$_2$)$_3$ 31%
26g: R^1=H, R^2=Ph   6%^{b}
^{a} in MeCN ^{b} at 120 °C
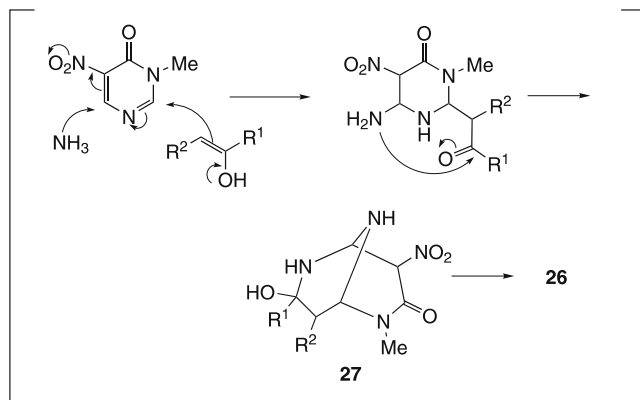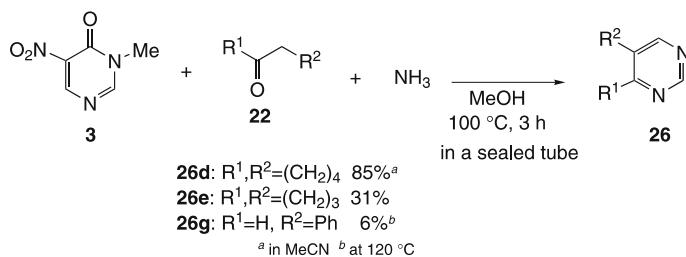
Scheme 12 Synthesis of pyrimidines by TCRT

Pyrimidine derivatives are frequently used as functional materials or are found in their partial structures. A great number of methods for construction of pyrimidine skeleton have been reported in which the majority is the condensation of a C – C – C unit (e.g., malonaldehyde, malononitrile, diethyl malonate) and an N – C – N unit (e.g., urea, guanidine) [46]. On the other hand, the general method involving a combination of C – N – C, C – C and N units is not known to our best of knowledge. Thus, the present TCRT will be an alternative method for the preparation of 4,5-disubstituted pyrimidines, however, this reaction suffers from limited scope of ketones. When cyclohexanone is employed, tetrahydroquinazoline **26d** is effectively formed

as a result of TCRT. To the contrary, yields of pyrimidines **26** are significantly diminished in reactions of pyrimidinone **3** with other ketones. In the case of acetophenone, only 6% 4-phenylpyrimidine **26g** is obtained even though the reaction is conducted at $120\,°C$ in a sealed tube. In each case, small amounts of nitroenamines **11a** (R = H) and **11b** (R = Me) are isolated, as shown in Scheme 7. This experimental fact indicates the competitive ammonolysis of nitropyrimidinone **3** prevents the TCRT.

5.3.3
TCRT Using Ammonium Acetate as the Nitrogen Source

As mentioned in last section, ammonia is not suitable for the nitrogen source in the TCRT due to competitive ammonolysis. In order to avoid this undesired reaction, less nucleophilic ammonium acetate is employed instead of ammonia. When a methanol solution of nitropyrimidinone **3** is heated with acetophenone **22g** and ammonium acetate, the formation of yellow precipitates is observed during the reaction. 4-Phenylpyrimidine **26g** is isolated from the reaction mixture in a considerably improved 49% yield under quite milder conditions compared with the TCRT using ammonia (Scheme 13) [44, 47].
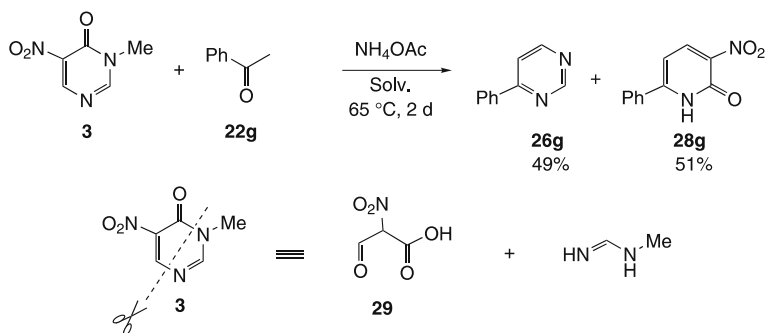
Scheme 13 TCRT leading to pyrimidines and 3-nitro-2-pyridones

The precipitated yellow solid during the reaction is 6-phenyl-3-nitro-2-pyridone **28g** whose C2 – C3 – C4 unit is derived from the C4 – C5 – C6 unit of pyrimidinone **3**. Another TCRT proceeds at the 4- and the 6-positions of pyrimidinone **3**, which behaves as the synthetic equivalent of α-nitro-formylacetic acid **29**.

Both pyrimidines [46] and 3-nitro-2-pyridones [48–53] are often found in biologically active compounds or their synthetic intermediates. The present TCRT will be a useful protocol for construction of a useful library, however, it is required to control the selectivity of these products from the viewpoint of atom economy. The addition of acetic acid is influential for the selectivity of this reaction, and the results are summarized in Table 3.

Table 3 Solvent effect on selectivity

| Solv.	AcOH/equiv.	Yield/%		Recovery/%
		26g	28g	3
MeOH	0	49	51	0
MeOH	1	40	56	0
MeOH	4	22	59	0
MeOH – AcOH	(3 : 1)	24	9	21
AcOH	–	65	14	0

When a stoichiometric amount of acetic acid is added to the reaction mixture, the yield of pyrimidine **26g** is diminished and **28g** is formed in a somewhat increased yield. On the other hand, the addition of a larger amount of acetic acid causes a dramatic change in the ratio of the two products, and pyrimidine **26g** is also formed as the major product when acetic acid is used as the solvent.

5.3.4
Structural Effects of the Ketones

The selectivity between pyrimidine **26** and nitropyridone **28** is varied with structural difference of ketones **22**. In a series of reactions using cyclic ketones, cycloheptanone **22n** is found to show unique reactivity [44]. While cyclic ketones having a five-, six- or eight-membered ring afford corresponding bicyclic pyrimidines **26e**, **26d** and **26o**, bicyclic pyridone **28n** is predominantly produced in the case of **22n** (Table 4). Although it has not been clarified why this different reactivity is observed, the selectivity is successfully inverted by conducting the reaction in acetic acid to give **26n** exclusively.

Electronic property of the ketone is also an important factor changing the selectivity of the present TCRT [54]. Several kinds of acetophenone derivatives are employed for studying the substituent effects, and the results are shown in Table 5. When acetophenone **22g** and 4-chloroacetophenone **22q** are employed, both products **26** and **28** are obtained in almost the same yields. In cases of electron-poor ketones **22j**, **22r** and **22s**, pyrimidines **26** are predominantly produced, however, total yields become lower. The diminished electron density on the carbonyl group is found to be influential for the lower reactivity and the predominant formation of pyrimidines **26**. On the contrary, the TCRT effectively proceeds in cases of electron-rich ketones **22i**, **22p**, **22t** and **22u** to furnish corresponding products in good total yields, in which pyridones **28** are formed prior to **26**. It is noteworthy that three isomeric methoxyacetophenones show almost the same reactivity, although 3-methoxy group only behaves as the electron-withdrawing group for the car-

Table 4 TCRT using cyclic ketones
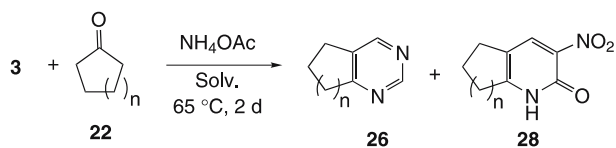
n	Solv.		Yield/%		Ratio
			26	28	26/28
1	MeOH	e	85	0	100/0
2	MeOH	d	71	0	100/0
3	MeOH	n	11	79	12/88
3	AcOH	n	90	0	100/0
4	MeOH	o	67	17	80/20

Table 5 Substituent effects on selectivity
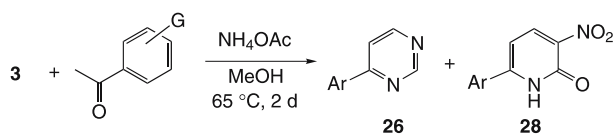
G		Yield/%		Ratio
		26	28	26/28
Ph	g	49	51	49/51
4-MeO	p	20	63	24/76
4-Me	i	25	75	25/75
4-Cl	q	37	41	47/53
4-NO$_2$	j	52	10	77/23
3-NO$_2$	r	38	25	60/40
2-NO$_2$	s	0	0	–
3-MeO	t	27	54	34/66
2-MeO	u	30	52	37/63

bonyl group. Hence, the electron density on the benzene ring seems more influential than that of the carbonyl group.

This tendency is applicable to hetaryl ketones **22k**, **22l** and **22v–z** as shown in Table 6. While almost equal amounts of **26v** and **28v** are obtained in the reaction with 3-acetylpyridine **22v**, pyridylpyrimidines **26w** and **26k** are predominantly afforded since the electron density on the acetyl group

Table 6 Synthesis of bihetaryl compounds
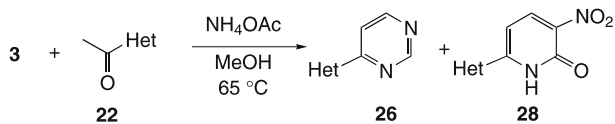
Het	Time/d			Yield/%		Ratio
				26	**28**	**26/28**
3-Pyridyl	2	v		44	38	54/46
4-Pyridyl	2	w		44	9	84/16
2-Pyridyl	2	k		49	1	98/2
2-Pyrrolyl	7	x		0	47	0/100
3-Pyrrolyl	7	y		0	68	0/100
2-Thienyl	7	z		0	72	0/100
2-Furyl	2	l		13	60	18/82

is diminished by the 2-pyridyl or the 4-pyridyl group. On the other hand, pyridones **28** are mainly produced when electron-sufficient heterocyclic compounds having an acetyl group **22x–z** and acetylfuran **22l** are employed.

5.3.5
Plausible Mechanisms

On the basis of the experimental results mentioned in the last section, a plausible mechanism for TCRT using aromatic ketone and ammonium acetate is proposed in Scheme 14. Since ammonium acetate is not nucleophilic, the TCRT proceeds in a somewhat different pathway from that using ammonia, as shown in Scheme 12.

The enol form of the ketone attacks at the 6-position of nitropyrimidinone **3** to give an adduct intermediate **30**. Affinity of the electron-rich ketone with electron-deficient pyrimidinone **3** realizes the effective TCRT to afford products **26** and **28** in a good total yield. The adduct **30** is considered to be a key intermediate for determining reaction paths leading to pyrimidine **26** or nitropyridone **28**. When the benzene ring is substituted with the electron-withdrawing group, enamine **31** is formed as a result of predominant amination of the more electrophilic carbonyl group **A**. The following intramolecular attack of the amino group occurs at the less-hindered 2-position to afford pyrimidine **26** via bicyclic intermediate **32** together with elimination of nitroacetamide. On the other hand, the carbonyl group **B** is more readily aminated to give **33** when electron-rich ketone is employed. The amino group of **33** attacks the carbonyl group **A** to yield pyridone **28** via the bicyclic intermediate **34** together with elimination of amidine.
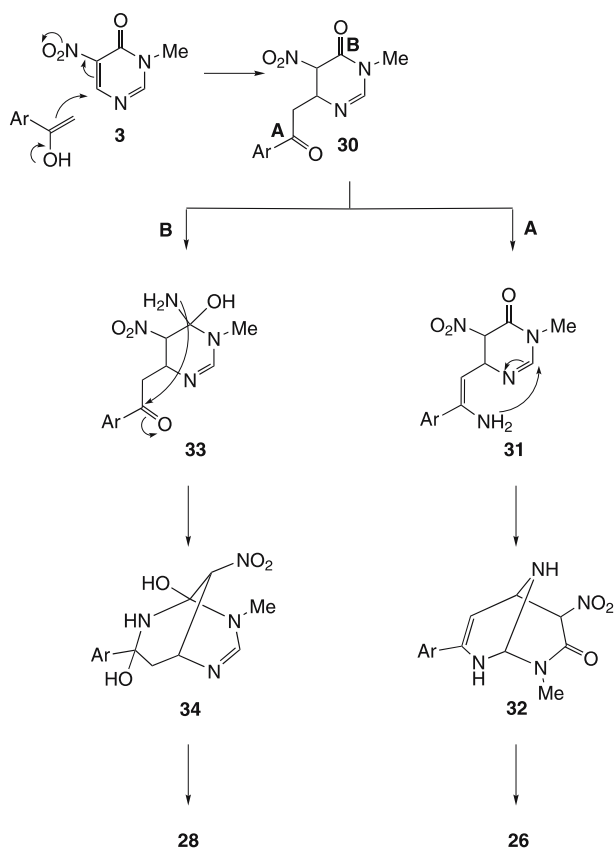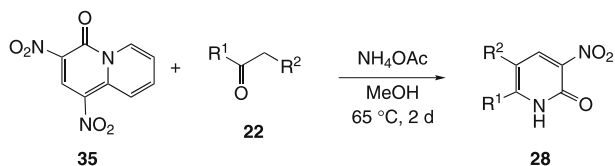
Scheme 14 A plausible mechanism for formation of pyrimidine and pyridone

5.3.6
Another Approach to 3-Nitro-2-pyridones

In the last sections, 3-nitro-2-pyridones **28** are synthesized by TCRT of nitropyrimidinone **3** with ketones **22** in the presence of ammonium acetate. The C2 – C3 – C4 unit of **28** is derived from the C4 – C5 – C6 unit of pyrimidinone **3**, which behaves as the synthetic equivalent of α-nitroformylacetic acid **29**. The same partial structure is also found in 1,3-dinitroquinolizin-4-one **35** [55], which is regarded as the dinitropyridone blocked with a benzene ring on the [*f*] face [56], and only a single kind of TCRT is expected to proceed. Nitropyridones **28** are actually prepared in moderate yields by TCRT upon treatment of quinolizinone **35** with ketones **22** in the presence of ammonium acetate as the nitrogen source (Table 7) [57].

Table 7 TCRT using dinitroquinolizinone

R^1	R^2		Yield/%
Ph	H	**g**	49
4-MeC$_6$H$_4$	H	**i**	47
4-NO$_2$C$_6$H$_4$	H	**j**	35
Me	H	**a**	58
i-Pr	H	**f**	23
$-(CH_2)_5-$		**n**	26

5.3.7
TCRT of Dinitropyridone Using Ammonium Acetate

As mentioned, ammonium acetate is indicated to be an effective promoter of the TCRT in addition to the role as nitrogen source. Ammonium acetate also enables the TCRT of dinitropyridone **1** with ketone [58].

When pyridone **1** is allowed to react with 4-methoxyacetophenone **22p** in the presence of ammonium acetate, the TCRT effectively proceeds to give 2-(4-methoxyphenyl)-5-nitropyridine **24p**. While the yields are low in cases of acetophenone **22g** and 4-nitroacetophenone **22q** because of competitive side reactions giving unidentified products, electron-rich acetophenones **22p** and **22u** reveal high reactivity to afford corresponding nitropyridines **24p** and **24u** in high yields. It is also possible to prepare trisubstituted pyridine **24h** and hetarylpyridines **24k** and **24l** by changing ketones. Compared to TCRT of **1** using ammonia described in Sect. 5.3.2, the present method is advantageous since solid ammonium acetate is easily treatable, and the reaction proceeds under milder conditions.

To the contrary, nitroaniline **23aa** is formed in addition to nitropyridine **24aa** in the reaction of pyridone **1** with butanone that has two kinds of α-hydrogens (Table 9). Although the reaction mixture is complicated because of side reactions in cases of methyl ketones, employment of ketones having longer alkyl chains is rather effective to give nitroanilines **23cc** and **23dd** in higher yields. On the other hand, reactions of **1** with cyclic ketones furnish only bicyclic nitropyridines **24d, 24e** and **24n** without detection of any corresponding nitroanilines since 2,6-bridged benzene is highly strained. When

Table 8 Synthesis of nitropyridines using ammonium acetate
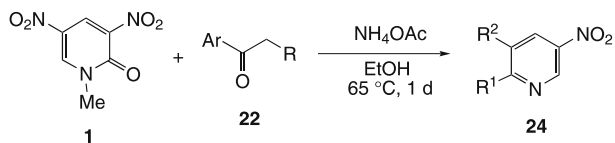
Ar	R		Yield/%
4-MeOC$_6$H$_4$	H	**p**	91
2-MeOC$_6$H$_4$	H	**u**	87
Ph	H	**g**	35
4-ClC$_6$H$_4$	H	**q**	65
4-NO$_2$C$_6$H$_4$	H	**j**	27
Ph	Me	**h**	26
2-Pyridyl	H	**k**	21
2-Furyl	H	**l**	73

Table 9 Synthesis of nitroanilines
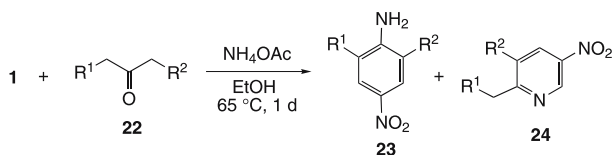
R^1	R^2		Yield/%	
			23	24
Me	H	**aa**	7	5
Pr	H	**bb**	17	12
Et	Et	**cc**	63	16
Pr	Pr	**dd**	45	9
Me	H	**aa**	7	5
$-(CH_2)_3-$		**d**	0	56
$-(CH_2)_2-$		**e**	0	85
$-(CH_2)_4-$		**n**	0	48
$-(CH_2)_9-$		**ee**	2	20

cyclododecanone is used to solve this problem, it is succeeded to prepare small amount of bridged nitroaniline **23ee**.

After the addition of ketone at the 4-position of pyridone **1**, the adduct **15′** is transformed to two kinds of enamines **36** and **37** by ammonium ion

(Scheme 15). The intramolecular nucleophilic attack of the amino group at the 6-position followed by elimination of nitroacetamide from the bicyclic intermediate **38** furnishes nitropyridines **24**. In this case, the β-carbon of the enamine does not attack due to the formation of a four membered ring. On the contrary, both the amino and the β-carbon can form a six-membered ring by nucleophilic addition at the 6-position in the case of adduct intermediate **37**. When the amino group attacks (route **A**), nitropyridine **24** is produced via bicyclic intermediate **39**. Nucleophilic attack of the β-carbon also occurs to give bicyclic intermediate **40** (route **B**), and elimination of nitroacetamide leads to nitroaniline **23**. The latter route is more predominant than the former one since the β-carbon is more nucleophilic than the amino group.
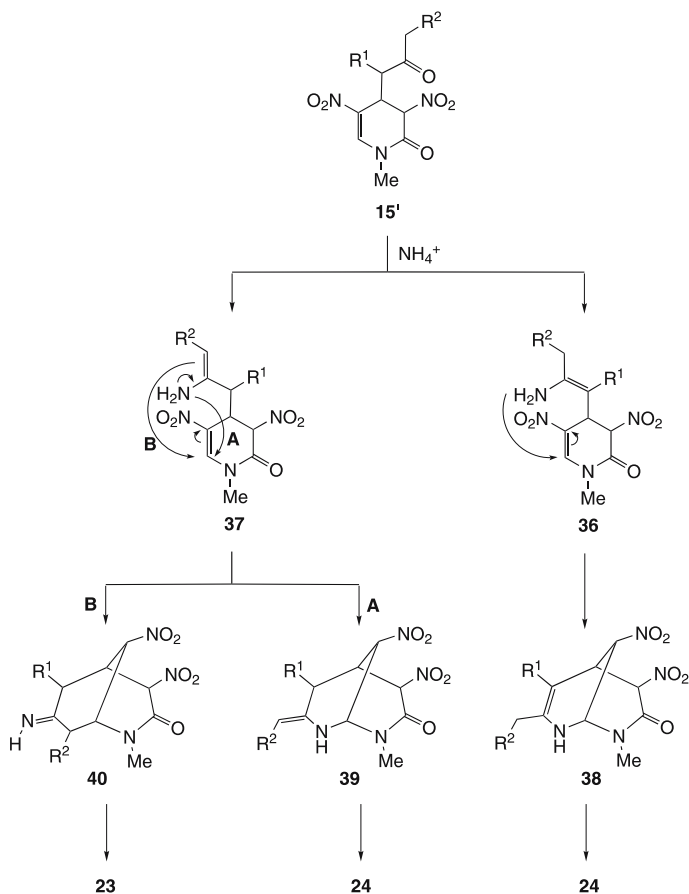
Scheme 15 A mechanism for formation of nitropyridine and nitrophenol

5.3.8
Synthesis of 4-Aminopyridine-3-carboxylates

When pyrimidinone **3** is treated with ethyl 3-oxobutanoate **19a** in the presence of ammonium acetate, a different type of TCRT proceeds, giving ethyl 4-aminopyridine-3-carboxylate **41a** (Table 10) [59]. In this reaction, pyrimidinone **3** behaves as the synthetic equivalent of activated diformylamine **5**, and the amino group at the 4-position is derived from ammonium acetate. Since 3-ethoxycarbonyl-4-pyridone **14a** prepared in Sect. 5.2 is intact under the same conditions, aminopyridine **41a** is not formed via pyridone **14a**. Furthermore, ammonium ion also causes no change on ethyl 3-oxobutanoate **19a**, which indicates enamine is not dinucleophilic reagent in the present reaction. Hence, the keto ester moiety is converted to the enaminone after the addition of **19a** to pyrimidinone **3**.

The keto ester **19** does not require an acetyl group, and it is possible to introduce a methyl or a methoxy group at the 5-position of **41**. Furthermore, β-keto amide and chloropropanone are usable for this TCRT, which enables the synthesis of aminopyridines **41g–i** possessing other functional group than the ester function at the 3-position.

On the basis of the above experimental facts, enaminones **42** are considered to be usable as the dinucleophilic reagents for the RTF reaction leading to 4-aminopyridine-3-carboxylic acid derivatives **41** (Table 11) [60]. Enaminones **42** are readily prepared by only mixing 1,3-dicarbonyl compounds **19** and amines without solvent. When enaminone **42i** derived from ethyl acetoacetate **19a** and propylamine is used, the RTF reaction proceeds to afford ethyl N-propyl-4-aminopyridine-3-carboxylate **41i** in 88% yield. The amino group of **41** is easily modified by changing amine, and pyridine-3-carboxylic

Table 10 TCRT leading to 4-aminopyridine-3-carboxylate
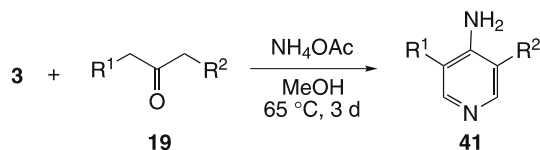
R^1	R^2		Yield/%
COOEt	H	**a**	97
COOMe	Me	**e**	97
COOMe	OMe	**f**	97
$CONH_2$	H	**g**	31
Cl	H	**h**	17

Table 11 RTF reaction using enaminones

R^1	R^2	R^3		Yield/%
COOEt	Pr	H	**i**	88
COOEt	*i*-Pr	H	**j**	79
COOEt	*p*-MeOC$_6$H$_4$	H	**k**	59
COOEt	Pr	Pr	**l**	73
COMe	Pr	H	**m**	28
COPh	Pr	H	**n**	21
COOEt	CH$_2$CH$_2$OH	H	**o**	80
COOEt	CH$_2$CHMeOH	H	**p**	70
COOEt	CHMeCH$_2$OH	H	**q**	82
COOEt	CMe$_2$CH$_2$OH	H	**r**	14

acid esters having an anilino group or a dialkylamino one, **41k** and **41l**, are readily prepared. Synthesis of 3-acylated 4-propylaminopyridines is also performed by use of enaminones **42m** and **42n** derived from β-diketones.

The present reaction is found to be applicable to enaminones **42o–r** derived from amino alcohol, which affords corresponding aminopyridines **41o–r** without observation of any influence of the hydroxy group. While α-branching enaminone **41q** effectively causes the RTF reaction as well as β-branching one **41p**, the reactivity of α,α-bisbranching enaminone **41r** is significantly diminished.

The functionality at the vicinal positions of obtained aminopyridines **41o–r** is useful for synthesis of [*c*]-fused bicyclic pyridines. For example, aminopyridine **41o** undergoes the intramolecular nucleophilic substitution under basic conditions to give bicyclic pyridine **43** in a quantitative yield (Scheme 16).
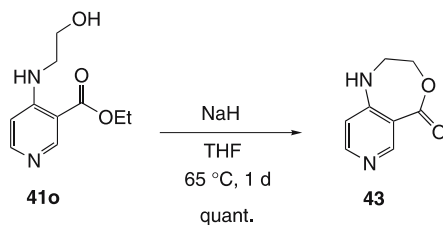
Scheme 16 Synthesis of [*c*]-fused bicyclic pyridine

5.4
Synthesis of Polyfunctionalized 2-Pyridones

All of the RTF reactions mentioned so far involve a combination of dielectrophilic substrates and dinucleophilic reagents, namely dinitropyridone **1** and nitropyrimidinone **3** cause RTF reactions upon treatment with dinucleophilic reagents. Meanwhile, nitropyrimidinones **2** and **3** readily react with primary amines to afford functionalized nitroenamines as shown in Sect. 4. Since the nitroenamines **10** and **11** have both nucleophilic and electrophilic sites, this structural feature is applicable to development of the new type of RTF reaction by use of regents having both electrophilic and a nucleophilic sites.

When cyclic secondary amine, morpholine (X = O), is added to a solution of nitropyrimidinone **3** in ethanol, a white solid immediately precipitates. Although empirical formula of the solid is $C_9H_{14}N_4O_4$, its ^1H NMR spectrum using dimethyl sulfoxide-d_6 as the solvent shows only signals for both starting materials. These experimental facts indicate that pyrimidinone **3** and morpholine forms adduct **44a**, however, it is easily splits into starting materials in the polar dimethyl sulfoxide solution. On the other hand, the adduct of pyrimidinone **3** with piperidine (X = CH$_2$) is soluble in ethanol, and N-iminopiperidine **45** is isolated by column chromatography on silica gel (Scheme 17). Both the C2 – N3 and the C6 – N1 bonds in adduct **44** are easily cleaved as a result of activation by secondary amine since the aromaticity of pyrimidinone **3** is destroyed. In other words, the N3 – C4 – C5 – C6 moiety of pyrimidinone **3** is considered to behave as the synthetic equivalent of
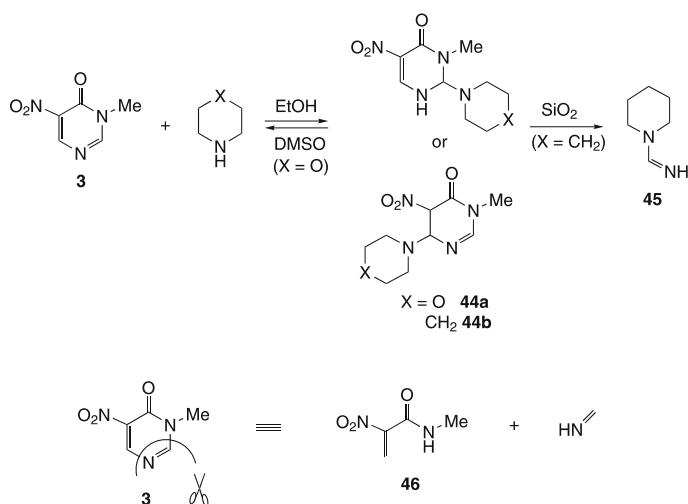
Scheme 17 Reaction of nitropyrimidinone with cyclic secondary amine

N-methyl-α-nitroacrylamide **46**, and the rest part, the N1 – C2 unit, behaves as the donor of an imino group [61].

When pyrimidinone **3** is allowed to react with 1,3-dicarbonyl compounds **19** in the presence of piperidine, polyfunctionalized pyridones **12** are prepared (Table 12) [62]. In the present reaction, β-keto esters **19b** and **19i**, diester **19k** and cyanoacetate **19l** are usable as the reagent to give corresponding pyridones **12**, however β-diketones **19c** and **19j** affords no RTF product, which is due to further decomposition of produced pyridones **12c** and **12j** under the employed conditions.

On the other hand, functionalized enamines **47** are isolated when sodium ethoxide is used as the base, in which a C – N unit of pyrimidinone **3** is transferred to active methylene compounds **19**. The severe conditions using stronger base prevents the isolation of pyridones **12** except for **12k** and **12l** that are stabilized by electron-donating hydroxy or amino groups. In these cases, two molecules of enolates are considered to attack at the 2- and the 6-positions of pyrimidinone **3** to give adduct intermediate **48**. Then, the ring opening reaction of **48** occurs together with elimination of α-methaneimidoyl keto ester **49**, and recyclization of **50** leads to pyridone **12** (Scheme 18). Modified ethyl acetoacetate **49** is converted to more stable enamine **47** by tautomerism.

Since the aminomethylene group is an equivalent of the formyl group, enamines **47** are regarded as the new building block whose central carbon is connected with three different types of carbonyl groups. Especially, enam-

Table 12 Synthesis of polyfunctionalized pyridones

R^1	R^2	R^3		Yield/%[a]		Yield/%[b]	
				12	47	12	47
MeCO	OEt	Me	**a**	67	0	0	70
PhCO	OEt	Ph	**i**	84	0	0	41
MeCO	Me	Me	**c**	0	0	0	38
PhCO	Me	Ph	**j**	0	0	0	12
COOEt	OEt	OH	**k**	31	0	78	41
CN	OEt	NH$_2$	**l**	67	0	70	47

[a] Base: Piperidine; time 24 h
[b] Base NaOEt; time 4 h
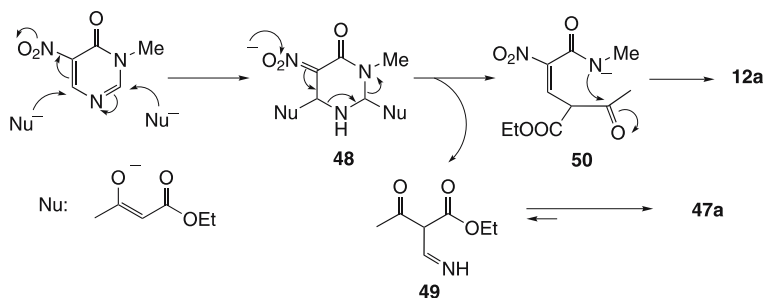
Scheme 18 A plausible mechanism for formation of pyridone and enamine
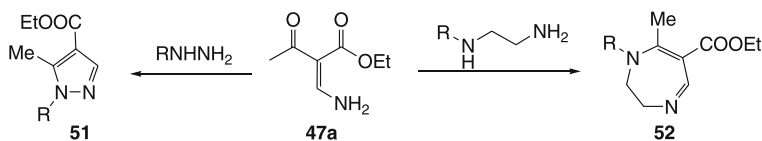
Scheme 19 Synthetic equivalent of tricarbonyl methane

ines derived from keto ester **47a** and **47i** can be employed as the synthetic equivalent of trifunctionalized methanes having a formyl, an acyl and an ethoxycarbonyl groups at the same carbon. Enamines **47** effectively yield various kinds of polyfunctionalized compounds such as pyrazoles **51** and diazepines **52** upon treatment with hydrazines and 1,2-diamines as shown in Scheme 19.

6
Summary

In this review, dinitropyridone **1** and nitropyrimidinone **3** are shown to be excellent substrates for RTF and the TCRT reactions. Dinitropyridone **1** behaves as the synthetic equivalent of nitromalonaldehyde **4** to give nitrated compounds such as nitroanilines **23** and nitropyridines **24**. Nitropyrimidinone **2** is also used as the masked nitromalonaldehyde. Nitropyrimidinone **3** reveals three kinds of reactivity. When the RTF reaction occurs at the 2- and the 6-positions, the C2 – N1 – C6 moiety of **3** is built in the new ring system in which pyrimidinone **3** behaves as the synthetic equivalent of activated diformylamine **5**. The RTF reaction at the 4- and 6-positions is also observed in reactions using ammonium acetate as the nitrogen source. In this case, pyrimidinone **3** behaves as the synthetic equivalent of α-nitroformylacetic acid **29**. Furthermore, pyrimidinone **3** is also usable as the equivalent of
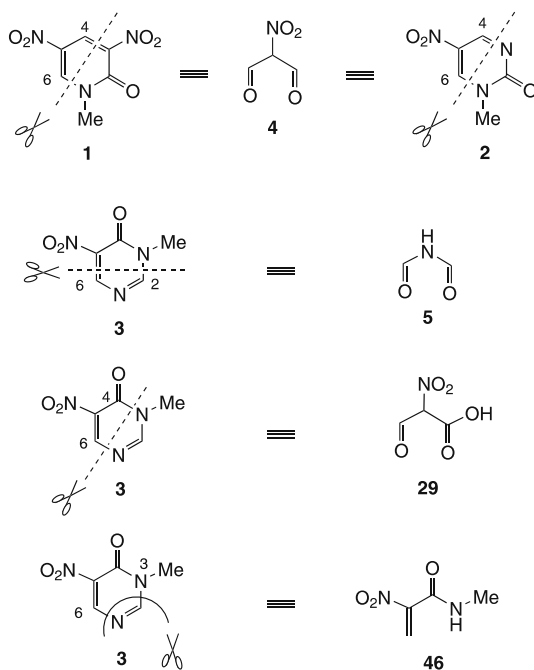
Scheme 20 Versatile reactivity of nitropyrimidinone

N-methyl-*α*-nitroacrylamide **46** to afford polyfunctionalized pyridones **12** in reactions with 1,3-dicarbonyl compounds **19** in the presence of piperidine. As a result, versatile azaheterocyclic compounds can be easily prepared from pyridone **1** and pyrimidinone **3**, and the synthetic utility of the RTF reaction has been considerably improved.

References

 1. Ono N (2001) The nitro group in organic chemistry. Wiley, New York
 2. Feuer H, Nielsen AT (1990) Nitro compounds. Wiley, New York
 3. Perekalin VV, Lipina ES, Berestovitskaya VM, Efremov DA (1994) Niroalkenes. Wiley, New York
 4. Bakke JM (2003) Pure Appl Chem 75:1403
 5. Katritzky AR, Lagowsky JM (1971) Chemistry of the heterocyclic N-oxides. Academic Press, London
 6. Nishiwaki N, Ariga M (2003) J Synth Org Chem Jpn 61:882
 7. Gomorov SP (2000) Heterocycles 53:1607
 8. van der Plas HC (2000) J Heterocycl Chem 37:427
 9. van der Plas HC (1999) Adv Heteocycl Chem, Vol 74. Academic Press, London
10. Nishiwaki N, Nakanishi M, Hida T, Miwa Y, Tamura M, Hori K, Tohda Y, Ariga M (2001) J Org Chem 66:7535

11. Ariga M, Nishiwaki N, Miwa Y, Tani K, Tohda Y (1997) Heterocycles 44:81
12. Nishiwaki N, Nogami T, Kawamura T, Asaka N, Tohda Y, Ariga M (1999) J Org Chem 64:6476
13. Prill EA, McElvain SM (1943) Org Synth Coll Vol 2:419
14. Fox JJ, Praag DV (1960) J Am Chem Soc 82:486
15. Bauer L, Wright GE, Mikrut BA, Bell CL (1965) J Heterocycl Chem 2:447
16. Tohda Y, Ariga M, Kawashima T, Matsumura E (1987) Bull Chem Soc Jpn 60:201
17. Nishiwaki N, Tohda Y, Ariga M (1996) Bull Chem Soc Jpn 69:1997
18. Bourget-Merle L, Lappert MF, Severn JR (2002) Chem Rev 102:3031
19. Dai X, Warren TH (2004) J Am Chem Soc 126:10085
20. Moore DR, Cheng M, Lobkovsky EB, Coates GW (2003) J Am Chem Soc 125:11911
21. Moore DR, Cheng M, Lobkovsky EB, Coates GW (2002) Angew Chem Int Ed 41:2962
22. Shimokawa C, Tachi Y, Nishiwaki N, Ariga M, Itoh S (2006) Bull Chem Soc Jpn 79:118
23. Yokota S, Tachi Y, Nishiwaki N, Ariga M, Itoh S (2001) Inorg Chem 40:5316
24. Shimokawa C, Yokota S, Tachi Y, Nishiwaki N, Ariga M, Itoh S (2003) Inorg Chem 42:8395
25. Nishiwaki N, Ogihara T, Takami T, Tamura M, Ariga M (2004) J Org Chem 69:8382
26. Nishiwaki N, Ogihara T, Tamura M, Asaka N, Hori K, Tohda Y, Ariga M (2002) Heterocycles 57:2170
27. Nakaike Y, Kamijo Y, Mori S, Tamura M, Nishiwaki N, Ariga M (2005) J Org Chem 70:10169
28. Nishiwaki N, Mizukawa Y, Terai R, Tohda Y, Ariga M (2000) Arkivoc ii:103
29. Nishiwaki N, Mizukawa Y, Ohta M, Terai R, Tohda Y, Ariga M (1996) Heterocycl Commun 2:21
30. Rajappa S (1999) Tetrahedron 55:7065
31. Rajappa S (1981) Tetrahedron 37:1453
32. Fanta PE, Stein RA (1960) Chem Rev 60:261
33. Fanta PE (1963) Org Synth Coll Vol 4:844
34. Nishiwaki N, Tamura M, Hori K, Tohda Y, Ariga M (2003) Molecule 8:500
35. Kashima C, Arao H, Hibi S, Omote Y (1989) Tetrahedron Lett 30:1561
36. Allenstein E, Sille F (1979) Chem Ber 111:921
37. Fltsch W, Hampel K, Hohenhorst M (1990) Liebigs Ann Chem p 397
38. Fltsch W, Hampel K, Hohenhorst M (1987) Tetrahedron Lett 28:4395
39. Matsumura E, Ariga M, Tohda Y (1979) Bull Chem Soc Jpn 52:2413
40. Nishiwaki N, Tohda Y, Ariga M (1997) Synthesis, p 1277
41. Matsumura E, Tohda Y, Ariga M (1982) Bull Chem Soc Jpn 55:2174
42. Tohda Y, Kawahara T, Eiraku M, Tani K, Nishiwaki N, Ariga M (1994) Bull Chem Soc Jpn 67:2176
43. Tohda Y, Eiraku M, Nakagawa T, Usami Y, Ariga M, Kawashima T, Tani K, Watanabe H, Mori Y (1990) Bull Chem Soc Jpn 63:2820
44. Nishiwaki N, Adachi T, Matsuo K, Wang H-P, Matsunaga T, Tohda Y, Ariga M (2000) J Chem Soc Perkin Trans 1, p 27
45. Nishiwaki N, Matsunaga T, Tohda Y, Ariga M (1994) Heterocycles 38:249
46. Brown DJ, Evans RF, Cowden WB, Fenn MD (1994) The chemistry of heterocyclic compounds, vol 52. Wiley, New York
47. Nishiwaki N, Wang H-P, Matsuo K, Tohda Y, Ariga M (1997) J Chem Soc Perkin Trans 1, p 2261
48. Hutter D, Benner SA (2003) J Org Chem 68:9839
49. Konakahara T, Ogawa R, Tamura S, Kakehi A, Sakai N (2001) Heterocycles 55:1737

50. Stadlbauer W, Fiala W, Fischer M, Hojas G (2000) J Heterocycl Chem 37:1253
51. Grag R, Gupta SP, Gao H, Babu MS, Debnath AK, Hansch C (1999) Chem Rev 99:3525
52. Olejniczak ET, Hajduk PJ, Marcotte PA, Nettesheim DG, Meadows RP, Edalji R, Holzman TF, Fesik SW (1997) J Am Chem Soc 119:5828
53. Pomel V, Rovera JC, Godard A, Marsais F, Queguiner G (1996) J Heterocycl Chem 33:1995
54. Nishiwaki N, Yamashita K, Azuma M, Adachi T, Tamura M, Ariga M (2004) Synthesis, p 1996
55. Thyagarajan BS, Gopalakrishnann PV (1964) Tetrahedron 20:1051
56. Ariga M, Matsumura E (1987) Bull Chem Soc Jpn 60:1198
57. Nishiwaki N, Ohtomo H, Tamura M, Hori K, Tohda Y, Ariga M (2001) Heterocycles 55:1581
58. Nishiwaki N, Tatsumichi H, Tamura M, Ariga M (2006) Lett Org Chem 3:629
59. Nishiwaki N, Azuma M, Tamura M, Hori K, Tohda Y, Ariga M (2002) Chem Commun, p 2170
60. Nishiwaki N, Nishimoto T, Tamura M, Ariga M (2006) Synlett, p 1437
61. Nishiwaki N, Morimura H, Matsushima K, Tamura M, Ariga M (2003) Heterocycles 61:19
62. Nishiwaki N, Matsushima K, Chatani M, Tamura M, Ariga M (2004) Synlett, p 703

Synthesis of Thalidomide

Norio Shibata (✉) · Takeshi Yamamoto · Takeshi Toru (✉)

Graduate School of Engineering, Nagoya Institute of Technology, Gokiso,
Showa-ku, 466-8555 Nagoya, Japan
nozshiba@nitech.ac.jp, toru@nitech.ac.jp

Abstract Despite the most notorious medical disaster caused by thalidomide in medical history, huge numbers of papers have been published about this drug since its formulation in 1956. While most of the early studies specifically concerned teratogenicity, recently there has been a resurgence of interest in thalidomide because of its potential for treating a number of otherwise intractable diseases, such as leprosy, human immunodeficiency virus replication in acquired immune deficiency syndrome, and cancer. Although the pharmacological aspects of the drug have been frequently reviewed, reviews focusing on thalidomide synthesis are rare. Here, the synthesis of thalidomide is reviewed in chronological order from the first report. We first aim to give an overview of the most conventional aspects of thalidomide. Subsequently, we will focus on the synthesis of racemic thalidomide, which is now commercially available. Finally, we will describe the asymmetric synthesis of thalidomide. To our knowledge, all the papers and patents concerning thalidomide synthesis have been introduced. Because of the number of papers and patents, we will not mention the preparation of thalidomide derivatives.

Keywords Asymmetric synthesis · Drug synthesis · Teratogenicity · Thalidomide

Abbreviations
CAN   Ceric ammonium nitrate
CDI N,N'-Carbonyldiimidazole
DCC N,N'-Dicyclohexylcarbodiimide
DIC N,N'-Diisopropylcarbodiimide
DMAP   4-(Dimethylamino)pyridine
DMF N,N-Dimethylformamide
DMSO   Dimethyl sulfoxide
EDC   1-Ethyl-3-(3-dimethylaminopropyl)carbodiimide
HMDS   Hexamethyldisilazane
HOBT   1-Hydroxybenzotriazole
MS-4 Å   Molecular sieves 4 Å

m.w.   Microwave
NMM   *N*-Methylmorpholine
PMB   *p*-Methoxybenzyl
PyBOP   Benzotriazole-1-yl-oxy-tris-pyrrolidino-phosphonium hexafluorophosphate
TFA   Trifluoroacetic acid
THF   Tetrahydrofuran
TIS   Triisopropylsilane

1
Introduction

Thalidomide [1–14] ((*N*-phthalimido)glutarimide, **1**) (Fig. 1) is conceivably
the most notorious drug in pharmaceutical history, with more than 7000 pa-
pers having been published so far. Thalidomide (**1**) was first marketed in West
Germany by Chemie Grunenthal GmbH as a clinically effective and extremely
safe non-barbiturate sedative hypnotic in 1956. It became a popular drug in
Europe, Canada, and Japan with a variety of names: Contergan®, Distaval®,
and Isomin®, for example. In 1961, Lenz and McBride independently realized
the unexpected potent teratogenicity of thalidomide (**1**) [15, 16]. The terato-
genic side effects, leading to birth defects such as limb reduction, produced
one of the most notorious medical disasters of modern medical history and
thalidomide (**1**) was consequently withdrawn from the market in 1962. How-
ever, the unique and broad physiological effects of thalidomide (**1**) have been
gradually revealed in succession with the discovery of its effectiveness toward
leprosy in 1965 [17]. It prompted recent reevaluation of its medical applica-
tions. Thus, thalidomide (**1**) was approved in the USA for the treatment of
a painful inflammation associated with leprosy in 1997.

The increasing interest in thalidomide (**1**) during the last decade is clearly
represented by the number of hits in the scientific literature dealing with
the word "thalidomide" under SciFinder® search. It is worth mentioning that
most of the documents were published in the last 10 years (Fig. 2). Most of
them concerned the biological, physiological, and clinical aspects of thalido-
mide (**1**) and they are now systematically well summarized [1–14]. However,
review of the synthetic side of thalidomide (**1**) is still rare. In this review, we
focus on the synthesis of racemic thalidomide (**1**), which is now commercially

1
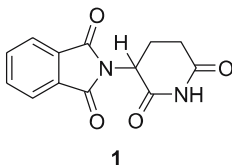
Fig. 1 Structure of thalidomide
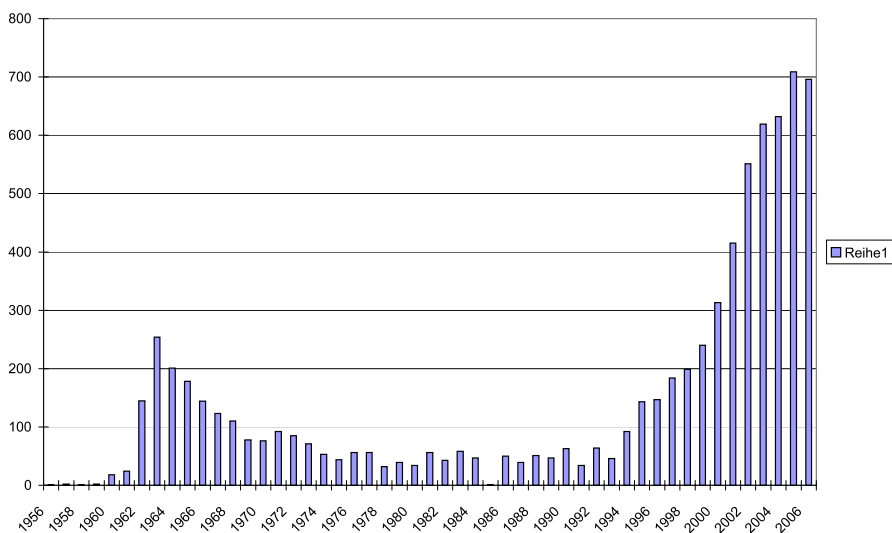
Fig. 2 Number of scientific documents on thalidomide

available. Next, we describe the asymmetric synthesis of thalidomide (**1**). To our knowledge, all the papers and patents concerning thalidomide (**1**) synthesis have been introduced. Because of the volume of papers and patents, we do not mention the preparation of thalidomide derivatives.

2
Synthesis of Thalidomide

On May 17, 1954, thalidomide was disclosed for the first time by the Chemie Grunenthal GmbH in Germany [18]. The preparation consists of three simple steps involving a reaction of glutamic acid with phthalic anhydride, followed by ring closure. Namely, *N*-phthaloyl glutamic acid, prepared from glutamic acid and phthalic anhydride in refluxing pyridine, was treated with acetic anhydride to give *N*-phthaloyl glutamic acid anhydride (**2**). This was melted with urea at 170–180 °C for 20 min to produce thalidomide (**1**) (Scheme 1).
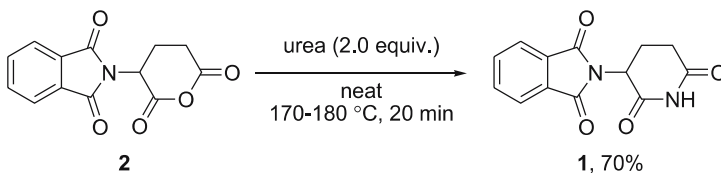
Scheme 1 First synthesis of thalidomide (**1**) in Chemie Grunenthal GMBH [18]

Dry gaseous ammonia can replace urea at the final high-temperature melt re-
action. The reaction product requires multiple recrystallizations from 95%
ethanol to furnish pure thalidomide (1) on a large scale.

Subsequent to this work, chemists at Dainippon Pharmaceutical Com-
pany in Japan focused on developing an alternative way to thalidomide (1)
(Scheme 2) [19, 20] that comprises the reaction of alpha-aminoglutarimide
(3) with phthalic anhydride (4) in refluxing pyridine for 1 h. They also
patented an additional sequence to thalidomide (1) that contains a Gabriel-
type substitution reaction of bromoglutarimide (6) prepared from piperidine-
2,6-dione (5), with potassium phthalimide (7) in N,N-dimethylformamide
(DMF) with heat. While the original Grunenthal route constructs the glu-
tarimide ring later on in the synthesis, the Japanese method cyclizes the ring
in the first stage of the preparation. Not surprisingly, the Grunenthal patent
described a route in which the bromoglutarimide (6) or aminoglutarimide (3)
was not involved.

These classical syntheses remained the available approaches for a long
time, despite the huge number of clinical studies on thalidomide in the last
third of the twentieth century. After a dormant period of more than 30 years,
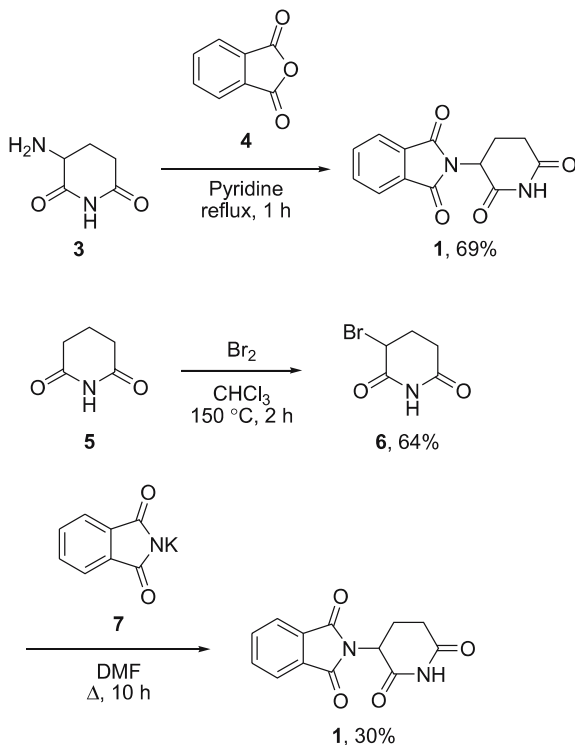
Scheme 2 Synthesis of thalidomide (1) in Dainippon Pharmaceutical Company [19, 20]

interest in the chemistry of thalidomide (**1**) revived, and in the late 1990s several groups succeeded in assembling this molecule in different ways, using advanced techniques for organic synthesis, microwave reaction, and solid-phase synthesis, for example.

In 1999, Muller et al. from Celgene Corporation reported a further improvement of the classical Grunenthal scheme that now allows commercial synthesis of thalidomide (**1**) [21–24]. The last step in the Grunenthal synthesis involves a high-temperature melt reaction that affords crude thalidomide (**1**) requiring multiple recrystallization. While the original synthesis begins with L-glutamic acid (**8**), crucial to the Celgene development is the finding that thalidomide (**1**) is prepared from L-glutamine (**11**) in only two steps in very high yield without requiring a purification sequence on the multigram scale. Namely, treatment of L-glutamine (**11**) with N-carbethoxyphthalimide (**10**) in water in the presence of Na_2CO_3 at room temperature produces N-phthaloyl-L-glutamine (**12**). Cyclization of N-phthaloyl-L-glutamine (**12**) to afford thalidomide (**1**) is accomplished by treatment with N,N'-carbonyldiimidazole (CDI) in the presence of a catalytic amount of 4-(dimethylamino)pyridine (DMAP) in tetrahydrofuran (THF) at reflux conditions (Scheme 3). Although enantiomerically pure L-glutamine (**11**) is the starting material, racemization occurs in this step. THF is a suitable solvent because of the low solubility of thalidomide (**1**) and the high solubility of the by-product, which provides an easy way for purification of the product. The procedure can easily be used to prepare thalidomide (**1**) in a 100-g scale in the laboratory, and it was successfully scaled up to the multikilogram scale in a pilot plant.

The microwave technique was introduced during the past decade in organic synthesis and has proved to be highly effective to promote many organic reactions [25–33]. Since the final step of the original thalidomide preparation requires the formation of the glutarimide ring with urea at very high temperature, the microwave irradiation strategy should be considered for improvement of the step. A Spanish group realized the idea of microwave-promoted synthesis of thalidomide (**1**) [34, 35]. The formation of the glutarimide ring was carried out in 63% yield by microwave irradiation of N-phthaloyl-L-glutamic acid (**9**) for 10 min in the presence of urea. The yield was improved to 85% under microwave irradiation for 15 min using thiourea instead of urea (Scheme 4). It is interesting to note that thalidomide (**1**) was also obtained in a one-pot procedure from L-glutamic acid (**8**), phthalic anhydride (**4**), and thiourea by microwave-induced double cyclocondensation in a 1000-W domestic microwave oven, although thalidomide (**1**) mixed with pyroglutamic acid was obtained in very low yield when the microwave reaction was performed using urea as a nitrogen donor for the formation of the glutarimide ring. The multimode microwave irradiation using thiourea takes advantage of the rapid, one-pot reaction and does not require a high-temperature melt reaction, although an application of this laboratory-scale
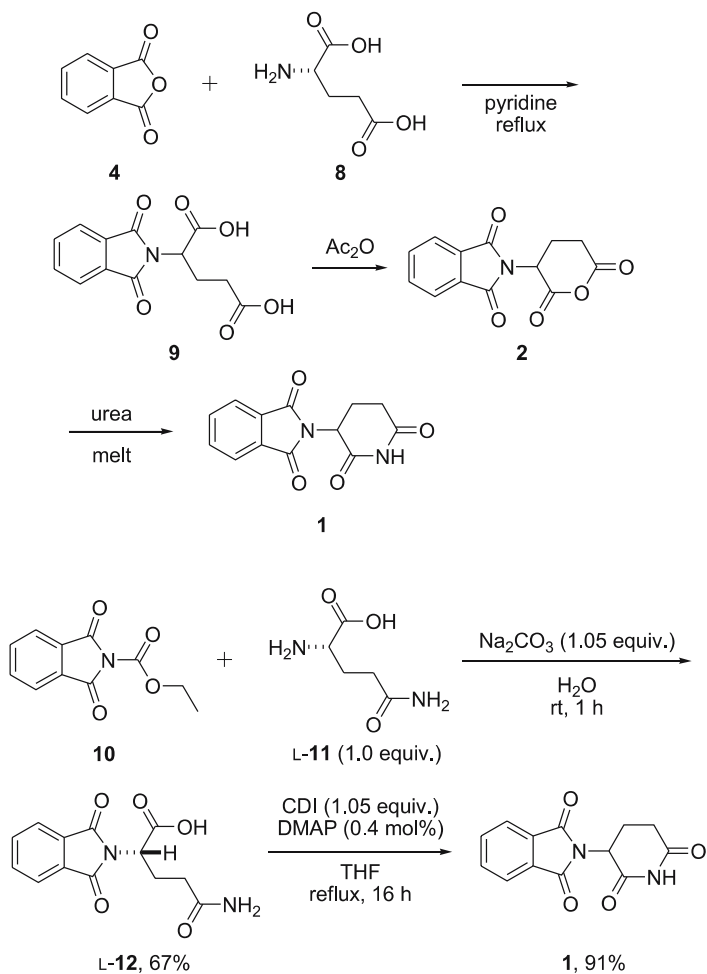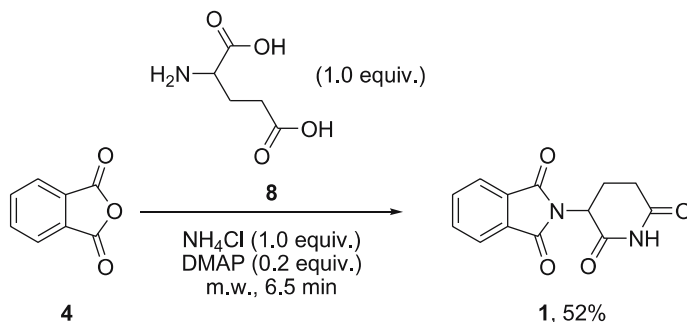
Scheme 3 Commercial synthesis of thalidomide (**1**) [21–24]
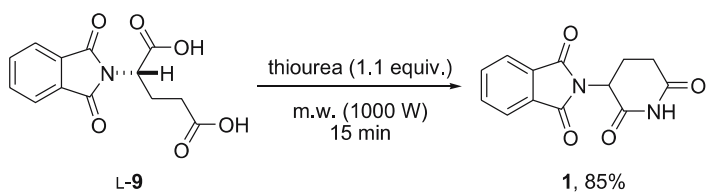
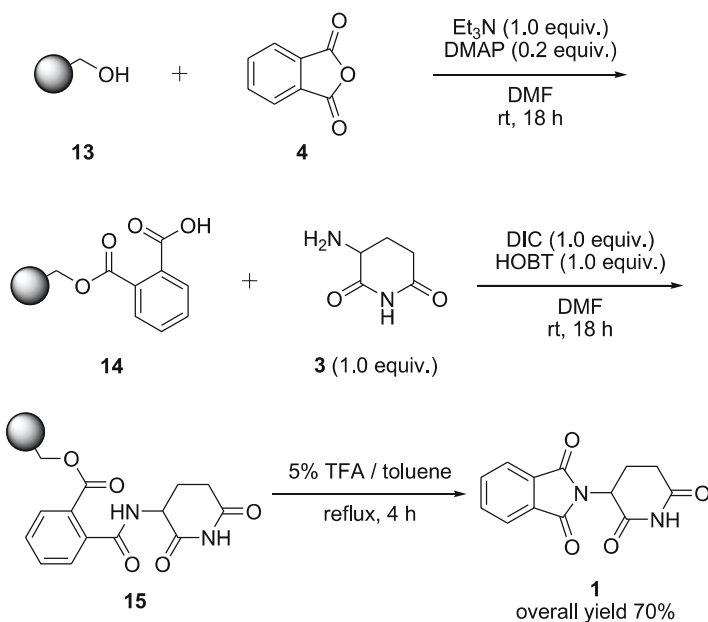**Scheme 4** Microwave synthesis of thalidomide (**1**) by Spanish group [34, 35]

reaction to the plant scale would be difficult to consider. An additional benefit of this procedure is that L-glutamic acid (**8**) is five times cheaper than L-glutamine (**11**).

Hijji and Benjamin also accomplished a microwave synthesis of thalidomide in acceptable yield in 2004 (Scheme 5) [36–39]. Ammonium chloride was found to be an effective source for nitrogen. Namely, phthalic anhydride (**4**), glutamic acid (**8**), and ammonium chloride were mixed in 1 : 1 : 1 ratio with a catalytic amount of DMAP and heated in a conventional microwave oven for 6.5 min. The mixture melted to a brown liquid. The heating continued for an additional 1 min to give thalidomide (**1**) in 52% yield in this two-step, one-pot reaction after solubilization, precipitation, and recrystallization.

Scheme 5 One-pot microwave synthesis of thalidomide (**1**) [36–39]

Combinatorial chemistry is an important new technology throughout the pharmaceutical and biochemical industries [40–53]. It results in reducing the time and costs involved in finding effective novel drugs. Furthermore, the biological assay of the combinatorial library provides the generation of pharmacophores of the lead compounds when it combines with a recent 3D quantitative structure–activity relationship (QSAR) technique [54–63]. An interesting approach toward the combinatorial library of thalidomide analogues, which is needed to generate an active antiangiogenic pharmacophore of thalidomide, was developed by Xiao et al. from the USA that centers upon the solid-phase synthesis of thalidomide (**1**) and its derivatives (Scheme 6) [64]. The method involves a straightforward three-step sequence starting from a resin-linked acid prepared from the coupling of hydroxymethyl polystyrene (**13**) with phthalic anhydride (**4**) in the presence of triethylamine and DMAP in DMF. The acid was then reacted with α-aminoglutarimide (**3**) in the presence of *N*,*N'*-diisopropylcarbodiimide (DIC) and 1-hydroxybenzotriazole (HOBT) followed by trifluoroacetic acid (TFA) treatment in toluene to form thalidomide (**1**) with an overall yield of 70%. The analogues were also synthesized with high yields. Purity was high enough for biological testing without further purification. The method can be extended to the synthesis of a combinatorial library of thalidomide analogues, which is needed to generate an active pharmacophore of thalidomide.

Scheme 6 Solid-phase synthesis of thalidomide (**1**) [64]

Chang et al. from Taiwan developed a series of thalidomide syntheses in 2002 to 2003 [65–67]. Unique in their approaches for the glutarimide ring construction of thalidomide (**1**) is a formal [3 + 3] cycloaddition strategy between α-toluenesulfonyl acetamide and unsaturated esters followed by desulfonylation and deprotection reactions. The method can avoid the high-temperature melt reaction required in the classical reaction. The total yield of thalidomide (**1**) was 18% in five steps from acrylate **16** (Scheme 7) and 30% in three steps from 2-phthalimidoacrylic acid methyl ester (**21**) (Scheme 8). For example, the formal [3 + 3] cycloaddition reaction of α,β-unsaturated ester, which was prepared from methyl propiolate and phthalimide, with the dianion intermediate obtained from *p*-methoxybenzyl (PMB)-α-toluenesulfonyl acetamide (**17**) and 2.2 equiv. sodium hydride produced the 5-phthalimide α-sulfonyl glutarimide derivative **20** in 58% yield. Treatment of **20** with 6% sodium amalgam and sodium phosphate in methanol produced crude PMB thalidomide, which was treated with ceric ammonium nitrate (CAN) in MeCN/H$_2$O to give thalidomide (**1**). A solid-phase approach was also applied in this strategy, treating an easily accessible polymer-supported **23** with α,β-unsaturated esters **24** (Scheme 9). The method may allow the rapid synthesis of thalidomide (**1**) and its derivatives.

Greig et al. from the USA claimed an improved method of preparation of thalidomide (**1**) (Scheme 10) [68]. Namely, thalidomide (**1**) was prepared in three steps (45, 99, 54%) starting from *N*-(*tert*-butoxycarbonyl)-L-glutamine
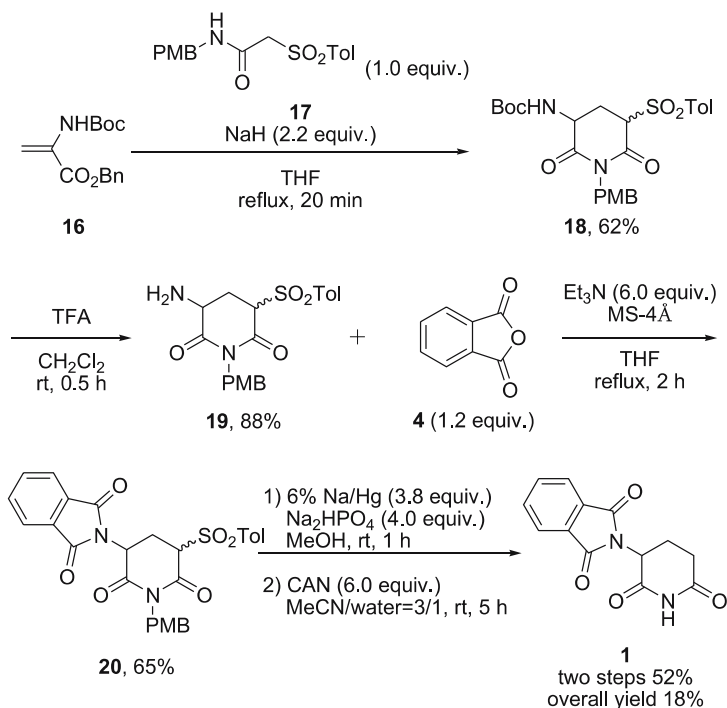
Scheme 7 Construction of thalidomide (**1**) via a formal [3 + 3] cycloaddition strategy from acrylate **16** [65]
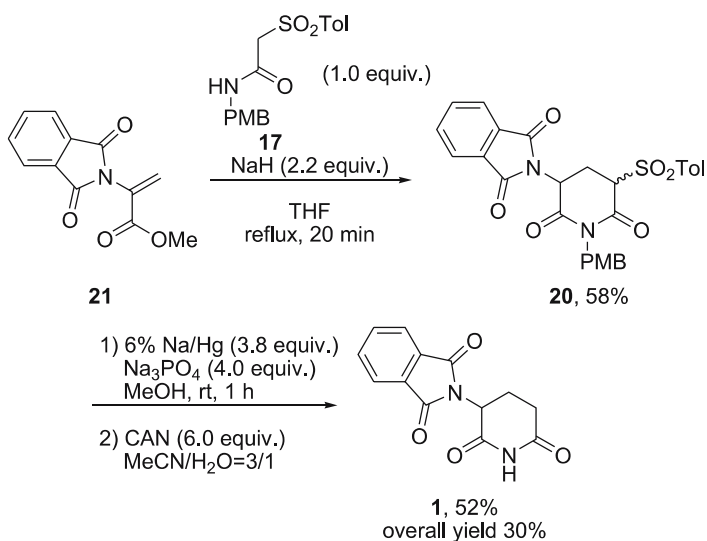
Scheme 8 Construction of thalidomide (**1**) via a formal [3 + 3] cycloaddition strategy from phthalimidoacrylate **21** [67]
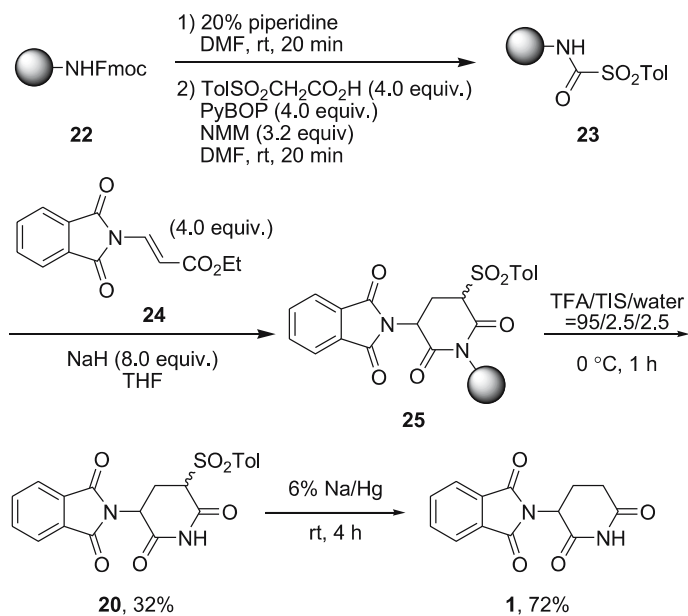
Scheme 9 Polymer-supported construction of thalidomide (**1**) via a formal [3 + 3] cycloaddition strategy [66]
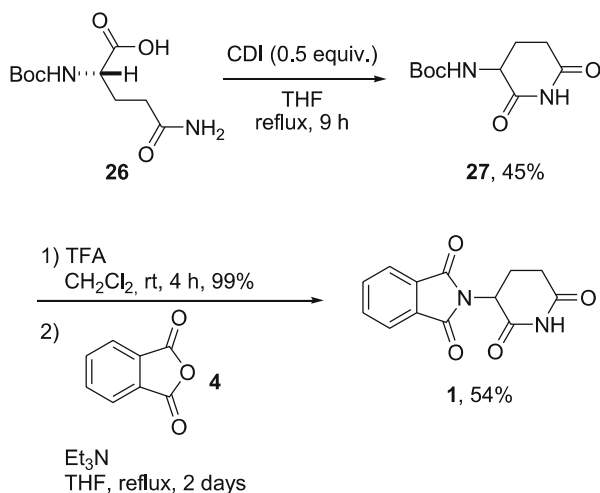
Scheme 10 Synthesis of Thalidomide (**1**) by Greig et al. [68]

(**26**) and involving intermediates 2,6-dioxo-3-(*tert*-butoxycarbonylamino)-piperidine (**27**) and 2,6-dioxo-3-aminopiperidine trifluoroacetate.

In 2003, a Chinese group reported a one-pot synthesis of thalidomide (**1**) in 24.1% yield by allowing phthalic anhydride (**4**) to be reacted with glu-

tamine (**11**) at $120 \pm 10\,°C$ for 40 min and $200 \pm 10\,°C$ for 2 h (Scheme 11). The authors commented that this method is more direct and convenient compared with traditional methods for thalidomide (**1**) synthesis [69].
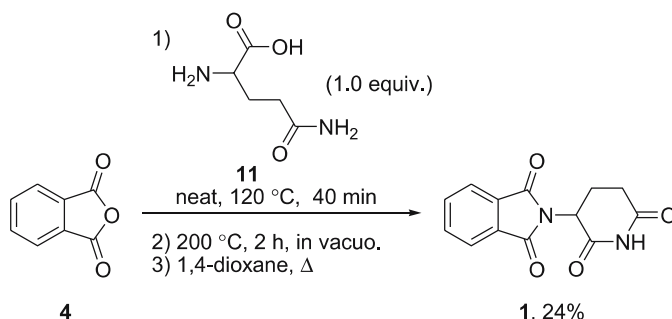
Scheme 11 One-pot synthesis of thalidomide (**1**) by Chinese group [69]

The method was again slightly modified by Zhang et al. in 2005 (Scheme 12) [70]. Thus, 1.48 g phthalic anhydride (**4**) was mixed with 1.40 g glutamine (**11**) in 5 mL water/5 mL triethylamine mixture to give a salt, which was refluxed with 3.56 g CDI in 15 mL THF for 14 h to give 1.82 g thalidomide (**1**).
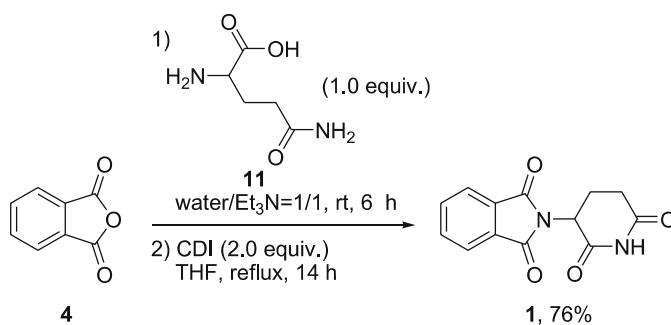
Scheme 12 Modified synthesis of thalidomide (**1**) [70]

Yuan et al. reported a one-step synthesis of thalidomide (**1**) by heating A mixture of phthalic anhydride (**4**) and L-glutamine (**11**) in vacuum. The method afforded thalidomide (**1**) directly with moderate yield (Scheme 13) [71].

Chemists in Italy investigated a process for the one-pot synthesis of thalidomide (**1**) directly from glutamine (**11**) using a variety of phthaloylating agents and condensing agents [72]. The method comprises reaction between glutamine (**11**) and a phthaloylating agent to give N-phthaloylglutamine (**12**), which is not isolated, but which is directly transformed into thalidomide (**1**) by the action of a condensing agent. The process is characterized by the
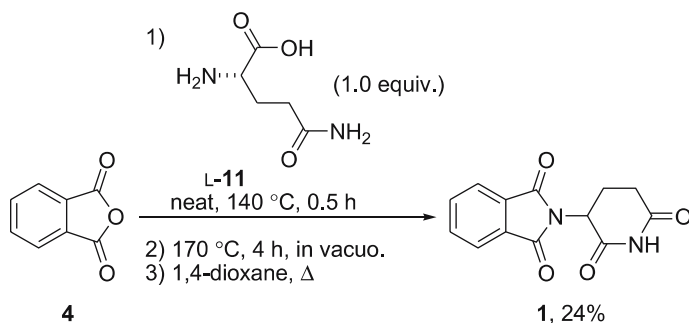
Scheme 13 One-pot synthesis of thalidomide (**1**) by Yuan et al. [71]

use of polar aprotic solvents other than THF, specifically pyridine. For instance, a mixture of L-glutamine (**11**) and phthalic anhydride (**4**) in pyridine was gradually heated to 80–85 °C, held at that temperature for 6 h, and then cooled to 40 °C. Next, CDI was added in portions under stirring for 2 h, followed by concentration, cooling, dilution with ethanol, addition of HCl to pH 7.0, warming to room temperature, and filtration. Thalidomide (**1**) was obtained in 60% yield based on L-**11**. When the reaction of L-glutamine (**11**) was carried out using dimethyl phthalate (**28**) in dimethyl acetamide instead of phthalic anhydride (**4**) in pyridine, the yield was slightly improved to 72% (Scheme 14).
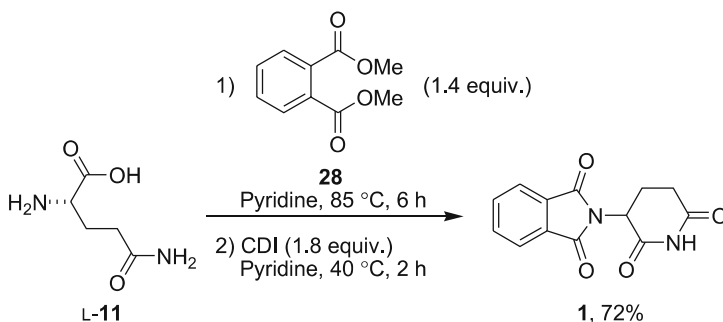
Scheme 14 One-pot synthesis of thalidomide (**1**) using dimethyl phthalate (**28**) [72]

The Celgene report of the practical synthesis of thalidomide (**1**) in 1999 has rekindled the synthetic interest in thalidomide (**1**) and a variety of methods have been documented as described. These synthetic procedures are straightforward transformations, and thus there seems to be no room for any improvement in the synthesis of thalidomide (**1**); however, a practical short synthesis using NaNH$_2$/liq. NH$_3$ methodology appeared as an alternative to the previous syntheses in 2005. Since most of the reported syntheses leave as

the final step the formation of the glutarimide ring, Varala and Adapa, in the Indian Institute of Chemical Technology, developed a novel protocol for the formation of the glutarimide ring from glutamic acid diesters by using the NaNH$_2$/liq. NH$_3$/Fe(NO$_3$)$_3$ methodology (Scheme 15) [73]. They initially attempted the cyclization of *N*-phthaloyl L-glutamic acid dimethyl ester (**29**) by using the NaNH$_2$/liq. NH$_3$/Fe(NO$_3$)$_3$; thalidomide (**1**) was obtained in a low yield (1.14 g, 45%). The low yield was probably due to the lability of the
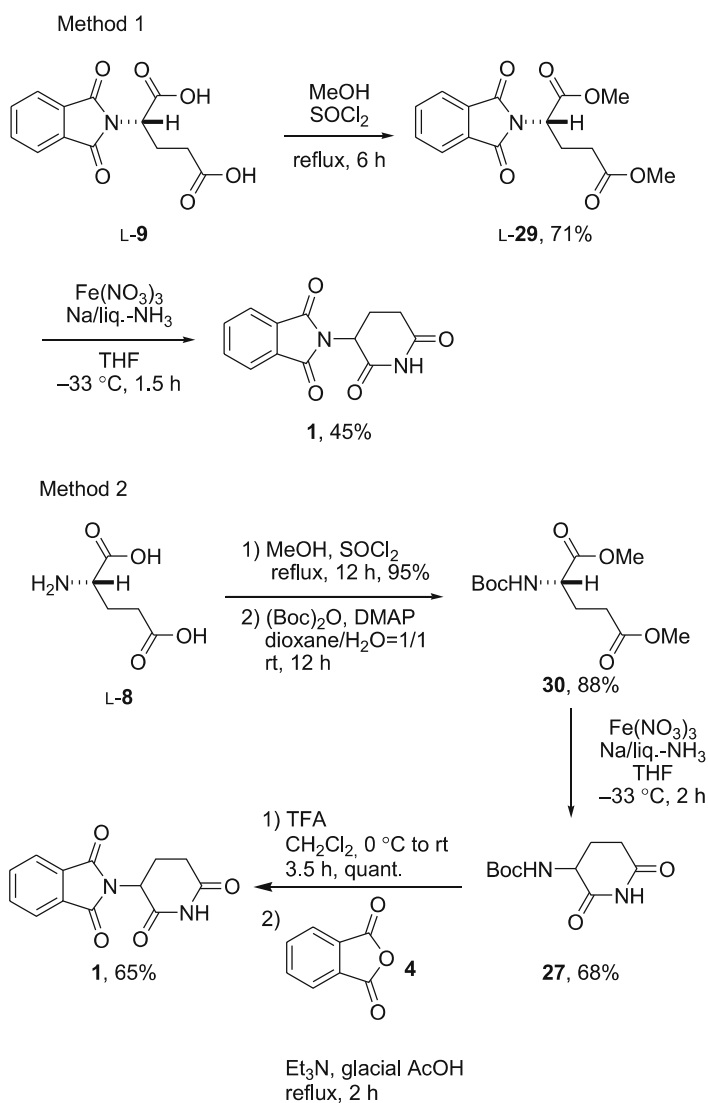
Scheme 15 Synthesis of thalidomide (**1**) via Na/Liquid NH$_3$ methodology [73]

phthalimide ring under these conditions; the starting material was changed to *tert*-butoxycarbonyl L-glutamic acid dimethyl ester (**30**). The ester **30** was treated with Na/liq. NH$_3$ at − 33 °C in THF to afford the glutarimide **27** in 2 h (68%). This imide **27** was then treated with TFA in CH$_2$Cl$_2$ in 3.5 h to remove the protective group and generate the corresponding aminoglutarimide trifluoroacetate in quantitative yield. Without further purification, this compound then was reacted with phthalic anhydride (**4**) in refluxing glacial acetic acid in the presence of triethylamine to furnish thalidomide (**1**) in 65% yield. Glacial acetic acid as solvent was found to be quite important in the condensation step.

3
Asymmetric Synthesis of Thalidomide

The question is whether thalidomide (**1**) is stereospecifically teratogenic. The recent revival of thalidomide in the clinical field has activated again an investigation of the molecular mechanism of the teratogenicity of thalidomide (**1**) and its analogues. Thalidomide (**1**) possesses an asymmetric center in the phthalimide ring. Since thalidomide was marketed as a racemate, it was conceivable that sedative effects might be associated with one enantiomer and the unexpected teratogenic side effects might be ascribed to the other enantiomer. Twenty years after the thalidomide disaster, only (*S*)-thalidomide (**1**) was proved to be teratogenic [74]. It was then concluded that the disaster could have been avoided if only the (*R*)-isomer had been marketed. However, it is presently unclear whether any of the actions of racemic thalidomide (**1**) can be separated out using a pure enantiomer. According to the reports, considerable chiral inversion took place after incubation of enantiomerically pure thalidomide (**1**) in aqueous media and it was catalyzed by serum albumin [75–78]. The strongly acidic hydrogen atom at the asymmetric center of thalidomide (**1**) rapidly epimerizes under physiological conditions (Fig. 3), rendering bioassay of the enantiomers difficult. Therefore, elucidation of the difference of biological activities between thalidomide enantiomers previously reported is said to be difficult. However, enantioselective inhibition of TNF-α release by thalidomide (**1**) has still been reported recently [79].
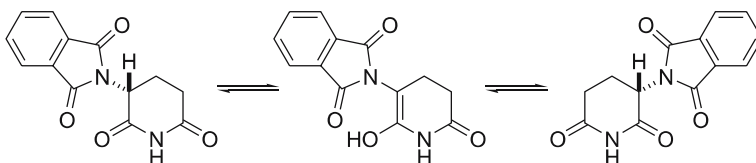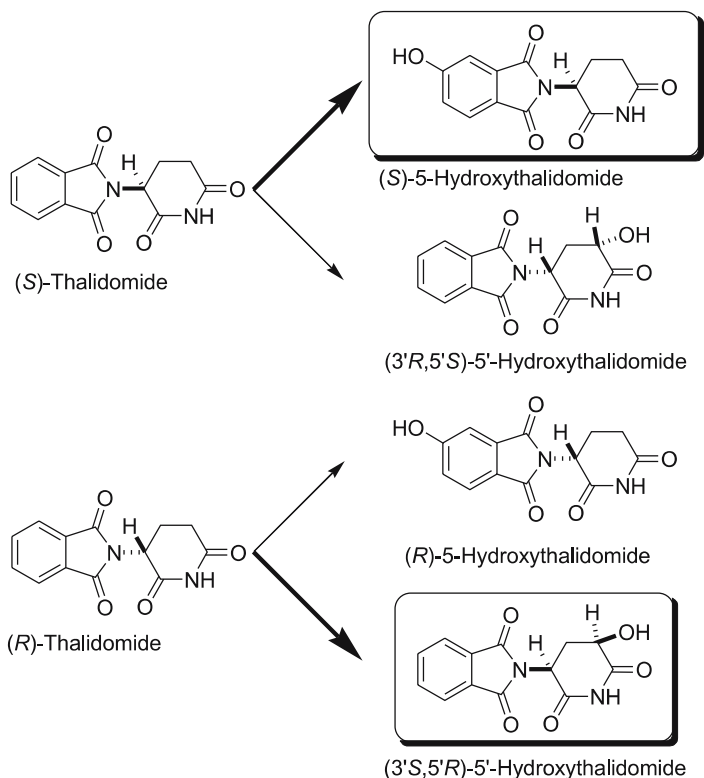

Fig. 3 Racemization of thalidomide (**1**)

The enantioselective metabolism of optically active thalidomide (**1**) has recently been intensively investigated (Scheme 16) [80]. While the (*S*)-isomer is found to be metabolized preferentially by hydroxylation of the phthaloyl ring, the (*R*)-isomer undergoes metabolic hydroxylation in the dioxopiperidine ring. Although it is impossible to find the relationship between the teratogenicity and enantioselective metabolism of thalidomide (**1**), the application of racemic thalidomide (**1**) in therapy is clearly controversial [81–84].

Scheme 16 The enantioselective metabolism of optically active thalidomide (**1**) [80]

As mentioned in the previous section, the synthesis of thalidomide (**1**) substantially consists of the cyclization of two imide rings. The glutarimide ring can be formed before the introduction of the phthalimido group; however, in most of the methods for the synthesis of racemic thalidomide (**1**) starting from glutamic acid (**8**) or glutamine (**11**), the final step is the formation of the glutarimide ring by a high-temperature melt reaction, a microwave-assisted reaction, or a *N*,*N*′-dicyclohexylcarbodiimide (DCC)-mediated peptide coupling reaction. Prior to the development of *N*-ethoxycarbonylphthalimide (**10**) for a phthaloylating reagent of amino acids, the preparation of optically ac-

tive *N*-phthaloylglutamic acid (**9**) was usually accompanied by racemization. Therefore, the problem is now in the formation of the glutarimide ring in the final step. Even when optically active L-glutamic acid (**8**) or L-glutamine (**11**) was employed for (*S*)-thalidomide (**1**) synthesis, racemization actually occurred during the formation of the glutarimide ring.

In 1964, in order to compare the pharmacological behavior of both antipodes of thalidomide (**1**), Casini and Ferappi in Italy examined the preparation of (*S*)-thalidomide (**1**) from *N*-phthaloyl-L-glutamine (**12**) for the first time [85]. Namely, treatment of *N*-phthaloyl-L-glutamine (**12**) with one equivalent of thionyl chloride, pyridine, and then triethylamine in dichloromethane at – 30 °C gave (*S*)-thalidomide (**1**), $[\alpha]_D^{20}$ – 62° (Scheme 17). Although the reported method was straightforward, it was devoid of many synthetic details.
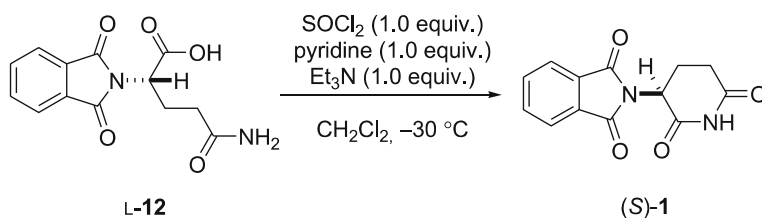
Scheme 17 Synthesis of (*S*)-thalidomide (**1**) from *N*-phthaloyl-L-glutamine (**12**) [85]

In 1965, Opliger et al. in the UK independently investigated the synthesis of optically pure thalidomide (**1**) [86, 87]. They first carefully examined the glutarimide ring formation from *N*-phthaloyl-L-glutamine (**12**) under a strategy similar to that of Casini and Ferappi, and found the methods are rather unreliable for avoiding racemization (Scheme 18). The active ester method was next examined by utilizing the cyanomethyl ester of *N*-phthaloyl-L-glutamine (**31**). As they expected, the cyanomethyl ester was rapidly cyclized at room temperature in dimethyl sulfoxide (DMSO) in the presence of one equivalent of sodium methoxide to give thalidomide (**1**) in 70% yield. The conditions employed were much milder than those previously reported; however, even racemic thalidomide (**1**) was produced.

The result suggested that the activation of the carboxyl group of glutamine derivatives increases the acidity of the C – H bond of the adjacent asymmetric carbon and thereby enhances the tendency to racemize. They thus came up with a new idea to use isoglutamine (**35**) instead of glutamine (**11**) as a starter. In this case, the carboxyl group to be activated for ring closure is removed from the vicinity of the asymmetric carbon atom (Fig. 4).
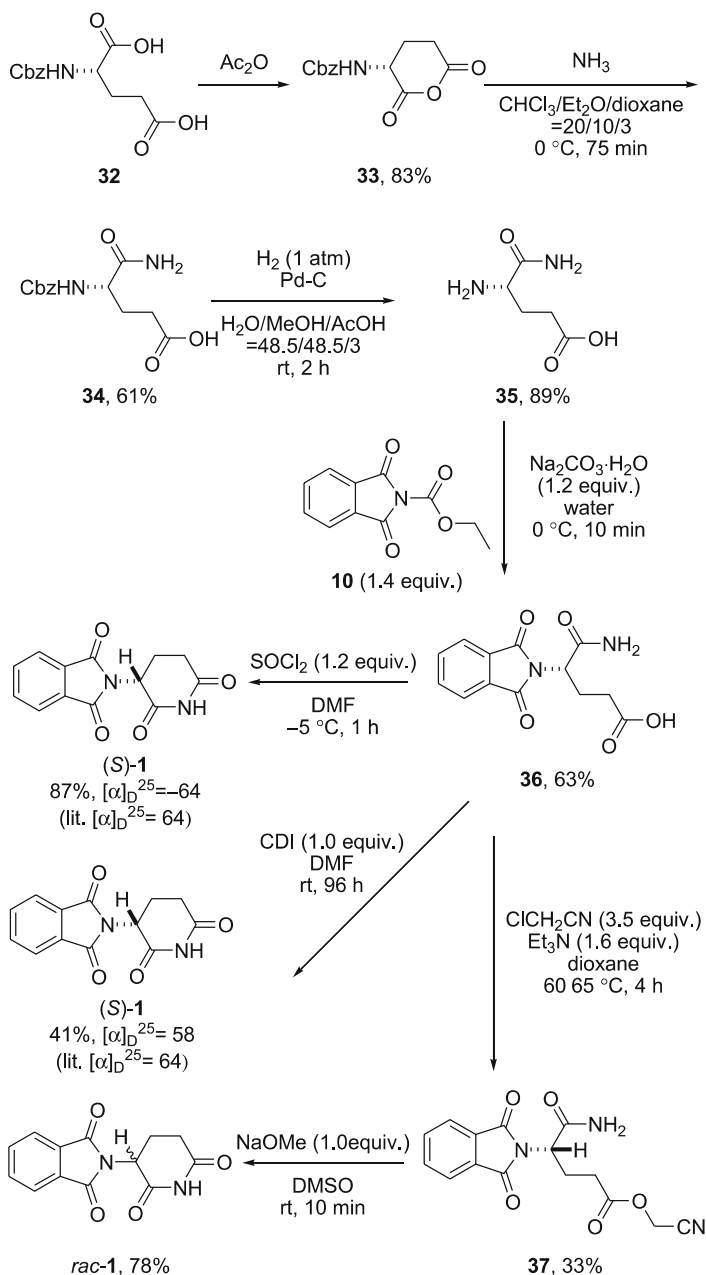
The preparations of optical isomers of thalidomide (**1**) were examined by a route based on D- and L-isoglutamine (**35**). The thalidomide isomers were obtained in high yields by treating the optical isomers of *N*-phthaloylisoglutamine (**36**) at 0 °C with thionyl chloride in DMF for 30 min. CDI
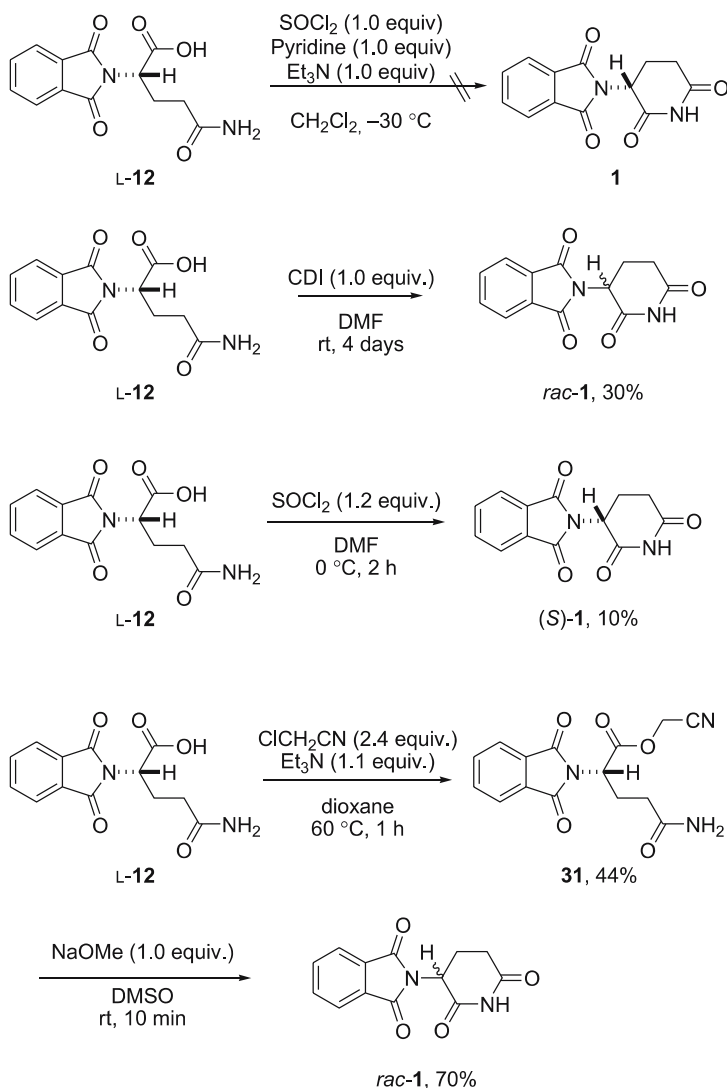
Scheme 18 Investigation of the synthesis of (S)-thalidomide (**1**) [86, 87]

was also found to be effective for glutarimide ring closure in the synthesis of (S)-thalidomide (**1**). In the course of the studies, Opliger et al. carefully compared the L-glutamine and L-isoglutamine derivatives as precursors of thalidomide (**1**) under the two conditions mentioned above, and concluded that (S)-thalidomide (**1**) is formed more readily and with less risk of racemization from the isoglutamine derivative.

While racemic thalidomide (**1**) is now commercially produced in only two steps from glutamine (**11**) and three steps from glutamic acid, these

Scheme 19 Synthesis of (S)-thalidomide (1) from N-phthaloyl-L-isoglutamine [86, 87]

early preparations of optically pure thalidomide are rather complicated and tedious. Therefore, enantioseparation by chiral HPLC was going to be the mainstream technique to obtain optically pure thalidomide (1) [88–96].
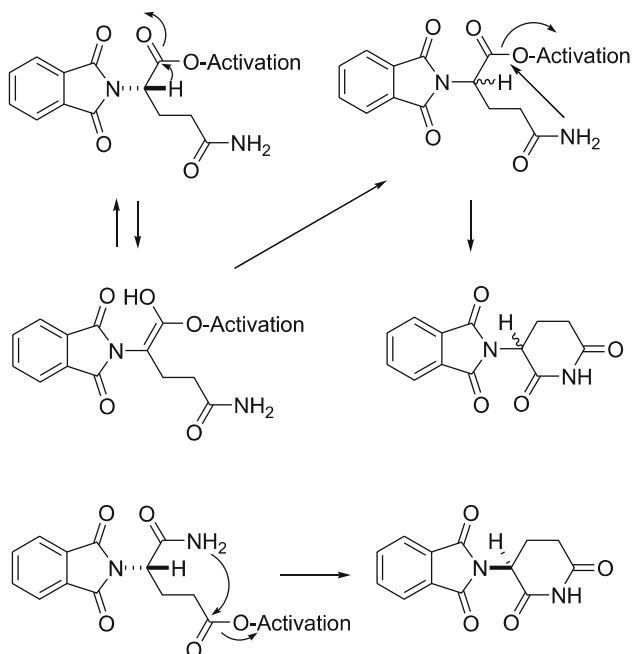
Fig. 4 New synthetic strategy for (S)-thalidomide (**1**)

The main difficulty confronted in the asymmetric synthesis of thalidomide (**1**) is the easy racemization due to the high acidity of the proton located on the asymmetric center. Galons et al. devised an effective strategy to avoid the racemization in the thalidomide (**1**) synthesis using benzyloxyamine (Scheme 20) [97]. The key step is the condensation of benzyloxyamine with Boc-glutamic phenyl ester (**39**), allowing the formation of the glutarimide ring under very mild conditions. The acidolysis of the Boc protective group followed by the phthalylation step led to *N*-benzyloxythalidomide (**41**). This compound was also obtained from (S)-phthaloylglutamic anhydride (**2**) in one step using benzyloxyamine, DCC, and pyridine in dichloromethane. The benzyloxy group was removed in two steps via *N*-hydroxythalidomide (**42**) to give (*R*)- or (*S*)-thalidomide (**1**) without racemization. Throughout the synthesis, the benzyloxy group located on the nitrogen plays important roles, not only as a protecting group of the glutarimide ring but also as an electron-donating group which effectively lowers the reactivity of the C = O groups and presumably reduces the acidity of the hydrogen on the stereogenic center.

This method seems to be easily reproducible, but again it requires multistep sequences. The same group reported a more simple route to optically active thalidomide (**1**) (Scheme 21) [98]. It is based on the condensation of the diacids with trifluoroacetamide in the presence of HOBT and 1-ethyl-
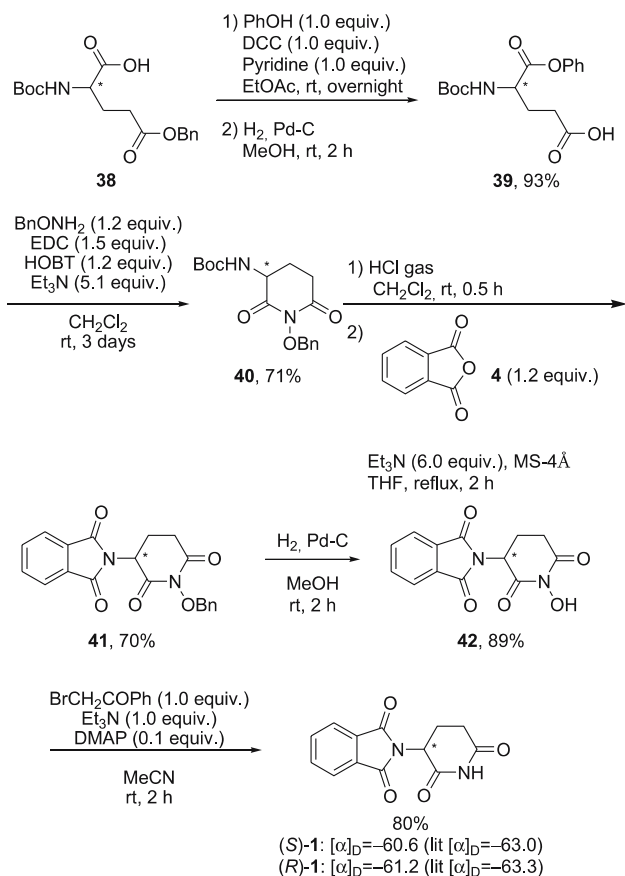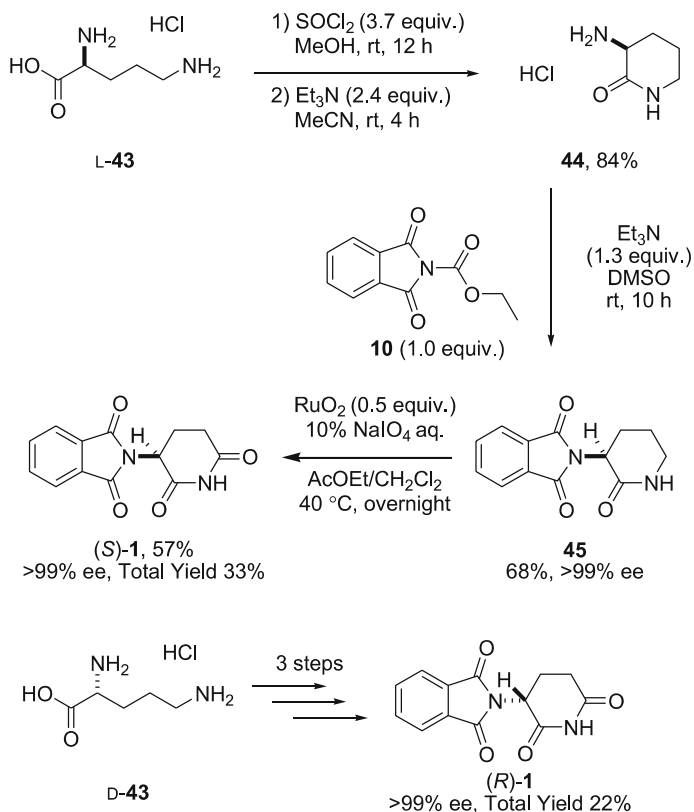
Scheme 20 Synthesis of (*S*)-or (*R*)-thalidomide (**1**) using benzyloxyamine [97]

3-(3-dimethylaminopropyl)carbodiimide (EDC). The enantiomeric purity of chiral thalidomide (**1**) was checked to be 88% ee by chiral HPLC analysis.

Although the Galones method with the use of EDC/HOBT cyclization of the *N*-phthaloylglutamic acid (**9**) with trifluoroacetamide is the most expeditious way to reach thalidomide enantiomers, partial racemization was observed. In 2001, we developed a three-step synthesis of enantiomerically pure (*R*)- and (*S*)-thalidomide (**1**) from ornithine (**43**) by the use of a racemization-free oxidation method, the ruthenium/metaperiodate system (Scheme 22) [99]. The point of our strategy is the ornithine as a precursor of thalidomide (**1**), instead of glutamine (**11**), glutamic acid (**8**), or isoglutamine (**34**). To avoid racemization, ornithine amide is used throughout the synthesis and it is converted to the glutarimide in the final step by oxidation. L-Ornithine (**43**) reacted with thionyl chloride in methanol followed by treatment with triethylamine to give the (*S*)-3-aminopiperidin-
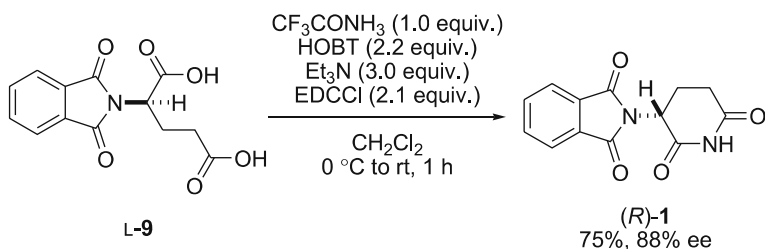
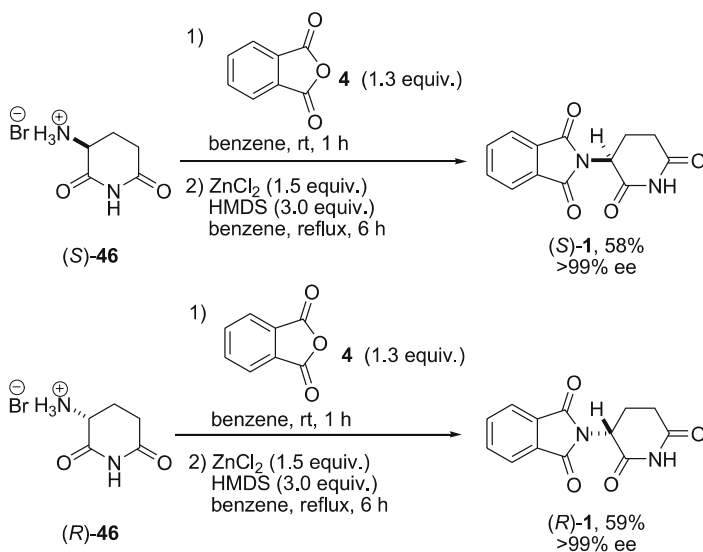**Scheme 21** Synthesis of (R)-thalidomide (**1**) using trifluoroacetamide [98]

Scheme 22 Synthesis of (S)- or (R)-thalidomide (**1**) from L- and D-ornithine [99]

2-one hydrochloride (**44**) in good yield. Protection of the amino moiety by the use of *N*-carboethoxyphthalimide (**10**) in DMSO furnished (S)-*N*-phthaloylpiperidin-2-one (**45**) as colorless crystals. Finally, oxidation using a catalytic amount of RuO₂ in the presence of excess sodium metaperiodate in a two-phase system gave (S)-thalidomide (**1**) in good yield without racemization. (R)-Thalidomide (**1**) can be prepared under the same conditions from

D-ornithine (**43**) with 99% ee in good yield. The advantage of the present method is that all the steps to thalidomide (**1**) can be performed without purification by silica-gel column chromatography; therefore, it is particularly useful for the practical synthesis of (*R*)- and (*S*)-thalidomides (**1**).

We have recently patented the preparation of optically active thalidomide (**1**) by the imidation reaction of aminopiperidinedione with phthalic anhydride (**4**) in the presence of hexamethyldisilazane and ZnCl$_2$ without racemization (Scheme 23) [100]. The process gives the thalidomide (**1**) in a reduced number of steps in a simple procedure and thereby is advantageous for industrial production of optically active thalidomide (**1**). Thus, a solution of 100 mg (*S*)-2-aminoglutarimide hydrobromide (**46**) in 5 mL benzene was treated with 92.0 mg phthalic anhydride (**4**), stirred for 1 h, treated with 98.0 mg ZnCl$_2$ and 0.304 mL hexamethyldisilazane (HMDS), refluxed at 80 °C for 6 h, and cooled to room temperature. After the usual workup, (*S*)-thalidomide (**1**) was obtained in 58% yield with > 99% ee. (*R*)-Thalidomide (**1**) can be prepared in the same way from (*R*)-**47** with 99% ee in good yield.

Scheme 23 Synthesis of (*S*)-or (*R*)-thalidomide (**1**) under HMDS induced phtaloylation conditions [100]

4
Concluding Remarks

The syntheses of thalidomide have been described. Both racemic and optically pure thalidomides (**1**) are now available with ease. Marketing of racemic

thalidomide (**1**) has already been resumed after a long break without clear interpretation of thalidomide (**1**) teratogenicity. Most of the thalidomide research reported recently has been done by the use of racemic thalidomide (**1**). We hope this review will serve to stimulate more active investigation of the chirality and biological activities of thalidomide (**1**).

References

1. Harousseau J-L (2006) Future Oncol 2:577
2. Lepper ER, Smith NF, Cox MC, Scripture CD, Figg WD (2006) Curr Drug Metab 7:677
3. Teo SK, Stirling DI, Zeldis JB (2005) Drug Discov Today 10:107
4. Frank ME, Macpherson GR, Figg WD (2004) Lancet 363:1802
5. Laffitte E, Revuz J (2004) Expert Opin Drug Saf 3:47
6. Botting J (2002) Drug News Perspect 15:604
7. Ng SSW, Brown M, Figg WD (2002) Biomed Pharmacother 56:194
8. Razza A (2002) Biochemist 24:21
9. Hashimoto Y (2002) Bioorg Med Chem 10:461
10. Stirling D (2001) Semin Oncol 28:602
11. Jacobson JM (2000) Expert Opin Pharmacother 1:849
12. Franks ME, Marcpherson GR, Figg WD (2004) Lancet 363:1802
13. Waldman AR (2000) Clin J Oncol Nurs 4:99
14. Stephens TD, Bunde CJ, Filmore BJ (2000) Biochem Pharmacol 59:1489
15. McBride WG (1961) Lancet 278:1358
16. Lenz W, Pfeiffer RA, Kosenow W, Hayman DJ (1962) Lancet 279:45
17. Sheskin J (1965) Clin Pharmacol Ther 6:303
18. Chemie Grunenthal (1957) GB Patent 768 821
19. Ose S, Umemoto S (1960) JP Patent 35 005 071
20. Ose S, Yoshimura Y, Saeki T (1960) JP Patent 35 005 277
21. Muller GW (1997) US Patent 5 698 579
22. Muller GW (1997) US Patent 5 605 914
23. Muller GW, Konnecke WE, Smith AM, Khetani VD (1999) Org Process Res Dev 3:139
24. Reepmeyer JC, Cox DC (1987) FDA monograph: guidelines to thalidomide synthesis. US Food & Drug Administration, Washington, DC
25. Caddick S (1995) Tetrahedron 51:10403
26. Perreux L, Loupy A (2001) Tetrahedron 57:9199
27. Lidstrom P, Tierney J, Wathey B, Westman J (2001) Tetrahedron 57:9225
28. Larhed M, Moberg C, Hallberg A (2002) Acc Chem Res 35:717
29. Kuhnert N (2002) Angew Chem Int Ed 41:1863
30. Blackwell HE (2003) Org Biomol Chem 1:1251
31. Kappe CO (2004) Angew Chem Int Ed 43:6250
32. Xu Y, Guo Q-X (2004) Heterocycles 63:903
33. Kirschning A, Solodenko W, Mennecke K (2006) Chem Eur J 12:5972
34. Seijas-Vazquez JA, Vazquez-Tato MP, Gonzalez-Bande C, Pacios-Lopez B (2003) ES Patent 2 190 707

35. Seijas JA, Vazquez-Tato MP, Gonzalez-Bande C, Martinez MM, Pacios-Lopez B (2001) Synthesis 999
36. Hijji YM, Benjamin E (2001) 5th International electronic conference on synthetic organic chemistry, 1–30 September 2001, p 1084
37. Hijji YM, Benjamin E (2002) 6th International electronic conference on synthetic organic chemistry, 1–30 September 2002, p 1084
38. Hijji YM, Benjamin E (2003) 7th International electronic conference on synthetic organic chemistry, 1–30 November 2003, p 1084
39. Hijji YM, Benjamin E (2004) 8th International electronic conference on synthetic organic chemistry, 1–30 November 2004, p 1084
40. Kassel DB (2001) Chem Rev 101:255
41. Amold FH (2001) Nature 409:253
42. Lehn J-M, Eliseev AV (2001) Science 291:2331
43. Schweizer F (2002) Angew Chem Int Ed 41:230
44. Brase S, Gil C, Knepper K (2002) Bioorg Med Chem 10:2415
45. Boger DL (2003) Bioorg Med Chem 11:1607
46. Brase S (2004) Acc Chem Res 37:805
47. Dolle RE (2004) J Comb Chem 6:623
48. Reymond J-L (2004) Angew Chem Int Ed 43:5577
49. Nefzi A, Ostresh JM, Yu J, Houghten RA (2004) J Org Chem 69:3603
50. Schwalbe T, Autze V, Hohmann M, Stimer W (2004) Org Process Res Dev 8:440
51. Spring DR (2005) Chem Soc Rev 34:472
52. Brown ED, Wright GD (2005) Chem Rev 105:759
53. Blotny G (2006) Tetrahedron 62:9507
54. Greco G, Novelino E, Martin YC (1998) Des Bioact Mol 219
55. Vedani A, Dobler M (2000) Prog Drug Res 55:105
56. Akamatsu M (2002) Curr Top Med Chem 2:1381
57. Mekenyan O (2002) Curr Pharm Des 8:1605
58. Schmieder P, Mekenyan O, Bradbury S, Veith G (2003) Pure Appl Chem 75:2389
59. Bultinck P, Winter HD, Langenaeker W, Tollenare J (eds) (2004) Computational Medicinal Chemistry for Drug Discovery, 1st ed. Marcel Dekker, New York
60. Debnath AK (2005) Curr Pharm Des 11:3091
61. Locuson CW, Wahlstrom JL (2005) Drug Metab Dispos 33:873
62. Allen DD, Geldenhuys WJ (2006) Life Sci 78:1029
63. Berger RD (2006) Drug Discov Today 11:429
64. Xiao Z, Schaefer K, Firestine S, Li P-K (2002) J Comb Chem 4:149
65. Chang M-Y, Chang C-H, Chen S-T, Chang N-C (2002) J Chin Chem Soc (Taipei) 49:383
66. Chang M-Y, Lin K-G, Chen S-T, Chang N-C (2003) J Chin Chem Soc (Taipei) 50:795
67. Chang M-Y, Chen S-T, Chang N-C (2003) Syn Commun 33:1375
68. Greig NH, Holloway H, Brossi A, Zhu X, Giordano T, Yu Q-S, Figg WD (2005) WO Patent 2 005 028 436
69. Gao L, Yuan X, Guo H, Liu X (2003) CN Patent 1 405 166
70. Zhang H (2005) CN Patent 1 597 680
71. Yuan X-H, Guo H-Q, Qiu X-P, Kang C-Q, Liu X-D, Gao L-X (2005) Gaodeng Xuexiao Huaxue Xuebao 26:1477
72. Alpegiani M, Mazzoni A, Vergani D, Cabri W (2005) EP Patent 1 602 654
73. Varala R, Adapa SR (2005) Org Proc Res Dev 9:853
74. Blaschke G, Kraft HP, Fickentscher K, Kohler F (1979) Arzneimittelforschung 29:1640
75. Winter W, Frankus E (1992) Lancet 339:365

76. Blaschke G, Knoche B (1994) J Chromatogr 2:183
77. Nishimura K, Hashimoto Y, Iwasaki S (1994) Chem Pharm Bull 42:1157
78. Wnendt S, Finkam M, Winter W, Ossing J, Rabbe G, Zwingenberger K (1996) Chirality 8:390
79. Sampaio EP, Sarno EN, Gallily R, Cohn ZA, Kaplan G (1991) J Exp Med 173:699
80. Meyring M, Mühlbacher J, Messer K, Kastner-Pustet N, Bringmann G, Mannschreck A, Blaschke G (2002) Anal Chem 74:3726
81. De Camp WH (1989) Chirality 1:2
82. Ed. Chirality (1990) Lancet 336:1100
83. Lien EJ (1995) J Drug Target 2:527
84. Wnendt S, Zwingenberger Z (1997) Nature 385:303
85. Casini G, Ferappi M (1964) Farmaco Ed Sci 19:563
86. Shealy YF, Opliger CE, Montgomery JA (1965) Chem Ind 1030
87. Shealy YF, Opliger CE, Montgomery JA (1968) J Pharm Sci 57:757
88. Blaschke G, Kraft HP, Fickentscher K, Kohler F (1979) Arzneimittelforschung 29:1640
89. Blaschke G, Kraft HP, Markgraf H (1980) Chem Ber 113:2318
90. Francotte E, Wolf RM (1992) J Chromatogr 595:63
91. Reepmeyer JC (1996) Chirality 8:11
92. Chankvetadz B, Schulte G, Blaschke G (1997) J Pharm Biomed Anal 15:1577
93. Meyring M, Chankvetadze B, Blaschke G (2000) J Chromatogr A 876:157
94. Meyring M, Muhlenbrock C, Blaschke G (2000) Electrophoresis 21:3270
95. Zhang Y, Watts W, Nogle L, McConnell O (2004) J Chromatogr A 1049:75
96. Murphy-Poulton SF, Boyle F, Gu XQ, Mather LE (2006) J Chromatogr B 831:48
97. Robin S, Zhu J, Galons H, Pham-Huy C, Claude JR, Tomas A, Viossat B (1995) Tetrahedron Asymmetry 6:1249
98. Flaih N, Pham-Huy C, Galons H (1999) Tetrahedron Lett 40:3697
99. Suzuki E, Shibata N (2001) Enantiomer 6:275
100. Iong J, Shibata N, Toru T (2005) JP Patent 2 005 336 157

Rational Drug Design of δ Opioid Receptor Agonist TAN-67 from δ Opioid Receptor Antagonist NTI

Hiroshi Nagase[1] (✉) · Hideaki Fujii[2] (✉)

[1]School of Pharmaceutical Science, Kitasato University, 5-9-1, Shirogane, Minatoku, Tokyo, Japan
nagaseh@pharm.kitasato-u.ac.jp

[2]Pharmaceutical Research Laboratories, Toray Industries, Inc., 6-10-1, Tebiro, Kamakura, Kanagawa, Japan
hideaki_fujii@nts.toray.co.jp

Abstract A highly selective nonpeptidic δ opioid receptor agonist TAN-67, (4aS^*, 12aR^*)-4a-(3-hydroxyphenyl)-2-methyl-1,2,3,4,4a,5,12,12a-octahydropyrido[3,4-*b*]acridine was designed on the basis of the message-address concept and the accessory site theory. (–)-TAN-67 is a potent and selective $δ_1$ opioid receptor agonist and shows strong antinociceptive, cardioprotective, and antiarrhythmic effects. By contrast, (+)-TAN-67 induced hyperalgesia, the opposite effect of antinociception. An important intermediate ketone for the TAN-67 synthesis, (4aS^*, 8aR^*)-4a-(3-methoxyphenyl)-2-methyl-6-oxodecahydroisoquinoline, has two structural features: a *trans*-fused bicyclic heterocycle and a quaternary carbon stereocenter at the bridgehead position. Syntheses of the intermediate ketone reported by some research groups are described. The synthesis of chiral TNA-67 is also shown.

Abbreviations

β-FNA	β-funaltrexamine
BNTX	7-benzylidenenaltrexone
CDI	1,1′-carbonyl diimidazole
COSY	correlated spectroscopy
CPM	cyclopropylmethyl
DPDPE	cyclic[D-Pen^2, D-Pen^5]enkephalin
DR	dose ratio
GABA	γ-aminobutyric acid
GPI	guinea pig ileum
i.t.	intrathecal
LAH	lithium aluminum hydride
MTPT	1-methyl-4-phenyl-1,2,3,6-tetrahydropyridine
MVD	mouse vas deferens
MVK	methyl vinyl ketone
NMDA	N-methyl D-aspartate
NMO	4-methylmorpholine N-oxide
NOE	nuclear Overhauser effect
NOESY	nuclear Overhauser effect spectroscopy
nor-BNI	nor-binaltrphimine
NTB	natoriben
NTI	naltrindole
OMI	oxymorphoindole
SIOM	spiroindanyloxymorphone
SNC-80	(+)-4-[(αR)-α-((2S,5R)-4-allyl-2,5-dimethyl-1-piperazinyl)-3-methoxybenzyl]-N,N-diethylbenzamide
TPAP	tetrapropylammonium perruthenate
WHO	World Health Organization

1
Introduction

1.1
Opioids

Morphine has a strong analgesic effect and has been used for the alleviation of postoperative and cancer pain since antiquity, but its use is now restricted because of its drug dependency. Morphine and its homologues were called opiates after opium, which was extracted from poppy seeds. This class of drugs are now termed opioids.

Sertürner isolated morphine in 1805 [1] and its structure was determined in the early 1990s [2–4]. A myriad of derivatives were synthesized in order to obtain strong analgesics without addiction, however, the separation of

the analgesic properties from addiction has not been achieved. The syntheses of derivatives at the time were based on the simplification of the morphine structure (Fig. 1). The three representative peptides (enkephalins, endorphins, and dynorphins) that showed the morphine-like analgesic effects were discovered in 1975 [5]. The peptides were not expected to be addictive because they were endogenous. Hundreds of peptide derivatives were synthesized and their analgesic and addictive effects were investigated in detail. Contrary to expectation, these synthesized peptides did show drug dependency. Moreover, their analgesic effects were not as strong as expected because their brain penetration was low (the area of action for the endogenous opioid peptides exists mainly in the brain). These circumstances caused a slow down in opioid research. However, in the course of the investigations, three types of receptors (μ, δ, and κ) were proposed, because it was difficult to explain the various pharmacological effects induced by synthesized compounds with just one receptor type. At the time, Portoghese et al. reported remarkable experimental results using β-FNA, a μ irreversible antagonist [6]. The results suggested that the addictive properties of morphine derivatives may be produced via the μ receptor. In mice whose μ receptors were blocked for a week with β-FNA, the administration of morphine induced strong analgesic effects but almost none of the undesirable morphine-like side effects such as drug dependency, constipation, respiratory depression, etc [7]. The experimental results strongly suggested that δ and κ receptors are involved in analgesic effects, but largely do not participate in the negative side effects. These findings imply that selective δ or κ agonists would be ideal analgesics, showing no side effects such as drug dependence, constipation, respiratory depression, etc. The challenge was in how to design a selective agonist for the δ or κ receptors.

1.2
The Message-Address Concept

A survey of the structures of the compounds synthesized at the time indicates that the strategy of drug design was the simplification of the morphine structure (Fig. 1). It is easy to presume that there was only one way to simplify inexpensively the complicated structure of morphine to obtain a compound showing analgesic effects comparable to or stronger than those of morphine. However, the smaller molecular size resulting from simplification could make it difficult to separate the drug dependency effects from the analgesic effects. i.e., to obtain receptor type selectivity for either the δ or κ receptor.

The structures of the endogenous opioid peptides were larger than that of morphine (Fig. 2). The upper row of Fig. 2 depicts dynorphin, which shows moderate selectivity for the κ receptor. Enkephalin also shows moderate selectivity for the δ receptor. Its structure is the portion of the dynorphin structure ending at dashed line b. The two peptides possess a common seg-
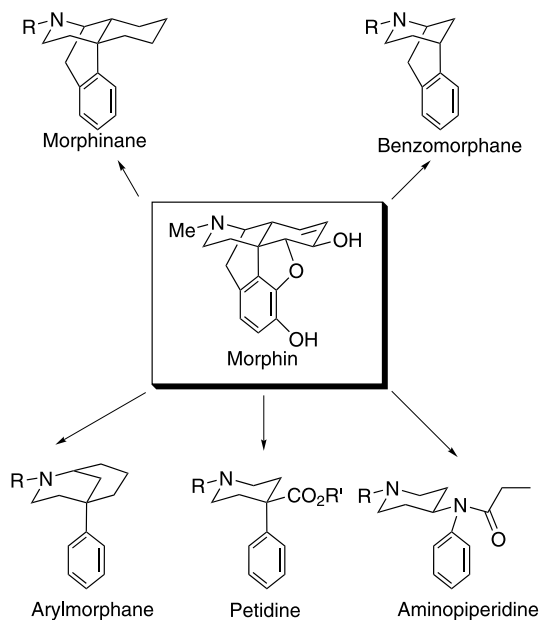
Fig. 1 Classical derivatization of morphin. Most of the derivatives were simplifications of the morphin structure
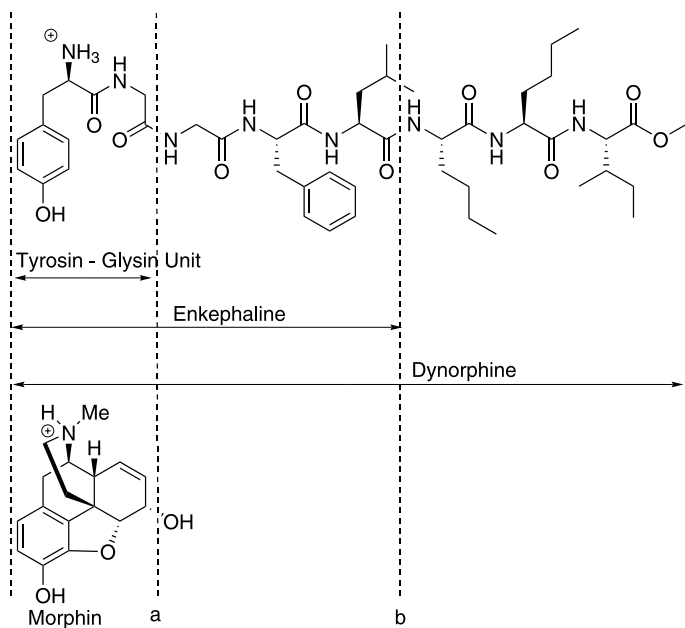

Fig. 2 Structural comparison of opioid peptides with morphine

ment, the tyrosine-glycin unit. The size of the morphine structure is similar to that of the tyrosine-glycin unit as shown in the lower row of Fig. 2. It might be possible to classify the opioid ligands according to two sites: the message site, which is the essential structure for binding the opioid to the opioid receptor, and the address site, which relates to the receptor type selectivity. This is the message-address concept (Fig. 3) [8–10]. According to the message-address concept, the μ, δ, and κ receptors have the smallest, intermediate, and largest address sites, respectively. Both the selective δ antagonist NTI and selective κ antagonist nor-BNI were designed on the basis of the concept as shown in Fig. 4 [8, 11, 12]. These two antagonists are listed in one of the rep-
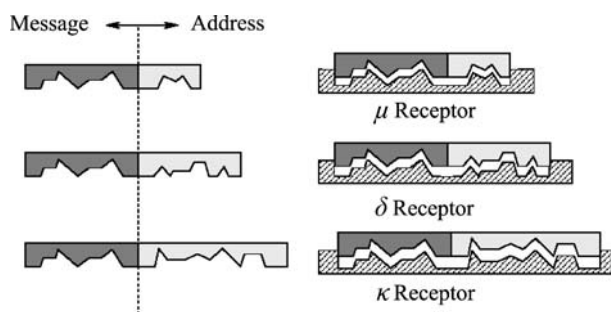
Fig. 3 The message-address concept
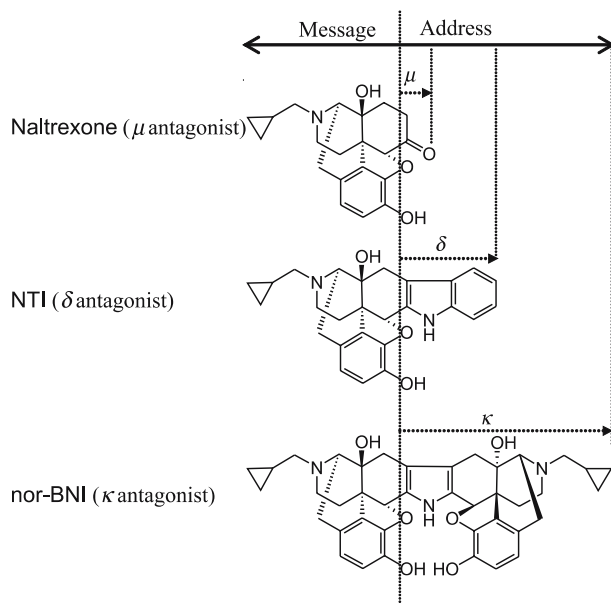
Fig. 4 Rationally designed selective antagonists and the message-address concept

resentative pharmacology textbooks (see also Goodman and Gilman's The Pharmacological Basis of Therapeutics) [13] as highly selective antagonists. With the selective δ and κ antagonists in hand, the next aim is the drug design and synthesis of the selective δ and κ agonists. In this article, we will describe in detail the drug design and synthesis of a selective δ agonist.

1.3
The Accessory Site Theory

The consideration of the structural difference between an agonist and an antagonist is an important basis of medicinal chemistry. An antagonist is larger than an agonist because antagonists have accessory sites (Fig. 5) [14]. According to theory, the removal of the accessory sites from the structure of a selective δ antagonist NTI could afford a δ agonist. The next issue is identifying the accessory site of the NTI. Consider the mechanism by which the agonist induces its agonistic activity. Figure 6 indicates that an agonist binds to a receptor and produces its agonistic activity. When the agonist approaches the cavity of the active site of the receptor, the pharmacophore interactions occur gradually between the agonist and the receptor. A pharmacophore interaction consists of a weak interaction such as ionic bonding, dipole–dipole interaction, π–π interaction, lipophilic interaction, hydrogen bonding, etc. The interactions are strengthened by the exclusion of water molecules to achieve a tight fit. When the agonist is tightly bound in the final state, the cavity binding site is smaller than the empty cavity. The binding-induced structural change of the receptor leads to the agonistic signal transductions. On the other hand, an antagonist possessing an accessory site restricts the conformational change of the receptor when the antagonist binds to the receptor. On the basis of the theory, we considered the model of NTI binding to the receptor (Fig. 7a). In the center of the cavity, three interactions take place between the receptor and the message site: an ionic bond, a π–π interaction,
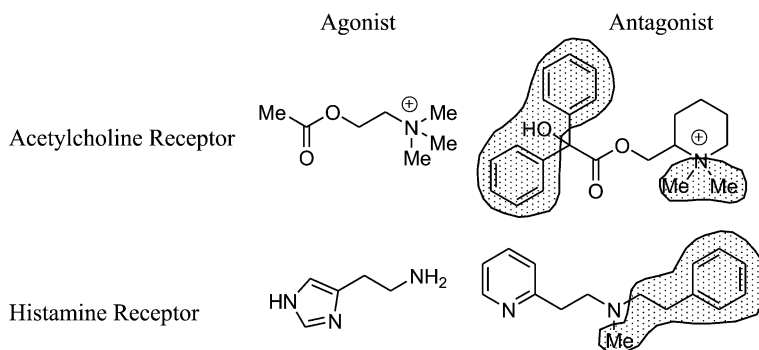

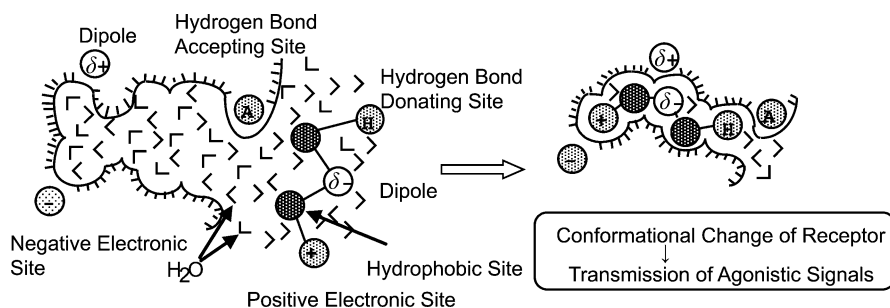**Fig. 5** The accessory site theory. The shaded areas show the accessory sites

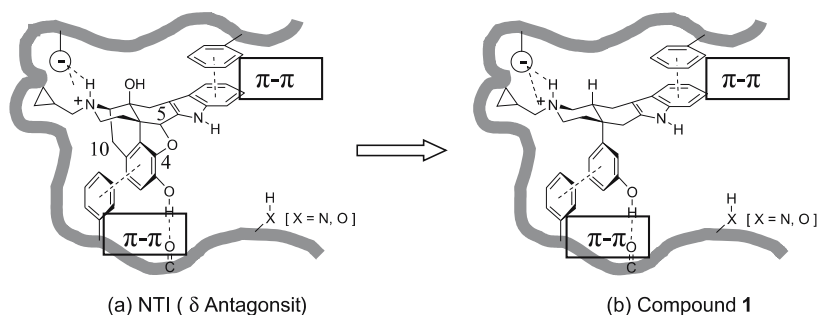**Fig. 6** Conceptual illustration of the interaction between agonist and receptor

Fig. 7 Binding model for NTI (**a**) and compound **1** (**b**) to the δ opioid receptor

and a hydrogen bond. The other interaction is between the receptor and the address site and is a π–π interaction. The interaction at the address site is what elicits the selectivity of the δ receptor. A more drastic shape change of the receptor is necessary for the production of agonistic activity. The free rotation of the phenol ring could make the receptor bind the compound more tightly. The 4,5-epoxy and C-10 methylene moieties of NTI, which conformationally fixed the phenol ring and disturbed the approach of the receptor to NTI, are expected to be accessory sites. Following the hypothesis, the indole derivative **1** shown in Fig. 7b was designed.

2
Synthesis of Indole Derivative 1

2.1
Synthesis of Key Intermediate Ketone 2

The usual synthesis of indole derivative **1** is easy to attain by converting the key intermediate ketone **2** to compound **1** by Fischer indolization (Scheme 1).
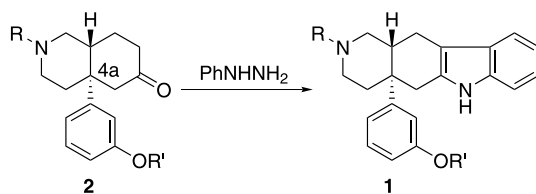
**Scheme 1** Synthesis of compound **1** by Fischer indole synthesis

Since the first synthesis of ketone **2** was reported by Rapoport et al. in 1977 [15], four research groups including our group have reported the synthesis of ketone **2** [16–19]. These syntheses will be described in the following sections. The structural feature of ketone **2** is the *trans*-decahydroisoquinoline skeleton possessing a quaternary carbon stereocenter at the bridgehead position. The key step is the construction of this characteristic structure.

2.2
Rapoport's Synthesis

Scheme 2 shows Rapoport's synthesis [15]. The cinnamic acid derivative **3** prepared from *m*-methoxy benzaldehyde [20] was ethylated by diethyl sulfate to give ethyl cinnamate derivative **4**, followed by Michael addition with ethyl cyanoacetate to afford compound **5**. Compound **5** was converted to lactam **6** by the reduction of the cyano group and subsequent cyclization. Selective reduction of the lactam moiety of **6** was achieved by treatment with trimethyloxonium fluoroborate followed by sodium borohydride reduction. Amine **8** was obtained by the reductive methylation of amine **7**. Amine **8** was converted to compound **9** by methylene lactam rearrangement [21], followed by selenium dioxide oxidation to provide compound **10**. Allylic rearrangement of compound **10** and subsequent hydrolysis gave compound **12**. The construction of the decahydroisoquinoline structure began with compound **12**,

Scheme 2 Rapoport's Synthesis: **a** Et_2SO_4, tris(2-hydroxypropyl)amine, acetone, Δ, 1.5 h, 88%; **b** Na, Ethyl cyanoacetate, EtOH, 93%; **c** PtO_2, H_2 (33–49 psi), 12N HCl/EtOH, 7 h; **d** toluene, reflux, 1 h, 100% for steps **c** and **d**; **e** trimethyloxonium fluoroborate, CH_2Cl_2, rt, 43 h; **f** $NaBH_4$, EtOH, 5–10 °C → rt, 24 h, 61% for steps **e** and **f**; **g** 10% Pd/C, CH_2O aq, H_2 (50 psi), EtOH, 12 h, 95%; **h** NaOH, MeOH, H_2O, reflux, 5 h; **i** Ac_2O, reflux, 1 h, 92% for steps **h** and **i**; **j** SeO_2, PhCl, 100 °C, 1 h; **k** HCO_2H, 25 °C, 27 h; **l** K_2CO_3, MeOH, 25 °C, 1.5 h, 90% for steps **j**, **k**, and **l**; **m** $MeC(OMe)_3$, *t*-$BuCO_2H$, diglyme, reflux, 18 h, 80%; **n** KOH, MeOH, H_2O, 25 °C, 20 h, 77%; **o** CDI/THF, $CHCl_3$, 25 °C, 1 h; **p** magnesium enolate prepared from $LiO_2CCH_2CO_2$-*t*-Bu + *i*-PrMgBr, THF, 16 h, 100% for steps **o** and **p**; **q** MeONa, MeOH, 7 h, 76% for *trans*-**17**, 18% for *cis*-**17**; **r** TFA, benzene, 25 °C, 3 h, then toluene reflux, 1 h, 81%; **s** ethylene glycol, TsOH · H_2O, benzene, Δ, 92%; **t** AlH_3, THF, – 78 °C, 1 min; **u** $LiAlH_4$, – 78 °C → 0 °C, 1 h at 0 °C; **v** 5% Rh/Al_2O_3, H_2 (50 psi), MeOH, 10 h, 83% for steps **t**, **u**, and **v**; **w** 1N H_2SO_4, 25 °C, 26 h, 99%
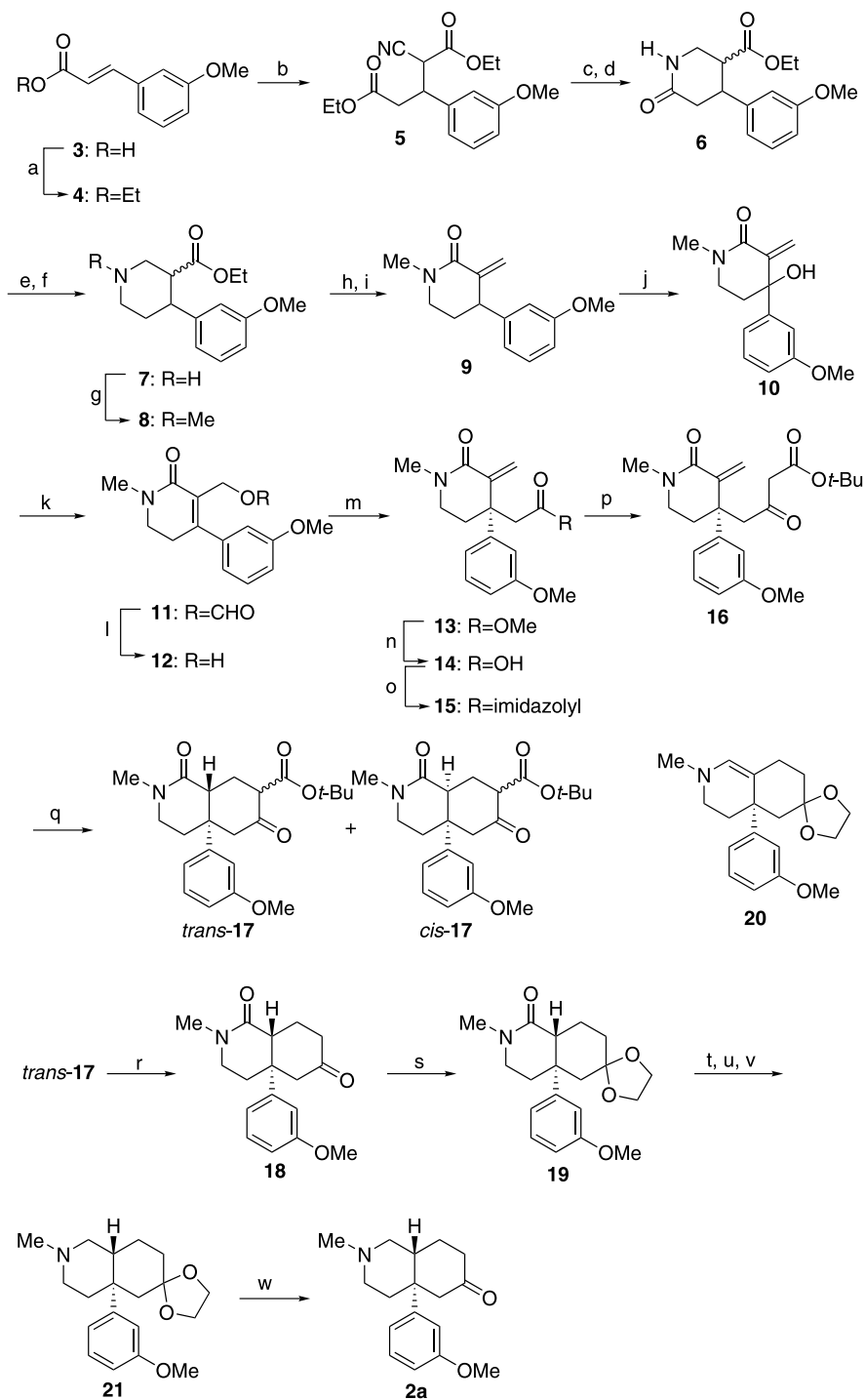
which was converted to compound **13** by Cleisen rearrangement, followed by transesterification via the acyl imidazole intermediate **15** and subsequent intramolecular Michael addition to yield decahydroisoquinoline *trans-* and *cis-* **17** with an 87 : 13 mixture of the diastereomers. The pure *trans-***17** was easily obtained by crystallization. Compound **19** was synthesized by decarboxylation of *trans-***17** following acetalization. The reduction of the amide moiety of compound **19** was achieved by stepwise reduction involving the addition of LAH to a cold solution of AlH_3 and compound **19** resulting in an 83:17 mixture of amine **21** and enamine **20**, followed by hydrogenation catalyzed by Rh/Al_2O_3. Finally, the objective ketone **2a** was obtained by deacetalization of compound **21**. Rapoport's method was a landmark for the synthesis of the ketone **2** possessing morphine-like structure; however the synthesis has many steps and is not practical.

2.3
Zimmerman's Synthesis

The synthesis of the ketone **2a** by Zimmeman et al. [16] is outlined in Scheme 3. The lithiated enamine **23** obtained by deprotonation of tetrahydropyridine **22** with *n*-butyl lithium was alkylated to give compounds **25** and **26**. The THP group of compounds **25** and **26** was removed, and the resulting alcohol was converted to bromides **27** and **28**, respectively. Bromides **27** and **28** were treated with acetic anhydride and TFA followed by refluxing in an acetonitrile solution in the presence of potassium carbonate to afford bicyclic enamines **31** and **32**. The acetyl groups of bicyclic enamines **31** and **32** were removed, yielding a mixture of compounds **33** and **34**, and compound **35**, respectively. Alcohols **36** and **37** were obtained by catalytic hydrogenation of the mixture of compounds **33** and **34**, and of compound **35**. Finally, both the alcohols **36** and **37** were converted to the desired ketone **2a** by Swern oxidation. The features of this synthesis are the construction of the quaternary carbon stereocenter [22] by alkylation of the lithiated enamine **23** and the stereoselective reduction of a bicyclic enamine by catalytic hydrogenation. However, this synthesis includes a poorly reproducible step and a labile intermediate. Moreover, the compound without a methoxy group corresponding to tetrahydropyridine **22**, that is 1-methyl-4-phenyl-1,2,3,6-tetrahydropyridine (MTPT), is reported to be highly neurotoxic [23]. Considering all the drawbacks and risks, this method is not practical.

2.4
Judd's Synthesis

Ketone **45** was synthesized by Judd et al. [17] as summarized in Scheme 4. The lithiated enamine **23** prepared from tetrahydropyridine **22** was alkylated, followed by refluxing in an acetonitrile solution in the presence of
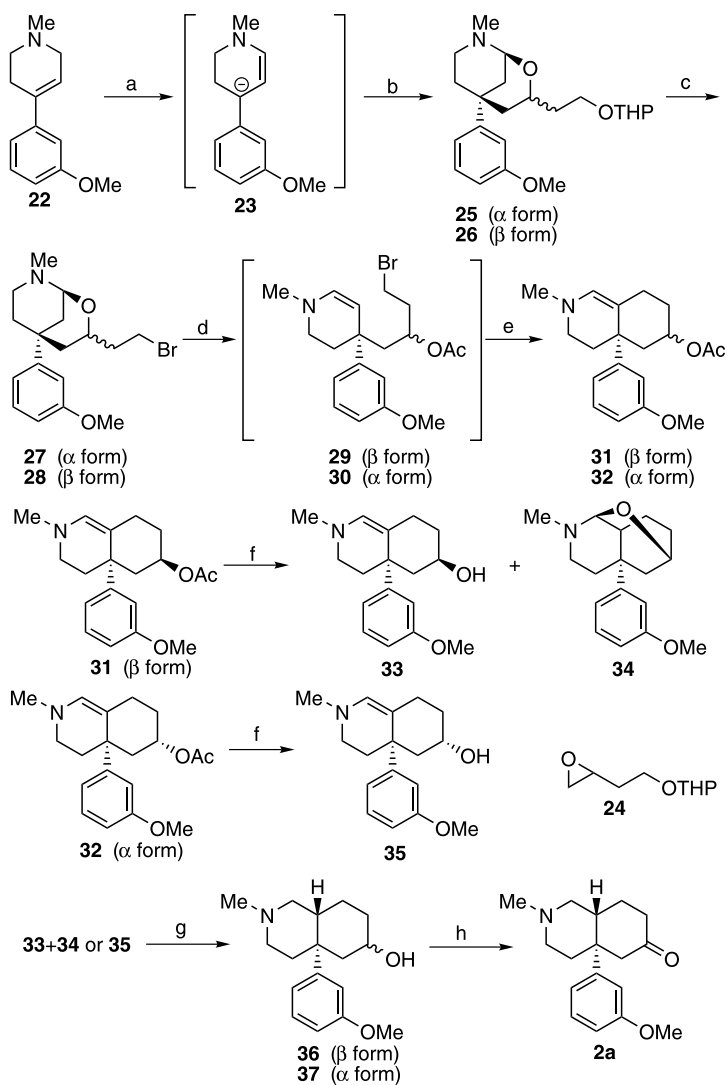
Scheme 3 Zimmerman's Synthesis: **a** *n*-BuLi, THF, 0 °C; **b** **24**, – 10 to – 5 °C, 40% for **25**, 34% for **26** for steps **a** and **b**, respectively; **c** HCl/Et$_2$O, then PPh$_3$, Br$_2$, THF, 10 °C to rt, 72% for **27**, 63% for **28**; **d** Ac$_2$O, TFA, rt; **e** K$_2$CO$_3$, MeCN, reflux, 75% for **31**, 61% for **32** for steps **d** and **e**, respectively; **f** K$_2$CO$_3$, MeOH, rt, 96% for **33** and **34**, 90% for **35**; **g** H$_2$ (60 psi), PtO$_2$, EtOH, 84% for **36**, 82% for **37**; **h** DMSO, (COCl)$_2$, CH$_2$Cl$_2$, – 55 °C, then Et$_3$N, 91% from **36**, 92% from **37**

sodium iodide and potassium carbonate to produce bicyclic enamine **38**. The bicyclic enamine **38** was converted to a methanesulfonate, and then reduced with sodium borohydride to give *trans*-decahydroisoquinoline **39**, selectively. The *N*-cyclopropylmethyl (CPM) derivative **42** corresponding to
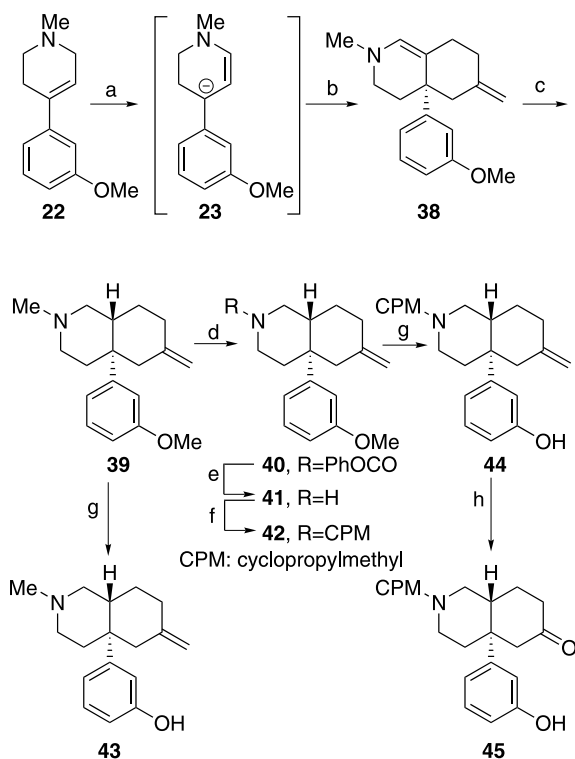
Scheme 4 Judd's Synthesis: **a** *n*-BuLi, THF, – 20 °C; **b** BrCH₂CH(= CH₂)CH₂CH₂Br, – 70 to – 40 °C, then NaI, K₂CO₃, MeCN, reflux, 29.5% for steps **a** and **b**; **c** MeSO₃H, MeOH, – 60 °C, then NaBH₄, rt, 83%; **d** ClCO₂Ph, *i*-Pr₂NEt, ClCH₂CH₂Cl, reflux, 88%; **e** KOH, EtOH, reflux, 74%; **f** CPMBr, DMF, 150 °C, 54%; **g** LiSMe, DMF, 125 °C, 60% for **43**, 33% for **44**; **h** OsO₄, NaIO₄, THF/H₂O, rt, 24%

the *N*-methyl compound **39** was obtained by the following sequence of reactions: first the conversion of methyl amine to carbamate, then the hydrolysis of the carbamate group, and the subsequent cyclopropylmethylation. The methoxy groups of compounds **39** and **42** were demethylated using lithium methylthiolate to provide compounds **43** and **44**, respectively. The desired ketone **45** was obtained by oxidation of compound **44** with osmium tetraoxide and sodium periodate. The characteristic of this synthesis is the construction of the quaternary carbon stereocenter by the alkylation of the lithiated enamine **23** and is the same as Zimmerman's synthesis, although Judd et al. attempted to shorten the synthesis steps by using a designed alkylating agent, 4-bromo-2-(bromomethyl)-1-butene. The formation of the characteristic *trans*-decahydroisoquinoline structure was achieved by the preparation of a kinetic iminium salt from bicyclic enamine **38** using methanesulfonic acid [22] and the subsequent hydride reduction of the kinetic iminium salt. Their synthesis also includes the suspected neurotoxin compound **22**.

2.5
Liras's Synthesis

Scheme 5 shows the synthesis of the ketone **2b** by Liras et al. [18]. Piperidone **46** was converted to enol triflate **47** using *N*-phenyltrifluoromethylsulfon-
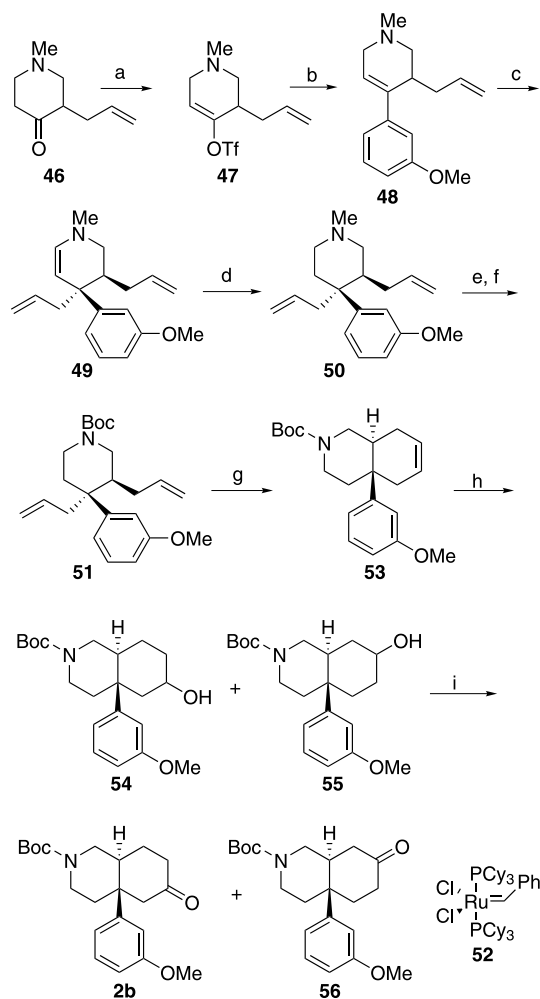

Scheme 5 Liras's Synthesis: **a** LHMDS, *N*-phenyltrifluoromethylsulfonimide, THF, – 78 °C to rt, 92%; **b** 3-methoxyphenylboronic acid, KBr, K$_3$PO$_4$, Pd(PPh$_3$)$_4$, 1,4-dioxane, 85 °C, 95%; **c** *sec*-BuLi, allyl bromide, THF, – 45 to – 78 °C to rt; **d** NaBH$_4$, MeOH, rt, 88% for steps **c** and **d**; **e** ClCO$_2$CHClCH$_3$, 1,2-dichloroethane, reflux, then MeOH reflux; **f** Boc$_2$O, Et$_3$N, CH$_2$Cl$_2$, rt, 80% for steps **e** and **f**; **g** Grubbs catalyst **52**, 1,2-dichloroethane, 60 °C, 93%; **h** 9-BBN, THF, reflux, 30% H$_2$O$_2$, EtOH, 6 *N* NaOMe, 100% (**54**:**55** = 3 : 1); **i** TPAP, NMO, CH$_2$Cl$_2$, rt, 88% for **2b** and 84% for **56**

imide, followed by Suzuki–Miyaura coupling to give tetrahydropyridine **48**. The lithiated enamine derived from the tetrahydropyridine **48** was diastereoselectively allylated, and then reduced with sodium borohydride to afford piperidine **50**. The *N*-methyl piperidine **50** was converted to *N*-Boc piperidine **51** for an easy conversion of the nitrogen substituent. Cyclization was achieved by a ring-closure-metathesis reaction of the piperidine **51** using the first generation Grubbs catalyst **52**, and then a hydroxyl group was installed on the resultant **53** by hydroboration to furnish *trans*-decahydroisoquinoline **54** and **55**. In the hydroboration step, the use of sterically hindered 9-BBN led to a 3 : 1 ratio of the separable isomeric alcohols **54** and **55**; however the use of the smaller borane-dimethyl sulfide complex resulted in a 1 : 3 ratio of alcohols **54** and **55**. Alcohols **54** and **55** were oxidized using tetrapropylammonium perruthenate (TPAP) to give ketone **2b** and **56**, respectively. The main feature of this synthesis is the construction of the quaternary carbon stereocenter by diastereoselective allylation of the lithiated enamine, which led to the determination of the decahydroisoquinoline structure. There are two drawbacks to this method. One is a low regioselectivity in the hydroboration step, resulting in the production of the desired ketone **2b** and its regioisomer **56**. Although obtaining two isomeric ketones is a benefit in view of the potential synthesis of various ligands, it is not of merit as the primary synthetic route for ketone **2**. A further drawback is the presence of intermediate **48** that has a similar structure to neurotoxic MTPT. Unfortunately, the toxicity of the compound **48** is not reported.
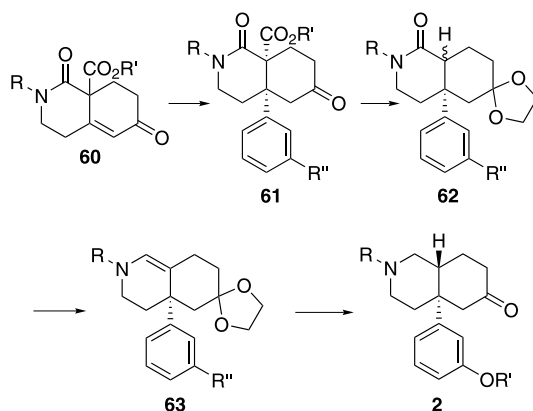
2.6
Nagase's Synthesis

Nagase et al. [19] planned to construct the quaternary carbon stereocenter without the alkylation of lithiated enamine **23** to avoid using the suspected neurotoxin tetrahydropyridine **22**. In general it is difficult to construct the quaternary carbon stereocenter by a 1,4-conjugated addition reaction, however, Finch et al. reported that the construction of the quaternary carbon stereocenter was achieved by 1,4-conjugated addition of a phenyl group [24] (Scheme 6). Although Finch's method did not provide the *trans*-decahydroisoquinoline but rather the *cis*-derivative, it suggests a method of
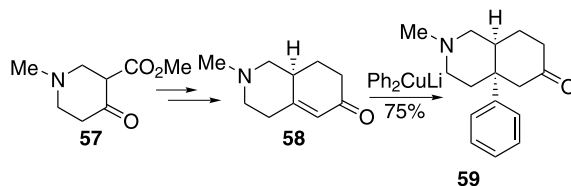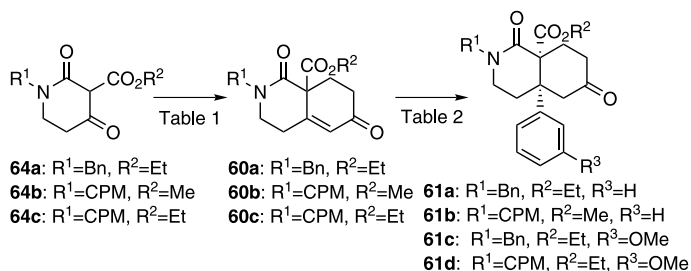

Scheme 6

constructing the quaternary carbon stereocenter by a 1,4-conjugated addition reaction. With Finch's method in mind, we planned a synthetic route to the *trans*-decahydroisoquinoline structure (Scheme 7). The synthesis of *trans*-decahydroisoquinoline **2** commenced with α,β-unsaturated ketone **60** which was converted to intermediate **61** by 1,4-conjugated addition. The amide carbonyl moiety of amide **62**, which was derived by decarboxylation of intermediate **61**, was partially reduced to afford the bicyclic enamine **63**, followed by stereoselective reduction [22] of the bicyclic enamine **63** to furnish the *trans*-decahydroisoquinoline **2**. The feature of our synthetic method is the utilization of the bicyclic enamine **63**, which opens the way to stereoinversion from the *cis*-form to the *trans*-form. The α,β-unsaturated ketones **60** were prepared from 2,4-piperidinediones **64** [25] by either the reported method [26] or by our modified procedure (Scheme 8). The results of the Robinson annulation for the preparation of the α,β-unsaturated ketones **60** are summarized in Table 1. Shultz's condition resulted in 50 and 42% yields of the α,β-unsaturated ketones **60** (entries 1, 2). However, the yield of ketone **60** was improved by varying between potassium *t*-butoxide or sodium hydride and sodium alkoxide as a base, benzene/*t*-butanol or benzene and ethanol

Scheme 7 Synthetic strategy

64a: R^1=Bn, R^2=Et   **60a**: R^1=Bn, R^2=Et
64b: R^1=CPM, R^2=Me   **60b**: R^1=CPM, R^2=Me   **61a**: R^1=Bn, R^2=Et, R^3=H
64c: R^1=CPM, R^2=Et   **60c**: R^1=CPM, R^2=Et   **61b**: R^1=CPM, R^2=Me, R^3=H
                                                              61c: R^1=Bn, R^2=Et, R^3=OMe
                                                              61d: R^1=CPM, R^2=Et, R^3=OMe

Scheme 8

Table 1 Results of Robinson annulation of **64**

Entry	Substrate	Reaction conditions	Product	Yield[a]
1	**64a**	MVK(1.7 eq), *t*-BuOK(0.12 eq), PhH/*t*-BuOH, 80 °C, 5 h	**60a**	50
2	**64b**	MVK(2.3 eq), NaH(0.1 eq), PhH, 42 °C, 46 h	**60b**	42
3	**64c**	MVK (2.25 eq), EtONa(0.12 eq), EtOH, rt, 7.5 h	**60c**	70
4	**64b**	MVK(2.5 eq), MeONa(0.12 eq), MeOH, rt, 10 h	**60b**	72
5	**64b**	MVK(2.3 eq), KOH(0.1 eq), 18-crown-6(0.1 eq), MeOH, rt, 22 h	**60b**	95

[a] isolated yield (%)

or methanol as a solvent, and reflux and room temperature as a reaction temperature (entries 3, 4). Moreover, the use of potassium hydroxide in the presence of 18-crown-6 provided the α,β-unsaturated ketone **60b** in 95% yield (entry 5). Next, the results of the 1,4-conjugated addition reaction of an aryl group to the α,β-unsaturated ketones **60** were shown in Scheme 8 and Table 2. As a model study, the reaction of the α,β-unsaturated ketone **60a** with lithium diphenylcuprate [27, 28], which was prepared from phenyl lithium and copper(I) iodide, afforded the 1,4-adduct **61a** in 51% yield (entry 1). Copper(I) iodide was the best reagent for the preparation of cuprate in our explorations. In the case of methyl ester **60b**, the 1,4-conjugated addition reaction barely proceeded, but the use of chlorotrimethlysilane [29, 30], which was the well-known accelerator of the 1,4-conjugated addition reaction, gave the objective product **61b** in 30% yield (entry 2). For the preparation of the designed compound **1**, the 1,4-conjugated addition reaction of the *m*-methoxyphenyl group to the α,β-unsaturated ketone **60** is essential. Considering the reaction efficiency, the reaction conditions of the 1,4-conjugated addition were investigated by use of the α,β-unsaturated ketones **60a** and **60c**, and copper(I) iodide as a copper reagent for the preparation of the cuprate. The optimal results were obtained by the following procedure: *m*-bromoanisole in THF was lithiated by *t*-butyl lithium, then the solvent was changed from THF to diethyl ether, followed by the addition of the resulting solution to copper(I) iodide suspended in diethyl ether. The cuprate prepared by the above procedure was added to the α,β-unsaturated ketone **60a** or **60c** in diethyl ether to give the 1,4-conjugated adduct **61c** or **61d** in moderate yield (entries 3, 4).

The stereochemistry of the obtained 1,4-conjugated adduct **61a** was assigned to be the structure shown in Fig. 8 by ^{1}H-NMR, COSY, and NOESY spectra, and a NOE experimental study. The observation of positive NOE enhancement on the proton combinations of $H_{Et} - H_o$, $H_{8ax} - H_o$, and

Table 2 Results of 1,4-conjugate addition of arylcuprates to **60**

Entry	ArLi	Condition of cuprate formation	Substrate	1,4-conjugate addition condition	Product	Yield[a]
1	PhLi(4.0 eq)	CuI(2.0 eq), Et_2O, 0 °C, 1 h	**60a**	Et_2O, 0 °C ~ rt, 1 h	**61a**	51
2	PhLi(4.0 eq)	CuI(2.0 eq), Et_2O, – 20 °C, then – 75 °C, TMSCl(4.0 eq)	**60b**	Et_2O/THF, – 75 °C ~ rt, 2 h	**61b**	30
3	m-bromoanisole(4.0 eq), t-BuLi(8.0 eq), THF, – 70 ~ – 25 °C, then THF → Et_2O at – 20 °C	CuI(2.0 eq), Et_2O, 0 °C, 10 min	**60a**	Et_2O, 0 °C ~ rt, 30 min	**61c**	40
4	m-bromoanisole(4.0 eq), t-BuLi(8.0 eq), THF, – 70 ~ – 25 °C, then THF → Et_2O at – 20 °C	CuI(2.0 eq), Et_2O, 0 °C, 10 min	**60c**	Et_2O, 0 °C ~ rt, 1 h	**61d**	50

[a] isolated yield (%)
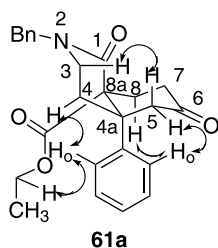
Fig. 8 NOE experiment of compound **61a**
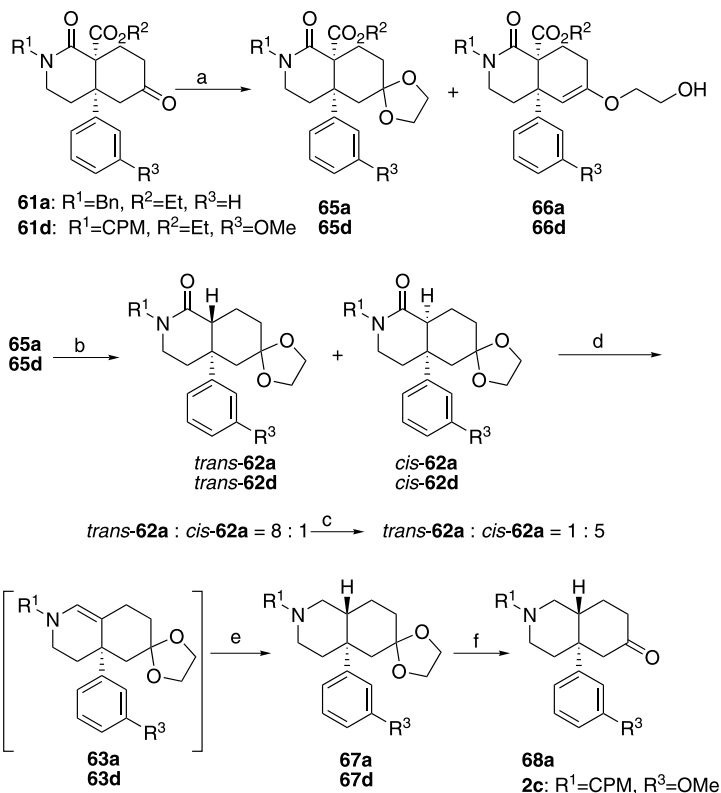
Scheme 9 Nagase's Synthesis: **a** ethylene glycol, p-TsOH · H$_2$O, PhH, reflux, 80% for **65a** with **66a** (20%), 72% for **65d** with **66d** (22%); **b** EtSH, NaH, DMF, 80 °C, 95% (*trans*-**62a** : *cis*-**62a** = 8 : 1), 95% (*trans*-**62d** : *cis*-**62d** = 8 : 1); **c** KOH, EtOH, Δ; **d** DIBALH, THF, 0 °C to rt, then 3N NaOHaq; **e** NaBH$_3$CN, HCl/MeOH, pH 3 $\sim$ 4, – 10 to 0 °C, 74% for **67a**, 80% for **67d** for steps **d** and **e**; **f** 1N H$_2$SO$_4$, rt, 100% for **68a**, 86% for **2c**

H$_{3ax}$ – H$_{5ax}$ strongly indicated that the 1,4-conjugated adduct **61a** should be the *cis*-fused decahydroisoquinoline structure bearing an axial 4a-phenyl group.

With the procedure for constructing the quaternary carbon stereocenter in hand, the conversion of the *cis*-form to the *trans*-form was explored in accordance with the synthetic plan shown in Scheme 9. The ketone moiety of the 1,4-conjugated adduct **61** was protected by an acetal group, followed by decarboxylation of compound **65** using sodium ethylthiolate to yield lactam *trans*-**62** and *cis*-**62** as an 8 : 1 diastereomixture [31]. The reason why the lactam *trans*-**62** was obtained as a major product is that the subsequent protonation after decarboxylation proceeded kinetically. This assertion is supported by experimental results in which the *trans*- and *cis*-lactam diastereomixture (8 : 1) in ethanol was refluxed in the presence of potassium hydroxide to afford a 1 : 5 mixture [15, 32, 33]. The mixture of the lactam *trans*-**62** and *cis*-**62** was reduced with DIBALH, followed by treatment with sodium hydroxide to give bicyclic enamine **63**. The kinetic iminium salt prepared from bicyclic enamine **63** with hydrochloric acid was reduced with sodium cyanoborohydride, leading to the *trans*-decahydroisoquinoline structure [22]. The acetal moiety of the resultant **67** was removed to provide the objective ketones **68a** and **2c**. This method enabled the construction of the *trans*-decahydroisoquinoline structure without an intermediate resembling the neurotoxic MPTP, and in fewer steps.

2.7
Synthesis of Indole Derivatives

The designed compound, indole **1** (R′ = H), was prepared by Fischer indole synthesis (Scheme 1) of ketone **2c** synthesized by the procedure described above with subsequent demethylation. Contrary to our expectation of a δ opioid agonist, the designed compound indole **1** (R = Me, R′ = H), was an antagonist. Nevertheless, compound **69** possessing a fluorine atom at the 7 position is one of indole **1**′s derivatives and showed weak agonistic activity (Fig. 9a). The indoles bearing halogen atoms other than fluorine (chlorine, bromine, and iodine) had no agonistic activity. Moreover, the 8-, 9-, or 10-fluoro indole derivatives also did not show any agonistic activity. From these results, we assumed that the significant agonistic character of the fluoro-substituted compound derives from its hydrogen bonding ability, because of the halogens, only the fluorine atom can form a hydrogen bond. The specific position (only 7-, not 8-, 9-, or 10-) of the substituent for the agonistic activity implies the importance of formation of the hydrogen bond at this position with the δ opioid receptor, which changes the receptor shape and leads to agonistic activity. In other words, this hydrogen-bond forming site, which we call the "fifth pharmacophore", should be necessary for its agonist character. We then designed a more favorable structure for forming a hydrogen bond with the fifth pharmacophore site to give a tighter fit with the receptor. On the basis of the above hypothesis, we designed the decahydroisoquinoline derivative fused quinoline, (±)-TAN-67. (±)-TAN-67 possesses a lone
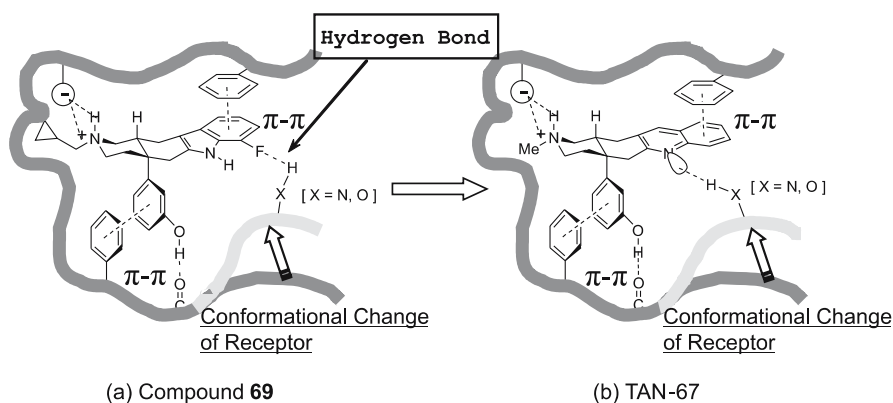
Fig. 9 Binding model for compound 69 (a) and b TAN-67 to the δ opioid receptor

electron pair on a nitrogen atom in the quinoline ring in order to form a hydrogen bond with the receptor more effectively than the 7-fluoro-indole compound **69** (Fig. 9b). The synthesis of (±)-TAN-67 started from ketone **2a** which reacted with *o*-aminobenzaldehyde in the presence of methanesulfonic acid to afford quinoline **70a**, followed by demethylation with potassium propylthiolate (Scheme 10). The *N*-demethyl and the *N*-CPM derivatives of
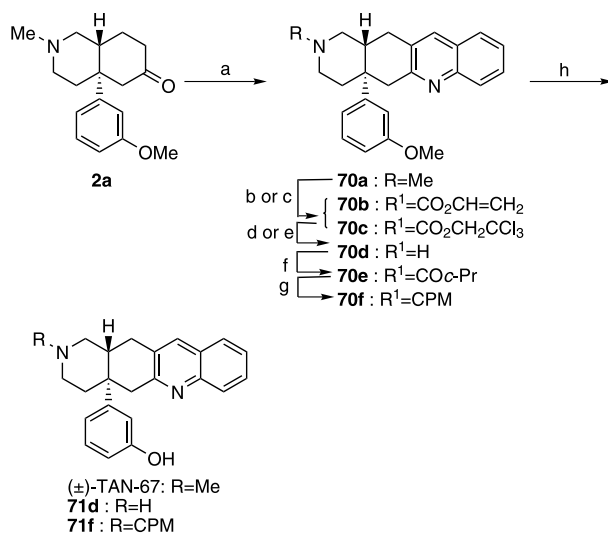
Scheme 10 **a** *o*-C$_6$H$_4$(NH$_2$)(CHO), MeSO$_3$H, EtOH, reflux, 79%; **b** ClCO$_2$CH = CH$_2$, proton sponge, CH$_2$Cl$_2$, 0 °C to rt, 75% for **70b**, **c** ClCO$_2$CH$_2$CCl$_3$, proton sponge, CH$_2$Cl$_2$, 54% for **70c**, **d** HCl/MeOH, rt, **e** Zn, AcOH, rt, **f** *c*-PrCOCl, Et$_3$N, THF, rt, 79% from **70b** for steps **d** and **f**, 60% from **70c** for steps **c** and **e**, **f** DIBALH, toluene, – 55 °C, 92%, **g** *n*-PrSH, *t*-BuOK, DMF, reflux, 74% for (±)-TAN-67, 57% for **71d**, 85% for **71f**

(±)-TAN-67 were also synthesized because it is well known that the 17 nitrogen substituents of the 4,5-epoxymorphinan derivatives, which seemingly correspond to the 2-nitrogen substituent of (±)-TAN-67, have a significant influence on opioid agonistic activities [35]. The N-methyl group of quinoline **70a** was converted to either carbamate **70b** or **70c** with vinyl chloroformate or trichloroethyl chloroformate, respectively, and subsequently reacted with hydrochloric acid/methanol or zinc/acetic acid to provide the N-demethyl derivative **70d**. The N-CPM derivative **70f** was prepared by cyclopropylcarbonylation of the N-demethyl derivative **70d** and subsequent reduction with DIBALH. The N-demethyl and N-CPM derivatives **70d** and **70f** were demethylated with potassium propylthiolate to give the (±)-TAN-67 derivatives **71d** and **71f**, respectively (Scheme 10).

3
Pharmacological Activities of (±) -TAN-67

The opioid receptor binding activities of (±)-TAN-67, its derivatives **71d** and **71f**, and DPDPE, a representative selective peptidic δ opioid receptor agonist, were assessed with a radio-ligand competition assay in guinea pig brain membranes (Table 3) [34, 36]. The Ki value is the index of affinity—the smaller its value, the higher the affinity. The synthesized compounds (±)-TAN-67 and its derivatives **71d** and **71f** showed comparable or higher selectivity for the δ opioid receptor than DPDPE, which is one of the most selective peptidic δ agonists. (±)-TAN-67 showed a higher selectivity for the δ receptor than it did for the μ and κ receptors (with a Ki ratio of 2071 for μ/δ and 1600 for κ/δ).

The opioid agonistic activities of (±)-TAN-67, its derivatives **71d** and **71f**, and DPDPE were evaluated on electrically stimulated guinea-pig ileum (GPI) and mouse vas deferens (MVD) preparations (Table 4) [34, 36]. It is known that μ and κ opioid receptors are predominantly expressed in GPI and the δ receptor is predominantly expressed in MVD [37, 38]. The IC_{50} value is the index of agonistic activity—the smaller its value, the more potent the agonistic

Table 3 Opioid receptor binding

Compound	Ki (nm)			Selectivity	
	δ	μ	κ	μ/δ	κ/δ
(±)-TAN-67	1.12 ± 0.42	2320 ± 720	1790 ± 602	2071	1600
71d	2.41 ± 0.86	452 ± 112	2130 ± 765	188	884
71f	0.90 ± 0.39	175 ± 65	42 ± 15	194	47
DPDPE	4.74 ± 1.35	911 ± 251	undetectable	192	undetectable

Table 4 Opioid agonist activity

Compound	MVD		GPI
	IC$_{50}$ (nM)	NTI DR	IC$_{50}$ (nM)
(±)-TAN-67	6.61 ± 1.25	96.2	26 470 ± 3211
71d	88.7 ± 9.3	165	135 026 ± 11 025
71f	0.25 ± 0.02	30.8	10 733 ± 1357
DPDPE	3.93 ± 0.49	76.5	11 300 ± 1085

activity. The NTI DR is the IC$_{50}$ value of the test compound in the presence of NTI divided by the IC$_{50}$ value of the test compound in the absence of NTI. The NTI DR index shows the extent to which the agonistic activity of the test compound was antagonized by the δ antagonist NTI. The larger the NTI DR value, the more the test compound induced agonistic activity via the δ opioid receptor. Although the *N*-demethyl compound **71d** was a weak agonist, (±)-TAN-67 and the *N*-CPM derivative **71f** showed comparable or stronger agonistic activity than DPDPE.

Morphine, a μ agonist, is well known to possess a methyl group as a 17-nitrogen substituent, and its derivative, *N*-CPM nor-morphine, showed weak analgesic effects itself but antagonized against antinociceptive effects induced by morphine (Fig. 10) [35]. It is also widely known that NTI has a CPM group as a 17-nitrogen substituent and is a δ antagonist but its derivative OMI whose 17-nitrogen substituent is a methyl group is a δ agonist (Fig. 10) [39, 40]. The result that the *N*-CPM derivative **71f** showed stronger agonistic activity than the *N*-methyl derivative (±)-TAN-67 was contrary to our expectation.

Morphin (μ agonist)   Partial agonist

OMI (δ agonist)   NTI (δ antagonist)
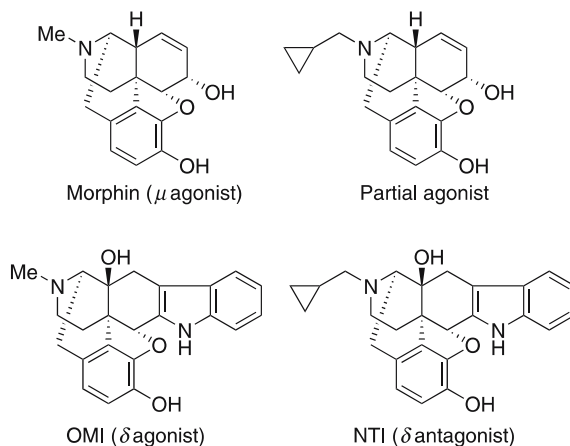
Fig. 10 17-nitrogen substituents of 4,5-epoxymorphinan derivatives and their opioid activities

The experimental finding that the *N*-CPM derivative **71f** was a δ agonist suggests that our working hypothesis for the drug design of a δ agonist is correct: the free rotation of the phenol ring allows the receptor to approach the compound, inducing the agonistic effects. The detailed investigations of the effects of (±)-TAN-67, which had both potent agonistic activity and a high δ receptor type selectivity, showed that the antinociceptive effects induced by (±)-TAN-67 were very weak in spite of the compound's activity in vitro [41]. Each enantiomer of a compound can, in general, induce different pharmacological effects. This is a well-known phenomenon in pharmacology—the incident involving Thalidomide is one of the most infamous and tragic examples. For the next step, we tried to synthesize the optically active compounds (+)- and (−)-TAN-67 to investigate their pharmacological effects.

4
Synthesis of Optically Active TAN-67

In one report, the enantiomers of the racemic compound **73**, whose structure resembles ketone **2a**, were separated by fractional recrystallization of the optically active mandelic acid salts [43]. Although we tried to optically resolve the optically active mandelic acid salts of the racemic ketone (±)-**2a**, no satisfying results were obtained. After several trials, the (+)- or (−)-di-*p*-toluoyl tartrate salt prepared from ketone (±)-**2a** was effectively fractionally recrystallized and finally provided the optically active ketones (+)-**2a** and (−)-**2a** [42]. The chiral ketone (−)-**2a** was converted to compound **73** via compound **72** by thioacetalization followed by desulfurization using Raney nickel
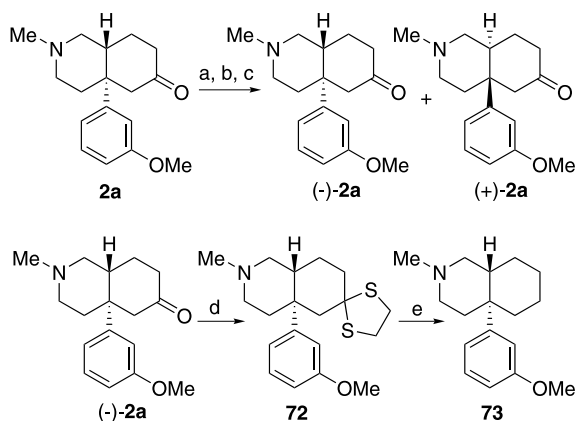
Scheme 11 a (−)- or (+)-di-*p*-toluoyl-L-tartaric acid; **b** fractional recrystallization from MeOH; **c** 5% NaOHaq, 27% for (−)-**2a**, 29% for (+)-**2a**; **d** HSCH$_2$CH$_2$SH, Et$_2$O · BF$_3$; **e** Raney Ni, EtOH, rt, 21% for steps **d** and **e**

(Scheme 11). The specific optical rotation of compound (−)-**2a** derived from the chiral ketone (−)-**2a** agreed with the reported rotation of **73** [43], showing that the absolute configuration of **73** was (4aS, 8aR) and corresponded to that of natural (−)-morphine [42].

5
Pharmacological Effects of (−)-TAN-67

Intrathecal (i.t.) treatment with (−)-TAN-67 showed strong dose-dependent analgesic effects in the mouse tail-flick test (ED_{50} = 17.1 nM/mouse, i.t.), suggesting that the active ingredient producing δ agonist activity was not (+)-but (−)-TAN-67 [36]. The antinociception induced by (−)-TAN-67 was significantly reduced by the treatment with the δ_1 antagonist BNTX, though it was not influenced by the administration of the δ_2 antagonist NTB. This result suggests that (−)-TAN-67 is highly selective for the δ_1 opioid receptor [44]. The term of δ_1 and δ_2 means the subtype of δ opioid receptor. Although some nonpeptidic δ agonists such as SIOM [45] and SNC-80 [46, 47] have been reported, no example is found of a compound such as (−)-TAN-67 showing receptor subtype selectivity.

(−)-TAN-67 has been reported to possess cardioprotective effects. Ischemia of part of a cardiac muscle induces not only necrosis of the muscle but also necrosis of the marginal muscle cell i.e., infarction. The necrosis of the marginal muscle is observed even when the ischemic condition is relieved due to bloodstream recirculation. The administration (infusion) of (−)-TAN-67 reduced the risk of the infarction, and its effect was the strongest among the reported drugs with these effects. The effects induced by (−)-TAN-67 were blocked by treatment with the δ_1 antagonist BNTX, suggesting that the effects of (−)-TAN-67 are mediated by a δ_1 opioid receptor [48]. Moreover, it has also been reported that (−)-TAN-67 showed antiarrhythmic effects via the δ_1 opioid receptor [49].

6
Pharmacological Effects of (+)-TAN-67

The i.t. administration of (+)-TAN-67 induced pain-like nociceptive behaviors, beyond our expectation [36, 44]. This observation implies that (+)-TAN-67 counteracted the analgesic effects produced by (−)-TAN-67. Treatment with (−)-TAN-67 actually reduced the hyperalgesic effects induced by (+)-TAN-67. The weak antinociceptive effect of (±)-TAN-67 in spite of its strong agonistic activities in vitro could result from the fact that both (+)- and (−)-TAN-67 have the opposite effects in vivo. It is worth noting that the pain-like behaviors induced by (+)-TAN-67 were not suppressed by morphine

treatment, suggesting that the hyperalgesia produced by (+)-TAN-67 could become a pain model in which morphine shows no or less analgesic effects. Moreover, the (+)-TAN-67-induced nociception was attenuated by the administration of a GABA agonist, an NMDA antagonist, and a protein kinase C inhibitor, indicating that the hyperalgesia resembled a neuropathic pain [50]. It is also interesting that the pain-like behaviors induced by (+)-TAN-67 are reduced by treatment with a δ or κ agonist.

7
Conclusion

Indole **1** was designed from the selective δ antagonist NTI to obtain a non-peptidic selective δ agonist on the basis of both the message-address concept, which is utilized for the drug design of receptor-type selective ligands in the opioid research field, and the accessory site theory, which gives an account of the structural difference between agonists and antagonists. Ketone **2**, the starting material for the synthesis of indole **1**, was synthesized by a new reduced step method without the neurotoxic intermediate or its derivatives (Nagase's synthesis). Contrary to our expectation, the designed compound **1** showed no agonistic activities. Then a fifth pharmacophore was proposed and TAN-67 was newly designed based on the structure-activity relationship studies on derivatives of compound **1**. TAN-67 was found to be a δ agonist and its active component (−)-TAN-67 showed strong antinociceptive, cardioprotective, and antiarrhythmic effects. Beyond our expectations, its enantiomer (+)-TAN-67 exhibited opposite, nociceptive effects. Although it is well known that the pharmacological effects of each enantiomer are different, it is rare that each enantiomer shows opposite effects as in the case of TAN-67. In the past, when one enantiomer exhibited narcotic properties, WHO has automatically regarded the other enantiomer as a narcotic drug as well. The case of TAN-67 is the first counterexample to this policy, and may lead WHO to change its opinion.

We expected that (−)-TAN-67 will be used for the detailed investigation of both the existence and the pharmacological effects of a δ₁ opioid receptor, and that the (+)-TAN-67-induced nociception may be a unique pharmacological model for the elucidation of pain mechanisms. Moreover, the hyperalgesia produced by (+)-TAN-67 could be one of the neuropathic pain models. We hope that the (+)-TAN-67-induced nociception will be used for the development of analgesics for neuropathic pain, for which morphine indicates little or no effect.

References

1. Sertürner FW (1805) Trommsdorf's J Pharmazie 13:234
2. Gulland JM, Robinson R (1923) J Chem Soc 980
3. Gulland JM, Robinson R (1925) Mem Proc Manchester Lit Phil Soc 69:79
4. Schöpf C (1927) Justus Liebigs Ann Chem 452:441
5. Hughes J, Smith TW, Kosterlitz HW, Forthergill LA, Morgan BA, Morris HR (1975) Nature 258:577
6. Portoghese PS, Larson DL, Sayre LM, Fries DS, Takemori AE (1980) J Med Chem 23:233
7. Delander GE, Portoghese PS, Takemori AE (1984) J Pharmacol Exp Ther 231:91
8. Portoghese PS (1989) Trends Pharmacol Sci 10:230
9. Portoghese PS, Sultana M, Takemori AE (1990) J Med Chem 33:1714
10. Portoghese PS (1991) J Med Chem 34:1757
11. Portoghese PS, Sultana M, Nagase H, Takemori AE (1988) J Med Chem 31:281
12. Portoghese PS, Nagase H, Lipkowski AW, Larson DL, Takemori AE (1988) J Med Chem 31:836
13. Reisene T, Pasternak GW (1996) In: Hardman JG, Limbird LE (eds) Goodman and Gilman's: the pharmacological basis of therapeutics. McGraw-Hill, New York, p 521
14. Nogrady T (1985) In: Medicinal chemistry, a biochemical approach. Oxford University Press, New York, p 68
15. Weller DD, Gless RD, Rapoport H (1977) J Org Chem 42:1485
16. Cantrell BE, Paschal JW, Zimmerman DM (1989) J Org Chem 54:1442
17. Judd DB, Brown DS, Lloyd JE, McElroy AB, Scopes DIC, Birch PJ, Hayes AG, Sheehan MJ (1992) J Med Chem 35:48
18. Liras S, Allen MP, Blake JF (2001) Org Lett 3:3483
19. Kawamura K, Kawai K, Miyamoto T, Ooshima K, Nagase H (1998) Heterocycles 48:267
20. Lock G, Bayer E (1939) Ber 72:1064
21. Lee DL, Morrow CJ, Rapoport H (1974) J Org Chem 39:893
22. Evans DA, Mitch CH, Thomas RC, Zimmerman DM, Robey RL (1980) J Am Chem Soc 102:5955
23. Zimmerman DM, Cantrell BE, Reel JK, Hemrick-Luecke SK, Fuller RW (1986) J Med Chem 29:1517
24. Finch N, Blanchard L, Puckett RT, Werner LH (1974) J Org Chem 39:1118
25. Iijima I, Homma K, Saiga Y, Matsuoka Y, Matsumoto M (1985) Eur Pat Appl 0149534 ((1986) Chem Abstr 104:19570y)
26. Schultz AG, Lucci RD, Napier JJ, Kinoshita H, Ravichandran R, Shannon P, Yee YK (1985) J Org Chem 50:217
27. Posner GH (1972) Organ React 19:1
28. Posner GH (1980) An introduction to synthesis using organocopper reagents. Wiley, New York
29. Corey EJ, Boaz NW (1985) Tetrahedron Lett 26:6019
30. Matsuzawa S, Horiguchi Y, Nakamura E, Kuwajima I (1989) Tetrahedron 45:349
31. Barlett PA, Johnson WJ (1970) Tetrahedron Lett 4459
32. Weller DD, Rapoport H (1976) J Am Chem Soc 98:6650
33. Gless RD, Rapoport H (1979) J Org Chem 44:1324
34. Nagase H, Kawai K, Hayakawa J, Wakita H, Mizusuna A, Matsuura H, Tajima C, Takezawa Y, Endoh T (1998) Chem Pharm Bull 46:1695
35. Casy AF, Pargitt RY (1986) In: Opioid analgesics, chemistry and receptors. Plenum Press, New York, p 30

36. Nagase H, Yajima Y, Fujii H, Kawamura K, Narita M, Kamei J, Suzuki T (2001) Life Sci 68:2227
37. Smith JAM, Leslie FM (1993) In: Hertz A (ed) Handbook of experimental pharmacology 104/I, opioid I. Springer, Berlin Heidelberg New York, p 63
38. Rees DC, Hunter JC (1990) In: Hansch C (ed) Comprehensive medicinal chemistry, Vol. 3. Pergamon Press, Oxford, p 812
39. Portoghese PS, Sultana M, Takemori AE (1990) J Med Chem 33:1714
40. Portoghese PS, Larson DL, Sultana M, Takemori AE (1992) J Med Chem 35:4325
41. Suzuki T, Tsuji M, Mori T, Misawa M, Endoh T, Nagase H (1995) Life Sci 57:155
42. Fujii H, Kawai K, Kawamura K, Mizusuna A, Onoda Y, Murachi M, Tanaka T, Endoh T, Nagase H (2001) Drug Des Discov 17:325
43. Zimmerman DM, Cantrell BE, Swartzendruber JK, Jones ND, Mendelsohn LG, Leander JD, Nickander RC (1988) J Med Chem 31:555
44. Tseng LF, Narita M, Mizoguchi M, Kawai K, Mizusuna A, Kamei J, Suzuki T, Nagase H (1997) J Pharmacol Exp Ther 280:600
45. Portoghese PS, Moe ST, Takemori AE (1993) J Med Chem 36:2575
46. Calderon SN, Rothman RB, Porreca F, Flippen-Anderson JL, McNutt RW, Xu H, Smith LE, Bilsky EJ, Davis P, Rice KC (1994) J Med Chem 37:2125
47. Bilsky JE, Calderson NS, Wang T, Bernstein NR, Davis P, Hruby JV, McNutt WR, Rothman BR, Rice KC, Porreca F (1995) J Pharmacol Exp Ther 273:359
48. Schultz J, Hsu AK, Nagase H, Gross GJ (1998) Am J Physiol 274:H909
49. Fryer RM, Hsu AK, Nagase H, Gross GJ (2000) J Pharmacol Exp Ther 294:451
50. Yajima Y, Narita M, Tsuda M, Imai S, Kamei J, Nagase H, Suzuki T (2000) Life Sci 68:719
51. Nagase H, Fujii H (2006) J Synth Org Chem Jpn 64:371

Tetrahydrobiopterin
and Related Biologically Important Pterins

Shizuaki Murata[1] (✉) · Hiroshi Ichinose[2] · Fumi Urano[3]

[1]Graduate School of Environmental Studies, Nagoya University, Chikusa-ku,
 464-8601 Nagoya, Japan
 murata@urban.env.nagoya-u.ac.jp

[2]Graduate School of Bioscience and Biotechnology, Tokyo Institute of Technology,
 Nagatsuda, Midori-ku, 226-8501 Yokohama, Japan

[3]Institute of Liberal Arts and Sciences, Nagoya University,
 Chikusa-ku, 464-8601 Nagoya, Japan

Abstract Some naturally occurring pteridine derivatives carry out various important metabolic transformations which produce and metabolize essential materials for life as cofactors in all kinds of living organisms. For example, the pteridine derivatives work in biosyntheses of amino acids, nucleic acids, neurotransmitters and nitrogen monoxides and metabolisms of purine and aromatic amino acids in the human body. Based on the mechanisms of the metabolisms, such compounds have long been interested in biological chemistry and medicinal chemistry. Some pteridine derivatives are practically used in chemotherapy or diagnosis for various diseases. In Sect. 1, we briefly review the history of pteridine and the biological significances of naturally occurring pteridine derivatives other than tetrahydrobiopterin, e.g., folic acid, molybdenum cofactor. Recent progress on the analysis and synthesis of tetrahydrobiopterin and its analogues is summarized in Sects 2 and 3. In Sects. 4 and 5, The biosynthesis of tetrahydrobiopterin and its functions in catecholamine and NO biosynthesis are described and Sect. 6 describes diseases caused by the deficiency of tetrahydrobiopterin.

Keywords Biopterin · Catecholamine biosynthesis · Dystonia · Hyperphenylalaninemia · NO biosynthesis · Pterin · Tetrahydrobiopterin

Abbreviations

ATP	adenosine triphosphate
BH4	(6R)-5,6,7,8-tetrahydrobiopterin
CD	circular dichroism
CSF	cerebrospinal fluid
DDATHF	5,10-dideazatetrahydrofolic acid
DHFR	dihydrofolate reductase
DHPR	dihydropterin reductase
DOPA	3,4-dihydroxyphenylalanine
DRD	DOPA-responsive dystonia
FAD	flavin adenine dinucleotide
FDCD	fluorescence detected circular dichroism
FMN	flavin mononucleotide
GCH	GTP cyclohydrolase I
GFRP	GTP cyclohydrolase I feedback regulatory protein
GTP	guanosine triphosphate
H2F	7,8-dihydrofolate
H4F	(6S)-5,6,7,8-tetrahydrofolate
HPLC	high-performance liquid chromatography
LC-MS/MS	liquid chromatography tandem mass spectrometry
MTX	methotrexate
NAD	nicotinamide adenine dinucleotide
NADP	nicotinamide adenine dinucleotide phospate
NOS	nitric oxide synthase
PAH	phenylalanine hydroxylase

PCD   pterin-4a-carbinolamine dehydratase
PKU   phenyl ketonuria
PTPS   pyruvoyltetrahydropterin synthase
SCF   supercritical fluid
SPR   sepiapterin reductase
TH   tyrosine hydroxylase
TPH   tryptophan hydroxylase
TPH$^{-/-}$ mice genetically deficient mice for TPH
TS   thymidylate synthase
XO   xanthine oxidase
XOR   xanthine oxidoreductase

1
Introduction

1.1
History of Pteridine and Pterin

The year 2007 marks the 150th anniversary of the chemistry of pteridine. In 1857, Wöhler and Hlasiwetz individually obtained yellow materials containing the first examples of pteridine derivatives. Approximately thirty years later, Hopkins isolated the first naturally occurring pteridine derivatives **1** and **2** from butterfly (*Pteridae*) wings. In honor of this discovery, designs of butterflies have been chosen as the symbol of pteridine in various symposia and scientific societies. Throughout the long history of the science of pteridine, there have been several momentous discoveries of biologically important derivatives, such as biopterin cofactor, folic acid (vitamin M or B9), molybdenum cofactor and neopterin. The significance of these materials is described in the following sections. Currently, pteridine derivatives are of great interest in a wide variety of fields from basic sciences to chemical industries, biology, pharmacology, medicine and nutrition. The following scientists deserve mention as important contributors to progress in the chemistry and biochemistry of pteridine: A. Albert (Canberra), M. Akino (Tokyo), D. J. Brown (Canberra), M. Goto (Tokyo), S. Matuura (Nagoya), T. Nagatsu (Nagoya), W. Pfleiderer (Konstantz), E. C. Taylor (Princeton), H. Wachter (Innsbruck) and M. Viscontini (Zurich). Thus, chemistry and biochemistry of pteridine have led the
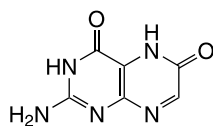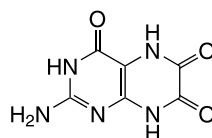
1   **2**

historical advances. Details of the history of the chemistry of pteridine have been summarized in various reviews [1, 2]. There are also useful databases on the biochemistry and clinical chemistry of biopterin and neopterin available for public use on the internet (biopterin: http://www.bh4.org/BH4_Start.asp; neopterin: http://www.neopterin.net/). Current information indicates that future applications of pterins could develop utilities in wider scientific and industrial fields in collaboration with basic chemistry and biochemistry. Unfortunately, for the last decade advances of pterin in chemistry have fallen behind those in biochemistry and molecular biology. At present, the modern science of pterins requires progress that benefits chemistry, thus, it is necessary to focus on the recent scientific advances of pterins. In this chapter, we would like to present a summary of biologically important pteridine derivatives as well as some aspects of the chemistry and biology of tetrahydrobiopterin and its related compounds.

1.2
The Structure of Pterins

Pterins belong to a family of nitrogen heterocyclic compounds and consist of 2-amino-4-hydroxypteridine. Due to keto-enol tautomerism (Eq. 1), pterin exists generally as the 4-keto, i.e. amido, form that is illustrated as 2-aminopteridin-4(3H)one (**4**) rather than the enol form (**3**). Various pterin derivatives have been unexceptionally isolated from almost all kinds of living organisms and almost all such pterin derivatives have carbon substituents on the C(6) position.
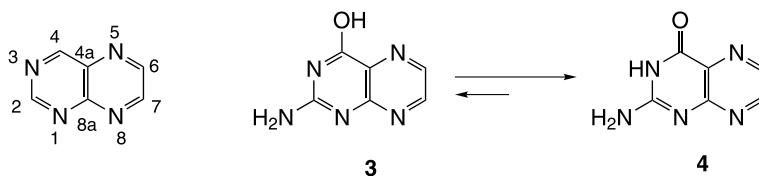
Equation 1

Naturally occurring pterin derivatives have existed in 3 oxidation states: pterin (**4**: aromatic), dihydropterin (e.g., **5–8**) and tetrahydropterin (**9**). In the present review, we do not refer to reduced pterin derivatives with reduced pyrimidine structures. The reduced pterin derivatives, dihydropterin and tetrahydropterin are readily oxidized to the corresponding aromatic form (**4**) under aerobic conditions. Based on the location to which hydrogen atoms are added, 4 kinds of dihydropterin have been defined: 7,8-dihydropterin (**5**), quinonoid dihydropterin (**6**), 5,6-dihydropterin (**7**) and 5,8-dihydropterin (**8**). Of these, only 7,8-dihydropterin derivatives can be stored for long periods under non-aerobic conditions. Indeed, several 7,8-
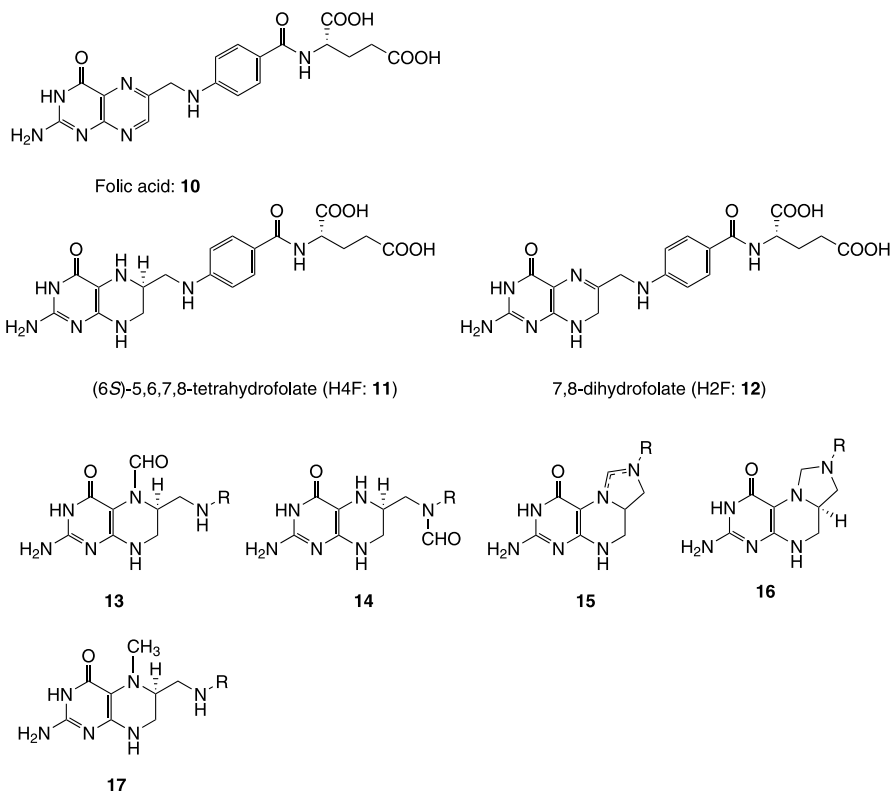
4

5   **6**   **7**   **8**

9
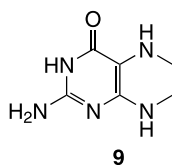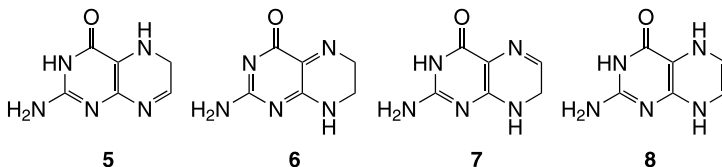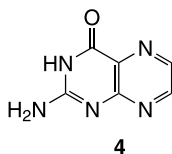
dihydropterin derivatives have been detected or isolated from biological tissues and fluids. Quinonoid dihydropterin derivatives are considered to be transient intermediates in the oxidative transformation of tetrahydropterin to aromatic pterin. The existence of a quinonoid dihydropterin derivative in biological samples has been reported and the details of the chemical characteristics of quinonoid dihydropterin are given in Sect. 3.6. 5,6-Dihydropterin derivatives are considered to be important intermediates in the chemical synthesis of pterin (see Sect. 3.3), but due to electrophilic activation induced by resonance (Eq. 2), they are immediately converted to the tetrahydropterin derivatives produced by the nucleophilic addition of a solvent or intramolecular alcohol group. There are a few examples of 5,8-dihydropterin, however, their chemical or biological importance remains unknown. The reasons for the stability of 7,8-dihydropterin and the instabilities of the other dihydropterins were examined in a theoretical study that found that 7,8-dihydro-6-methylpterin was more than 30 kJ/mol stabilized in comparison with other isomers [3]. It is known that many biologically active pterin derivatives, such as folic acid, molybdenum cofactor and biopterin work as tetrahydropterin derivatives.
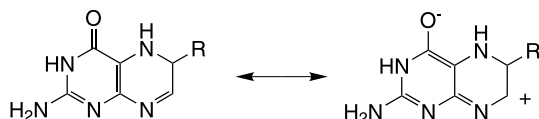
Equation 2

1.3
Folic Acids

Folic acids, the monoglutamate structure which is given as **10,** are widely distributed in almost all kinds of living organisms and are well known as very important cofactors in the metabolic systems of nucleic acids as well as in amino acid biosynthesis. The biologically active form of folic acid is (6*S*)-5,6,7,8-tetrahydrofolate (H4F: **11**). Biosynthesis of **11** is carried out from **10** by the action of dihydrofolate reductase (DHFR) through 7,8-dihydrofolate (H2F: **12**). There are several C_1 homologues of **11** in different oxidation states, such as 5-formyl- (**13**) and 10-formyl- (**14**), 5,10-methenyl- (**15**), 5,10-methylene- (**16**) and 5-methyltetrahydrofolate (**17**) in various metabolic processes. These C_1 derivatives are transformed to each other by biological redox processes and are known as intermediates in C_1 (methyl or formyl) transfer reactions, such as biosyntheses of methionine and thymidine. For example, the biosynthesis of thymidine in mitochondria is illustrated in Scheme 1. Here, H4F (**11**) receives the methylene unit from serine and is converted to **16.** Migration of the C_1 unit from **16** to uridine is carried out by the action of

Folic acid: **10**

(6*S*)-5,6,7,8-tetrahydrofolate (H4F: **11**)   7,8-dihydrofolate (H2F: **12**)

13   **14**   **15**   **16**

17
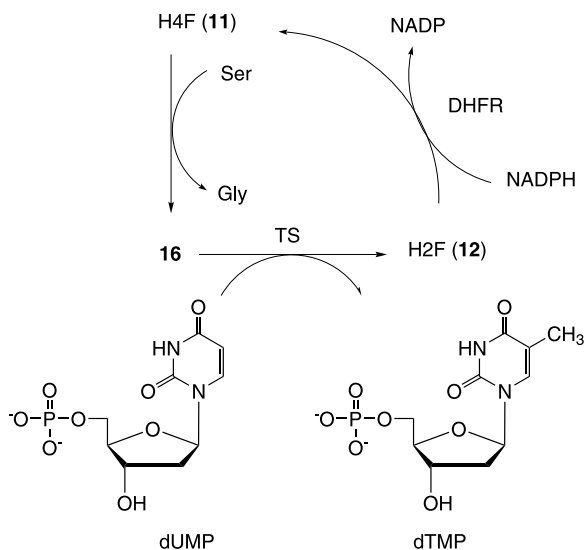
Scheme 1 Thymidine biosynthesis

thymidylate synthase (TS) and affords thymidine and H2F (**12**). Finally, H2F is reduced back to H4F through the action of DHFR. In order to maintain sufficient concentrations of H4F in the living cell, both the biosynthesis and the reproduction processes of H4F carried out by DHFR are essential in all kinds of living organisms.

When the action of DHFR is obstructed, fatal tetrahydrofolate (H4F) deficiency may occur in the living organism to retard the biosynthesis of essential nutrients [4, 5]. Since the effect of H4F deficiency is more severe in cells that are in a growing state than those that are stationary, compounds with an inhibiting activity against DHFR have selective cytotoxic activities toward growing cells. There is a large series of antifolate drugs which have been developed to kill tumor cells based on this concept. Because of their structural similarity, various pteridine derivatives such as methotrexate (MTX: **18**) and 5,10-dideazatetrahydrofolic acid (DDATHF: **19**) are considered to be basic candidates for new antifolate drugs. Sixty years have passed since the development of MTX with anti-tumor activity and it still remains one of the best-selling drugs in the world [6–11]. Recently, the clinical application
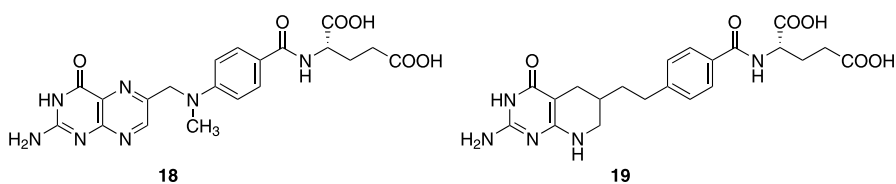
of anti- folate drugs and MTX has been widely expanded to treat various immunodeficiency syndromes and parasitic diseases like rheumatism and malaria [12, 13]. It is known that, due to differences in the gene transcription of DHFR proteins between the human host and the malaria parasite *Plasmodium falciparum*, the synthesis of DHFR in the protozoa is selectively inhibited by anti- folate drugs [14–17]. Thus, the significance of the chemistry of pterin derivatives increases as we learn more about its associated medical and molecular biological sciences.

1.4
Methanopterin

Methanopterin (**20**) is a folate analogue that is isolated from an archaebacteria, *Methanosarcina thermophila*, and the bacteria produces methane from CO_2 under anaerobic conditions [18–24]. In the methane-producing metabolic process (Scheme 2), tetrahydromethanopterin (**21**) is known to work as a cofactor for the reduction of the C_1 unit. Here, **21** accepts a formyl group that originates from CO_2 and transforms it into the formyl
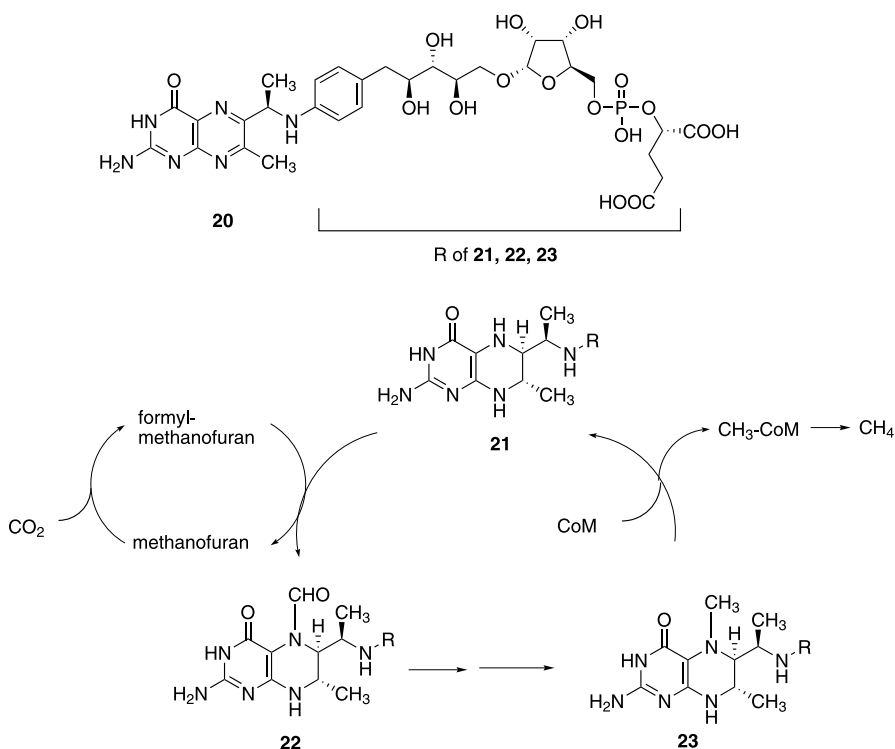
Scheme 2 Methanopterin and methane biosynthesis

derivative **22**. Then, similar to folate metabolism, a process occurs in which the formyl group on the cofactor is reduced to a methyl group through various reduction steps. In the final reducing step to methane, the methyl group of **23** is transferred to another cofactor (CoM).

1.5
Molybdenum Cofactor

Molybdenum cofactor (**24**) is a unique monometallic complex of tetrahydromolybdopterin (**25**) with molybdenum and is found in many different animals as a cofactor for generally distributed xanthine oxidoreductase (XOR) and xanthine oxidase (XO) [25–30]. It is known that these enzymes contain iron and molybdenum in the active site and work in the redox processes of a wide variety of substrates. In the active site of XOR, electrons are passed from an electron-rich substrate to an electron-deficient cofactor, nicotinamide adenine dinucleotide (NAD), through the molybdenum cofactor, metal atoms (molybdenum and iron) and flavin adenine dinucleotide (FAD). In the human body, XOR works in purine metabolism, carrying out the two steps of the oxidation of hypoxanthine (**26**) to xanthine (**27**) and then to urate (**28**), as shown in Scheme 3. Finally, **24** is converted to urothion (**29**) in the metabolic process and is excreted into the urine. XOR also promotes the reversed reduction process that occurs in the presence of nicotinamide adenine dinucleotide hydride (NADH), while XO only carries out the oxidation process. XO requires molecular oxygen as its electron acceptor, which produces toxic active oxygen species like O_2^- and H_2O_2 as a result of the reduction process. These toxic species promote apoptosis. Therefore, there has been interest in **24**, XOR and XO in clinical and biochemical research on various syndromes caused by active oxygens and on uratemia and gout [31]. In addition, the electron transfer mechanism and the unique metal complex
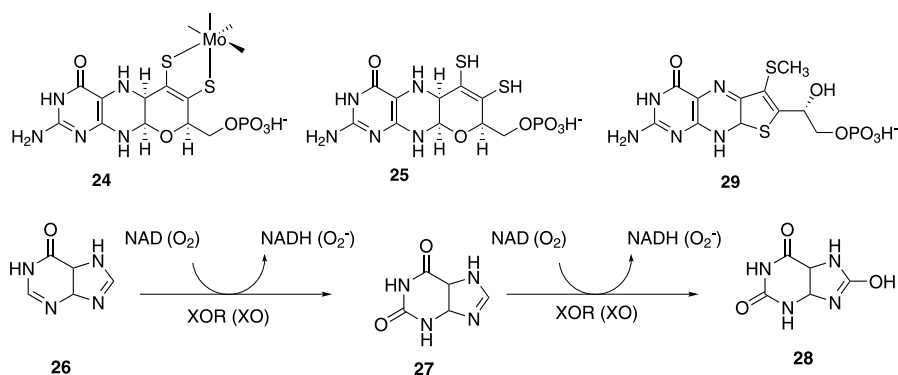
Scheme 3 Molybdenum cofactor in purine metabolism

structure of **24** are of particular interest in bioinorganic chemistry and cata-
lytic chemistry [32–40]. Tungsten cofactor, which is a complex of **25** with
tungsten metal, also exists.

2
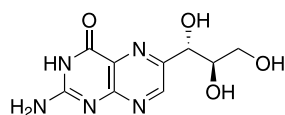# Analysis and Structure of Biopterin and Neopterin

## 2.1
Structure of Biopterin and Neopterin

Both biopterin (**30**) and neopterin (**31**) belong to the family of naturally oc-
curring 6-hydroxypropylpterin and are isolated as major pterins from almost
all higher animals. Due to the existence of 2 chiral centers on the propyl
side chain, 4 diastereomers are possible in biopterin and neopterin, and iso-
mers **32–37** are found and considered to be minor or exceptional pterins. The
absolute configurations of biopterin and neopterin are $1'R,2'S$ and $1'S,2'R$, re-
spectively, and expedient notations of L-*erytho*, for biopterin, and D-*erythro*,
for neopterin, have frequently been used. Following these notations, the di-
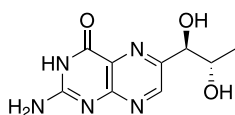
30: Biopterin (L-*erytho*-Biopterin)   **31**: Neopterin (D-*erythro*-Neopterin)
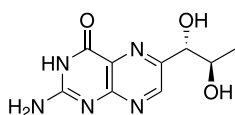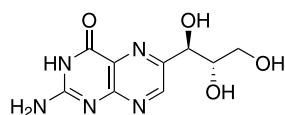
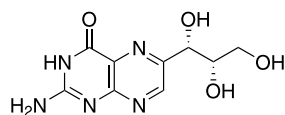**32**   **33**
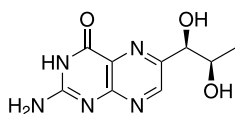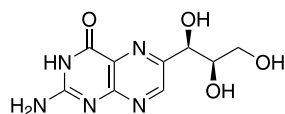
**34**   **35** (D-*threo*)
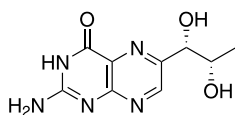
36 (L-*threo*)   **37**

astereomers of biopterin and neopterin with $1'S,2'S$ and $1'R,2'R$ configurations, **34–37**, are named L-*threo* and D-*threo*, respectively. On the other hand, in some papers the names "dictyopterin" and "monapterin" are used for the diastereomeric isomers of biopterin and neopterin with $1'S,2'S$ and $1'R,2'R$ configurations, respectively. In the present review, to avoid unnecessary confusion, we use the names "biopterin" and "neopterin" without the S and R representations, indicating the cases of **30** and **31**, respectively. To refer to the chirality or diastereoisomerism, the other compounds are named on the basis of biopterin and neopterin with the S/R symbol of their configuration, for example, **32**: $(1'S,2'R)$-biopterin, **35**: $(1'R,2'R)$-neopterin, etc.

Structurally unique derivatives of biopterin and neopterin such as glycosides and oncopterin, have been identified from different types of biological samples. There are several examples of the glycoside derivatives of biopterin and neopterin, such as **38** and **39**, which have been obtained from microorganisms and seaweeds, however, their biological functions remain unclear [41–45]. Oncopterin (**40**), which has 1,3-diaminopropane substituent at the C(2) position of biopterin, was isolated as a cancer-specific biopterin derivative from urine samples of patients [46]. Analogous pterin derivatives **41** and **42** were designed on the basis of the structure of **40**; they promote unique structural mutations on higher- order structure of DNA [47, 48].
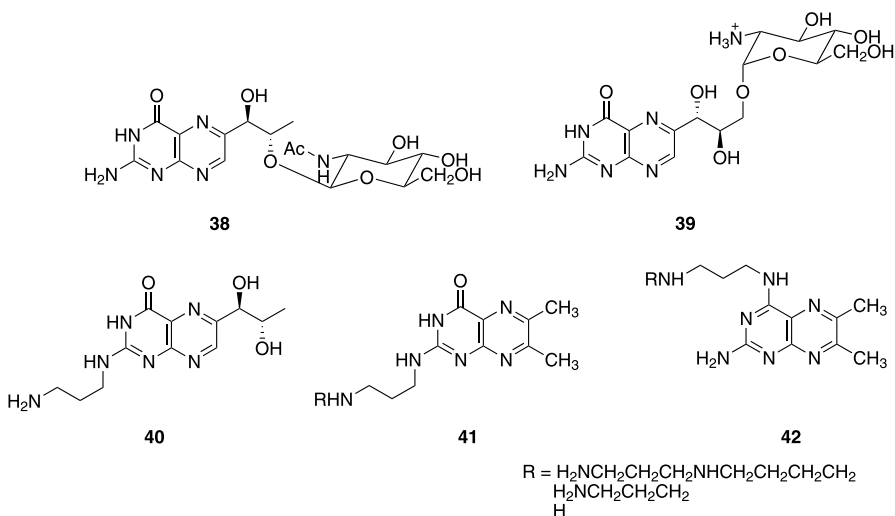
2.2
Analysis of Biopterin and Neopterin by HPLC

Recent progress in the high-performance liquid chromatography (HPLC) technique, e.g., developments in high-performance reversed phase columns and highly sensitive and specific detectors, has contributed to advances in

purification and analysis of naturally occurring pterin derivatives [49–54]. Because pterin derivatives of fully aromatic forms generally emit strong fluorescent light, it is possible to analyze them at very low concentrations using the HPLC system with a fluorescence detector (excitation: λ_{max} 350 nm; emission: λ_{max} 450 nm). The oxidation potential of tetrahydropterin derivatives is generally lower, and tetrahydropterins can be selectively detected by an electrochemical detector. A typical HPLC chart of a mixture of biopterin (**30**), neopterin (**31**), pterin (**4**), 7,8-dihydrobiopterin (**44**) and tetrahydrobiopterin (**43**) is shown in Fig. 1, and we note that retention volumes increase in the sequences of tetrahydropterin, dihydropterin, and aromatic pterin.

Conditions
Column: Inertsil® ODS-3, 3 x 250 mm,
Eluant: 0.1 M NaPO$_4$ buffer (pH 3.0) containing 3 mM sodium octyl sulphate, 0.1 mM EDTA, 0.1 mM ascorbic acid, and 5% MeOH
Flow rate: 0.4 ml/min
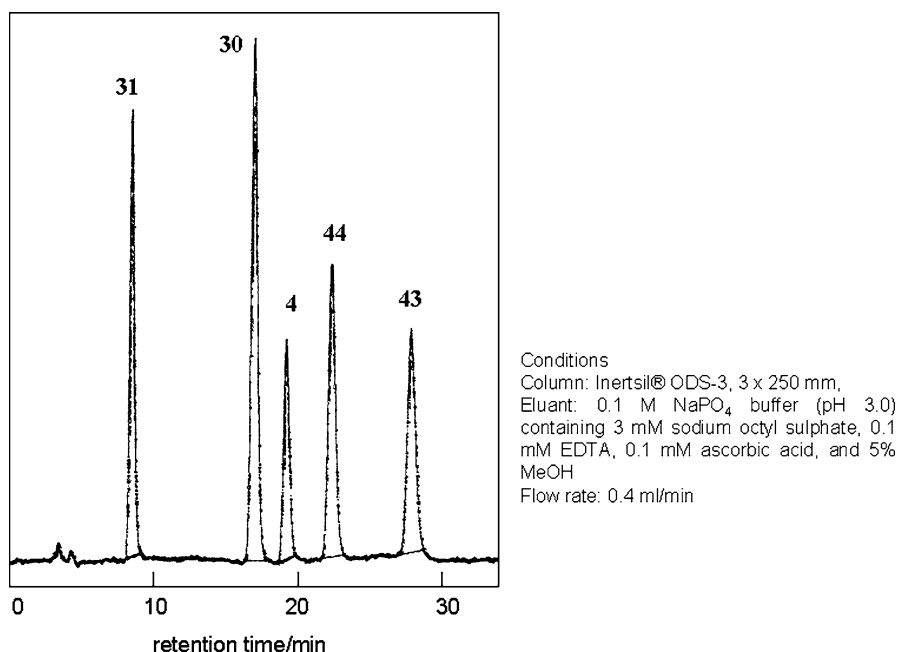
Fig. 1 HPLC analysis of a mixture of biopterins and related pterins

A convenient HPLC technique known as the Fukushima-Nixon method has been widely used for selective analyses of tetrahydrobiopterin and tetrahydroneopterin in biological samples [49]. This method allows the estimation of concentrations of tetrahydropterins based on difference in the concentrations of the corresponding aromatic pterins in the samples, which are prepared in situ by treatment with iodine under acidic and basic conditions. The Fukushima-Nixon method does not require special techniques or equipment for the chemical reaction; the sample is simply subjected to oxidation just before its injection into the HPLC column. For example, tetrahydrobiopterin (**43**) was selectively oxidized to biopterin (**30**) by iodine in the presence of
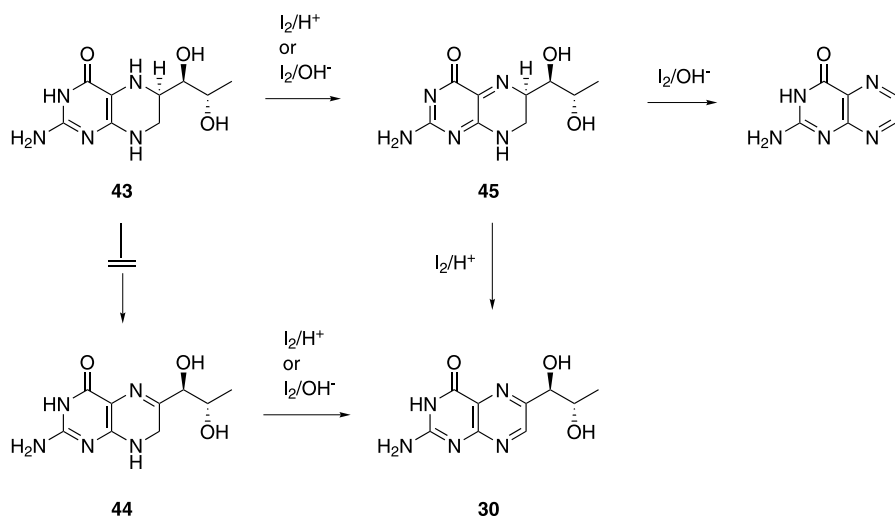
Scheme 4 Oxidation of **43** in the Fukushima–Nixon method

hydrochloric acid (0.1 M) with over 85% recovery. In contrast, the recovery of **30** was less than 13% when oxidation was carried out under basic conditions. More than 80% of **30** was successfully recovered from the oxidation of 7,8-dihydrobiopterin (**44**) under both acidic and basic conditions. As illustrated in Scheme 4, the oxidation of **43** proceeds not through stable **44** but through quinonoid dihydrobiopterin (**45**), in which the dihydroxypropyl side chain readily dissociates in a basic solution. The mechanism of the degradation of **45** is described in Sect. 3.6 below. The concentrations of **44** and **43**, which are given as [**44**] and [**43**], respectively, can be obtained by Eqs. 1 and 2, and here, [**30**], [**30**/*a*] and [**30**/*b*] express the concentrations of **30** observed in the control, acidic oxidation and basic oxidation samples, respectively.

$$[44] = [30/b] - [30] \tag{1}$$
$$[43] = [30/a] - [30/b] . \tag{2}$$

2.3
Circular Dichroism (CD)
and Fluorescence Detected Circular Dichroism (FDCD)

Approximately 30 years ago, when researchers first became interested in the biological significance of tetrahydrobiopterin (**43**), as described in Sect. 4, the absolute configuration of **43** was one of the big problems facing the chemistry and biochemistry of pteridine. The $1'R,2'S$ configuration of the side chain had already been determined by comparison with authentic sugars, however, it was difficult to prove the 6R configuration due to the instability of **43**. In the 1980s, this problem was finally solved by X-ray crystallographic

43   **46**   **47**
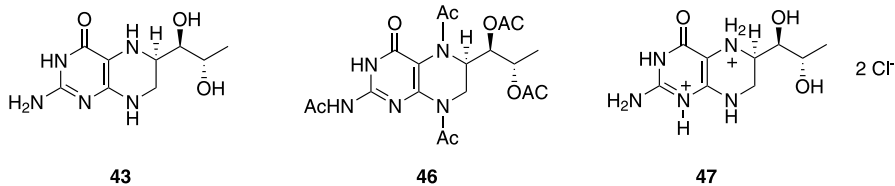
analyses and CD spectra. Single crystals of the pentaacetyl derivative of **43**, that is **46**, was prepared, and X-ray analysis of the crystal confirmed its 6R configuration [55–58]. The chemical derivation of fully acetylated derivatives has been used as a convenient stabilization technique for labile tetrahydropterin derivatives. However, from the viewpoint of practical supply of **43** for pharmaceutical use, it was essential to prepare **43** as a stable form. A few years later, pure crystals of tetrahydrobiopterin dihydrochloride (**47**) were obtained [59]. Tetrahydrobiopterin (**43**) is so stable in the crystal form of **47** that it can be stored for long periods, even under aerobic conditions, and the successful provision of **47** has brought a large breakthrough in its biochemical and pharmaceutical applications.

X-ray analysis of **47** not only directly confirmed its 6R configuration but also uncovered the twisted-chair conformation of the tetrahydropterin ring [60, 61]. The dihydroxypropyl group (R of structure **48**) was found to locate at the quasi-equatorial position and its CD spectrum could be empirically rationalized by its conformational relation with 2-methyl-1,2,3,4-tetrahydronaphthalene. It is predictable that tetrahydropterins with 6R and 6S configurations (**48** and **49**, respectively) afford plus and minus CD signs, respectively, at a λ 265 nm, and the absolute configurations of newly isolated 6-substituted tetrahydropterin derivatives can easily be determined. In contrast, the CD spectra of fully acetylated 6R and 6S acetyltetrahydropterin derivatives, such as **46** and its (6S)-epimer, did not provide general information on their conformations even though these compounds indicated distinct CD spectra. However, the relationships of the CD behaviors of the acetyl derivatives with their absolute structures could be explained on the basis of boat conformations **50** and **51** [63].

There was no obvious explanation for the side-chain chirality of biopterin or its related aromatic pterin derivatives in the CD spectra. This fact requires that structural determination of all newly found pterins must be carried out by comparison with optically active authentic samples. Indeed, almost all compounds have been obtained as aromatic pterins through the exploration of naturally occurring rare pterins and their structures have been generally determined by chemical syntheses from sugar derivatives, as descried in Sect. 3.2. From the viewpoint of characteristic fluorescence emissions, the application of FDCD to the configurational analyses of aromatic pterin derivatives has been carried out in previous studies [64, 65]. Since FDCD analysis of aromatic pterins is approximately 100 times more sensitive than normal
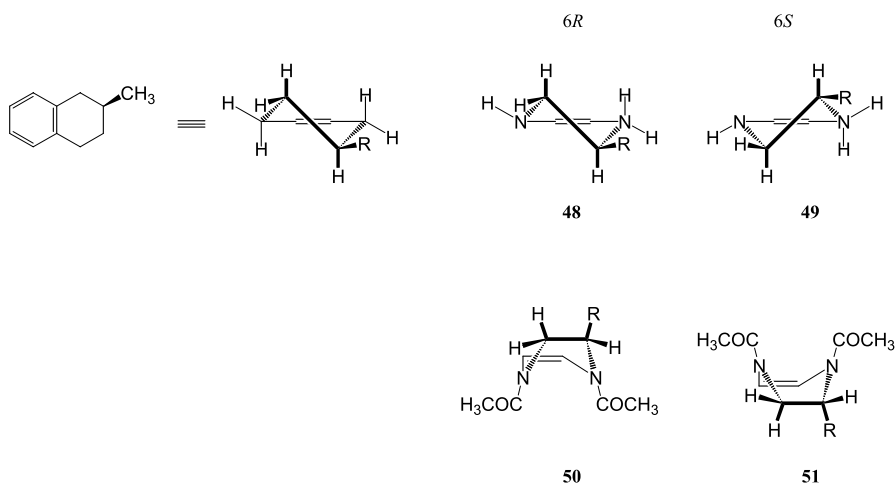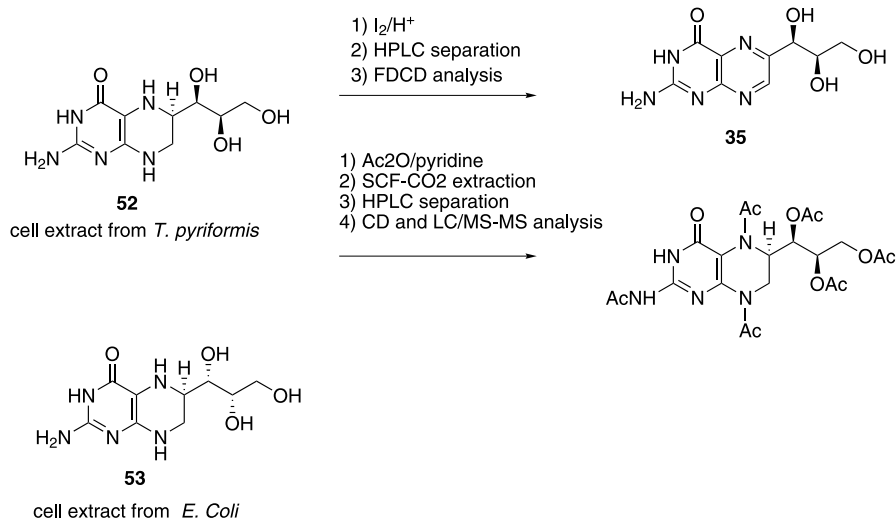
Fig. 2 Conformations of 6R and 6S tetrahydropterins

CD analysis and is insensitive to chiral contaminants, this method is useful in the present analyses of the sample in high dilution. The results of the application of the advanced techniques mentioned herein the analyses of naturally occurring rare pterins are described in the next section.

2.4
Exploration of Naturally Occurring Rare Pterins

There are several exceptional microorganisms in which generally existing biopterin and neopterin are not detected. For example, *Tetrahymena pyriformis* and *Escherichia coli*, both of which have been frequently used in biology laboratories, contain significant amounts of the diastereomeric isomers of neopterin instead of biopterin. The isolation of the pterins from cell extracts of *T. pyriformis* and *E. coli* was carried out by HPLC separation. The structures of the aromatic pterins from *T. pryiformis* and *E. coli*, both of which were isolated after iodine oxidation of corresponding samples under acidic condition, were determined by FDCD spectra as (1′R,2′R)-neopterin (**35**) and (1′S,2′S)-neopterin (**37**), respectively [64, 65]. On the other hand, Fukushima–Nixon HPLC analyses indicated that these pterins exist as tetrahydropterins in the living cell. Freeze-dried cell homogenate of *T. pryiformis* was treated with a mixture of acetic anhydride and pyridine and a fraction including crude acetylated pterin derivative was obtained by supercritical fluid (SCF) CO_2 extraction followed by silica-gel column chromatography. The structure of the hexaacetylated tetrahydroneopterin in *T. pryiformis* was determined as **54**, which was derived from (1′R,2′R,6R)-tetrahydroneopterin (**52**) by CD and liquid chromatography tandem mass spectrometry (LC-

1) I$_2$/H$^+$
2) HPLC separation
3) FDCD analysis

1) Ac2O/pyridine
2) SCF-CO2 extraction
3) HPLC separation
4) CD and LC/MS-MS analysis

52
cell extract from *T. pyriformis*

35

53
cell extract from *E. Coli*

Scheme 5 Isomeric tetrahydroneopterin in *T. pyriformis* and *E. coli*

MS/MS) spectra [66]. In the same manner (Scheme 5), the pterin derivative in *E. coli* was determined as (1*S*,2*S*,6*R*)-tetrahydroneopterin (**53**) [67].

3
Synthesis of Tetrahydrobiopterin and Related Pterins

3.1
Problems in the Synthesis of Tetrahydrobiopterin

In the first year of the 20th century, there was a new finding concerning the synthesis of pteridine, known as Gabriel–Coleman synthesis. In this method, pteridine derivatives are generally produced through the condensation of 2,3-diaminopyrimidine **55** with α-diketone (Eq. 5). One century has passed since the development of Gabriel–Coleman synthesis, however, modern synthetic procedures of tetrahydrobiopterin (**43**) conceptually depend on this synthe-

55
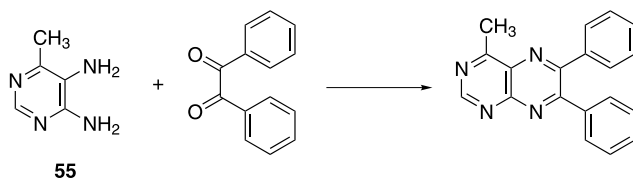
Equation 5
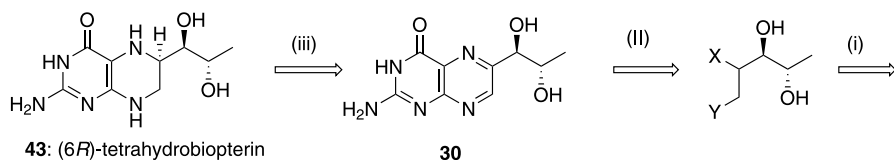
Scheme 6 Retrosynthetic route of tetrahydrobiopterin

sis. Three key processes have been identified in the retrosynthetic path of **43** (Scheme 6): enantioselective synthesis of the side chain, regioselective formation of biopterin (**30**), and stereoselective reduction of **30** to **43**. Recent progress on these steps is described in the following sections.

Alternatively, it is a significant problem that the synthetic precursors of biopterin (**30**) as well as **30** itself are insoluble not only in common organic solvents but also in water under neutral conditions, making it difficult to apply most of the organic reactions available in organic solvents. Additionally, there are few suitable purification procedures for large amounts of insoluble **30** and its intermediates. Because the low solubility problem is caused by the hydrogen-bonding self association of **30**, the introduction of protecting groups which block the hydrogen bond at C(2)-NH$_2$ and/or N(3)-H is effective in preventing the problem. Several examples of protected biopterin derivatives **56** [67] and **57**, which are so easily soluble in common organic solution that they can be applied to organic reactions, have been identified. Protection on the 1′ and 2′ hydroxyl groups, such as dimethyl acetal derivative **58**, is not effective in increasing solubility, however.
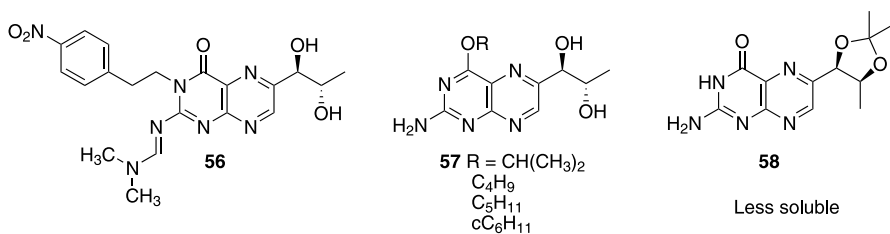

3.2
Enantioselective Synthesis of the Side Chain

In almost all procedures for various chiral 6-hydroxyalkylpterin derivatives as well as those for biopterin (**30**) and neopterin (**31**), preparation of the chiral building block for the C(6) substituent has been carried out using naturally occurring sugar derivatives. This method is conceptually natural since the hydroxypropyl side chains of **30** and **31** are derived from D-ribose of guanosine

triphosphate (GTP) in their biosyntheses. Generally, in chemical synthesis, a C_5 building unit is necessary to construct pterin with a hydroxypropyl side chain and the remaining two carbons are converted to C(6) and C(7) of the pterin ring. Therefore, as shown in Scheme 7, pentose derivatives with exact chiral centers at the C(3) and C(4) positions are necessary to build up the structures. Based on this viewpoint, either D-ribose (59) or D-arabinose (60), both of which are readily available, is suitable to serve as the precursor of 31, and indeed, 31 has been synthesized from 60 on a practical scale.
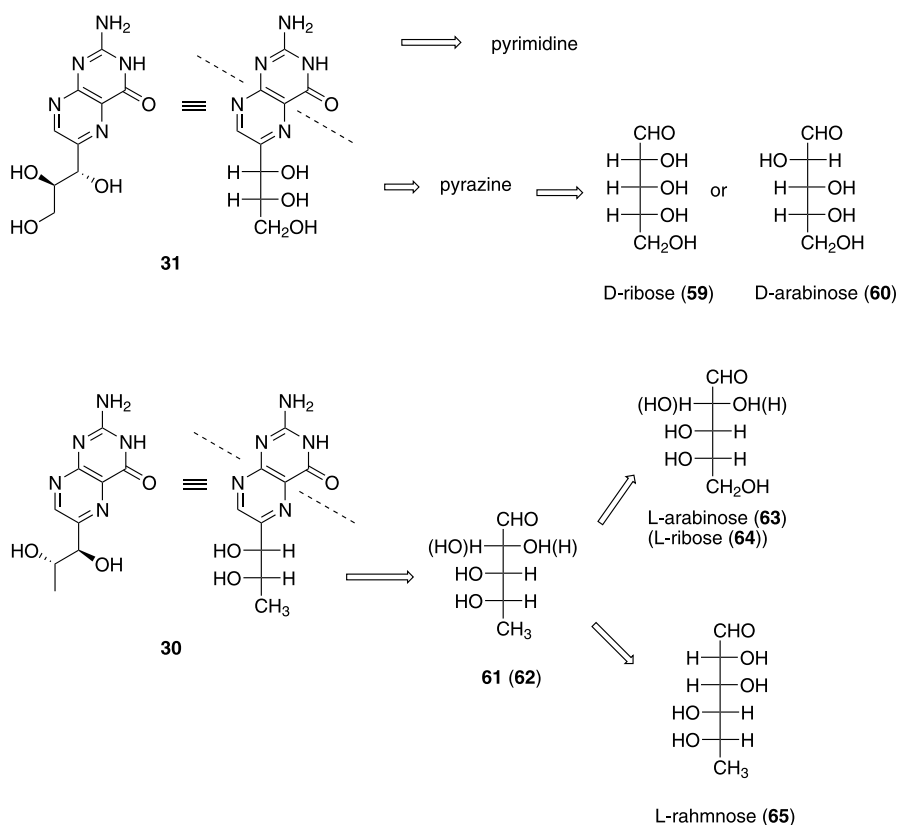

Scheme 7 Relation of biopterin and neopterin to sugars

However, it is rather difficult to search a library of natural sugars for an appropriate sugar derivative for the synthesis of 30. It is necessary to find either 5-deoxy-L-arabinose (61) or 5-deoxy-L-ribose (62), neither of which is available from natural resources [69]. Chemical derivation from easily available sugars is the only way to obtain 61 and 62,however, simple deoxygenation of the terminal alcohol group from L-arabinose (63) and L-ribose (64) generally requires a multi-step process. For example, the deoxygenative transformation
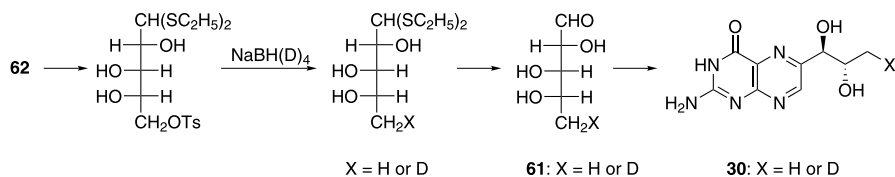
Scheme 8 Deoxygenation of sugar

of **63** to 5-deoxy-L-arabinose (**61**) was carried out by multi-step reactions including protection of the aldehyde terminal, tosylation of the terminal alcohol, hydride substitution by $NaBH_4$ and deprotection of the aldehyde. This method was applied to the synthesis of deuterium-labeled biopterin (X = D), in which the reductive cleavage of the tosylate was carried out by $NaBD_4$ (Scheme 8) [70]. In contrast, L-ribose, which is not obtained from natural resources, is not suitable as a precursor for 5-deoxy-L-ribose (**62**). The precursor **62** could be synthesized from D-isomer **59** using C_1 homologation with a Grignard reagent followed by C_1 cleavage, as illustrated in Scheme 9 [71]. In practice, to avoid such a complicated deoxygenation process, L-rhamnose (**65**), which is a naturally occurring terminal deoxyhexose available on the market, has been chosen as a suitable starting material for **30**. The same chiral structure that appears as the C(2)–C(4) unit of **62** is found in the C(3)–C(6) region of **65**. Therefore, the transformation of **65** to **62** can easily be carried out by conversion of the terminal aldehyde to 1,1-disulfone followed by C_1 degradation under basic conditions, as shown in Scheme 10. Finally, the 5-deoxy-L-arabinose (**62**) thus obtained was converted to acetyl derivatives of phenylhydrazone **66** when it was used in the synthesis of **30** [72–75].
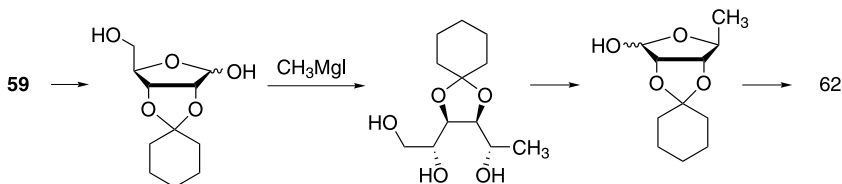
Scheme 9 Preparation of L-deoxyribose
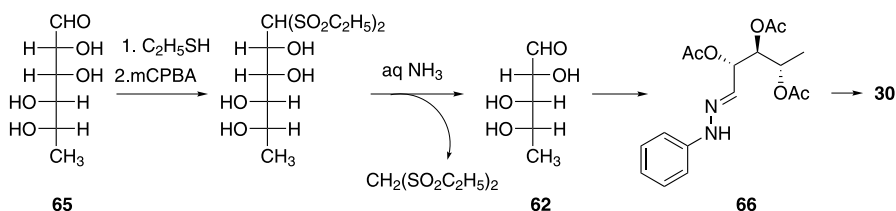
Scheme 10 Practical synthesis of 5-deoxy-L-arabinose
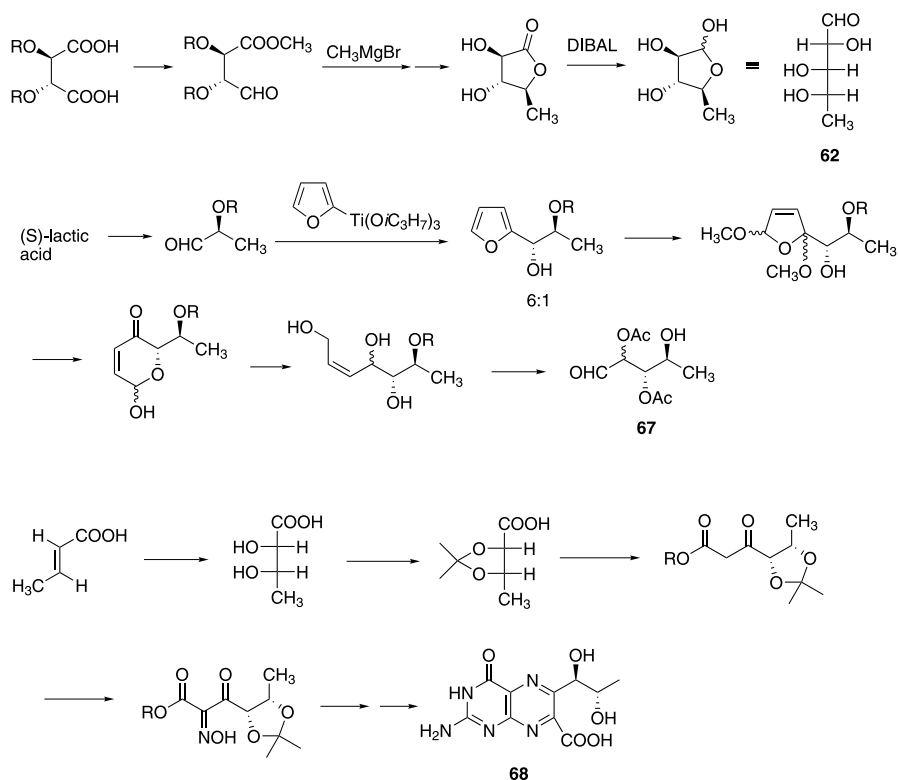
Scheme 11 Examples for stereoselective synthesis of the side chain units

Various attempts to synthesize biopterin independent of naturally occurring sugars have been carried out (Scheme 11). L-Tartalic acid and (S)-lactic acid were converted to 5-deoxy-L-arabinose (**62**) and its derivative (**67**), respectively [76–78]. However, these procedures required multiple steps and cannot be replaced by the procedure using L-rahmnose (**65**). The stereoselective process of biopterin 7-carboxylic acid (**68**) starting from *E*-2-butenoic acid, which is a bulk industrial chemical, looked attractive because the process is thoroughly independent of natural chiral resources, however, it is not applicable to the synthesis of biopterin (**30**) [79].

3.3
Regioselective Formation of Biopterin by Pyrazine Ring Formation

The application of Gabriel–Coleman synthesis to the synthesis of biopterin (**30**) is reliable, however, it has a serious problem in that the condensation of the pyrimidine precursor with asymmetrically substituted sugar derivatives is sometimes less regioselective or even nonregioselective. For example,

it is generally possible to produce both isomeric 6-methylpterin (**70**) and 7-methylpterin (**71**) in the reaction of triaminopyrimidine **69** with methylglyoxal. Furthermore, the simple Gabriel–Coleman synthesis is not satisfactory for the synthesis of 6-substituted pterin because the major product of the reaction is **71** [80, 81]. There is a difference in the electron densities of the two amino groups with respect to the condensation because the electron withdrawing effects of pyrimidine are not identical (Scheme 12). The amino group at the C(5) position is more electron-rich (nucleophilic) than that at the C(6) position. When an asymmetrically substituted dicarbonyl compound, such as 2-ketopropanal, reacts with **69**, the coupling between the more nucleophilic NH_2 at C(5) and the more electrophilic aldehyde preferably occurs in the first step, giving the imine intermediate **72**, which was cyclized to **71**.
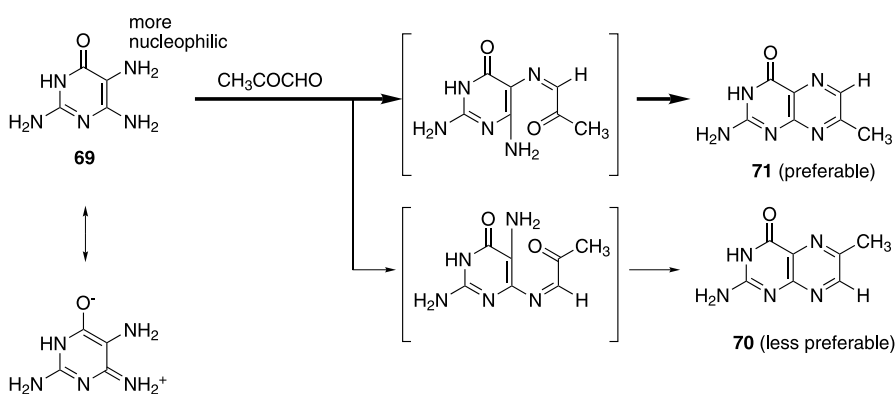
**Scheme 12** Nonregioselective reaction

However, the fact that the coupling reaction between reactive amino and carbonyl groups occurred preferably in the first stage suggests a valuable idea for designing regioselective cyclization. In the precursor of the α-dicarbonyl compound, if the carbonyl group which is converted to the C(6) carbon is more reactive than the other, cyclization would selectively proceed to the 6-substituted pterin. Indeed, a regioselective reaction of **73** with 2,3,4-pentantrione (**74**) (Scheme 13) occurred to give 6-acetyl-7-methylpteridine (**75**), which was used as a precursor in methanopterin synthesis [82]. Here,
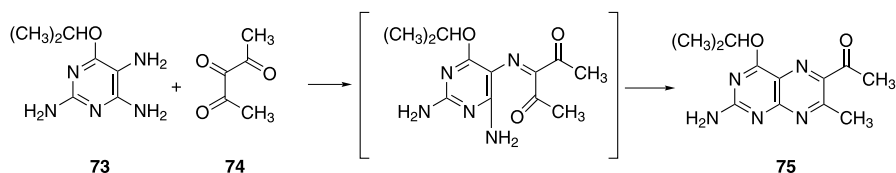
**Scheme 13** Regioselective pterin formation

the coupling reaction of electron-rich NH_2 on C(5) with the most electron-deficient carbon (C(3)) was preferable to afford the intermediate.

Based on this concept, various equivalents for the α-dicarbonyl compounds were used. Among them, phenylhydrazone derivatives of sugars were identified as particularly important precursors for the synthesis of naturally occurring 6-substituted pterins because they could be easily prepared from optically active sugars. In practice, large-scale syntheses of biopterin (30) and neopterin (31) were accomplished by Gabriel–Coleman synthesis using phenylhydrazone derivatives of the corresponding pentose. The reaction proceeded regioselectively and the mechanism was explained by the following intramolecular rearrangement (Scheme 14). The hydrazone 66 was rearranged to α-aminoketone derivative 76 (Amadori rearrangement) and the pterin-forming condensation initiated from the coupling reaction with 76 gave the imine intermediate 77. Tautomeric rearrangement in 77 afforded phenylhydrazone again, and this was cyclized to the 5,6-dihydropterin derivative 78 [72–75]. The acetyl groups of 66 were used to prevent side-chain cleavage during the cyclization.
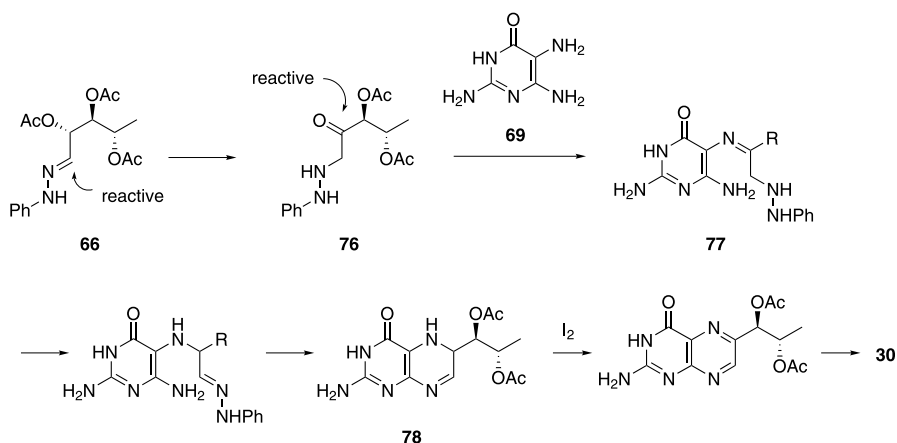
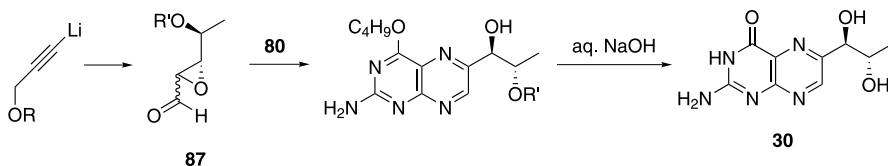**Scheme 14** Selective ring formation of biopterin

α,β-Epoxyaldehyde (79), a modified sugar derivative, could be used in Gabriel–Coleman-type cyclization instead of α-ketoaldehyde because the epoxide group was rather electrophilic [83]. Based on the mechanism of Gabriel–Coleman synthesis, the major cyclization product of protected pyrimidine 80 with 79 was expected to be 7-substituted pteridine. However, as shown in Scheme 15, the reaction regioselectively gave the 6-substituted pteridine, 5,6-dihydro-6-1′-hydroxyalkylpteridine (81), which existed as the tetrahydropteridine derivative of the methanol adduct (82). Oxidation of 81 by treatment with iodine and formic acid, followed by deprotection by aqueous NaOH, gave 6-hydroxyalkylpterin (83) [84].
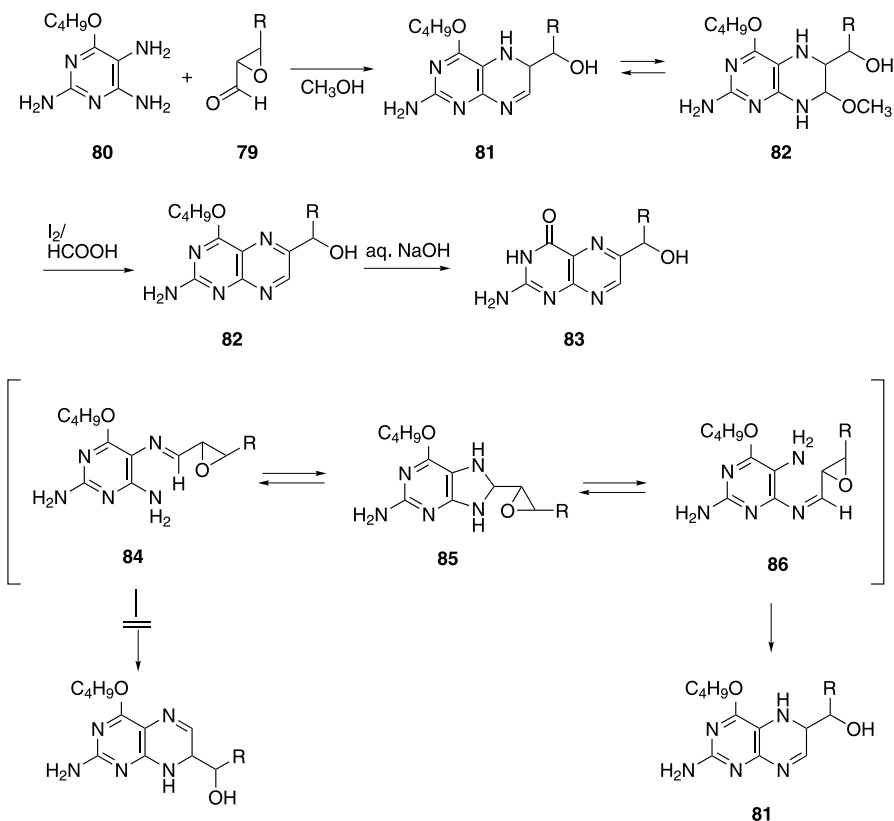
**Scheme 15** Pterin-forming condensation with epoxyaldehyde

In the first step of the reaction, the predicted coupling reaction between the reactive centers, C(5)–NH$_2$ and aldehyde, occurred to give **84**. Because the nucleophilicity of C(6)–NH$_2$ is not strong enough to induce the ring-opening attack to **84**, nucleophilic addition of the amino group to the C=N bond occurred instead, yielding the tetrahydropurin intermediate **85**. The isomeric imine intermediate **86** was formed by the ring opening of **85** and the pteridine-forming ring-opening by reactive C(5)–NH$_2$ gave **81**. This reaction was applied to the synthesis of biopterin (**30**), as shown in Scheme 16 [84].
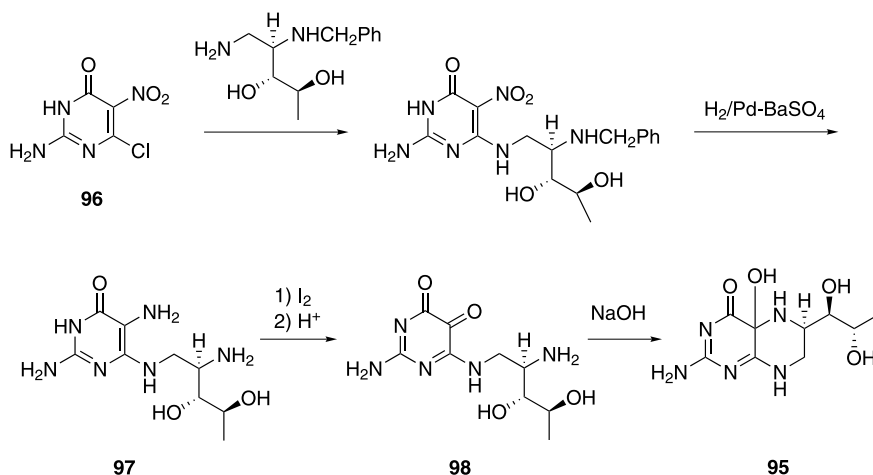

Scheme 16 Synthesis of biopterin

The optically active precursor **87** was prepared by combination of usual synthetic transformations and the butyl protective group which could be easily removed by alkaline hydrolysis made the substrate and intermediates soluble in organic solvents and applicable to usual purification by silica-gel column chromatography. Therefore, there are various opportunities to apply modern synthetic reactions to this pteridine synthesis.

Since nitroso and nitro group were considered to be precursors of amino groups, nitrosopyrimidine and nitropyrimidine were employed to the regioselective synthesis of pterin through stepwise pyrazine ring formation (Scheme 17) [85]. The reaction of 6-amino-5-nitrosopyrimidine (**88**) with phenylacetaldehyde in the presence of base was carried out through stepwise pyrazine ring formation to selectively give 6-phenylpterin derivative **89**. Here, the reactive amino group, C(5)–NH$_2$, of the pyrimidine substrate was masked, and the first coupling occurred between C(6)–NH$_2$ and aldehyde to give the intermediate **90**. In the second step, the condensation of the active methylene group with the nitroso group in **90** regioselectively yielded **89** [86]. Because of the existence of a strongly electron-withdrawing nitro group, the N(8) nitrogen atom of pteridine was brought to the pyrimidine by nucleophilic C – N bond-forming substitution. The reaction of 6-chloro-5-nitropyrimidine **91** with α-aminoketone **92** afforded the 6-aminopyrimidine intermediate **93**, and the reduction of the nitro group of **93** (X = O) to the amino group (X = H) followed by C = N bond-forming cyclization gave 6-substituted 7,8-dihydropteridine **94** [87].
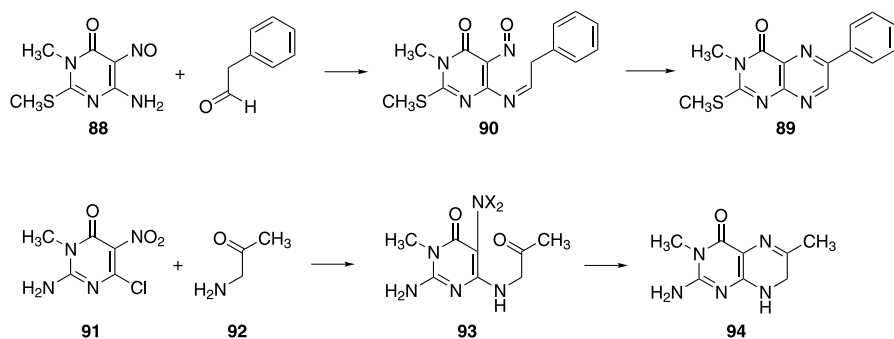
Scheme 17 Regioselective pterin formation

Stepwise pyrazine ring-formation using 5-nitropyrimidine was applied to the synthesis of 4a-hydroxytetrahydrobiopterin (**95**), which is an interesting intermediate in the metabolism of aromatic amino acids (see Sect. 5.2). As illustrated in Scheme 18, the 5-aminopyrimidine **97** prepared from chloronitropyrimidine **96** by nucleophilic substitution followed by catalytic hydrogenation was oxidized under acidic conditions to *o*-quinone derivative **98**.

Scheme 18 Synthesis of 4a-hydroxytetrahydrobiopterin

Finally, the intramolecular cyclization of **98** under basic conditions gave **95** and its 6-methyl and propyl derivatives [88, 89].

3.4
## Synthesis of Pterin by Pyrimidine Ring Formation

Pyrimidine-forming condensation in pyrazine intermediates is another pteridine synthetic method (Eq. 6) [90, 91]. It is important for this method to selectively prepare asymmetrically substituted pyrazine precursors **99** suitable for 6-substituted pteridine. Similar methods, which were used in the regioselective Gabriel–Coleman synthesis, were employed in the synthesis of the precursor. For example, the pyrazine precursor **100** of $(1'R,2'R)$-neopterin (**37**) synthesis was selectively prepared from D-xylose (Scheme 19) [92]. The reaction of α-ketooxime **101** with aminocyanoacetate followed by the reduction of pyrazine N-oxide **102** gave **100**. The cyclization of **100** with diethyl acetal of urea afforded **37**. The significance of this procedure was not clear in the practical synthesis of biopterin (**30**), however, pyrimidine ring formation methods have been used for the syntheses of biologically interesting pteridine derivatives. For example, urothion (**29**) and its related compound were synthesized from **103** by the reaction with guanidine (Scheme 20) [93, 94].
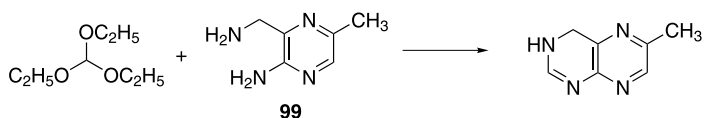

**Equation 6**
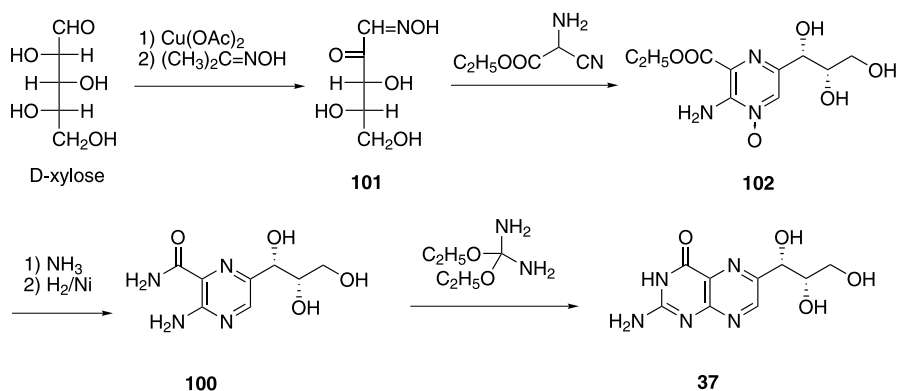
Scheme 19 Pyrimidine ring formation
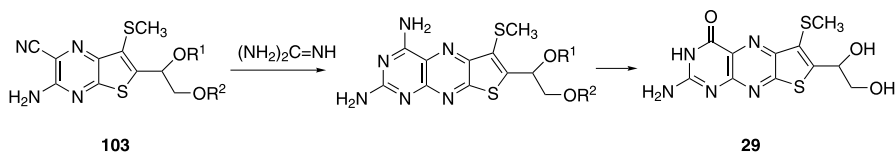
Scheme 20 Synthesis of urothion

The palladium (II)-catalyzed coupling reaction of bromopyrazine deriva-
tive **104** with acetylene derivatives afforded the corresponding alkynylpyr-
azine intermediates **105**, which were transformed to 6-alkynylpterin **107**
through **106**. The acetylene derivative reacted with 6-chloropterin **108** under
similar conditions to give **107** (Scheme 21) [95–98]. 6-Alkynylpterin **109** was
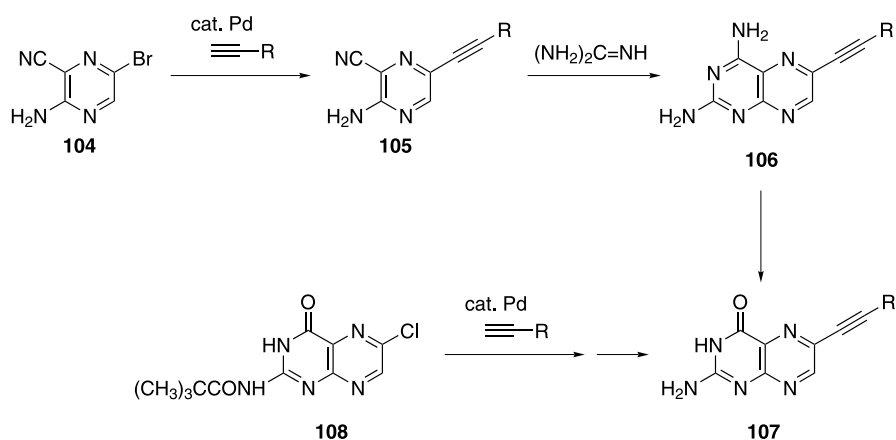
Scheme 21 Synthesis of 6-alkynylpterin using palladium catalyzed coupling

X = (CH₃)₃CCO
Cp = η⁵-cyclopentadienyl
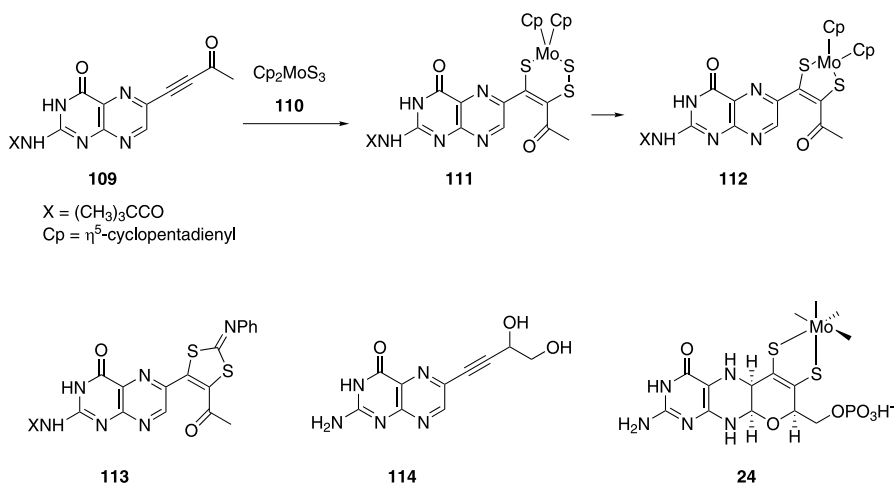
Scheme 22 Synthesis of molybdenum cofactor

converted to **111** and **112**, which are model compounds of molybdenum co-factor (**24**), by the action of the η^5-cyclopentadiene complex of molybdenum **110** (Scheme 22). Similarly, the related compounds **113** and **114** were synthesized from **109**. The palladium-catalyzed coupling reaction was employed to the synthesis of antifolate DDATHF (**19**).

3.5
Stereoselective Reduction of Biopterin to (6*R*)-Tetrahydrobiopterin

The reduction of pteridine to tetrahydropteridine was generally carried out by the action of various chemical reductants, such as NaBH$_4$ and LiAlH$_4$, and catalytic hydrogenation over palladium or platinum. In order to increase the biological usefulness of (6*R*)-tetrahydrobiopterin (**43**) for the purpose of pharmaceutical and clinical use, a provision of large amounts of isomerically pure **43** is required. Only 2 methods exist, neither of which is suitable to prepare isomerically pure **43** from biopterin (**30**) on a large scale. (6*R*)-and (6*S*)-tetrahydrobiopterin, **43** and **115**, respectively, can be separated by HPLC using a strong cation-exchange column [60, 62, 99]. Another possibility is stepwise reduction through 7,8-dihydrobiopterin (**44**), which is known to be an intermediate in the reduction process of **30**. Dihydropterin **44** can be isolated when the reduction is carried out under milder conditions, such as under Zn/aq. NaOH or NaS$_2$O$_3$ [100], and further reduction to **43** was performed by enzymatic reduction with DHFR (Scheme 23) [55, 57, 101]. Due to the poor solubility and high instability of **30**, reduction to tetrahydrobiopterin was used to carry out the reaction in aqueous acidic solution. Although the yield of the hydrogenation of **30** was generally high, the stereo-
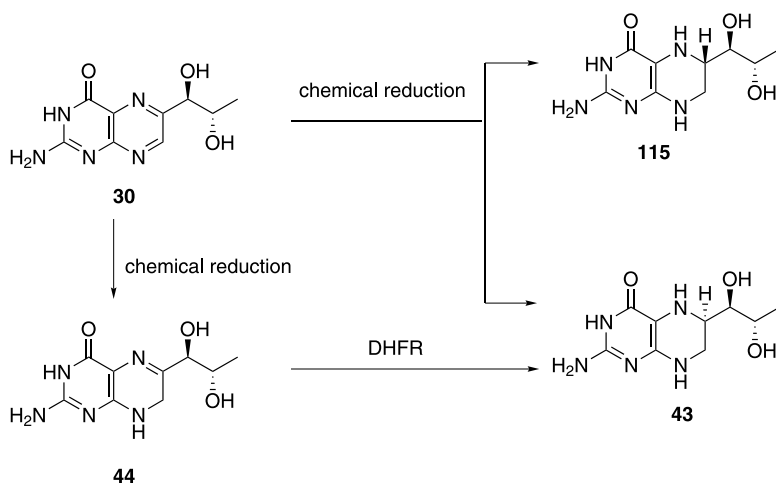
Scheme 23 Reduction of biopterin

selectivity was not satisfactory. For example, catalytic hydrogenation of **30** under an atmospheric pressure of hydrogen over PtO_2 at pH 2 gave a mixture of **43** and **115** at a ration of ca. 2:1 [102]. The catalytic hydrogenation under basic conditions was not taken into consideration to a significant extent because the conditions retard the rate of reduction while accelerating the oxidative degradation of the product. However, the *R/S* stereoselectivity was significantly improved when catalytic hydrogenation over PtO_2 was carried out in a basic solution. In an alkaline phosphate buffer solution (pH 10.8), **30** was reduced to **43** at 8:1 selectivity and a large amount of isomerically pure (6*R*)-tetrahydrobiopterin was obtained as crystals of diammonium salt (**47**) upon treatment with HCl (Scheme 24) [60].
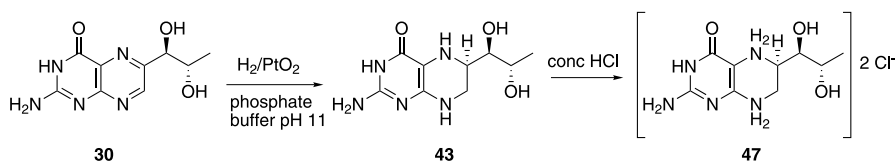

**Scheme 24** Practical synthesis of biopterin

3.6
Quinonoid Dihydrobiopterin and 4a-Hydroxytetrahydrobiopterin

Quinonoid (6*R*)-dihydrobiopterin (**45**) was expected to be a labile compound which readily isomerizes to 7,8-dihydrobiopterin (**44**). When a so-

lution of (6R)-tetrahydrobiopterin (**43**) in high concentration was oxidized by the action of hydrogen peroxide and potassium iodide in the presence of hydrochloric acid, **45** precipitated out as ammonium salt [103, 104]. Despite the expected instability, the **45** thus obtained was so stable in the solid phase that it could be stored for long periods. However, it decomposed immediately when it was dissolved in a buffer solution. Depending on the pH of the solution, there were 3 major decomposition processes of **45**, as given in Scheme 25. The expected isomerization to **44** was observed as the major pathway only under neutral conditions. Under basic conditions, the formation of pterin **4** was predominant over isomerization to **44**, and this degradation contributed significantly to the Fukushima–Nixon HPLC method mentioned above in Sect. 2.2. The disproportionation of **45** to an equimolar mixture of **30** and **43** occurred at pH 3.5. The reduction of **45** to **43** was carried out not only by the action of the enzyme (Sect. 5.2), but also nonenzymatically by common chemical reducing agents such as $NaBH_4$, ascorbic acid and NADH. Since the isomerization of **43** to the epimer **115** was not observed, the chemical reduction was deemed to have occurred not from **44** but directly from **45**. In a solution of $NaHSO_3$, **45** was stabilized as the adduct **116**, and **45** was recovered when HSO_3^- was removed by oxidation.
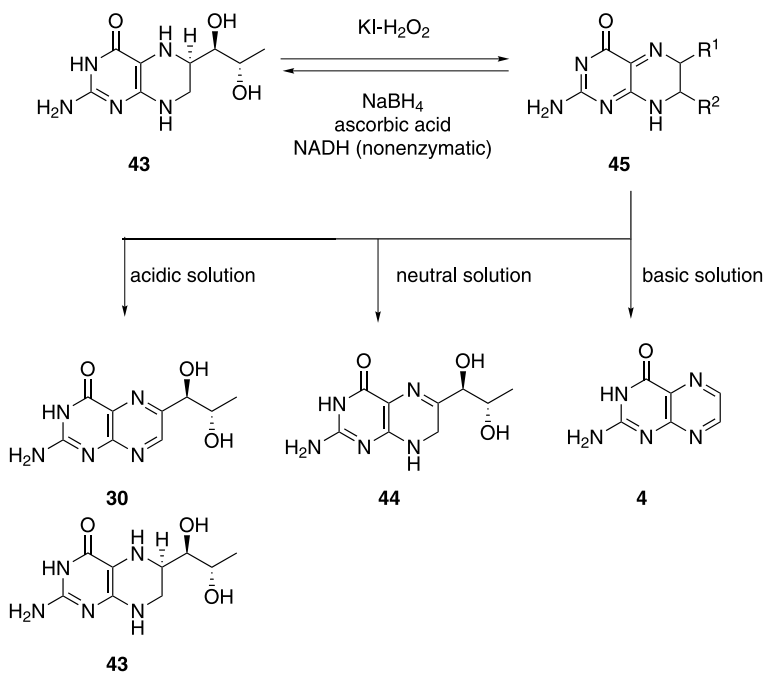
**Scheme 25** Quinonoid dihydrobiopterin
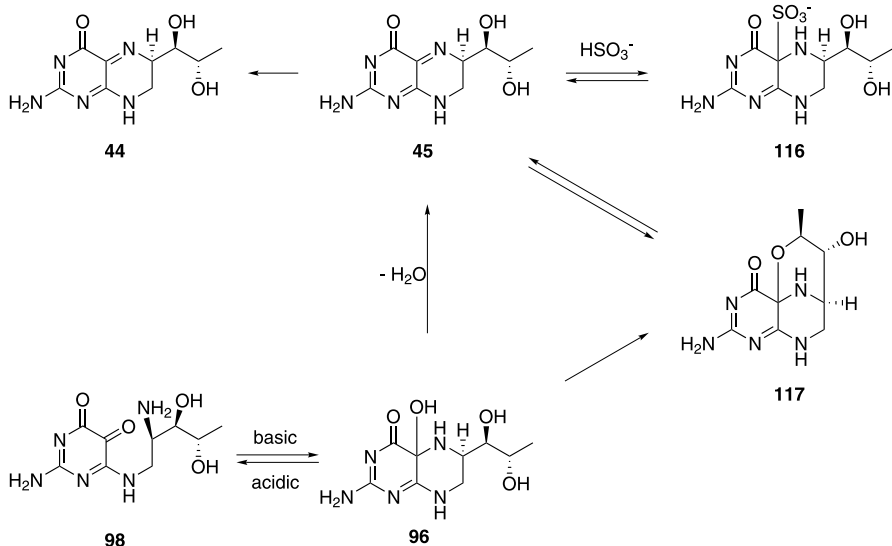
Scheme 26 Quinonoid dihydrobiopterin and 4a-hydroxytetrahydrobiopterin

In combination with the findings on quinonoid (6R)-dihydrobiopterin (**45**), the success of the preparation of the other key intermediate, 4a-hydroxytetrahydrobiopterin (**96**), with a short lifetime contributed to the investigation on the aromatic amino acid hydroxylation process (Sect. 4.1) [88, 89, 104]. Under basic conditions, the precursor **98** cyclized to **96**, and the degradation of **96** to **44** proceeded through **45** and the tetrahydropterin derivative **117** (Scheme 26). The fact that the first dehydroxylation step of the degradation, **96** to **45**, readily occurred nonenzymatically together with the structural resemblance in **96**, **116** and **117** would suggest new targets for chemical investigation.

3.7
Sepiapterin and (6R)-Pyruvoyltetrahydropterin

Sepiapterin (**118**) was isolated from various insects such as *Drosophia melanogaster*, *Bombyx mori* and *Lucilia cuprina* as a yellow eye pigment and its structure was determined as (R)-7,8-dihydro-6-lactoylpterin [105–111]. Related 6-acyl-7,8-dihydropterin derivatives such as deoxysepiapterin (**119**) and sepiapterin-C (**120**) were isolated together with **118** [108, 112]. Because **118** is a side-product in biosynthesis of (6R)-tetrahydrobiopterin (**43**), **118** are distributed over almost all animals. Chemical synthesis of sepiapterin (**118**) was incidentally performed by air oxidation of **43** [111, 113, 114], while to carry out systematic synthesis of 6-acyl-7,8-dihydropterin as well as **118**, was rather difficult. For example, only a few methods of describing the syn-

118 **119** **120**
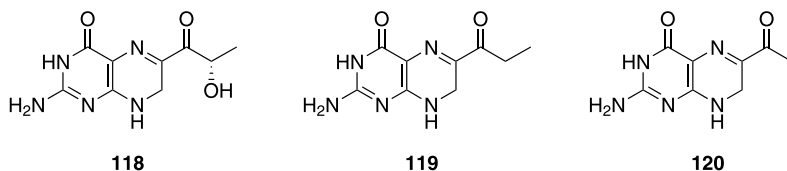
thesis of **119** and **120** exist. 6-Acyl-7,8-dihydropterin was synthesized by the partial reduction (see Sect. 3.5) of the aromatic derivative (**121**), which was prepared by the following methods: acylation of pterin and oxidation of 6-hydroxyalkylpterin. The acylation of pterin was performed by reaction with α-ketobutyric acid in the presence of thiamine [115] or with propanal under radical conditions (Scheme 27) [116], and it is necessary for regioselective acylation to block the undesired C(7) position. On the other hand, chemoselective oxidation of the hydroxyalkyl group to the acyl group was difficult, because there are many possibilities in oxidation of 6-hydroxyalkylpterin, e.g., side-chain cleavage and formation of N-oxides. Ruthenium(IV) catalyzed oxidation of 6-hydroxyalkylpteridines (**81**) selectively proceeded to give 6-acylpteridines (**122**), which were transformed to **121** and **123** [117].
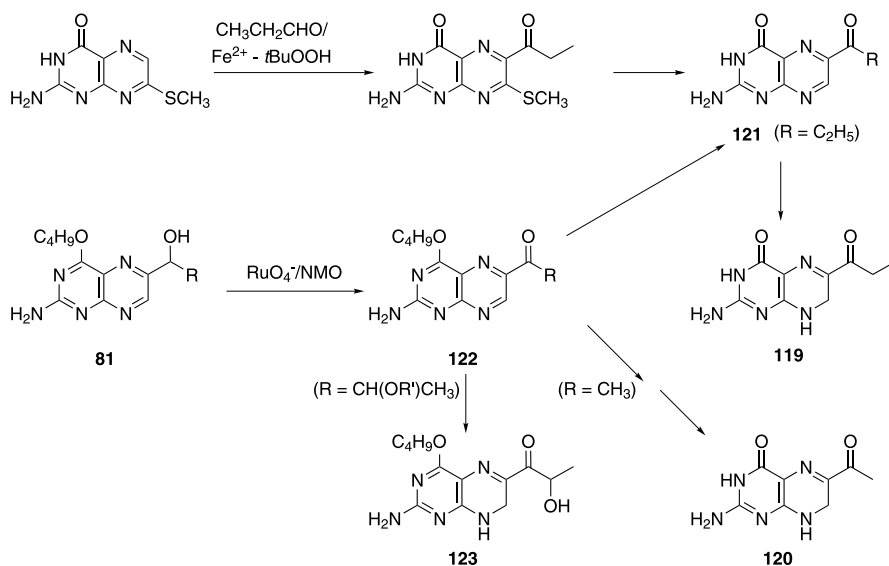
Scheme 27 Synthesis of deoxysepiapterin

Sequential keto-enol tautomeric isomerization (Eq. 7) could convert **118** to the tetrahydropterin derivative, the structure of which is widely accepted as (6R)-pyruvoyltetrahydropterin (**124**). Contrary to the importance of **124** in the biosynthesis of tetrahydrobiopterin (**43**) (Sect. 5.1), thus far, only a few
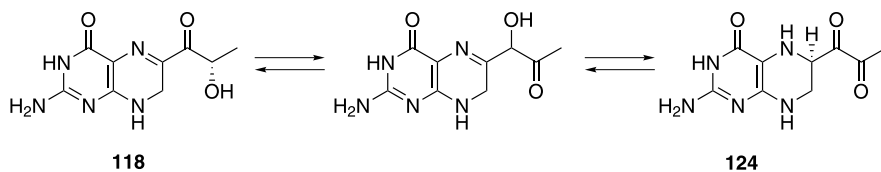
Equation 7

chemical investigations on **124** prepared in situ by an enzymatic method have been carried out by only using biochemical and analytical (HPLC, NMR and MS) methods [118–121]. Since either synthesis or isolation of **124** has not been successful, chemical properties and the proposed structures of these compounds are unclear. Theoretical studies on **124** predicted the structure and stability, and the potential of **124** is only slightly higher than the tautomeric isomer, sepiapterin (**118**) [3, 118].

4
Biological Action of (6*R*)-Tetrahydrobiopterin (BH4)

4.1
BH4 as a Cofactor for Aromatic Amino Acid Hydroxylase

One of the best characterized physiological functions of (6*R*)-tetrahydrobiopterin (BH4, **43**) is the action as a cofactor for aromatic amino acid hydroxylases (Scheme 28). There are three types of aromatic amino acid hydroxylases; phenylalanine hydroxylase [PAH; phenylalanine monooxygenase (EC 1.14.16.1)], tyrosine hydroxylase [TH; tyrosine monooxygenase (EC 1.14.16.2)] and tryptophan hydroxylase [TPH; tryptophan monooxygenase (EC 1.14.16.4)]. PAH converts L-phenylalanine (**125**) to L-tyrosine (**126**), a reaction important for the catabolism of excess phenylalanine taken from the diet. TH and TPH catalyze the first step in the biosyntheses of catecholamines and serotonin, respectively. Catecholamines, i.e., dopamine, noradrenaline and adrenaline, and serotonin, are important neurotransmitters and hormones. TH hydroxylates L-tyrosine (**126**) to form L-DOPA (3,4-dihydroxyphenylalanine, **127**), and TPH catalyzes the hydroxylation of L-tryptophan (**128**) to 5-hydroxytryptophan (**129**). The hydroxylated products, **127** and **129**, are decarboxylated by the action of aromatic amino acid decarboxylase to dopamine (**130**) and serotonin (**131**), respectively.

In 2003, Walther and Bader discovered a new TPH isoform from the study on TPH$^{-/-}$ mice (mice genetically deficient in TPH) [123, 124]. They found the amount of serotonin in the brain of homozygous TPH$^{-/-}$ mice was unchanged, although, the amounts of serotonin in the peripheral tissues were almost depleted in the knockout mice. They searched another TPH in the
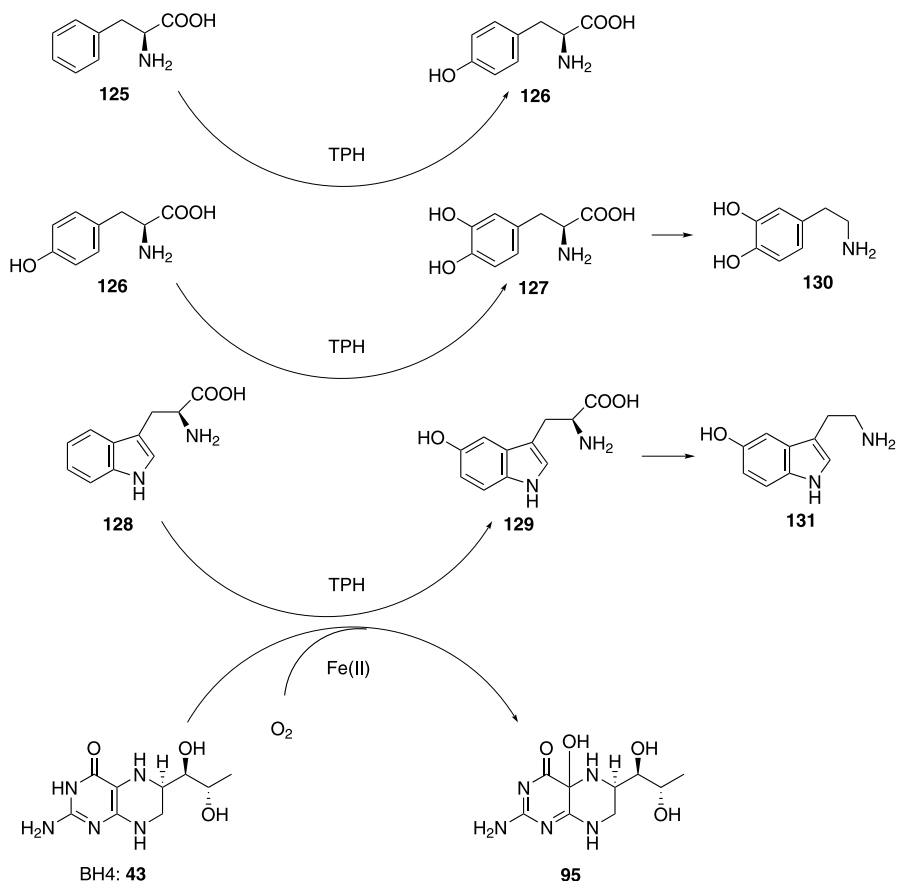
Scheme 28 (6R)-Tetrahydrobiopterin in hydroxylation of aromatic amino acids

mouse genome through the sequence homology with the previously identified TPH (now called TPH1), and found a brain-specific isoform of TPH, referred to as TPH2. Human TPH1 and TPH2 share 72% sequence homology and have high sequence identity within the COOH-terminal catalytic domain.

PAH, TH and TPH are highly homologous enzymes. These enzymes catalyze a hydroxylation reaction of aromatic amino acids that requires reduced pterin cofactor **43**, molecular oxygen, and iron (Scheme 28). Iron is present at the active sites of the enzymes. Ferrous iron (Fe(II)) is essential for the catalysis, although, the iron was found to be in the ferric form (Fe(III)) when the enzymes were purified from tissues or cells. The ferric iron at the active site of the enzymes was found to be reduced to the ferrous form by BH4 [125]. Thus, BH4 serves a bi-functional role for aromatic amino acid hydroxylases; one is the reduction of iron at the active sites from the ferric form to the ferrous form and the other is an electron donor for the hydroxylation reaction.

4.2
BH4 as a Cofactor for Nitric Oxide Synthase

In 1989, BH4 was found to be a cofactor for nitric oxide synthase (NOS) [126, 127]. BH4 is also involved in dimerization of NOS, as NOS is catalytically active in a homodimer structure. Three isoforms of NOS exist; neuronal NOS (NOS 1), inducible NOS (NOS 2) and endothelial NOS (NOS 3). BH4 is essential for all NOS isoforms. The NOS isoforms share approximately 50–60% sequence homology. Each NOS polypeptide is comprised of oxygenase and reductase domains. An N-terminal oxygenase domain contains iron protoporphyrin IX (heme), BH4 and an arginine binding site, and a C-terminal reductase domain contains flavin mononucleotide (FMN), and a reduced nicotin-amide adenine dinucleotide phosphate (NADPH) binding site.

NOS catalyzes two sequential monooxygenase reactions. First, NOS hydroxylates L-arginine (**132**) to generate an enzyme-bound intermediate, N-hydroxy-L-arginine (**133**). Then, **133** is further oxidized to generate nitric oxide (·NO) and citrulline (**134**) [128] (Scheme 29).
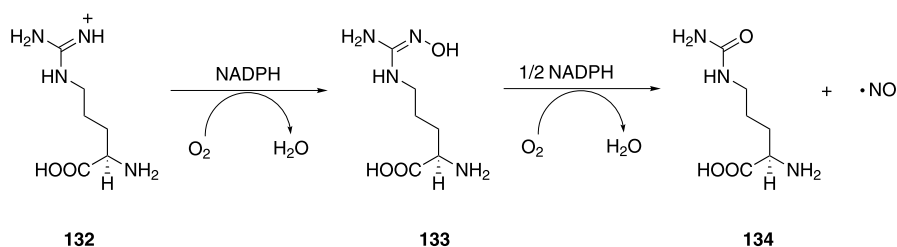
Scheme 29 The reaction catalyzed by NO synthase

Affinities between NOSs and BH4 are stronger than those between aromatic amino acid hydroxylases and BH4, so the purified NOS from animal tissues still contain 0.2–0.5 BH4 molecules per heme moiety [128]. BH4 tightly binds to endothelial and neural NOSs with dissociation constants in the nanomolar range, and this binding is reported to stabilize the dimeric structure of NOS [129–131], whereas aromatic amino acid hydroxylases do not have BH4 in the proteins. BH4 functions as a one electron donor to a heme-dioxy enzyme intermediate. The BH4 radical remains bound in NOS and is subsequently reduced back to BH4 by an electron provided by the NOS reductase domain [128].

4.3
BH4-Dependent Regulation of the TH Protein

Sumi-Ichinose et al. found that the TH protein content in the brain, especially at the nerve terminals, was significantly decreased in BH4-deficient mice pro-

duced by disruption of the second gene for the biosynthesis of BH4 [132]. Interestingly, the protein amount of TPH, which, like TH, utilizes BH4 as a cofactor, was unaffected. The TH protein level was recovered by repeated administration of BH4. The findings suggested that the intracellular concentration of BH4 regulates the level of TH protein in the cell.

Urano et al. found that preincubation of recombinant human TH with a nearly stoichiometric amount of BH4 resulted in irreversible inactivation of TH in spite of its cofactor role, whereas oxidized biopterin, which has no cofactor activity, did not affect the enzyme activity [133]. They showed that TH was inactivated by BH4 in competition with the binding of dopamine at concentrations far less than the K_m value toward BH4. Sequential addition of BH4 to TH resulted in a gradual decrease in the intensity of the fluorescence and CD spectra without changing their entire profiles. Sedimentation analysis demonstrated the association of TH molecules with each other in the presence of BH4, and studies using gel-permeation chromatography, turbidity measurements and transmission electron microscopy demonstrated the formation of amorphous aggregates with a large molecular weight following the association of the TH proteins. The results suggest that BH4 greatly accelerates the aggregation of TH at concentrations less than the K_m value [133].

BH4 acts bifunctionally in the reaction with TH. One function is the reduction of iron at the active site from the ferric to the ferrous state and the other is hydroxylation of the substrate by acting as an electron donor [125, 134]. The TH and ferric iron complex, designated as TH-Fe(III) in Scheme 30, reacts with both catecholamines and BH4. Because the affinity for both compounds is comparable in magnitude, their intracellular concen-
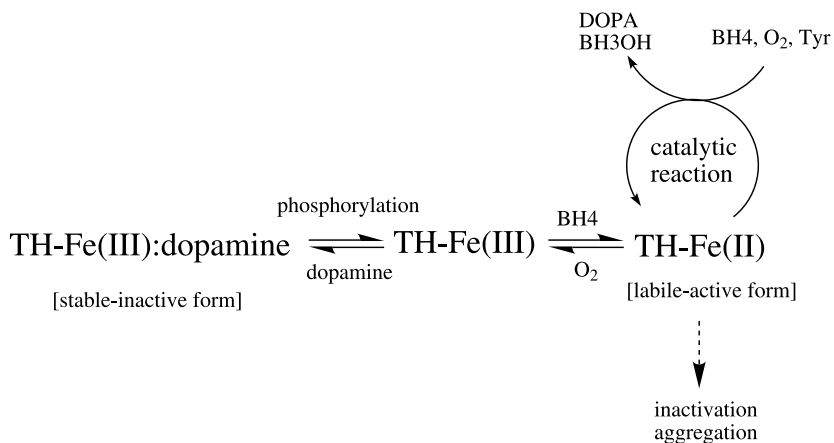
Scheme 30 Proposed mechanism for regulating the amount of TH protein by BH4 and catecholamines

trations would be important determinants for the fate of TH-Fe(III). When TH-Fe(III) reacts with catecholamine, the complex is stable and protected from pterin-mediated inactivation until TH is phosphorylated. When TH-Fe(III) reacts with BH4, ferric iron is reduced to its ferrous form and ready for the catalytic reaction. At this point, if the intracellular BH4 concentration ([BH4]) is high enough for the reaction, [BH4] $> \sim K_m$, TH catalyzes the hydroxylation reaction, generating DOPA from tyrosine (Scheme 30). Because the K_m values of phosphorylated TH toward BH4 were shown to be around 10–$30 \mu M$ [135, 136], more than $10 \mu M$ BH4 would be necessary for efficient catalysis. Indeed, the intracellular concentration of BH4 in the striatum was assumed to be approximately $10 \mu M$, i.e., around the K_m value [137]. When the concentration of catecholamine becomes high enough to bind to the iron at the active site, TH would form a stable complex with dopamine, thus halting the catalytic reaction. However, when the BH4 synthesis is suppressed and the concentration of BH4 is decreased to less than the K_m value, [BH4] $< K_m$, the hydroxylation reaction hardly proceeds. Since BH4 can still react with TH to make the unstable complex TH-Fe(II), even at a concentration less than the K_m value, the TH protein would be inactivated and aggregated. This aggregated TH would be degraded rapidly in the cell, most likely by the ubiquitin-proteasome system [138] or it may accumulate as insoluble aggregates. As a result, the amount of TH protein would be decreased when the intracellular concentration of BH4 is decreased.

5
# Biosynthesis of BH4 and Related Metabolic Processes

5.1
The de novo Pathway

BH4 is synthesized in vivo by three sequential reactions by GTP cyclohydrolase I (GCH; EC 3.5.4.16), pyruvoyltetrahydropterin synthase (PTPS; EC 4.6.1.10), and sepiapterin reductase (SPR; EC 1.1.1.153) (Scheme 31).

GCH catalyses the hydrolytic release of formate from GTP (135) followed by cyclization to dihydroneopterin triphosphate (136) [139]. GCH is the rate-limiting enzyme for the biosynthesis of BH4 (43), and the cellular BH4 content is regulated mainly by the activity of this enzyme.

Various hormones and cytokines are known to induce the expression of the GCH gene in neural, lymphocytic and endothelial cells, and in different cell lines, resulting in an increased BH4 content [140–144]. At the post-transcriptional level, BH4 was shown to inhibit, and phenylalanine to stimulate, GCH activity through interaction with GFRP, a GTP cyclohydrolase I feedback regulatory protein [145]. GCH, which is a homodecameric protein,
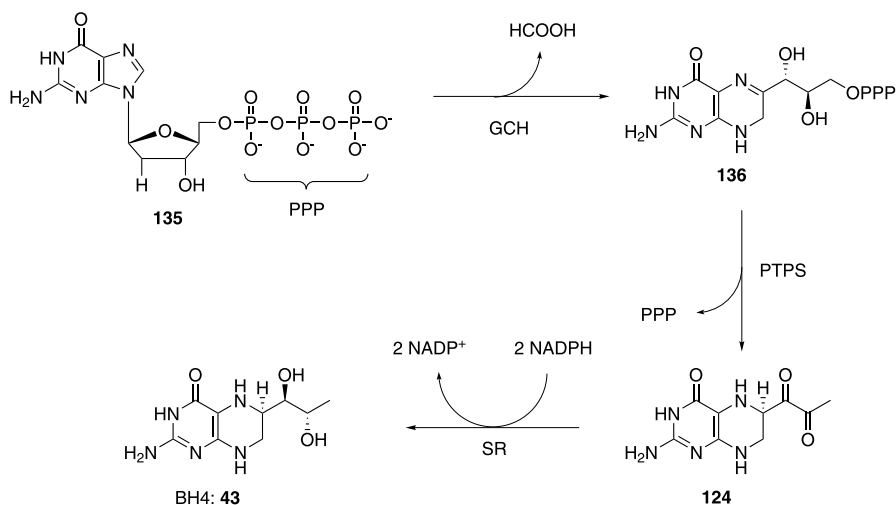
Scheme 31 Biosynthesis of tetrahydrobiopterin from GTP

shows positive cooperativity against the GTP substrate [146] and phenylalanine changes the substrate velocity curve from sigmoidal to hyperbolic [147]. By crystallographic analysis using purified *Escherichia coli* enzyme [148] and an N-terminally truncated form of the recombinant human enzyme [149], Zn(II) was shown to be bound to the active center of the homodecameric GCH enzyme.

Suzuki et al. examined the effect of various divalent cations on purified recombinant human GCH expressed in *Escherichia coli* to clarify the molecular mechanism of action of divalent cations on the GCH enzymatic activity [150]. They demonstrated that GCH utilizes metal-free GTP as the substrate for the enzyme reaction. Inhibition of the GCH activity by divalent cations such as Mg(II) and Zn(II) was due to a reduction in the concentration of metal-free GTP substrate by complex formation. Many nucleotide-hydrolyzing enzymes such as G proteins and kinases recognize Mg-GTP or Mg-ATP complex as their substrate. In contrast with these enzymes, Suzuki et al. demonstrated that GCH activity is dependent on the concentration of Mg-free GTP [150].

5.2
Recycling Pathway

BH4 is converted to 4a-hydroxytetrahydrobiopterin (**95**) with incorporating one atom of dioxygen in the C(4a) position of pterin by the hydroxylation reaction catalyzed by aromatic amino acid hydroxylases (Scheme 32). The formation of **95** was observed in the reaction catalyzed by all three hydroxylases using UV spectroscopy [151]. Dehydration of **95** was carried out by the action
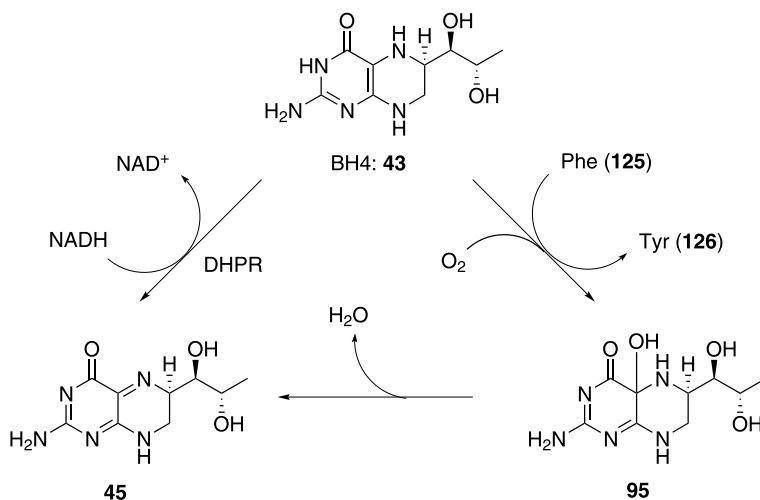
Scheme 32 Recycling pathway of tetrahydrobiopterin

of pterin 4a-carbinolamine dehydratase (PCD; EC 4.2.1.96) to give quinonoid dihydrobiopterin (**45**), and **45** is reduced to BH4 by dihydropteridine reductase (DHPR; EC 1.6.99.7).

PCD deficient patients excrete 7-biopterin (**137**), called primaterin, in their urine [152–154], which had not been observed in normal mammals. The mechanism of the 7-substituted pterin synthesis from 6-substitute has been proposed [155, 156] (Scheme 33). When **95** is rapidly dehydrated to **45** via PCD, the dihydroxypropyl side chain of **95** is retained at its 6-position. However, in the absence of PCD activity, the rate of conversion of unstable **95** is slow. Therefore, its pyrazine ring is opened to give **98**, and recyclization of **98** to the 7-substituted pterin derivative proceeds via spiro intermediate **138** [89, 156].
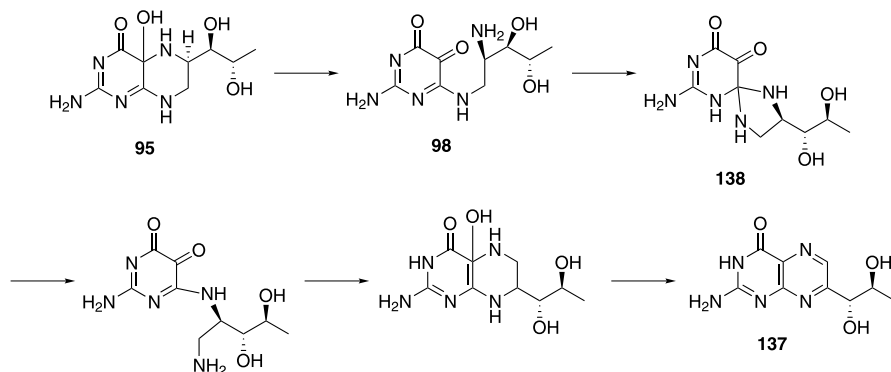
Scheme 33 Mechanism of isomerization to 7-biopterin

6
Deficiency of BH4

6.1
Malignant-Type Hyperphenylalaninemia

Two types of inherited disorders caused by mutations of genes related to BH4 are known. Autosomal dominant mutations in the GCH gene are causative for DOPA-responsive dystonia (DRD) [157, 158]. Malignant hyperphenylalanine-mia or atypical phenylketonuria (PKU) is caused by recessive mutations of genes encoding BH4-biosynthetic or recycling enzymes [159].

Most of hyperphenylalaninemia are caused by a mutation in the PAH gene. About 5% of hyperphenylalaninemia is caused by genetic defects in the BH4-metabolizing enzymes, and called malignant-type or atypical hyperpheny-lalaninemia. Patients with malignant-type hyperphenylalaninemia develop neurological symptoms due to deficiency of catecholamines and serotonin, as well as hyperphenylalaninemia. For example, patients with GTP cyclohy-drolase deficiency show severe retardation of development, severe muscular hypotonia of the trunk and hypertonia of extremities, convulsions, and fre-quent episodes of hyperthermis without infection [160, 161].

6.2
Dopa-Responsive Dystonia

DOPA-responsive dystonia (DRD) is a disorder characterized by childhood or adolescent onset dystonia and by the dramatic response to low-dose L-DOPA, a precursor of dopamine. DRD is a hereditary disorder in an autosomal dom-inant trait with reduced penetrance, and constitutes approximately 5 to 10% of primary dystonia in childhood and adolescence. DRD is caused by the dys-function of nigro-striatal dopaminergic neurons, as indicated by the dramatic effect of L-DOPA. Although Parkinson's disease is also caused by the dysfunc-tion of nigro-striatal dopaminergic neurons due to the degeneration of the dopaminergic neurons, the differences in symptoms, i.e. dystonia in DRD and parkinsonism in Parkinson's disease, has not yet been clarified.

Ichinose et al. cloned the human GCH gene and mapped the gene to chro-mosome 14q22.1–q22.2 within the DRD locus, which had been identified by linkage analysis [162]. They proved that the GCH gene is the causative gene for DRD based on the identification of mutations of the gene in the patients and decreases in the enzyme activity expressed in mononuclear blood cells [163]. About 100 different mutations (missense, nonsense and frameshift mutations) in the coding region or in the exon-intron junctions of the GCH gene have been reported in patients with DRD all over the world. Up-to-date information on mutations found in BH4-synthesizing en-zymes is tabulated in a BIOMDB database [164]. DRD patients were heterozy-

gous in terms of the mutations, bearing both a mutated gene and a normal gene.

The findings demonstrated that DRD is caused by a partial BH4 deficiency in the brain. In general, disorders caused by an inborn error of metabolism show recessive inheritance, as half of the enzyme activity is usually sufficient enough to maintain homeostasis in vivo. To the contrary, DRD is a dominant disorder with low penetrance, even though the causative gene for DRD is that for an enzyme, GCH. The marked decrease (to approximately 20% of controls) in the neopterin content in the CSF (cerebrospinal fluid) from DRD patients suggests that GCH activity in the brain of DRD patients is also about 20% of that for normal individuals. Because neopterin is a metabolite of dihydroneopterin triphosphate, the product of GCH, the neopterin content in the CSF is thought to reflect the GCH activity in the brain.

Genetic analysis of DRD families has proved the presence of asymptomatic carriers, who have the same mutations as the patients. Therefore, there must be some unknown biochemical difference between patients and asymptomatic carriers. Takahashi et al. reported that the CSF of an asymptomatic carrier showed a higher neopterin level than that of patients [165], although this was the only case examined. The observation supports the idea that GCH activity in the brain is an important factor in the development of DRD symptoms. It seems to be essential that GCH activity in the brain must decrease to less than 20% of the normal level to cause the symptoms shown in DRD. Interestingly, it is known that there must be an 80% loss of striatal dopamine content before the symptoms appear in Parkinson's disease [166]. In accordance with this concept, mutations in the GCH gene and a decrease in the dopamine and BH4 levels in the striatum to less than 20% of the normal values were confirmed in one autopsy case of DRD [166]. Thus, dopamine deficiency in DRD patients was shown to be caused by mutated GCH, reduced GCH activity, a low BH4 content, and low TH activity [163]. The results suggest high susceptibility of the nigrostriatal dopaminergic neurons to a deficiency of BH4 and dopamine. In other words, dystonia-parkinsonism would be the first symptom when BH4 is gradually depleted in the brain.

References

1. Brown DJ (1988) Fused pyrimidines Part 3: Pteridines. Wiley, New York
2. Pfleiderer W (1992) J Heterocyclic Chem 29:583
3. Landge SS, Murata S (2006) Heterocycles 68:405
4. Gates M (1947) Chem Rev 41:63
5. Sauberlich HE, Baumann CA (1948) J Biol Chem 172:65
6. Henderson ES, Adamson RH, Denham C, Oliverio VT (1965) Cancer Res 25:1008
7. Henderson ES, Adamson RH, Oliverio VT (1965) Cancer Res 25:1018
8. Taylor EC, Harrington PJ, Flecher SR, Beardsley GP, Moran RG (1985) J Med Chem 28:914

9. Palmer DC, Skotnicki JS, Taylor EC (1988) In: Ellis GP, West GB (eds) Progress in medicinal chemistry. Elsevier, Amsterdam, p 85
10. Taylor EC, Wong GSK (1988) J Org Chem 54:3618
11. Taylor EC, Yoon C-M (1994) J Org Chem 59:7096
12. Leonard PA, Clegg DO, Carson CC, Cannon GW, Egger MJ, Ward JR (1987) Clin Rheumatol 6:575
13. Songsiridej N, Furst DE (1990) Bailliere's Clin Rheumatol 4:575
14. Laing ABG (1972) Trans Royal Soc Tropical Med Hygiene 66:518
15. Goldberg D (2002) Science 296:482
16. Zhang K, Rathod PK (2002) Science 296:545
17. Nzila AM, Kokwaro G, Winstanley PA, Marsh K, Ward SA (2004) Trends Parasitol 20:109
18. Jones W, Nagel DP Jr, Whitman WB (1987) Microbiol Rev 51:135
19. DiMarco AA, Bobik TA, Wolfe RS (1990) Annu Rev Biochem 59:355
20. White RH (1990) Biochemistry 29:5397
21. White RH (1991) J Bacteriol 173:1987
22. White RH (1996) Chirality 8:332
23. White RH (1996) Biochemistry 35:3447
24. Rasche ME, White RH (1998) Biochemistry 37:11343
25. Hille R (1996) Chem Rev 96:2757
26. Collison D, Garner CD, Joule JA (1996) Chem Soc Rev 25
27. Romao MJ, Huber R (1998) In: Hagen AF, Arendsen AF (eds) Metal Sites in Proteins and Models: Redox Centers. Springer, Berlin, p 70
28. Xia M, Dempski R, Hille R (1999) J Biol Chem 274:3323
29. Enroth C, Eger BT, Okamoto K, Nishino T, Nishino T, Pai EF (2000) Proc Nat Acad Sci USA 97:10723
30. Kuwabara Y, Nishino T, Okamoto K, Matsumura T, Eger BT, Pai EF, Nishino T (2003) Proc Natl Acad Sci USA 100:8107
31. Elion GB (1989) Science 244:41
32. Young CG, Wedd AG (1997) Chem Comm 1251
33. Davies ES, Beddoes RL, Collison D, Dinsmore A, Docrat A, Joule JA, Wilson CR, Garner CD (1997) J Chem Soc Dalton Trans 3985
34. Lorber C, Donahue JP, Goddard CA, Nordlander E, Holm RH (1998) J Am Chem Soc 120:8102
35. Donahue JP, Goldsmith CR, Nadiminti U, Holm RH (1998) J Am Chem Soc 120:12869
36. Musgrave KB, Donahue JP, Lorber C, Holm RH, Hedman B, Hodgson KO (1999) J Am Chem Soc 121:10297
37. Kaufmann HL, Liable-Sands L, Rheingold AL, Brugmayer SJN (1999) Inorg Chem 38:2592
38. Ilich P, Hille R (2002) J Am Chem Soc 124:6796
39. Maiti NC, Tomita T, Kitagawa T, Okamoto K, Nishino T (2003) J Biol Inorg Chem 8:327
40. Sen S, Roy PS (2005) Transit Metal Chem 30:797
41. Lin X, White RH (1988) J Bacteriol 170:1396
42. Cha KW, Pfleiderer W, Yim JJ (1995) Helv Chim Acta 78:600
43. Noguchi Y, Ishii A, Matsushima A, Haishi D, Yasumuro K-I, Moriguchi T, Wada T, Kodera Y, Hiroto M, Nishimura H, Sekine M, Inada Y (1999) Marine Biotec 1:207
44. Choi YK, Hwang YK, Kang YH, Park YS (2001) Pteridines 12:121
45. Hanaya T, Soranaka K, Harada K, Yamaguchi H, Suzuki R, Endo Y, Yamamoto H, Pfleiderer W (2006) Heterocycles 67:299

46. Sugimoto T, Ogiwara S, Teradaira R, Fujita K, Nagatsu T (1992) Biogenic Amines 9:77
47. Chen N, Zinchenko AA, Murata S, Yoshikawa K (2005) J Am Chem Soc 127:10910
48. Chen N, Zinchenko AA, Murata S, Yoshikawa K (2005) Chem Eur J 11:4835
49. Fukushima T, Nixon JC (1980) Anal Biochem 102:176
50. Klein R (1992) Anal Biochem 203:134
51. Werner E, Werner-Felmayer G, Wachter H (1996) J Chromatogr B 684:51
52. Tomandl J, Tallova J, Tomandlova M, Palyza V (2003) J Sep Sci 26:674
53. Carru C, Zinellu A, Sotgia S, Serra R, Usai MF, Pintus GF, Pes GM, Deiana L (2004) Biomed Chromatogr 18:360
54. Furrer H-J, Bieri JH, Viscontini M (1979) Helv Chim Acta 62:2577
55. Ganguly SN, Viscontini M (1982) Helv Chim Acta 65:1090
56. Prewo R, Bieri JH, Ganguly SN, Viscontini M (1982) Helv Chim Acta 65:1094
57. Armarego WLF, Waring P, Paal B (1982) Aust J Chem 35:785
58. Armarego WLF, Randles D, Taguchi H, Whittaker MJ (1984) Aust J Chem 37:355
59. Matsuura S, Murata S, Sugimoto T (1984) Chem Lett 735
60. Matsuura S, Sugimoto T, Murata S, Sugawara Y, Iwasaki H (1985) J Biochem (Tokyo) 98:1341
61. Sugimoto T, Murata S, Matsuura S, Nagatsu T (1987) Synth Org Chem Jpn 46:564
62. Chen N, Ikemoto K, Komatsu S, Murata S (2005) Heterocycles 65:2917
63. Sugimoto T, Ikemoto K, Murata S, Tazawa M, Nomura T, Hagino Y, Ichinose H, Nagatsu T (2001) Heterocycles 54:283
64. Chen N, Ikemoto K, Sugimoto T, Murata S (2002) Heterocycles 56:387
65. Sugimoto T, Ikemoto K, Murata S, Tazawa M, Nomura T, Hagino Y, Ichinose H, Nagatsu T (2001) Helv Chim Acta 84:918
66. Ikemoto K, Sugimoto T, Murata S, Tazawa M, Nomura T, Hagino Y, Ichinose H, Nagatsu T (2001) Biol Chem 383:325
67. Yao Q, Pfleiderer W (2003) Helv Chim Acta 86:1
68. Viscontini M, Provenzale R, Ohlgart S, Mallevialle J (1970) Helv Chim Acta 53:1202
69. Adler C, Curtius H-C, Datta S, Viscontini M (1990) Helv Chim Acta 73:1058
70. Mori K, Kikuchi H (1989) Liebigs Ann Chem 1267
71. Sugimoto T, Matsuura S (1975) Bull Chem Soc Jpn 48:3767
72. Sugimoto T, Matsuura S (1979) Bull Chem Soc Jpn 52:181
73. Kappel M, Mengel R, Pfleiderer W (1984) Liebigs Ann Chem 1815
74. Schircks B, Viscontini M (1985) Helv Chim Acta 68:1639
75. Fernandez A-M, Duhamel L (1996) J Org Chem 61:8698
76. Fernandez A-M, Plaquevent J-C, Duhamel L (1997) J Org Chem 62:4007
77. Mori K, Kikuchi H (1989) Liebigs Ann Chem 963
78. Pastor SD, Nelson AL (1984) J Heterocycl Chem 21:657
79. Brown DJ (1988) Fused pyrimidines Part 3: Pteridines. Wiley, New York, pp 57–61
80. Murata S, Kiguchi K, Sugimoto T (1998) Heterocycles 48:1255
81. Heizmann G, Pfleiderer W (1989) Biol Chem Hoppe-Seyer 370:384
82. Murata S, Sugimoto T, Matsuura S (1987) Heterocycles 26:883
83. Murata S, Sugimoto T, Ogiwara S, Mogi K, Wasada H (1992) Synthesis 303
84. Brown DJ (1988) Fused pyrimidines Part 3: Pteridines. Wiley, New York, pp 108–130
85. Pfleiderer W, Hutzenlaub W (1973) Chem Ber 106:3149
86. Zondler H, Forrest HS, Lagowski JM (1967) J Heterocyclic Chem 4:12
87. Bailey SW, Chandrasekaran RY, Ayling JE (1992) J Org Chem 57:4470
88. Bailey SW, Rebrin I, Boerth SR, Ayling JE (1995) J Am Chem Soc 117:10203
89. Brown DJ (1988) Fused pyrimidines Part 3: Pteridines. Wiley, New York, pp 143–158

90. Albert A, Ohta K (1970) J Chem Soc (C) 1540
91. Jacobi PA, Martinelli M, Taylor EC (1981) J Org Chem 46:5416
92. Taylor EC, Reiter LA (1982) J Org Chem 47:528
93. Taylor EC, Reiter LA (1989) J Am Chem Soc 111:285
94. Taylor EC, Ray PS (1987) J Org Chem 52:3997
95. Taylor EC, Ray PS, Darwish IS (1989) J Am Chem Soc 111:7664
96. Taylor EC, Doetzer R (1991) J Org Chem 56:1816
97. Piato RS, Eriksen KA, Greaney MA, Stiefel EI, Goswami S, Kilpatrick L, Spiro TG, Taylor EC, Rheingold AL (1991) J Am Chem Soc 113:9372
98. Bailey SW, Ayling JE (1978) J Biol Chem 253:1598
99. Schricks B, Bieri JH, Viscontini M (1978) Helv Chim Acta 61:2731
100. Nagai M (1968) Ach Biochem Biophys 126:426
101. Schricks B, Bieri JH, Viscontini M (1977) Helv Chim Acta 60:211
102. Matsuura S, Sugimoto T, Murata S (1985) Tetrahedron Lett 26:4003
103. Matsuura S, Murata S, Sugimoto T (1985) Tetrahedron Lett 27:585
104. Hadron IEE, Mitchell HK (1951) Proc Natl Acad Sci USA 37:650
105. Nawa S (1960) Bull Chem Soc Jpn 33:1555
106. Pfleiderer W (1964) Angew Chem Int Ed Engl 3:114
107. Brown DJ (1988) Fused pyrimidines Part 3: Pteridines. Wiley, New York, pp 273–275
108. Mazda T, Tsusue M, Sakate S (1980) Insect Biochem 10:357
109. Summers KM, Howells AJ (1980) Insect Biochem 10:151
110. Pfleiderer W (1979) Chem Ber 112:2750
111. Sugiura K, Takikawa S, Tsusue M, Goto M (1973) Bull Chem Soc Jpn 46:3312
112. Schircks B, Bieri JH, Viscontini M (1978) Helv Chim Acta 43:630
113. Woo HJ, Kang JY, Choi YK, Park YS (2002) Microbiology 68:3138
114. Nawa S, Forrest HS (1962) Nature 196:169
115. Baur R, Sugimoto T, Pfleiderer W (1984) Chem Lett, p 1025
116. Landge SS, Kudoh K, Yamada Y, Murata S (2007) Heterocycles 71:911
117. Switchenko AC, Brown GM (1985) J Biol Chem 260:2945
118. Milstein S, Kaufman S (1985) Biochem Biophys Res Commun 128:1099
119. Smith GK, Nichol CA (1986) J Biol Chem 261:2725
120. Ghisla S, Kuster T, Steinerstauch P, Leimbacher W, Richter WJ, Raschdorf F, Dahinden R, Curtius H-C (1990) Eur J Biochem 187:651
121. Katoh S, Sueoka T, Kurihara T (1991) Biochem Biophys Res Commun 176:52
122. Walther DJ, Peter JU, Bashammakh S, Hortnagl H, Voits M, Fink H, Bader M (2003) Science 299:76
123. Walther DJ, Bader M (2003) Biochem Pharmacol 66:1673
124. Ramsey AJ, Hillas PJ, Fitzpatrick PF (1996) J Biol Chem 271:24395
125. Kwon NS, Nathan CF, Stuehr DJ (1989) J Biol Chem 264:20496
126. Tayeh MA, Marletta MA (1989) J Biol Chem 264:19654
127. Wei C-C, Crane BR, Stuehl DJ (2000) Chem Rev 103:2365
128. Mayer B, Wu C, Gorren AC, Pfeiffer S, Schmidt K, Clark P, Stuehr DJ, Werner ER (1997) Biochemistry 36:8422
129. Presta A, Siddhanta U, Wu C, Sennequier N, Huang L, Abu-soud HM, Erzurum S, Stuehr DJ (1998) Biochemistry 37:298
130. Hemmens B, Gorren AC, Schmidt K, Werner ER, Mayer B (1998) Biochem J 332:337
131. Sumi-Ichinose C, Urano F, Kuroda R, Ohye T, Kojima M, Tazawa M, Shiraishi H, Hagino Y, Nagatsu T, Nomura T, Ichinose H (2001) J Biol Chem 276:41150
132. Urano F, Hayashi N, Arisaka F, Kurita H, Murata S, Ichinose H (2006) J Biochem 139:625

133. Fitzpatrick PF (1999) Annu Rev Biochem 68:355
134. Nasrin S, Ishinose H, Hidaka H, Nagatsu T (1994) J Biochem 116:393–398
135. Daubner SC, Lauriano C, Haycock JW, Fitzpatrick PF (1992) J Biol Chem 267:12639
136. Levine RA, Miller LP, Lovenberg W (1981) Science 214:919
137. Doskuland AP, Flatmark T (2002) Eur J Biochem 269:1561
138. Schramek N, Bracher A, Bacher A (2001) J Biol Chem 276:2622
139. Werner ER, Werner FG, Fuchs D, Hausen A, Reibnegger G, Yim JJ, Pfleiderer W, Wachter H (1990) J Biol Chem 265:3189
140. Werner FG, Werner ER, Fuchs D, Hausen A, Reibnegger G, Schmidt K, Weiss G Wachter H (1993) J Biol Chem 268:1842
141. Zhu M, Hirayama K, Kapatos G (1994) J Biol Chem 269:11825
142. Ziegler I, Hültner L, Egger D, Kempkes B, Mailhammer R, Gillis S, Rodl W (1993) J Biol Chem 268:12544
143. Ziegler I, Schott K, Lübbert M, Herrmann F, Schwuléra U, Bacher A (1990) J Biol Chem 265:17026
144. Harada T, Kagamiyama H, Hatakeyama K (1993) Science 260:1507
145. Hatakeyama K, Harada T, Suzuki S, Watanabe Y, Kagamiyama H (1989) J Biol Chem 264:21660
146. Yoneyama T, Brewer JM, Hatakeyama K (1997) J Biol Chem 272:9690
147. Nar H, Huber R, Auerbach G, Fischer M, Hösl C, Ritz H, Bracher A, Meining W, Eberhardt S, Bacher A (1995) Proc Natl Acad Sci USA 92:12120
148. Auerbach G, Herrmann A, Bracher A, Bader G, Gütlich M, Fischer M, Neukamm M, Garrido-Franco M, Richardson J, Nar H, Huber R, Bacher A (2000) Proc Natl Acad Sci USA 97:13567
149. Suzuki T, Kurita H, Ichinose H (2004) Eur J Biochem 271:349
150. Fitzpatrick PF (2003) Biochemistry 42:14083
151. Curtius HC, Kuster T, Matasovic A, Blau N, Dhondt JL (1988) Biochem Biophys Res Commun 153:715
152. Ayling JE, Bailey SW, Boerth SR, Giugliani R, Braegger CP, Thöny B, Blau N (2000) Mol Genet Metab 70:179
153. Curtius HC, Matasovic A, Schoedon G, Kuster T, Guibaud P, Giudici T, Blau N (1990) J Biol Chem 265:3923
154. Adler C, Ghisla S, Rebrin I, Haavik J, Heizmann CW, Blau N, Kuster T, Curtius HC (1992) Eur J Biochem 208:139
155. Davis MD, Kaufman S, Milstien S (1991) Proc Natl Acad Sci USA 88:385
156. Segawa M, Ohmi K, Itoh S, Aoyama M, Hayakawa H (1971) Shinryo (Tokyo) 24:667
157. Segawa M, Hosaka A, Miyagawa F, Nomura Y, Imai H (1976) Adv Neurol 14:215
158. Thöny B, Blau N (2006) Human Mutat 27:870
159. Niederwieser A, Blau N, Wang M, Joller P, Atarés M, Cardesa-Garcia J (1984) Eur J Pediatr 141:208
160. Dhondt J-L, Farriaux J-P, Boudha A, Largilliére C, Ringel J, Roger M-M, Leerning RJ (1985) J Pediatr 106:954
161. Ichinose H, Ohye T, Matsuda Y, Hori T, Blau N, Burlina A, Rouse B, Matalon R, Fujita K, Nagatsu T (1995) J Biol Chem 270:10062
162. Ichinose H, Ohye T, Takahashi E, Seki N, Hori T, Segawa M, Nomura Y, Endo K, Tanaka H, Tsuji S, Fujita K, Nagatsu T (1994) Nat Genet 8:236
163. Blau N, Thöny B, Dianzani I (2001) BIOMDB: Database of mutations causing tetrahydrobiopterin deficiency. http://www.bh4.org/biomdb1.html
164. Takahashi H, Levine RA, Galloway MP, Snow BJ, Calne DB, Nygaard TG (1994) Ann Neurol 35:354

165. Bernheimer H, Birkmayer W, Hornykiewicz O, Jellinger K, Seitelberger F (1973) J Neurol Sci 20:415
166. Furukawa Y, Nygaard TG, Gütlich M, Rajput AH, Pifl C, DiStefano L, Chang LJ, Price K, Shimadzu M, Hornykiewicz O, Haycock JW, Kish SJ (1999) Neurology 53:1032

Preparation, Structure, and Biological Properties of Phosphorus Heterocycles with a C – P Ring System

Mitsuji Yamashita

Biomedical Materials Laboratory, Nano Material Research Division,
Department of Research, Graduate School of Science and Technology,
Shizuoka University, Hamamatsu 432-8561, Japan
tcmyama@ipc.shizuoka.ac.jp

Abstract Phosphoric acid esters, phosphates, have three P – O bonds around the central P(V) atom in the molecule. Replacing a phosphate P – O bond by a P – C bond and reducing the number of oxygen atoms one by one, converts phosphates into phosphonates, phosphinates, and phosphine oxides. *Phospha* sugar is a pseudo-sugar whose hemiacetal ring of the sugar contains a phosphorus atom with a C – P – C bond in the heterocycle, and is not yet found in nature. Research on phosphorus heterocycles is not as popular as that on nitrogen heterocycles, nevertheless the research is quite challenging.

Keywords Phospha sugar · Phosphorus heterocycle · P – C compound · Phospholene · Phospholane

1
Introduction

A large number of phosphorus compounds possess P – O bond(s) as phosphate esters (e.g., DNA, RNA, ATP, phospholipids, etc.) and these phosphates play important roles in living systems. Unlike a P – O bond, a P – C bond constructs phosphorus molecules, which are relatively reduced molecules compared to compounds constructed with a P – O bond. Both of the two
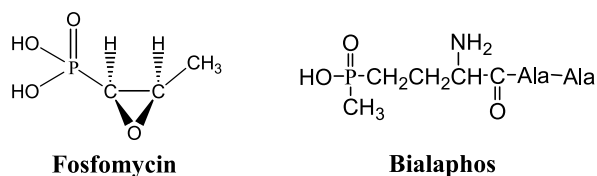
Fosfomycin   **Bialaphos**

Fig. 1 Biologically active phosphorus–carbon (P–C) bonded compounds (Fosfomycin and Bialaphos)

types of phosphorus components are often found in nature, for example, phospholipids (such as phosphorylchorine) and phosphonolipids are found in cell membranes. 2-Aminoethylphosphonic acid, one of the naturally occurring P – C compounds, was first found by Kandatsu and Horiguchi in 1959 [1] when the chemistry and biochemistry of P – C bonded compounds started. P – C bonded compounds must play important roles in living systems, nevertheless there have not been enough studies on P – C compounds, especially cyclic compounds with a P – C bond.

Among P – C bonded compounds, Fosfomycin and Bialaphos are well known (Fig. 1). They are obtained from fermentation broth and act as antibiotics and herbicides.

In the field of carbohydrates, besides normal sugars (such as glucose, ribose, etc.), pseudo-sugars are also naturally occurring sugar analogues. Pseudo-sugars contain a carbon (*carba* sugars), nitrogen (*aza* sugars), sulfur (*thia* sugars), etc., instead of an oxygen atom in the hemiacetal ring of monosaccharides and have important biological activities. Replacement of the oxygen atom of sugars (represented in the Haworth equation) by a phosphorus atom gives other pseudo-sugars named *phospha* sugars, which have a C – P – C bond. However, *phospha* sugars are not found in nature as are *carba*, *aza*, and *thia* sugars. Nevertheless, *phospha* sugars present a challenge for developing new carbohydrate chemistries and for finding new biologically important materials.

This chapter focuses on the preparation, structure, and biological properties of heterocycles of a C – P ring system having a C – P – C bond and a C – P – O bond.

2
Aliphatic Phosphorus Heterocycles with a C – P – C Ring

2.1
Four-, Five-, and Six-Membered Aliphatic Rings (Smaller Than Six-Membered)

Phosphorinic, phospholanic, and phosphetanic acids are four-, five-, and six-membered phosphorus heterocycles, respectively, with a cyclic phosphinic

acid structure where a C – P – C bond forms the heterocycle. Ethyl phosphorinate is prepared by the reaction of 1,3-dibromopropane and magnesium with ethyl phosphorodichloridate by the two-step intramolecular Grignard coupling reaction in 43% yield. The hydrolysis of the ethyl ester with concentrated hydrochloric acid produces phosphorinic acid in 74% yield. The same reaction procedure produces phospholanic and phosphetanic acids **1–3** via ethyl esters **4–6** (Scheme 1) [2].
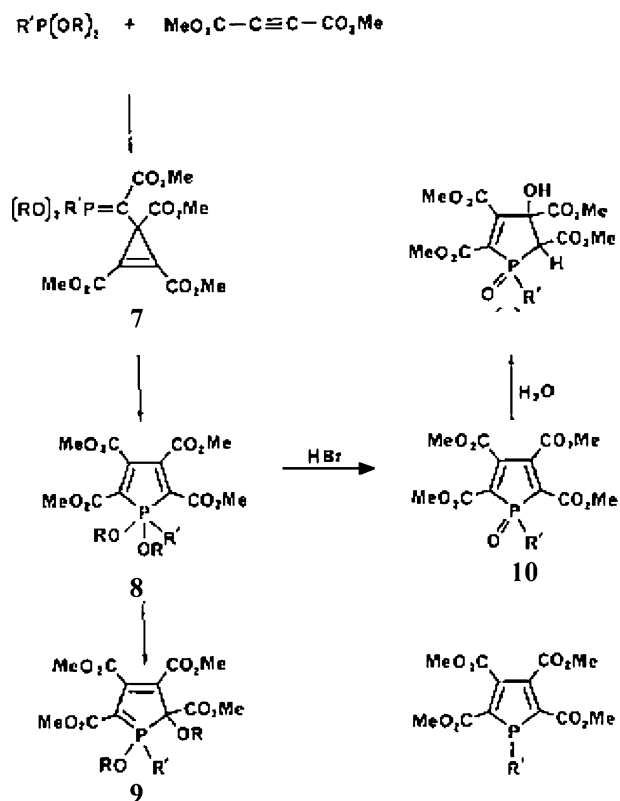

$$4; n = 3 \ (43\%)$$
$$5; n = 2 \ (30\%)$$
$$6; n = 1 \ (7.5\%)$$

$$1; n = 3 \ (74\%)$$
$$2; n = 2 \ (91\%)$$
$$3; n = 1 \ (88\%)$$
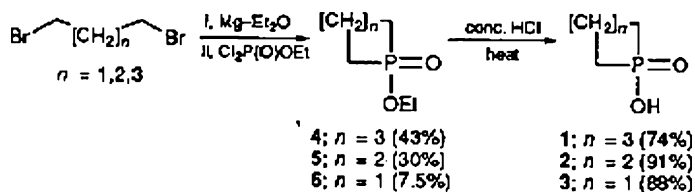
Scheme 1 Production of phospholanic and phosphetanic acids **1–3** via ethyl esters **4–6**

Reaction of dialkyl arylphosphonites or dialkyl alkylphosphonites with two molar equivalents of dimethyl acetylenedicarboxylate, through an analogous pathway to the reaction of trimethyl phosphate with the acetylenedicarboxylate, proceeds smoothly for 30 min at –70 °C to give phosphorus ylide **7** initially in almost quantitative yield. The ylide (^{31}P NMR: δ_P 69.8 ppm) converts to affords the λ^5-phosphole **8**, and then to cyclic ylide **9**. Addition reaction of hydrogen bromide to the λ^5-phosphole **8** at –70 °C occurs for dealkylation of the λ^5-phosphole giving the oxo-phosphole **10** (δ_P 38.7 ppm) (Scheme 2) [3].
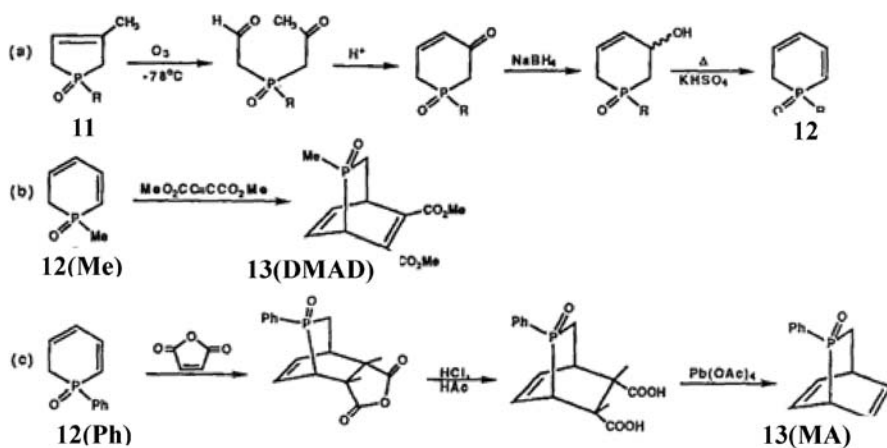
1,6-Dihydrophosphinine derivatives **12** are prepared from 3-methyl-3-phospholene 1-oxides **11** by an oxidative ring opening reaction with ozone and a ring-forming intramolecular aldol reaction. The diene in the heterocyles of 1,6-dihydrophosphine derivatives reacts with alkyes (such as dimethyl acetylenedicarboxylate (DMAD)) or maleic anhydride (MA) to produce bicyclic systems of phosphorus heterocycles of 2-phosphabicyclo[2.2.2] oct-5-ene and 2-phosphabicyclo[2.2.2]octa-5,7-diene 2-oxide ring systems **13** **(DMAD)** or **13 (MA)**, respectively (Scheme 3).

From the bicyclic phosphorus heterocycles, highly reactive species Me-P = CH$_2$ and Ph-P = CH$_2$ are generated by retro Diels–Alder reaction via reduction of phosphorus(V) to reduced phosphorus(III) of the heterocycles **14** on treatment with trichlorosilane (Scheme 4).

The 3-phospholene 1-oxide derivative is a potential heterocycle for easily producing chemically modified phosphorus heterocycles because the compound possesses a reactive C=C double bond, allylic methylene, an electron-deficient methylene group α-positioned to phosphorus, etc. 4-Chloro-1,6-dihydrophosphinie derivatives **16A** and **16B** are prepared from dichlorocarbene adducts **15** with 1-(R)-3-ethylphospholene 1-oxide (Scheme 5) [4].

R'P(OR)$_2$ + MeO$_2$C—C≡C—CO$_2$Me

(RO)$_2$R'P=C $\overset{\text{CO}_2\text{Me}}{\underset{}{}}$ CO$_2$Me

MeO$_2$C $\overset{}{\underset{}{}}$ CO$_2$Me

7

MeO$_2$C $\quad$ CO$_2$Me

MeO$_2$C $\overset{}{\underset{}{}}$ CO$_2$Me

RO$\overset{}{\underset{\text{OR}}{}}$R'

8

$\xrightarrow{\text{HBr}}$

MeO$_2$C $\quad$ CO$_2$Me

MeO$_2$C $\overset{}{\underset{}{}}$ CO$_2$Me

O $\quad$ R'

10

MeO$_2$C $\overset{\text{OH}}{\underset{}{}}$ CO$_2$Me

MeO$_2$C $\overset{}{\underset{}{}}$ CO$_2$Me

$\quad$ H

O $\quad$ R'

$\Big\uparrow$ H$_2$O

MeO$_2$C $\quad$ CO$_2$Me

MeO$_2$C $\overset{}{\underset{}{}}$ CO$_2$Me

RO $\overset{\text{OR}}{\underset{}{}}$ R'

9

MeO$_2$C $\quad$ CO$_2$Me

MeO$_2$C $\overset{}{\underset{}{}}$ CO$_2$Me

$\overset{}{\underset{}{}}$ R'

Scheme 2 Preparation of cyclic ylide **9** and oxo-phosphole **10**

(a) $\xrightarrow[-78°C]{O_3}$ $\xrightarrow{H^+}$ $\xrightarrow{NaBH_4}$ $\xrightarrow[KHSO_4]{\Delta}$

11 $\qquad\qquad\qquad\qquad\qquad\qquad\qquad\qquad\qquad$ **12**

(b) **12(Me)** $\xrightarrow{MeO_2C\mathrm{C≡C}CO_2Me}$ **13(DMAD)**

(c) **12(Ph)** $\longrightarrow$ $\xrightarrow[HAc]{HCl}$ $\xrightarrow{Pb(OAc)_4}$ **13(MA)**

Scheme 3 Preparation of **13** (DMAD) and **13** (MA) from 3-methyl-3-phospholene 1-oxides **11**
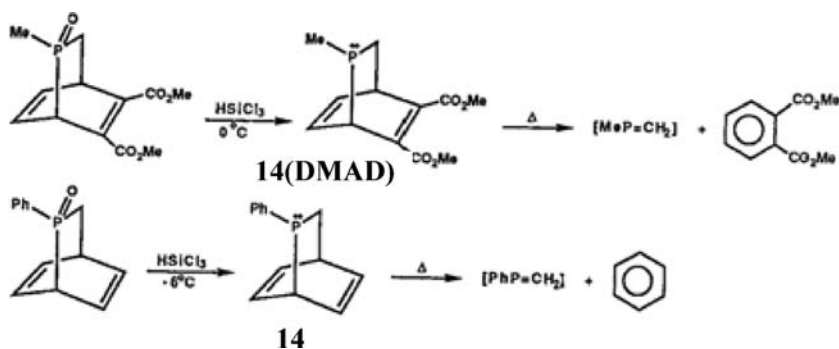
**Scheme 4** Generation of highly reactive species Me-P $=$ CH$_2$ and Ph-P $=$ CH$_2$
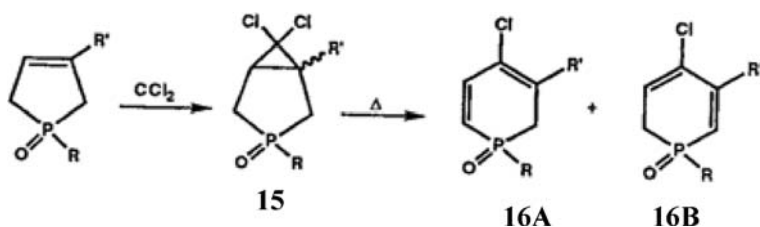
Scheme 5 Preparation of 4-chloro-1,6-dihydrophosphinie derivatives **16A** and **16B**

Me-P $=$ CH$_2$ is a reactive phosphine and the freshly prepared species reacts with isoprene to give Diels–Alder adducts of phophinines with six-membered phosphorus heterocycles **17–20** (Scheme 6).

The ring enlargement reaction of 3-phospholenes is separately reported by using phase transfer catalyst, then convenient preparation of 1-alkyl-1,2-di-
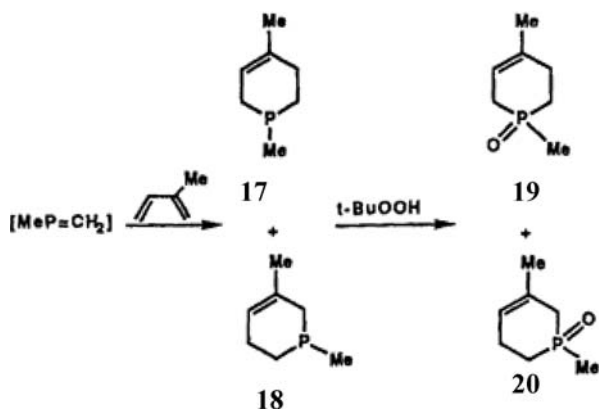
Scheme 6 Reaction of Me-P $=$ CH$_2$ with isoprene to give Diels–Alder adducts of phophinines with phosphorus heterocycles **17–20**

and 1,2,3,6-tetrahydrophosphinine 1-oxides (via thermolysis of the adduct) and cyclopropane ring opening (effected by silver nitrate) of 3-phospholene with dichlorocarbine intermediate [5, 6].

Regioisomeric 1,2-dihydrophosphinine 1-oxides **21A**, **21B**, and **24** undergo the Diels–Alder cyclization with dimethyl acetylenedicarboxylate (DMAD) to give 2-phosphabicyclo[2.2.2]octane derivatives **22A**, **22B**, and **25** (Schemes 7 and 8). The 1,2-dihydrophosphinine 1-oxides **26** react with phenylmaleimide to give the corresponding tricyclic heterocycles **27** (four isomers) (Scheme 9).
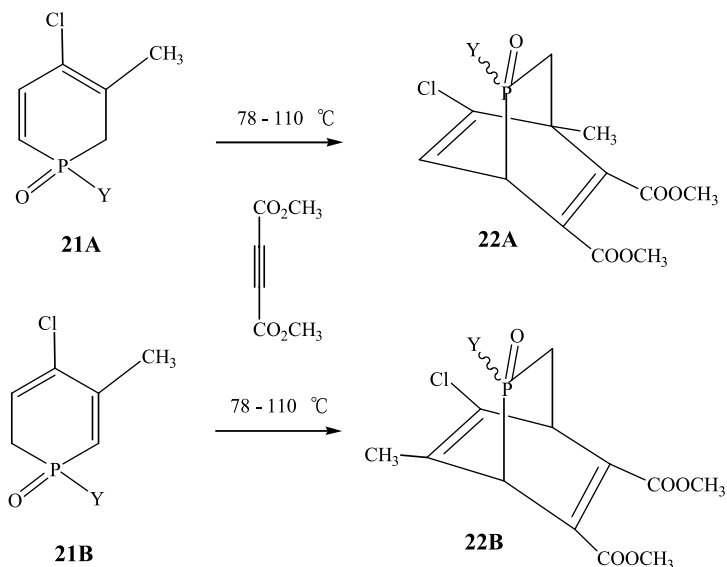
Y = Ph (a), Me (b), MeO (c), EtO (d), n-PrO (e), i-PrO (f)

Scheme 7 Regioisomeric 1,2-dihydrophosphinine 1-oxides **21A** and **21B** undergo the Diels–Alder cyclization with DMAD to give **22A** and **22B**
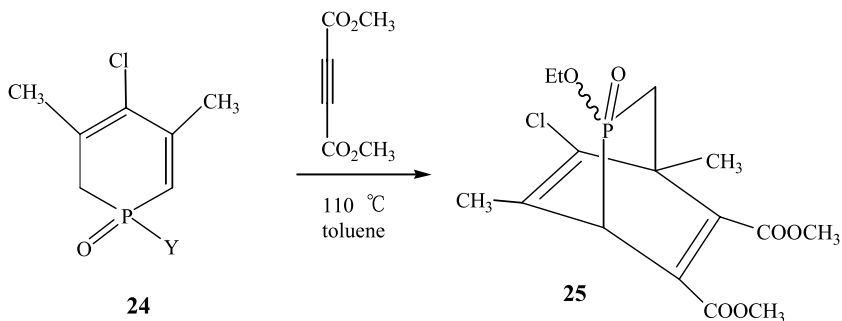

Scheme 8 Reaction of **24** with DMAD to give **25**

Substitution of the phosphinate ester group by dimethylamine via the chloride, and thionation of the P=O group of the 2-phosphabicyclo[2.2.2]octane P-oxide derivatives **28** with diphosphorus pentasulfide affords the corresponding amide **29** and P-sulfide **30** (Scheme 10). The thionation is also achieved with Lawesson's reagent [7, 8]. Thermolysis of **28** proceeds a retro Diels–Alder reaction to give **31**.

Two diasteromers of phosphorus heterocycles **33A** and **33B** are prepared from 3,4-dimethyl-3-phospholene **32** via the carbene adduct forma-
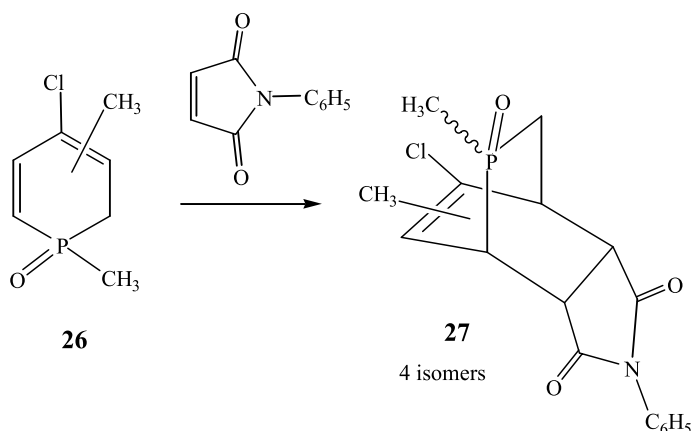
Scheme 9 1,2-Dihydrophosphinine 1-oxides **26** react with phenylmaleimide to give the corresponding tricyclic heterocycles **27**
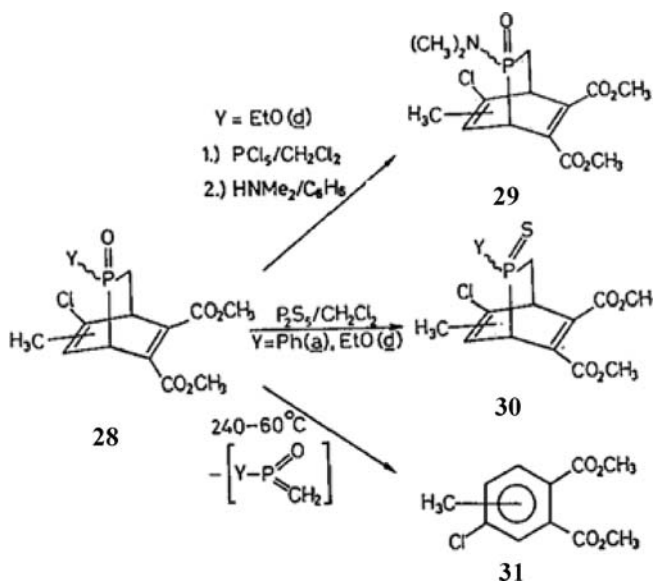

Scheme 10 Reactions of 2-phosphabicyclo[2.2.2]octane P-oxide derivatives **28** to give **29–31**

tion (Scheme 11). 1-Amino-3-phosphabicyclo[3.1.0]hexane 3-oxides **35** and **39a–c** are prepared separately and selectively from 1-amino-3-methyl-3-phospholene 1-oxide (**34**) and 1-ethoxy-3-methyl-3-phospholene (**36**) by dichlorocarbene addition to the 3-phospholene double bond under phase transfer catalyst (PTC) and substitution of the 1-chloro derivative of the bicyclic system with amines, respectively (Scheme 12) [9, 10].

3-Phosphabicyclo[3.1.0]hexane 3-oxides **40A** and **40B** and dihydrophosphinine 1-oxide derivatives, 1,6-dihydro- and 1,2-dihydrophosphinine deriva-
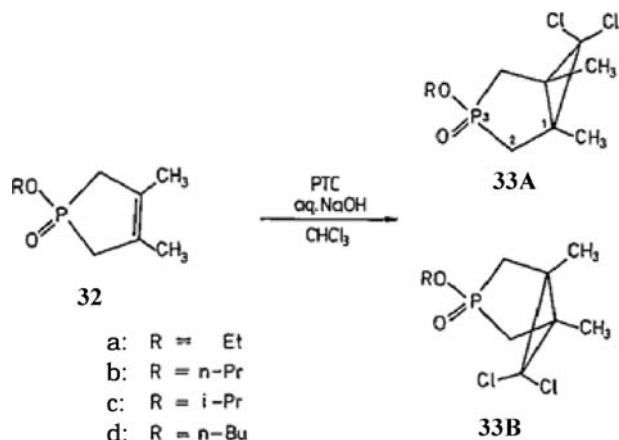

Scheme 11 Preparation of diastereomers of phosphorus heterocycles **33A** and **33B** from 3,4-dimethyl-3-phospholene **32**
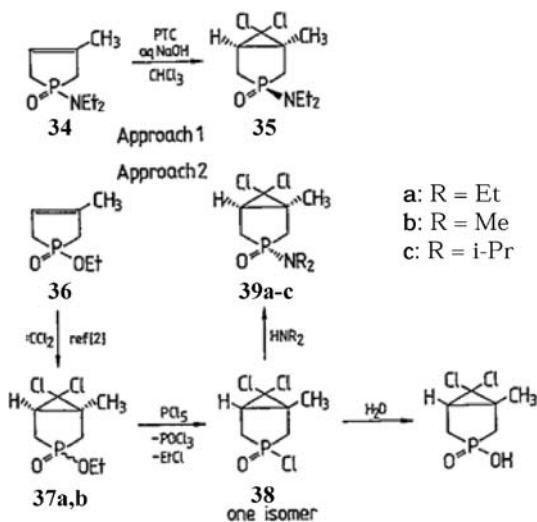
Scheme 12 Selective preparation of 1-amino-3-phosphabicyclo[3.1.0]hexane 3-oxides **35** and **39a–c** from **34**

tives, **42A** and **42B**, respectively, are transformed into the corresponding 3-sulfide **41** and 1-sulfides **43A** and **43B** by oxygen–sulfur exchange with diphosphorus pentasulfide (Scheme 13) [11].
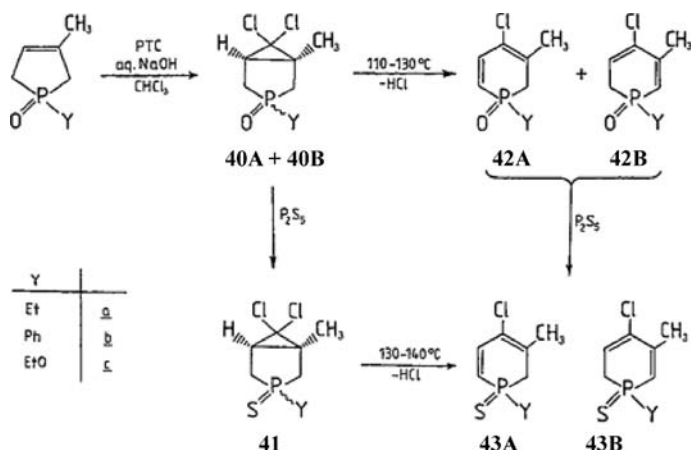
Scheme 13 Oxygen–sulfur exchange transforms **40A**, **40B**, **42A**, and **42B** into the corresponding sulfides

2.2
Phospha Sugars and Substituted Phospholanes

Phospha sugars (e.g., **44–46** in Fig. 2) are the phosphorus analogues of *aza* sugars.
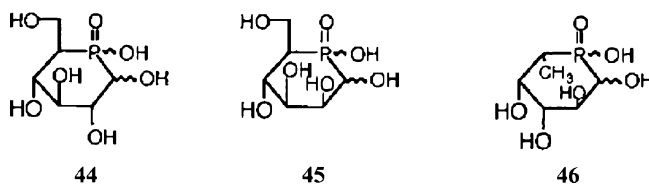

Fig. 2 Examples of *phospha* sugars

D-Galactopyranose analogues of *phospha* sugars, e.g., 3,6-di-*O*-benzyl-5-deoxy-5-hydroxyphosphinyl-α,β-D-galactopyranose (**48**), which have a phosphorus atom instead of an oxygen atom in the hemiacetal ring of sugars, are prepared by the intramolecular addition reaction of a P – H group of the 5-phosphino sugar derivative **47** to an aldehyde group, via hemiacetal ring opening under acidic conditions (Scheme 14). By a similar reaction pathway, *phospha* sugar analogues of D-glucose [12, 13], D-mannose [14], and L-fucose [15] have been synthesized [16].
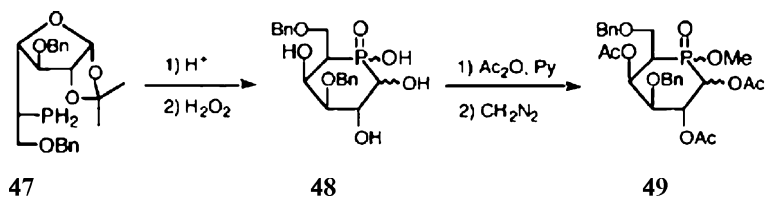
Scheme 14 Conversion of 5-phosphino sugar derivative **47** to **49**

These *phospha* sugar analogues are acetylated into **49a–d** and the structure of the acetates of the *phospha* sugars are analyzed by NMR spectrometry to elucidate the conformation (Table 1).

D-Ribofuranose-type *phospha* sugars **50** (R=OH, Et, and Ph) and 2-deoxy-D-ribofuranose analogues **51** (R=OH and Me) in Fig. 3 have been prepared via longer reaction pathways by a similar ring closing intramolecular addition re-action of a P – H group to an aldehyde of sugars shown in Scheme 14 [17–20].

To improve the preparative method of *phospha* sugars from sugar start-ing materials [21, 22], the Arbzov reaction and Grignard coupling reac-tion have been applied to a reaction of 1,4-dibromobutane. The reaction of 1,4-dibromobutane (**53**) with dimethyl phenylphosphonite to give ethyl (4-bromobutyl)phenylphosphinate (**54**) and successive intramolecular substi-tution of the 4-bromo substituent with phosphinyl anion affords 1-phenyl-phospholane 1-oxide (**56a**) in 40% yield. It can also be prepared from
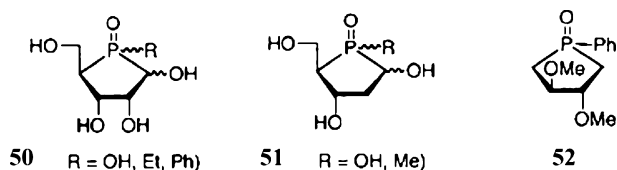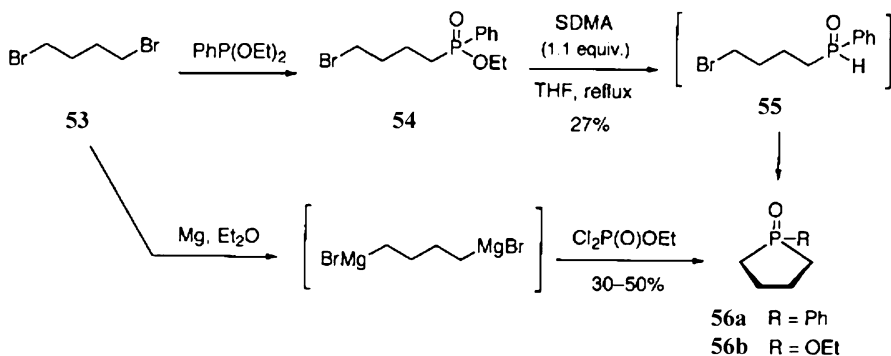

Fig. 3 Tetro- and pentofuranose-type *phospha* sugars

Scheme 15 Preparation of **56a** and **56a** from 1,4-dibromobutane (**53**)

Table 1 ^{1}H and ^{31}P NMR parameters for compounds **49a–d** in CDCl$_3$

Chemical shifts (δ)

Compound	H-1	H-2	H-3	H-4	H-5	H-6	H-6′	POMe	AcO-1,2,4a	CH$_2$O-3,6b,c	^{31}P
49a	5.61	5.69	3.80	5.98	2.52	3.78	3.62	3.65	2.13, 2.11, 1.98	4.75, 4.46; 4.52, 4.48	39.6
49a	5.61	5.69	3.80	5.98	2.52	3.78	3.62	3.65	2.13, 2.11, 1.98	4.75, 4.46; 4.52, 4.48	39.6
49b	5.24	5.69	3.49	5.90	2.26	3.84	3.65	3.66	2.16, 2.13, 1.95	4.72, 4.41; 4.53, 4.49	39.7
49c	5.68	5.38	3.76	5.99	2.67	3.89	3.59	3.78	2.12, 2.03, 1.98	4.735, 4.46; 4.49, 4.49	39.2
49d	5.40	5.50	3.49	5.96	2.37	3.91	3.54	3.85	2.10, 2.06, 1.94	4.73, 4.39; 4.495, 4.48	39.2

Coupling constants (Hz)

| Compound	$J_{1,2}$	$J_{1,P}$	$J_{2,3}$	$J_{2,P}$	$J_{3,4}$	$J_{4,5}$	$J_{4,P}$	$J_{5,6}$	$J_{5,6′}$	$J_{5,P}$	$J_{6,6′}$	$J_{6,P}$	$J_{6′,P}$	J_{POMr}
49a	2.8	14.6	10.4	0.5	2.9	2.8	34.5	4.9	9.2	15.9	9.8	5.8	9.5	11.0
49b	10.7	5.5	9.8	2.7	2.5	2.7	35.5	5.8	8.5	13.8	9.8	6.1	10.7	11.0
49c	3.0	15.6	10.4	0.5	3.0	2.9	33.9	3.5	9.2	16.6	9.5	9.5	4.0	11.0
49d	10.9	3.7	9.9	1.8	2.9	2.9	36.0	3.6	9.5	14.5	9.5	7.3	4.0	10.7
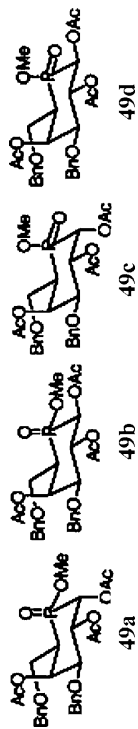
1,4-dibromobutane via a Grignard coupling reaction. By the same reaction with ethyl phosphonous dichloroide, **56b** is also prepared in 54% yield (Scheme 15). By analogy, (3R,4R)-3,4-dimethoxy-1-phenylpholane 1-oxide (**52**) as well as **59** can be prepared from 1-bromo-1,4-dideoxy-4-[(R and S)-ethoxy(phenyl)phosphinoyl]-2,3-di-O-methyl-L-threitols (**57**) in 78% yield (Scheme 16) [23].
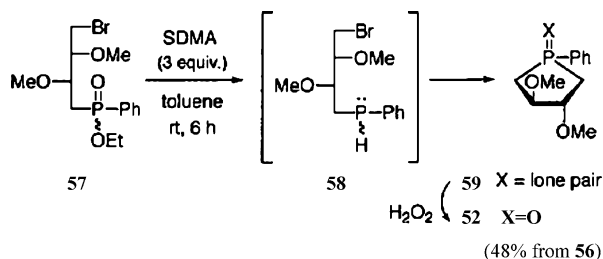

Scheme 16 Preparation of **52** and **59** from **57**

Two moles of bis-Grignard reagent **60**, or a α,ω-dibromoalkane such as 1,4-dibromobutane with magnesium, and benzothiadiphosphole **61** (a phosphorus donating reagent) gives 1-alkylpholane **62a–c** and the 1-sulfide **63a–c** via the hypothetical intermediates **A′** and **A** in a one-pot synthesis (Schemes 17 and 18). The ring size of the product is reported as being from
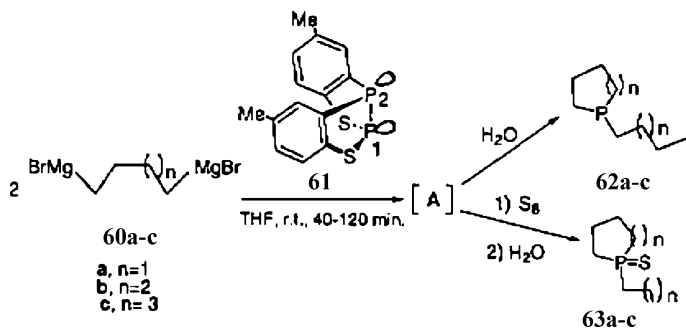

Scheme 17 One-pot synthesis of **62** and **63** from **60** and **61**
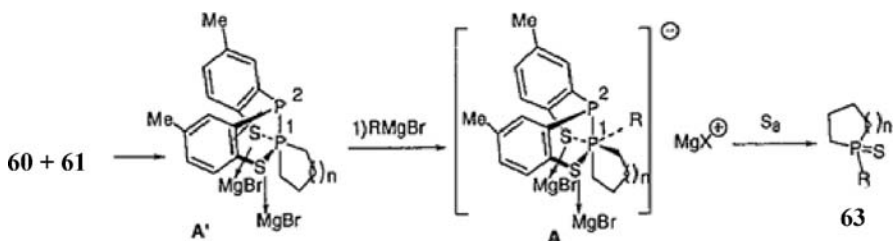

Scheme 18 Hypothetical intermediates **A′** and **A**

five to seven ($n = 1$–3) and the phospholane with a P(III) moiety in the ring is converted into the 1-sulfide **63** by the action of sulfur [24].

The 2- and 3-phospholenes are prepared by the McCormack reaction and are good candidates as starting materials for the preparation of five- and six-membered phosphorus heterocycles [25–27]. From 1-methoxy-3-methyl-2-phospholene **64** or 1-methoxy-2,3-diacetoxy-3-methylphospholane **67**, 1-aryoxy-3-methyl-2-phospholenes **66a–c** (Scheme 19), or 1-aryoxy-2,3-diacetoxy-3-methylphospholane **69** (Scheme 20) with a substituted phenyl group at phosphorus, or 1-aryl-3-methyl-2-phospholenes **71a–g** (Scheme 21) are prepared by a substitution reaction and/or a Grignard coupling reaction [28, 29].
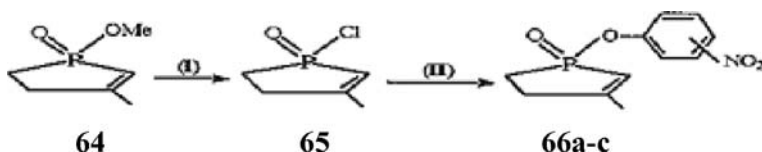
Scheme 19 Preparation of 1-aryoxy-3-methyl-2-phospholenes **66a–c**
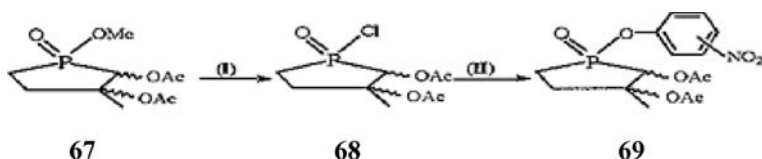
Scheme 20 Preparation of 1-aryoxy-2,3-diacetoxy-3-methylphospholane **69**
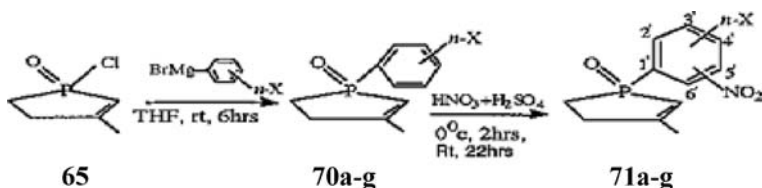
Scheme 21 Preparation of 1-aryl-3-methyl-2-phospholenes **71a–g**

The structure of dinitro derivative **70e** is elucidated by X-ray single crystal structure analysis (Fig. 4).

Novel preparative methods for *phospha* sugars (e.g., **74–77, 83, 89–91**) and/or phosphorus heterocycles (up to now *phospha* sugars have not been found in natural products) have been extensively developed starting from phosphorus heterocycles such as phospholenes, unlike traditional sugar chemistry in which sugar starting materials (e.g., **72, 78, 94, 92, 93**) are mainly used (Schemes 22–25) [30–33].
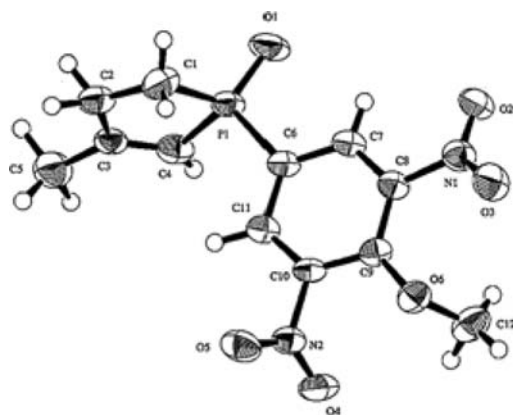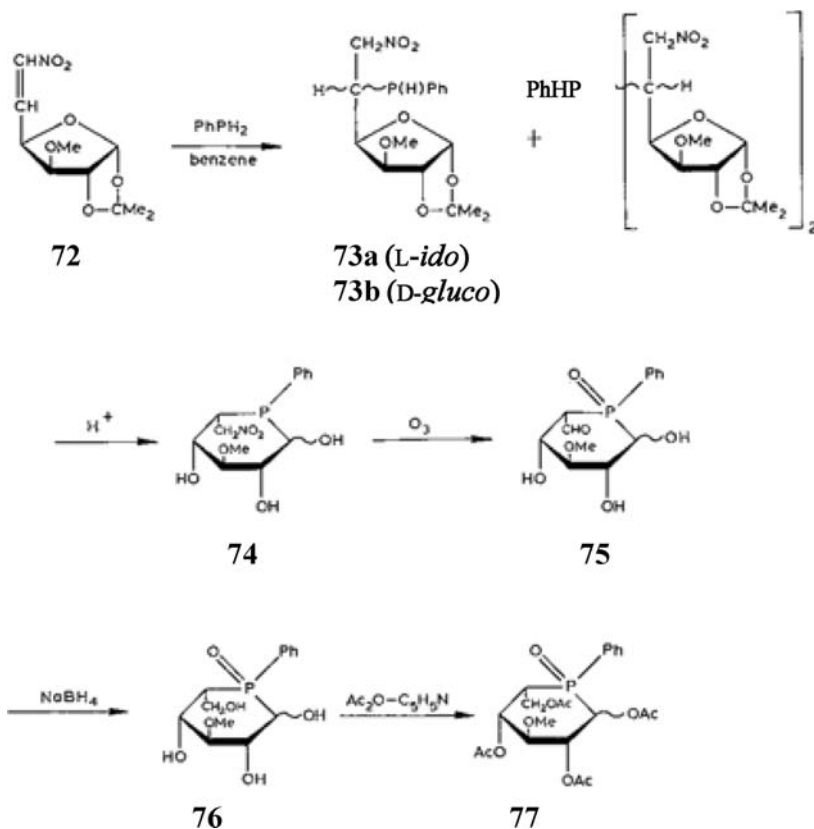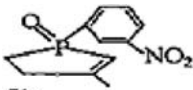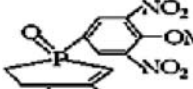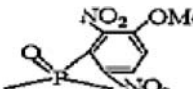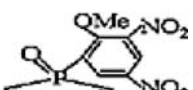
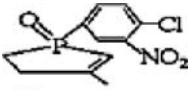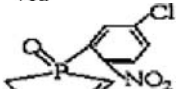**Fig. 4**   ORTEP   drawing   of   1-(4′-ethoxy-3′,5′-dinitrophenyl)-3-methyl-2-phosphlene 1-oxide (**70e**)

Scheme 22 Novel preparative methods for *phospha* sugars **74–77**

Table 2 Product structures, physical and ^{31}P NMR data of **71a–g**

Entry	Substrate	Product	Yield (%)	MP (°C)	^{31}P-NMR (ppm)
1	**70a**	71a	80	117–120	59.90
2	**70b**	71b	56	ND^a	77.28
3	**70c**	71c	55	ND^a	76.57
4	**70d**	71d	50	ND^a	77.92
5	**70e**	71e	75	170–173	57.96
6	**70f**	71f	71	162–166	56.65
7	**70g**	71g	70	155–159	58.18

^{a} Not determined due to syrupy state

The structure of **93a** was elucidated by X-ray single crystal structure analysis to be the 6-deoxy-D-*gluco*-type *phospha* sugar (Fig. 5).

[4 + 2] Cycloaddition of phosphorus(III) halides to 1,3-dienes (such as 1,3-butadiene, 1,3-pentadiene, and 2-methyl-1,3-butadiene) followed by solvolysis is known to produce cyc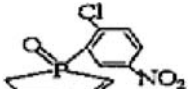lic unsaturated phosphorus heterocycles, i.e., 2- and 3-pholene 1-oxide derivatives **94** and **95**, respectively, depending on the chloride and bromide of the phosphorus halides (Fig. 6) [34–36].
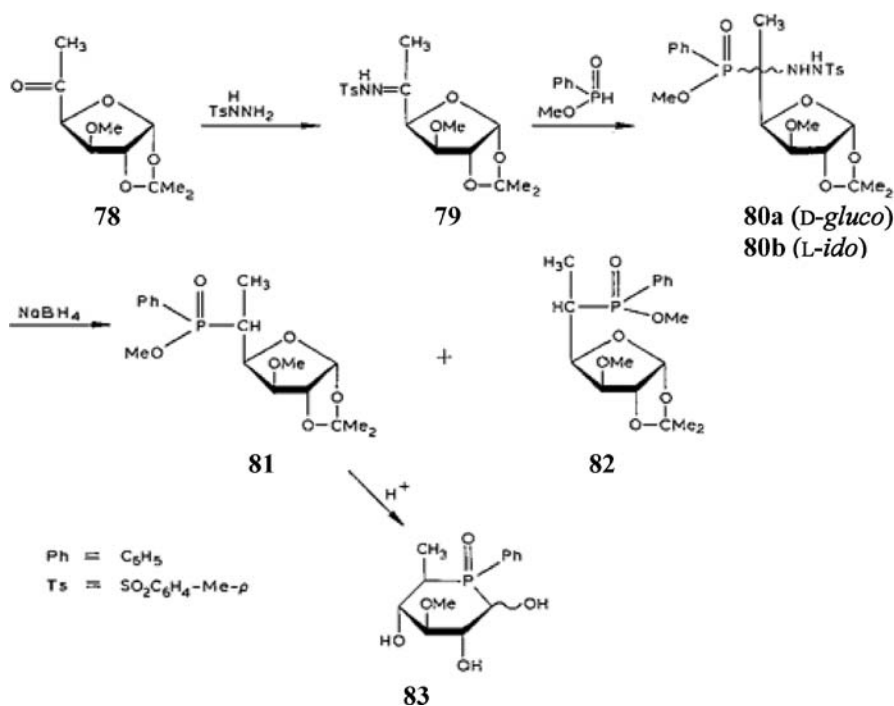
Scheme 23 Novel preparative methods for *phospha* sugar **83**

The carbon–carbon double bond of 2-phospholene heterocycles **94a–c** is first converted into *cis*-diols **96a–c** (2,3-dihydroxyphospholane derivatives or α,β-D,L-*glycero*-tetrofuranose-type *phospha* sugars) with osmium tetroxide in the presence of a co-oxidant (Scheme 26) and the structure is confirmed by X-ray single crystal structure determination. The ORTEP drawing and the structure of two possible enantiomers **96A** and **96B** are shown in Fig. 7. Compared with the traditional *phospha* sugar preparation procedure, the novel preparative method for *phospha* sugars is much more convenient and is able to develop new *phospha* sugar chemistries and phospholane chemistries because the variation of substituents of **94** and **95** is rather easy and the pathway is short.

The *cis*-diole **96** can be converted into the corresponding acetate **97** and acetonide **98** for confirmation of the structure (Scheme 27).

Using the new preparative method, combined with reactions at the allylic position in the phospholene 1,2,3,4-tetrasubstituted-phospholanes, a series of the tetrofuranose-type *phospha* sugars can be prepared (Scheme 28 and Tables 3 and 4) [37, 38].

Addition of bromine, in an aqueous organic solvent medium or in organic solvents/water systems, to the carbon–carbon double bond of 2-phospholenes **94** produces 2-bromo-3-hydroxyphospholanes, which correlates to a 1-deoxy-
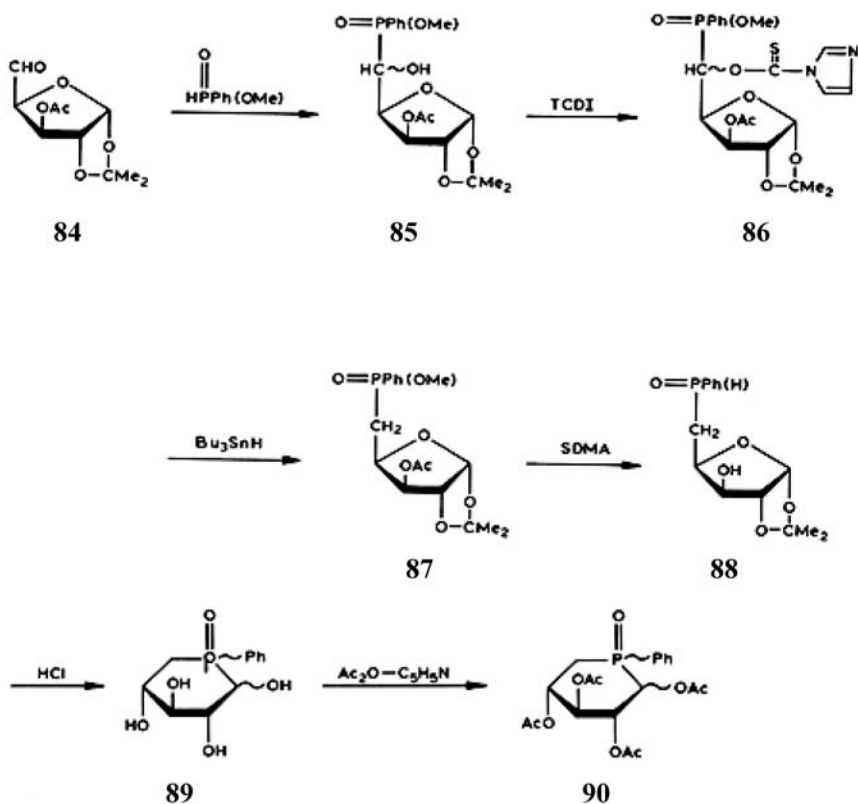
Scheme 24 Novel preparative methods for *phospha* sugars 89 and 90

93a,b
(D-*gluco* type and L-*ido* type)
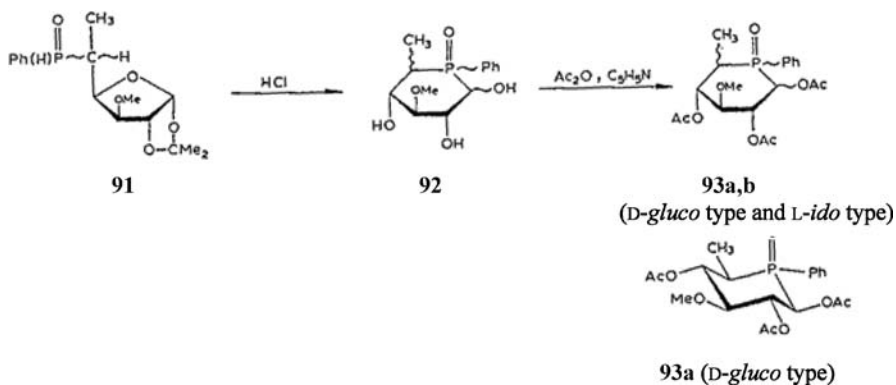
93a (D-*gluco* type)

Scheme 25 Novel preparative methods for *phospha* sugars 93
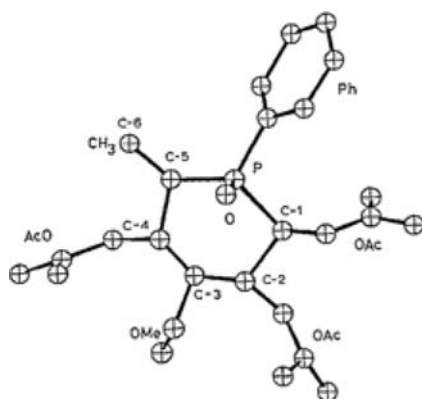
Fig. 5 Computer-generated drawing of compound **93a** (D-*gluco* type)
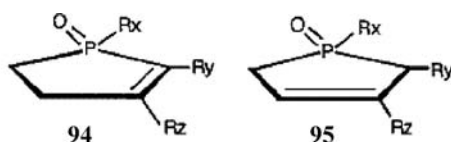
Rx=Alkyl, Aryl (e.g., Ph), Alkoxyl (e.g., OMe, OEt), Halogen, etc.
Ry, Rz=Alkyl (e.g., Me), Hydrogen, etc.

a; Rx=Ph, Ry=H, Rz=Me   b; Rx=Ph, Ry=Rz=H
c; Rx=OMe, Ry=H, Rz=Me   d; Rx=OMe, Ry=Rz=H
e; Rx=OEt, Ry=H, Rz=Me   f; Rx=OEt, Ry=Rz=H
g; Rx=O^{i}Pr, Ry=H, Rz=Me   h; Rx=O^{i}Pr, Ry=Rz=H
i; Rx=Ph, Ry=Me, Rz=H

Fig. 6 Substituted 2- and 3-phospholene 1-oxides **94** and **95**
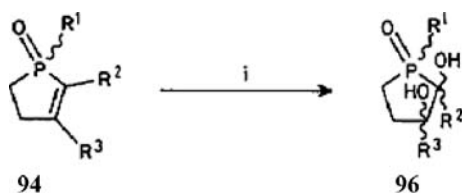
a; R^1 = Ph, R^2 = H, R^3 = Me
b; R^1 = Ph, R^2 = Me, R^3 = H
c; R^1 = OMe, R^2 = H, R^3 = Me

Reagents: i. OsO$_4$–MClO$_4$.

Scheme 26 The carbon–carbon double bond of 2-phospholene heterocycles **94a–c** is converted into *cis*-diols **96a–c**
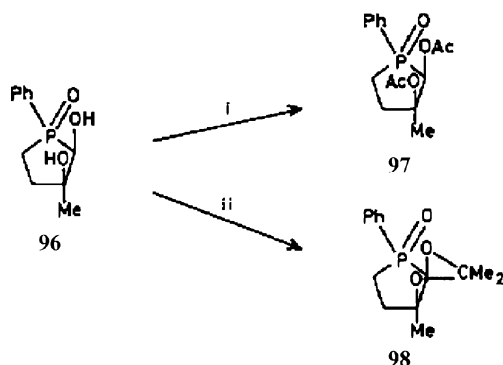
Reagents: i, Ac₂O–pyridine; ii, H⁺, acetone.

Scheme 27 **96** can be converted into the corresponding acetate **97** and acetonide **98**
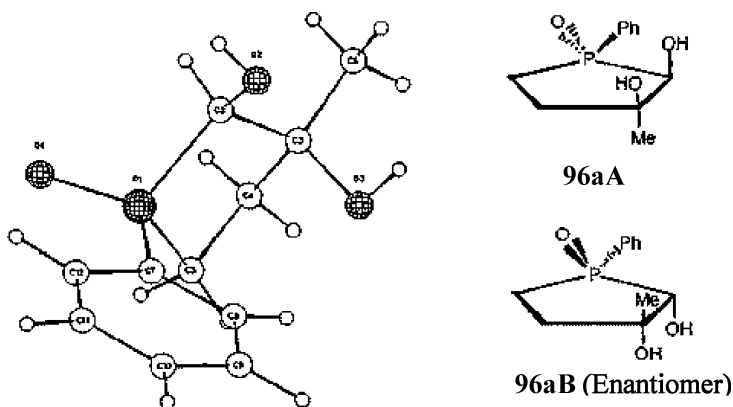
Fig. 7 ORTEP drawing of *cis*-diol **96a** and representation of the enantiomers **96aA** and **96aB**

Table 3 *cis*-Dihydroxylation of 2-phospholene 1-oxides **94**

Phos- pholene no.	Reaction conditions			Reaction product		
	Reagent	Temperature (°C)	Time (h)	No.	Yield (%)	MS (m/z)[a]
94a	OsO_4-$KClO_3$	45–50	18	**96a**	91	226
94a	OsO_4-$KClO_3$	45–50	18	**96a**	66	226
94a	OsO_4-$Ba(ClO_3)_2$	45–50	18	**96a**	65	226
94a	OsO_4-$^tBuO_2H$	45–50	24	**96a**	20	226
94b	OsO_4-$KClO_3$	35	48	**96b**	82	212
94c	OsO_4-$KClO_3$	55–60	24	**96c**	35	178
94i	OsO_4-$KClO_3$	45–50	18	**96i**	42	226

[a] MS data indicate the molecular ion peak (M*) in *m/z*.

Table 4 Preparation of 4-acyloxy-2-phospholene 1-oxides and 4-acyloxy-2,3-*cis*-dihydroxyphospholane 1-oxides

2-Phospholene no.	Substituents			R′	Product yield (%)			
	Rx	Ry	Rz		99	100	101	102
94b	Ph	H	H	Me	100	61	45	69
94c	OMe	H	Me	Me	100	55	71	75
94c	OMe	H	Me	Ph		67	41	78
94d	OMe	H	H	Me	98	75	63	68
94e	OEt	H	Me	Me	100	90	74	80
94e	OEt	H	Me	Ph		83	69	76
94f	OEt	H	H	Me	100	51	51	52
94f	OEt	H	H	Ph		93	93	46
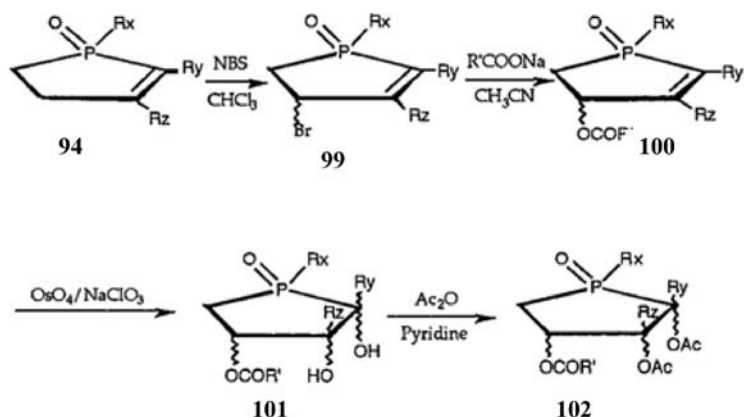
94b, 99b:	Rx=Ph, Ry=Rz=H;
94d,99d:	Rx=OMe, Ry=Rz=H;
94f,99f:	Rx=OEt, Ry=Rz=H.

94c,99c: Rx=OMe, Ry=H, Rz=Me;
94e,99e: Rx=OEt, Ry=H, Rz=Me;

100b-102b: Rx=Ph, Ry=Rz=H, R'=Me;
100c'-102c': Rx=OMe, Ry=H, Rz=Me, R'=P
100e-102e: Rx=OEt, Ry=H, Rz=Me, R'=Me;
100f-102f: Rx=OEt, Ry=Rz=H, R'=Me;

100c,102c: Rx=OMe, Ry=H, Rz=Me, R'=Me;
100d,102d: Rx=OMe, Ry=Rz=H, R'=Me;
100e',102e': Rx=OEt, Ry=H, Rz=Me, R'=Ph;
100f',102f': Rx=OEt, Ry=Rz=H, R'=Ph.

Scheme 28 Preparation of a series of tetrofuranose-type *phospha* sugars

1-bromotetrofuranose-type *phospha* sugar. Replacement of the bromo substituent by nitrogen nucleophiles introduces a nitrogen substituent on the 2-position of phospholanes to give 2-amino-3-hydroxy-1-phenylphospholane 1-oxide (**104E**; the *erythro* form diastereomer, where the oxygen atom of the P=O group and the nitrogen atom of the 2-amino group locate on the same

side of the heterocycle), which is an analogue of *phospha* sugar *N*-glycoside (Scheme 29 and Table 5) [39].
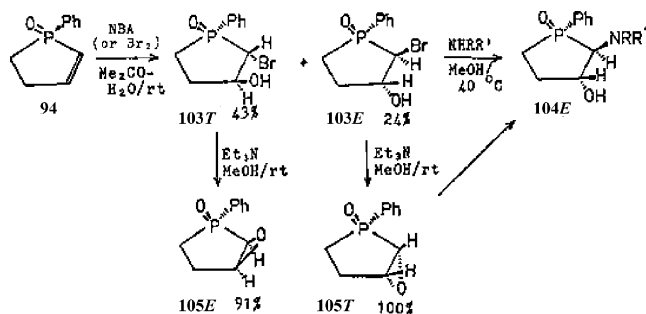
Scheme 29 Preparation of *phospha* sugar *N*-glycosides **104Ea–d**

2,3,4-Tri-*O*-acetyl-1-phenylpholane **108**, the peracetate of a tetro-furanose-type *phospha* sugar, is synthesized from 2-pholene **94** and/or 3-pholene **95**. The bromo group of 2-bromopholanes **103** is re-placed by various nucleophiles to afford glycosides **104**, i.e., *O*-glycosides, *S*-glycosides (e.g., **109**), *N*-glycosides (e.g., **104** and **111**), and *P*-glycosides (e.g., **110**), via intermediary formed epoxide **105** from **103** and/or directly prepared 2,3-epoxypholane **105** (Schemes 30–33) [40–43]. These struc-tures are determined by X-ray crystallography (ORTEP drawings are shown in Figs. 8–10).
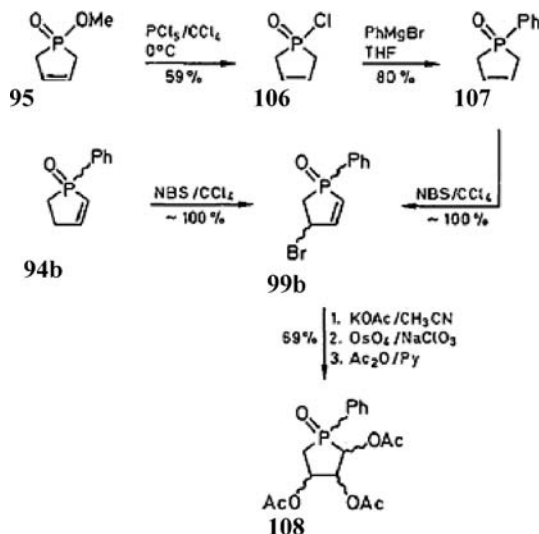
Scheme 30 Synthesis of 2,3,4-tri-*O*-acetyl-1-phenylpholane **108**

Table 5 Preparation and properties of compounds 104*E*, 105*E*, and 105*T*

Starting material	Amine	Reaction conditions[a]		Product No.	R	R′	Product properties		NMR[b]	MS[c]
		Solvent	Temp (°C)				Mp (°C)	Yield (%)		
103*E*	MeNH$_2$	MeOH-H$_2$O	40	104*E*	Me	H	Syrup	56	2.76	225
103*E*	*i*-PrNH$_2$	MeOH	40	104*E*	*i*-Pr	H	138.5–140	75	2.78	253
103*E*	*t*-BuNH$_2$	MeOH	40	104*E*	*t*-Bu	H	184–185	55	2.82	267
103*E*	Et$_2$NH	MeOH	40	104*E*	Et	Et	Syrup	84	2.88	267
103*E*	Et$_3$N	Et$_3$N	Room temp	105*E*	–	–	Syrup	100	3.36	194
103*T*	Et$_3$N	Et$_3$N	Room temp	105*T*	–	–	116–118	91	3.39	194

[a] The reaction was carried out for 2 days

[b] ^{1}H-NMR (60 MHz, TMS, CDCl$_3$): δ value for H-1

[c] MS datum (in m/z observed) for molecular ion (M$^+$)

Scheme 31 Synthesis of various glycosides by replacement of the bromo group of 2-bromophospholanes **103**

$$R^1 = \text{Me and Et}$$
$$R^2 = \text{Ac, Bz, and THP}$$
$$R^3 = \text{OMe and Ph}$$

Scheme 32 Synthesis of *P*-glycoside **110**

Scheme 33 Synthesis of *N*-glycoside **111**

2,3-Epoxyphospholanes **105** are directly prepared from 2-phospholenes **94**. Epoxidation of **94** with sodium peroxide give a single diastereomer of *erythro* **105E** (X-ray analysis gives the ORTEP drawing in Fig. 10) in stereospecific and stereoselective manner (Scheme 34 and Table 6). However, 2,3-epoxidation of
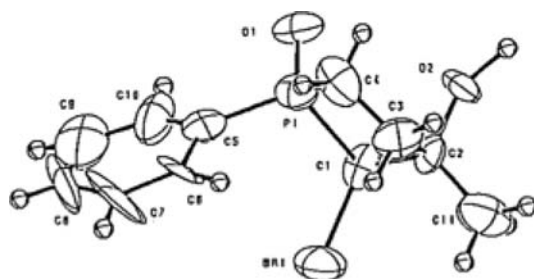
Fig. 8 ORTEP drawing of 2-bromo compound **103**
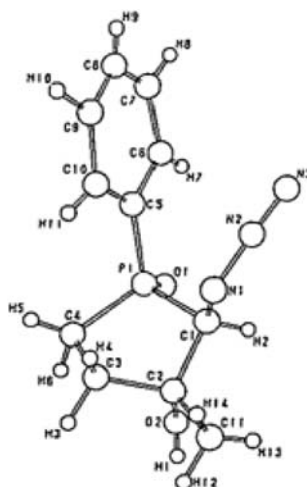
Fig. 9 ORTEP drawing of 2-azide compound **110a**
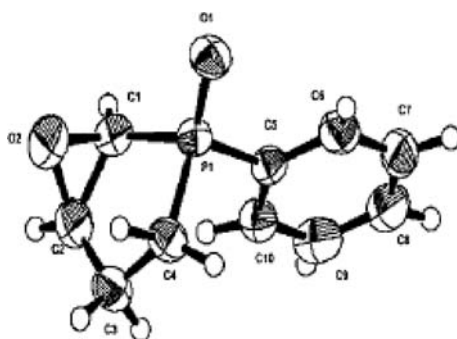
Fig. 10 ORTEP drawing of 2,3-epoxyphospholane **105a**

2-pholsenes **94** by the action of hydrogen peroxide affords the diastere-omer mixture of *threo* **105T** and *erythro* **105E** [44, 45].
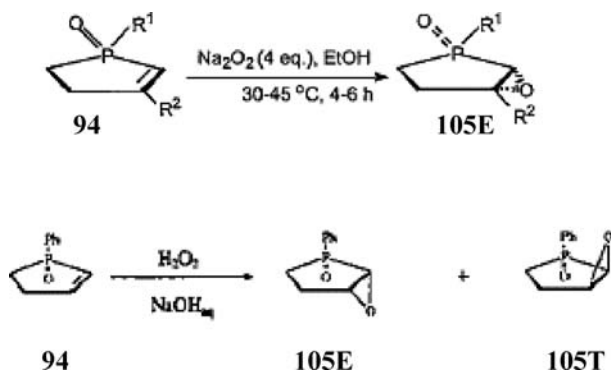
Scheme 34 Direct preparation of 2,3-epoxyphospholanes **105** from 2-phospholenes **94**

Table 6 Epoxidation of 2-phospholene **94**

R1	R2	Time (h)	Yield (%)
Ph	H	5	76
$C_6H_4 - NO_2$ (*m*)	H	6	80
$C_6H_4 - OMe$ (*p*)	H	6	75
C_6H_4-Cl (*m*)	H	6	77
OMe	H	4	70
Ph	Me	6	No epoxidation
OMe	Me	6	No epoxidation

Combination of 2-bromophospholanes as the glycosyl donor (Fig. 11) and monosaccharides as the glycosyl accepter gives disaccharides of *phospha* sugars (Table 7 and Fig. 12). The disaccharide-forming reaction proceeds for 2-bromo-3-methoxyphospholanes **111** (glycosyl donor type III and IV) but not for 2-bromo-3-hydroxyphospholanes **105** (glycosyl donor type I and II) [46].
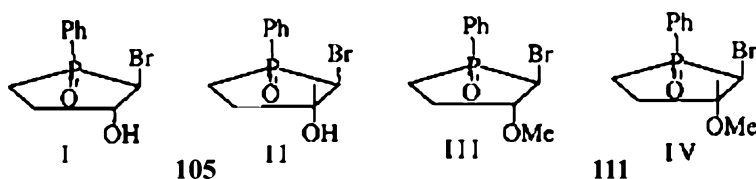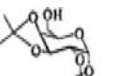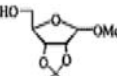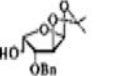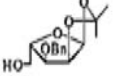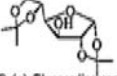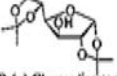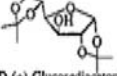
Fig. 11 Different types of 2-bromo-3-hydroxy/methoxy-phospholane-based glycosyl donors (**105** I and II/**111** III and IV)

Table 7 Preparation of deoxy sugar–sugar disaccharides **112–116**

Entry	Donor	Acceptor	Disaccharide	Yield (%)[a]
1	**111-III**	D-(+)-Glucosediacetonide	**112**	42
2	**111-III**	D-(+)-Galactosediacetonide	**113**	44
3	**111-III**	D-(-)-Riboseacetonide	**114**	42
4	**111-III**	L-(-)-Xyloseacetonide	**115**	39
5	**111-III**	L-(-)-Arabinoseacetonide	**116**	41
6	**111-III**	D-(+)-Mannosediacetonide		91
7	**111-I**	D-(+)-Glucosediacetonide		88
8	**111-II**	D-(+)-Glucosediacetonide		92
9	**111-IV**	D-(+)-Glucosediacetonide		95

[a] Percentage yield for entry 4 was calculated after purification by column chromatography and recycle GPC analysis
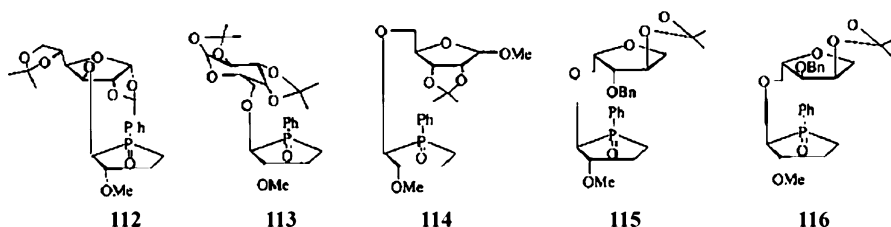
Fig. 12 Structures of *phospha* sugar disaccharides **112–116**

Phospha sugar nucleosides have not yet been shown to be naturally occurring. Some analogues of *phospha* sugar nucleosides (e.g., **118**) are prepared from 2-bromo-3-hydroxyphospholanes **94** or **103** by nucleophilic substitution reaction with nitrogen nucleophiles (Schemes 35 and 36, and Table 8). However, the nucleophilic substitution reaction (or electrophilic substitution reaction in the presence of catalyst) of 2-bromo-3-hydroxyphospholanes **94**
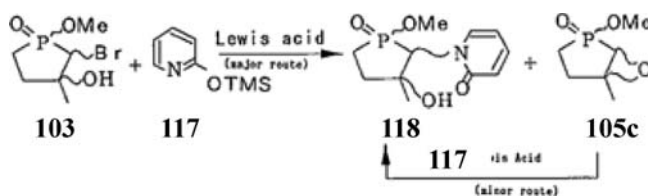
Scheme 35 Preparation of *phospha* sugar nucleoside **118** from 2-bromo-3-hydroxyphospholane **103** by nucleophilic substitution reaction with nitrogen nucleophiles
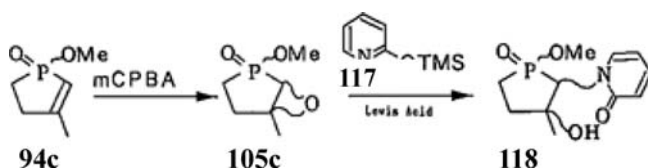
Scheme 36 Preparation of **118** from 2-bromo-3-hydroxyphospholane **94c**

Table 8 Preparation of *phospha* sugar nucleoside **118** by the reaction of 2-bromophospholane **103c** with cyclic base **117**

Solvent	Lewis acid/eq.	Yield (%)
ClCH$_2$CH$_2$Cl	SnCl$_4$/0.1	4.4
DMF	SnCl$_4$/0.1	11.0
CH$_3$CN	SnCl$_4$/0.1	21.5
CH$_3$CN	SnCl$_4$/0.5	28.0
CH$_3$CN	BF$_3$-OEt$_2$/0.5	62.0

with nucleic acids does not give any nucleosides of *phospha* sugars, because of the lower nucleophilicity of the nucleic acid than that of amine nucleopholes (Scheme 37) [47].
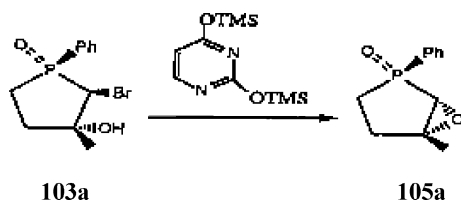
Scheme 37 Nucleophilic substitution reaction of 2-bromo-3-hydroxyphospholane **103a** with nucleic acids does not give *phospha* sugar nucleosides

The alternative preparative methods for *phospha* sugar nucleosides are reported by cycloaddition or cyclocondensation of 2-aminophospholanes, *N*-glycosides of *phospha* sugars, with acrylates. Such sugar-modified and/or nucleic acid-modified nucleosides (e.g., Ribavirin, AZT, 4′-thio ddC, Aristeromycin, etc.) are known and have biological activities such as anti-HIV, anticancer, antibacterial, etc. 1,3-Cycloaddition of 2-azidophospholane with alkynes gives triazole analogues of the *phospha* sugar nucleoside **119** (Scheme 38 and Table 9). The structure of Ribavirin analogue **119cB** was determined by X-ray analysis (Fig. 13) [48].
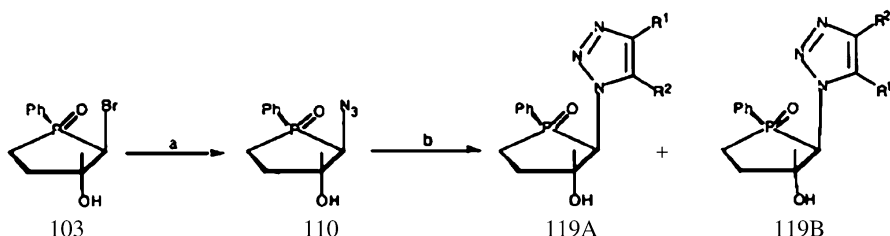
Scheme 38 Alternative preparative method for *phospha* sugar nucleosides: *a* NaN$_3$, DMF, 70 °C, 24 h; *b* substituted acetylenes (R^{1}CCR^2 are shown in Table 9), DME, reflux

2-Amino-3-hydroxyphospholane **111a**, prepared from 2-azido-3-hydroxy-phospholane **110a** by hydrogenolysis, reacts with substituted acrylamide derivatives and undergoes the double condensation reaction to produce the pyrimidine or uracil nucleosides (e.g. **120**) of *phospha* sugars via the acyclic uracylphospholane derivatives (Scheme 39, Table 10, and Fig. 14). The results of conformational analysis and X-ray crystallographic analysis are shown in Figs. 15 and 16 [49].

1-Amino acid derivatives of 2-phospholene and 3-methyl-2-phospholene 1-oxides are prepared by the reaction of 1-chloro-2-phospholene 1-oxide with

Table 9 1,3-Dipolar cycloaddition of azide **110** with various alkynes **a–j**

Alkyne	R′	R²	Reaction time (h)	Product	Yield (%)	Mp (°C)
a	CO₂Me	CO₂Me	12	**119aB**	79	205–206
b	CO₂Et	CO₂Et	16	**119bB**	84	175–176
c	CH₂OH	CH₂OH	75	**119cB**	68	205–206
d	CO₂H	CO₂H	24	**119dB**	79	175–176
e	H	SiMe₃	24	**119eB**	57	221–222
f	H	CH₂OH	48	**119fB**	36	184–185
			48	**119fA**	38	227–228
g	H	CMe₂OH	120	**119gB**	42	204–205
			120	**119gA**	25	215–216
h	H	CO₂Me	12	**119hB**	49	206–207
			12	**119hA**	37	219–220
i	H	Ph	96	**119iB**	33	230–232
			96	**119iA**	17	228–229
j	H	CMe₃	36	**119jB**	55	224–227
			36	**119jA**	21	247–250
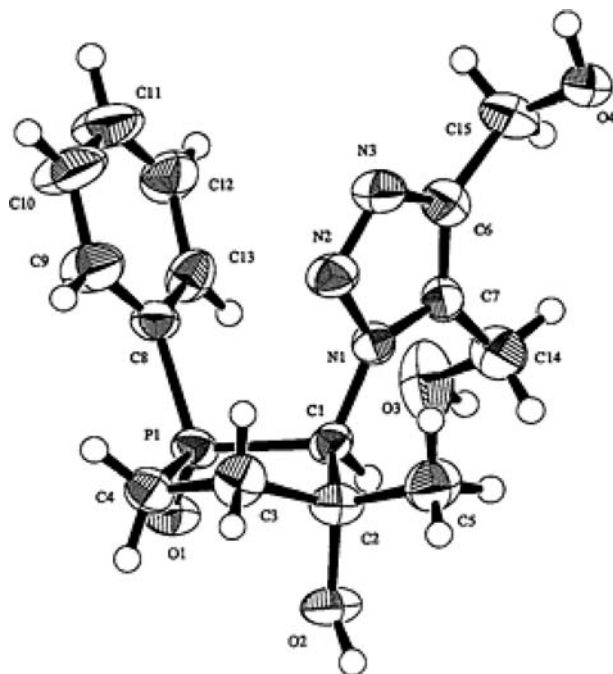
Fig. 13 ORTEP drawing of nucleoside **119cB**
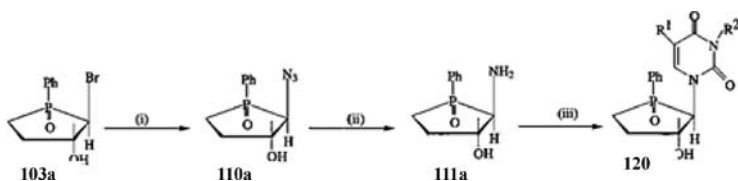
Scheme 39 Synthesis of pyrimidine or uracil nucleosides of *phospha* sugars

Table 10 Deoxy *phospha* sugar pyrimidine nucleosides **120a–g** prepared via Scheme 39

Compound	R^1	R^2	Yield (%)
120a	CN	Me	88
120b	CN	*p*-ClBn	68[a]
120c	CN	H	82
120d	COMe	H	75
120e	CO$_2$Et	H	73
120f	Me	H	72
120g	H	H	76

[a] Percentage yield of compound **120b** was decreased due to steric hindrance of *p*-ClBn substituent on the uracil ring
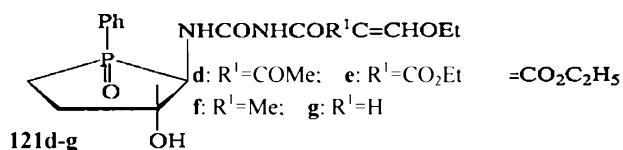
Fig. 14 2-Uncyclized substituted uracil phospholane derivatives **121d–g**
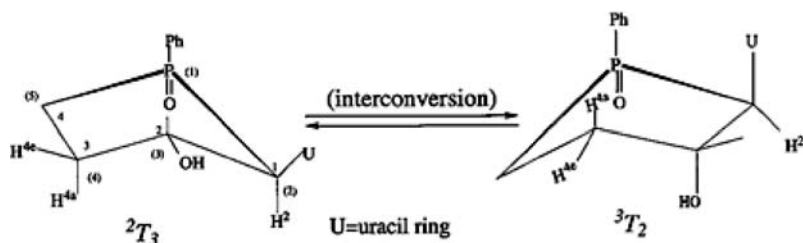
Fig. 15 Favored conformations for the phospholane ring of **120a–g** based on ^{1}H NMR analysis in solution

an amino acid (such as L-alanine, L-leucine, L-valine, and L-phenylalanine) at –78 °C as the diastereomer mixture (Table 11) [50]. Evaluated bioassay of acyclic analogues of phosphinic acid and phosphoric acid peptide derivatives
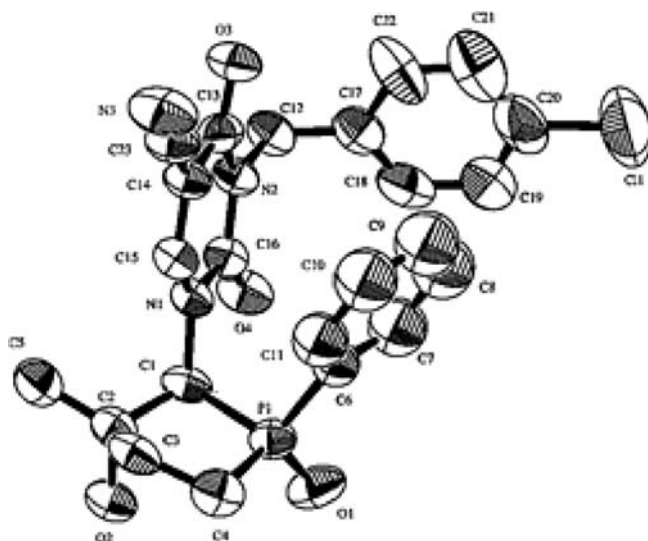
Fig. 16 Crystal structure of compound **120b**. Selected bond length(Å), bond angle (°), and torsion angles (°): P-1-C-1, 1.861(8); P-1-C-4, 1.800(10); C-1-P-1-C-4, 97.0(4); P-1-C-4-C-3-C-2, 34.7(8); C-1-P-1-C-4-C-3, −12.3(6)

shows the presence of inhibitors of aspartic proteases, pepsin, pencillopepsin, and carboxypeptidase A (Fig. 17) [51, 52]. Biologically, cyclophosphamide is known to act as an antitumor drag, so the amino acid derivatives of *phospha* sugars may exert an important bioactivity (Schemes 40 and 41) [53].

The prepared amino acid derivatives of phospholenes **124a–j** are shown in Table 11.

2,3-Dibromo-3-methyl-1-phenylphospholane 1-oxide (**125**) prepared from 1-phenyl-3-methyl-2-phospholene 1-oxide and bromine in the presence of

Table 11 Prepared amino acid derivatives of phospholenes **124a–j**

Entry	Substrate	Product	Isolated yield (%)
1	**122a, 123a**	**124a : 124a′**	34 : 36
2	**122a, 123b**	**124b : 124b′**	32.5 : 33.5
3	**122a, 123c**	**124c : 124c′**	32 : 32
4	**122a, 123d**	**124d : 124d′**	33 : 34
5	**122b, 123a**	**124e : 124e′**	36 : 32
6	**122b, 123b**	**124f : 124f′**	31 : 32
7	**122b, 123c**	**124g : 124g′**	30 : 31
8	**122b, 123d**	**124h : 124h′**	33 : 32
9	**122a, 123i**	**124i : 124i′**	34 : 34
10	**122a, 123j**	**124j : 124j′**	31 : 34
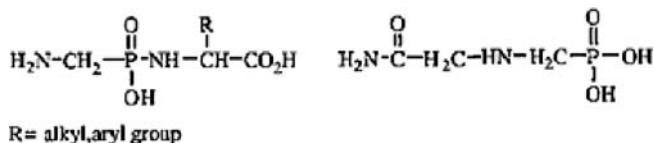
Fig. 17 General structures of amino acid derivatives linked with phosphates and exhibiting potential biological activity
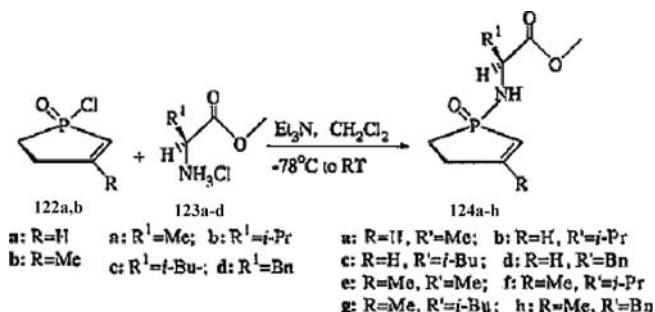
Scheme 40 Preparation of amino acid derivatives of *phospha* sugars 124a–h
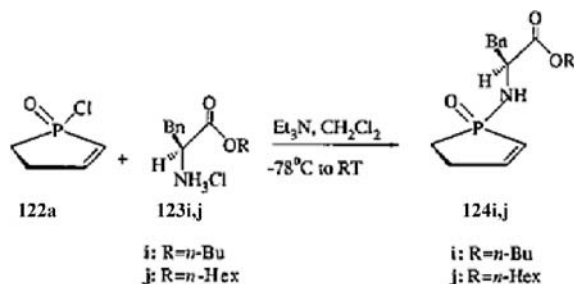
Scheme 41 Preparation of amino acid derivatives of *phospha* sugars 124i–j

catalyst consists of diastereoisomers (Fig. 18). The mixture and the isolated diastereomers of the dibromophospholane show quite specific and selective antitumor activity for leukemia as well as stomach cancer, e.g., Imatinib [54]. Some of these *phospha* sugars and/or epoxides and bromides of phosopholanes have recently been found to be highly active anticancer agents.
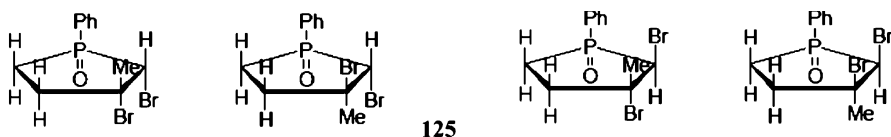
Fig. 18 Diastereomers of 2,3-dibromophospholanes 125

Allylic oxidation of 2-phospholenes affording 4-oxophospholanes **126** as the new starting materials for pentofuranose and C1-homologation of 2,3-epoxy-phospholanes to prepare pentofuranose-type *phospha* sugars are also reported (Scheme 42 and Table 12) [55–57]. ORTEP drawing of **126a** is shown in Fig. 19.

An alternative method for preparation of 4-oxophospholanes **126** is oxidation of 3-hydroxyphospholane **127**. Alkylation of **126** at the methylene of the 5-position, where acidic property is expected by the two electron-withdrawing groups of adjacent P=O and C=O groups to the methylene corresponding to two ester groups of maleate, gives mono- and di-alkylation products **128** and **129**, respectively (Scheme 43).

From 3-phospholenes **95**, pentofuranose- and hexofuranose-type *phospha* sugars are prepared. Thus, all four kinds of pentofuranose-type *phospha* sugars (i.e., xylose, lyxose, ribose, and arabinose) are available from 3-phospholene as the starting material. Alkylation of **95** by a C1 unit provides the pentofuranose structure. The alkylation under LDA base and alkyl halides proceeds to give **130** (Table 13), whose *cis*-dihydroxylation affords **131**. The
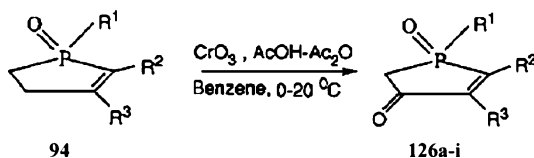
Scheme 42 Allylic oxidation to prepare 4-oxo-2-phospholene 1-oxides **126**

Table 12 Allylic oxidation of 2-phospholenes **94** to prepare **126**

2-Phospholenes **94**			Product[a]	Reaction time[b] (h)	Conv. (%)	Isol. yield (%)	Molar ratio of CrO_3 to substrate
R^1	R^2	R^3					
Ph	H	H	**126a**	4	85	62	2 : 1
OMe	H	Me	**126b**	4	90	60	2 : 1
OMe	H	H	**126c**	4	86	55	2 : 1
3-ClC$_6$H$_4$	H	Me	**126d**	5	80	60	3 : 1
4-OMe-3,5-(NO$_2$)$_2$C$_6$H$_2$	H	Me	**126e**	6	78	62	3 : 1
4-OMeC$_6$H$_4$	H	Me	**126f**	5	82	64	3 : 1
Ph	Br	H	**126g**	5	70	55	2 : 1
Ph	Br	Me	**126h**	4	75	60	2 : 1
Ph	OMe	H	**126i**	5	88	66	2 : 1

[a] From [17]
[b] From [18]
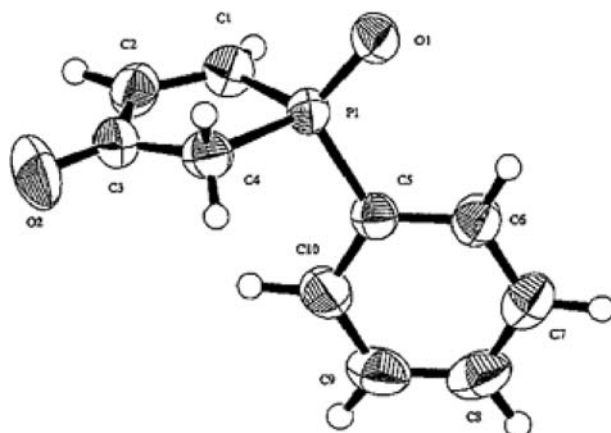
Fig. 19 ORTEP drawing of compound **126a**
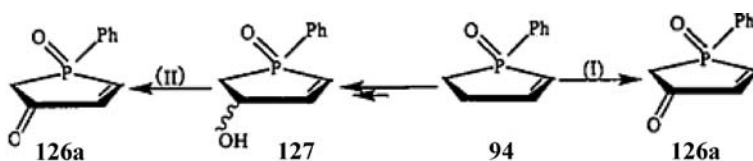
(I) 5CrO₃, Ac₂O-AcOH, CH₂Cl₂, 0-10°C, 5 hrs
(II) 3MnO₂, CHCl₃, RT, 6-8 hrs
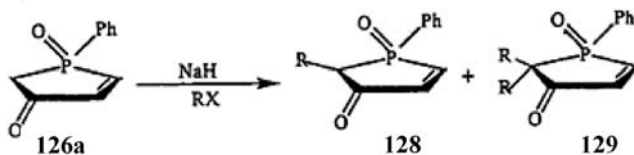
Entry	Number of Moles of NaH	RX	Temp °C	Reaction time	Alkylation total yield (%)	Mono-alkylation yield (%)	Dialkylation yield (%)
1	1.4	1.5CH₃I	−5° to 0°C	2–3 hrs	40	90	10
2	2.4	3CH₃I	RT	6–8 hrs	42	—	100
3	1.4	1.5C₆H₅CH₂Br	0–5°C	4–5 hrs	52	100	—

Scheme 43 Preparation of **126a** from **94** and its conversion to mono- and di-alkylation products

structural studies by X-ray single crystal analysis of acetonide **133** (Fig. 20) from **131** and 2-benzyl-3,4-dihydroxy-1-methoxyphospholane 1-oxide **131b** (Fig. 21) show that they have the $^3T_2$ conformation. Structural studies of 1,4-

Table 13 Alkylation of 3-phospholene derivatives

R of phospholene 95	Alkyl halide R′X	C-Alkylated product		
		Number	Yield (%)	Diastereomer excess (%)
Me	MeI	**130a**	44	95
Me	BnBr	**130b**	69	100
i-Pr	MeI	**130c**	55	100
Me	BnOCH$_2$Cl	**130d**	61	100
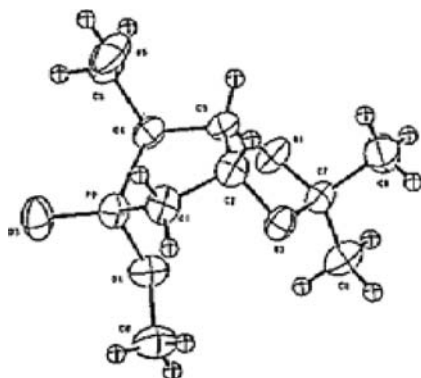
Fig. 20 Structure of acetonide **133** for the *cis*-dihydroxyl group of **132** by X-ray analysis

dideoxy-4-[(S)-methoxyphosphinyl]-D-ribofuranose have revealed that the compound has $^3T_2$ conformation [58–60].

The pentofuranose-type *phospha* sugar **132** is converted into the acetonide **133**, whose structure determined by X-ray analysis is represented in Fig. 20.
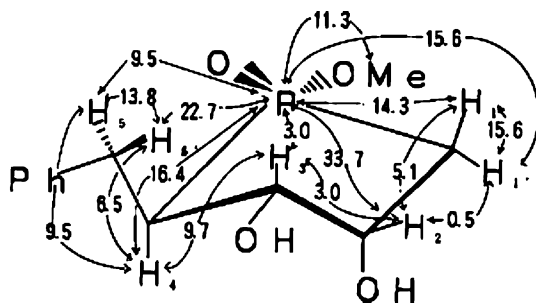
Fig. 21 ^{1}H-NMR spectral analysis and the conformation for 2-benzyl-3,4-dihydroxy-phospholene **131b**
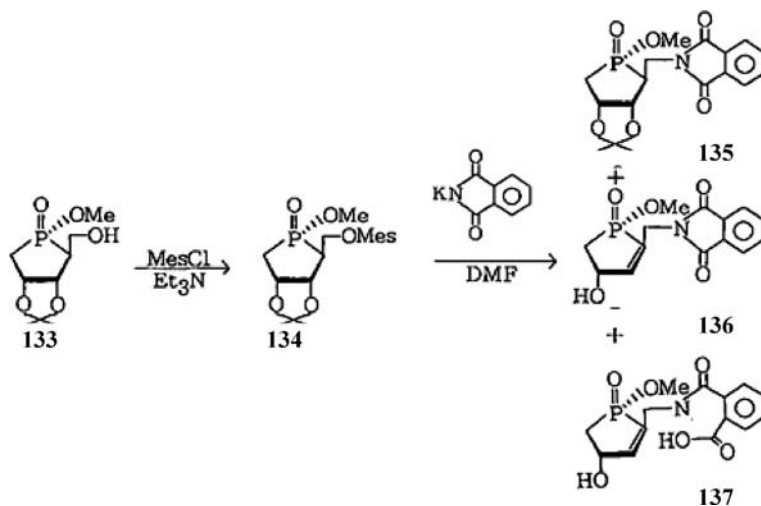
Scheme 44 Preparation of phthalated *phospha* sugars **137-136** by nucleophilic substitution reaction with potassium phthalimide

Acetonide **133** is converted into the phthalimide derivative **135** and further reaction products **136** and **137** via substitution of mesylate **134** with potassium phthalimide (Scheme 44).

The carbon–carbon double bond in alkylated 3-phospholene **130** is oxidized with OsO$_4$-NaClO$_3$ to the *cis*-diol **131**. For epoxidation of 3-phospholene **130d**, *m*-chloroperbenzoic acid (mCPBA) converts the *endo* 3,4-olefin to 3,4-epoxypholanes **134E** and **134T**, which give benzyloxymethylated 2-phospholenes **135a–d** (Scheme 45). *cis*-Hydroxylation of the double bond of phospholenes **135a–d** with osminium tetroxide affords all of the four pentofuranose types (*xylo*-, *lyxo*-, *ribo*-, and *arabino*-pentofuranose *phospha* sugars), **137X**, **140L**, **144R**, and **144A** (Schemes 46 and 47). These is the first case of successful preparation of pentofuranose-type *phospha* sugars from 3-phospholenes **95**.

Addition of methyl 2-methoxycarbonylethylphosphinate to methyl cyclohexenonate (**145** (R = Me)) gives methyl 2-methoxycarbonylethyl-2'-methoxycarbonylcyclohexylphosphinate (**147**), which is successively cyclized by the reaction in the presence of sodium *t*-pentoxide in *t*-pentyl alcohol and finally affords methyl 1-methoyl-1,4-dioxo-2,3-4a,5,6,7,8,8a-octahydro-1λ^5-phosphinoline-3-carboxylate (**149**) with the advantage of a *cis* ring fused bicyclic single stereoisomer formation in 45% yield (Scheme 48) [61].

The reaction of 1,2-dihydrophosphinine oxides **150A** and **150B** with tetracyanoethylene (TCNE) does not follow the Diels–Alder reaction, but rather follows the reaction of two moles of dihydrophosphinine (both of the two double bond isomers) with one mole TCNE to give a 2:1 cyclic adduct, via the 1:1 adduct, due to the ionic or radical nature of TCNE. The
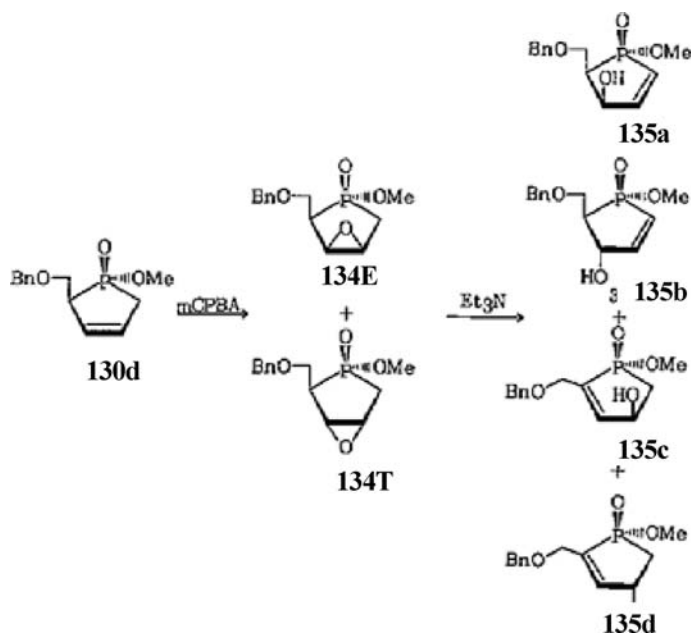
Scheme 45 Isomerization of epoxides **134** prepared from 3-phospholene **130d** to 2-phospholenes **135a–d**
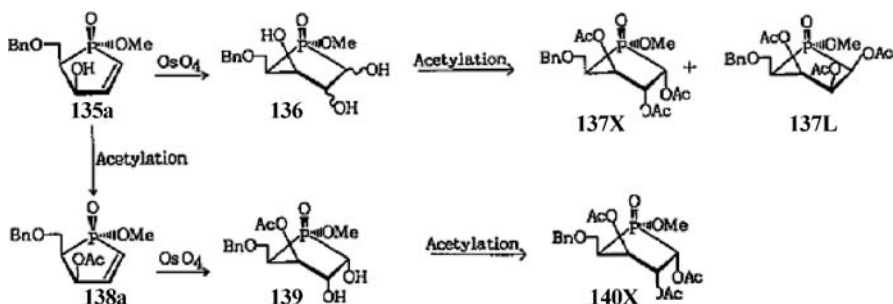
Scheme 46 Preparation of α-D-*xylo*- and β-D-*lyxo* furanose-type *phospha* sugars **137X** and **137L** from **135a**

final product is the bisphosphorus tricyclic adduct, 2,8-diphenylphosphatricyclo[5.3.1.1^{2,6}]dodecatriene **151** in 42–65% yields (Scheme 49) [62].

The photochemical properties of 2,5-dihydrophosphole 1-oxides in the presence of methanol significantly differ according to the P-substituent (the Y group in Scheme 50) on the phosphorus heterocycles. In the case where Y is an aryl group, (1-aryl substituted)-2,5-dihydro-3-methylphosphole 1-oxides (aryl = phenyl, 4-methylphenyl, 2-methylphenyl, etc.) **152** undergo photolysis to give methyl arylphophinites **153** in good to excellent yields
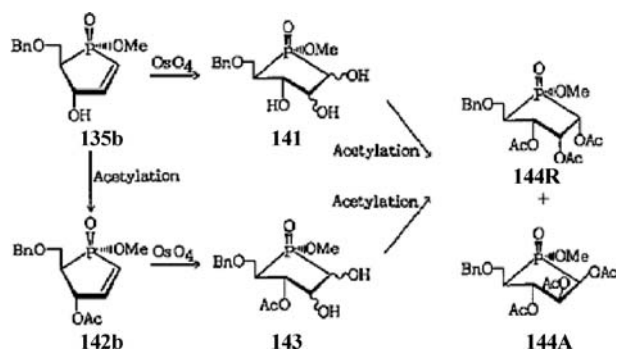
Scheme 47 Preparation of α-D-*ribo*- and β-D-*arabino*-pentofuranose-type *phospha* sugars **144R** and **144A** from **135b**
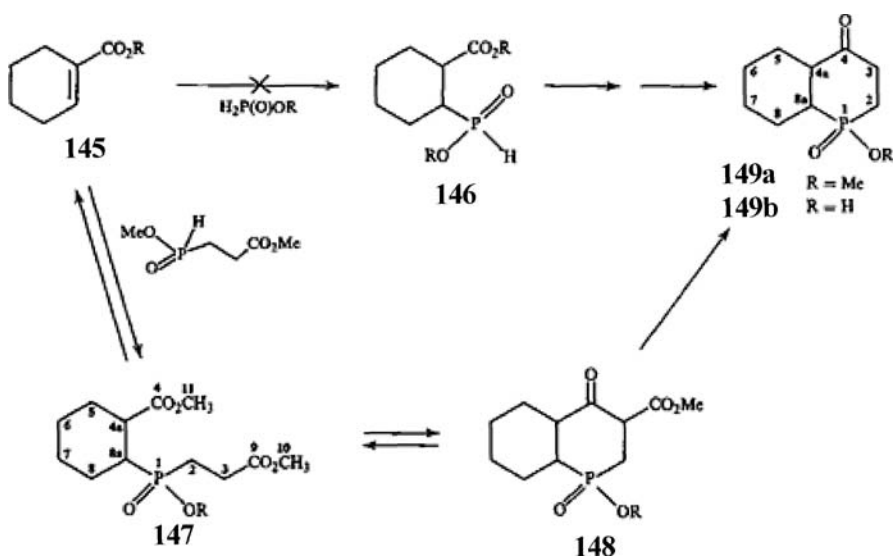
Scheme 48 Preparation of **149** from **145** after successive cyclization
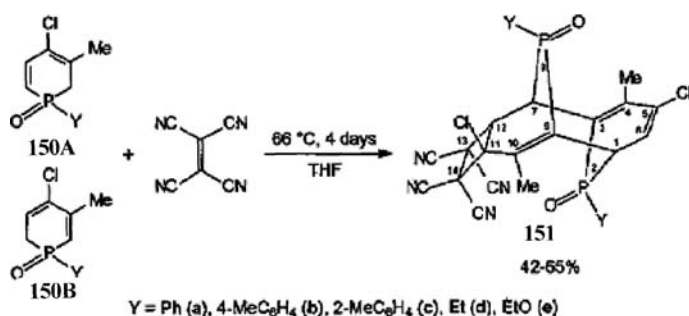
Scheme 49 Reaction of 1,2-dihydrophosphinine oxides with tetracyanoethylene to form **151**
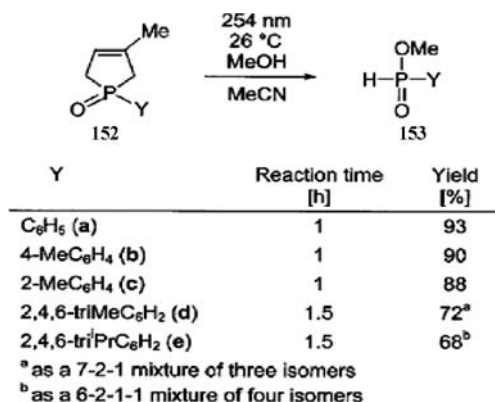
Scheme 50 Yield of methyl arylphophinites after photolysis of 152 with various P-substituents

(68–93% yield). Whereas (1-alkyl or 1-alkoxy substituted)-2,5-dihydro-3-methylphosphole 1-oxides (alkyl or alkoxy = ethyl, cyclohexyl, and ethoxy) react much slower to give methyl alkylphosphonite in little or no yield [63].

Reaction of 4-(hydroxyl methylphosphinyl)butanoic acid (154) with thionyl chloride followed by successive treatment with copper powder, potassium iodide, and potassium carbonate affords 1-methyl-2-oxophospholane 1-oxide (155) in 65% yield. 3-Bromo-, 3-amino-, 3-acethylamino-1-methyl-2-oxophospholanes (156–158) are prepared by substitution of the 3-methylene position (Scheme 51) [64].
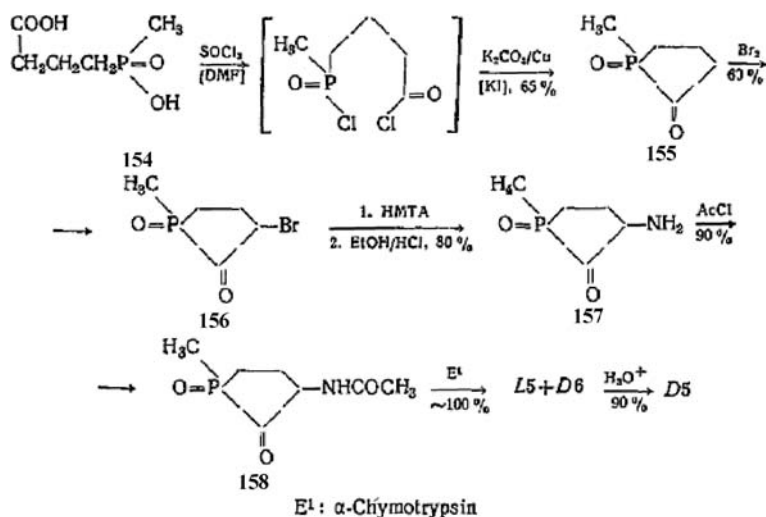
Scheme 51 Preparation of 1-methyl-2-oxophospholanes 156–158

2.3
Seven-Membered Aliphatic Rings

Dibenzo[b,f]phosphepin systems **159–161** (Fig. 22) are prepared from 10,11-dihydro-5-phenyl-5*H*-bibenzo[b,f]phosphepin 5-oxide (**159b**). New members in the 10,11-dihydro-5-phenyl-5*H*- bibenzo[b,f]phosphepin series, includ-

a: X= :, R=Ph   **e:** X= O, R=OMe
b: X= O, R=Ph   **f:** X= O, R=H
c: X= O, R=OH   **g:** X= O, R=Me₂N(CH₂)₃
d: X= O, R=Cl   **h:** X= :, R=Me₂N(CH₂)₃
                          i: X= S, R=Ph
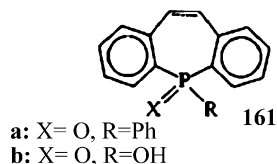
c: X= O, R=Cl
d: X= O, R=H
e: X= O, R=Me
a: X= O, R=Ph   **f:** X= :, R=Ph
b: X= O, R=OH   **g:** X= S, R=Ph

Fig. 22 Bibenzo[b,f]phosphepins **159–161**
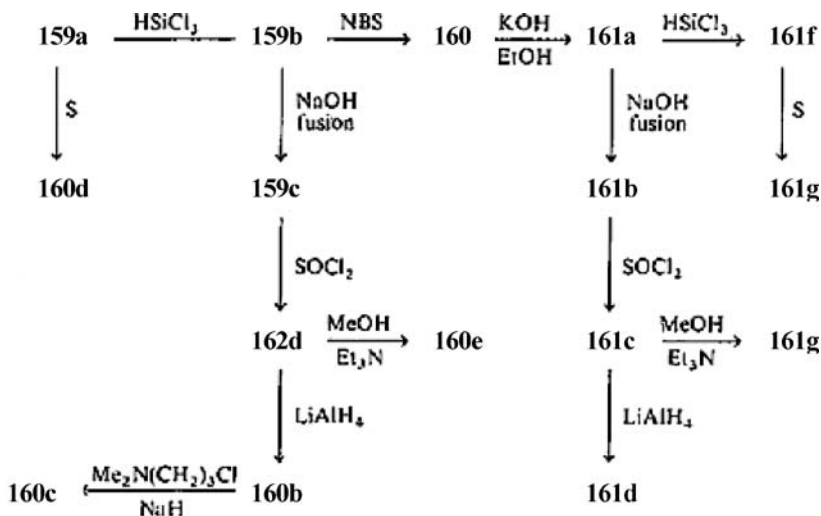
Scheme 52 Preparation of dibenzo[b,f]phosphepin systems **159–161** from 10,11-dihydro-5-phenyl-5*H*-bibenzo[b,f]phosphepin 5-oxide (**159b**)

ing the antidepressant drug imipramine (the nitrogen analogue of the phosphorus heterocycle) are also prepared. Products of nucleophilic substitution at the tetrahedral phosphorus atom in 10,11-dihydro-5-phenyl-5H-bibenzo[b,f]phosphepin 5-oxide (**159b**) appear to be determined by the relative apicophilicity of the nucleoside (Schemes 52 and 53) [65].
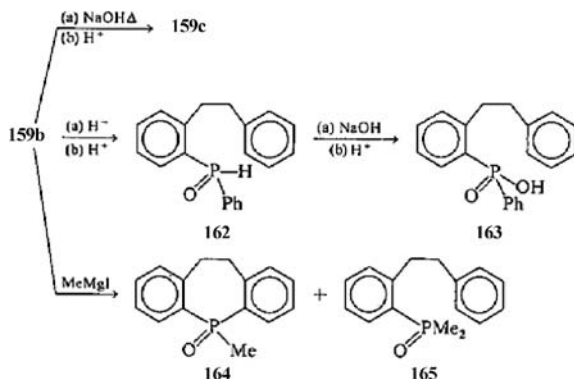
Scheme 53 Products **162–165** of nucleophilic substitution at the tetrahedral phosphorus atom in **159b**

Tetrahydrophosphinine oxide **166** reacts with dichlorocarbene under phase-transfer catalytic conditions giving 7,7-dichloro-1-methyl-3-phenyl-3-phosphabicyclo[4.1.0]heptane (**167**) in 71% yield. Heating the phosphabicyclo[4.1.0]heptane **167** at 220 °C makes the bicyclic ring opening and the simultaneous elimination of hydrogen chloride gives 4-chloro-3-methyl-1-phenyl-2,7-dihydrophosphepin 1-oxide (**168**), a seven-membered phosphorus heterocycle, in 67% yield (Scheme 54) [66].
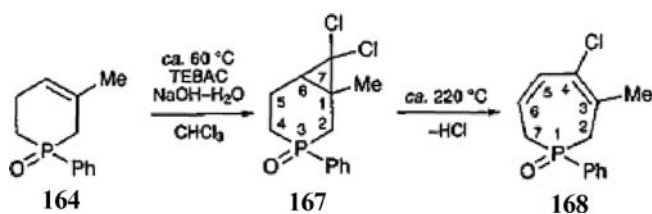
Scheme 54 Preparation of the seven-membered phosphorus heterocycle **168**

3
Aromatic Phosphorus Heterocycles with a C – P – C Bond

In contrast to the fact that benzene or pyridine and their derivatives have an aromaticity, the phosphorus analogues (phosphinines or phos-
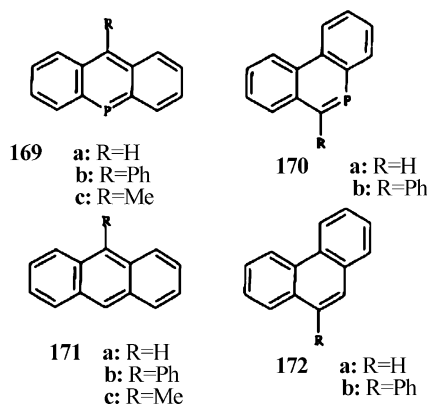
Scheme 55 Phenyldibenzo[b,d]phosphaheterocycles 169–172
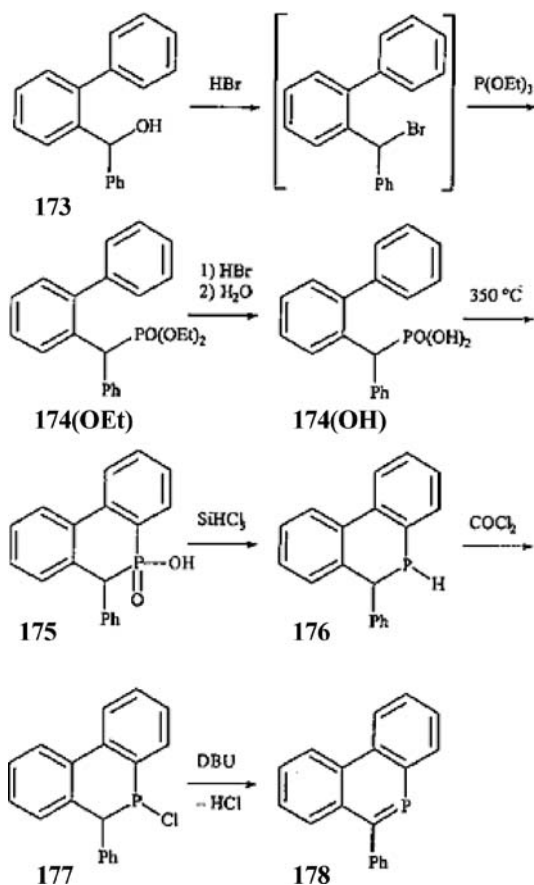
Scheme 56 Preparation of the stable 6-phenyldibezo[b,d]phosphinine 178

phabenzenes [67–69]) tend to be less stable both thermally and towards oxygenation, especially aromatic rings that are annelated to the heterocycles. For example, [9]phosphaanthracene and [5]phosphaphenanthrene are too unstable to be isolated in a pure form; however, introduction of a phenyl group into these phosphorus heterocyclic rings increases the thermal stability (compounds **169–170** in Scheme 55). Therefore, it becomes possible to isolate these phenyldibenzo[b,d]phosphaheterocycles, e.g., 6-phenyl-dibezo[b,d]phosphinine, and to obtain them in a pure form (compound **178** in Scheme 56) [70].

4
Phosphorus Heterocycles with a C – P – O Bond

Physarum phospholipids (PHYLPA), isolated from myxoamoebae of *Physarum polycephalum*, is an inhibitor of eukaryotic DNA polymerase [71]. PHYLPA inhibits the proliferation of human fibroblasts cultured in a chemically defined medium.

Fluoromethylene phosphonate analogues **179** of carbocyclic phosphatidic acid (ccPA) and the novel cyclic phosphonothioate **180** (Fig. 23) are prepared from benzyl glycidol ether (**181**) via nucleophilic ring opening by lithium diethyl methylphosphonate giving γ-hydroxy phosphonate (dimethyl 4-(benzyloxy)-3-hydroxybutylphosphonate (**182**)), which is then cyclized by intramolecular transesterification with pyridinium *p*-toluenesulfonate (PPTS). According to Scheme 57 phosphates **185** are interconverted into thiophosphates **186** by Lawesson's reagent, and then the endocyclic hydroxymethyl group is carboxylated. Mono- and difluorophosphonates (**180Fa,b**) are prepared from diethyl 1-fluoro-3,4-dihydroxybutyl- (**189Fa**) and 1,1-difluoro-3,4-dihydroxybutyl-phosphonates (**189Fb**) via intramolecular dehydration with DCC to form cyclic phosphonate (Schemes 57 and 58) [72].
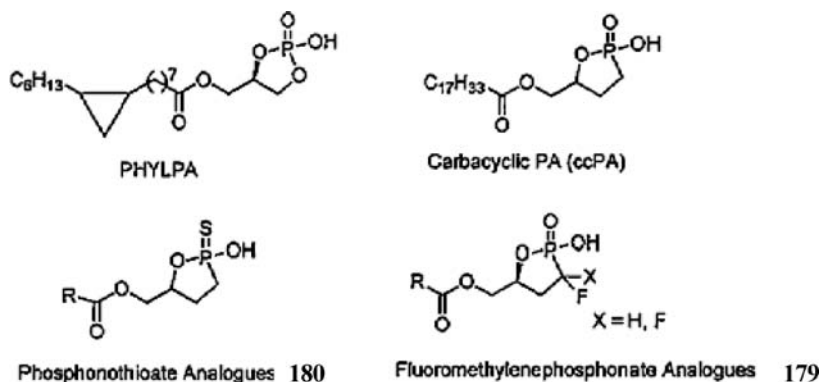
Fig. 23 Cyclic phosphatidic acids and their carbacyclic analogues
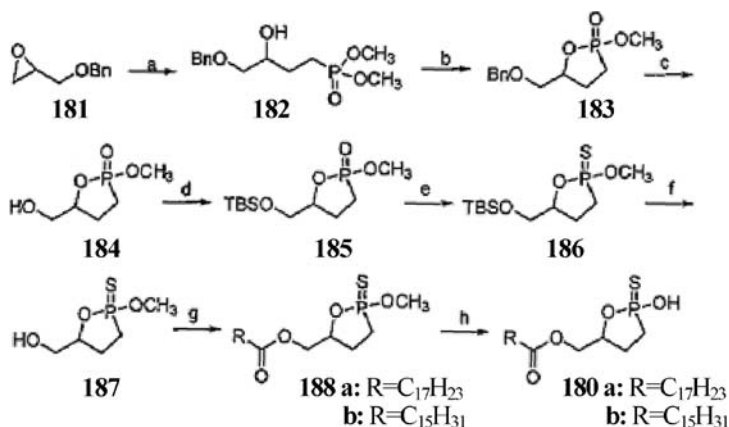
Scheme 57 Preparation of cyclic phosphonothioate analogues from benzyl glycidol ether (**181**)
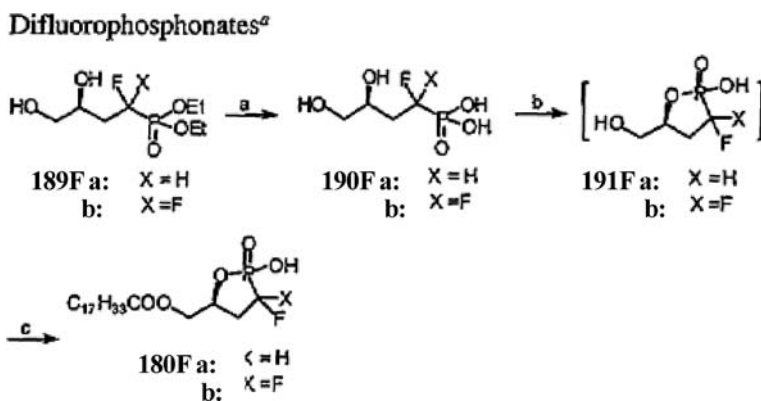
Scheme 58 Preparation of mono- and difluorophosphonates (**180Fa,b**)

Phosphole oxide, which is a phosphorus analogue of pyrrole and thiophene and has a heterocyclic structure with a C–P–C linkage, easily dimerizes to give the Diels–Alder dimer (**195**) (Scheme 61) having a tricyclic heterocyclic structure with two C–P–C linkage. The reaction of the Diels–Alder dimer with *m*-chloroperbenzoic acid (mCBPA) occurs at the bridging C–P bond to give an oxygen insertion product, 2,3-oxaphosphabicyclo[2.2.2]octane ring system **192**. The 2,3-oxaphosphabicyclo[2.2.2]octane ring system is a cyclic phosphinate ester system, which is of significance because of the thermal or photochemical fragmentation to release the phosphorus–oxygen bridge and to generate the low-coordinate metaphosphate species **193** (Scheme 59).

Thionation of 2,3-oxaphosphabicyclo[2.2.2]octane system **192** with Lawesson's reagent (**196**) gives the corresponding cyclic thiophosphate **194**. Accord-

192 a: R=OEt   193 a: R=OEt
    b: R=NMe₂   b: R=NMe₂
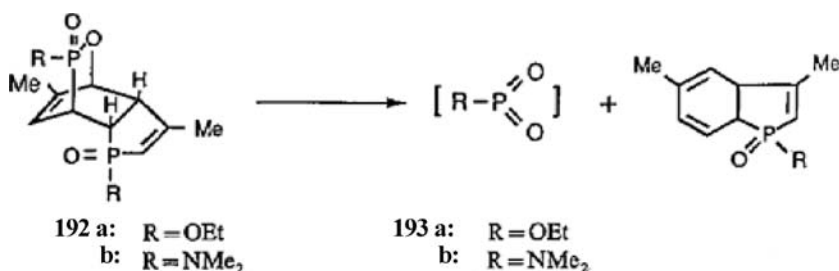
Scheme 59 Fragmentation of 2,3-oxaphosphabicyclo[2.2.2]octane ring system to give the metaphosphate species **193**

ing to the same procedure, the phosphoryl group of the Diels–Alder dimer **195** is converted into the thiophosphoryl group of compound **197** (or **197′**), which on treatment with mCPBA reproduces the original compound **195** (Schemes 60–62) [73].

Cyclic phosphonate formation is reported. By using ring-closing metathesis (RCM), allyl allylphosphonates **198** prepare allylphostone derivatives having a C – P – O linkage in the heterocycles. The functionalization (such as oxidation of the C=C double bond, regioisomerization of the double bond, etc.) of allylphostone **199** or vinylphostone gives a variety of phosphono sug-

194a   193a
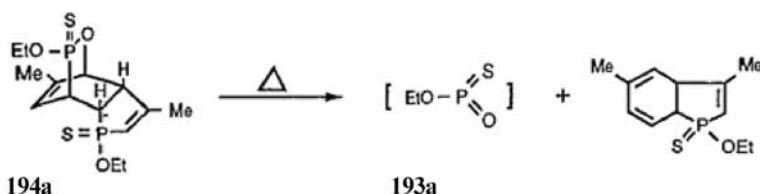
Scheme 60 Fragmentation of cyclic thiophosphate **194**

195a   196   Ar = 4-MeOC₆H₄   197   197′
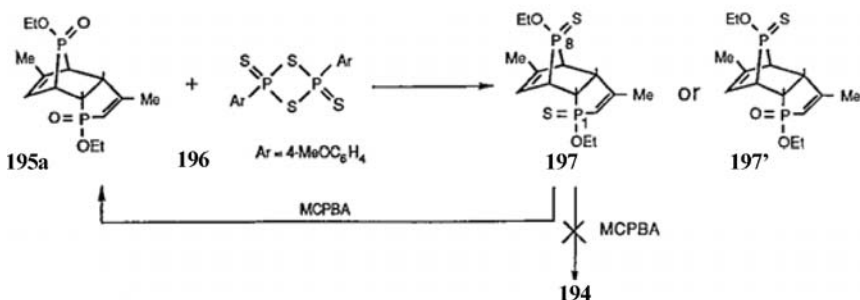
Scheme 61 Conversion of the phosphoryl group of the Diels–Alder dimer **195** into the thiophosphoryl group of compound **197**
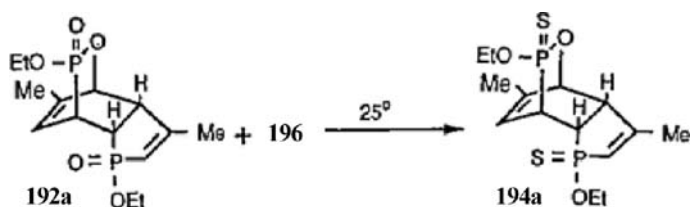
Scheme 62 Thionation of **192** with Lawesson's reagent to give the corresponding cyclic thiophosphate **194**

ars **200** having a C – P – O bond in the ring (Scheme 63). Thus, phosphono sugars **201–206** with a cyclic phosphonate structure are prepared (Schemes 64 and 65) [74].
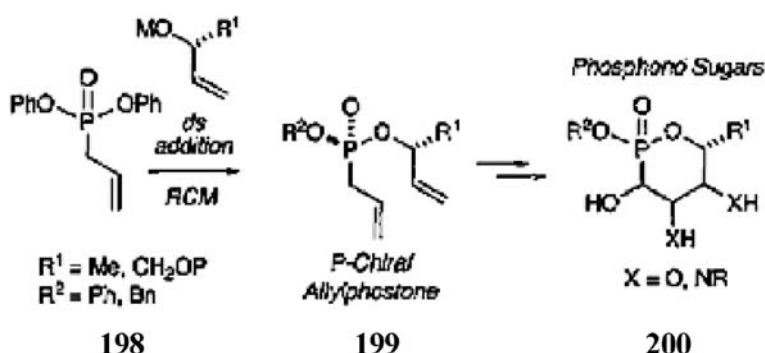
Scheme 63 Preparation of phosphono sugars **200** from allyl allylphosphonates **198**
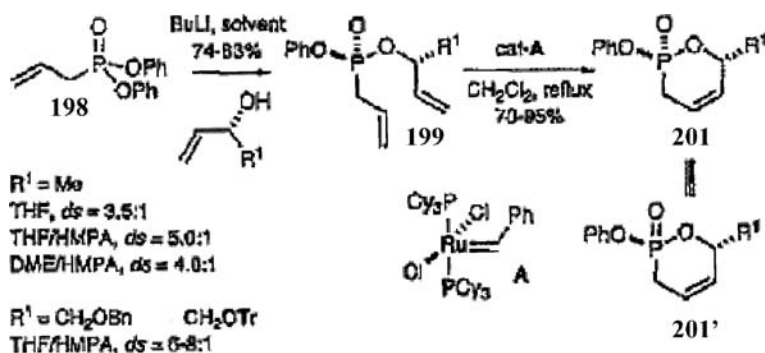
Scheme 64 Preparation of phosphono sugars **201** and **201′**

Phosphono sugars, (2*R*,4*R*,5*R*)- and (2*S*,4*R*,5*R*)-4,5-dimethoxy-2-oxo-2-phenyl-1,2-oxaphosphorinates (**211A** and **211B**), are prepared from 1,4-dibromo-1,4-dideoxy-2,3-di-*O*-methyl-L-threitol (**209**), being prepared from
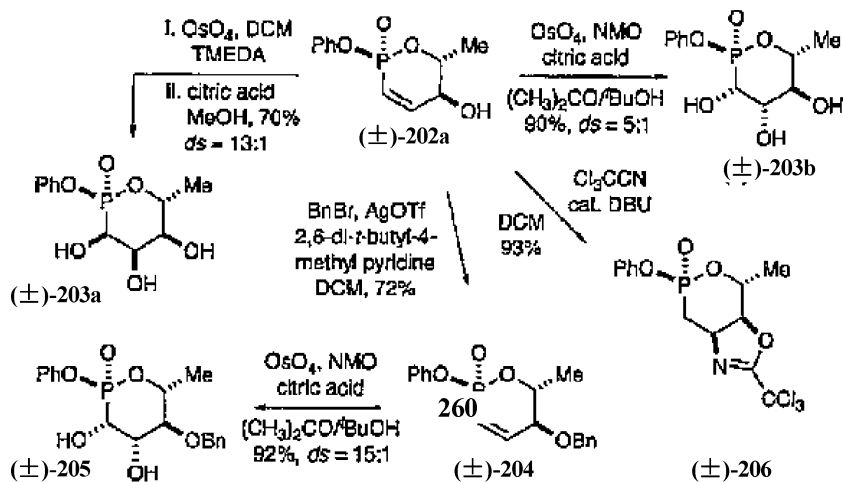
Scheme 65 Preparation of phosphono sugars 202–206
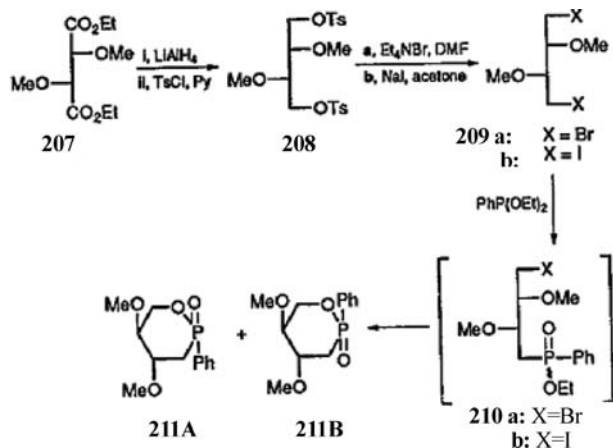
Scheme 66 Preparation of phosphono sugars **211A** and **211B**

diethyl 2,3-di-*O*-methyl-L-tartrate (**207**) by nucleophilic substitution of di-tosylate **208** with bromide, by the Arbuzov reaction of **209** with diethyl phenylphosphonite in 42% and 47% yield, respectively (Scheme 66) [75].

5
Conclusion

The research on organophosphorus chemistry and phosphorus heterocy-cles is quite active and extensive, and we have studied synthetic procedures,

structures, and activities of phosphorus heterocycles. However, for practical purposes, these research results are not comprehensive but sectional. This chapter has focused on the syntheses and structure, as well as the biological activity, of the P – C bonded compounds. According to the development of the life sciences in 21st century, one of the most important research targets in this field is an innovation in chemotherapy by development of molecular targeting anticancer drugs. We are expecting that *phospha* sugars may be a potential agent for leukemia as well as for solid cancers [76]. If our present knowledge on phosphorus heterocycles is developed by collaboration of chemistry with engineering and medicine we may achieve an improvement in chemotherapy for cancer and in the quality of life for the patient.

References

1. Kandatsu M, Horiguchi M (1984) In: Hori T, Horiguchi M, Hayashi A (eds) Biochemistry of natural C – P compounds. Maruzen, Tokyo, chaps 1 and 6
2. Wong S-C, Carruthers NI, Chan T-M (1993) J Chem Res (S):268
3. Caesar JC, Griffiths DV (1987) Phosphor Sulf 29:123–127
4. Quin LD, Tang J-S (1991) Heteroatom Chem 2(2):283–295
5. Keglevich G, Toke L, Kovacs A, Toth G, Ujszaszy K (1993) Heteroatom Chem 4(1):61–72
6. Kelevich G, Brlik J, Janke F, Toke L (1990) Heteroatom Chem 1(5):419–424
7. Keglevich G, Quin LD (1995) Magyar Kemiai Folyoirat 101:282–292
8. Quin LD, Osman FH, Day Ro, Hughes AN, Wu XP, Wang LQ (1989) New J Chem 13:375–381
9. Keglevich G, Toke L, Kovacs A, Toth G, Ujszaszy K (1993) Heteroatom Chem 4(1):61–72
10. Keglevich G, Kovacs A, Toke L, Ujszaszy K, Argay G, Czugler M, Kalman A (1993) Heteroatom Chem 4(4):329–335
11. Keglevich G, Toke L, Lovasz C, Ujszaszy K, Szalontai G (1994) Heteroatom Chem 5(4):395–401
12. Yamamoto H, Hanaya T, Kawamoto H, Inokawa S, Yamashita M, Armour M-A, Nakashima TT (1985) J Org Chem 50:3516
13. Richter T, Luger P, Hanaya T, Yamamoto H (1989) Carbohydrate Res 193:9
14. Hanaya T, Hirose K, Yamamoto H (1993) Heterocycles 36:2557
15. Hanaya T, Yasuda K, Yamamoto H (1993) Bull Chem Soc Jpn 66:2315
16. Hanaya T, Sugiyama K, Fujii Y, Akamatsu A, Yamamoto H (2001) Heterocycles 55(7):1301–1309
17. Hanaya T, Yamamoto H (1989) Bull Chem Soc Jpn 62:2320
18. Yamamoto H, Nakamura Y, Inokawa S, Yamashita M, Armour M-A, Nakashima TT (1984) J Org Chem 49:1364
19. Hanaya T, Noguchi A, Armour M-A, Hogg AM, Yamamoto H (1992) J Chem Soc Perkin Trans 1, p 295
20. Hanaya T, Noguchi A, Yamamoto H (1991) Carbohydr Chem 209:C9
21. Polniaszek RP, Foster AL (1991) J Org Chem 56:3137
22. Yabui A, Yamashita M, Oshikawa T, Hanaya T, Yamamoto H (1995) Chem Lett, p 93

23. Hanaya T, Kawase S, Yamamoto H (2005) Heterocycles 66:251–261
24. Baccolini G, Boga C, Negri U (2000) Synlett (11):1685–1687
25. Quin LD, Quin GS (2000) A guide to organophosphorus chemistry. Wiley-Interscience, New York
26. Dahl O, Edmundson RS (1996) In: Hartley FR (ed) The chemistry of organophosphorus compounds. Wiley, Chichester, chaps 1 and 2
27. Majoral J-P, Igau A, Cadierno V, Zablocka M (2002) In: Majoral J-P (ed) New aspects in phosphorus chemistry I. Springer, Berlin
28. Reddy VK, Rao LN, Oshikawa T, Takahashi M, Yamashita M (2002) Phosphor Sulf Silicon 177:1801–1806
29. Reddy VK, Onogawa J, Rao LN, Oshikawa T, Takahashi M, Yamashita M (2002) J Heterocycl Chem 39:69–75
30. Yamashita M, Nakatsukasa Y, Yoshida H, Ogata T, Inokawa S, Hirotsu K, Clardy J (1979) Carbohydr Res 70:247–261
31. Inokawa S, Yamamoto K, Kawata Y, Kawamoto H, Takagi K, Yamashita M (1980) Carbohydr Res 86:C11–12
32. Yamashita M, Yamada M, Tsunekawa K, Oshikawa T, Seo K, Inokawa S (1983) Carbohydr Res 121:C4–C5
33. Seo K, Yamashita M (1985) Carbohydr Res 141:335–339
34. Emsley J, Hall D (1976) The chemistry of phosphorus. Harper & Row, London, p 157
35. Quin LD, Barket Tp (1967) J Chem Soc Chem Commun, p 288
36. McCormack WB (1963) Org Syn 43:73
37. Yamashita M, Uchimura M, Iida A, Parkanayi L, Clardy J (1988) J Chem Soc Chem Commun, pp 569–570
38. Yamashita M, Yabui A, Suzuki K, Kato Y, Uchimura M, Iida A, Mizuno H, Ikai K, Oshikawa T, Parkanayi L, Clardy J (1997) Carbohydr Res, pp 499–519
39. Yamashita M, Iida A, Ikai K, Oshikawa T, Hanaya T, Yamamoto H (1992) Chem Lett, pp 407–410
40. Ikai K, Iida A, Yamashita M (1989) J Syn Org Chem (8):595–597
41. Totsuka H, Maeda M, Reddy VK, Takahashi M, Yamashita M (2004) Heterocycl Commun 10(4–5):295–300
42. Miyamoto M, Yamashita M, Oshikawa T (1992) Bull Chem Soc Jpn 65(7):2004–2006
43. Yamashita M, Suzuki K, Kato Y, Iida A, Ikai K, Reddy PM, Oshikawa T (1999) J Carbohydr Chem 18(8):915–935
44. Yamashita M, Reddy VK, Rao LN, Haritha B, Maeda M, Suzuki K, Totsuka H, Takahashi M, Oshikawa T (2003) Tetrahedron Lett 44:2339–2341
45. Totsuka H, Maeda M, Reddy VK, Takahashi M, Yamashita M (2004) Heterocycl Commun 10(4–5):295–300
46. Haritha B, Reddy VK, Oshikawa T, Yamashita M (2004) Tetrahedron Lett 45:1923–1927
47. Yamashita M, Ikai K, Takahashi C, Oshikawa T (1993) Phosphor Sulf Silicon 79:293–296
48. Yamashita M, Reddy PM, Kato Y, Reddy VK, Suzuki K, Oshikawa T (2001) Carbohydr Res 336:257–270
49. Yamashita M, Reddy VK, Reddy PM, Kato Y, Haritha B, Suzuki K, Takahashi M, Oshikawa T (2003) Tetrahedron Lett 44:3455–3458
50. Harith B, Reddy VK, Takahashi M, Yamashita M (2004) Tetrahedron Lett 45:5339–5341
51. Bartret PA, Hanson JE, Giannousis PP (1990) J Org Chem 55:6268–6274

52. Jacobsen NE, Bartlett PA (1981) J Am Chem Soc 103:654–657
53. Yamashita M, Yamada M, Sugiura M, Nomoto H, Oshikawa T (1987) Nippon Kagaku Kaishi (7):1207–1213
54. Yamashita M, Fujie M, Nakamura S (2007) Japan patent application 2007-35083
55. Reddy VK, Rao LN, Maeda M, Haritha B, Yamashita M (2003) Heteroatom Chem 14(4):320–325
56. Yamashita M, Rao LN, Reddy VK, Maeda M, Oshikawa T, Takahashi M (2002) Phosphor Sulf Silicon 177:1661–1665
57. Yamashita M, Iida A, Oshikawa T, Kakehi A (1994) Chem Lett, pp 23–26
58. Yamashita M, Yabui A, Suzuki K, Kumagai S, Oshikawa T (1996) Phosphor Sulf Silicon 109–110:405–408
59. Yamashita M, Yabui A, Oshikawa T, Hanaya T, Yamamoto H (1994) Heterocycles 38(7):1449–1452
60. Yabui A, Yamashita M, Oshikawa T, Hanaya T, Yamamoto H (1993) Chem Lett, pp 93–96
61. Franisal N, Gallagher MJ (1987) Aust J Chem 40:1353–1363
62. Kovacs J, Ire T, Ludanyi K, Toke L, Keglevich G (2004) Synth Commun 34(6):1033–1039
63. Szelke H, Kovacs J, Keglevich G (2005) Synth Commun 35:2927–2934
64. Natchev IA (1990) Bulgarian Acad Sci 23(4):511–515
65. Segall Y, Shirin E, Granoth I (1980) Phosphor Sulf 8:243–254
66. Keglevich G, Thanh HTT, Ludanyi K, Novak T, Ujszaszy K, Toke L (1998) J Chem Res (S):210–211
67. Floch PL (2001) In: Mathey F (ed) Phosphorus–carbon heterocyclic chemistry: the rise of a new domain. Pergamon, Amsterdam, chap 5.2
68. Nyulaszi L (2001) Chem Rev 101:1229
69. Mathey F (2003) Angew Chem Int Ed 42:1578
70. de Koe P, Bickelhaupt F (2003) Z Naturforsh 58b:782–786
71. Murakami K, Shioda M, Kaji K, Yoshida S, Murofushi H (1992) J Biol Chem 267:21512–21517
72. Xu Y, Jiang G, Tsukahara R, Fujikawa Y, Tigyi G, Prestwich GD (2006) J Med Chem 49:5309–5315
73. Quin LD, Osman FH, Day Ro, Hughes AN, Wu XP, Wang LQ (1989) New J Chem 13:375–381
74. Stoianova DS, Whitehead A, Hanson PR (2005) J Org Chem 70:5880–5889
75. Hanaya T, Akamatsu A, Kawase S, Yamamoto H (1995) J Chem Res (S):194–195
76. Yamashita M, Niimi T, Fujie M, Reddy VK, Totsuka H, Haritha B, Reddy MK, Nakamura S, Asai K, Suyama T, Yu G, Takahashi M, Oshikawa T (2007) 17th International Conference on Phosphorus Chemistry (ICPC), Xiamen, China, 15–21 April 2007

The Role of the Membrane Actions of Phenothiazines and Flavonoids as Functional Modulators

K. Michalak[1] (✉) · O. Wesołowska[1] · N. Motohashi[2] · A. B. Hendrich[1]

[1]Department of Biophysics, Wrocław Medical University, ul. Chałubińskiego 10,
 50-368 Wrocław, Poland
 michalak@biofiz.am.wroc.pl

[2]Meiji Pharmaceutical University, 2-522-1 Noshio, Kiyose-shi, 204-8588 Tokyo, Japan

Abstract Phenothiazine derivatives as well as flavonoids belong to heterocyclic compounds that exert numerous effects on biological systems. The structure of these compounds enables their specific interactions with different membrane proteins and also nonspecific interactions with the lipid phase of membranes. In the present review we focus on the influence of phenothiazines and flavonoids on lipid bilayers and other model systems, and on two groups of membrane proteins: transporters involved in the phenomenon of multidrug resistance and ion channels. Most of the compounds described in this paper interact with membranes and affect different properties of lipid bilayers. Modification of membrane properties should contribute to mechanisms underlying certain types of biological activity of the discussed molecules. Structural features essential for the modulatory effects exerted by phenothiazines and flavonoids on multidrug transporters are presented. Also various types of response of voltage-

gated and chemically activated ion channels to the presence of heterocyclic compounds are reviewed.

Abbreviations
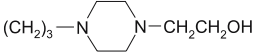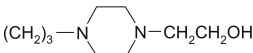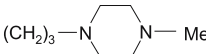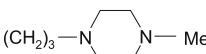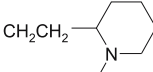
ABC	ATP-binding cassette
ANS	1-Anilinonaphthalene-8-sulfonic acid
BCPCF	2′,7′-Bis(3-carboxypropyl)-5-(and -6)-carboxyfluorescein
BCRP	Breast cancer resistance protein
C	(+)-Catechin
CFTR	Cystic fibrosis transmembrane conductance regulator
CHO	Chinese hamster ovary cell line
cmc	Critical micelle concentration
CPZ	Chlorpromazine
CTAB	Hexadecyltrimethylammonium bromide
ΔH	Phase transition enthalpy
DHA	Docosahexanoic acid
DHS	Dehydrosilybin
DMPC	Dimyristoylphosphatidylcholine
DMPE	Dimyristoylphosphatidylethanolamine
DMPG	Dimyristoylphosphatidylglycerol
DMPS	Dimyristoylphosphatidylserine
DPH	1,6-Diphenyl-1,3,5-hexatriene
DPPC	Dipalmitoylphosphatidylcholine
DPPH	1,1-Diphenyl-2-picrylhydrazyl
DPPS	Dipalmitoylphosphatidylserine
DSC	Differential scanning calorimetry
EC	(−)-Epicatechin
ECg	(−)-Epicatechin gallate
EGCg	(−)-Epigallocatechin gallate
ESR	Electron spin resonance
FPhMS	2-Trifluoromethyl-10-[4-(methanesulfonylamido)butyl]-phenothiazine
GABA	Gamma-aminobutyric acid
GSH	Glutathione
HCN	Cyclic nucleotide-gated channel
hERG	Human *ether-a-go-go*-related gene encoded channel
HPS	3-(*N*-Hexadecyl-*N*,*N*-dimethylammonio)propanesulfonate
IC_{50}	Concentration causing 50% inhibition
IFG8	7-*tert*-Butyl(dimethylsilyl)-genistein
IFG10	7,4′-Bis[*tert*-butyl(dimethylsilyl)]-genistein
IFG12	7-*tert*-Butyl(dimethylsilyl)-4′-acetyl-genistein
IFG18	7-*O*-Palmitate-genistein
$InsP_3$	Inositol 1,4,5-triphosphate
K_p	Partition coefficient
LPC	Lysophosphatidylcholine
MDCK	Madin–Darby canine kidney cell line
MDR	Multidrug resistance

MRP1   Multidrug resistance-associated protein
MX   Mitoxantrone
nAChR   Nicotinic acetylcholine receptor
NBD   Nucleotide binding domain
NMDA   *N*-Methyl-D-aspartic acid
NMR   Nuclear magnetic resonance
NPN   *N*-Phenyl-1-naphthylamine
PA   Phosphatidic acid
PC   Phosphatidylcholine
PE   PE
PG   Phosphatidylglycerol
P-gp   P-glycoprotein
PhA   Phenothiazine acetylamides
PhM   Phenothiazine maleates
PhMC   Phenothiazine methoxycarbonylamides
PhMS   Phenothiazine methanesulfonylamides
PI   Phosphatidylinositol
POPC   1-Palmitoyl-2-oleoyl phosphatidylcholine
PS   Phosphatidylserine
PTK   Protein tyrosine kinase
QSAR   Quantitative structure–activity relationship
Rh123   Rhodamine 123
SDPS   Phosphatidylserine containing docosahexanoic acid
SDS   Sodium dodecyl sulfate
SM   Sphingomyelin
SOPC   L-α,β-Oleoyl-γ-palmitoyl phosphatidylcholine
TDZ   Thioridazine
TFP   Trifluoperazine
T_m Main phase transition temperature
TTX   Tetrodotoxin
VSCC   Voltage-sensitive calcium channel

1
Introduction

Phenothiazine derivatives as well as flavonoids belong to heterocyclic compounds that exert numerous effects on biological systems. Despite the structural differences (compare structures presented in Figs. 1 and 2 for phenothiazines and flavonoids, respectively), these two groups of compounds share at least one common feature: the highly hydrophobic multiring system in the core of their molecules and more or less hydrophilic substitutions located around this lipophilic moiety that make them well suited for interaction either with the lipid phase of membranes or with membrane proteins. As will be presented in this review, nonspecific interactions with lipids and specific interactions with proteins could contribute to the mechanisms underlying various biological activities of phenothiazines and flavonoids.

	Name	R_1	R_2
1	promethazine	$CH_2CH(Me)N(Me)_2$	H
2	perphenazine	$(CH_2)_3-N\underset{}{\bigcirc}N-CH_2CH_2OH$	Cl
3	fluphenazine	$(CH_2)_3-N\underset{}{\bigcirc}N-CH_2CH_2OH$	CF_3
4	prochlorperazine dimaleate	$(CH_2)_3-N\underset{}{\bigcirc}N-Me$ * $(2C_4H_4O_4)$	Cl
5	trifluoperazine (TFP)	$(CH_2)_3-N\underset{}{\bigcirc}N-Me$	CF_3
6	thioridazine (TDZ)	$CH_2CH_2-\underset{}{\bigcirc}$	SMe
7	diethazine	$CH_2CH_2NEt_2$	H
8	promazine	$(CH_2)_3NMe_2$	H
9	chlorpromazine (CPZ)	$(CH_2)_3NMe_2$	Cl
10	methochlorpromazine	$(CH_2)_3N^+Me_3$	Cl
11	triflupromazine	$(CH_2)_3NMe_2$	CF_3
12	phenothiazine maleates (PhM)	$(CH_2)_nNH_2$; n = 3 or 4	H or Cl or CF_3
13	phenothiazine acetylamides (PhA)	$(CH_2)_nNHCOCH_3$; n = 3 or 4	H or Cl or CF_3
14	phenothiazine methoxycarbonyl-amides (PhMC)	$(CH_2)_nNHCO_2CH_3$; n = 3 or 4	H or Cl or CF_3
15	phenothiazine methanesulfonyl-amides (PhMS)	$(CH_2)_nNHCSO_2CH_3$; n = 3 or 4	H or Cl or CF_3
16	2-trifluoromethyl-10-(4-[methane-sulfonylamid]butyl)-phenothiazine (FPhMS)	$(CH_2)_4NHCSO_2CH_3$	CF_3
17	trimeprazine	$CH_2CH(Me)CH_2NMe_2$	H
18	methotrimeprazine (levomepromazine) maleate	$CH_2CH(Me)CH_2NMe_2$ * $(C_4H_4O_4)$	OMe
19	chloracizine	$CO(CH_2)NEt_2$	Cl
20	oxomemazine	$CH_2CH(Me)CH_2NMe_2$	H
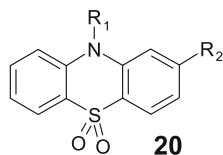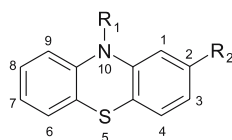
Fig. 1 Chemical structures of phenothiazine derivatives

Phenothiazines are commonly used as tranquillizers but they also exert many other biological effects. Among others they were shown to act as antimicrobial agents against aerobic and anaerobic bacteria [1]. Antiplasmid activity of various phenothiazine derivatives was demonstrated in many types of bacteria [2–5]. Recently, Spengler et al. [6] noted that the mutagenic and antiplasmid effects of heterocyclic compounds were correlated with the energy of their highest occupied molecular orbitals. An important feature of phenothiazine drugs is also their activity against *Mycobacterium tuberculosis* (for a review see Amaral et al. [7]) and *Staphylococcus aureus* [8]. Apart from effects on bacteria phenothiazines could also act as antifungal agents, as was shown with respect to *Saccaromyces cerevisiae* [9] and *Candida albicans* [10]. In many studies on cancer cells, various phenothiazine derivatives were proved to act as antitumor [11, 12], antimutagenic, chemopreventive [13–15], antiproliferative, or pro-apoptotic agents [16–18].

The spectrum of flavonoid biological effects is very broad; the best known are their estrogenic, antitumor, antimicrobial, antiallergic, and antiinflammatory activities (for review, see Cushnie [19]). At least some of these activities are based on non-membrane-related mechanisms, like flavonoid-induced cell cycle arrest. Most of them, however, are claimed in the literature to appear as a consequence of antioxidative properties of flavonoids.

During the last decade our knowledge of the membrane-related processes has substantially increased, and therefore more attention is now paid to studies on different aspects of drug–membrane interactions. The aim of this review is to present current knowledge concerning membrane-related mechanisms of biological activity of phenothiazines and flavonoids. Studying an interaction of these classes of compounds with selected membrane proteins, such as multidrug resistance transporters or ion channels, is important for a better understanding of molecular events which govern substrate transport and inhibition processes in the case of these proteins.

2
Influence of Phenothiazine Derivatives and Flavonoids on Properties of Model and Natural Membranes

2.1
Interaction of Phenothiazines with Model Systems

Phenothiazine derivatives used in medicine are amphiphilic compounds with a relatively hydrophobic ring system and hydrophilic side groups, often bearing a positive charge under physiological conditions (see Fig. 1 for chemical structures). Their amphiphilic character is the main feature determining the self-aggregation of phenothiazines, and their interaction with detergents, model lipid bilayers, and natural membranes.

In aqueous solutions phenothiazine drugs behave as classical detergents, i.e., they tend to aggregate. The critical micelle concentrations (cmc) for phenothiazines in water were reported to range from 10^{-5} M for trifluoperazine (TFP) (**5**) and 10^{-3} M for thioridazine (TDZ) (**6**) up to 10^{-2} M for chlorpromazine (CPZ) (**9**), promazine (**8**), and promethazine (**1**) [20]. Phenothiazines formed roughly spherical micelles consisting of 6–15 molecules, which underwent spherical-to-rod transition at higher salt concentrations. Elevated electrolyte concentration also caused the decrease of cmc and the increase of aggregation number [20]. The opposite changes in cmc and aggregation number occurred in association with pH decrease. The cmc of CPZ (**9**) increased one order of magnitude when the pH was lowered from 7.3 to 5.6 [21]. CPZ (**9**) micelles were vulnerable to temperature and pH; changes of these parameters gave rise to micelle phase transitions. Light scattering and electron spin resonance (ESR) experiments demonstrated that at low pH the micelles were less ordered than at high pH. The authors concluded that at low pH CPZ (**9**) molecules were more protonated and therefore electrostatic repulsive interactions were stronger, which imposed a more loosely packed structure of the micellar interior. Temperature exerted the opposite effect— CPZ (**9**) micelles became less ordered at higher temperatures.

The interaction of two phenothiazines, TFP (**5**) and CPZ (**9**), with detergent micelles of different character was thoroughly investigated [22–26]. First, the binding of **5** and **9** to cationic, zwitterionic, and neutral detergent micelles was studied by means of absorption spectroscopy [22]. In the presence of surfactants, the pK values of both drugs were shifted to lower values. As lower binding constants were recorded for cationic detergents than for neutral ones, it was suggested that electrostatic interaction played a crucial role in the interaction of phenothiazine derivatives with detergent micelles. The authors also pointed out the fact that only taking into account two protonation states (two pK values) of TFP (**5**) could correctly explain the data obtained for this drug. In conclusion it was proposed that TFP (**5**) was able to penetrate deeper into the micelle interior than CPZ (**9**). Similar localization of both drugs inside anionic detergent sodium dodecyl sulfate (SDS) micelles was also postulated [23]. In this system the pK values of CPZ (**9**) and TFP (**5**) were increased in the presence of detergent. The process of phenothiazine association with SDS micelles was much more complex than in the case of neutral and cationic detergents, being biphasic and dependent on drug and surfactant concentrations. Further studies of CPZ (**9**) and TFP (**5**) interactions with SDS micelles were conducted using the small-angle X-ray scattering technique [24, 25]. The dramatic shape and size changes of SDS micelles associated with binding of phenothiazines were shown. Pure detergent micelles were ellipsoid, whereas drug–detergent aggregates were cylindrical. Such drug-associated transitions were not observed for micelles of zwitterionic detergent 3-(*N*-hexadecyl-*N*,*N*-dimethylammonio)propanesulfonate (HPS). However, later studies where

another zwitterionic detergent—lysophosphatidylcholine (LPC)—was used demonstrated that binding of CPZ (**9**) and TFP (**5**) caused the micelles' shape to change from ellipsoid to cylindrical in this system, too [26]. Additionally, the LPC micelles gained a non-null overall surface micelle charge in the presence of phenothiazines. A model of phenothiazine derivative association with both zwitterionic detergents was proposed. The differences in phenothiazine derivative accommodation by the two detergents were attributed to dissimilar orientation of the detergent polar headgroup according to the drug molecule. In conclusion, the results of all studies on CPZ (**9**) and TFP (**5**) binding to detergent micelles pointed to such a localization of drug molecules in the micelle that the protonated phenothiazine side group was placed near the polar head region of detergent molecules, whereas the hydrophobic ring system was immersed in the interior of the micelle [26].

Determining the partition coefficients (K_p) of phenothiazine derivatives between water and lipid bilayers is an important step toward characterization of the interaction of the drugs with biological membranes. CPZ (**9**) partitioned easily into model phosphatidylcholine (PC) membranes up to the concentration 3×10^{-5} M; at higher CPZ (**9**) concentrations membrane lysis occurred [27]. It was also shown that the partition coefficient was dependent on the lipid hydrocarbon chain length (smaller K_p in membranes composed of long-chain lipids), bilayer phase state (smaller K_p in gel state), and cholesterol content in the membrane (reduced K_p in the presence of cholesterol). Other studies demonstrated that the phenothiazine partition coefficient between buffer and liposomes also depended on pH [28]. Unprotonated forms of phenothiazine derivatives partitioned into lipid bilayers to a greater extent than protonated forms. The K_p for CPZ (**9**) was distinctly higher than for methochlorpromazine (**10**) that bore a permanent positive charge and could not be deprotonated. Even below lytic concentrations, the interaction of CPZ (**9**) with liposomes was not just simple partitioning. CPZ (**9**) was demonstrated to occupy different binding sites in the membrane depending on drug concentration [29]. The authors claimed that at intermediate CPZ (**9**) concentrations (above 2×10^{-6} M), next to drug partitioning into the lipid bilayer some type of electrostatic interaction of CPZ (**9**) with anionic groups of membrane components also took place. On the other hand, Banerjee et al. [30], based on calorimetric experiments, suggested that binding of CPZ (**9**) and imipramine with dipalmitoylphosphatidylcholine (DPPC) liposomes could not be ruled solely by electrostatic interactions. It was proposed that nonspecific "dilution" of drugs into a hydrophobic lipid phase was crucial for their interaction with membranes ("simple partition" model). Next, Binford and Palm [31] showed that partition coefficients of CPZ (**9**) and TDZ (**6**) obtained for model dimyristoylphosphatidylcholine (DMPC) vesicles and for erythrocyte ghosts were similar, which suggested a lack of influence of membrane proteins on phenothiazines binding to the erythrocyte membranes.

There are different methods to determine membrane/buffer partition co-
efficients of drugs; however, they usually demand physical separation of the
lipid and aqueous phases and subsequent drug concentration measurement
in both phases. Such techniques are time-consuming; moreover, the sepa-
ration process may disturb the equilibrium state between the two phases.
Therefore, the method of second derivative spectrophotometric determin-
ation of partition coefficients of phenothiazines was introduced [32]. The
method did not demand a separation step; it was based on the fact that the
background signal coming from liposomes can be eliminated when second
derivative spectra instead of absorption spectra are recorded. It should be
pointed out that second derivative spectrophotometry could be used for K_p
determination only when the absorption maxima of the drug in water and
in the lipid phase were different. The usefulness of this method was first
demonstrated for CPZ (**9**) and promazine (**8**) [32]; later on it was also used
for triflupromazine (**11**) [33]. It was also shown that the size of liposomes
used as membrane models had no influence on the obtained partition coef-
ficient values, whereas increased cholesterol content in PC vesicles resulted
in lower K_p values for phenothiazines. The same method was used to com-
pare membrane binding of CPZ (**9**), triflupromazine (**11**), and promazine (**8**)
and their *N*-monodemethylated derivatives [34]. Partition coefficient values
of these derivatives were similar to those of the parent compounds. Both for
parent drugs and for the derivatives the highest K_p value was observed for
the compound having a $-CF_3$ group substituted at position 2 of the ring,
smaller for the Cl-substituted one, and smallest for the compound possess-
ing an H atom at this position. Investigation of membrane/buffer partition
coefficients of phenothiazine derivatives as a function of temperature brought
Takegami et al. [35] to the conclusion that binding of these drugs to phospho-
lipid bilayers is an enthalpy/entropy driven process. The observed negative
enthalpy change of drug–membrane binding was most probably caused by fa-
vorable electrostatic interaction of the positively charged side chain amino
group of phenothiazine derivatives with negatively charged phosphate groups
of PC molecules. Positive entropy change was attributed to the enhancement
of disorder in the acyl chain region of the bilayer caused by phenothiazine
ring insertion. The affinity of CPZ (**9**) and triflupromazine (**11**) for model
membranes containing, apart from PC, also phosphatidylserine (PS) or phos-
phatidylethanolamine (PE) was studied by the same group [36]. It was ob-
served that partition coefficient values for both drugs were slightly reduced
when PE was present in the liposomes. On the other hand, K_p values in-
creased in accordance with PS content in model membranes, which suggested
a higher affinity of phenothiazines for PS than for PC. Second derivative spec-
trophotometry in combination with ^{13}C nuclear magnetic resonance (NMR)
was used to demonstrate that pK values of promazine (**8**), CPZ (**9**), and tri-
flupromazine (**11**) bound to a PC bilayer were smaller than those measured
in aqueous solution by about one unit [37].

The role of the structure of phenothiazine derivatives in their binding to model membranes was recently studied by Hendrich et al. [38] and Pola et al. [39] by means of second derivative spectrophotometry. Two groups of derivatives were studied: phenothiazine maleates (**12**) [38] and phenothiazine acetylamides (**13**) [39] (see Fig. 1 for chemical structures). Both studies have clearly shown that partition coefficients between buffer and PC liposomes were dependent on the type of ring substituent at position 2 and also on the length of the alkyl chain connecting the ring system with the side chain amino group. For both groups partition coefficients increased in the order H < Cl < CF_3-substituted compounds. When derivatives with the same ring substituents were compared, it came out that derivatives possessing a longer (four carbon atoms) linker between the ring system and amino group partitioned into PC bilayers better than compounds with a shorter (three carbon atoms) linker. The type of ring substituent was previously recognized to be important for surface activity of phenothiazines [40]. Recent studies of Gerebtzoff et al. [41] have shown that substitution of an H atom at position 2 of the phenothiazine ring by a chlorine or a trifluoromethyl residue enhanced not only the surface activity and lipid/water partition coefficients of these drugs but also the permeability coefficients. The authors also calculated the increase of negative free enthalpy change of phenothiazines partitioning into the membrane associated with the replacement of the hydrogen atom by Cl or a $-CF_3$ group (ΔG was -1.3 and -4.5 kJ/mol, respectively).

Different model systems mimicking biological membranes and diverse experimental techniques are used to study the effect of phenothiazine derivatives on phospholipid assemblies. The Langmuir technique has been used to study CPZ (**9**) interaction with monolayers formed from phospholipids with different polar heads [42]. It was shown that the surface area of negatively charged lipids such as PS, phosphatidylglycerol (PG), and phosphatidic acid (PA) increased dramatically when CPZ (**9**) was introduced to the system. In contrast, CPZ (**9**) did not induce such an effect in monolayers composed of neutral lipid species (PC or PE). The pronounced effect of CPZ (**9**) on PS, PG, and PA might suggest the preferential role of electrostatic forces in the drug's interactions with anionic lipids. However, the comparison of the effect of CPZ (**9**) with that exerted by simple monovalent cations makes the authors conclude that CPZ (**9**) interacted with lipid acyl chains. This hypothesis was corroborated by further studies in which monolayers composed of saturated or unsaturated PS species were used [43]. It was demonstrated that the work of insertion of CPZ (**9**) between lipid molecules was the smallest, when the most unsaturated PS species was used to form the monolayer. Therefore, the CPZ-induced increase of the surface area of a single lipid molecule was proportional to the packing density of a given phospholipid. Similar results were obtained by de Matos Alves Pinto et al. [44], who studied the interaction of promethazine (**1**) and TDZ (**6**) with PC and PA monolayers. The authors

found that the most important parameters that ruled the drug–membrane interaction were both features of the monolayer (mechanical properties and thermodynamic stability) and the drug itself (molecular size, shape, and charge). The maximal surface pressure that allowed drug penetration was bigger in PC monolayers that had higher surface stability as compared with PA model membranes. This parameter was also dependent on drug's molecular size, being inversely proportional to the molecular volume of the drug. This correlation, however, was not valid in the case of protonated forms of phenothiazines, probably because of electrostatic interactions between the charged drug and phospholipids.

The Langmuir technique was also used by Hidalgo et al. [45] in their study of CPZ (**9**) and TFP (**5**) interaction with monolayers formed from zwitterionic PC and anionic PG. The surface pressure and dipole moment of PG monolayers were seriously affected by both CPZ (**9**) and TFP (**5**). At the same time, phenothiazine derivatives exerted almost no effect on PC model membranes. Only small differences between the actions of CPZ (**9**) and TFP (**5**) were observed; these were attributed to different protonation properties of the two drugs. Additionally, a kind of cooperative effect of phenothiazine derivatives on PG monolayers was noticed, i.e., phospholipid molecules that were not direct neighbors of the drug molecule were also affected by its presence. The use of Brewster angle microscopy allowed the presence of domains in the CPZ:PG monolayers to be observed, too. Further studies by the same group, in which attenuated total reflection infrared spectroscopy was employed, showed that CPZ (**9**) affected only the headgroup region of the monolayer without changing the conformational order of the phospholipid acyl chains [46]. It was suggested that predominant interactions took place between CPZ (**9**) and phosphate groups of lipids. An explanation for the cooperative effect exerted by CPZ (**9**) on PG monolayers was proposed. This effect could be based on the disruption of the hydrogen-bonding network at the phospholipid/water interface by the drug. According to the authors, such an interaction might produce a conformational change not only in the headgroup region but also in the hydrophobic tail region.

Monolayers composed of zwitterionic DPPC and different amounts of anionic PS were used by Jutila et al. [47] in the study of the influence of three neuroleptic drugs (including CPZ) on membrane lateral heterogeneity. It was revealed that in DPPC:brain PS monolayers, CPZ (**9**) increased the average area per lipid molecule. The importance of specific interactions between phenothiazine derivatives and PS was emphasized by the authors. Additionally, microscopic studies of DPPC:brain PS monolayers labeled by the fluorescent probe NBD-PC showed that CPZ (**9**) modulated the domain morphology of the monolayers, increasing the gel–fluid domain boundary length.

Molecular dynamics simulations have been performed to investigate the interactions between CPZ (**9**) and DPPC in Langmuir monolayers [48]. The results of computer simulations revealed that the unprotonated form of the

drug is preferentially located in the lipid tail region of the phospholipids, having little contact with the aqueous phase. The precise orientation and conformation of the CPZ (**9**) molecule inside the monolayer depended on lipid surface density. CPZ (**9**) exerted a "cholesterol-like" effect in DPPC monolayers. The drug promoted ordering of the lipid tails at lower lipid surface densities and induced a local distortion of the acyl chains in the most dense monolayers modeled (area per lipid of 50 $Å^2$).

Self-assembled PC monolayers on mercury electrodes were also used to study the effect of TFP (**5**) and TDZ (**6**) on the electrochemical properties of model membranes [49]. From these experiments it was deduced that phenothiazine derivatives tended to reduce the order of DPPC monolayers. Voltammetric study of levomepromazine (**18**) interaction with stable thin liquid films formed from lecithin on a glassy carbon electrode showed that the permeability of the model membrane to the small solutes was increased in the presence of the drug [50]. The effect of TDZ (**6**) on the transport of neurotransmitters and ions has been recently studied by Nagapa et al. [51]. The authors aimed to test the hypothesis according to which all surface-active drugs, when added to an aqueous phase, spontaneously form a liquid membrane at the interface and modify the transport across the phase boundary. Such a behavior might alter the permeability of cell membranes in the presence of surface-active drugs, like phenothiazine derivatives. It was demonstrated that TDZ (**6**) alone as well as its mixtures with cholesterol and sphingomyelin (SM) modified strongly the membrane permeability for sodium, potassium, and calcium ions and also for biogenic amines. The authors therefore concluded that a "liquid membrane phenomenon" might be important for biological actions of TDZ (**6**) as a neuroleptic drug.

Membrane interactions have been recognized to be important in many biological actions of phenothiazines. Apart from being neuroleptic drugs, many phenothiazines are also able to modulate the multidrug resistance (MDR) of cancer cells and pathological microorganisms. MDR in its most typical form is caused by the expression of transmembrane pumps that transport chemotherapeutics outside the cells, in this way enabling them to survive. Recently the dependencies between drug–membrane interactions and phenothiazine MDR-modulatory properties were reviewed by Tsakovska and Pajeva [52]. The role of phenothiazine–lipid interaction in MDR reversal was also reviewed by Michalak et al. [53]. Passive transport of anticancer drugs is one of the crucial factors governing their accumulation inside the cells. It was therefore studied whether MDR modulators, among them TDZ (**6**), were able to alter the permeability of PC : PA : cholesterol liposomes [54]. The results demonstrated that only the compounds bearing a positive charge and being active MDR modulators caused the leakage of the dye Sulphan Blue from the liposomes. The authors pointed out the importance of the net positive charge of the drugs for being both effective anti-MDR agents and perturbers of the liposome membrane.

Pajeva et al. [55] studied the interaction of a series of phenothiazines with PC and PS model membranes by means of differential scanning calorimetry (DSC) and NMR techniques with the aim of elucidating the role of drug–membrane binding in anti-MDR function of phenothiazines. After addition of phenothiazines to DPPC membranes a shift of the main phase transition temperature (T_m) to lower temperatures, the broadening of the transition peak, and no change in enthalpy (ΔH) were observed. Such changes in transition profiles were attributed to the presence of phenothiazine derivatives in the hydrophobic/hydrophilic interface of model DPPC membranes. The picture that emerged from DSC experiments with phenothiazines and dipalmitoylphosphatidylserine (DPPS) membranes was much more complicated. Apart from lowering of T_m and calorimetric peak broadening, a drug concentration-dependent decrease in ΔH was recorded in this system. Moreover, an additional drug-induced, low-temperature peak appeared in thermograms of phenothiazine : DPPS mixtures. This "new" peak according to the authors was due to strong electrostatic interactions of the cationic drug with negatively charged PC molecules. The NMR technique was used to measure the proton relaxation times of CPZ (9), TFP (5) and triflupromazine (11) in bovine brain PS bilayers. The concentration-dependent reduction of proton relaxation times was recorded in all cases. Additionally, a correlation was found between the MDR modulatory potency of phenothiazine derivatives and their ability to alter the biophysical properties of phospholipid bilayers. Further work by the same group concentrated on membrane actions of *trans*-flupentixol (75), an MDR modulator being structurally related to phenothiazines [56]. It was shown that modulator–membrane interactions might facilitate the penetration of anticancer drugs inside resistant cancer cells.

DSC has been used as a tool to characterize the interactions of phenothiazine derivatives with phospholipid membranes since the 1970s. The most intensively studied drug was CPZ (9), probably due to its common use in the treatment of psychiatric disorders. Cater et al. [57] found that CPZ (9) caused a melting temperature decrease and transition peak broadening in DPPC membranes. Virtually the same results were obtained later on by Frenzel et al. [58] in DPPC mixtures with CPZ (9) and diethazine (7). It was, however, noticed that at high CPZ (9) concentrations (above 15 mol %) the calorimetric peaks became narrow again. The conclusions about CPZ (9) location in DPPC membranes were very similar to those drawn by Pajeva et al. [55]. CPZ-induced lowering of T_m and transition peak broadening accompanied by the decrease of transition enthalpy was also recorded by Jutila et al. [47] in DPPC and DPPS:brain PS model membranes. The interaction of CPZ (9) with negatively charged phospholipids was also studied by means of microcalorimetry. It was demonstrated that in PA and PG model membranes, higher CPZ (9) concentrations induced the appearance of a new calorimetric peak at lower temperatures than the main transition peak [59]. The

authors concluded that phase separation occurred, and CPZ-rich and CPZ-poor domains were present in the bilayer. Similar conclusions were drawn by Fernandez et al. [60] based on their DSC study of CPZ (**9**) interaction with PG multilayers.

Apart from microcalorimetry, ^{13}C and ^{31}P NMR techniques have also been widely used to study the interactions of phenothiazines with model membranes. CPZ (**9**) was found to stabilize the bilayer arrangement of egg PE, the lipid that relatively easily adopted the inverted hexagonal packing mode [61]. In DPPC multilayers the presence of CPZ (**9**) or diethazine (**7**) resulted in enhanced mobility in the acyl chain region of the model membrane and a mobility reduction of the polar DPPC headgroups [58]. The authors proposed that phenothiazine derivatives are incorporated into membranes in such a way that the ring system is placed not far beyond the lipid's glycerol backbone and the cationic side chain is located near the polar headgroups. A similar model of CPZ (**9**) location in PC membranes was proposed by Nerdal et al. [62] as the result of magic angle spinning solid-state ^{13}C NMR experiments. Further interest of this research group was attracted by the interaction of CPZ (**9**) with mixed lipid systems containing both PC and PS. It was shown that CPZ (**9**) interacts preferentially with PS (with its phosphate and the carboxyl group of serine) producing an enhancement of the mobility of the phospholipid polar headgroup [63]. It was also noticed that the degree of phospholipid acyl chain unsaturation partly determined the way in which CPZ (**9**) interacted with membranes. Docosahexanoic acid (DHA) is a highly unsaturated fatty acid that is found at a level of about 50% in the phospholipids of neuronal membranes. As medically important actions of CPZ (**9**) are concentrated on neurons, SDPS (PS containing DHA) was used in NMR experiments, and binding of the drug to this phospholipid was studied [64]. The results of the study demonstrated that in the mixture containing PC and PS possessing different acyl chains, the addition of CPZ (**9**) did not change the mobility of the saturated acyl chains and the choline headgroup of PC. At the same time, NMR measurements allowed detection of the reduced mobility of DHA and the increased mobility of the PS headgroup. A model of CPZ (**9**) interaction with SDPS was proposed. According to this model, the positive charge of the drug was in the vicinity of the negative charge of lipid phosphates, whereas the phenothiazine ring was incorporated near the carbons C-4 and C-5 of the unsaturated fatty acid. Model membranes composed of DPPC and SDPS have also been studied by Song et al. [65]. In this system the presence of lipid microdomains, whose formation is probably due to the hydrophobic mismatch between the two phospholipids, was recorded. The addition of CPZ (**9**) resulted in more uniform membrane packing, i.e., the disappearance of phase separation. The authors claimed that the presence of the drug affected the area occupied by a SDPS molecule in the bilayer and probably the thickness of the bilayer, too.

Fluorescence spectroscopy has also been employed to study CPZ–membrane interactions. Chen et al. [66] exploited CPZ (**9**) intrinsic fluorescence to study binding of the drug to PC liposomes. As CPZ (**9**) fluorescence strongly increased upon addition of PC vesicles to the aqueous drug solution, it was concluded that CPZ had significant affinity for the lipid phase. However, when anionic PS was introduced to the system, a further increase of CPZ (**9**) fluorescence intensity was recorded. It was therefore likely that CPZ (**9**) interacted preferentially with the negatively charged lipid. Fluorescence probes located in different membrane regions were employed to study CPZ (**9**) interaction with synaptosomal plasma membrane vesicles isolated from bovine brain [67]. The use of pyrene derivative Py-3-Py as a probe allowed the authors to demonstrate that the lateral mobility in the membranes was decreased by CPZ (**9**) in a concentration-dependent manner, and the ordering effect was more pronounced in the inner monolayer. A decreased annular lipid fluidity was also observed. Furthermore, the drug was found to have a clustering effect on membrane proteins.

The ESR technique has been employed by Louro et al. [68] to investigate the interaction of the protonated form of CPZ (**9**) with carboxyl groups at the membrane surface. Spin-labeled stearic acid was used both to provide the carboxyl groups and to monitor the CPZ-induced changes in PC liposomes. The results of this study demonstrated strong binding of the drug to the model membrane; however, the distribution of the drug in the membrane surface was not likely to be uniform. In conclusion, the authors suggested that there is an increased affinity of CPZ (**9**) for carboxyl groups present in the vicinity of the membrane surface.

ESR experiments also brought interesting findings when dealing with CPZ (**9**) binding to model and natural membranes containing various amounts of cholesterol. It was shown that CPZ (**9**) in low concentrations increased the degree of order (calculated from ESR spectra) in multilayers composed of ox brain white matter phospholipids containing 5% of cholesterol [69]. However, raising the concentration of the drug eventually produced disorder in model membranes. Pang and Miller [70] employed two spin probes, 5-doxyl stearic acid and 1-acyl-2[8(4,4-dimethyloxazolidine-*N*-oxyl)]palmitoyl phosphatidylcholine, to study the interaction of CPZ (**9**) with PC:PA liposomes. The drug increased the order parameter of both probes in a concentration-dependent manner. When 5-doxyl stearic acid, whose spin label was localized closer to the membrane's surface in comparison to the other probe, was used, the ordering effect of the drug was more pronounced. It was evident that CPZ (**9**) exerted a "cholesterol-like" effect on model membranes, but the increase in order parameter in the presence of the drug was two to three times less than that in the presence of cholesterol. The authors also noticed that the ordering effect of CPZ (**9**) became smaller when the amount of cholesterol in the membrane was raised (up to 33 mol %). The modulatory effect of cholesterol on CPZ-induced changes of lipid order in

model membranes has also been observed by Wisniewska and Wolnicka-Glubisz [71]. The effect of the drug depended mainly on the phase state of the bilayer. In cholesterol-free liposomes, formed from saturated DMPC or unsaturated L-α,β-oleoyl-γ-palmitoyl phosphatidylcholine (SOPC), CPZ (**9**) increased order parameter and rotational mobility of spin-labeled stearic acid above T_m, and decreased these parameters below T_m. The addition of 30 mol % of cholesterol changed the situation completely. In DMPC liposomes the presence of cholesterol reduced CPZ (**9**) partitioning into the membrane. Moreover, the clear increase in lipid motion, i.e., membrane disordering, was visible at temperatures both above and below T_m in DMPC liposomes containing CPZ (**9**) and cholesterol. The influence of cholesterol on CPZ-containing SOPC membranes was not so strong. The ordering effect of CPZ (**9**) observed in pure SOPC liposomes above T_m was reduced by cholesterol, but unlike in DMPC–cholesterol membranes, no fluidizing effect was observed instead. Below T_m CPZ (**9**) induced an increase in lipid motion but this effect was much smaller in the presence of cholesterol as compared with pure SOPC membranes. Summing up, it was shown that CPZ (**9**) alone induced a "cholesterol-like" effect on phospholipid bilayers, but the effect of the drug was strongly abolished when cholesterol itself was present in the membranes.

The modulation of the effect exerted by CPZ (**9**) on membranes in the presence of cholesterol and SM was also studied in respect of membrane stability against the solubilization by detergents [72]. It was observed that CPZ (**9**) in concentrations below the cmc behaved as a mild detergent, inducing the leakage of fluorescent probe 6-carboxyfluorescein from PC liposomes. At higher drug concentrations complete liposome solubilization occurred. The addition of cholesterol or SM to the liposomes did not change the ability of CPZ (**9**) to induce fluorescent dye leakage. As in the case of membrane resistance to detergents, cholesterol increased while SM, surprisingly, decreased liposome resistance against solubilization by detergents.

When applied in high concentration CPZ (**9**) had the tendency to change the lipid packing mode of model membranes. Studies by freeze–fracture electron microscopy demonstrated that CPZ (**9**) induced the formation of a hexagonal phase in cardiolipin [73] and in dioleoyl phosphatidic acid membranes [74]. It should be noticed that CPZ-induced adaptation of non-bilayer organization by these negatively charged lipids was observed only in CPZ : lipid molar ratios as high as 1 : 1 or even 2 : 1. On the other hand, a structural analysis by X-ray diffraction showed that CPZ (**9**) (at 33 mol %) reduced the thickness of a model DPPC membrane by almost 50% [75]. The observation was attributed by the authors to the formation of an interdigitated phase. The possibility of the existence of such a phase at high CPZ (**9**) concentrations was also suggested by Frenzel et al. [58] as they observed that the calorimetric peaks, broadened at low CPZ (**9**) concentrations, became narrow again at high concentrations of the drug.

Besides CPZ (**9**), TFP (**5**) is another phenothiazine derivative whose interaction with membranes is relatively well known. In the extensive study of Hendrich et al. [76], the influence of TFP (**5**) on model membranes formed from zwitterionic lipids (DMPC and DPPC) and negatively charged dimyristoylphosphatidylglycerol (DMPG) was investigated by means of DSC and fluorescence spectroscopy. For all lipids lowering of T_m, calorimetric peak broadening, and ΔH decrease were recorded in the presence of the drug. The extent of drug-induced changes in thermotropic membrane properties depended, however, on both phospolipid headgroup type and the acyl chain length. It was shown that the transition temperature of DMPC was affected more seriously that that of DMPG, whereas ΔH of DMPG was reduced more strongly than that of DMPC. Moreover, the biophysical properties of DPPC, which possessed longer acyl chains than DMPC, were altered by TFP (**5**) to a much smaller extent than the PC species with shorter acyl chains. Additionally, it was noticed that above given drug:lipid molar ratios the calorimetric peaks recorded in zwitterionic lipid clearly consisted of two components, i.e., phase separation was induced by TFP (**5**) in both DMPC and DPPC bilayers. Fluorescence spectroscopy was used to further study the phenomenon of phase separation in PC membranes. The fluorescent probe Laurdan, whose spectral properties are sensitive to the hydration of the lipid bilayer, was employed. The results of fluorescence spectroscopy experiments demonstrated that the main phospholipid phase transition temperature of DPPC bilayers was reduced by TFP (**5**). The observation of phase separation in PC but not in PG bilayers was also confirmed. The existence of microdomains in TFP (**5**):PC mixed membranes was attributed by the authors to the dissimilar interactions of two protonation forms of TFP (**5**) with PC molecules. On the other hand, the formation of TFP-induced domains was not observed by DSC in model membranes formed from the other zwitterionic lipid, dimyristoylphosphatidylethanolamine (DMPE) [77]. The effects exerted by TFP (**5**) on DMPE model membranes were qualitatively similar to the effects of the drug on DMPC. However, stronger lowering of T_m was recorded in DMPC than in DMPE, while drug-induced ΔH reduction was almost the same in the two lipid systems studied.

The interactions of TDZ (**6**) with model membranes composed of different phospholipids were also studied by the same group [78]. Calorimetric studies demonstrated that TDZ (**6**) altered the thermotropic properties of negatively charged DMPC membranes to a larger extent than of zwitterionic phospholipids (PC and PE). The character of the drug-induced changes of the transition parameters of all studied lipids indicated that TDZ (**6**), similarly to other phenothiazine derivatives, was likely to be localized close to the polar/apolar interface of the bilayers. Experiments in which fluorescent probe 1,6-diphenyl-1,3,5-hexatriene (DPH) was employed revealed that TDZ (**6**) reduced the mobility of lipid molecules in a concentration-dependent manner and thus decreased membrane fluidity. The influence of TDZ (**6**) on isolated

rat mitochondria was also studied [79]. As TDZ exhibited strong antioxidant activity it was hypothesized that this effect could be mediated by the interaction of the drug with the mitochondial membrane. To test this hypothesis, experiments with two fluorescent probes were performed. After the addition of TDZ (**6**) the fluorescence intensity of the probe localized near the lipid polar headgroups increased, while the fluorescence of the probe incorporated into the hydrophobic region of the membrane was strongly reduced. It was concluded that TDZ (**6**) interacted with the inner mitochondrial membrane, probably not far from its surface, and such an interaction was important for antioxidant activity of the drug.

The newly synthesized phenothiazine derivative 2-trifluoromethyl-10-[4-(methanesulfonylamido)butyl]-phenothiazine (FPhMS, see Fig. 1 for chemical structure) was also extensively studied in the context of its interaction with lipid bilayers. DSC was used to study the influence of this compound on model membranes formed from DMPE [80], DPPC [81], DMPC, and DMPG [82]. In all the studied lipid systems FPhMS (**16**) lowered T_m, caused broadening of transition peaks, and induced the decrease of ΔH. Melting temperatures were found to be reduced by the phenothiazine derivative to a similar extent when different lipids possessing acyl chains of the same length were compared.

Transition enthalpy was reduced most strongly in DMPC membranes, whereas in DMPE and DMPG the scope of FPhMS-induced change was smaller. Such results confirmed the supposition that FPhMS (**16**) localization inside the membrane is similar to that of other phenothiazines. Additionally, this compound was observed to induce phase separation in DMPE membranes [80]. Two components were clearly visible in the thermograms of FPhMS/DMPE mixtures starting from a drug : lipid molar ratio of 0.04. When the amount of the phenothiazine derivative in the membrane was raised the maximal temperatures of the two components converged, and a single calorimetric peak was finally observed at a FPhMS : lipid molar ratio of 0.12. The existence of phase separation in FPhMS/DMPE mixed membranes was attributed by the authors to the putative two spatial orientations of the phenothiazine derivative side chain in the region of DMPE polar headgroups that were interconnected by the tight network of hydrogen bonds. On the other hand, in model membranes composed of DPPC the phenothiazine derivative showed a biphasic effect on the main phospholipid phase transition parameters as recorded by DSC [81]. Up to a drug : lipid molar ratio of 0.08 FPhMS (**16**) caused the decrease of T_m. At higher molar ratios an increase was observed, and at a drug:lipid molar ratio of 0.12 the melting temperature reached almost the value typical for pure DPPC; however, the calorimetric peaks remained broad. The dependence of ΔH on FPhMS (**16**) concentration was also biphasic but this effect was not as pronounced as in the case of T_m. ESR experiments were performed at a FPhMS:DPPC molar ratio of 0.06 at room temperature (below T_m of DPPC). It was found that the presence of

the phenothiazine derivative caused the restriction of motional freedom of spin labels located at different depths inside the membrane (close to the surface, at the 5th, 7th, and 16th carbon atoms of the DPPC acyl chain). During the same study experiments with the use of fluorescent probe DPH, which is located deep in the membrane core, were performed. The analysis of DPH fluorescence polarization as a function of temperature revealed that FPhMS (**16**) decreased the melting temperature of DPPC.

Additionally, it was observed that the phenothiazine derivative increased DPH polarization in both DPPC and DMPC liposomes at temperatures above T_m. Similar observations were made for liposomes composed of egg PC that were in the liquid-crystalline state at room temperature. At temperatures at which DPPC or DMPC were in the gel state the addition of FPhMS (**16**) caused a concentration-dependent decrease of DPH polarization degree. It was concluded that the effect of FPhMS (**16**) on membranes to some extent resembled the effect of cholesterol, since the addition of the phenothiazine derivative caused an increase of membrane fluidity in the gel state and a decrease of fluidity in the liquid-crystalline state of the bilayer. Many experimental works demonstrated that the electrostatic interaction of phenothiazines and negatively charged lipids might be specific and crucial for the biological functions of these drugs. Wesolowska et al. [82] studied the interactions of FPhMS (**16**) with anionic lipids. The results of this study brought some interesting and unexpected observations that slightly changed the picture emerging from previous works dealing with this subject. As was described above, the cooperativity of the main phospholipid phase transition in DMPC was affected more strongly by the phenothiazine derivative than in DMPG. It suggested deeper penetration of this compound into the membranes composed of neutral phospholipid. Further, interaction of FPhMS (**16**) with liposomes composed of pure PC, pure PS, or mixtures of these two lipids in different proportions was examined. Fluorescence spectroscopy showed that DPH polarization was increased in the presence of the drug in all model membranes; however, the phenothiazine-induced effect was the biggest in pure PC bilayers and the smallest in pure PS model membranes. Just the opposite results were obtained when quenching of fluorescence of *N*-phenyl-1-naphthylamine (NPN) in the presence of FPhMS (**16**) was studied. NPN is localized much closer to the membrane surface than DPH. Here, the most pronounced quenching was recorded in PS membranes, while NPN fluorescence in pure PC liposomes was affected to a lesser extent. Based on the results reviewed above, it was concluded that FPhMS (**16**) was located closer to the membrane surface in the anionic lipid than in the zwitterionic one. Such findings were in general compatible with a model assuming the interaction of the positively charged phenothiazine derivative side chain with the polar headgroups region of phospholipids, while the aromatic ring system of the drug was inserted between lipid acyl chains. Electrostatic interaction between FPhMS (**16**) and negatively charged PS or PG could anchor this compound and

thus keep it closer to the membrane surface than in the neutral PC model membrane.

Four groups of new phenothiazine derivatives were synthesized: phenothiazine maleates (PhM) (**12**), phenothiazine acetylamides (PhA) (**13**), phenothiazine methoxycarbonylamides (PhMC) (**14**), and phenothiazine methanesulfonylamides (PhMS) (**15**) with the aim of their putative application as MDR modulators [9]. The chemical structures of these compounds are presented in Fig. 1. Within each group three different types of ring substituent at position 2 were possible ($-$ H, $-$ Cl, and $-$ CF$_3$) and two lengths of alkyl chain between the ring system and side chain amino group (three and four carbon atoms). The interaction of these new derivatives with model membranes composed of different lipids was studied in a systematic way and the results were presented in a series of papers [9, 38, 83]. Calorimetrically recorded changes in transition parameters of DPPC were the most pronounced in the case of trifluoromethyl-substituted derivatives [9]. PhM (**12**) were identified as the most effective perturbers of DPPC model membranes, whereas other groups of derivatives altered T_m and ΔH in a similar way. All new phenothiazine derivatives were also found to quench NPN fluorescence strongly in liposomes formed from bovine brain PS. The quenching potency decreased in the order: PhM > PhMS > PhMC > PhA. PhMC (**14**) and PhMS (**15**) possessing four carbon atom linkers between the phenothiazine nucleus and side chain group were studied in more detail [83]. Calorimetric analysis of the influence of these compounds on the thermotropic properties of DPPC, DMPE, and DMPG was performed. When the effect of PhMC (**14**) on the melting temperature of the three lipids was analyzed, it was found that chlorine- and trifluoromethyl-substituted compounds decreased T_m more strongly than H-substituted ones. In PhMS (**15**) all derivatives similarly affected T_m in DPPC and DMPG. Only in the case of DMPE was a dramatic drug-induced drop in T_m recorded for Cl- and CF$_3$-substituted compounds. Analysis of the influence of PhMC (**14**) and PhMS (**15**) on ΔH of lipids gave no clear picture—different derivatives were found to be most effective in different phospholipids. Both PhMC (**14**) and PhMS (**15**) turned out to be quenchers of NPN fluorescence in PS liposomes. The quenching effectiveness in the two groups decreased in the order: CF$_3$- > Cl- > H-substituted compounds. Hydrogen- and chlorine-substituted derivatives from both groups of phenothiazines quenched the fluorescence similarly; however, CF$_3$-substituted PhMS (**15**) was a twofold stronger NPN quencher than CF$_3$-substituted PhMC (**14**). Both groups of phenothiazine derivatives were also observed to increase DPH fluorescence polarization in PS model membranes. The effect of PhMC (**14**) and PhMS (**15**) was similar. In both groups the strongest DPH polarization increase was caused by CF$_3$-substituted compounds followed by Cl- and H-substituted ones. In the case of both PhMC (**14**) and PhMS (**15**) a significant correlation was found between their membrane-perturbing activity and MDR-modulating efficiency, which could suggest that interactions with

membranes might be important for the MDR reversing action of these phenothiazine derivatives.

PhM (**12**) have also been found to quench NPN fluorescence and increase DPH polarization in PS membranes [38]. Again, CF$_3$-substituted compounds were found to be both the most effective NPN quenchers and the most potent agents inducing DPH polarization increase. Additionally, it was observed that derivatives possessing four carbon atoms in the alkyl chain between the phenothiazine ring and side chain group were more effective in altering the fluorescence of both NPN and DPH than derivatives with a three carbon atom linker. The compounds with a longer alkyl bridge connecting the phenothiazine nucleus with the side chain group were also shown to influence the transition parameters of DPPC, DMPE, and DMPG to a greater extent than phenothiazines with the shorter linker. The melting temperature and enthalpy were reduced in the presence of all PhM (**12**); however, the most pronounced drop of T_m was found in mixtures of DMPG with CF$_3$-substituted compounds. On the other hand, ΔH was reduced most strongly in the case of CF$_3$-substituted compounds mixed with DMPE. Generally, the effects exerted by PhM (**12**) on the biophysical properties of model membranes were correlated with their lipophilicity but not with their MDR-modulating potency. It was therefore concluded that the mechanism of anti-MDR activity of PhM (**12**) is different from those of PhMC (**14**) and PhMS (**15**), in spite of the relatively similar chemical structures of all groups of phenothiazine derivatives.

2.2
Interaction of Flavonoids with Model Phospholipid Membranes

Flavonoids constitute a large and divergent group of plant-derived compounds characterized by a very wide spectrum of biological activities (for chemical structures see Fig. 2 and Table 1). Flavonoids have been commonly reported to protect cells (e.g., cardio- or hepatoprotection) against injuries caused by external factors. Antioxidant activity is often claimed to be the cause of such cell-protective properties of flavonoids. As membrane lipids are cell components that tend to be the most vulnerable to being oxidized by free radicals, the antioxidant activity of flavonoids has been proposed, and subsequently demonstrated, to be correlated with the ability of these compounds to change the biophysical properties of model and biological membranes [84–86]. The antioxidant properties of flavonoids have been recently reviewed by Heim et al. [87].

Different model systems and different methods are used to evaluate the antioxidant properties of flavonoids. The stable free radical 1,1-diphenyl-2-picrylhydrazyl (DPPH), which changes color after being reduced by an antiradical compound, was employed to study the antioxidant properties of isoflavones genistein (**42**) and daidzein (**40**), flavones apigenin (**23**) and lute-

olin (**25**), and flavonols quercetin (**29**) and kaempferol (**28**) [88]. Only luteolin (**25**), quercetin (**29**), and kaempferol (**28**) turned out to be effective scavengers of the DPPH radical, whereas the other compounds were inactive in this respect. Madsen et al. [89] used an ESR assay based on competition between the spin trap and flavonoids in scavenging peroxyl radicals. Twelve different compounds belonging to flavanones, flavones, flavanols, and flavonols have been tested. The study revealed that flavonols were the most potent scavengers of radicals among all the flavonoids tested. The simultaneous presence of the 2,3-double bond and 3-hydroxyl group in the flavonoid molecule as well as the catechol (benzene 1,2-diol) group in ring B were also identified as markers of the high antioxidant activ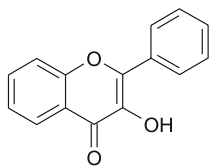ity of flavonoids. Additionally, the authors pointed to the importance of the hydrophilic/lipophilic balance of the flavonoid molecule for its radical scavenging properties. Similar conclusions were also drawn by Yang et al. [90] who determined the oxidation potentials of 30 flavonoids using an electrochemical method. It was noticed that both too high and too low lipophilicity of the flavonoid was devastating for its antioxidant properties. Canola oil constitutes another popular model system to study antioxidant properties of chemicals. Quercetin (**29**) was found to be the most protective against lipid oxidation in this system, followed by kaempferol (**28**), myricetin (**31**), and morin (**30**), while apigenin (**23**) was inactive [91]. The authors concluded that the crucial factors for flavonoid antioxidant activity included the total number and the location of hydroxyl groups, with the 3-OH group being extremely important. Vaya et al. [92] employed low-density lipoprotein as a model system to study the inhibition of chemically induced lipid oxidation by 20 flavonoids belonging to five different subclasses. Quantum chemical calculations of the geometry of the flavonoids and their corresponding radicals demonstrated that abstraction of a hydrogen atom from the 3-OH group was the most energetically favorable, and that was why the presence of this group in the flavonoid structure was so important for its antioxidant activity. Additionally, it was shown that the energy of radical formation at position 3 was dependent on the structure of rings B and C.

The antioxidant activity of flavonoids in liposomes has also been extensively studied. Gordon and Roedig-Penman [93] used liposomes formed from egg PC to compare the antioxidant potencies of myricetin (**31**) and quercetin (**29**) with that of known antioxidant α-tocopherol. Myricetin (**31**) was found to be more effective than α-tocopherol, while the ability of quercetin (**29**) to protect liposomes against oxidation depended strongly on its concentration and pH. Arora et al. also studied different isoflavones [94] and flavonoids [95] in liposomal systems. For both groups of compounds the spatial pattern of hydroxyl groups in the molecule (especially in ring B) was identified to govern the ability of flavonoids to protect PC liposomes against oxidation. Additionally, it was demonstrated that the relative antioxidant potency of flavonoids was dependent not only on their chemical structure but also on the system used to initiate lipid peroxidation. Both groups of flavonoids pro-

flavone   flavonol   flavanone
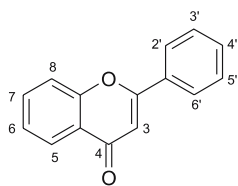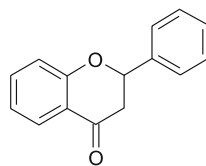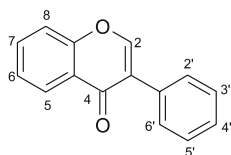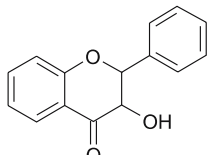
isoflavone   flavanol
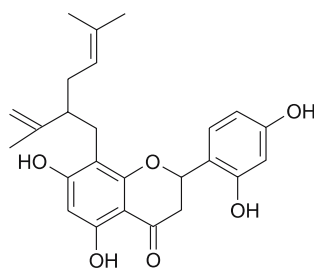
51 sophoraflavonone G
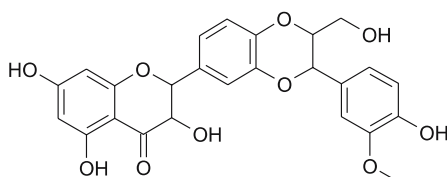
52 silybin (flavanolignan)   **53** dehydrosilybin
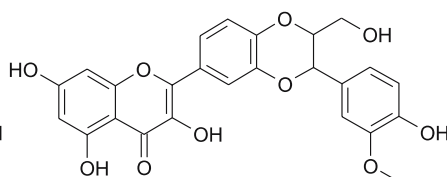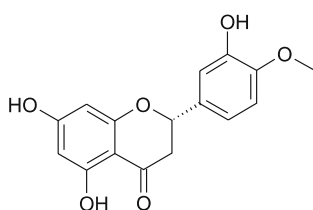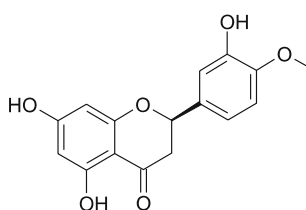
34 hesperetin   **35** neohesperetin

tected liposomes better against oxidation induced by Fe^{2+} or Fe^{3+} ions than by peroxyl radicals. It might suggest that apart from the radical scavenging ability of flavonoids, their metal chelating properties were also important for liposome protection. The high effectiveness of quercetin (**29**) and rutin (**50**) in complexing Cu^{2+} and Fe^{2+} but not Pb^{2+} ions in lipid bilayers was demon-

54 licoisoflavone A

55 licoisoflavone B

56 IFG8

57 IFG10

58 IFG12

59 IFG18

60 sophoraisoflavone A

61 6,8-diprenylgenistein

62 artelastin
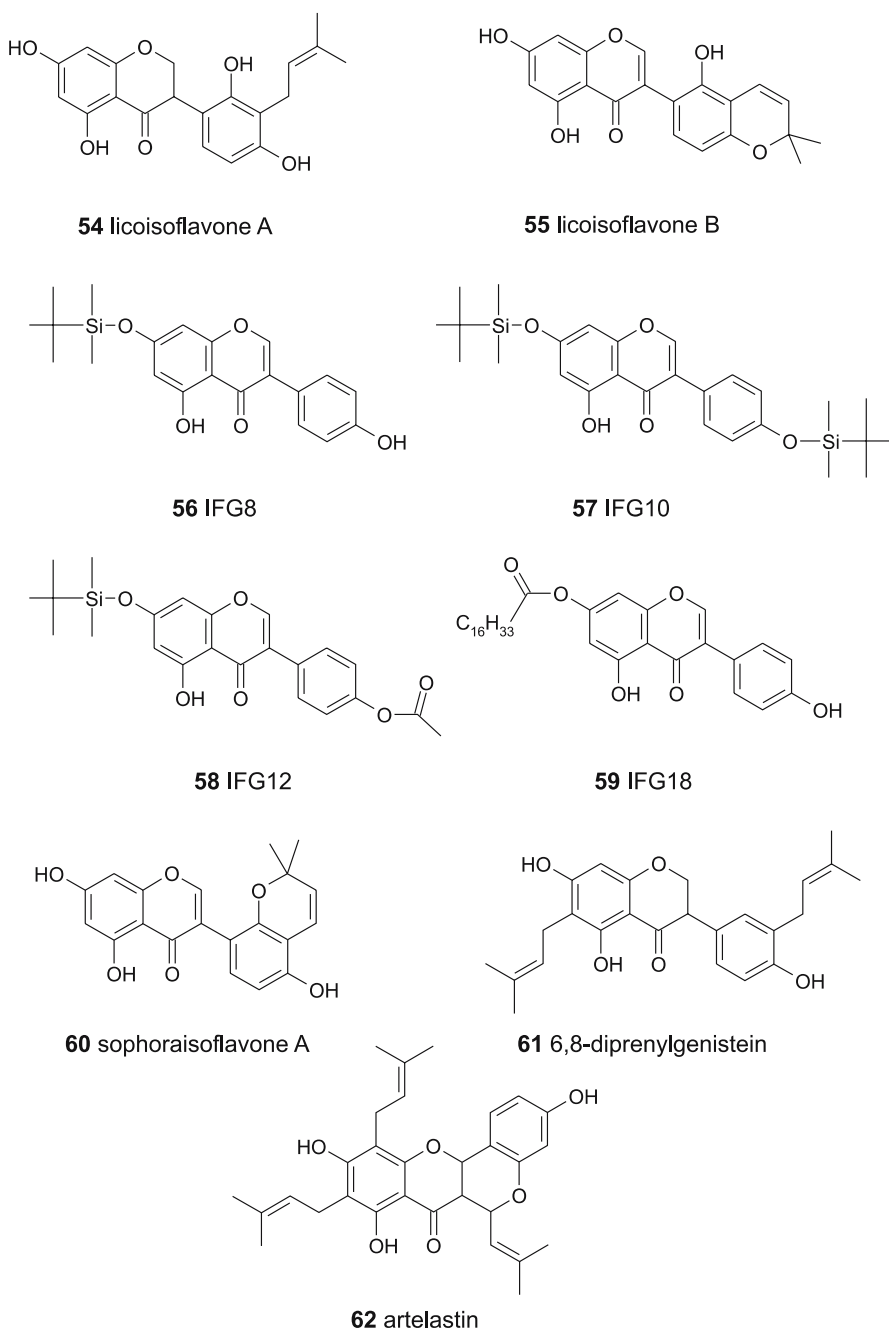
Fig. 2 Chemical structures of flavonoids (basic types of flavonoids and some selected examples)

Table 1 Chemical substitutions at different ring positions for various types of flavonoids

#	Compound/position	3	5	6	7	2′	3′	4′	5′
Flavones:									
21	flavone	H	H	H	H	H	H	H	H
22	chrysin	H	OH	H	OH	H	H	H	H
23	apigenin	H	OH	H	OH	H	H	OH	H
24	acacetin	H	OH	H	OH	H	H	OCH$_3$	H
25	luteolin	H	OH	H	OH	H	OH	OH	H
26	baicalein	H	OH	OH	OH	H	H	H	H
Flavonols:									
27	galangin	OH	OH	H	OH	H	H	H	H
28	kaempferol	OH	OH	H	OH	H	H	OH	H
29	quercetin	OH	OH	H	OH	H	OH	OH	H
30	morin	OH	OH	H	OH	OH	H	OH	H
31	myricetin	OH	OH	H	OH	H	OH	OH	OH
32	fisetin	OH	H	H	OH	H	H	H	H
Flavanones:									
33	naringenin	H	OH	H	OH	H	H	OH	H
34	hesperetin [a]	H	OH	H	OH	H	OH	OCH$_3$	H
35	neohesperetin [a]								
Flavanols:									
36	catechin [a]	OH	OH	H	OH	H	H	OH	H
37	epicatechin [a]								
38	epigallocatechin	OH	OH	H	OH	H	OH	OH	OH
39	taxifolin	OH	OH	H	OH	H	OH	OH	H
Isoflavones:									
40	daidzein		H	H	OH	H	H	OH	H
41	formononetin		H	H	OH	H	H	OCH$_3$	H
42	genistein		OH	H	OH	H	H	OH	H
43	biochanin A		OH	H	OH	H	H	OCH$_3$	H
44	prunetin		OH	H	OCH$_3$	H	H	OH	H
45	irisolidone		OH	OCH$_3$	OH	H	H	OCH$_3$	H
Flavonoid glycosides:									
46	genistin		OH	H	O-Glc [b]	H	H	OH	H
47	hesperidin [a]	H	OH	H	O-Glc-Rha [b]	H	OH	OCH$_3$	H
48	neohesperidin [a]								
49	naringin	H	OH	H	O-Glc-Rha [b]	H	H	OH	H
50	rutin	O-Glc-Rha [b]	OH	H	OH	H	OH	OH	H

[a] Stereoisomers, see Fig. 2
[b] Glc = glucose; Rha = rhamnose

strated by a spectrophotometric method [96]. Heart microsomes were used in the study of antioxidant and metal chelating properties of a large group of flavonoids [97]. The catechol structure in ring B and the presence of the 2,3-double bond and 3-OH group were the structural features identified to be important for antioxidant activity. Additionally, it was stressed that the 3-OH group might constitute a chelation site for Fe^{2+} ions. Foti et al. [98] studied the protective action of isoflavones on normal and cancer lymphocytes against oxidative damage induced by hydrogen peroxide. Both genistein (**42**) and daidzein (**40**) were found to reduce DNA damage but only daidzein (**40**) was shown to reduce lipid peroxidation in the cells.

Apart from the ability to protect cells against oxidative damage flavonoids can, under certain circumstances, exert prooxidative effects. Such a prooxidant activity of many flavonoids was demonstrated [99, 100], and was shown to depend both on the flavonoid structure and on the presence of external factors (e.g., Cu^{2+} ions).

Flavonoids are polyphenolic compounds that combine in their molecules three hydrophobic aromatic rings with lots of hydrophilic side substituents (mainly hydroxyl groups). Such structures are likely to interact with lipid bilayers or detergent molecules that contain spatially separated hydrophobic and hydrophilic regions. Liu and Guo [101] studied the interaction of morin (**30**) with cationic detergent hexadecyltrimethylammonium bromide (CTAB). The results suggested that morin (**30**) was bound to the detergent micelles by its ring B, and that the angle between ring B and the rest of the molecule changed during binding. It was also shown that morin–detergent interaction was an endothermic process driven by weak intermolecular forces (both hydrophobic and electrostatic). Interaction of quercetin (**29**) with micelles of anionic detergent SDS and cationic CTAB was studied by the same authors [102]. It was demonstrated that quercetin (**29**) incorporates into micelles formed from both detergents. Different interaction modes were proposed, however, for the quercetin–SDS and quercetin–CTAB systems. The authors concluded that ring B of morin (**30**) is most likely to interact with SDS molecules, while rings A and C constituted the most probable site of interaction with cationic detergent.

The affinity of flavonoids for phospholipid membranes has been unequivocally demonstrated by many authors. Many biological functions of these compounds are also believed to be the result of flavonoid interactions with cell membranes. Partition coefficients for a large group of flavonoids between water and olive oil were determined, and it was shown that the hydrophobicity of the compounds is inversely proportional to the number of OH groups.

Additionally, it was noticed that flavones were slightly more hydrophobic than flavanones possessing the same number of hydroxyl groups [103]. Flavonols turned out to be the least hydrophobic from all the compounds studied. The degree of DPH fluorescence quenching in PC liposomes by flavonoids was used as a measure of the relative membrane affinity of these

compounds. The test showed that flavonols, although less hydrophobic than flavanones, exhibited a substantially higher affinity for liposomes. According to the authors flavones were likely to easily intercalate into the PC bilayer due to the more planar configuration of their molecules as compared to flavanones. The octanol:water partition coefficients for a series of isoflavonoids and their affinity for egg PC vesicles were measured by Kato et al. [104]. It was shown that high lipophilicity was characteristic for the compounds with a 5-OH group combined with a methoxy group at the 4′ position. The authors postulated that these groups formed an intramolecular hydrogen bond and in this way an additional aromatic ring was formed. More hydrophobic isoflavonoids were found to be more effective quenchers of fluorescence of both 2- and 12-anthroyloxy stearic acid probes incorporated into PC liposomes. Lipophilicity of the studied isoflavonoids was correlated with their cytotoxicity for Chinese hamster lung fibroblast V79 cells. The same cell line was used to investigate the toxicity of four flavonols: myricetin (**31**), quercetin (**29**), galangin (**27**), and kaempferol (**28**) [105]. Again it was found that more hydrophobic compounds were more toxic to the cells.

On the other hand, the results of Ollila et al. [106] demonstrated that the interactions between flavonoids and DPPC immobilized on a chromatographic column were not governed by compound hydrophobicity but by the number of OH groups in the flavonoid molecule. Affinity for the DPPC membrane measured as retention time was higher for the compounds possessing large numbers of hydroxyl groups. This suggested that both polar and nonpolar forces were important for flavonoid–biomembrane interactions. Kajiya et al. [107] in their study on binding of four tea catechins to PC liposomes demonstrated that such factors as the number of OH groups, the presence of the galloyl moiety, and the stereochemical structure governed the affinity of flavonoids for phospholipid bilayers (see Fig. 3 for chemical structures). Moreover, it was shown that raising the salt concentration in the aqueous medium resulted in an increased amount of catechins bound with the model membrane. The introduction of a negative charge by adding 10% of PS to PC liposomes resulted in lower amounts of catechins associated with the membrane. The importance of the stereochemical structure of tea catechins for their interaction with lipid membranes was studied in more detail [108]. Catechins can be classified into *cis* and *trans* types that differ by the configuration of the hydrogens at the 2 and 3 positions of ring C. The authors found that both the octanol:buffer partition coefficient and the amount of flavonoid incorporated into liposomes were higher in the case of *cis*-catechins. *Cis*-catechins also turned out to be more effective quenchers of fluorescence of 2-anthroyloxy stearic acid than the corresponding *trans*-catechins, which might reflect a higher membrane affinity of *cis*-stereoisomers.

Human colon adenocarcinoma cell line Caco-2 constitutes a popular model to study the absorption of different compounds into enterocytes and their transport through the monolayer of epithelial cells. Murota et al. [88]

36a (+)-catechin (trans form) **36b** (-)-catechin (trans form)

37a (+)-epicatechin (cis form) **37b** (-)-epicatechin (cis form)

38 (-)-epigallocatechin

63 (-)-epicatechin gallate

64 (-)-epigallocatechin gallate
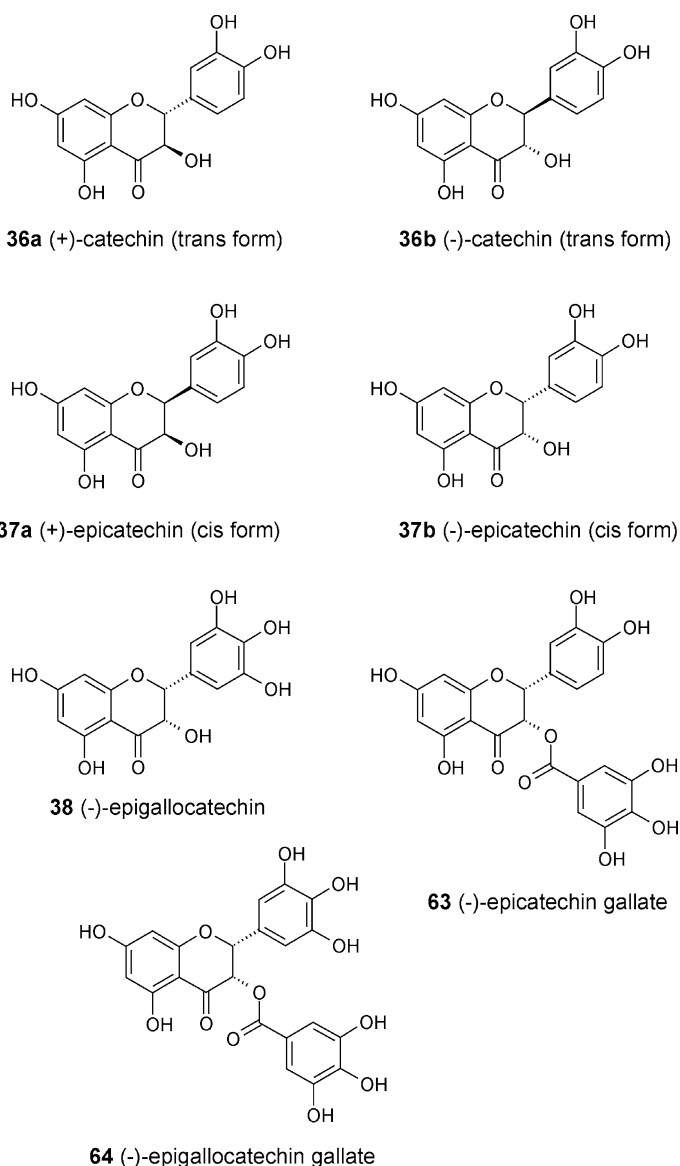
Fig. 3 Stereochemical structures of catechin isomers

showed that some degree of hydrophobicity is needed for flavonoids to enter and be transported by these cells, as isoflavone aglycones were bound and transported more efficiently than their glucosides. On the other hand, strong binding to cell membranes was likely to diminish transport through the monolayer of Caco-2 cells, as shown for a group of flavonoids by Tammela et al. [109]. The authors demonstrated that high membrane affinity was

accompanied by poor apical to basolateral transport. Flavonoids interacted strongly with membranes and were most probably accumulated within the cells and/or cell membranes, which led to their low ability to penetrate the monolayer of epithelial cells.

The influence of flavonoids on membrane permeability and integrity was studied by many authors. Depending on flavonoid concentration and the model system used both protective and disruptive activities of flavonoids were recorded. Catechins [85] and other flavonoids [110] were found to protect PC:PS liposomes against detergent-induced lysis. Ollila et al. [106] noticed that the ability of flavonoids to induce the leakage of fluorescent probe calcein entrapped in PC liposomes was correlated with the hydrophobicity of the compounds. However, not only hydrophobicity but also flavonoid location inside the membrane might be important for its action on membrane permeability. Gallic esters of catechins (gallates) were found to be more hydrophobic and have higher affinity for lipid bilayers than catechins themselves [111]. In spite of this fact, catechins induced calcein efflux from PC liposomes even at the lowest concentrations tested, whereas catechin gallates protected the liposome membrane when used at concentrations below 1 nM. The authors concluded that such an effect was due to more superficial location of catechin gallates as compared to the corresponding catechins. The conclusion was additionally supported by the observation that catechin gallates but not catechins quenched the fluorescence of 2-anthroyloxy stearic acid whose fluorophore is located near the membrane surface. At high concentrations, however, catechin gallates induced stronger carboxyfluorescein efflux from liposomes formed from a lipid mixture extracted from *Escherichia coli* than catechins [112].

As flavonoids constitute an extremely large and divergent group of compounds, one may expect that the scope of membrane-associated effects exerted by these compounds would be very broad and that different flavonoids would change the biophysical properties of membranes in a dissimilar way. Surprisingly, virtually all publications in which the effect of flavonoids on membrane fluidity was studied came to similar conclusions. Furusawa et al. [113] employed two fluorescent probes: DPH, buried deep in the membrane hydrophobic core, and TMA-DPH which possessed the same fluorophore but anchored closer to the membrane surface by a cationic trimethylammonium (TMA) phenyl group. The authors reported a significant increase of fluorescence polarization of both probes in the presence of quercetin (**29**) and its derivatives commonly found in the brownish scale of onion. The same probes were used to study the membrane action of epigallocatechin gallate (EGCg) (**64**), genistein (**42**), daidzein (**40**), quercetin (**29**), and apigenin (**23**) [114]. Again, the membrane rigidifying effect of flavonoids was observed. Additionally, it was found that the ability of flavonoids to decrease membrane fluidity was significantly affected by membrane composition. The more cholesterol was present in the PC bilayer the weaker rigidifying ac-

tion of flavonoids was recorded. Surprisingly, no effect of two catechins on the DPH fluorescence polarization in mixed PS:PC liposomes was reported by Verstraeten et al. [85]. Arora et al. [115] employed a series of fatty acid probes fluorescently labeled by the anthroyloxy moiety at different positions to study the interactions of a series of isoflavonoids and flavonoids with PC model membranes. All compounds studied significantly increased the fluorescence anisotropy of these probes. The rigidifying effect was the most pronounced deep in the membrane core, as flavonoids changed the fluorescence anisotropy of 16-anthroyloxy palmitic acid most prominently. The comparison of the effect of flavonoids on PC bilayers with that exerted by cholesterol revealed that flavonoids in the membranes behaved similarly to this steroid. Anthroyloxy fatty acids were also used to study the action of 26 polyphenolic compounds on PC liposomes [86]. Flavanols and flavonols decreased membrane fluidity. Again, a more pronounced effect was recorded when the fluorescence anisotropy of 16-anthroyloxy palmitic acid was studied than for 6-anthroyloxy stearic acid. On the other hand, isoflavones and flavanones exerted almost no effect on membrane fluidity. In the case of flavanones, it was attributed to the tilted configuration of their molecules as compared to the planar structure of flavonols.

In a series of papers Tsuchiya [116–118] employed two fluorescent probes, 1-anilinonaphthalene-8-sulfonic acid (ANS) and NPN, to study the effect of the flavonoids on membrane fluidity. ANS binds close to the polar heads of phospholipid molecules, whereas NPN is located deeper in the membrane and probes its hydrophobic/hydrophilic interface. The effect of naringenin (**33**) and its more hydrophobic derivative possessing the 8-lavandulyl moiety (sophoraflavanone G (**51**)) on the fluorescence polarization of the two probes was compared [117]. Both compounds were shown to decrease the fluidity of model PC membranes, sophoraflavanone G (**51**) being more active than naringenin (**33**). It was hypothesized that the reduction of the fluidity of bacterial membranes was the cause of the antimicrobial activity of sophoraflavanone G (**51**). The same model system was used to demonstrate the ability of eight catechins from green tea to rigidify phospholipid bilayers [116]. Both ANS and NPN polarization degree was increased in the presence of catechins; however, the effect of these compounds on the hydrophilic region of the membrane was slightly more pronounced. A higher membrane affinity of *cis*-catechins than the *trans* forms was recorded in this model system, too [118], as *cis*-catechins turned out to be more effective membrane rigidifying agents than the *trans* stereoisomers.

In a more detailed study Caturla et al. [112] investigated the interaction of four catechins with PC and PE model membranes by fluorescence spectroscopy, microcalorimetry, and infrared spectroscopy. DPH fluorescence anisotropy was monitored as a function of temperature and it was observed that catechins either did not change or increased DPH anisotropy. The membrane rigidifying effect of (–)-epicatechin (EC) (**37b**) was the most

pronounced when DMPC was in the gel state, whereas (–)-epicatechin gallate (ECg) (**63**) exerted a stronger effect on lipid in the liquid-crystalline phase. The plots of DPH anisotropy versus temperature revealed that only ECg (**63**) reduced the T_m of DMPC strongly enough to be detected by fluorescence spectroscopy. Microcalorimetry demonstrated that only ECg (**63**) and (–)-EGCg (**64**) were able to change the main phospholipid phase transitions of DMPC, whereas EC (**37b**) and (+)-catechin (C) (**36a**) were inactive in this respect. This was in agreement with measured liposome : buffer partition coefficients that were substantially higher for ECg (**63**) and EGCg (**64**) than for C (**36**) and EC (**37**). Both ECg (**63**) and EGCg (**64**) reduced T_m and caused calorimetric peak broadening. Additionally, in the case of ECg (**63**) at concentrations above 15% cooperativity of the transition increased again. Additional experiments on quenching of intrinsic fluorescence of catechins by lipids spin-labeled at different depths brought the authors to the conclusion that catechin gallates (especially ECg (**63**)) were located deeper in the membranes than non-galloylated catechins. This conclusion was, however, opposite to that reached previously by Hashimoto et al. [111]. Yoshioka et al. [119] employed ESR spectroscopy to characterize the binding of (+)-catechin (**36a**) to DPPC membranes. TEMPO, the spin probe superficially associated with the lipid bilayer, was used to demonstrate that C (**36**) stabilized the membrane surface, which resulted in an increase of the lipid melting temperature. (+)-Catechin (**36a**) also caused a rise in 5-doxyl stearic acid order parameter and hindered the motion of alkyl chains, as judged by the rotational correlation time of 16-doxyl stearic acid. The authors concluded that the effects of C (**36**) on the membrane core were due to its strong interaction with polar lipid headgroups without flavonoid penetration deep into the phospholipid bilayer.

Many flavonoids exhibit relatively intensive intrinsic fluorescence. Tomeckova et al. [120] attempted to employ it to characterize the interaction of some chalcones and flavonoids, i.e., naringenin (**33**), naringin (**49**), and quercetin (**29**), with the outer membrane of rat mitochondria. It was observed that polarization of the flavonoid fluorescence increased when mitochondria were added to the reaction buffer, which was attributed to the process of compound binding to the membrane. Interaction of the plant flavonoid fisetin (**32**) with PC model membranes was investigated in detail by Sengupta et al. [121]. The fluorescence anisotropy of fisetin (**32**) was monitored as a function of temperature. It was demonstrated that this parameter was useful to detect the main phase transition of DPPC. Fisetin's anisotropy was relatively high at temperatures below the T_m of the phospholipid and was significantly lowered when DPPC was in the liquid-crystalline state. The authors concluded that flavonoid fluorescence anisotropy might serve as a useful indicator of the rigidity of the local microenvironment of the fluorophore. This was probably caused by relatively deep incorporation of fisetin (**32**) into lipid bilayers and its localization in motionally constrained sites. New highly fluorescent

derivatives of flavonols were designed and were demonstrated to be useful for studying the interdigitation of lipid bilayers [122]. 3-Hydroxyflavone derivatives anchored in lipid bilayers at a relatively precise depth through their attached ammonium groups were demonstrated to probe the hydration and polarity of lipid bilayers simultaneously [123].

DSC was also employed to study the interactions of flavonoids with model membranes. Saija et al. investigated the thermotropic behavior of DPPC bilayers in the presence of quercetin (**29**), naringenin (**33**), hesperetin (**34**) [124], and rutin (**50**) [84]. All flavonoids, with the exception of rutin (**50**), caused a concentration-dependent decrease of T_m accompanied by the broadening of calorimetric peaks. None of the flavonoids changed the transition enthalpy of DPPC. The lowering of the lipid melting temperature was time-dependent; the effect was more pronounced immediately after preparation of the probe and diminished with time. Additionally, it was observed that the influence of quercetin (**29**) and hesperetin (**34**) on T_m was biphasic. Raising the concentration of the flavonoids resulted in a T_m decrease that reached a minimum at a flavonoid:DPPC mole ratio of 0.09 in the case of quercetin (**29**) and 0.18 for hesperetin (**34**). In the presence of higher amounts of the flavonoids the melting temperature increased again, not reaching, however, the values typical for pure DPPC. The authors claimed that the studied flavonoids induced a fluidizing effect on DPPC bilayers; however, since no other researchers reported such an effect of flavonoids, this conclusion should be treated with caution. The biphasic effect of the compounds on T_m was attributed to their differential solubility in lipid bilayers in gel and liquid-crystalline phases. As an alternative explanation the possibility that flavonoids left the lipid bilayer when applied in high concentrations was considered. The changes caused by quercetin (**29**) in the thermotropic properties of DPPC membranes observed by Wojtowicz et al. [125] were very similar. In addition, the mobility of spin probes 5- and 16-doxyl stearic acid in the presence of quercetin (**29**) was studied. Based on calorimetric results and on the observation that only the motional freedom of 5-doxyl stearic acid was affected by the flavonoid, it was concluded that quercetin (**29**) was most likely located at the polar/apolar interface of the membrane.

Microcalorimetry was also employed by Lehtonen et al. [126] in their study on binding of daidzein (**40**) to model membranes formed from different phospholipids. It was found that daidzein (**40**) strongly perturbed the main phospholipid phase transition of both DMPC and dimyristoylphosphatidylserine (DMPS). The melting temperature of both lipids was decreased by the isoflavone in a concentration-dependent manner. In the case of DMPC, but not DMPS, the lowering of transition enthalpy was additionally recorded. The difference in the interaction of daidzein (**40**) with zwitterionic and negatively charged phospholipids was also noticed when turbidity measurements were performed on liposomes treated by the isoflavone. Strong liposome aggregation then occurred, and its extent depended on the type of phospholipid

used. The most pronounced aggregation was observed in the case of anionic lipids, such as PS, PG, PA, and phosphatidylinositol (PI). The aggregation-promoting effect of daidzein (**40**) was reduced in the presence of cholesterol. It was concluded that the properties of the bilayer surface were drastically changed by daidzein (**40**), and it was proposed that the membrane hydration was lowered in the presence of the isoflavone. The addition of cholesterol reduced the daidzein-dependent effect as cholesterol was known to increase the hydration of lipid bilayers.

Movileanu et al. [127] used reconstituted planar PC bilayers (black lipid bilayers) to study the effect exerted by quercetin (**29**) on their electrical properties. Quercetin inserted into model membranes, which resulted in an increase in their conductance and electrical capacitance. Clear pH dependence of quercetin (**29**) binding to membranes was observed. Capacitance changes were the most pronounced at low pH, which was attributed to the deeper insertion of quercetin (**29**) into the bilayer in acidic conditions. The authors postulated that quercetin inside the membrane interacted with both the hydrophobic domain and polar headgroups of PC.

The use of ^{1}H magic angle spinning NMR spectroscopy allowed Scheidt et al. [128] to precisely determine the localization of flavone (**21**), chrysin (**22**), luteolin (**25**), and myricetin (**31**) in model 1-palmitoyl-2-oleoyl phosphatidylcholine (POPC) membranes. The presence of the flavonoids changed the chemical shift of NMR signals derived from different portions of the POPC molecule. Since the biggest shifts were induced in signals of PC fragments located near the flavonoid molecules, the precise localization of the compounds inside model membrane could be calculated. It was shown that all lipid segments were affected by the flavonoids, i.e., their distribution in the membrane was very broad. The center of distribution was located at the level of the glycerol region. The precise membrane location was dependent on the number of hydroxyl groups in the flavonoid molecule. More polar compounds tended to be biased toward the polar headgroups region. The spatial orientation of the flavonoid inside the membrane was governed by the position of the molecule's polar center. It was deduced that in the case of luteolin (**25**) and myricetin (**31**) ring B was pointing toward the aqueous phase while ring A was inserted deeper in the acyl chain region of the bilayer. The opposite orientation was postulated for chrysin (**22**), whereas no preferential orientation was found for flavone (**21**), which indicated a high molecular mobility of this compound inside the membrane. The same method was employed by Siarheyeva et al. [129] in a study dealing with the interaction of a large group of multidrug transporter substrates (including quercetin (**29**)) with model DMPC membranes. Quercetin's distribution inside the lipid bilayer was relatively broad. The most probable location of the flavonoid molecule was the layer located below the headgroup phosphates and above the first segments of the lipid acyl chain. The interaction of EGCg (**64**), one of the tea catechins, with DMPC membranes was studied by means of solid-

state ^{31}P and ^{2}H NMR [130]. In the presence of EGCg (**64**) the ^{31}P chemical shift anisotropy was decreased, which suggested that the motions of phospholipid headgroups were affected by the flavonoid. The above data confirmed the localization of EGCg (**64**) not far from the polar headgroup region of the membrane.

Hendrich et al. [131] combined DSC and absorption spectroscopy to study membrane actions of isoflavones isolated from *Sophora japonica*: formononetin (**41**), irisolidone (**45**), licoisoflavone A (**54**), and 6,8-diprenylgenistein (**61**). The two latter compounds were substituted by at least one prenyl group, whereas formononetin (**41**) and irisolidone (**45**) were more polar. It was found that both formononetin (**41**) and irisolidone (**45**) caused strong aggregation of liposomes, the effect of 6,8-diprenylgenistein (**61**) was weaker, and licoisoflavone A (**54**) promoted no liposome aggregation. Liposomes composed of negatively charged phospholipids (PI or PS) were slightly more affected by isoflavones than the ones formed from neutral PC. DSC experiments revealed that all isoflavones were incorporated into DPPC model membranes and caused a drop of both T_m and ΔH and transition peak broadening. Interestingly, the thermotropic behavior of DPPC was the most influenced by licoisoflavone A (**54**) and 6,8-diprenylgenistein (**61**), while irisolidone (**45**) and formononetin (**41**) exerted less pronounced effects. Additionally, it was noticed that licoisoflavone A-induced changes in transition enthalpy and cooperativity were biphasic. At an isoflavone : lipid molar ratio as high as 0.2 the calorimetric peak resharpened again, and also ΔH increased slightly as compared to the licoisoflavone A:DPPC molar ratio of 0.1. Based on the above data, the authors proposed that aggregation-promoting formononetin (**41**) and irisolidone (**45**) bound close to the liposome surface, whereas isoflavones possessing prenyl groups in their structure penetrated the bilayer more deeply and were located near the polar/apolar membrane interface. In the next paper of this research group, the interaction of two pairs of isoflavones with PC bilayers was investigated [132]. After ingestion isoflavones are subjected to many metabolic processes, among others O-demethylation which transforms formononetin (**41**) to daidzein (**40**) and biochanin A (**43**) to genistein (**42**). The results of DSC experiments revealed some similarities between metabolically related compounds. All isoflavones decreased the main phospholipid phase transition of DPPC. The effect of daidzein (**40**) and formononetin (**41**) was quite weak and not concentration-dependent. On the other hand, clear concentration dependence was visible in the case of genistein (**42**) and biochanin A (**43**). Both compounds caused a slight increase of T_m at an isoflavone : lipid molar ratio of 0.2 accompanied by a strong decrease at higher concentrations. The magnitude of changes was, however, much bigger for genistein (**42**) than for biochanin A (**43**). Genistein (**42**) and biochanin A (**43**) also caused a decrease in phase transition cooperativity, whereas daidzein (**40**) and formononetin (**41**) did not induce the broadening of transition peaks. None of the isoflavones studied exerted

a significant effect on the transition enthalpy. The authors concluded that the ability of isoflavones to influence the biophysical properties of lipid bilayers was not changed after the process of O-demethylation. In addition, it was proposed that all the studied isoflavones were located close to the membrane surface. This proposition was supported by the fact that genistein (**42**), in spite of being the most polar compound of all, exerted the most pronounced effects on DPPC model membranes.

Superficial membrane localization was also proposed for flavanolignan–silybin (**52**) on the basis of the results obtained by means of fluorescence spectroscopy, ESR, and microcalorimetry [133]. It was found that generalized polarization of the fluorescent probe Laurdan was not changed by the presence of the flavonoid. The fluorophore of Laurdan is located at the level of the glycerol backbone and fluorescence emission spectra of this probe are highly sensitive to lipid bilayer hydration. On the other hand, generalized polarization of more shallowly located Prodan was lowered by silybin (**52**). DSC experiments demonstrated that silybin (**52**) reduced the transition temperature of DMPC but ΔH was affected very weakly. Silybin-induced changes in the thermotropic properties of PC possessing longer acyl chains (DPPC) were almost negligible. Additionally, it was observed that the appearance of calorimetric peaks of silybin/DPPC mixtures evolved with time. This could be caused by the escape of the flavonoid from the densely packed DPPC membrane, as proposed by Saija et al. [124] for quercetin (**29**) and hesperetin (**34**). The interaction of silybin (**52**) with only the surface of the lipid bilayer was corroborated by ESR spectroscopy. Only the spectral parameters of superficial spin probe TEMPO palmitate were affected by the flavonoid, while the mobility of 5-doxyl and 16-doxyl stearic acid was not changed. The ability of silybin (**52**) to induce efflux of calcein entrapped inside egg PC liposomes was also found to be very limited.

2.3
Interaction of Phenothiazines with Erythrocyte Membranes

Mammalian erythrocytes are highly specialized cells characterized by an extremely simplified structure whose main task is the transport of gases (oxygen and carbon dioxide) inside a body. They are biconcave membrane sacks filled with hemoglobin. Red blood cells are devoid of internal membranes; also, the structure of their membrane and membrane skeleton is well known. That is why erythrocytes constitute a good and relatively simple model of biological membranes and are often used in studies on the interactions of drugs with lipid bilayers. Marroum and Curry [134] investigated the partitioning of six phenothiazines into red blood cells. It was found that the partition rate of the drugs between erythrocytes and buffer was not correlated with the phenothiazine lipophilicity, which was measured by determination of partition coefficients in hexane/buffer systems. This suggested that other mechanisms,

not only simple partitioning, accounted for the interaction of phenothiazines with the erythrocyte membrane. The authors proposed two possible explanations for that. First, they noticed that all the phenothiazines studied would be in their cationic forms at physiological pH—therefore, electrostatic interactions between the drugs and membrane could overrule lipophilicity in partitioning. Second, specific binding of phenothiazines to some components of the cell membrane or to some targets inside the cell could also result in an apparent lack of correlation between phenothiazine lipophilicity and red blood cell partitioning. A twinned titration flow calorimetry method was used to characterize the thermodynamics of binding of five phenothiazine derivatives to erythrocyte ghosts and intact red blood cells [135, 136]. When binding of the drugs to erythrocyte ghosts was studied it turned out that the process was entropy driven, as a large positive entropy change (ΔS) and small negative enthalpy change (ΔH) were observed during binding. Phenothiazines were characterized by a relatively high affinity to erythrocyte ghosts; the binding constants lay in the range of 10^4–$10^5\,\mathrm{M}^{-1}$. The picture changed dramatically when binding of phenothiazine drugs to intact erythrocytes was analyzed. In this case, both ΔS and ΔH showed large negative values. Additionally, the affinity of drugs for red blood cells was larger the more hydrophobic the substituent present at position 2 of the phenothiazine ring (see Fig. 1). The results demonstrated unequivocally that different mechanisms ruled the interaction of phenothiazine derivatives with erythrocyte ghosts and with intact cells. It was suggested that in whole erythrocytes phenothiazines bound and/or penetrated the inner monolayer of the membrane and reacted with intracellular components, such as hemoglobin.

The ESR technique was employed to study the interactions of 11 phenothiazines with erythrocyte ghost membranes [137]. All the drugs were observed to induce spin-label immobilization. In the majority of cases the immobilization effect was stronger for phenothiazine derivatives possessing a hydrophobic substituent at position 2 of the ring ($-\mathrm{SCH_3}$ or $-\mathrm{CF_3}$) than for those with more hydrophilic residues ($-\mathrm{COCH_3}$ or $-\mathrm{H}$). A correlation was found between the ability of the drug to induce spin-label immobilization and its antisickling potency. Olivier et al. [138] investigated binding of two spin-labeled CPZ (**9**) derivatives to human intact erythrocytes. The fraction of the probes partitioned into erythrocytes depended neither on temperature nor on spin-label concentration. In ESR spectra of both spin-labeled CPZ (**9**) derivatives two components were found: a slow-motion component and a fast-motion component. The ratio of the two components depended on temperature, and the slow-motion component was observed to prevail at low temperatures. The authors drew the conclusion that two binding sites for phenothiazine derivatives existed in erythrocyte membranes. An ESR study [139] on CPZ (**9**), chlorpromazine sulfoxide, and TFP (**5**) binding to both erythrocyte ghosts and intact red blood cells gave opposite results than those obtained before [137]. Stearic acid spin probes labeled at the 5th, 7th, and

12th carbon atoms showed the increase in motional freedom in the presence of phenothiazine derivatives [139]. Since it was demonstrated that phenothiazines exerted no effect on the fluidity of erythrocyte-extracted vesicles depleted of spectrin and actin, the authors came to the conclusion that skeletal proteins might constitute the putative membrane target for phenothiazine drugs.

The conformation and dynamics of erythrocyte membrane proteins were also significantly influenced by TFP (5), as demonstrated by means of fluorescence spectroscopy [140]. Fluorescence energy transfer between membrane protein tryptophans and 1-aniline-8-naphthalene sulfonate molecules was increased in the presence of TFP (5) in erythrocyte ghosts, which suggested a decrease of apparent distance separating energy donors (tryptophans) and acceptors (ANS molecules). It was concluded that TFP-induced alterations in the structure of membrane proteins led to the rearrangement of the surrounding lipids. Specific binding of CPZ (9) to spectrin was also demonstrated in erythrocyte ghosts [141]. As a consequence, a concentration-dependent increase in membrane stability was observed after the addition of TFP (5).

The effect of phenothiazine derivatives on the stability and integrity of erythrocyte membranes depends on the drug concentration. At high concentrations hemolysis occurs, but at low concentrations stabilizing effects of phenothiazines were reported. Born and Housley [142] have shown that CPZ (9) and TDZ (6) at concentrations below 20 μM protected human erythrocytes against hypotonic lysis. The pretreatment of red blood cells with trypsin and neuraminidase diminished the antihemolytic effect of phenothiazine derivatives. It was therefore suggested that positively charged drugs interacted strongly with the negatively charged sialic acid moieties of glycoproteins on the erythrocyte surface. That is why sialic acid removal by enzymes abolished the antihemolitic activity of phenothiazines. TFP (5) was also observed to protect erythrocytes against hypotonic lysis when used at a concentration below 20 μM [143]. Similar protective concentrations were reported for TFP (5) and CPZ (9) by Hagerstrand and Isomaa [144]. The authors noticed that the protective action of phenothiazines and other amphiphilic compounds was not related to drug-induced shape changes in erythrocytes. They proposed that intercalation of low amounts of amphiphiles into the erythrocyte membrane caused rearrangements within the bilayer which were associated with an increase of membrane permeability. It was suggested that rapid efflux of ions through the amphiphile-treated membrane decreased the difference in osmotic pressure between the cell interior and hypotonic buffer, thereby protecting cells from being lysed.

At high concentrations phenothiazine derivatives are known to induce erythrocyte hemolysis. Many groups studied this process; parameters such as hemolysis onset, 50%, and completion have been widely used to characterize phenothiazine-induced membrane disruption. TFP (5) was reported to

cause 50% hemolysis at ca. 90 μM concentration [143], whereas TDZ (**6**) induced such an effect at 110 μM, and CPZ (**9**) only at 370 μM [78]. In the latter study it was also noticed that the drug concentration range between hemolysis onset and completion was much narrower in the case of TDZ (**6**) than of CPZ (**9**). The hemolytic activity of PhM (**12**) was also investigated [9]. Derivatives possessing $-CF_3$ at position 2 of the phenothiazine ring were more active than Cl- and H-substituted ones. Additionally, it was observed that PhM (**12**) with a four carbon atom linker connecting the ring with the side chain amino group were more potent hemolysis-inducing agents than derivatives with a three carbon atom alkyl bridge. It must be noted, however, that simple comparison of hemolytic parameters obtained in different studies may be misleading because of the different amounts of erythrocytes used in hemolytic experiments. As was demonstrated by Malheiros et al. [143], not drug concentration but drug : lipid ratio should be used to correctly describe the hemolysis process. This study and the subsequent one [145] provided lots of details dealing with the mechanisms of TFP-induced erythrocyte hemolysis. The partition coefficient of TFP (**5**) between erythrocyte ghost and buffer was measured and it was found to be slightly lower than in model PC liposomes. This was explained by the presence of significant amounts of cholesterol in red blood cell membranes that reduced the drug partitioning into the bilayer. This finding is compatible with the results of earlier studies on model phospholipid membranes [27, 33]. It was also observed that, similar to the case of some detergents [22] and PC liposomes [37], the TFP (**5**) pK value was shifted down from 8.1 in water to 7.62 in the presence of erythrocyte membranes [143]. The pK value of 7.62 in erythrocytes indicated that two protonation forms (cationic and neutral) of TFP (**5**) were present in membranes at physiological pH. The neutral form bound to the membrane more strongly than the cationic one, and the authors pointed out the importance of hydrophobic drug–membrane interactions for the hemolytic effect of TFP (**5**). It was also noticed that TFP (**5**) induced hemolysis at concentrations above the cmc, therefore the possibility of the formation of TFP (**5**) micelles inside erythrocyte membranes was also taken into consideration when the hemolytic mechanism of phenothiazines was discussed [143]. Significant amounts of cholesterol and phospholipids were released from erythrocyte membranes following the incubation with TFP (**5**) at hemolytic concentrations [146], which suggested that drug-induced membrane disorganization occurred. Freeze–fracture electron microscopy was used to show that CPZ (**9**) at concentrations above 3 mM induced the formation of transient holes in the erythrocyte membrane [147]. Additionally, some round patches were visible on the membrane surface, which suggested that phase separation occurred in the presence of the phenothiazine derivative. It was concluded that the mechanism of CPZ-induced hemolysis consisted of intermittent opening of gaps at phase boundaries. Aki and Yamamoto [136, 148] studied the thermodynamics of the erythrocyte hemolysis process caused by a series of phenothiazines.

It was shown that the more hydrophobic phenothiazine was, the lower was the concentration at which 50% of hemolysis occurred. Binding of the drug to erythrocytes was a strongly exothermic process. After drug binding sites in the erythrocyte membrane became saturated, hemolysis started, which was accompanied by a large endothermic effect of hemoglobin release. A correlation was found between the strength of phenothiazine–membrane binding (ruled by the drug's hydrophobicity) and the hemolytic potency of phenothiazine derivatives.

Apart from the influence of phenothiazine derivatives on red blood cells' membrane integrity, the ability of the drugs to induce shape changes of erythrocytes was also reported. This phenomenon has been observed for many drugs and detergents. Normally, erythrocytes are biconcave disks; the treatment by various amphiphiles may transform them into stomatocytes or echinocytes. Stomatocytic cells are cup-shaped, and small invaginations on their membrane surface are visible under the microscope. On the other hand, lots of protuberances are visible on the surface of echinocytes, which gives the cells a characteristic crenated appearance. Many phenothiazine derivatives have been shown to transform human erythrocytes to stomatocytes, e.g., CPZ (**9**) [149], TFP (**5**) [144, 146], TDZ (**6**) [78], PhM (**12**), PhA (**13**), PhMC (**14**) and PhMS (**15**) [9]. Additionally, it was shown that erythrocyte ghosts were also able to adopt a stomatocytic shape in the presence of phenothiazine derivatives; however, the concentration of CPZ (**9**) required to achieve this effect was much higher than in the case of intact erythrocytes [141]. Electron and fluorescence microscopic observations revealed that following the treatment with CPZ (**9**) endovesicles were released from the membranes of stomatocytic erythrocytes to the interior of the cells [150]. Further studies demonstrated that endovesicles formed during CPZ (**9**) or TFP (**5**) treatment of erythrocytes were usually clustered in one of two regions of the cell [151]. In some endovesicles the membrane was budding off into the lumen of the vesicles, which could eventually lead to the formation of smaller vesicles inside the endovesicles.

What is the mechanism of drug-induced erythrocyte shape changes? The most widely accepted answer was given by Sheetz and Singer [152] who proposed the "bilayer couple" hypothesis. According to this, two halves of a closed membrane bilayer might respond dissimilarly to various perturbations while remaining coupled to one another. As the majority of amphiphiles that turn erythrocytes to echinocytes were negatively charged and the majority of stomatocytogenic agents were cationic, it was proposed that echinocytogenic drugs intercalated preferentially into the exterior half of the erythrocyte membrane, and cup-forming substances were distributed mainly in the cytoplasmic leaflet. When the area of one of the membrane leaflets expanded independently from the other leaflet, shape changes of red blood cells would be observed (for schematic representation see Fig. 4). The asymmetry of amphiphile distributions inside the erythrocyte membrane was
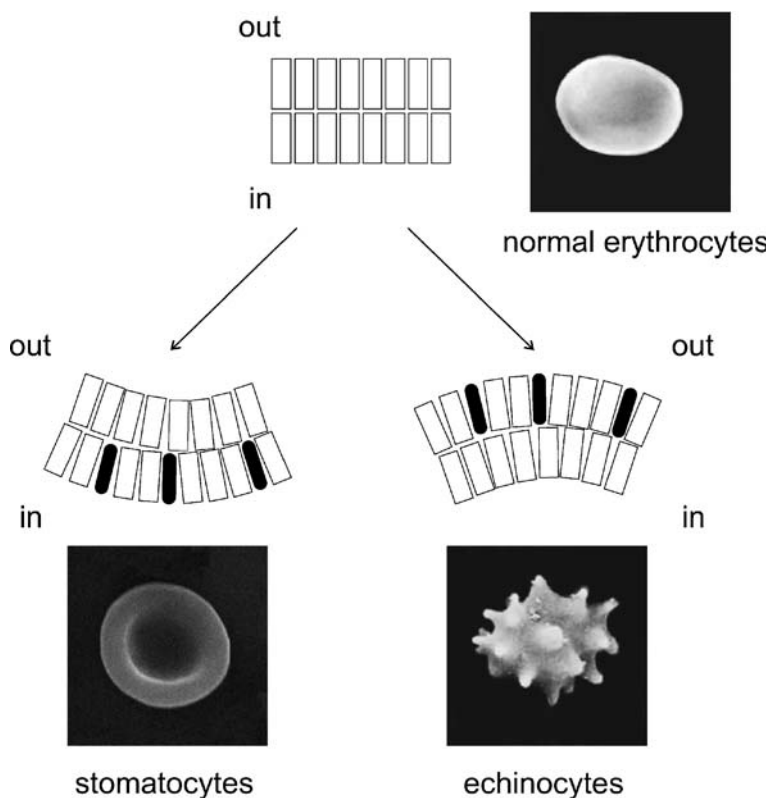
Fig. 4 Schematic representation of "bilayer couple" hypothesis

proposed to be determined by the charge of an amphipathic compound and its rate of diffusion across the membrane. The exclusive presence of negatively charged PS in the cytoplasmic half of the bilayer was assumed to be the main reason for cationic amphiphiles' preferential localization in the inner membrane monolayer. To prove this hypothesis erythrocytes were treated by CPZ (**9**) and methochlorpromazine (**10**) [152]. The latter compound possessed a quaternary amine group that could not be discharged, which was why this phenothiazine derivative could not penetrate into the cytoplasmic half of the bilayer. According to the assumptions, it was demonstrated that CPZ (**9**) induced the transformation of erythrocytes into stomatocytes, while methochlorpromazine (**10**) treatment resulted in echinocyte formation. The exclusive location of a quaternary analogue of CPZ (**9**) in the outside membrane leaflet was also demonstrated by Elferink [153]. On the other hand, CPZ (**9**) was suggested to bind preferentially to polyphosphoinositide lipids that were present in the cytoplasmic half of the erythrocyte membrane [66]. Isomaa et al. [149] pointed to the shape of amphiphile molecules as an important factor governing erythrocyte shape changes induced by different compounds.

They proposed that after the first stage of amphiphile binding to the membrane, when the majority of guest molecules are partitioned into the outer monolayer, membrane rearrangement occurred that corrected the imbalance of the area between the two monolayers. The authors claimed that this process was necessary to maintain the membrane stability and to explain some level of membrane protection (e.g., against hypotonic lysis) observed at low concentrations of amphiphiles. The formation of transient non-bilayer structures in the membrane, for instance inverted micelles, was proposed to constitute the mechanism of this rearrangement. The authors concluded that the ratio between the areas of the monolayers might be the main factor determining the shape attained by erythrocytes in the presence of amphiphiles. However, according to them, the imbalance between the two membrane halves was not solely due to preferential intercalation of amphiphiles to a given monolayer, but was the net result of membrane rearrangement processes.

CPZ (**9**) has been demonstrated not only to induce erythrocyte shape changes but also to cause the rearrangement of phospholipids between the two membrane monolayers. Normally, the erythrocyte membrane is highly asymmetric, with PC and SM located in the outer monolayer, while PE and PS are exclusively located in the inner half of the membrane. The analysis of the amounts of different types of phospholipids accessible to enzymatic digestion revealed that the addition of CPZ (**9**) to erythrocytes resulted in PC and SM movement to the inner monolayer, transient elevation of the amount of PE in the outer monolayer, and no rearrangement of PS [154]. It was noticed that the lipid distribution changes occurred at the same time as when drug-induced endocytosis took place. Radiolabeled PC was employed to study the effect of CPZ (**9**) on erythrocytes during prolonged incubations [155]. It was demonstrated that at 37 °C radioactive PC was partially translocated to the cytoplasmic half of the bilayer, while no CPZ-induced PC movement was recorded at 0 °C. As erythrocytes gained stomatocytic shape in the presence of phenothiazine derivative at all temperatures, it was concluded that shape changes are not related to lipid scrambling. Rosso et al. [156] studied the transport of spin-labeled phospholipid derivatives using the ESR technique. It was found that CPZ (**9**) had no effect on PC and SM translocation, while a reduction of the transport rate of PE and PS was recorded. This effect was proposed to be mediated by aminophospholipid translocase. It was suggested that the influence of CPZ (**9**) on the protein activity was responsible for the observed changes in PE and PS transport. Additionally, it was demonstrated that CPZ (**9**) addition to erythrocytes caused sudden passage of a fraction of both PE and PS from the inner monolayer to the outer one, but this effect was visible only at the very moment when CPZ (**9**) passed through the membrane. Contrary to the previous work [155], Schrier et al. [157] claimed, based on ESR experiments, that CPZ-induced lipid scrambling in combination with aminophospholipid translocase activity were the processes responsible for generating stomato-

cyting shape of erythrocytes in the presence of phenothiazine derivative. In the presence of CPZ (**9**), significant amounts of both PC and SM were moved from the outer membrane monolayer inward. The opposite translocation of PE and PS was not recorded, but the authors claimed it was caused by very fast transport of these two lipids backward by aminophospholipid translocase. According to the proposed model of erythrocyte stomatocytosis, the transporter flipped back PS and PE inward faster than scrambled PC and SM could diffuse outward. This process was postulated to produce the expansion of the inner monolayer area, i.e., stomatocytosis. Flow cytometric experiments, in which the advantage was taken of the ability of fluorophore-labeled annexin V to bind PS exposed on an erythrocyte surface, gave contradictory results. Hagerstrand et al. [158] demonstrated that CPZ (**9**) was not able to induce significant PS exposure, while Akel et al. [159] showed that PS exposure on the erythrocyte surface was elevated in the presence of the drug, and this effect was more pronounced under conditions of cellular stress (like glucose depletion, osmotic stress, etc.). Also, the importance of erythrocyte shape change for PS exposure was a matter of controversy. Hagerstrand et al. [158] concluded that shape changes and PS scrambling were not related. On the other hand, Wolfs et al. [160], who followed PS appearance on the erythrocyte surface by an enzymatic assay, came to the conclusion that PS exposure rate is enhanced in echinocytes and reduced in stomatocytes.

2.4
Interaction of Flavonoids with Erythrocyte Membranes

The literature reports dealing with the effect of flavonoids (Fig. 2 and Table 1) on red blood cells and their membranes are rather scarce. Chen et al. [91] concentrated on antioxidant properties of flavonoids. Flavonoids were found to effectively protect erythrocytes against free radical-induced lysis. When the flavonoids were used at 0.25 mM concentration, quercetin (**29**) turned out to be the most potent protective agent, followed by myricetin (**31**), morin (**30**), kaempferol (**28**), and apigenin (**23**). Quercetin was also an active antihemolytic agent at a concentration two times lower. Since the activity order of the flavonoids recorded in erythrocytes was slightly different than in canola oil, the authors noticed that the antioxidant activity of the flavonoids was governed not only by their chemical structure but also was determined by their interactions with phospholipids, hemoglobin, iron, and other components of red blood cells. The ability of flavonoids to protect erythrocytes against the lysis induced by water-soluble free radicals was the subject of the study of Dai et al. [161], too. Four flavonols and their glycosides were studied. It was demonstrated that the compounds possessing hydroxyl groups at both positions 3′ and 4′ of ring B (*ortho*-dihydroxyl) were much more active antihemolytic agents than the flavonoids without such an arrange-

ment. In addition, it was noticed that the erythrocyte protective effect of the flavonols was additive with the effect of α-tocopherol.

Lopez-Revuelta et al. [162] concentrated on membrane cholesterol and its influence on the antioxidant effectiveness of flavonoids against oxidative damage of red blood cells. Quercetin (**29**) was found to be superior to rutin (**50**) in protecting erythrocytes against lipid peroxidation, reactive oxygen species formation, and in preserving cellular integrity. The two flavonoids performed similarly when alteration in membrane fluidity, lipid and glutathione loss, and percentage of hemoglobin oxidation were measured. Both quercetin (**29**) and rutin (**50**) turned out to be effective antioxidant agents in normal erythrocytes and in those artificially enriched in cholesterol. When the cells were depleted of cholesterol the protective activity of both flavonoids was seriously reduced. The ability of flavonoids to lower membrane fluidity (measured as DPH fluorescence anisotropy increase) was also visible only in the presence of cholesterol. The authors concluded that flavonoids incorporated preferentially into the membranes containing cholesterol, and claimed that in cholesterol-depleted erythrocytes flavonoids would be located mainly in the cytoplasm.

The influence of quercetin (**29**) on red blood cells and erythrocyte ghosts was studied in detail by Pawlikowska-Pawlega et al. [163] by means of ESR spectroscopy. The use of spin labels localized at different depths inside the erythrocyte membrane revealed that quercetin (**29**) affected only the polar region of the membrane without changing the biophysical properties of the hydrophobic core. The increase in protein–protein interactions in human erythrocyte membranes in the presence of the flavonoid was also recorded. Additionally, quercetin (**29**) was found to protect erythrocytes against hypotonic lysis. Its presence, however, accelerated heat-induced hemolysis. Observation of cells in a scanning electron microscope showed the quercetin-induced changes in erythrocyte shape. In the presence of the flavonoid numerous irregular cells with extrusion on their surface (echinocytes) or cells with ruffled edges were found.

Echinocytic transformation of erythrocytes was also recorded in the presence of the extract from leaves of the Chilean plant *Ugni molinae* [164]. This extract is known to contain many polyphenols, tannins, and flavonoids. To explain the shape changes induced in erythrocytes by the compounds present in the extract, the authors appealed to the bilayer couple hypothesis and assumed that echinocyte formation was due to polyphenol incorporation mainly into the outer monolayer of the erythrocyte membrane. Fluorescence spectroscopy experiments on erythrocyte ghosts showed that low concentrations (up to 0.1 mM) of *U. molinae* extract caused an increase of both DPH anisotropy and Laurdan generalized polarization. Further raising of the plant extract concentration resulted in a significant drop of the two parameters. The authors concluded that the components of the extract perturbed the packing of phospholipid acyl chains and polar headgroups,

first ordering and afterward disordering them as the extract concentration increased.

3
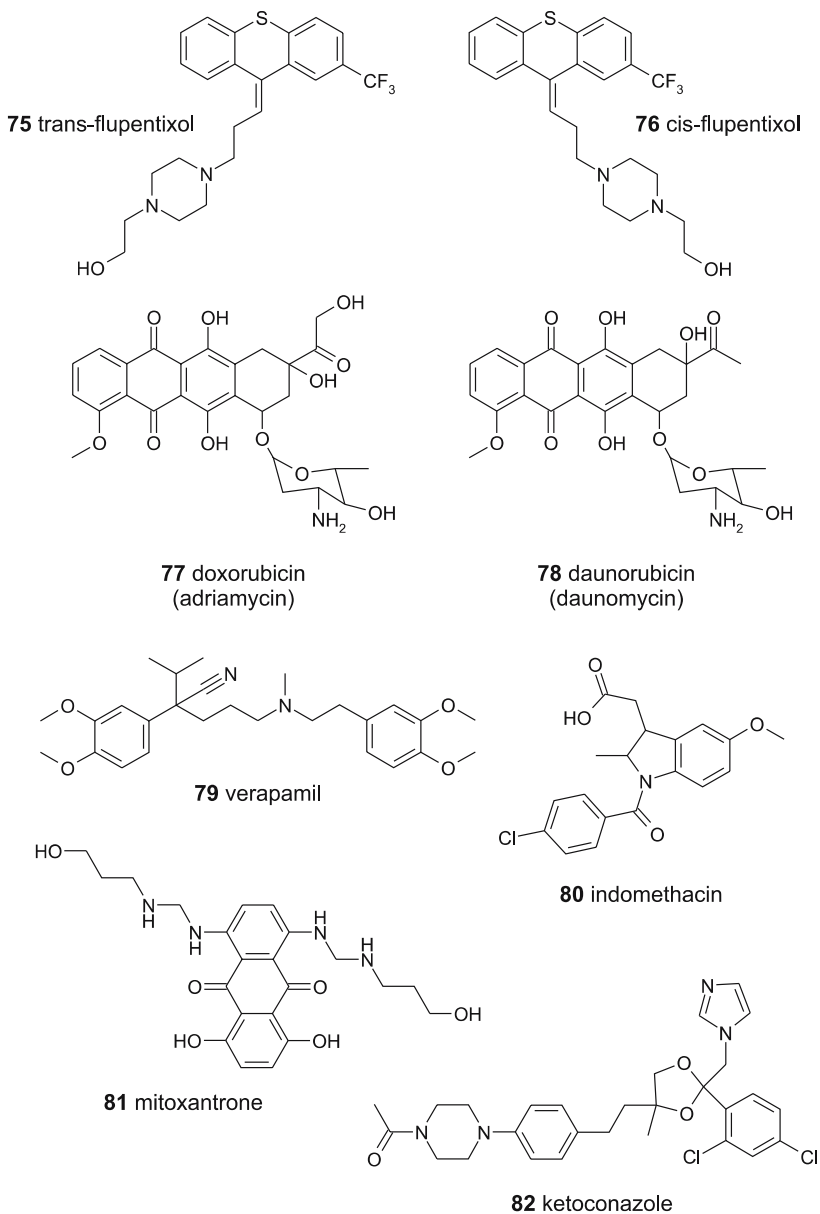# Modulation of MDR Transporters by Phenothiazines and Flavonoids

3.1
Phenothiazines and Related Compounds as Modulators of MDR Transporters

MDR represents a major obstacle in the successful therapy of cancer. MDR is a cellular mechanism, which reduces the chemosensitivity of tumors to structurally different cytostatic drugs such as anthracyclines, vinca alkaloids, and others (see Fig. 5). This form of drug resistance occurs in cultured tumor cell lines as well as in human cancers. The MDR phenomenon was originally detected in cultured tumor cells which were selected for resistance to a single anticancer agent and developed resistance to a variety of chemically unrelated compounds. The study of the molecular mechanism of MDR has provided one of the most exciting areas within cancer research. In multidrug-resistant cells the intracellular concentration of cytostatic drugs is reduced due to the action of drug efflux pumps expressed in tumor cell membranes. Their transport activity is responsible for maintaining the intracellular concentration of cytotoxic agents below a killing threshold. Among the best characterized multidrug efflux pumps in cancer cells are P-glycoprotein (P-gp, MDR1, ABCB1), multidrug resistance-associated protein (MRP1, ABCC1), and breast cancer resistance protein (BCRP, ABCG2) [165, 166]. These proteins belong to the ATP-binding cassette (ABC) superfamily. ABC transporters present in both prokaryotes and eukaryotes are built from a combination of membrane-spanning helices and cytoplasmic ATP-binding domains. Primary structures of P-gp and MRP1 share only approximately 15% amino acid identity.

The best characterized multidrug transporter is P-gp which is a membrane protein encoded by the mdr1 gene. The most intriguing feature of P-gp is its ability to interact with a large number of structurally and functionally different amphiphilic compounds. P-gp expression can be acquired during the course of treatment (e.g., in leukemias, lymphomas, ovarian carcinomas) or it is constitutive (e.g., in colorectal and renal cancers). In normal tissues of mammals P-gp is localized on the luminal surface of transporting epithelia in liver, kidney, small intestine, testes, and blood–brain barrier.

TFP (5) was the first phenothiazine demonstrated to modulate MDR in drug-resistant P338 murine leukemia cells. TFP (5) enhanced intracellular accumulation of vincristine and adriamycin (77) in resistant tumor cells by inhibiting outward transport of these anticancer drugs [167]. Studies per-

formed by Hait and Pierson [168] using the same cell line showed that the sensitivity of multidrug-resistant cancer cells to the cytotoxic compound, dequalinium, could be completely restored by nontoxic concentrations of TFP (**5**), and that TFP (**5**) also increased the sensitivity of these cells to doxorubicin (**77**). Fluphenazine (**3**) was shown to inhibit P-gp function in

75 trans–flupentixol

76 cis-flupentixol

77 doxorubicin
(adriamycin)

78 daunorubicin
(daunomycin)

79 verapamil

80 indomethacin

81 mitoxantrone

82 ketoconazole

83 topotecan   **84** camptothecin

85 ^{125}I-iodoarylprazosin   **86** forskolin
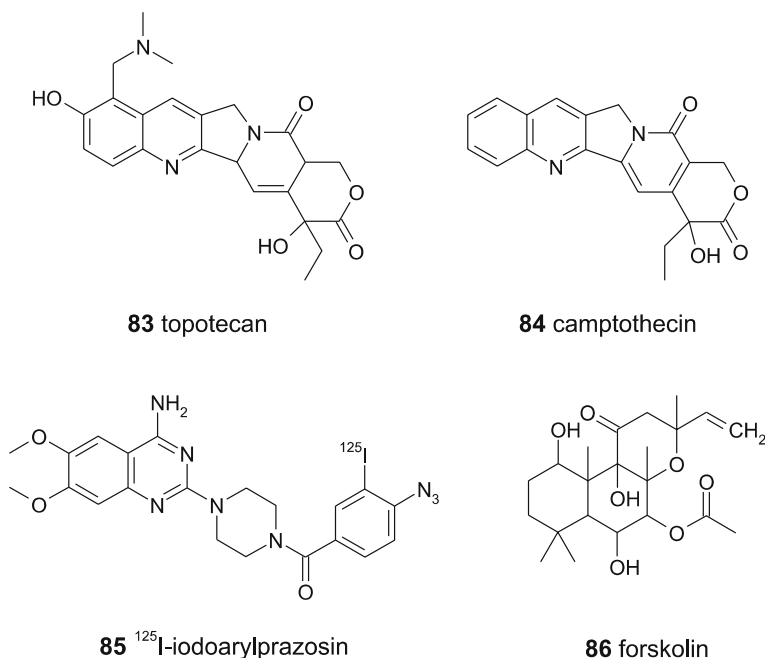
Fig. 5 Structures of selected drugs and chemicals appearing in this review

two leukemic resistant cell lines L121C and L5178 and in human adreno-carcinoma cell line KB-V-1 [169]. Barbieri et al. [170] demonstrated that quinolizidinyl derivatives of phenothiazine increased doxorubicin (**77**) cyto-toxicity in resistant ovarian cancer cells (A2780-DX3). The presence of the rigid quinolizidine ring in the structure of the studied compounds seemed to be favorable for their anti-MDR activity.

Recent studies on multidrug reversal in mouse lymphoma and MDR/COLO 320 cells have shown that phenothiazine derivatives, namely perphenazine (**2**) and prochlorperazine dimaleate (**4**), effectively inhibited rhodamine efflux [171]. Other phenothiazine derivatives such as promethazine (**1**), ox-omemazine (**20**), methotrimeprazine maleate (**18**), triflupromazine (**11**), and trimeprazine (**17**) differently modulated intracellular rhodamine accumulation in these resistant cells. The effect of some substitution in the phenothiazine ring was studied in mouse lymphoma cells expressing P-gp [172]. The 3,7,8-trihydroxy- and 7,8-dihydroxychlorpromazine derivatives were effective P-gp inhibitors, whereas 7,8-diacetoxy-, 7,8-dimethoxy-, 7-semicarbazone-, and 5-oxo-chlorpromazine derivatives exerted only a moderate effect.

The mechanism of modulation of P-gp-mediated MDR remains poorly understood. Several mechanisms of MDR reversal were proposed. Modulators may act as substrates for P-gp and inhibit drug transport in a competitive way. They may also interact with the sites of protein molecules other than

substrate binding sites and affect drug efflux by an allosteric effect. The modulating agents may also influence the ATPase activity of P-gp.

It has been demonstrated that *cis-* (**76**) and *trans-*flupentixol (**75**) (see Fig. 5) inhibited the photoaffinity labeling of P-gp by substrate analogues [173]. Binding of several MDR modulators, among them TFP (**5**), to P-gp was shown by means of fluorescence quenching of the MIANS probe [174] or P-gp tryptophan fluorescence [175]. CPZ (**9**) is likely a P-gp substrate, as was shown in studies of its transport in membrane vesicles obtained from multidrug-resistant CCRF-CEM cells [176], and therefore it was used as a competitive inhibitor of drug transport mediated by P-gp [177].

Recombinant human P-gp allows for screening of drug binding to P-gp from changes of substrate-induced ATPase activity of the protein. The affinity of the atypical antipsychotics (e.g., quetiapine, risperidone) and conventional antipsychotics (CPZ and haloperidol) for P-gp was determined by Boulton et al. [178] with this method. ATPase activity was quantified by determining the increase in inorganic phosphate concentration observed as a result of ATP hydrolysis. All of the antipsychotics studied stimulated ATPase activity at low concentrations and inhibited it at high concentrations. Drug transport by P-gp requires communication between substrate binding sites and nucleotide binding domains (NBD). Recent results obtained by Maki et al. [179] demonstrated that MDR modulator *cis-*flupentixol (**76**) and its closely related analogues effectively disrupted functional cross-talk between substrate and ATP-binding sites of P-gp by an allosteric effect without affecting the functions of these two domains. Maki and Dey [180] also documented in their recent studies that thioxanthene derivative *cis-*flupentixol (**76**), unlike most other P-gp inhibitors, facilitated interaction of the protein with its substrate ^{125}I-iodoarylprazosin (**85**). The authors concluded that modulation of P-gp function by *cis-*flupentixol (**76**) was mediated through interaction of modulator with P-gp at a site which was specific for tricyclic compounds containing thioxanthene or the phenothiazine backbone. Allosteric modulation of P-gp by flupentixols involved conformational changes which mimicked catalytic transition intermediates [181].

Phenothiazines were likely to be the substrates competing with ketoconazole (**82**) for binding sites on yeast multidrug transporter Pdr5p. This drug transporter displays a homology to P-gp. The synergistic effect with ketoconazole (**82**) observed for two phenothiazine derivatives, 2-chloro-10-aminobutyl-phenothiazine maleate and 2-trifluoromethyl-10-aminobutyl-phenothiazine maleate, was stronger than that of commercially available phenothiazines [182].

Apart from direct interaction of modulators with P-gp their influence on phospholipid bilayer properties was also suggested as an important molecular mechanism responsible for MDR reversal. The "vacuum cleaner" hypothesis assumes that P-gp substrates are recognized within the lipid phase during their diffusion across the cell membrane. An alteration of lipid phase prop-

erties in the presence of modulators may affect substrate binding to transporter molecules or enhance the passive diffusion of drugs across the lipid bilayer, resulting in their increased intracellular accumulation. Studies on reconstituted proteoliposomes demonstrated that the composition of the lipid environment of P-gp played an important role in MDR modulator–protein interaction [183]. Biophysical properties of the membrane lipid phase influence substrate recognition, P-gp conformation, and its ATPase activity (see review by Ferte et al. [184]). Hydrophobicity is an important determinant for the MDR reversing activity of modulators and this indicates the significance of modulator–lipid membrane interactions in MDR reversal. The membrane lipid environment modulates both modulator and substrate interactions with P-gp [185].

Bebawy et al. [186] demonstrated that CPZ (**9**) and vinblastine inhibited each other's transport in a human lymphoblastic leukemia cell line (CCRF-CEM/VLB$_{100}$). CPZ (**9**) reversed resistance to vinblastine but not to fluorescently labeled colchicine and it increased resistance to colchicine. Colchicine was supposed to be transported from the inner leaflet of the membrane and vinblastine from the outer leaflet. CPZ (**9**) was assumed to be located in the inner membrane leaflet where it interacts with anionic groups of phospholipids and it may inhibit vinblastine transport via allosteric interactions. The authors concluded that transport of P-gp substrates and its modulation by CPZ (**9**) (or verapamil (**79**)) are dependent on substrate localization inside the membrane. Contrary to CPZ (**9**) location in the inner leaflet of the membrane, other modulators and substrates of P-gp were proved to be rather localized within the interface region of the membrane. The location of seven P-gp substrates and two modulators within neutral phospholipid bilayers was examined by NMR spectroscopy by Siarheyeva et al. [129]. The substrates and the modulators of P-gp were found in the highest concentrations within the membrane interface region. The role of drug–lipid membrane interactions in MDR and its reversal was reviewed in detail elsewhere [53, 187].

The anti-MDR activity of phenothiazines, thioxantenes, and structurally related heterocyclic compounds has been studied by many researchers and some common structural features important for anti-MDR activity have been determined. Hydrophobicity of the ring system, kind of side chain, and the ring substituents at position 2 were revealed as important factors for P-gp inhibition. Ford et al. [188] examined MDR reversal activity of more than 20 phenothiazine derivatives in a human breast cancer cell line (MCF-7/DOX) and showed that substituents at position 2 in the tricyclic phenothiazine ring that increased hydrophobicity, such as Cl or CF$_3$, also improved the anti-MDR activity of phenothiazines (see Fig. 1). The alkyl bridge connecting the phenothiazine ring with the side group containing four carbon atoms was optimal. A favorable structural feature that increased modulator potency was the presence of a side chain containing tertiary amine. A cyclic amine rather than a noncyclic one further increased the anti-MDR potency. Ramu and

Ramu [189] studied the anti-MDR activity of 38 phenothiazines and almost 200 structurally related compounds in the resistant P338 murine leukemia cells. They also observed that the kind of substitution at position 2 of the phenothiazine ring was important for anti-MDR potency, and substituents like $-SOCH_3$ and $-SO_2N(CH_3)_2$ more strongly increased this potency than $-CF_3$. Apart from the above mentioned structural features of phenothiazine modulators, the significance of some minimal distance between the phenothiazine ring and positively charged side chain was suggested by Pajeva and Wiese [190, 191].

Unlike the results obtained by Ford and coworkers [188], Molnar et al. [192] did not observe the effect of the length of side chain on MDR reversal for other phenothiazine derivatives, i.e., phthalimidophenothiazines. Derivatives with butyl or propyl chains revealed a similar ability to reduce MDR in mouse T lymphoma cells.

More recently, Barbieri et al. [170], when studying a small group of quinolizidinyl phenothiazine derivatives, also observed that $-Cl$, $-CF_3$, or $-OCH_3$ substituents at position 2 of the phenothiazine ring increased the ability of the compounds to reverse the resistance of ovarian cancer cells to doxorubicin (**77**). Konya et al. [193] investigated an effect of newly synthesized phenothiazines on P-gp-mediated efflux of calcein-AM in drug-sensitive Madin–Darby canine kidney (MDCK) and drug-resistant MDCK : mdr1 cells, and observed that the most active compounds contain a methoxy group, carbonyl group, methyl group, and trimethoxybenzyl group. Some of the examined phenothiazine derivatives were more effective than verapamil (**79**) and as active as cyclosporine.

Tsakovska [194] used methods of molecular modeling to investigate a group of 25 phenothiazines and structurally related compounds. The role of hydrophobicity of modulators and hydrogen-bond acceptor interactions in MDR reversal were revealed. The piperazine moiety with a tertiary nitrogen was identified as the most favorable type of side chain for effective MDR modulators.

Contrary to the results of most quantitative structure–activity relationship (QSAR) studies on phenothiazine type modulators, Dearden et al. [195] found that molecular size, polarity, or polarizability better than other structural features of the compounds correlated with MDR reversing ability, P-gp associated ATPase activity, and inhibition of drug efflux from the blood–brain barrier. They did not find evidence that hydrogen bonding or hydrophobicity played a role in MDR reversal.

The modulatory effects of different phenothiazines and structurally related compounds in MDR caused by P-gp overexpression have been recently reviewed by Tsakovska and Pajeva [52]. Fifteen newly synthesized *N*-acylphenothiazines [196] were examined as putative MDR reversing agents in mouse T lymphoma cells transfected with MDR1 gene by flow cytometry using the standard functional assay with rhodamine 123 (Rh123). The chem-

ical structures and name abbreviations of these new phenothiazine derivatives are given in Fig. 1. PhM (**12**), PhA (**13**), PhMC (**14**) and PhMS (**15**) inhibited Rh123 outward transport in P-gp overexpressing resistant lymphoma cells [197]. In each group of the studied phenothiazine derivatives three different substituents occurred at position 2: – H, – Cl, and – CF$_3$. Apart from PhM (**12**), phenothiazine derivatives possessing trifluoromethyl or chlorine substitution at position 2 of the ring system were usually more active than hydrogen-substituted ones. For PhA (**13**), PhMC (**14**), and PhMS (**15**) a correlation was observed between lipophilicity of the compounds and anti-MDR potency [83]. Modulator–lipid bilayer interactions were suggested to be at least one of the important factors responsible for MDR reversal by these compounds.

PhM (**12**) constituted a separate group and no correlation between MDR reversal ability and lipophilicity was observed in the same cell model [38]. Their ability to inhibit the P-gp-mediated efflux of cyanine fluorescent dye DiOC$_2$(3) out of resistant mouse T lymphoma cells and their influence on lipid membrane properties were studied. The results of flow cytometric functional tests revealed that all PhM (**12**) under study were effective MDR reversing agents. For this group of phenothiazine derivatives, no clear relationship was found between their lipophilicity or perturbation exerted by phenothiazines in model lipid membranes composed of different lipids and their ability to modulate P-gp transport activity. The molecular mechanism of MDR reversal for PhM (**12**) was probably different than that for the rest of the studied phenothiazine derivatives [197]. The positive charge density is much higher in PhM (**12**) than in the other studied derivatives because of the presence of the primary amino group, which is smaller than the amido groups of the rest of the compounds. Moreover the maleate moiety might likely change the phenothiazine derivatives' electron-donor properties. In this case a direct interaction of PhM (**12**) with P-gp should be taken into account.

The choice of a cell line to study MDR modulator potency was very important for future potential application in human cancer treatment. PhM (**12**) that were quite effective in resistant mouse lymphoma cells were only slightly active in drug-resistant human sarcoma cell line MES-SA/Dx5 [198]. The drug-sensitive human sarcoma cell line MES-SA and its multidrug-resistant counterpart MES-SA/Dx5 were applied as a model system for evaluation of MDR modulator activities. Examination performed by the flow cytometric Rh123 accumulation test demonstrated that the well-known P-gp modulators verapamil (**79**) and TFP (**5**) reduced MDR in MES-SA/Dx5 cells. In resistant MES-SA/Dx5 cells, verapamil (**79**) and TFP (**5**) restored the drug accumulation pattern which was typical for sensitive cells. However, the effectiveness of PhM (**12**) was very low. The most active compounds were derivatives with an H atom at position 2 of the phenothiazine ring, followed by Cl-substituted and CF$_3$-substituted compounds.

The effect of PhM on multidrug resistance- associated protein (MRP1) was also examined by determining the influence of these modulators on MRP1 transport and ATPase activity [199]. Contrary to the inhibitory effect of PhM against P-gp-mediated drug efflux, stimulation of MRP1-mediated efflux of fluorescent substrate 2′,7′-bis(3-carboxypropyl)-5-(and -6)-carboxyfluorescein (BCPCF) was detected in human erythrocytes. Erythrocytes were chosen as a good model to study MRP1 activity because this transporter is expressed in these cells under physiological conditions. The highest stimulation was observed for the derivatives with the H atom substituted at position 2 of phenothiazine ring. It was also observed that PhM with four carbon atoms in the alkyl bridge connecting the phenothiazine nucleus with the side chain amino group were more effective than compounds with a three carbon atom alkyl bridge. The increased BCPCF efflux out of erythrocytes in the presence of phenothiazine modulators was caused by the stimulation of an active transport system, as was shown both in inside-out membrane vesicles prepared from erythrocyte membranes and in whole erythrocytes. In this study it was demonstrated for the first time that inhibitors of P-pg transport activity could stimulate another MDR transporter, in that case MRP1.

3.2
Flavonoids as Inhibitors of Multidrug Transporters: P-gp, MRP1, and BCRP

3.2.1
Modulation of P-gp by Flavonoids

Among plant-derived polyphenols some effective inhibitors of ABC transporters were found [200]. Flavonoids (Fig. 2 and Table 1) which are integral components of our common diet are especially promising candidates for modulators of MDR because of their low toxicity.

Chieli et al. [201] have studied the influence of flavonols (kaempferol (**28**), galangin (**27**), quercetin (**29**)) on P-gp activity in cultured hepatocytes. In cultured hepatocytes spontaneously overexpressing functional P-gp, flavonols inhibited Rh123 efflux but increased the efflux of doxorubicin (**77**). The flavonols may modulate differently the transport of P-gp substrates in normal rat hepatocytes. The chemico-physical properties of substrates were crucial for a stimulatory or inhibitory effect of flavonols. Since P-gp is expressed in many normal tissues and it may constitute a part of the cellular defense system against xenobiotics, it was of interest to examine the role of certain flavonoids in facilitating the removal of xenobiotics from various kinds of cells by P-gp stimulation. Critchfield et al. [202] have shown that in P-gp expressing HCT-15 colon cells, adriamycin (**77**) accumulation was strongly inhibited in the presence of galangin (**27**), kaempferol (**28**), and quercetin (**29**). Flavonoid-induced stimulation of P-gp-mediated efflux was rapid. The

authors concluded that some flavonoids may stimulate activity of P-gp and therefore acceleration of adriamycin (**77**) efflux was observed. Flavonoid-stimulated efflux was completely blocked by MDR reversing agents such as verapamil (**79**), vinblastine, and quinidine. An opposite inhibitory effect of quercetin (**29**) was demonstrated in experiments on purified and reconstituted P-gp [203].

The effect of different flavonoids on the activity of P-gp in cancer cell lines overexpressing this transporter was studied by Ferte et al. [204], Di Pietro et al. [205], Boumendjel et al. [206, 207], and Zhang and Morris [208]. It has been proved that some flavonoids bind to the nucleotide binding site of P-gp and they directly effect its function [209]. Boumendjel et al. [206] have tested a series of flavonol derivatives for their binding affinity toward the NBD of P-gp. They found that the 5,7-dihydro-4′-*n*-octylflavonol derivative displayed affinity toward the P-gp domain 93-fold greater than galangin (**27**) used as reference compound.

Studies carried out on recombinant cytosolic nucleotide binding domain (NBD2) of P-gp revealed that incubation of NBD2 with flavonoids led to quenching of intrinsic protein fluorescence. Quercetin and apigenin (**23**) were shown to bind strongly to purified NBD2, as was concluded from complete quenching of protein fluorescence. Flavonoids such as kaemferol, galangin (**27**), and genistein (**42**), which are effective modulators of P-gp, also interact with purified cytosolic NBD2. The same flavonoids were found to bind to NBD1. The authors proposed a tentative model for binding of these compounds to P-gp cytosolic domains, and they suggested that flavonoid molecules overlapped both ATP and steroid binding sites. The binding of flavonoids to nucleotide binding sites was probably due to the structural similarity between flavonoids and the adenine moiety of ATP. Hydroxylation at position 3 in addition to ketone at position 4 is essential for the ability of these modulators to mimic the adenine moiety of ATP [209].

Since most P-gp effectors are hydrophobic, it was of interest to study flavonoids substituted with different hydrophobic groups, for example the isoprenyl group [210]. Isoprenylated flavonoids are natural compounds which constitute a class of plant secondary metabolites. Comte et al. [210] have synthesized a series of C- or O-substituted hydrophobic derivatives of chrysin (**22**). Increasing the hydrophobicity of substituents at positions 6, 7, or 8 increased the affinity of binding to the purified cytosolic domain of P-gp. Isoprenylated derivatives also increased intracellular daunomycin (**78**) accumulation in K562/R7 leukemic cells.

Silybin (**52**) is a naturally occurring flavanolignan from milk thistle. Dehydrosilybin (**53**) and isoprenoid dehydrosilybins were also recognized as potent inhibitors of P-gp [211]. These compounds were tested for their binding affinity toward domain NBD2 of P-gp. Oxidation of silybin to flavonol dehydrosilybin (**53**) increased the affinity three times. Prenylation and geranylation led to a further increase in affinity [207]. C-isoprenylated deriva-

tives of dehydrosilybin (**53**) with their high affinities for direct binding to P-gp were also found to be very effective modulators of P-gp [207, 211]. Isoprenoid dehydrosilybins are the best flavonoids with high affinities for direct binding to P-gp. It was also demonstrated that the presence of 5-OH, 3-OH, and a 2,3-double bond in the flavonoid molecule facilitated flavonoid–NBD2 interaction [207]. The double bond in that position confers a planar structure to the flavonoid molecule. The importance of the 2,3-double bond for interaction of flavonoids with P-gp was also suggested by Kitagawa [212]. Oxidized and prenylated derivatives of silybin also exhibit high binding affinity to the recombinant cytosolic domain of *Leishmania* P-gp transporter and reverse drug resistance of *Leishmania tropica* [213].

Recently, Limtrakul et al. [214] have shown that flavonols quercetin (**29**) and kaempferol (**28**), and isoflavones genistein (**42**) and daidzein (**40**), markedly increase the sensitivity of the multidrug-resistant human cervical carcinoma KB-V1 cells to vinblastine and paclitaxel. The flavonols inhibited P-gp activity in MDR KB-V1 cells more efficiently than isoflavones.

Kitagawa et al. [215] have studied the effects of flavonoids naringenin (**33**) (flavanone), baicalein (**26**) (flavone), kaempferol (**28**), quercetin (**29**), myricetin (**31**), morin (**30**), and fisetin (**32**) (flavonols), as well as two glycosides of quercetin (**29**), on P-gp function in multidrug-resistant P-gp overexpressing KB-C2 cells. Kaempferol and quercetin (**29**) increased the accumulation of Rh123 in resistant cells. The effects of other flavonoids on the accumulation of daunorubicin (**78**) were in the order of kaempferol > quercetin, baicalein > myricetin > fisetin, morin. Quercetin-3-*O*-glucoside and rutin (**50**) had no effect. The difference in the number and position of hydroxyl groups in flavonoid molecules by themselves seemed to have little effect; however, the effects corresponded with the partition coefficients. These results suggested that hydrophobicity as well as planar molecular structure was important for the inhibitory effects of flavonoids on P-gp-mediated transport.

Vaclavikova et al. [216] have investigated the effect of 13 flavonoid derivatives—aurones, chalcones, flavones, flavonols, chromones, and isoflavones—on ^{14}C-paclitaxel transport in two human breast cancer cell lines, the doxorubicin-resistant NCI/ADR-RES and sensitive MDA-MB-435. The compounds with known binding affinity toward the NBD of P-gp were selected. The four aurones studied most effectively inhibited P-gp-related transport in the resistant line in comparison with other groups of flavonoids. The aurones also most effectively increased the intracellular accumulation of paclitaxel and decreased its efflux. The results obtained did not always correlate with the binding of flavonoid derivatives to P-gp, so this indicated that the binding was not the only factor influencing the transport of paclitaxel. The different aspects of inhibition of P-gp by polyphenols was recently reviewed by Kitagawa [212].

3.2.2
Modulation of MRP1 by Flavonoids

Generally much more is known about the influence of flavonoids on P-gp than on transporter MRP1. Multidrug resistance-associated protein (MRP1) is another multidrug transporter identified in a number of MDR human tumor cell lines that do not express P-gp. It is a member of a family of multidrug resistance- associated proteins (MRP1-MRP9). The profile of anticancer drugs expelled in the presence of MRP is similar but not identical to that of P-gp. MRP1 has been identified in a number of different types of tumors, but it is not clear yet to what extent it is responsible for clinical resistance. MRP1 overexpression in selected in vitro MDR cell lines occurs frequently in lung cancer and leukemia cell lines and often precedes P-gp overexpression. Resistance modulators active against P-gp are less or not effective in reversing MRP1-mediated resistance. It is not fully understood how MRP1 carries out drug efflux; however, the mechanism is probably different from those responsible for P-gp-mediated drug efflux. The MDR-associated protein MRP1 has a major role in the export of large organic anions, including glutathione (GSH) conjugates. MRP1 can specifically transport the cysteinyl leukotriene (LTC4) and some other GSH conjugates. GSH is required for the effective expulsion of the anticancer agents [217]. Like P-gp, MRP1 is expressed not only in resistant tumor cells, but also in normal human tissues. These include the epithelial cells lining the airways and the gastrointestinal tract. Also other multidrug resistance proteins that belong to the MRP group of transporters (MRP1-MRP9) are constitutively expressed in normal tissues [218, 219].

Genistein (**42**) was the first flavonoid found to be a potent inhibitor of MRP1 transport activity [220, 221]. It has been suggested that flavonoids interact directly with the substrate binding site of MRP1 [221] and may act as competitive inhibitors [220]. The influence of dietary flavonoids on modulation of MRP1 transport and ATPase activities has been studied by Leslie et al. [222]. In these studies flavonoid glycosides such as genistin (**46**) or naringin (**49**) have been recognized as much less effective MRP1 inhibitors than aglycons.

Flavonoids are now regarded as a class of MDR modulators that directly interact with nucleotide and steroid binding domains of P-gp. However, the molecular mechanism leading to inhibition of MRP1 transport activity by these compounds is still far from being fully understood. Apart from interaction with NBD or substrate binding sites, the stimulation of GSH transport carried by MRP1 and depletion of cellular GSH was also proposed as a possible mechanism of MRP1-mediated resistance reversal by flavonoids [223].

Recently Trompier et al. [224] proved the direct interaction of different flavonoids with recombinant NBD from human MRP1. Especially high affinity was detected for flavanolignan dehydrosilybin (DHS) (**53**). DHS

(**53**) strongly inhibited leukotriene C4 transport by membrane vesicles from MRP1-transfected cells and chemosensitized the cells to vincristine. The authors of these studies suggested that the DHS (**53**) binding site overlapped the ATP-binding site in the NBD of MRP1. Binding affinities toward NBD1 were further increased for prenylated and geranylated derivatives of DHS (**53**). Although the relationship between ATPase activity of ABC transporters and transport of their substrates is not fully understood, it is assumed that compounds that stimulate the ATPase activity of MDR transporter interact with the protein. The results of this study indicated multiple binding sites for DHS and its derivatives on both cytosolic and transmembrane domains of MRP1 [224].

Wu et al. [225] have investigated the interaction of six common polyphenols—quercetin (**29**), silymarin (a standard mixture of flavanolignans), resveratrol (**67**), naringenin (**33**), daidzein (**40**), and hesperetin (**34**)—with MRP1, MRP4, and MRP5. Quercetin and silymarin inhibited MRP1-, MRP4-, and MRP5- mediated transport more effectively than the rest of the polyphenols. Both compounds significantly influenced the ATPase activity of MRP1 but they had no effect on ^{32}P-8-azidoATP[αP] binding to the protein. This suggests that quercetin (**29**) and silymarin most likely interact with the substrate binding sites of MRP1 rather than nucleotide binding sites. Nguyen et al. [226] have studied the influence of 22 flavonoids on the transport of daunomycin (**78**) and vinblastine in Panc-1 cells, which are a human pancreatic adenocarcinoma cell line expressing MRP1. Biochanin A (**43**), genistein (**42**), quercetin (**29**), chalcone (**65**), silymarin, phloretin (**66**), morin (**30**), and kaempferol (**28**) at $100\,\mu$M concentrations all significantly increased the accumulation of both daunomycin (**78**) and vinblastine in these cells. Morin (**30**) was a very effective modulator that increased daunomycin (**78**) and vinblastine accumulation which achieved the level of 500% of the control. Morin (**30**) and other flavonoids influenced te cellular content of GSH; however, only morin (**30**) increased GSH concentration, and instead other flavonoids decreased cellular GSH.

Very recently van Zanden et al. [227, 228] investigated the effect of a large group of flavonoids on MRP1 transport activity in transfected MDCKII cells. Most of the flavonoids studied in this work were able to inhibit MRP1 activity. Among the best inhibitors were methoxylated flavonoids, such as 5,7,3′,4′-tetramethoxyflavone, diosmetin, chrysoeriol, tamarixetin, and isorhamnetin. Their IC$_{50}$ values were low and ranged between 2.7 and 14.3 μM. The structural characteristics of flavonoids regarding efficient MRP1 inhibition have been found. In particular the total number of methoxylated moieties, total number of hydroxyl groups, and the dihedral angle between the B and C rings were revealed as essential for inhibitory potency. A planar structure of the molecule due to the presence of the 2,3-double bond seemed to be necessary for high potency of flavonoid inhibitors of MRP1, while lipophilicity of the compounds was not decisive for the modulator activity [227]. Flavonoids

without a C2–C3 double bond like eriodictyol, taxifolin (**39**), and catechin (**36**) did not inhibit MRP1 [229].

It is worth mentioning a very interesting possibility to use flavonoids for imaging of MRP1. Recently, a series of apigenin (**23**) halogenated derivatives were synthesized and evaluated as potential radioligands [230]. Apigenin and its synthetic derivatives tested were likely not transported by MRP1 and selective binding of these compounds to MRP1 was proposed. These properties of flavonoid radioligands would be beneficial for PET or SPECT imaging of MRP1-related MDR.

3.2.2.1
Inhibition of MRP1 by Natural and Synthetic Flavonoids in Erythrocytes

The human erythrocyte may be a useful cell model in studies of MRP1 efflux pump activity and inhibitor potency of different modulators. In our studies [231, 232] it has been shown that genistein (**42**) and many other plant-derived polyphenolic compounds influence transport of BCPCF, the fluorescent substrate of MRP1, in erythrocytes. Structure–activity relationships for these compounds as MRP1 modulators are not well known. The significance of the hydrophobicity of chemical groups substituted at position 8 in ring A (and hydroxyl groups at positions 5 and 7) has been pointed out. The presence of a hydrophobic prenyl, geranyl, or lavandulyl group at position 8 in ring A of flavanones markedly increased inhibitor potency. The geranyl group was more efficient than the prenyl group. The presence of a hydroxyl group at position 5 in ring A increased the inhibitory potency of flavonoids, as was observed for genistein (**42**) and daidzein (**40**) [232].

In our recent investigations the inhibition of erythrocyte MRP1 by the representatives of different classes of natural flavonoids (flavones, isoflavones, flavonols, flavanolignans) and synthetic genistein derivatives have been examined by determination of MRP1 fluorescent substrate efflux out of erythrocytes [233]. We compared the inhibition potency of different plant-derived flavonoids and four new synthetic genistein derivatives. In the new synthetic isoflavones different substitutions were introduced to the genistein (**42**) molecule to obtain much more hydrophobic compounds than genistein (**42**) itself. The new synthetic genistein derivatives were 4′-O- and 7-O-substituted silyl derivatives: 7,4′-bis[*tert*-butyl(dimethylsilyl)]-genistein (IFG10 (**57**)), 7-*tert*-butyl(dimethylsilyl)-4′-acetyl-genistein (IFG12 (**58**)), 7-*tert*-butyl(dimethylsilyl)-genistein (IFG8 (**56**)), and genistein substituted with a palmitate acyl chain, 7-O-palmitate-genistein (IFG18 (**59**)) (see Fig. 2). The maximal achieved inhibition (> 90%) recorded for some natural flavonoids was higher than that for indomethacin (**80**), a well-known MRP1 inhibitor, and for all the synthetic genistein derivatives studied. Morin (**30**) and silybin (**52**) were especially good inhibitors. In the structure of both compounds the 7-OH moiety is not substituted. Morin (**30**), a flavonol with five polar

unsubstituted hydroxyl groups, was shown to be one of the most effective inhibitors of BCPCF efflux. The concentration of morin (**30**) that caused 50% inhibition of MRP1 activity (IC$_{50}$) recorded in erythrocytes was lower than the IC$_{50}$ value obtained previously by Nguyen et al. [226] in a cancer cell line overexpressing MRP1. Taking into account the IC$_{50}$ values, the potency of silybin (**52**) to inhibit BCPCF efflux was similar to that of morin (**30**) or licoisoflavone B (**55**) [233]. The IC$_{50}$ value obtained in our study for silybin (**52**) was similar to that recorded by Trompier et al. [224] for inhibition of LTC4 transport by this flavanolignan. Two of the four synthetic genistein derivatives studied, IFG10 (**57**) and IFG12 (**58**), and natural flavonoids apigenin (**23**), sophoraisoflavone A (**60**), and genistein (**42**), were also shown to be MRP1 inhibitors; their IC$_{50}$ values were significantly higher than those for the most active compounds [233]. Isoflavone prunetin (**44**) was not active, while synthetic isoflavones IFG8 (**56**) and IFG18 (**59**) were only slightly effective; however, their IC$_{50}$ values were not achieved within all ranges of concentration studied. In the novel synthetic genistein derivatives, the hydrogen atom in 7-OH and 4′-OH groups was replaced by substituents that strongly increased genistein (**42**) hydrophobicity. Comparing the effects exerted by the three derivatives with *tert*-butyl(dimethylsilyl) substitution at position 7 (IFG10 (**57**), IFG12 (**58**), and IFG8 (**56**)), it was evident that for effective inhibitors (IFG10 (**57**) and IFG12 (**58**)) the hydrogen of the 4′-OH group was also substituted by the *tert*-butyl(dimethylsilyl) (IFG10 (**57**)) or acetyl group (IFG12 (**58**)). IFG8 (**56**) with no substitution at position 4′ only slightly affected BCPCF efflux. Also IFG18 (**59**), a compound substituted with the palmitate acid chain at position 7 but not substituted at position 4′, was a very weak inhibitor of MRP1. We concluded that substitution of the hydroxyl group at position 4′ in ring B with a less polar group was crucial for the inhibitory activity of these derivatives. In contrast, substitution of 7-OH by a less polar group did not increase inhibitory activity. Isoflavones IFG8 (**56**) and IFG18 (**59**), which differed from genistein (**42**) by substitution of the hydrogen in 7-OH with a *tert*-butyl(dimethylsilyl) group (IFG8 (**56**)) or palmitate acid chain (IFG18 (**59**)), were less active than the precursor compound. A similar structure–activity relationship could be observed for the pair of plant-derived isoflavones, genistein (**42**) and prunetin (**44**). The exchange of the hydroxyl group 7-OH of genistein (**42**) for a methoxy group (7-OCH$_3$) in prunetin (**44**) results in a strong decrease of inhibitory potency. Two other natural isoflavones which are effective inhibitors of MRP1, licoisoflavone B (**55**) and sophoraisoflavone A (**60**), have no substitution at position 7. In licoisoflavone B (**55**) group 4′-OH is replaced by a prenyl group and in sophoraisoflavone A (**60**) this group is not substituted but a prenyl group formed an additional ring attached to ring B, increasing the hydrophobicity of the flavonoid.

Increasing the inhibitory potency by substitution of a hydroxyl group at position 4′ of the isoflavone molecule, which was observed in the group of

synthetic compounds [233] and in some natural flavonoids, is not a general rule, however. We did not observe any difference in BCPCF efflux inhibition in the case of pairs of isoflavones, daidzein/formonetin and genistein/biochanin A [132]. In each pair the compounds differed by a methoxy substituent at position 4′, which was present in formononetin (**41**) and biochanin A (**43**) but not in daidzein (**40**) and genistein (**42**). Formononetin (**41**) and daidzein (**40**) were not effective inhibitors of MRP1 activity. Instead the OH group substituted at position 5 in genistein (**42**) and biochanin A (**43**) seemed to be beneficial for inhibition and this result confirmed our previous observation made for a large group of flavonoid compounds [232].

3.2.3
Modulation of BCRP by Flavonoids

Breast cancer resistance protein (BCRP, ABCG2) is a member of the ABCG "half-transporter" subfamily since it has only six transmembrane domains and one ATP-binding site, in contrast to other ABC transporters which consist of 12 transmembrane domains and have two ATP-binding sites. It confers resistance to anticancer drugs such as mitoxantrone (MX) (**81**), topotecan (**83**), and camptothecin (**84**) [234]. Recently, many studies have revealed that plant-derived polyphenols, flavonoids and stilbenes, are able to modulate BCRP function in cancer cell lines [235–237]. In the presence of quercetin (**29**), hesperetin (**34**), silymarin (a standard mixture of flavanolignans), daidzein (**40**), and resveratrol (**67**), the increase in accumulation of BCRP substrates MX (**81**) and Bodipy-FL-prazosin in BCRP-overexpressing cells was observed. These polyphenols also stimulated the BCRP-associated ATPase activity, as was determined using inside-out vesicles prepared from BCRP-transformed bacterial cells [235].

A more than threefold increase in MX (**81**) accumulation in BCRP-overexpressing cells (MCF-7 MX100 and NCI-H460 MX20) was also demonstrated for apigenin (**23**), biochanin A (**43**), chrysin (**22**), genistein (**42**), kaempferol (**28**), and naringenin (**33**) [237]. Imai et al. [236] demonstrated that not only aglycones (genistein (**42**), naringenin (**33**), acacetin (**24**), and kaempferol (**28**)) but also some glycosylated flavonoids, such as naringenin-7-glucoside, effectively inhibited transporter BCRP overexpressed in K562 cells. Some sulfate conjugates and glucoronides have also been shown to be transported by BCRP [238].

Recently performed studies on structure–activity relationships for inhibition of BCRP by flavonoids showed that the presence of the 2,3-double bond in ring C, ring B attached at position 2, an OH group at position 5, lack of hydroxylation at position 3, and hydrophobic groups substituted at positions 6, 7, 8, or 4′ are favorable for BCRP modulation [239]. The studies were carried out with five flavonoid subclasses: flavones, isoflavones, flavanones, flavonols, and chalcones (Figs. 2 and 6). For several compounds the 50% in-

crease in MX (**81**) accumulation in BCRP-overexpressing cells was observed at very low, micromolar flavonoid concentrations. The IC_{50} values are likely much lower than the intestine concentrations of flavonoids delivered from a common diet. The studied flavonoids demonstrated potencies to inhibit BCRP transporter that differed by even more than 2000-fold. IC_{50} values for increasing MX (**81**) accumulation in MCF-7 MX100 cells ranged from 0.07 μM for 7,8-benzoflavone to 183 μM for sylibin. 7,8-Benzoflavone and 2′-hydroxy-α-naphthoflavone were the most active BCRP inhibitors that had IC_{50} values below 0.1 μM [239]. The mechanisms by which flavonoids inhibit the BCRP efflux pump are currently under investigation.

In addition to the modulating effect exerted by flavonoids on P-gp, MRP1, and BCRP function, the antiproliferative activity of these polyphenols is well documented [240]. However, some flavonoids with estrogen activity, such as prenylated flavones, showed at low concentrations a proliferative effect in estrogen-dependent human breast cancer cells. At higher concentrations inhibition of DNA synthesis was observed. It was noticed that artelastin (**62**), a prenylated flavone, exhibited a biphasic effect on DNA synthesis in estrogen-dependent MCF-7 cells, stimulatory at low concentrations and inhibitory at high concentrations. A proliferative effect was observed only in the presence of those prenylated flavones that possessed an isopentyl group at C-8 and an additional ring linking C-3 and C-2′ atoms [241].

4
Effects Exerted by Phenothiazines and Flavonoids on Ion Channel Properties

4.1
Influence of Phenothiazines on Ion Channels

Cardiotoxicity is a very well known side effect of phenothiazine drug (see Fig. 1) administration. The main cardiotoxic effect is the induction of different types of arrhythmia, which are mostly the result of QT interval prolongation [242]. This prolongation can be associated with a potentially lethal ventricular arrhythmia known as torsades de pointes [242, 243]. The mechanism of the influence of phenothiazines on QT interval prolongation is complex, but on the molecular level there is increasing evidence that different types of myocardial ion channels are involved [243].

QT interval prolongation induced by phenothiazines suggests that potassium channels responsible for the repolarization phase of myocardial action potential are naturally the first candidates for the possible interaction with these drugs. Wooltorton and Mathie [244] using a whole-cell voltage clamp found that in isolated rat sympathetic neurons, CPZ (**9**) inhibited mostly delayed rectified potassium current, leaving the transient K^+ current almost

unchanged. As was found by Kon et al. [245], CPZ (**9**) interfered with different components of potassium current in isolated rat ventricular myocytes. It inhibited inward-rectifying K^+ current, time-independent outward currents, transient outward K^+ current, and ATP-dependent potassium current. When applied in higher concentrations (50 μM) CPZ (**9**) also caused a significant increase of myocyte resting potential, from – 79 to – 27 mV.

CPZ (**9**) and TFP (**5**) are the phenothiazine derivatives known to induce QT prolongation and torsades de pointes. Both compounds were found to influence the delayed rectifier potassium current in guinea pig cardiomyocytes, and especially its rapidly activating component conducted by protein encoded by human *ether-a-go-go*-related gene (hERG); see [246] for CPZ (**9**) and [247] for TFP (**5**). As was shown using channels expressed in *Xenopus* oocytes, CPZ (**9**) and TFP (**5**) acted as potent dose- and potential-dependent hERG channel blockers. It was also found that this block was use-dependent. Experiments performed on guinea pig cardiomyocytes confirmed that CPZ (**9**) and TFP (**5**) affected rapidly activating potassium current leaving the slow activating one unchanged. The final conclusion drawn in both papers was that arrhythmias induced by CPZ (**9**) and TFP (**5**) may result from the inhibition of the rapidly activating component of outward potassium current.

Inhibition of hERG channels expressed in Chinese hamster ovary (CHO) cells by TDZ (**6**) and other antipsychotic drugs was investigated by Kongsamut et al. [248]. The ability of the studied drugs to block hERG channels (IC_{50} value for TDZ (**6**) was 191 nM) was compared with their affinity to dopamine D_2 and $5-HT_{2A}$ receptors as well as with the QT interval prolongation induced by these drugs. This comparison showed that when hERG IC_{50} and receptor binding potencies were separated by less than a log unit, significant QT prolongation might be expected. In recent work devoted to elucidation of the mechanism of hERG block induced by TDZ (**6**) [249], a potential binding site for the drug on channel protein was found. Comparing the influence of TDZ (**6**) on wild-type and mutant hERG channels expressed in HEK293 cells, Milnes et al. discovered that S6 helix point mutation F656A almost completely abolished TDZ-induced block. This result allowed the conclusion that the TDZ (**6**) binding site was located in the channel vestibule and drug molecules bound preferentially to the channel in the open state. The mechanism of the block of hERG potassium channels expressed in *Xenopus* oocytes was also studied by Thomas et al. [250]. As in other experiments performed on hERG channels, CPZ (**9**) induced a dose-dependent block with IC_{50} value 21.6 μM. The analysis of the block, based on its voltage dependence, revealed that hERG currents were inhibited by drug molecules bound to the channels in closed and open states, while block of the inactivated channel state was less pronounced. The reversed frequency dependence suggested that a different amount of closed-channel block occurred during the time between the pulses. The general conclusion of this work was that block of hERG currents by CPZ (**9**) underlay the clinically observed QT interval prolongation.

The same experimental model (CHO cells) was used by Kim and Kim [251] in the study of hERG channel inhibition by TDZ (**6**), CPZ (**9**), TFP (**5**), and perphenazine (**2**). The phenothiazine derivatives studied in this work showed different potency to block hERG channels; the IC_{50} values for TDZ (**6**), perphenazine (**2**), TFP (**5**), and CPZ (**9**) were 224, 1003, 1406, and 1561 nM, respectively. Exclusively for TDZ (**6**) the hERG channel inhibition was voltage-dependent, and the amount of block was greater at more positive potentials. Inhibition caused by other phenothiazine derivatives studied herein showed no voltage dependence. It is worth emphasizing that IC_{50} values obtained by two independent research groups using the same experimental model— Kongsamut et al. [248] and Kim and Kim [251]—were very close.

Kv1.3 voltage-gated potassium channels present in lymphocytes are known to play an important role in setting the resting membrane potential, cell mitogenesis, and volume regulation. In the whole-cell patch-clamp study Teisseyre and Michalak [252] have demonstrated that TFP (**5**) was blocking these channels in a concentration-, voltage-, and time-dependent manner. TDZ (**6**) additionally studied in this work showed effects similar to those of TFP (**5**). According to the authors of this paper the exact molecular mechanism of Kv1.3 potassium channel blocking by TFP (**5**) remained to be elucidated.

TFP (**5**) was found to be a very effective blocker of human Kv2.1 potassium channels expressed in human glioblastoma cells [253]. As for other types of channels, for Kv2.1 the TFP-induced block was also dose-dependent ($IC_{50} = 1.21\,\mu M$). Some of the other, non-phenothiazine drugs were even more effective blockers; for the most potent, fluspirilene (an antipsychotic agent), substantial block was observed at 30 nM.

CPZ (**9**), triflupromazine (**11**), and fluphenazine (**3**) inhibited HIT-T15 pancreatic β-cell ATP-sensitive potassium channels in a dose-dependent manner [254]. Reversible inhibition of these channels was observed when they were activated by ATP depletion or by treatment with the channel opener diazoxide. The IC_{50} values for CPZ (**9**), triflupromazine (**11**), and fluphenazine (**3**) were 1, 4, and 6 μM, respectively.

The potassium channels present in neuronal membranes could also be affected by phenothiazine derivatives. In the study performed by Ogata et al. [255] it was shown that CPZ (**9**) interfered with several types of potassium channels present in membranes of neurons of the newborn rat cultured dorsal root ganglia. Reversible reduction of the amplitude was found for transient and delayed rectified K^+ currents, while inward rectified K^+ current remained unaffected by CPZ (**9**). The block of delayed rectified K^+ current by CPZ (**9**) was, however, less potent than block of the transient one. The hyperpolarizing shift of the steady-state inactivation curve for transient K^+ current indicated that CPZ (**9**) binds preferably to the channels in the inactivated state.

Lee et al. [256] showed that CPZ (**9**), TFP (**5**), and TDZ (**6**) effectively inhibited activity of Ca^{2+}-activated large conductance potassium channels

in neurons dissociated from the rat motor cortex. Inhibition was voltage-independent. The butyrophenone drugs also studied in this work were as effective potassium channel inhibitors as phenothiazines, while atypical neuroleptics were much less effective. Since all compounds studied herein were lipophilic, Lee et al. [256] concluded that channel inhibition was caused by specific drug–channel interaction but not by membrane perturbation induced by neuroleptics. The Ca^{2+}-activated, large conductance potassium channels from charophyte plants resemble Maxi-K channels from animal cells, mainly due to very similar kinetic properties. As was found by thorough analysis of the channel kinetics, the presence of TFP (**5**) generated a new, low-conductance state in these potassium channels [257]. This new state was not recorded in previous studies performed by McCann and Welsh [258] and by Kihira et al. [259] because the methods of data analysis used in both these works classified the low-conductance state as a closed one.

Also, Ca^{2+}-activated small conductance potassium channels (SK channels) could be affected by the presence of different antipsychotic drugs. Rat SK2 subtype channels expressed in HEK293 cells were blocked by a group of tricyclic antipsychotic drugs, including CPZ (**9**) and TFP (**5**) [260]. Inhibition of rat SK2 channels was dose-dependent; K_D values calculated from the fitted dose–response curves were 12.75 and 7.6 μM for CPZ (**9**) and TFP (**5**), respectively. The potency of drugs studied in this paper to inhibit rSK2 channels was not correlated with their pK_a values. Terstappen et al. [261] have shown that other subtypes of SK channels, human SK3 channels expressed in CHO cells, were blocked by several types of tricyclic antidepressants, including four phenothiazines. This inhibition was dose-dependent; the IC_{50} values were 13, 31, 32.7, and 48.1 μM for fluphenazine (**3**), promethazine (**1**), CPZ (**9**), and TFP (**5**), respectively. A direct binding of blocker molecules with channel protein was indicated in experiments on displacement of ^{125}I-apamin by antipsychotic drugs. Terstappen et al. [261] pointed also to the possibility that phosphorylation of the SK3 channel and/or accessory subunit might be involved in its modulation. The influence of tricyclic antidepressants and a variety of other compounds on the huge set of different potassium channels was reviewed by Mathie [262].

Phenothiazine derivatives also exerted some effects on the properties of different types of calcium channels. Two types of voltage-gated Ca^{2+} channels, differing in voltage- and time-dependent kinetics, were blocked by CPZ (**9**) [263]. This block was reversible, concentration-dependent, and enhanced by membrane depolarization. Hyperpolarizing shift of the steady-state inactivation curve showed a higher affinity of CPZ (**9**) for channels in the inactivated state than in the resting state. Ogata et al. [263] also concluded that gating kinetics of activation of both channel types was not affected by CPZ (**9**).

Inhibition of voltage-gated L-type Ca^{2+} channels was recorded by Ito et al. [264] and by Lee et al. [265] in rat neuronal cell line pheochromocytoma

(PC12) cells. Inhibition of L-type Ca^{2+} currents by phenothiazine drug was also found in invertebrate neurons. Investigations performed by Cruzblanca et al. [266] revealed that TFP (**5**) caused reversible and dose-dependent reduction of L-type Ca^{2+} currents in *Helix aspersa* (brown snail) neurons. The efficacy of inactivation of this current was enhanced by this drug. The possibility that calcium currents were altered by the influence of TFP (**5**) on the protein kinase C (PKC) activity was excluded in this paper.

Also, T-type calcium channels could be affected by phenothiazine derivatives. CPZ (**9**) caused a dose-dependent and reversible block of T-type calcium channels in mouse neuroblastoma cells [267]. Neither the activation nor inactivation kinetics of these channels was altered by CPZ (**9**); however, the block was voltage-dependent. Results obtained by Ogata et al. [267] indicated greater affinity of CPZ (**9**) to channels in the inactivated state. In another study performed on mouse spermatogenic cells, Lopez-Gonzalez et al. [268] have shown that the effects exerted by TFP (**5**) on T-type Ca^{2+} channels were very similar to those exerted by W7, a very well known calmodulin antagonist. Both these compounds decreased T currents in a concentration-dependent manner, with IC_{50} values of 12 and 10 μM for TFP (**5**) and W7, respectively. Additionally this research team found that W7 altered the channels' voltage dependence on activation and slowed both the activation and inactivation kinetics.

CPZ (**9**) also showed some inhibitory effects with respect to the calcium current produced by combined expression of α_{1E} and β_3 subunits of voltage-sensitive calcium channels (VSCCs) [269]. The authors of this article suggested that this effect could be the result of either direct interaction of the drug with channel protein or indirect alteration of the properties of the lipid bilayer surrounding the VSCC molecules.

Background (or B-type) calcium channels present in membranes of heart myocytes are responsible for the resting calcium influx in cardiac cells. It was found that the activity of these channels could be altered by phenothiazine derivatives. CPZ (**9**) and TFP (**5**) activated the B-type Ca^{2+} channels present in rat ventricular [270] and human atrial myocytes [271, 272]. As was recorded using the patch-clamp technique, the TFP- and CPZ-induced activation of B-type Ca^{2+} channels appeared in approximately 20% of rat ventricular myocyte patches. CPZ-activated channels were voltage-independent in the physiological range of membrane potentials [270]. As in rat, in human myocytes micromolar concentrations of CPZ (**9**) also induced complex gating behavior with several levels of elementary conductances. The CPZ-induced increased activity of B-type Ca^{2+} channels was observed in about 25% of examined cells and was voltage-independent [271]. Despite the thorough description of background calcium channel activity induced by phenothiazine derivatives, Antoine et al. [271] have not provided any explanation of the molecular mechanism of this process. B-type Ca^{2+} channels are also present in the membranes of red blood cells. As was found by Pinet et al. [273], their

properties and also their ability to be activated by CPZ (**9**) remained almost unchanged after reincorporation into the membranes of giant liposomes.

The influence of CPZ (**9**) and TFP (**5**) on the release of calcium from the intracellular stores was shown by Quamme et al. [274] in a study on the activation of Ca^{2+}-activated Cl^- current in native *Xenopus* oocytes. Although the relation between phenothiazine derivative-induced intracellular Ca^{2+} concentration increase and Cl^- current appearance was convincingly proved, Quamme et al. [274] have not presented any explanation of the mechanism of the observed phenomena.

Release of calcium ions from the intracellular stores is triggered by inositol 1,4,5-triphosphate ($InsP_3$). $InsP_3$ receptor is a tetramer channel protein which could be affected by, among others, calmodulin antagonists like phenothiazine derivatives. CPZ (**9**), TFP (**5**), and fluphenazine (**3**) were found to bind to and alter the properties of $InsP_3$ receptors of pig cerebellar microsomes [275]. It was shown that the presence of phenothiazine drugs alters the fast component of Ca^{2+} release, leaving the slow component unchanged. As was suggested in this paper, the inhibition of calcium current carried by $InsP_3$ receptor was rather caused by the alteration of channel gating properties than by affecting the $InsP_3$ binding to the receptor molecule.

Like other channel types, voltage-gated sodium channels can also be affected by the presence of phenothiazine derivatives. In voltage-clamp experiments Bolotina et al. [276] found that CPZ (**9**), as well as chloracizine (**19**), blocked sodium channels in the inactivated state. Whole-cell patch-clamp studies revealed that CPZ (**9**) induced a dose-dependent and reversible block of sodium channels in mouse neuroblastoma cells [267]. This block was also use-dependent, because train depolarizations caused cumulative increase of block. Since the steady-state inactivation curve was shifted toward negative potentials by exposure to CPZ (**9**), Ogata et al. [267] concluded that this drug showed greater affinity to the channels in the inactivated state. Two types of voltage-gated sodium channels—tetrodotoxin (TTX)-sensitive and TTX-resistant—were found to be blocked by another neuroleptic phenothiazine derivative, fluphenazine (**3**) [277]. The mechanism of channel block by this drug resembled that caused by local anesthetics, i.e., neuroleptic molecules bound with high affinity to the channel in the inactivated state. Fluphenazine (**3**) showed no appreciable effect on the voltage dependence of sodium channel activation.

Awayda et al. [278] suggested that CPZ-induced alteration of epithelial sodium channels (ENaC) could be a result of the influence exerted by the pheniothiazine derivative on the membrane fluidity. To demonstrate it they used epithelial sodium channels expressed in *Xenopus laevis* oocytes as a model, and compared the effects of CPZ (**9**) and temperature on the ENaC activity. They have shown that a decrease of membrane order caused either by the increase of temperature or by incorporation of drug molecules into the membrane affected the conductance of epithelial sodium channels in a very

similar way. Awayda et al. [278] concluded that they could not exclude the possibility that the effects on ENaC might result from the combination of the alteration of lipid order and membrane capacitance. The last effect might be a consequence of membrane thickness change induced by CPZ (**9**) or increased mobility of lipid hydrocarbon chains.

Apart from causing very well known cardiotoxic effects, phenothiazine derivatives can accumulate in lung epithelial cell membranes and therefore cause severe respiratory disorders. In the study performed by Ito et al. [279] it was found that CPZ (**9**) inhibited transepithelial Cl^- transport, mainly due to two mechanisms: influence on the beta-adrenergic receptor and inhibition of basolateral potassium channels. The authors of this study also suggested that the recorded effects could result from the electrostatic interactions between the drug molecules and negatively charged components of the inner leaflet of the plasma membrane.

Large conductance chloride channels (Maxi Cl^- channels) present in membranes of fibroblast cells were another class of chloride channels that were affected by the presence of phenothiazine derivatives. As described by Valverde et al. [280], these channels become activated by CPZ (**9**) and triflupromazine (**11**). Activation was dose-dependent for both drugs; the half-maximal responses (EC_{50}) were 21 and 23 µM for CPZ (**9**) and triflupromazine (**11**), respectively. The effects of the drugs were observed exclusively for applications in the extracellular bathing solution. The authors of this paper provided no information about the possible physiological role of Maxi Cl^- channel activation by phenothiazine drugs.

The activity of ligand-gated channels could also be affected by the presence of phenothiazine derivatives. CPZ (**9**) affected the nicotinic acetylcholine receptors (nAChRs) of mouse muscle cells [281]. Two kinds of effects were recorded: CPZ (**9**) decreased the frequency of channel opening and decreased the mean channel opening time. The first effect was potential-independent and was interpreted as a closed channel block. The second one, in which CPZ (**9**) acted as an open channel blocker, was dependent on membrane potential as well as on the concentration of the drug. Benoit and Changeux [281] concluded that CPZ (**9**) bound to a site within the nAChR ionic channel. This suggestion was strongly supported by a previous study performed by Revah et al. [282], who showed that CPZ (**9**) bound to the amino acids located in the hydrophobic and putative transmembrane region MII of the *Torpedo marmorata* nAChR γ-subunit. As proved by Lee et al. [265], inhibition of nAChRs by CPZ (**9**) was involved in the inhibition of catecholamine secretion in rat pheochromocytoma (PC12) cells. Catecholamine secretion was also inhibited by the block of voltage-gated calcium channels by CPZ (**9**), but to a lesser extent than by the block of nAChRs involved with this drug. In the next paper devoted to the problem of the influence of antipsychotic drugs on catecholamine secretion, Park et al. [283] compared the influence of CPZ (**9**) with that of the atypical drug clozapine. Using bovine adrenal chromaffin cells as

a model they found that both these drugs blocked nAChRs and VSCCs; however, clozapine was a less effective blocker than CPZ (**9**).

GABA$_A$ receptors are another site of action of CPZ (**9**) in neurons of the central nervous system. Mozrzymas et al. [284] have found that CPZ (**9**) reduced the amplitude and accelerated the decay of miniature inhibitory post-synaptic currents. Using ultrafast γ-aminobutyric acid (GABA) applications and model simulations, they demonstrated that CPZ (**9**) decreased the binding and increased the unbinding constants of the neurotransmitter to GABA$_A$ receptors.

N-Methyl-D-aspartic acid (NMDA) receptors also belong to the group of ligand-gated channels that are affected by the presence of phenothiazine derivatives. Using a functional neurochemical assay, Lidsky et al. [285] have shown that CPZ (**9**) and TDZ (**6**) at low concentrations augmented NMDA receptor activity while at higher concentrations they suppressed it. In contrast promazine (**8**), which shows no dopamine receptor D2 effects, does not influence NMDA receptors either. Whole-cell patch-clamp experiments performed by Zarnowska and Mozrzymas [286] revealed that in cultured rat hippocampal neurons, CPZ (**9**) slowed down the NMDA receptor deactivation in a dose-dependent manner. Thus, CPZ (**9**) stabilized the open conformation of these channels, presumably by fixing them in a bound state.

4.2
Influence of Flavonoids on Ion Channels

Compared with phenothiazines, much less is known about the effects exerted by different types of flavonoids on the properties of ionic channels. These compounds exert mostly beneficial effects on human health, acting mainly as nonspecific antioxidants that cause almost no side effects. Therefore, there was only a limited need to study specific interactions of flavonoids with different types of ionic channels.

Choi et al. [287] described the interaction of (–)-epigallocatechin-3-gallate (EGCg, Fig. 3) with the rat brain Kv1.5 potassium channels expressed in CHO cells. EGCg (**64**) inhibited Kv1.5 channels in a dose-dependent manner with an IC$_{50}$ of 101.2 μM. Interaction with EGCg (**64**) did not alter the ion selectivity of Kv1.5 channels. Pretreatment of the CHO cells with genistein (**42**) did not influence the inhibitory potency of EGCg (**64**). Inhibition was voltage-independent, and neither activation nor inactivation voltage dependencies were altered by EGCg (**64**). The results suggested that EGCg (**64**) interacted directly with channel protein and bound preferentially with the channel in a closed state [287]. The block occurred presumably due to pore occlusion by the catechin molecule. In a further study the effect of EGCg (**64**), (–)-epigallocatechin (**38**), (–)-epicatechin-3-gallate (ECg, **63**), and (–)-epicatechin (EC, **37b**) on ATP-sensitive potassium channels (K_{ATP}) expressed in *Xenopus* oocytes was evaluated by Baek et al. [288]. Intracellular EGCg (**64**) applica-

tion inhibited K_{ATP} current in cloned as well as native (in β-cells) channels, and the effect was only partly reversible after EGCg (**64**) wash-out. Since ECg (**63**) also inhibited K_{ATP} currents and EC (**37b**) as well as EGCg (**64**) were ineffective, it appeared that for inhibitory activity the gallic acid ester moiety was a critical structural factor of green tea catechins. The authors of this paper suggested that the gallic acid ester moiety exerted its effects via the modulation of the lipid bilayer properties.

In the study performed by Zitron et al. [289] the activity of 22 flavonoids against hERG channels expressed either in *Xenopus* oocytes or in HEK cells was screened. The studied flavonoids belonged to different subgroups (see Fig. 2): flavanone glycosides (neohesperidin (**48**), hesperidin (**47**), naringin (**49**)), flavanone aglycones (galangin (**27**), hesperetin (**34**), naringenin (**33**)), flavone glycosides (rutin (**50**)), and flavone aglycones (flavone (**21**), chrysin (**22**), fisetin (**32**), kaempferol (**28**), morin (**30**), quercetin (**29**), myricetin (**31**), apigenin (**23**)). Also, furanocoumarin (bergapten (**69**), methoxalen (**70**), psoralen (**68**)) and coumarin derivatives (scopoletin (**72**), umbelliferone (**73**), coumarin (**71**), 7-ethoxycoumarin (**74**)) were studied (see Fig. 6 for chemical structures). Ten of these flavonoids profoundly inhibited hERG currents in a dose-dependent manner. The most active were naringenin (**33**), morin (**30**), and hesperetin (**34**). The IC_{50} values for these flavonoids differed, depending on the type of cells in which hERG channels were expressed. In *Xenopus* oocytes the IC_{50} values were 102.3, 111.4, and 288.8 μM for naringenin (**33**), morin (**30**), and hesperetin (**34**), respectively. In HEK cells the IC_{50} for naringenin (**33**) was 36.5 μM. Flavone, quercetin (**29**), kaempferol (**28**), methoxalen (**70**), umbelliferone (**73**), scopoletin (**72**), and 7-ethoxycoumarin (**74**) also belonged to the group of active flavonoids. The authors correlated the obtained results with the in vivo measured QT interval prolongation induced by grapefruit juice, in which naringenin (**33**) is the major flavonoid component.

T lymphocyte Kv1.3 potassium channels were also inhibited by genistein (**42**) in a protein tyrosine kinase (PTK)-independent way [290]. Daidzein (**40**) that was also studied in this work did not influence the properties of Kv1.3 potassium channels. The genistein-induced inhibition occurred much faster than was observed for neuronal Kv1.3 channels expressed in HEK293 cells [291], for which a PTK-dependent mechanism of genistein (**42**) action was proposed. On the other hand, PTK-independent inhibition of myocyte Kv1.3 channels by genistein (**42**) was reported by Washizuka et al. [292].

Extensive studies have been performed on the influence of flavonoids on the properties of the cystic fibrosis transmembrane conductance regulator (CFTR) channel. The best-known CFTR channel activator is genistein (**42**) [293, 294], but this channel could also be activated by apigenin (**23**), kaempferol (**28**), and quercetin (**29**) [295], which appeared to be even more potent activators than genistein (**42**). CFTR channel activation by genistein (**42**) was not accompanied by an increase of intracellular cAMP level, which
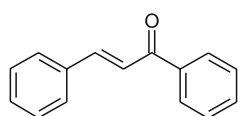
65 chalcone
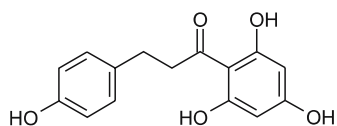
66 phloretin
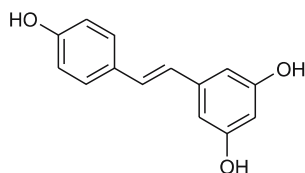
67 resveratrol
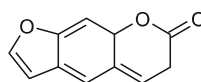
68 psoralen
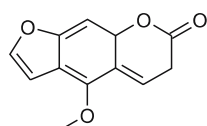
69 bergapten
(5-methoxypsoralen)
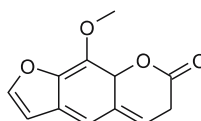
70 methoxalen
(8-methoxypsoralen)
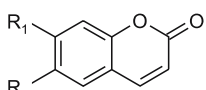
Name	R₁	R₂

Name	R_1	R_2
71 coumarin	H	H
72 scopoletin	OH	OMe
73 umbelliferone	OH	H
74 7-ethoxycoumarin	OEt	H

Fig. 6 Chemical structures of chalcone and coumarin derivatives

suggested that channel stimulation did not involve direct activation of protein kinase A [293]. Whole-cell patch-clamp experiments have shown that the effect exerted on CFTR by genistein (**42**) was dose-dependent and the EC$_{50}$ of flavonoid was approximately 100 μM [296]. Daidzein (**40**), a flavonoid structurally related to genistein (**42**), was also studied by Shuba et al. but it appeared that it was at least one order of magnitude less effective than genistein (**42**). In a further study Chiang et al. [294] investigated the activation of CFTR channels in guinea pig ventricular myocytes by genistein (**42**), and found that this process was protein kinase A and tyrosine kinase independent. In almost parallel work, French et al. [297] confirmed that CFTR activation was protein kinase A and tyrosine kinase independent; however, they have shown simultaneously that phosphorylation of the CFTR channel prior to genistein (**42**)

application was necessary for its activation. These authors proposed a direct binding of genistein (**42**) with a second NBD of the CFTR channel as a putative mechanism of channel stimulation. Using a site-directed mutagenesis, Melin et al. [298] experimentally confirmed this suggestion and showed that the signature motif LSHGH of the NBD2 was responsible for switching on and off the response of CFTR channels to the presence of genistein (**42**). In a later study on the influence of curcumin on CFTR channels, Berger et al. [299] also found that pre-phosphorylation of CFTR and the presence of ATP were necessary for its activation. Investigations performed on wild-type CFTR channels were supplemented by experiments in which mutant CFTR channels were also explored. Illek et al. [300] have found that the G551D mutant of CFTR, the third commonest causing cystic fibrosis mutation, was also activated by genistein (**42**). Using the most common CFTR mutation—ΔF508 CFTR—Bebok et al. [301] have shown that even this channel could be activated by genistein (**42**), while other wild-type stimulators (forskolin (**86**), β_2-adrenergic or A_{2B}-adenosine receptor agonists) failed to activate ΔF508 CFTR. In another paper Lim et al. [302] have shown that apigenin (**23**), genistein (**42**), kaempferol (**28**), and quercetin (**29**) did not change the expression of ΔF508 CFTR in bronchial epithelial cells. Except for kaempferol (**28**), however, these flavonoids increased the Cl^- conductance of the epithelial cell membranes.

Contrary to the activation of chloride current, genistein (**42**) partly inhibited the pacemaker currents recorded in the cardiac sinoatrial myocytes [303–305]. As was shown by Yu et al. [304], the exact effects of genistein (**42**) depended on the subtype of hyperpolarization-activated cyclic nucleotide-gated (HCN) channels involved in interaction with the flavonoid. For different HCN subtypes expressed in *Xenopus* oocytes it was found that genistein (**42**) had no effect on HCN1-carried currents, while it significantly decreased currents carried by HCN2 and HCN4 channels. Daidzein (**40**) apparently exerted no effects either on HCN1 or on HCN2 currents. In a recent study devoted to the elucidation of the mechanism of genistein-induced block of HCN channels, Altomare et al. [305] have found that this block was independent of the presence of ATP; also, inhibition of tyrosine kinase by herbimycin did not influence the effects exerted by the flavonoid. Direct interaction of genistein (**42**) with HCN channels, responsible for pacemaker currents, was proposed as a possible mechanism of isoflavone action.

Apart from HCN channels, genistein (**42**) also acted on other types of channels present in cardiac cells. Chiang et al. [306] examined the impact of this isoflavone on the L-type calcium and cAMP-dependent chloride currents in guinea pig ventricular myocytes. Using the voltage-clamp technique they found that genistein (**42**) reversibly inhibited L-type calcium currents in a dose-dependent manner. Surprisingly daidzein (**40**), which was ineffective with respect to many other channel types, also decreased L-type calcium currents in myocytes. Opposite to calcium currents, the cAMP-dependent

chloride current was augmented by the presence of genistein (**42**) but not by daidzein (**40**). Direct interaction of genistein (**42**) with L-type calcium channels was also proposed by Yokoshiki et al. [307] as one of the possible mechanisms of inhibition.

Unlike genistein (**42**), quercetin (**29**) [308, 309] and myricetin (**31**) [310] enhanced the calcium current carried by L-type calcium channels of the myocytes from rat tail artery. The character of voltage-, concentration-, and frequency-dependent calcium current changes induced by myricetin (**31**) [310] allowed the conclusion that this flavonoid exerted its effect on L-type calcium channels by binding preferentially to the channels in the inactivated state. Quercetin stimulated L-type calcium channels in rat pituitary GH3 cells in a dose-dependent manner [309]. The EC_{50} value was about 7 μM, and many facts suggested direct interaction between ion channels and flavonoid. In NG 108-15 neuronal cells quercetin (**29**) caused inhibition of TTX-sensitive sodium current.

Also, the T-type calcium channels could be regulated by interaction with flavonoids. In a study on the influence of genistein (**42**) on the T-type calcium channels ($Ca_V 3.1$) expressed in HEK293 cells, Kurejova et al. [311] have demonstrated that external application of flavonoid caused the dose-dependent inhibition of the channel activity (IC_{50} = 24.7 μM). A decrease of calcium current amplitude was accompanied by deceleration of channel activation and acceleration of its inactivation. Genistin (**46**), which was also studied by Kurejova et al. [311], exerted no effects on the properties of $Ca_V 3.1$ channels. Intracellular applications of both genistein (**42**) and genistin (**46**) caused no effects as well. According to the interpretation of these results genistein (**42**) molecules directly interact with the voltage sensor and occlude the channel pore.

In contrast to many other potassium channels (see below), the inward rectifying K^+ channels in guinea pig ventricular myocytes were directly blocked by genistein (**42**) and daidzein (**40**) [312]. Both flavonoids inhibited inward rectifying K^+ current in a dose-dependent manner. The opposite effect (i.e., stimulation) was observed when the influence of naringenin (**33**) on the Ca^{2+}-activated K^+ channels of rat tail artery myocytes was studied [313]. Channel activation was dose-dependent and reversible after flavonoid wash-out. The final conclusion of this work was that the vasorelaxant effect of naringenin (**33**) could be due to activation of Ca^{2+}-activated K^+ channels.

Several examples demonstrated that flavonoids could also interfere with the activity of ligand-gated channels. The possibility that glycine receptors of hypothalamic neurons could be modulated by genistein (**42**) was tested by Huang et al. [314], and they found that flavonoid blocked channels in a voltage-dependent manner. Additionally it was shown that daidzein (**40**) also inhibited glycine-activated channels. The results obtained in this work suggested that glycine receptor block was caused by direct flavonoid–channel interaction, and was not mediated by a PTK. On the other hand, a phosphory-

lation pathway was proposed to explain the influence of genistein (**42**) on such ligand-gated channels as NMDA receptors [315] and GABA$_A$ receptors [316].

Chrysin was presumably the first flavonoid that was found to interact with GABA$_A$ receptors [317]. Since this discovery many laboratories focused their efforts on the research of flavonoid–GABA$_A$ receptor interactions, because it appeared that these compounds possessed anxiolytic properties. Today a huge group of natural [318, 319] and synthetic [320, 321] flavonoids have been tested regarding their ability to interfere with GABA$_A$ receptors. Also theoretical calculations, i.e., 3D-QSAR studies, were performed [322] to elucidate the optimal structural features of flavonoids with respect to their binding with GABA$_A$ receptor binding sites. Different aspects of flavonoid–GABA$_A$ receptor interactions were recently reviewed by Wang et al. [323].

The idea that genistein (**42**) could modulate the ionic channel activity by a phosphorylation-independent mechanism was proposed by Hwang et al. [324]. Using a model of gramicidin A channels in planar lipid bilayers, they have demonstrated that genistein (**42**) could alter the channel properties (conductivity and lifetime) by changing the hydrophobic mismatch and/or bilayer mechanical properties. Gramicidin channel properties were also profoundly altered by daidzein (**40**) and phloretin (**66**), while genistin (**46**) showed apparently no effects.

Genistein (**42**) was found to affect many other types of channels, but the main proposed mechanism of these interactions was indirect. In most cases a PTK pathway was suggested as a putative explanation of the observed effects. Since genistein (**42**) is a well-known inhibitor of this kinase, we will not focus on those papers and only a short list will be presented. Such a mechanism was mentioned in the case of inhibition of ATP-sensitive K$^+$ channels [325], cardiac slowly activating delayed-rectifier K$^+$ current [326], L-type calcium channels [327, 328] (contrary to the direct interaction proposed by Chiang et al. [306] and Yokoshiki et al. [307]), P/Q-type calcium channels in rat hippocampal neurons [329], and carotid baroreceptor activity [330]. A PTK-dependent mechanism was also proposed as the explanation of potentiation of neuronal α7 nAChRs by genistein (**42**) [331].

In several papers direct and/or indirect flavonoid–ion channel interactions were proposed as a putative explanation of the observed phenomena. Thus, the inhibition of Ca^{2+} and activation of K$^+$ channels in rat thoracic aorta was suggested to explain the mechanism of vasorelaxation induced by luteonin [332]. An EGCg (**64**) influence on calcium channels sensitive to diphenylamine-2-carboxylate was proposed as one of the mechanisms underlying the EGCg-induced alteration of intracellular calcium levels in nonexcitable cells [333]. Direct interaction with the protein molecule was suggested as a mechanism of stimulation of mitochondrial Ca^{2+} uniporter by genistein (**42**), genistin (**46**), kaempferol (**28**), and quercetin (**29**) [334]. Interactions of a group of flavonoids with different types of potassium channels were proposed to explain the vasorelaxant properties of these compounds [335].

References

1. Bourlioux P, Moreaux JM, Su WJ, Boureau H (1992) APMIS Suppl 30:40
2. Molnar J, Foldeak S, Nakamura MJ, Gaizer F, Gutmann F (1991) Xenobiotica 21:309
3. Molnar J, Foldeak S, Nakamura MJ, Rausch H, Domonkos K, Szabo M (1992) APMIS Suppl 30:24
4. Motohashi N, Sakagami H, Kurihara T, Ferenczy L, Csuri K, Molnar J (1992) Anticancer Res 12:1207
5. Molnar A, Amaral L, Molnar J (2003) Int J Antimicrob Agents 22:217
6. Spengler G, Molnar A, Schelz Z, Amaral L, Sharples D, Molnar J (2006) Curr Drug Targets 7:823
7. Amaral L, Kristiansen JE, Viveiros M, Atouguia J (2001) J Antimicrob Chemother 47:505
8. Kristiansen MM, Leandro C, Ordway D, Martins M, Viveiros M, Pacheco T, Molnar J, Kristiansen JE, Amaral L (2006) In Vivo 20:361
9. Motohashi N, Kawase M, Molnar J, Ferenczy L, Wesolowska O, Hendrich AB, Bobrowska-Hagerstrand M, Hagerstrand H, Michalak K (2003) Arzneimittelforschung 53:590
10. Sharma S, Kaur H, Khuller GK (2001) Microbiol Lett 199:185
11. Wuonola MA, Palfreyman MG, Motohashi N, Kawase M, Gabay S, Nacsa J, Molnar J (1997) Anticancer Res 17:3409
12. Wuonola MA, Palfreyman MG, Motohashi N, Kawase M, Gabay S, Molnar J (1997) Anticancer Res 17:3425
13. Tanaka M, Molnar J, Kidd S (1997) Anticancer Res 17:381
14. Tanaka M, Wayda K, Molnar J, Parkanyi C, Aaron JJ, Motohashi N (1997) Anticancer Res 17:839
15. Azuine MA, Tokuda H, Takayasu J, Enjyo F, Mukainaka T, Konoshima T, Nishino H, Kapadia GJ (2004) Pharmacol Res 49:161
16. Zhelev Z, Ohba H, Bakalova R, Hadjimitova V, Ishikawa M, Shinohara Y, Baba Y (2004) Cancer Chemother Pharmacol 53:267
17. Gil-Ad I, Shtaif B, Levkovitz Y, Dayag M, Zeldich E, Weizman A (2004) J Mol Neurosci 22:189
18. Karmakar P, Natarajan AT, Poddar RK, Dasgupta UB (2001) Toxicol Lett 125:19
19. Cushnie TP, Lamb AJ (2005) Int J Antimicrob Agents 26:343–356
20. Schreier S, Malheiros SVP, de Paula E (2000) Biochim Biophys Acta 1508:210
21. Wajnberg E, Tabak M, Nussenzveig PA, Lopes CMB, Louro SRW (1988) Biochim Biophys Acta 944:185
22. Caetano W, Tabak M (1999) Spectrochim Acta A 55:2513
23. Caetano W, Tabak M (2000) J Colloid Interface Sci 225:69
24. Caetano W, Gelamo EL, Tabak M, Itri R (2002) J Colloid Interface Sci 248:149
25. Caetano W, Barbosa LRS, Itri R, Tabak M (2003) J Colloid Interface Sci 260:414
26. Barbosa LRS, Caetano W, Itri R, Homem-de-Mello P, Santiago PS, Tabak M (2006) J Phys Chem B 110:13086
27. Luxnat M, Galla HJ (1986) Biochim Biophys Acta 856:274
28. Welti R, Mullikin LJ, Yoshimura T, Helmkamp GM Jr (1984) Biochemistry 23:6086
29. Zachowski A, Durand P (1988) Biochim Biophys Acta 937:411

30. Banerjee S, Bennouna M, Ferreira-Marques J, Ruysschaert JM, Caspers J (1999) J Colloid Interface Sci 219:168
31. Binford JS Jr, Palm WH (1994) Biophys J 66:2024
32. Kitamura K, Imayoshi N, Goto T, Shiro H, Mano T, Nakai Y (1995) Anal Chim Acta 304:101
33. Takegami S, Kitamura K, Kitade T, Hasegawa K, Nishihira A (1999) J Colloid Interface Sci 220:81
34. Takegami S, Kitamura K, Takahashi K, Kitade T (2002) J Pharm Sci 91:1568
35. Takegami S, Kitamura K, Kitade T, Kitagawa A, Kawamura K (2003) Chem Pharm Bull (Tokyo) 51:1056
36. Takegami S, Kitamura K, Kitade T, Takashima M, Ito M, Nakagawa E, Sone M, Sumitani R, Yasuda Y (2005) Chem Pharm Bull (Tokyo) 53:147
37. Kitamura K, Takegami S, Kobayashi T, Makihara K, Kotani C, Kitade T, Moriguchi M, Inoue Y, Hashimoto T, Takeuchi M (2004) Biochim Biophys Acta 1661:61
38. Hendrich AB, Wesolowska O, Pola A, Motohashi N, Molnar J, Michalak K (2003) Mol Membr Biol 20:53
39. Pola A, Michalak K, Burliga A, Motohashi N, Kawase M (2004) Eur J Pharm Sci 21:421
40. Zografi G, Munshi MV (1970) J Pharm Sci 59:819
41. Gerebtzoff G, Li-Blatter X, Fischer H, Frentzel A, Seelig A (2004) ChemBioChem 5:676
42. Varnier Agasoster AV, Tungodden LM, Cejka D, Bakstad E, Sydnes LK, Holmsen H (2001) Biochem Pharmacol 61:817
43. Varnier Agasoster A, Holmsen H (2001) Biophys Chem 91:37
44. de Matos Alves Pinto L, Pinheiro Malheiros SV, Senges Lino AC, de Paula E, Perillo MA (2006) Biophys Chem 119:247
45. Hidalgo AA, Caetano W, Tabak M, Oliveira ON Jr (2004) Biophys Chem 109:85
46. Hidalgo AA, Pimentel AS, Tabak M, Oliveira ON Jr (2006) J Phys Chem B 110:19637
47. Jutila A, Soderlund T, Pakkanen AL, Huttunen M, Kinnunen PKJ (2001) Chem Phys Lipids 112:151
48. Pickholz M, Oliveira ON Jr, Skaf MS (2006) J Phys Chem B 110:8804
49. Moncelli MR, Becucci L (1996) Bioelectrochem Bioenerg 39:227
50. Karabaliev M, Kochev V (2001) Electrochem Commun 3:742
51. Nagappa AN, Kole PL, Srinivas D, Vivek D, Ullas DP, Srivastava RC (2005) Colloids Surf B Biointerfaces 43:21
52. Tsakovska I, Pajeva I (2006) Curr Drug Targets 7:1123
53. Michalak K, Wesolowska O, Motohashi N, Molnar J, Hendrich AB (2006) Curr Drug Targets 7:1095
54. Castaing M, Brouant P, Loiseau A, Santelli-Rouvier C, Santelli M, Alibert-Franco S, Mahamoud A, Barbe J (2000) J Pharm Pharmacol 52:289
55. Pajeva IK, Wiese M, Cordes HP, Seydel JK (1996) J Cancer Res Clin Oncol 122:27
56. Pajeva I, Todorov DK, Seydel J (2004) Eur J Pharm Sci 21:243
57. Cater BR, Chapman D, Hawes SM, Saville J (1974) Biochem Soc Trans 2:971
58. Frenzel J, Arnold K, Nuhn P (1978) Biochim Biophys Acta 507:185
59. Hanpft R, Mohr K (1985) Biochim Biophys Acta 814:156
60. Fernandez MR, Keyzer H, Dea MK, Dea PK (1992) The interaction of chlorpromazine with phospholipid multilayers. In: Keyzer H (ed) Thiazines and structurally related compounds. Krieger, Malabar, p 187
61. Hornby AP, Cullis PR (1981) Biochim Biophys Acta 647:285

62. Nerdal W, Gundersen SA, Thorsen V, Hoiland H, Holmsen H (2000) Biochim Biophys Acta 1464:165
63. Gjerde AU, Holmsen H, Nerdal W (2004) Biochim Biophys Acta 1682:28
64. Chen S, Gjerde AU, Holmsen H, Nerdal W (2005) Biophys Chem 117:101
65. Song C, Holmsen H, Nerdal W (2006) Biophys Chem 120:178
66. Chen JY, Brunauer LS, Chu FC, Helsel CM, Gedde MM, Huestis W H (2003) Biochim Biophys Acta 1616:95
67. Jang HO, Jeong DK, Ahn SH, Yoon CD, Jeong SC, Jin SD, Yun I (2004) J Biochem Mol Biol 37:603
68. Louro SRW, Anteneodo C, Wajnberg E (1998) Biophys Chem 74:35
69. Neal MJ, Butler KW, Polnaszek CF, Smith ICP (1976) Mol Pharmacol 12:144
70. Pang KY, Miller KW (1978) Biochim Biophys Acta 511:1
71. Wisniewska A, Wolnicka-Glubisz A (2004) Biophys Chem 111:43
72. Ahyayauch H, Requero MA, Alonso A, Bennouna M, Goni FM (2002) J Colloid Interface Sci 256:284
73. Cullis PR, Verkleij AJ, Ververgaert PHJ (1978) Biochim Biophys Acta 513:11
74. Verkleij AJ, de Maagd R, Leunissen-Bijvelt J, de Kruijff B (1982) Biochim Biophys Acta 684:255
75. McIntosh TJ, McDaniel RV, Simon SA (1983) Biochim Biophys Acta 731:109
76. Hendrich AB, Wesolowska O, Michalak K (2001) Biochim Biophys Acta 1510:414
77. Hendrich AB, Wesolowska O, Michalak K (2001) Curr Top Biophys 25:67
78. Hendrich AB, Lichacz K, Burek A, Michalak K (2002) Cell Mol Biol Lett 7:1081
79. Rodrigues T, Santos AC, Pigoso AA, Mingatto FE, Uyemura SA, Curti C (2002) Br J Pharmacol 6:136
80. Wesolowska O, Hendrich AB, Motohashi N, Michalak K (2001) Curr Top Biophys 25:71
81. Hendrich AB, Wesolowska O, Komorowska M, Motohashi N, Michalak K (2002) Biophys Chem 98:275
82. Wesolowska O, Hendrich AB, Motohashi N, Kawase M, Dobryszycki P, Ozyhar A, Michalak K (2004) Biophys Chem 109:399
83. Hendrich AB, Wesolowska O, Motohashi N, Molnar J, Michalak K (2003) Biochem Biophys Res Commun 304:260
84. Saija A, Scalese M, Lanza M, Marzullo D, Bonina F, Castelli F (1995) Free Radic Biol Med 19:481
85. Verstraeten SV, Keen CL, Schmitz HH, Fraga CG, Oteiza PI (2003) Free Radic Biol Med 34:84
86. Erlejman AG, Verstraeten SV, Fraga CG, Oteiza PI (2004) Free Radic Res 38:1311
87. Heim KE, Tagliaferro AR, Bobilya DJ (2002) J Nutr Biochem 13:572
88. Murota K, Shimizu S, Miyamoto S, Izumi T, Obata A, Kikuchi M, Terao J (2002) J Nutr 132:1956
89. Madsen HL, Andersen CM, Jorgensen LV, Skibsted LH (2000) Eur Food Res Technol 211:240
90. Yang B, Kotani A, Arai K, Kusu F (2001) Anal Sci 17:599
91. Chen ZY, Chan PT, Ho KY, Fung KP, Wang J (1996) Chem Phys Lipids 79:157
92. Vaya J, Mahmood S, Goldblum A, Aviram M, Volkova N, Shaalan A, Musa R, Tamir S (2003) Phytochemistry 62:89
93. Gordon MH, Roedig-Penman A (1998) Chem Phys Lipids 97:79
94. Arora A, Nair MG, Straasburg GM (1998) Arch Biochem Biophys 356:133
95. Arora A, Nair MG, Straasburg GM (1998) Free Radic Biol Med 24:1355

96. Soczynska-Kordala M, Bakowska A, Oszmianski J, Gabrielska J (2001) Cell Mol Biol Lett 6:277
97. van Acker SA, van den Berg DJ, Tromp MN, Griffioen DH, van Bennekom WP, van der Vijgh WJ, Bast A (1996) Free Radic Biol Med 20:331
98. Foti P, Erba D, Riso P, Spadafranca A, Criscuoli F, Testolin G (2005) Arch Biochem Biophys 433:421
99. Cao G, Sofic E, Prior RL (1997) Free Radic Biol Med 22:749
100. Galati G, Sabzevari O, Wilson JX, O'Brien PJ (2002) Toxicology 177:91
101. Liu W, Guo R (2005) J Colloid Interface Sci 290:564
102. Liu W, Guo R (2006) J Colloid Interface Sci 302:625
103. van Dijk C, Driessen AJM, Recourt K (2000) Biochem Pharmacol 60:1593
104. Kato R, Kajiya K, Tokumoto H, Kumazawa S, Nakayama T (2003) Biofactors 19:179
105. Kajiya K, Ichiba M, Kuwabara M, Kumazawa S, Nakayama T (2001) Biosci Biotechnol Biochem 65:1227
106. Ollila F, Halling K, Vuorela P, Vuorela H, Slotte JP (2002) Arch Biochem Biophys 399:103
107. Kajiya K, Kumazawa S, Nakayama T (2002) Biosci Biotechnol Biochem 66:2330
108. Kajiya K, Kumazawa S, Nakayama T (2001) Biosci Biotechnol Biochem 65:2638
109. Tammela P, Laitinen L, Galkin A, Wennberg T, Heczko R, Vuorela H, Slotte JP, Vuorela P (2004) Arch Biochem Biophys 425:193
110. Oteiza PI, Erlejman AG, Verstraeten SV, Keen CL, Fraga CG (2005) Clin Dev Immunol 12:19
111. Hashimoto T, Kumazawa S, Nanjo F, Hara Y, Nakayama T (1999) Biosci Biotechnol Biochem 63:2252
112. Caturla N, Vera-Samper E, Villalain J, Mateo CR, Micol V (2003) Free Radic Biol Med 34:648
113. Furusawa M, Tsuchiya H, Nagayama M, Tanaka T, Nakaya K, Iinuma M (2003) J Health Sci 49:475
114. Tsuchiya H, Nagayama M, Tanaka T, Furusawa M, Kashimata M, Takeuchi H (2002) Biofactors 16:45
115. Arora A, Byrem TM, Nair MG, Strasburg GM (2000) Arch Biochem Biophys 373:102
116. Tsuchiya H (1999) Pharmacology 59:34
117. Tsuchiya H, Iinuma M (2000) Phytomedicine 7:161
118. Tsuchiya H (2001) Chem Biol Interact 134:41
119. Yoshioka H, Haga H, Kubota M, Sakai Y, Yoshioka H (2006) Biosci Biotechnol Biochem 70:395
120. Tomeckova V, Guzy J, Kusnir J, Fodor K, Marekova M, Chavkova Z, Perjesi P (2006) J Biochem Biophys Methods 69:143
121. Sengupta B, Banerjee A, Sengupta PK (2004) FEBS Lett 570:77
122. Bondar OP, Pivovarenko VG, Rowe ES (1998) Biochim Biophys Acta 1369:119
123. Klymchenko AS, Mely Y, Demchenko AP, Duportail G (2004) Biochim Biophys Acta 1665:6
124. Saija A, Bonina F, Trombetta D, Tomaino A, Montenegro L, Smeriglio P, Castelli F (1995) Int J Pharm 124:1
125. Wojtowicz K, Pawlikowska-Pawlega B, Gawron A, Misiak LE, Gruszecki WI (1996) Folia Histochem Cytobiol 34:49
126. Lehtonen JY, Adlercreutz H, Kinnunen PK (1996) Biochim Biophys Acta 1285:91
127. Movileanu L, Neagoe I, Flonta ML (2000) Int J Pharm 205:135
128. Scheidt HA, Pampel A, Nissler L, Gebhardt R, Huster D (2004) Biochim Biophys Acta 1663:97

129. Siarheyeva A, Lopez JJ, Glaubitz C (2006) Biochemistry 45:6203
130. Kumazawa S, Kajiya K, Naito A, Saito H, Tuzi S, Tanio M, Suzuki M, Nanjo F, Suzuki E, Nakayama T (2004) Biosci Biotechnol Biochem 68:1743
131. Hendrich AB, Malon R, Pola A, Shirataki Y, Motohashi N, Michalak K (2002) Eur J Pharm Sci 16:201
132. Lania-Pietrzak B, Hendrich AB, Zugaj J, Michalak K (2005) Arch Biochem Biophys 433:428
133. Wesolowska O, Lania-Pietrzak B, Kuzdzal M, Stanczak K, Mosiadz D, Dobryszycki P, Ozyhar A, Komorowska M, Hendrich A B, Michalak K (2007) Acta Pharmacol Sin 28:296
134. Marroum PJ, Curry SH (1993) J Pharm Pharmacol 45:39
135. Aki H, Yamamoto M (1990) J Pharm Pharmacol 42:637
136. Aki H, Yamamoto M (1991) Biochem Pharmacol 41:133
137. Jones GL, Woodbury DM (1978) J Pharmacol Exp Ther 207:203
138. Olivier JL, Chachaty C, Wolf C, Daveloose D, Bereziat G (1989) Biochem J 264:633
139. Minetti M, Di Stasi AM (1987) Biochemistry 26:8133
140. Ruggiero AC, Meirelles NC (1998) Mol Genet Metab 64:148
141. Enomoto A, Takakuwa Y, Manno S, Tanaka A, Mohandas N (2001) Biochim Biophys Acta 1512:285
142. Born GVR, Housley GM (1983) Br J Pharmacol 79:481
143. Malheiros SVP, de Paula E, Meirelles NC (1998) Biochim Biophys Acta 1373:332
144. Hagerstrand H, Isomaa B (1991) Chem Biol Interact 79:335
145. Malheiros SVP, Meirelles NC, de Paula E (2000) Biophys Chem 83:89
146. Malheiros SVP, Brito MA, Brites D, Meirelles NC (2000) Chem Biol Interact 126:79
147. Lieber MR, Lange Y, Weinstein RS, Steck TL (1984) J Biol Chem 259:9225
148. Aki H, Yamamoto M (1990) Biochem Pharmacol 39:396
149. Isomaa B, Hagerstrand H, Paatero G (1987) Biochim Biophys Acta 899:93
150. Hagerstrand H, Isomaa B (1989) Biochim Biophys Acta 982:179
151. Hagerstrand H, Isomaa B (1992) Biochim Biophys Acta 1109:117
152. Sheetz MP, Singer SJ (1974) Proc Natl Acad Sci USA 71:4457
153. Elferink JGR (1977) Biochem Pharmacol 26:2411
154. Schrier SL, Chiu DTY, Yee M, Sizer K, Lubin B (1983) J Clin Invest 72:1698
155. Chen JY, Huestis WH (1997) Biochim Biophys Acta 1323:299
156. Rosso J, Zachowski A, Devaux PF (1988) Biochim Biophys Acta 942:271
157. Schrier SL, Zachowski A, Devaux PF (1992) Blood 79:782
158. Hagerstrand H, Holmstrom TH, Bobrowska-Hagerstrand M, Eriksson JE, Isomaa B (1998) Mol Membr Biol 15:89
159. Akel A, Hermle T, Niemoeller OM, Kempe DS, Lang PA, Attanasio P, Podolski M, Wieder T, Lang F (2006) Eur J Pharmacol 532:11
160. Wolfs JLN, Comfurius P, Bevers EM, Zwaal RFA (2003) Mol Membr Biol 20:83
161. Dai F, Miao Q, Zhou B, Yang L, Liu ZL (2006) Life Sci 78:2488
162. Lopez-Revuelta A, Sanchez-Gallego JI, Hernandez-Hernandez A, Sanchez-Yague J, Llanillo M (2006) Chem Biol Interact 161:79
163. Pawlikowska-Pawlega B, Gruszecki WI, Misiak LE, Gawron A (2003) Biochem Pharmacol 66:605
164. Suwalsky M, Orellana P, Avello M, Villena F, Sotomayor CP (2006) Food Chem Toxicol 44:393
165. Ambudkar SV, Kimchi-Sarfaty C, Sauna ZE, Gottesman MM (2003) Oncogene 22:7468
166. Schinkel AH, Jonker JW (2003) Adv Drug Deliv Rev 55:3

167. Tsuruo T, Iida H, Tsukagoshi S, Sakurai Y (1982) Cancer Res 42:4730
168. Hait WN, Pierson NR (1990) Cancer Res 50:1165
169. Szabo D, Szabo G Jr, Ocsovszki I, Aszalos A, Molnar J (1999) Cancer Lett 139:115
170. Barbieri F, Alama A, Tasso B, Boido V, Bruzzo C, Sparatore F (2003) Invest New Drugs 21:413
171. Pajak B, Molnar J, Engi H, Orzechowski A (2005) In Vivo 19:1101
172. Molnar J, Hever A, Fakla I, Fischer J, Ocsovski I, Aszalos A (1997) Anticancer Res 17:481
173. Ford JM, Bruggemann EP, Pastan I, Gottesman MM, Hait WN (1990) Cancer Res 50:1748
174. Liu R, Sharom FJ (1996) Biochemistry 35:11865
175. Liu R, Siemiarczuk A, Sharom FJ (2000) Biochemistry 39:14927
176. Syed SK, Christopherson RI, Roufogalis BD (1996) Biochem Mol Biol Int 39:687
177. Sandstrom R, Karlsson A, Lennernas H (1998) J Pharm Pharmacol 50:729
178. Boulton DW, DeVane CL, Liston HL, Markowitz JS (2002) Life Sci 71:163
179. Maki N, Moitra K, Silver C, Ghosh P, Chattopadhyay A, Dey S (2006) Biochemistry 45:2739
180. Maki N, Dey S (2006) Biochem Pharmacol 72:145
181. Ghosh P, Moitra K, Maki N, Dey S (2006) Arch Biochem Biophys 450:100
182. Kolaczkowski M, Michalak K, Motohashi N (2003) Int J Antimicrob Agents 22:279
183. Sharom FJ (1997) Biochem Soc Trans 25:1088
184. Ferte J (2000) Eur J Biochem 267:277
185. Romsicki Y, Sharom FJ (1999) Biochemistry 38:6887
186. Bebawy M, Morris MB, Roufogalis BD (2001) Br J Cancer 85:1998
187. Hendrich AB, Michalak K (2003) Curr Drug Targets 4:23
188. Ford JM, Prozialeck WC, Hait WN (1989) Mol Pharmacol 35:105
189. Ramu A, Ramu N (1992) Cancer Chemother Pharmacol 30:165
190. Pajeva IK, Wiese M (1997) Quant Struct-Act Relat 16:1
191. Pajeva IK, Wiese M (1998) J Med Chem 41:1815
192. Molnar J, Molnar A, Mucsi I, Pinter O, Nagy B, Varga A, Motohashi N (2003) In Vivo 17:145
193. Konya A, Andor A, Satorhelyi P, Nemeth K, Kurucz I (2006) Biochem Biophys Res Commun 346:45
194. Tsakovska IM (2003) Bioorg Med Chem 11:2889
195. Dearden JC, Al-Noobi A, Scott AC, Thomson SA (2003) SAR QSAR Environ Res 14:447
196. Motohashi N, Kawase M, Saito S, Kurihara T, Satoh K, Nakashima H, Premanathan M, Arakaki R, Sakagami H, Molnar J (2000) Int J Antimicrob Agents 14:203
197. Wesolowska O, Molnar J, Motohashi N, Michalak K (2002) Anticancer Res 22:2863
198. Wesolowska O, Paprocka M, Kozlak J, Motohashi N, Dus D, Michalak K (2005) Anticancer Res 25:383
199. Wesolowska O, Mosiadz D, Motohashi N, Kawase M, Michalak K (2005) Biochim Biophys Acta 1720:52
200. Morris ME, Zhang S (2006) Life Sci 78:2116
201. Chieli E, Romiti N, Cervelli F, Tongiani R (1995) Life Sci 57:1741
202. Critchfield JW, Welsh CJ, Phang JM, Yeh GC (1994) Biochem Pharmacol 48:1437
203. Shapiro AB, Ling V (1997) Biochem Pharmacol 53:587
204. Ferte J, Kuhnel JM, Chapuis G, Rolland Y, Lewin G, Schwaller MA (1999) J Med Chem 42:478

205. Di Pietro A, Conseil G, Perez-Victoria JM, Dayan G, Baubichon-Cortay H, Trompier D, Steinfels E, Jault JM, de Wet H, Maitrejean M, Comte G, Boumendjel A, Mariotte AM, Dumontet C, McIntosh DB, Goffeau A, Castanys S, Gamarro F, Barron D (2002) Cell Mol Life Sci 59:307
206. Boumendjel A, Bois F, Beney C, Mariotte AM, Conseil G, Di Pietro A (2001) Bioorg Med Chem Lett 11:75
207. Boumendjel A, Di Pietro A, Dumontet C, Barron D (2002) Med Res Rev 22:512
208. Zang S, Morris ME (2003) Pharm Res 20:1184
209. Conseil G, Baubichon-Cortay H, Dayan G, Jault JM, Barron D, Di Pietro A (1998) Proc Natl Acad Sci USA 95:9831
210. Comte G, Daskiewicz JB, Bayet C, Conseil G, Viorney-Vanier A, Dumontet C, Di Pietro A, Barron D (2001) J Med Chem 44:763
211. Maitrejean M, Comte G, Barron D, El Kirat K, Conseil G, Di Pietro A (2000) Bioorg Med Chem Lett 10:157
212. Kitagawa S (2006) Biol Pharm Bull 29:1
213. Perez-Victoria JM, Perez-Victoria FJ, Conseil G, Maitrejean M, Comte G, Barron D, Di Pietro A, Castanys S, Gamarro F (2001) Antimicrob Agents Chemother 45:439
214. Limtrakul P, Khantamat O, Pintha K (2005) J Chemother 17:86
215. Kitagawa S, Nabekura T, Takahashi T, Nakamura Y, Sakamoto H, Tano H, Hirai M, Tsukahara G (2005) Biol Pharm Bull 28:2274
216. Vaclavikova R, Boumendjel A, Ehrlichova M, Kovar J, Gut I (2006) Bioorg Med Chem 14:4519
217. Cole SPC, Deeley RG (2006) Trends Pharmacol Sci 27:438
218. Borst P, Oude Elferink R (2002) Annu Rev Biochem 71:537
219. Gottesman MM, Fojo T, Bates SE (2002) Nat Rev Cancer 2:48
220. Versantvoort CH, Broxterman HJ, Lankelma J, Feller N, Pinedo HM (1994) Biochem Pharmacol 48:1129
221. Hooijberg JH, Broxterman HJ, Heijn M, Fles DL, Lankelma J, Pinedo HM (1997) FEBS Lett 413:344
222. Leslie EM, Mao Q, Oleschuk CJ, Deeley RG, Cole SPC (2001) Mol Pharmacol 59:1171
223. Leslie EM, Deeley RG, Cole SP (2003) Drug Metab Dispos 31:11
224. Trompier D, Baubichon-Cortay H, Chang XB, Maitrejean M, Barron D, Riordon JR, Di Pietro A (2003) Cell Mol Life Sci 60:2164
225. Wu CP, Calgano AM, Hladky SB, Ambudkar SV, Barrand MA (2005) FEBS J 272:4725
226. Nguyen H, Zhang S, Morris ME (2003) J Pharm Sci 92:250
227. Van Zanden JJ, Wortelboer HM, Bijlsma S, Punt A, Usta M, van Bladeren PJ, Rietjens IM, Cnubben NHP (2005) Biochem Pharmacol 69:699
228. Van Zanden JJ, Mul A, Wortelboer HM, Usta M, van Bladeren PJ, Rietjens IM, Cnubben NHP (2005) Biochem Pharmacol 69:1657
229. Van Zanden JJ, Geraets L, Wortelboer HM, Van Bladeren PJ, Rietjens IM, Cnubben NHP (2004) Biochem Pharmacol 67:1607
230. Mavel S, Dikic B, Palakas S, Emond P, Greguric I, Gomez de Gracia A, Mattner F, Garrigos M, Guilloteau D, Katsifis A (2006) Bioorg Med Chem 14:1599
231. Bobrowska-Hagerstrand M, Wrobel A, Rychlik B, Bartosz G, Soderstrom T, Shirataki Y, Motohashi N, Molnar J, Michalak K, Hagerstrand H (2001) Blood Cells Mol Dis 27:894
232. Bobrowska-Hagerstrand M, Wrobel A, Mrowczynska L, Soderstrom T, Shirataki Y, Motohashi N, Molnar J, Michalak K, Hagerstrand H (2003) Oncol Res 13:463
233. Lania-Pietrzak B, Michalak K, Hendrich AB, Mosiadz D, Grynkiewicz G, Motohashi N, Shirataki Y (2005) Life Sci 77:1879

234. Litman T, Druley TE, Stein WD, Bates SE (2001) Cell Mol Life Sci 58:931
235. Cooray HC, Janvilisri T, Van Veen HW, Hladky SB, Barrand MA (2004) Biochem Biophys Res Commun 317:269
236. Imai Y, Tsukahara S, Asada S, Sugimoto Y (2004) Cancer Res 64:4346
237. Zhang S, Yang X, Morris ME (2004) Mol Pharmacol 65:1208
238. Suzuki M, Suzuki H, Sugimoto Y, Sugiyama Y (2003) J Biol Chem 278:22644
239. Zhang S, Yang X, Coburn RA, Morris ME (2005) Biochem Pharmacol 70:627
240. Middleton E, Kandaswami C, Theoharides TC (2000) Pharmacol Rev 52:673
241. Pedro M, Lourenco CF, Cidade H, Kijjoa A, Pinto M, Nascimento MSJ (2006) Toxicol Lett 164:24
242. Welch R, Chue P (2000) J Psychiatry Neurosci 25:154
243. Zareba W, Lin DA (2003) Psychiatr Q 74:291
244. Wooltorton J, Mathie A (1993) Br J Pharmacol 110:1126
245. Kon K, Krause E, Gogelein H (1994) J Pharmacol Exp Ther 271:632
246. Lee S, Choi SY, Youm JB, Ho WK, Earm YE, Lee CO, Jo SH (2004) J Cardiovasc Pharmacol 43:706
247. Choi S, Koh YS, Jo SH (2005) J Pharmacol Exp Ther 313:888
248. Kongsamut S, Kang J, Chen XL, Roehr J, Rampe D (2002) Eur J Pharmacol 450:37
249. Milnes J, Witchel HJ, Leaney JL, Leishman DJ, Hancox JC (2006) Biochem Biophys Res Commun 351:273
250. Thomas D, Wu K, Kathofer S, Katus HA, Schoels W, Kiehn J, Karle CA (2003) Br J Pharmacol 139:567
251. Kim K, Kim EJ (2005) Drug Chem Toxicol 28:303
252. Teisseyre A, Michalak K (2003) Biochem Pharmacol 65:551
253. Wible B, Murawsky MK, Crumb WJ Jr, Rampe D (1997) Brain Res 761:42
254. Muller M, De Weille JR, Lazdunski M (1991) Eur J Pharmacol 198:101
255. Ogata N, Tatebayashi H (1993) Br J Pharmacol 109:1239
256. Lee K, McKenna F, Rowe IC, Ashford ML (1997) Br J Pharmacol 121:1810
257. Laver D, Cherry CA, Walker NA (1997) J Membr Biol 155:263
258. McCann J, Welsh MJ (1987) J Gen Physiol 89:339
259. Kihira M, Matsuzawa K, Tokuno H, Tomita T (1990) Br J Pharmacol 100:353
260. Dreixler J, Bian J, Cao Y, Roberts MT, Roizen JD, Houamed KM (2000) Eur J Pharmacol 401:1
261. Terstappen G, Pula G, Carignani C, Chen MX, Roncarati R (2001) Neuropharmacology 40:772
262. Mathie A, Wooltorton JR, Watkins CS (1998) Gen Pharmacol 30:13
263. Ogata N, Narahashi T (1990) J Pharmacol Exp Ther 252:1142
264. Ito K, Nakazawa K, Koizumi S, Liu M, Takeuchi K, Hashimoto T, Ohno Y, Inoue K (1996) Eur J Pharmacol 314:143
265. Lee I, Park TJ, Suh BC, Kim YS, Rhee IJ, Kim KT (1999) Biochem Pharmacol 58:1017
266. Cruzblanca H, Gamino SM, Bernal J, Alvarez-Leefmans FJ (1998) Invert Neurosci 3:269
267. Ogata N, Yoshii M, Narahashi T (1990) J Physiol 420:165
268. Lopez-Gonzalez I, De La Vega-Beltran JL, Santi CM, Florman HM, Felix R, Darszon A (2001) Dev Biol 236:210
269. McNaughton N, Green PJ, Randall AD (2001) Acta Physiol Scand 173:401
270. Lefevre T, Coraboeuf E, Ghazi A, Coulombe A (1995) J Membr Biol 147:147
271. Antoine S, Lefevre T, Coraboeuf E, Nottin R, Coulombe A (1998) J Mol Cell Cardiol 30:2623

272. Antoine S, Pinet C, Coulombe A (2001) J Membr Biol 179:37
273. Pinet C, Antoine S, Filoteo AG, Penniston JT, Coulombe A (2002) J Membr Biol 187:185
274. Quamme G (1997) Biochim Biophys Acta 1324:18
275. Khan S, Dyer JL, Michelangeli F (2001) Cell Signal 13:57
276. Bolotina V, Courtney KR, Khodorov B (1992) Mol Pharmacol 42:423
277. Zhou X, Dong XW, Priestley T (2006) Brain Res 1106:72
278. Awayda M, Shao W, Guo F, Zeidel M, Hill WG (2004) J Gen Physiol 123:709
279. Ito Y, Sato S, Son M, Kume H, Takagi K, Yamaki K (2002) Toxicol Appl Pharmacol 183:198
280. Valverde M, Hardy SP, Diaz M (2002) Steroids 67:439
281. Benoit P, Changeux JP (1993) Neurosci Lett 160:81
282. Revah F, Galzi JL, Giraudat J, Haumont PY, Lederer F, Changeux JP (1990) Proc Natl Acad Sci USA 87:4675
283. Park T, Bae S, Choi S, Kang B, Kim K (2001) Biochem Pharmacol 61:1011
284. Mozrzymas J, Barberis A, Michalak K, Cherubini E (1999) J Neurosci 19:2474
285. Lidsky T, Yablonsky-Alter E, Zuck LG, Banerjee SP (1997) Brain Res 764:46
286. Zarnowska E, Mozrzymas JW (2001) Neurosci Lett 315:1
287. Choi B, Choi JS, Min DS, Yoon SH, Rhie DJ, Jo YH, Kim MS, Hahn SJ (2001) Biochem Pharmacol 62:527
288. Baek W, Jang BC, Lim JH, Kwon TK, Lee HY, Cho CH, Kim DK, Shin DH, Park JG, Lim JG, Bae JH, Bae JH, Yoo SK, Park WK, Song DK (2005) Biochem Pharmacol 70:1560
289. Zitron E, Scholz E, Owen RW, Luck S, Kiesecker C, Thomas D, Kathofer S, Niroomand F, Kiehn J, Kreye VA, Katus HA, Schoels W, Karle CA (2005) Circulation 111:835
290. Teisseyre A, Michalak K (2005) J Membr Biol 205:71
291. Fadool D, Holmes TC, Berman K, Dagan D, Levitan IB (1997) J Neurophysiol 78:1563
292. Washizuka T, Horie M, Obayashi K, Sasayama S (1998) J Mol Cell Cardiol 30:2577
293. Illek B, Fischer H, Santos GF, Widdicombe JH, Machen TE, Reenstra WW (1995) Am J Physiol 268:C886
294. Chiang C, Chen SA, Chang MS, Lin CI, Luk HN (1997) Biochem Biophys Res Commun 235:74
295. Illek B, Fischer H (1998) Am J Physiol 275:L902
296. Shuba L, Asai T, Pelzer S, McDonald TF (1996) Br J Pharmacol 119:335
297. French P, Bijman J, Bot AG, Boomaars WE, Scholte BJ, de Jonge HR (1997) Am J Physiol 273:C747
298. Melin P, Thoreau V, Norez C, Bilan F, Kitzis A, Becq F (2004) Biochem Pharmacol 67:2187
299. Berger A, Randak CO, Ostedgaard LS, Karp PH, Vermeer DW, Welsh MJ (2005) J Biol Chem 280:5221
300. Illek B, Zhang L, Lewis NC, Moss RB, Dong JY, Fischer H (1999) Am J Physiol 277:C833
301. Bebok Z, Collawn JF, Wakefield J, Parker W, Li Y, Varga K, Sorscher EJ, Clancy JP (2005) J Physiol 569:601
302. Lim M, McKenzie K, Floyd AD, Kwon E, Zeitlin PL (2004) Am J Respir Cell Mol Biol 31:351
303. Shibata S, Ono K, Iijima T (1999) Br J Pharmacol 128:1284
304. Yu H, Lu Z, Pan Z, Cohen IS (2004) Pflugers Arch 447:392

305. Altomare C, Tognati A, Bescond J, Ferroni A, Baruscotti M (2006) Br J Pharmacol 147:36
306. Chiang C, Chen SA, Chang MS, Lin CI, Luk HN (1996) Biochem Biophys Res Commun 223:598
307. Yokoshiki H, Sumii K, Sperelakis N (1996) J Mol Cell Cardiol 28:807
308. Saponara S, Sgaragli G, Fusi F (2002) Br J Pharmacol 135:1819
309. Wu S, Chiang HT, Shen AY, Lo YK (2003) J Cell Physiol 195:298
310. Fusi FSG, Saponara S (2005) J Pharmacol Exp Ther 313:790
311. Kurejova M, Lacinova L (2006) Arch Biochem Biophys 446:20
312. Chiang C, Luk HN, Chen LL, Wang TM, Ding PY (2002) J Biomed Sci 9:321
313. Saponara S, Testai L, Iozzi D, Martinotti E, Martelli A, Chericoni S, Sgaragli G, Fusi F, Calderone V (2006) Br J Pharmacol 149:1013
314. Huang R, Dillon GH (2000) Neuropharmacology 39:2195
315. Wang Y, Salter MW (1994) Nature 369:233
316. Wan Q, Man HY, Braunton J, Wang W, Salter MW, Becker L, Wang YT (1997) J Neurosci 17:5062
317. Wolfman C, Viola H, Paladini A, Dajas F, Medina JH (1994) Pharmacol Biochem Behav 47:1
318. Wang H, Hui KM, Chen Y, Xu S, Wong JT, Xue H (2002) Planta Med 68:1059
319. Huen M, Hui KM, Leung JW, Sigel E, Baur R, Wong JT, Xue H (2003) Biochem Pharmacol 66:2397
320. Viola H, Marder M, Wasowski C, Giorgi O, Paladini AC, Medina JH (2000) Biochem Biophys Res Commun 273:694
321. Marder M, Estiu G, Blanch LB, Viola H, Wasowski C, Medina JH, Paladini AC (2001) Bioorg Med Chem 9:323
322. Huang X, Liu T, Gu J, Luo X, Ji R, Cao Y, Xue H, Wong JT, Wong BL, Pei G, Jiang H, Chen K (2001) J Med Chem 44:1883
323. Wang F, Shing M, Huen Y, Tsang SY, Xue H (2005) Curr Drug Targets CNS Neurol Disord 4:575
324. Hwang T, Koeppe RE 2nd, Andersen OS (2003) Biochemistry 42:13646
325. Ogata R, Kitamura K, Ito Y, Nakano H (1997) Br J Pharmacol 122:1395
326. Missan S, Linsdell P, McDonald TF (2006) J Physiol 573:469
327. Ji E, Yin JX, Ma HJ, He RR (2004) Sheng Li Xue Bao 56:466
328. Nakayama S, Ito Y, Sato S, Kamijo A, Liu HN, Kajioka S (2006) FASEB J 20:1492
329. Potier B, Rovira C (1999) Brain Res 816:587
330. Ma H, Liu YX, Wang FW, Wang LX, He RR, Wu YM (2005) Acta Pharmacol Sin 26:840
331. Cho C, Song W, Leitzell K, Teo E, Meleth AD, Quick MW, Lester RA (2005) J Neurosci 25:3712
332. Jiang H, Xia Q, Wang X, Song J, Bruce IC (2005) Pharmazie 60:444
333. Kim H, Yum KS, Sung JH, Rhie DJ, Kim MJ, Min DS, Hahn SJ, Kim MS, Jo YH, Yoon SH (2004) Naunyn Schmiedebergs Arch Pharmacol 369:260
334. Montero M, Lobaton CD, Hernandez-Sanmiguel E, Santodomingo J, Vay L, Moreno A, Alvarez J (2004) Biochem J 384:19
335. Calderone V, Chericoni S, Martinelli C, Testai L, Nardi A, Morelli I, Breschi MC, Martinotti E (2004) Naunyn Schmiedebergs Arch Pharmacol 370:290

Author Index Volumes 1–8

The volume numbers are printed in italics

Subject Index